frontiers | Research Topics

Endocrinology, lipids, and disease: unraveling the links

Edited by
Prem Prakash Kushwaha, Dirk Müller-Wieland, Matthias Blüher and Robert Kiss

Coordinated by
Ashutosh Prince

Published in
Frontiers in Endocrinology

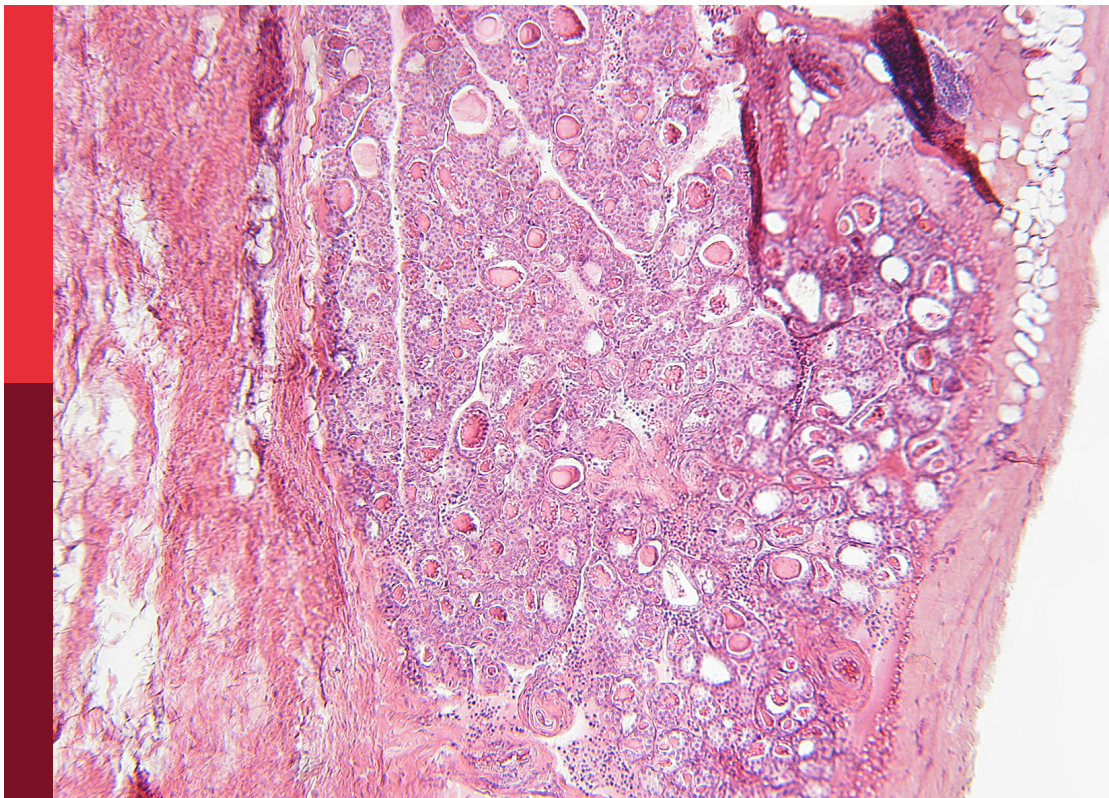

ISSN 1664-8714
ISBN 978-2-8325-6891-0
DOI 10.3389/978-2-8325-6891-0

Generative AI statement
Any alternative text (Alt text) provided alongside figures in the articles in this ebook has been generated by Frontiers with the support of artificial intelligence and reasonable efforts have been made to ensure accuracy, including review by the authors wherever possible. If you identify any issues, please contact us.

About Frontiers

Frontiers is more than just an open access publisher of scholarly articles: it is a pioneering approach to the world of academia, radically improving the way scholarly research is managed. The grand vision of Frontiers is a world where all people have an equal opportunity to seek, share and generate knowledge. Frontiers provides immediate and permanent online open access to all its publications, but this alone is not enough to realize our grand goals.

Frontiers journal series

The Frontiers journal series is a multi-tier and interdisciplinary set of open-access, online journals, promising a paradigm shift from the current review, selection and dissemination processes in academic publishing. All Frontiers journals are driven by researchers for researchers; therefore, they constitute a service to the scholarly community. At the same time, the *Frontiers journal series* operates on a revolutionary invention, the tiered publishing system, initially addressing specific communities of scholars, and gradually climbing up to broader public understanding, thus serving the interests of the lay society, too.

Dedication to quality

Each Frontiers article is a landmark of the highest quality, thanks to genuinely collaborative interactions between authors and review editors, who include some of the world's best academicians. Research must be certified by peers before entering a stream of knowledge that may eventually reach the public - and shape society; therefore, Frontiers only applies the most rigorous and unbiased reviews. Frontiers revolutionizes research publishing by freely delivering the most outstanding research, evaluated with no bias from both the academic and social point of view. By applying the most advanced information technologies, Frontiers is catapulting scholarly publishing into a new generation.

What are Frontiers Research Topics?

Frontiers Research Topics are very popular trademarks of the *Frontiers journals series*: they are collections of at least ten articles, all centered on a particular subject. With their unique mix of varied contributions from Original Research to Review Articles, Frontiers Research Topics unify the most influential researchers, the latest key findings and historical advances in a hot research area.

Find out more on how to host your own Frontiers Research Topic or contribute to one as an author by contacting the Frontiers editorial office: frontiersin.org/about/contact

Endocrinology, lipids, and disease: unraveling the links

Topic editors

Prem Prakash Kushwaha — Case Western Reserve University, United States
Dirk Müller-Wieland — University Hospital RWTH Aachen, Germany
Matthias Blüher — Leipzig University, Germany
Robert Kiss — McGill University, Canada

Topic coordinator

Ashutosh Prince — Cleveland State University, United States

Citation

Kushwaha, P. P., Müller-Wieland, D., Blüher, M., Kiss, R., Prince, A., eds. (2025). *Endocrinology, lipids, and disease: unraveling the links*. Lausanne: Frontiers Media SA. doi: 10.3389/978-2-8325-6891-0

Table of contents

frontiers | Frontiers in Endocrinology

TYPE Editorial
PUBLISHED 04 September 2025
DOI 10.3389/fendo.2025.1687649

OPEN ACCESS

EDITED AND REVIEWED BY
Ralf Jockers,
Université Paris Cité, France

*CORRESPONDENCE
Ashutosh Prince
a.prince65@csuohio.edu

RECEIVED 18 August 2025
ACCEPTED 25 August 2025
PUBLISHED 04 September 2025

CITATION
Prince A, Kushwaha PP, Blüher M, Müller-Wieland D and Kiss R (2025) Editorial: Endocrinology, lipids, and disease: unraveling the links. *Front. Endocrinol.* 16:1687649. doi: 10.3389/fendo.2025.1687649

Editorial: Endocrinology, lipids, and disease: unraveling the links

Ashutosh Prince[1,2]*, Prem Prakash Kushwaha[1,2], Mathias Blüher[3], Dirk Müller-Wieland[4] and Robert Kiss[5]

[1]Department of Biological, Geological and Environmental Science, Cleveland State University, Cleveland, OH, United States, [2]Centre of Gene Regulation in Health and Disease, Cleveland State University, Cleveland, OH, United States, [3]Helmholtz Institute for Metabolic, Obesity and Vascular Research (HI-MAG) of the Helmholtz Zentrum München at the University of Leipzig and University Hospital Leipzig, Leipzig, Germany, [4]Klinik für Kardiologie, Angiologie und Internistische Intensivmedizin, Universitätsklinikum RWTH Aachen, Aachen, Germany, [5]Research Institute of the McGill University Health Centre, McGill University, Montreal, QC, Canada

KEYWORDS

lipocrinology, endocrine regulation, lipid-based biomarkers, metabolic syndrome, extracellular vesicles, triglyceride-glucose (TyG) index

Editorial on the Research Topic
Endocrinology, lipids, and disease: unraveling the links

Introduction

The conventional view of lipids as a structural components or energy reservoirs have recently gained a more dynamic paradigm. Lipids are now a central molecular regulator in endocrine biology—act as active signaling molecules that profoundly shape hormone synthesis, secretion, and systemic action. This conceptual shift is at the heart of lipocrinology: the integration of lipid metabolism with endocrine function. The eighteen contributions assembled in this Research Topic, *Endocrinology, Lipids, and Disease: Unraveling the Links*, collectively advance this perspective, interweaving together key findings from molecular biology, systems-level pathophysiology, clinical diagnostics, and therapeutic innovation. This Research Topic moved beyond isolated observations to construct a cohesive, multi-scale narrative of how the intricate crosstalk between lipids and hormones governs metabolic health and disease.

Foundational mechanisms: from cellular machinery to systemic networks

At the most fundamental level, endocrine function is dependent on lipid biology. The mini-review by Aderhold and Alexaki provides a coherent overview of this within the adrenal gland, illustrating how specific lipids—including cholesterol, diacylglycerol, and phosphoinositides—are not just substrates but critical regulators of both steroidogenesis in the cortex and catecholamine exocytosis in the medulla. This work establishes the lipid-mediated orchestration of hormonal relay as a core cellular process.

Expanding from the cell to the system, the perspective by Łukowski et al. described a transformative model for type 1 diabetes, a classically defined autoimmune endocrinopathy. They proposed hypothesis at the Endocannabinoidome-Microbiota

(ECBoM) axis as a systemic disorder arising from a dysfunctional interplay between gut dysbiosis, lipid-derived endocannabinoid signaling, and immune dysregulation. This perspective, which emphasizes a network-based approach, redirects the cause of the condition from the pancreatic islet to a more comprehensive disruption in metabolic and immune balance. It implies that the autoimmune disorder is a secondary effect resulting from an imbalance among lipids, microbes, and the immune system on a systemic level.

Advancing the diagnostic frontier with integrated biomarkers

A prominent theme emerging from this Research Topic is the validation of biomarkers by apprehending the functional states of metabolic dysregulation. The triglyceride-glucose (TyG) index, a substitute for insulin resistance, is a key example. Zeng et al. demonstrate its potent predictive value in a cohort of patients with acute myocardial infarction, showing that a high TyG index independently predicts the formation of left ventricular aneurysms and cardiac death. Complementing this, Yan et al. employed machine learning algorithms on a large NHANES dataset, identifying the TyG index and its derivatives as the most powerful predictors of all-cause and cardiovascular mortality among eight lipid-related indicators in individuals with diabetes or prediabetes.

This principle of integrated risk assessment extends to other markers. Zhou et al. reveal that impaired sensitivity to thyroid hormones, even in euthyroid individuals, is strongly associated with the severity of metabolic syndrome, highlighting that tissue-level hormone resistance is a metabolic disruptor. Markers of visceral adiposity also show significant prognostic power. Pan et al. report a robust, L-shaped inverse correlation between the Lipid Accumulation Product (LAP) and osteoporosis in American adults, uncovering a critical lipid-bone axis. Similarly, work by Ding et al. associates perirenal fat thickness—a specific visceral fat depot—with hypertension and an elevated 10-year cardiovascular disease risk, emphasizing the endocrine influence of ectopic fat on vascular tone. Further illuminating the complexity of multi-organ damage, Jin et al. (Xue et al.) demonstrate how Advanced Glycation End Products (AGEs) interact with metrics like the TyG-BMI index to predict the risk of diabetic nephropathy, showcasing the synergy between glycation and lipotoxicity in driving renal disease.

Lipids and hormones in concert: diverse organ impacts of lipocrinology

The research presented illustrates that disruptions in the lipid-endocrine axis are not confined to classic metabolic organs but have far-reaching systemic consequences. In the liver, Meyer et al. uncover a mechanistic basis for sex differences in metabolic-associated steatotic liver disease (MASLD). Their preclinical model showed that female mice are protected from severe liver damage due to preferential lipid partitioning into adipose tissue, a process modulated by the differential expression of estrogen receptors that underscores the powerful influence of the hormonal milieu on organ-specific disease susceptibility. In reproductive health, Tu and Fang utilize integrative bioinformatics to link endometriosis directly to fatty acid metabolism. They identify six hub genes, including *PTGS2* and *ACSL4*, that resides at the nexus of lipid metabolism and inflammation, providing a molecular framework for understanding endometriosis as a metabolic-inflammatory disease and suggesting novel therapeutic targets. The systemic reach extends to the neuro-endocrine axis, where Liu et al. identify shared genetic variants and biological pathways between obesity and depression, particularly those related to inflammation and metabolic regulation. This finding points to a common genetic architecture underlying these frequently co-occurring conditions. Furthering this connection, Su et al. reported from a large prospective cohort that sufficient serum 25-hydroxyvitamin D levels are associated with a nearly 50% lower risk of sleep disorders in individuals with prediabetes or diabetes, highlighting the role of this fat-soluble hormone in regulating central processes beyond calcium homeostasis.

Therapeutic horizons: modulating lipid-endocrine pathways

Moreover, a deeper mechanistic understanding must translate into improved therapies. Several articles in this Research Topic explore interventions that target the lipid-endocrine network. A study by a separate Leng et al. cohort demonstrates that Ebenatide, a GLP-1 analogue, not only improves glycemic indices but also significantly reduces the TyG index and fat mass in patients with type 2 diabetes, showing the efficacy of hormonal agents in modifying both glucose and lipid pathways.

The therapeutic potential of natural compounds is also highlighted. Zong et al. review the evidence for lactoferrin, a natural protein, as a pleiotropic agent that can alleviate insulin resistance and inflammation via multiple signaling pathways, including PI3K/Akt. In a preclinical model of non-alcoholic steatohepatitis (NASH), Liu et al. showed that active vitamin D3 mitigates liver damage by modulating fatty acid metabolism, oxidative stress, and inflammation, positioning it as a potent metabolic regulator. Beyond pharmacology and nutraceuticals, *Zhang* et al. present a meta-analysis indicating that acupuncture can significantly improve glycemic and triglyceride profiles in patients with T2DM, suggesting that non-drug modalities can effectively restore lipid-hormonal balance.

Synthesis: embracing complexity and future directions

The ultimate understanding offered by this Research Topic highlights the intricate and non-linear characteristics of these biological systems. The work by Yan et al., for instance, describes

a U-shaped association between serum uric acid and metabolic risk, challenging simplistic linear assumptions and revealing that both low and high levels of a metabolite can be associated with pathology. This reflects the importance of maintaining metabolic homeostasis within a specific physiological range. The identification of shared genetic loci for obesity and depression by Tian et al. further strengthens that these clinical phenotypes are the emergent properties of embedded, interconnected biological networks.

Taken together, these eighteen articles chart the course of a field moving decisively toward an integrated, systems-level perspective. They firmly establish that lipids are not passive molecular integrity but active endocrine modulators that integrate cellular machinery, hormonal feedback loops, and systemic networks. The consistent outperformance of composite biomarkers like the TyG index and LAP signals a necessary evolution in clinical diagnostics, while therapeutic successes with agents like GLP-1 analogues and even non-traditional interventions like acupuncture highlight the promise of targeting the lipid-endocrine axis directly. This Research Topic solidifies *lipocrinology* as an essential conceptual framework, driving the field toward a more holistic and summarized approach to understanding the endocrine and metabolic diseases.

Author contributions

AP: Validation, Formal Analysis, Writing – review & editing, Conceptualization, Methodology, Writing – original draft, Resources, Investigation, Supervision. PK: Resources, Visualization, Formal Analysis, Supervision, Writing – original draft, Conceptualization, Writing – review & editing, Investigation, Methodology. MB: Writing – review & editing, Writing – original draft, Conceptualization, Formal Analysis. DM-W: Conceptualization, Writing – review & editing, Writing – original draft, Formal Analysis, Visualization. RK: Writing – original draft, Writing – review & editing, Conceptualization, Formal Analysis.

Conflict of interest

The authors declare that the research was conducted in the absence of any commercial or financial relationships that could be construed as a potential conflict of interest.

The author(s) declared that they were an editorial board member of Frontiers, at the time of submission. This had no impact on the peer review process and the final decision.

Generative AI statement

The author(s) declare that Generative AI was used in the creation of this manuscript. ChatGPT LLM and Grammarly were used for rephrasing and grammatical editing.

Any alternative text (alt text) provided alongside figures in this article has been generated by Frontiers with the support of artificial intelligence and reasonable efforts have been made to ensure accuracy, including review by the authors wherever possible. If you identify any issues, please contact us.

Publisher's note

frontiers | Frontiers in Medicine

TYPE Original Research
PUBLISHED 04 September 2024
DOI 10.3389/fmed.2024.1428593

OPEN ACCESS

EDITED BY
Prem Prakash Kushwaha,
Case Western Reserve University,
United States

REVIEWED BY
Norbert Stefan,
University of Tübingen, Germany
Wen Wang,
First Affiliated Hospital of Xi'an Jiaotong University, China

*CORRESPONDENCE
Xiaochun Weng
✉ weng04230409@163.com

RECEIVED 06 May 2024
ACCEPTED 27 August 2024
PUBLISHED 04 September 2024
CORRECTED 22 August 2025

CITATION
Jin X, Xu J and Weng X (2024) Correlation between ratio of fasting blood glucose to high density lipoprotein cholesterol in serum and non-alcoholic fatty liver disease in American adults: a population based analysis. *Front. Med.* 11:1428593.
doi: 10.3389/fmed.2024.1428593

Correlation between ratio of fasting blood glucose to high density lipoprotein cholesterol in serum and non-alcoholic fatty liver disease in American adults: a population based analysis

Xianjing Jin[2], Jing Xu[3] and Xiaochun Weng[1]*

[1]Department of Ultrasound, The Second Affiliated Hospital and Yuying Children's Hospital of Wenzhou Medical University, Wenzhou, China, [2]Department of Ultrasound, Wenzhou Yongjia County Traditional Chinese Medicine Hospital, Wenzhou, China, [3]Department of Endocrinology, The Second Affiliated Hospital and Yuying Children's Hospital of Wenzhou Medical University, Wenzhou, China

Background: Based on previous research, elevated fasting blood glucose (FBG) and decreased high-density lipoprotein cholesterol (HDL-C) levels are associated with non-alcoholic fatty liver disease (NAFLD). It is hypothesized that the prevalence of NAFLD may be proportional to the FBG-to-HDL-C ratio (GHR).

Methods: In this study, 3,842 participants from the National Health and Nutrition Examination Survey (NHANES) (2013–2020) were investigated. Liver steatosis was assessed using vibration-controlled transient elastography (VCTE). NAFLD was defined as controlled attenuation parameter (CAP) ≥288 dB/m.

Results: After adjusting for race, gender, age, diabetes, BMI, moderate activities, uric acid, albumin, ALT, GGT, ALP, total bilirubin and creatinine, multiple logistic regression analysis indicated a positive correlation between GHR and the prevalence of NAFLD (OR = 1.22, 95% CI = 1.17–1.28). Additionally, multiple linear regression analysis showed a positive correlation between GHR and the severity of liver steatosis according to CA *p*-values (β = 4.97, 95% CI: 4.28, 5.66). According to the subgroup analysis, the correlation was stronger in other race, participants at the age <50 years old and those with non-diabetes. In this study, a non-linear relationship and saturation effect between GHR and the prevalence of NAFLD was also revealed, characterized by an inverted L-shaped curve, with an inflection point of 7.443. Finally, the receiver operating characteristic (ROC) analysis suggested that the area under the curve (AUC) of GHR (AUC = 0.731) significantly exceeded that of FBG and HDL-C.

Conclusion: Elevated GHR levels are independently associated with the severity of liver steatosis and the increased prevalence of NAFLD in American adults.

KEYWORDS

fasting blood glucose, fatty liver, obesity, diabetes, dyslipidemia

Introduction

The prevalence and incidence of NAFLD are increasing worldwide (1–4), with rates from 13% in Africa (1) to 42% in Southeast Asia (4). In the United States, the prevalence of NAFLD is currently 35.3% (5) and continues to increase (4). Due to the increase of prevalence, NAFLD is increasingly recognized as a significant factor to liver fibrosis, cirrhosis, liver transplantation and hepatocellular carcinoma (HCC), resulting in a substantial socioeconomic burden on society (4, 6) and a rising cause of liver-related mortality globally (3). Therefore, it is necessary to discover a cost-effective and efficient biomarker for early detection and staging of fatty liver disease (7).

NAFLD has been found to have a strong and reciprocal correlation with type 2 diabetes mellitus (T2DM), obesity, hypertension and dyslipidemia, serving as a hepatic manifestation of metabolic syndrome (MetS) (2, 8). Several studies have demonstrated the significant impact of blood glucose in serum on the initiation and advancement of NAFLD. Specifically, it has been shown that the concentrations of elevated 24 h glucose can increase hepatic *de novo* lipogenesis (DNL) in NAFLD patients (9). Furthermore, HDL-C, commonly known as "good cholesterol," is crucial in binding lipid molecules, such as triglyceride (TG) and cholesterol, thereby actively contributing to the process of clearing cholesterol and ultimately preventing the progression of NAFLD (10). Due to the opposite trend between glucose and HDL-C, there is a greater difference in GHR between non NAFLD and NAFLD groups, making it a potential biomarker for diagnosing NAFLD. To our knowledge, it is the first study to report the effectiveness of GHR in the diagnosis of NAFLD.

In this study, the data collected from the NHANES (2013–2020) cohort were adopted to examine and evaluate the correlation between GHR and the prevalence of NAFLD in American adults.

Materials and methods

Research design and research population

The data analyzed in this study were obtained from NHANES (2013–2020), with a stratified, multi-stage probability and complex sample of uninstituted population in the United States. The cross-sectional surveys were conducted by NCHS.

The study focuses exclusively on subjects aged 18 years old and above (n = 27,654), among which, 23,812 subjects were excluded: (1) those with missing data on FBG, HDL-C or transient elastography (TE); (2) those who self-reported high levels of alcohol consumption, defined as exceeding 14 drinks for females and 21 drinks for males weekly; (3) those with viral hepatitis, severe kidney dysfunction, liver diseases caused by drugs. Consequently, 3,842 subjects aged 18–80 years old were included in the final analysis (Figure 1).

The implementation of NHANES was approved by the Ethics Review Board of NCHS, and all subjects have provided the informed consent in written (11).

Vibration controlled transient elastography

In the database of NHANES (2013–2020), liver vibration controlled transient elastography (VCTE) in participants was measured with the FibroScan 502 V2 Touch (Echosens), which was well-suited for studying NAFLD, a condition characterized by fatty liver disease. In order to assess liver steatosis in patients with fatty liver disease, validated parameters such as controlled attenuation parameter (CAP) were adopted (12, 13). The VCTE results were considered effectively to follow certain criteria, including obtaining at least 10 LSMs after fasting for at least 3 h, and interquartile range (IQR)/median less than 30% (14). It is used to determine that CAP values (≥288 dB/m) were NAFLD status (15).

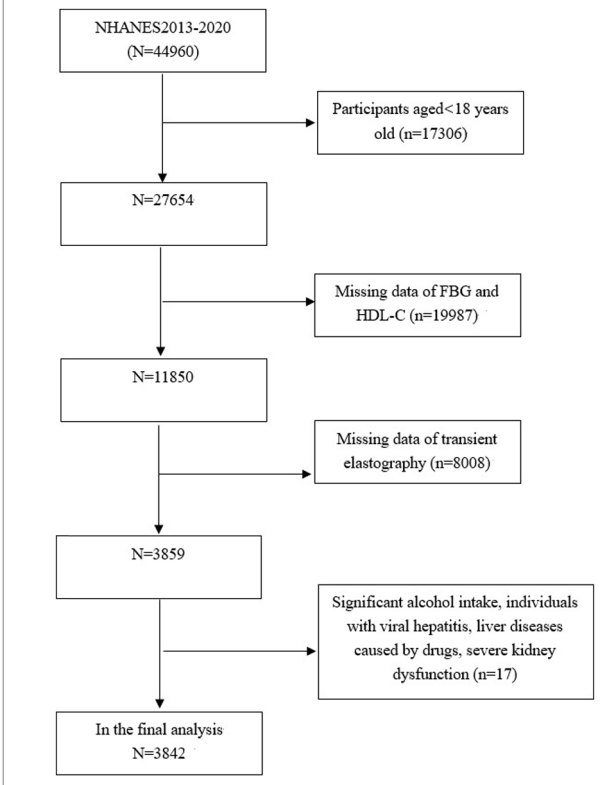

FIGURE 1
Flowchart of the sample selection from the 2013–2020 NHANES.

Research variables

The following covariates, including ALT, age, BMI, gender, history of diabetes, race [non-Hispanic White, non-Hispanic Black, Hispanic (American Mexican, and Hispanic other), and other race/multiracial], moderate activities, weight, TC, albumin, GGT, creatinine, ALP, LDL-C, FBG, HDL-C, total bilirubin, and triglyceride (TG) were included. Details of NAFLD and other covariate acquisition process were available at www.cdc.gov/nchs/nhanes/.

Statistical analysis

GHR was determined by calculating the ratio of FBG (mmol/L) to HDL-C (mmol/L). Continuous data in this analysis were presented as weighted mean ± standard deviation (SD). Categorical variables were represented as weighted proportions, and subjects were stratified into quartiles based on their GHR levels. The differences among the groups

for categorical variables were assessed with the weighted χ^2 test, while a weighted linear regression model was employed for continuous variables. Furthermore, the relationship between GHR and NAFLD status was examined with a weighted multivariate logistic regression model. In addition, the correlation between GHR and liver steatosis was explored through a weighted multivariate linear regression analysis, and assessed by liver CAP. The potential impacts of gender, BMI, age, moderate activities, diabetes and race on the relationship between GHR and NAFLD were examined through subgroup analyses. To identify any potential non-linear relationships between GHR and NAFLD probabilities, smooth curving fits and generalized additive models were utilized. The AUC was calculated through ROC analysis to evaluate the diagnostic ability of GHR, FBG and HDL-C for identification of NAFLD. Moreover, the statistical significance of the difference between two AUC values was assessed by MedCalc version 12.1.4.0 (MedCalc software, Belgium). Statistical analyses were performed with EmpowerStats software and R, with a significance ($p < 0.05$).

Results

Baseline characteristics of participants

A total of 3,842 participants aged 18–80 years old were included in the study, with a prevalence of NAFLD of 35.2%. The distribution of participant characteristics stratified by serum GHR quartiles (Q1: <3.49; Q2: 3.49–4.42; Q3: 4.42–5.66; Q4: >5.66) has been presented in Table 1. Compared with the bottom quartile, those in the top quartile of GHR were more likely to be the elderly and males, with a higher proportion of Mexican Americans, a higher prevalence of NAFLD, diabetes, and the increased levels of ALT, weight, GGT, BMI, ALP, creatinine, FBG, uric acid, TG, and CAP. In contrast, the proportion of moderate activities, and the levels of albumin, TC, HDL-C were lower ($p < 0.05$).

Correlation between GHR and the risk of NAFLD

Three weighted multivariate regression models were constructed to test the relationship between the prevalence of NAFLD and GHR (Table 2). The unadjusted model revealed a positive correlation between the levels of GHR and the probabilities of NAFLD [OR = 1.44, 95% CI: (1.38, 1.50)]. After adjusting for race, gender, age (Model 2), diabetes, BMI, moderate activities, uric acid, albumin, ALT, GGT, ALP, total bilirubin and creatinine (Model 3), the positive correlation was remained in Model 2 [OR = 1.41, 95% CI: (1.35, 1.47)] and Model 3 [OR = 1.22, 95% CI: (1.17, 1.28)]. Moreover, compared with the lowest level of GHR (Q1) in Model 3 (p for trend <0.001), the risk of NAFLD in subjects in quartiles 2, 3 and 4 increased by 0.35, 0.96 and 2.72, respectively. This results indicate that adults with elevated GHR are more likely to develop NAFLD than those with reduced GHR.

Correlation between GHR and the severity of liver steatosis

A multivariate linear regression analysis was performed between CAP and GHR (Table 3). GHR in Model 3 was dramatically and positively correlated with the severity of liver steatosis according to CAP values ($\beta = 4.97$, 95% CI: 4.28, 5.66) ($p < 0.001$).

Subgroup analysis

The consistency of the correlation between GHR and the prevalence of NAFLD across different demographic variables was evaluated through subgroup analyses. As displayed in Table 4, the results indicate that the positive correlation between GHR and the risk of NAFLD remains consistent regardless of BMI, gender, and moderate activities ($p > 0.05$ for all). The correlation between GHR and the risk of NAFLD was stronger among other race (OR = 1.42, p interaction =0.011), participants with age <50 years old (OR = 1.38, p interaction <0.001), and those with non-diabetes (OR = 1.36, p interaction <0.001).

Non-linearity and threshold effect analysis between GHR and NAFLD

A generalized additive model and smooth curve fittings were employed to illustrate the non-linear relationship and saturation effect between GHR and NAFLD, as depicted in Figures 2, 3. Among the participants, the correlation between GHR and NAFLD displayed an inverted L-shaped curve, with inflection points of 7.443 (as Table 5). Below the threshold of 7.443, a significant effect value of 1.359 was observed, while the value dropped to 1.076 when GHR exceeded 7.443.

ROC analysis

The ROC in Figure 4 and Table 6 presents the diagnostic performance of GHR, FBG and HDL-C in identifying NAFLD. The AUC for GHR in the ROC analysis was notably higher than that of FBG and HDL-C at 0.731 (95% CI: 0.714–0.747), with a sensitivity of 66.0%, a specificity of 68.8% and a cutoff of 4.73.

Discussion

An elevated GHR demonstrated a significant correlation with the prevalence of NAFLD in a large adult population in the United States in this cross-sectional study. Through subgroup analyses and interaction assessment, a stronger correlation was discovered in other race, participants with age <50 years old and those with non-diabetes. The analysis revealed an inverted L-shaped relationship between GHR and the prevalence of NAFLD, with a notable inflection point at a GHR measurement of 7.443. Furthermore, GHR exhibited a superior diagnostic accuracy for NAFLD compared to FBG and HDL-C alone.

Numerous studies have shown that glucose stimulates hepatic *de novo* lipogenesis (DNL) by activating carbohydrate-responsive element-binding protein (ChREBP) (16, 17). Moreover, studies have shown that fluctuations in glucose levels contribute to hepatic apoptosis, fibrosis, and inflammation by increasing oxidative stress in both *in vitro* and *in vivo* (18, 19). Conversely, HDL-C has been found to inhibit the retention, buildup, and oxidation of LDL-C, thereby exerting a protective effect. HDL-C facilitates the removal of dietary cholesterol through the reverse

TABLE 1 Weighted characteristics of the study population based on GHR quartiles.

Characteristic	Q1	Q2	Q3	Q4	*p*-value
Number	960	961	963	958	
Age, year	48.5 ± 18.4	47.1 ± 18.5	48.8 ± 17.9	53.1 ± 16.4	<0.001
NAFLD, %					<0.001
Yes	14.2	23.8	36.8	62.4	
No	85.8	76.2	63.2	37.6	
Sex, %					<0.001
Male	27.4	43.5	56.8	65.7	
Female	72.6	56.5	43.2	34.3	
Race, %					<0.001
Mexican American	9.5	14.2	15.5	17.9	
Other Hispanic	8.8	9.0	12.0	11.9	
Non-Hispanic White	37.8	32.4	37.1	37.1	
Non-Hispanic Black	26.7	25.8	19.8	17.1	
Other Race	17.2	18.5	15.6	16.0	
Moderate activities, %					<0.001
Yes	47.6	41.2	38.5	34.5	
No	52.4	58.8	61.5	65.5	
Diabetes					<0.001
Yes	3.8	5.7	10.6	38.1	
No	96.2	94.3	89.4	61.9	
Weight, kg	71.4 ± 17.7	79.8 ± 21.3	86.9 ± 21.3	94.6 ± 24.2	<0.001
BMI, kg/m^2	26.2 ± 5.9	28.8 ± 7.5	30.8 ± 7.1	33.2 ± 7.8	<0.001
GHR	2.89 ± 0.45	3.95 ± 0.27	5.00 ± 0.35	8.12 ± 3.41	<0.001
Albumin, g/dL	4.05 ± 0.34	4.04 ± 0.33	4.03 ± 0.33	3.99 ± 0.33	<0.001
ALT, U/L	19.5 ± 28.7	19.1 ± 11.5	22.8 ± 15.4	28.0 ± 21.5	<0.001
GGT, IU/L	29.2 ± 48.9	29.5 ± 83.1	29.9 ± 29.2	39.4 ± 47.9	<0.001
ALP, IU/L	72.7 ± 25.2	76.5 ± 22.9	78.7 ± 23.5	84.3 ± 29.8	<0.001
Total bilirubin, μmol/L	8.6 ± 5.0	8.2 ± 5.0	8.4 ± 4.7	8.4 ± 5.0	<0.001
Creatinine, mmol/L	74.1 ± 26.2	77.1 ± 36.6	80.7 ± 43.0	82.2 ± 47.0	<0.001
Uric acid, μmol/L	290.9 ± 77.7	313.3 ± 80.3	340.7 ± 80.4	353.8 ± 91.0	<0.001
FPG, mmol/L	5.3 ± 0.5	5.6 ± 0.6	6.0 ± 0.8	8.2 ± 3.3	<0.001
TC, mmol/L, mmol/L	4.98 ± 0.98	4.76 ± 1.03	4.69 ± 1.03	4.54 ± 1.12	<0.001
TG, mmol/L	0.94 ± 0.42	1.16 ± 0.58	1.44 ± 0.73	2.05 ± 1.84	<0.001
LDL-C, mmol/L	2.72 ± 0.86	2.86 ± 0.90	2.90 ± 0.90	2.71 ± 0.97	0.059
HDL-C, mmol/L	1.89 ± 0.38	1.43 ± 0.16	1.20 ± 0.17	1.02 ± 0.21	<0.001
CAP, dB/m	231.2 ± 54.3	249.3 ± 55.8	271.6 ± 58.1	304.4 ± 58.7	<0.001

Values are mean ± SD or number (%). $p < 0.05$ was deemed significant. BMI, body mass index; AC, arm circumference; HbA1c, glycosylated hemoglobin; TC, total cholesterol; TG, triglyceride; HDL-c, high density lipoprotein cholesterol; LDL-c, low density lipoprotein cholesterol; ALT, alanine aminotransferase; GGT, gamma-glutamyl transpeptidase; ALP, alkaline phosphatase; LSM, liver stiffness measurements; CAP, controlled attenuation parameter.

cholesterol transport pathway and exhibits antioxidant and anti-inflammatory properties (20). Therefore, a decrease in HDL-C levels may lead to impaired cholesterol efflux and antioxidant function, potentially contributing to the development of NAFLD (21). Studies have demonstrated a strong correlation between low HDL-C levels and the severity and progression of NAFLD (22, 23). The combination of HDL-C with other biomarkers has shown promising predictive value for NAFLD, with the monocyte-to-HDL-C ratio and uric acid-to-HDL-C ratio identified as independent predictors of the risk of NAFLD and severity (24, 25). Additionally, previous studies have indicated a significant correlation between the sdLDL-to-HDL-C ratio and NAFLD (26). Guo et al. (27) posited that elevated GHR levels were significantly correlated with heightened all-cause mortality among non-diabetic individuals with coronary artery disease undergoing percutaneous

TABLE 2 Association between GHR and NAFLD status in logistic regression analysis.

	Model 1 OR (95% CI) *p*-value	Model 2 OR (95% CI) *p*-value	Model 3 OR (95% CI) *p*-value
GHR	1.44 (1.38, 1.50), <0.001	1.41 (1.35, 1.47), <0.001	1.22 (1.17, 1.28), <0.001
AC (Quartile)			
Q1	Reference	Reference	Reference
Q2	1.87 (1.48, 2.35), <0.001	1.90 (1.51, 2.40), <0.001	1.35 (1.05, 1.75), 0.022
Q3	3.55 (2.85, 4.42), <0.001	3.55 (2.83, 4.45), <0.001	1.96 (1.52, 2.52), <0.001
Q4	9.41 (7.55, 11.73), <0.001	8.95 (7.12, 11.24), <0.001	3.72 (2.86, 4.84), <0.001
p for trend	<0.001	<0.001	<0.001

Model 1: None covariates were adjusted. Model 2: Gender, age and race were adjusted. Model 3: Gender, age, race, diabetes, moderate activities, BMI, albumin, uric acid, ALT, GGT, ALP, total bilirubin, creatinine.

TABLE 3 Associations between GHR and CAP value in linear regression analysis.

	Model 1 *β* (95% CI) *p*-value	Model 2 *β* (95% CI) *p*-value	Model 3 *β* (95% CI) *p*-value
GHR	9.31 (8.60, 10.01), <0.001	8.60 (7.89, 9.32), <0.001	4.97 (4.28, 5.66), <0.001
GHR (Quartile)			
Q1	Reference	Reference	Reference
Q2	18.10 (13.02, 23.18), 0.001	18.69 (13.66, 23.71), <0.001	7.44 (2.97, 11.91), <0.001
Q3	40.45 (35.38, 45.53), <0.001	39.85 (34.75, 44.95), <0.001	18.19 (13.51, 22.87), <0.001
Q4	73.18 (68.09, 78.26), <0.001	70.01 (64.82, 75.20), <0.001	36.79 (31.69, 41.89), <0.001
p for trend	<0.001	<0.001	<0.001

Model 1: None covariates were adjusted. Model 2: Gender, age and race were adjusted. Model 3: Gender, age, race, diabetes, moderate activities, BMI, albumin, uric acid, ALT, GGT, ALP, total bilirubin, creatinine.

TABLE 4 Association between GHR and NAFLD stratified by gender, age, race, diabetes, moderate activities and BMI.

	OR (95% CI) *p*-value	*p* for interaction
Stratified by gender		0.204
Male	1.17 (1.11–1.23), <0.001	
Female	1.29 (1.20–1.38), <0.001	
Stratified by race		0.011
Mexican American	1.24 (1.10, 1.39), <0.001	
Other Hispanic	1.16 (1.04, 1.29), 0.009	
Non-Hispanic White	1.25 (1.15, 1.37), <0.001	
Non-Hispanic Black	1.10 (1.02, 1.19), 0.016	
Other Race	1.42 (1.26, 1.60), <0.001	
Stratified by age		<0.001
Age <50 years old	1.38 (1.27, 1.50), <0.001	
Age ≥50 years old	1.17 (1.11, 1.22), <0.001	
Stratified by BMI		0.139
BMI <30 kg/m^2	1.31 (1.23, 1.39), <0.001	
BMI ≥30 kg/m^2	1.19 (1.12, 1.26), <0.001	
Stratified by diabetes		<0.001
Non-diabetes	1.36 (1.27, 1.46), <0.001	
Diabetes	1.09 (1.03, 1.16), 0.002	
Stratified by moderate activities		0.126
No	1.20 (1.14, 1.27), <0.001	
Yes	1.27 (1.18, 1.37), <0.001	

Gender, age, BMI, race, moderate activities, diabetes (not adjusted for in the subgroup analyses), albumin, uric acid, ALT, GGT, ALP, total bilirubin, creatinine were adjusted.

coronary intervention. So far, it is the first study to assess the relationship between GHR and NAFLD. The study revealed a significant correlation between elevated GHR levels and an increased prevalence of NAFLD in American adults, suggesting the potential importance of further exploration into the role of GHR in health outcomes.

Analyses on ROC revealed that GHR demonstrated the superior predictive utility for NAFLD compared to single biomarkers such as FBG and HDL-C. GHR may serve as a more effective indicator for clinical adjunct diagnosis of NAFLD due to the divergent trends observed in FBG and the levels of HDL-C. Additional research was warranted to investigate potential correlations between GHR and other metabolic conditions, such as hypertension, insulin resistance, and cardiovascular risk.

The findings suggest a notably stronger correlation between GHR and the prevalence of NAFLD among individuals under 50 years old and those with non-diabetes. As individuals ageing, body composition, metabolism, and the presence of coexisting diseases undergo changes (28–30). Additionally, dietary irregularities and insufficient exercise in young individuals can lead to excessive fat accumulation, potentially influencing GHR (31). Importantly, NAFLD is often overlooked for the aforementioned population. Therefore, GHR should be considered as an important factor for identifying NAFLD, especially for the aforementioned population.

Additionally, the study revealed an inverted L-shaped correlation between GHR and NAFLD, with the inflection point of 7.443. The discrepancy in the correlation between GHR and NAFLD on either side of the inflection point may be attributed to the influence of other variables. Analysis on Supplementary Table S1 indicated that individuals with GHR ≥7.443 exhibited higher levels or proportions than those with GHR <7.443 in male gender, BMI, weight, FBG, ALT, GGT, ALP, creatinine, uric acid and TG. However, abnormalities in these indicators were closely linked to NAFLD (32–34). When the level of GHR exceeded 7.443, the impact of GHR on NAFLD was found to be relatively weak, likely due to the presence of other risk factors for NAFLD. The study underscores the importance of targeting GHR levels in clinical interventions aimed at preventing NAFLD, with a particular emphasis on maintaining GHR levels below 7.443. Lower GHR levels below the threshold may significantly reduce the risk of NAFLD. This inflection point can serve as novel evidence supporting the management of GHR.

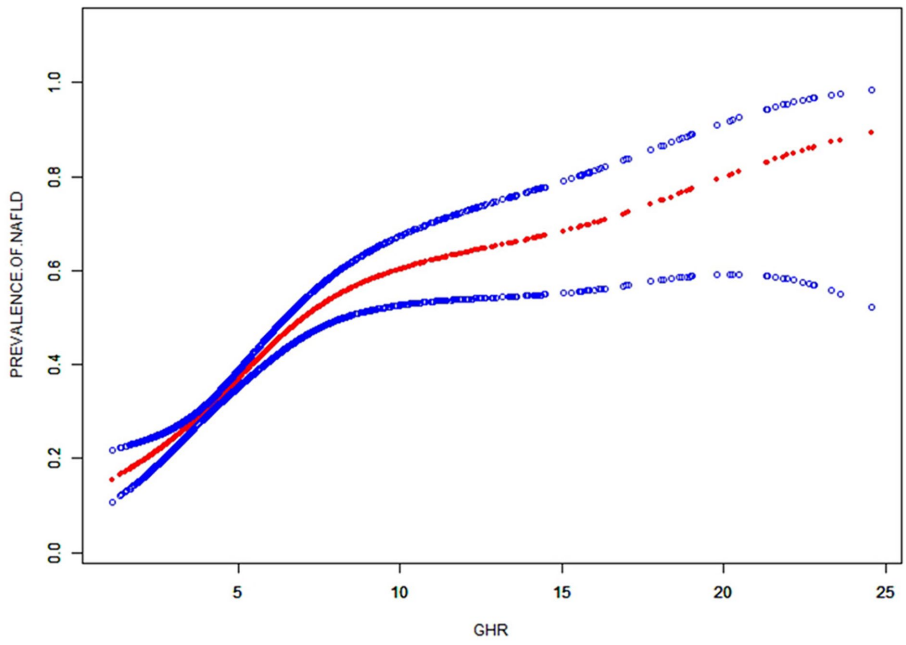

FIGURE 2
The smooth curve fit for the association between GHR and prevalence of NAFLD. Solid redline represents the smooth curve fit between variables. Blue bands represent the 95% of confidence interval from the fit. Adjusted for: race, gender, age, diabetes, BMI, moderate activities, uric acid, albumin, ALT, GGT, ALP, total bilirubin and creatinine.

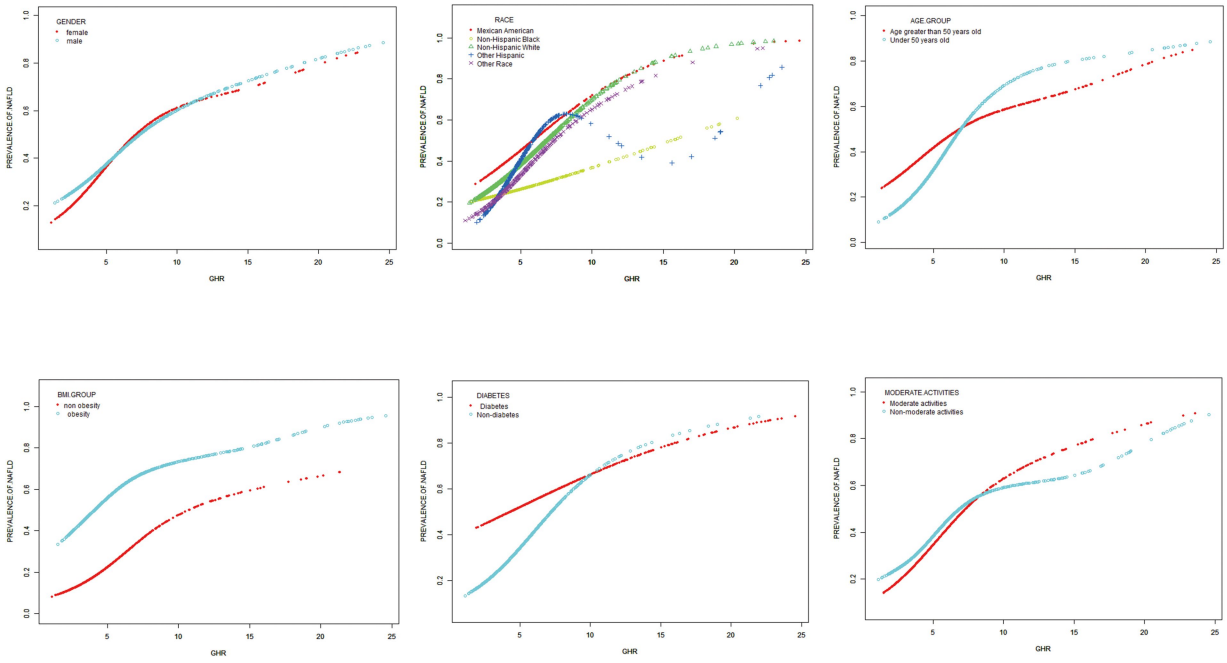

FIGURE 3
Subgroups analysis for the association between GHR and prevalence of NAFLD by gender, BMI, race, age, diabetes, moderate activities. Adjusted for: race, gender, age, diabetes, BMI, moderate activities, uric acid, albumin, ALT, GGT, ALP, total bilirubin and creatinine.

Notably, the study benefits from a large sample size and the national representativeness of Americans. In addition, various indicators in the model were adjusted to enhance the reliability of the findings. Nonetheless, this study is subject to certain limitations. Firstly, the establishment of a causal relationship between GHR and NAFLD was not feasible through cross-sectional studies. Secondly, the diagnosis of NAFLD relied on CAP values rather than the gold standard liver biopsy. Thirdly, the study was restricted to American adults, necessitating further prospective cohort research to validate and generalize the present results in a broader population.

TABLE 5 Threshold effect analysis of GHR on NAFLD using the two-piecewise linear regression model.

GHR	Adjusted OR (95% CI) *p*-value
Fitting by the standard linear model	1.218 (1.164, 1.274), <0.001
Fitting by the two-piecewise linear model	
Inflection point	7.443
GHR <7.443	1.359 (1.267, 1.457), <0.001
GHR >7.443	1.076 (1.005, 1.153), 0.0348
Log likelihood ratio	<0.001

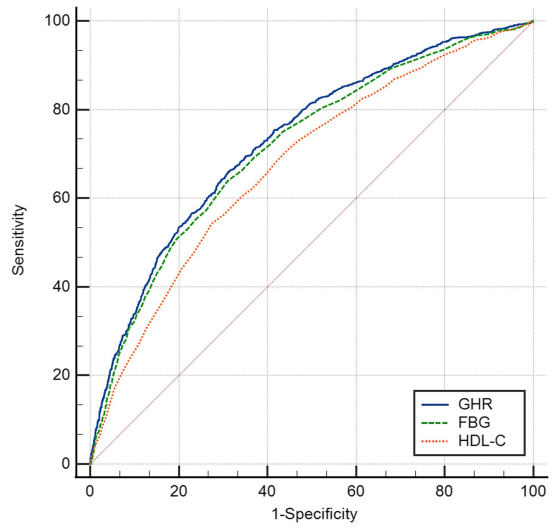

FIGURE 4
Receiver operating characteristic curves of GHR to identify NAFLD.

TABLE 6 The AUC for each index to discriminate NAFLD.

	AUC	95% CI	Cutoff value	Sensitivity	Specificity
GHR[a,b]	0.731	0.714–0.747	4.727	0.660	0.688
FBG[b]	0.715	0.698–0.732	5.855	0.639	0.690
HDL-C	0.676	0.658–0.694	1.205	0.659	0.688

[a]Indicates a significant difference as compared to FBG.
[b]Indicates a significant difference as compared to HDL-C.

Conclusion

In summary, elevated GHR was found to be independently associated with an increased risk of NAFLD and the severity of liver steatosis in a sizable cohort of American adults. This correlation was particularly pronounced among individuals of other races, those under 50 years old, and those without diabetes. These findings underscore the potential utility of GHR as a biomarker for identifying individuals at the heightened risk for NAFLD, thereby facilitating early detection and intervention strategies for this common liver disorder.

Data availability statement

Publicly available datasets were analyzed in this study. This data can be found here: NHANES, www.cdc.gov/nchs/NHANEs/.

Ethics statement

The studies involving humans were approved by National Center for Health Statistics Ethics Review Board. The studies were conducted in accordance with the local legislation and institutional requirements. The participants provided their written informed consent to participate in this study.

Author contributions

XJ: Writing – original draft. JX: Conceptualization, Investigation, Writing – original draft. XW: Writing – review & editing.

Funding

The author(s) declare that no financial support was received for the research, authorship, and/or publication of this article.

Acknowledgments

The authors thank the NHANES database for providing the data source for this study.

Conflict of interest

The authors declare that the research was conducted in the absence of any commercial or financial relationships that could be construed as a potential conflict of interest.

Correction note

A correction has been made to this article. Details can be found at: 10.3389/fmed.2025.1683822.

Publisher's note

Supplementary material

The Supplementary material for this article can be found online at: https://www.frontiersin.org/articles/10.3389/fmed.2024.1428593/full#supplementary-material

References

1. Younossi ZM, Koenig AB, Abdelatif D, Fazel Y, Henry L, Wymer M. Global epidemiology of nonalcoholic fatty liver disease-meta-analytic assessment of prevalence, incidence, and outcomes. *Hepatology*. (2016) 64:73–84. doi: 10.1002/hep.28431

2. Younossi Z, Anstee QM, Marietti M, Hardy T, Henry L, Eslam M, et al. Global burden of NAFLD and NASH: trends, predictions, risk factors and prevention. *Nat Rev Gastroenterol Hepatol*. (2018) 15:11–20. doi: 10.1038/nrgastro.2017.109

3. Paik JM, Golabi P, Younossi Y, Mishra A, Younossi ZM. Changes in the global burden of chronic liver diseases from 2012 to 2017: the growing impact of NAFLD. *Hepatology*. (2020) 72:1605–16. doi: 10.1002/hep.31173

4. Estes C, Razavi H, Loomba R, Younossi Z, Sanyal AJ. Modeling the epidemic of nonalcoholic fatty liver disease demonstrates an exponential increase in burden of disease. *Hepatology*. (2018) 67:123–33. doi: 10.1002/hep.29466

5. Le MH, Yeo YH, Li X, Li J, Zou B, Wu Y, et al. 2019 global NAFLD prevalence: a systematic review and meta-analysis. *Clin Gastroenterol Hepatol*. (2022) 20:2809–2817.e28 e28. doi: 10.1016/j.cgh.2021.12.002

6. Wong RJ, Cheung R, Ahmed A. Nonalcoholic steatohepatitis is the most rapidly growing indication for liver transplantation in patients with hepatocellular carcinoma in the U.S. *Hepatology*. (2014) 59:2188–95. doi: 10.1002/hep.26986

7. Araujo AR, Rosso N, Bedogni G, Tiribelli C, Bellentani S. Global epidemiology of non-alcoholic fatty liver disease/non-alcoholic steatohepatitis: what we need in the future. *Liver Int*. (2018) 38:47–51. doi: 10.1111/liv.13643

8. Stefan N, Cusi K. A global view of the interplay between non-alcoholic fatty liver disease and diabetes. *Lancet Diabetes Endocrinol*. (2022) 10:284–96. doi: 10.1016/S2213-8587(22)00003-1

9. Smith GI, Shankaran M, Yoshino M, Schweitzer GG, Chondronikola M, Beals JW, et al. Insulin resistance drives hepatic de novo lipogenesis in nonalcoholic fatty liver disease. *J Clin Invest*. (2020) 130:1453–60. doi: 10.1172/JCI134165

10. Katsiki N, Mikhailidis DP, Mantzoros CS. Non-alcoholic fatty liver disease and dyslipidemia: an update. *Metabolism*. (2016) 65:1109–23. doi: 10.1016/j.metabol.2016.05.003

11. Zipf G, Chiappa M, Porter KS, Ostchega Y, Lewis BG, Dostal J. National Health and Nutrition Examination Survey: plan and operations, 1999–2010. *Vital Health Stat*. (2013) 1:1–37.

12. Ferraioli G, Soares Monteiro LB. Ultrasound-based techniques for the diagnosis of liver steatosis. *World J Gastroenterol*. (2019) 25:6053–62. doi: 10.3748/wjg.v25.i40.6053

13. Cassinotto C, Boursier J, de Ledinghen V, Lebigot J, Lapuyade B, Cales P, et al. Liver stiffness in nonalcoholic fatty liver disease: a comparison of supersonic shear imaging, FibroScan, and ARFI with liver biopsy. *Hepatology*. (2016) 63:1817–27. doi: 10.1002/hep.28394

14. Ciardullo S, Perseghin G. Statin use is associated with lower prevalence of advanced liver fibrosis in patients with type 2 diabetes. *Metabolism*. (2021) 121:154752. doi: 10.1016/j.metabol.2021.154752

15. Rinella ME, Neuschwander-Tetri BA, Siddiqui MS, Abdelmalek MF, Caldwell S, Barb D, et al. AASLD practice guidance on the clinical assessment and management of nonalcoholic fatty liver disease. *Hepatology*. (2023) 77:1797–835. doi: 10.1097/HEP.0000000000000323

16. Yamashita H, Takenoshita M, Sakurai M, Bruick RK, Henzel WJ, Shillinglaw W, et al. A glucose-responsive transcription factor that regulates carbohydrate metabolism in the liver. *Proc Natl Acad Sci USA*. (2001) 98:9116–21. doi: 10.1073/pnas.161284298

17. Koo SH, Dutcher AK, Towle HC. Glucose and insulin function through two distinct transcription factors to stimulate expression of lipogenic enzyme genes in liver. *J Biol Chem*. (2001) 276:9437–45. doi: 10.1074/jbc.M010029200

18. Chandrasekaran K, Swaminathan K, Chatterjee S, Dey A. Apoptosis in HepG2 cells exposed to high glucose. *Toxicol In Vitro*. (2010) 24:387–96. doi: 10.1016/j.tiv.2009.10.020

19. Yin X, Zheng F, Pan Q, Zhang S, Yu D, Xu Z, et al. Glucose fluctuation increased hepatocyte apoptosis under lipotoxicity and the involvement of mitochondrial permeability transition opening. *J Mol Endocrinol*. (2015) 55:169–81. doi: 10.1530/JME-15-0101

20. Crudele L, De Matteis C, Piccinin E, Gadaleta RM, Cariello M, Di Buduo E, et al. Low HDL-cholesterol levels predict hepatocellular carcinoma development in individuals with liver fibrosis. *JHEP Rep*. (2023) 5:100627. doi: 10.1016/j.jhepr.2022.100627

21. Karami S, Poustchi H, Sarmadi N, Radmard AR, Ali Yari F, Pakdel A, et al. Association of anti-oxidative capacity of HDL with subclinical atherosclerosis in subjects with and without non-alcoholic fatty liver disease. *Diabetol Metab Syndr*. (2021) 13:121. doi: 10.1186/s13098-021-00741-5

22. Mato JM, Alonso C, Noureddin M, Lu SC. Biomarkers and subtypes of deranged lipid metabolism in non-alcoholic fatty liver disease. *World J Gastroenterol*. (2019) 25:3009–20. doi: 10.3748/wjg.v25.i24.3009

23. Feng G, Feng L, Zhao Y. Association between ratio of gamma-glutamyl transpeptidase to high-density lipoprotein cholesterol and prevalence of nonalcoholic fatty liver disease and metabolic syndrome: a cross-sectional study. *Ann Transl Med*. (2020) 8:634. doi: 10.21037/atm-19-4516

24. Huang H, Wang Q, Shi X, Chen Y, Shen C, Zhang J, et al. Association between monocyte to high-density lipoprotein cholesterol ratio and nonalcoholic fatty liver disease: a cross-sectional study. *Mediat Inflamm*. (2021) 2021:6642246. doi: 10.1155/2021/6642246

25. Xie Y, Huang K, Zhang X, Wu Z, Wu Y, Chu J, et al. Association of serum uric acid-to-high-density lipoprotein cholesterol ratio with non-alcoholic fatty liver disease in American adults: a population-based analysis. *Front Med*. (2023) 10:1164096. doi: 10.3389/fmed.2023.1164096

26. Yang S, Xu J. Elevated small dense low-density lipoprotein cholesterol to high-density lipoprotein cholesterol ratio is associated with an increased risk of metabolic dysfunction associated fatty liver disease in Chinese patients with type 2 diabetes mellitus. *J Diabetes Investig*. (2024) 15:634–42. doi: 10.1111/jdi.14148

27. Guo QQ, Zheng YY, Tang JN, Wu TT, Yang XM, Zhang ZL, et al. Fasting blood glucose to HDL-C ratio as a novel predictor of clinical outcomes in non-diabetic patients after PCI. *Biosci Rep*. (2020) 40:BSR20202797. doi: 10.1042/BSR20202797

28. Smith HJ, Sharma A, Mair WB. Metabolic communication and healthy aging: where should we focus our energy? *Dev Cell*. (2020) 54:196–211. doi: 10.1016/j.devcel.2020.06.011

29. Jafari Nasabian P, Inglis JE, Reilly W, Kelly OJ, Ilich JZ. Aging human body: changes in bone, muscle and body fat with consequent changes in nutrient intake. *J Endocrinol*. (2017) 234:R37–51. doi: 10.1530/JOE-16-0603

30. Goodpaster BH, Park SW, Harris TB, Kritchevsky SB, Nevitt M, Schwartz AV, et al. The loss of skeletal muscle strength, mass, and quality in older adults: the health, aging and body composition study. *J Gerontol A*. (2006) 61:1059–64. doi: 10.1093/gerona/61.10.1059

31. Correa-Rodriguez M, Gonzalez-Jimenez E, Fernandez-Aparicio A, Luis Gomez-Urquiza J, Schmidt-RioValle J, Rueda-Medina B. Dietary energy density is associated with body mass index and fat mass in early adulthood. *Clin Nurs Res*. (2021) 30:591–8. doi: 10.1177/1054773819883192

32. Semmler G, Balcar L, Wernly S, Volkerer A, Semmler L, Hauptmann L, et al. Insulin resistance and central obesity determine hepatic steatosis and explain cardiovascular risk in steatotic liver disease. *Front Endocrinol*. (2023) 14:1244405. doi: 10.3389/fendo.2023.1244405

33. Xing Y, Chen J, Liu J, Ma H. Associations between GGT/HDL and MAFLD: a cross-sectional study. *Diabetes Metab Syndr Obes*. (2022) 15:383–94. doi: 10.2147/DMSO.S342505

34. Huang XJ, Yin M, Zhou BQ, Tan XY, Xia YQ, Qin CX. Impact renaming non-alcoholic fatty liver disease to metabolic associated fatty liver disease in prevalence, characteristics and risk factors. *World J Hepatol*. (2023) 15:985–1000. doi: 10.4254/wjh.v15.i8.985

frontiers | Frontiers in Endocrinology

TYPE Original Research
PUBLISHED 29 October 2024
DOI 10.3389/fendo.2024.1422086

OPEN ACCESS

EDITED BY
Matthias Blüher,
Leipzig University, Germany

REVIEWED BY
Oscar Perez-Mendez,
Monterrey Institute of Technology and Higher Education (ITESM), Mexico
Arianna Toscano,
University Hospital of Policlinico G. Martino, Italy

*CORRESPONDENCE
Songhe Shi
ssh@zzu.edu.cn

RECEIVED 23 April 2024
ACCEPTED 07 October 2024
PUBLISHED 29 October 2024

CITATION
Su D, An Z, Chen L, Chen X, Wu W, Cui Y, Cheng Y and Shi S (2024) Association of triglyceride-glucose index, low and high-density lipoprotein cholesterol with all-cause and cardiovascular disease mortality in generally Chinese elderly: a retrospective cohort study.
Front. Endocrinol. 15:1422086.
doi: 10.3389/fendo.2024.1422086

Association of triglyceride-glucose index, low and high-density lipoprotein cholesterol with all-cause and cardiovascular disease mortality in generally Chinese elderly: a retrospective cohort study

Donghai Su[1], Zhantian An[2], Liyuan Chen[3], Xuejiao Chen[1], Wencan Wu[1], Yufang Cui[1], Yulin Cheng[1] and Songhe Shi[1]*

[1]Department of Epidemiology and Health Statistics, College of Public Health, Zhengzhou University, Zhengzhou, Henan, China, [2]Department of Orthopedics, Hongxing Hospital, 13th Division, Xinjiang Production and Construction Corps, Hami, Xinjiang, China, [3]Department of Epidemiology and Health Statistics, College of Public Health and Management, Wenzhou Medical University, Wenzhou, Zhejiang, China

Background: The impact of baseline triglyceride-glucose (TyG) index and abnormal low or high-density lipoprotein cholesterol (LDL-C or HDL-C) levels on all-cause and cardiovascular disease (CVD) mortality remains unclear. This study aimed to investigate the relationship between TyG index and LDL-C or HDL-C and all-cause and CVD mortality.

Methods: This retrospective cohort study analyzed data from health examinations of 69,068 older adults aged ≥60 in Xinzheng City, Henan Province, China, between January 2013 and January 2023. Cox proportional risk regression models were used to estimate the hazard ratio (HR) and 95% confidence interval (CI) of the TyG index and LDL-C or HDL-C about all-cause and CVD mortality. Restricted cubic spline was used to assess the dose-response relationship.

Results: During 400,094 person-years of follow-up (median follow-up 5.8 years [interquartile range 3.0-9.12]), 13,664 deaths were recorded, of which 7,045 were due to CVD. Compared with participants in the second quartile of the TyG index, participants in the fourth quartile had a 16% increased risk of all-cause mortality (HR: 1.16, 95% CI: 1.12,1.22), and an 8% increased risk of CVD mortality (HR: 1.08, 95% CI: 1.01,1.16). Similar results were observed in LDL-C and HDL-C, with all-cause and CVD mortality risks for participants in the fourth quartile compared with participants in the third quartile for LDL-C of (HR: 1.07, 95% CI: 1.02,1.12) and (HR: 1.09, 95% CI: 1.01,1.17), respectively. The risk of all-cause and CVD mortality in participants in the fourth quartile group compared with those in the second HDL-C quartile group was (HR: 1.10, 95% CI: 1.05,1.16) and (HR: 1.11, 95% CI: 1.04,1.18), respectively. We found that the TyG index was nonlinearly associated with all-cause and CVD mortality (P non-linear <0.05), and LDL-C was nonlinearly associated with all-cause mortality (P non-linear <0.05) but linearly

associated with CVD mortality (P non-linear >0.05). HDL-C, on the other hand, was in contrast to LDL-C, which showed a non-linear association with CVD mortality. We did not observe a significant interaction between TyG index and LDL-C or HDL-C (P >0.05).

Conclusion: TyG index and LDL-C or HDL-C increased the risk of all-cause and CVD mortality, especially a high TyG index combined with abnormal LDL-C.

KEYWORDS

triglyceride-glucose index, low density lipoprotein cholesterol, high density lipoprotein cholesterol, all-cause mortality, cardiovascular disease mortality

1 Background

Cardiovascular diseases (CVD) are the major cause of death and premature mortality in China (1, 2). The burden of CVD continues to increase annually, with approximately 330 million CVD patients in China. CVD is attributable to 2 out of every 5 deaths in China (3). The Global Burden of Disease (GBD) Study reports that the total prevalence of CVD worldwide has increased from 271 million in 1990 to 523 million in 2019. Additionally, the number of deaths has increased from 12.1 million to 18.6 million, and this trend is continuing (4).

Insulin resistance (IR), physiologically defined as a state of reduced responsiveness of insulin-targeted tissues to high physiologic insulin levels, is recognized as a causative driver of many modern diseases, including metabolic syndrome (Mts), type 2 diabetes mellitus (T2DM), and CVD complications (5). The main factors contributing to the development of IR are increased oxidative stress, hyperglycemia, and elevated lipid levels (6). Although advances have been made in therapies to help control blood glucose levels, CVD complications remain a major cause of morbidity and mortality in this population (7). The Homeostasis Model Assessment of Insulin Resistance (HOMA-IR) is the most widely used surrogate indicator of IR but has limitations due to its complexity and cost, and it cannot be used in populations receiving insulin therapy (7). The triglyceride glucose (TyG) index is a low-cost and convenient tool for assessing IR in diabetic and non-diabetic patients (8, 9). Using HIEC and HOMA-IR as reference methods, the diagnostic accuracy of the TyG index in identifying IR has been tested in several studies. The highest sensitivity for HIEC was 96% and the highest specificity for HOMA-IR was 99% (8). The TyG index has also shown good performance in the estimation of IR in diabetic and non-diabetic patients compared to HOMA-IR (8). In addition, the TyG index does not require insulin quantification and can be used in all people, regardless of their insulin therapy status (9). However, fewer studies have been conducted on the association between the TyG index and CVD mortality.

IR not only makes individuals susceptible to CVD, it also enhances the effects of dyslipidemia (10). Dyslipidemia, mainly low or high-density lipoprotein cholesterol (LDL-C or HDL-C) in the abnormal range, is considered one of the major risk factors for CVD (11). Previous epidemiological studies have suggested that a higher TyG index is an important risk factor for all-cause and, in particular, CVD mortality (12, 13). However, these studies were all conducted in the general population. Furthermore, while a causal association between LDL-C and CVD mortality has been demonstrated (14), there are conflicting results regarding the relationship between HDL-C and CVD mortality. For example, some studies have suggested that higher HDL-C may be a better preventive factor for CVD (15), while others have found that high HDL-C levels are associated with an increased risk of CVD (16). Some studies have suggested a U-shaped pattern of all-cause and CVD mortality associated with LDL-C (17, 18), with some studies showing a linear relationship (19). It is also worth noting that there is limited research on the effect of the interaction between the TyG index and LDL-C or HDL-C on mortality risk.

To our knowledge, over the past 20-30 years, the health status of China's total population has improved dramatically, with a significant increase in life expectancy, which has also meant a rapid and sustained increase in the aging population. Aging is considered to be an immutable factor that cannot be analyzed as a major influencing factor, so studies focusing on the elderly population are crucial. At the same time, the elderly are at high risk for CVD (20). Therefore, we wanted to explore the relationship

Abbreviations: ASCVD, Atherosclerotic Cardiovascular Disease; BMI, Body mass index; CDC, Center for Disease Control and Prevention; CHD, Coronary heart disease; CMD, Cardiovascular multimorbidity disease; CMM, Cardiovascular metabolic multimorbidity; CVD, Cardiovascular disease; DBP, Diastolic blood pressure; FPG, Fasting plasma glucose; GBD, Global Burden of Disease; HDL-C, High-density lipoprotein cholesterol; HOMA-IR, Homeostasis model assessment of insulin resistance; IQR, Interquartile range; IR, Insulin resistance; LDL-C, Low-density lipoprotein cholesterol; MI, Myocardial infarction; Mts, Metabolic syndrome; NO, Nitric oxide; RHR, Resting heart rate; SBP, Systolic blood pressure; SD, Standard deviation; TC, Total cholesterol; TG, Triglyceride; TyG, Triglyceride-glucose; T2DM, Type 2 diabetes mellitus; WC, Waist circumference.

between TyG index and LDL-C or HDL-C with all-cause and CVD mortality and to investigate the interaction between TyG index and LDL-C or HDL-C on risk in the elderly population.

2 Methods

2.1 Study design and population

The data analyzed were obtained from the Resident Health Examinations Database of Xinzheng City, Henan Province, Central China, which is a large-scale cohort study of older adults aged 60 years and older conducted by the Centers for Disease Control (CDC) and Prevention of Xinzheng City and contains sociodemographic and mortality information on the population of Xinzheng City. Since January 1, 2011, Xinzheng City has been providing free annual health examinations to senior citizens aged 60 and older. At the initial examination, the physician creates a health profile for each resident, which includes basic demographic information (age, gender, marital status, etc.), blood indicators (fasting plasma glucose (FPG), triglycerides (TG), total cholesterol (TC), etc.), urinalysis, eye examination, chest X-ray, and other functions. For this study, we obtained follow-up information from 2013 to 2023 from a total of 56,069 eligible older adults. The Framingham study revealed that premature development of CVD in first-degree relatives, such as parents or siblings, is associated with an elevated risk of subsequent development in the offspring. The presence of genetic factors may lead to the occurrence of heart disease, stroke, heart failure, and other serious illnesses (serious mental illness and cancer) in several family members (21). Consequently, individuals with a family history of CVD such as coronary heart disease (CHD), stroke, and myocardial infarction (MI) at the start of the study were excluded. Participants with any of the following were excluded: (1) Exclude participants with a family history of CVD (n=550); (2) Exclude those with missing FPG, TG, TC, LDL-C, and HDL-C at baseline (n=1066); (3) Exclude those with missing one or more of the covariates of smoking, alcohol consumption, physical activity, waist circumference (WC), body mass index (BMI) at baseline (n=281); (4) Exclude participants with serious illnesses, including serious mental illness and cancer (n=685); and (5) Exclude participants with no follow-up records (n=2004). The process of screening the data is presented in Figure 1.

2.2 Statement

The study was approved by the Ethics Committee of Zhengzhou University (ID: ZZUIRB2019-019), and the research team obtained permission to use the data from the Zhengzhou Health Commission. All studies were conducted by the Declaration of Helsinki, and informed consent was obtained from all participants or their legal guardians.

2.3 Data collection

Standardized questionnaires were administered by trained researchers, and participants completed a questionnaire on sociodemographic characteristics, personal disease history, and

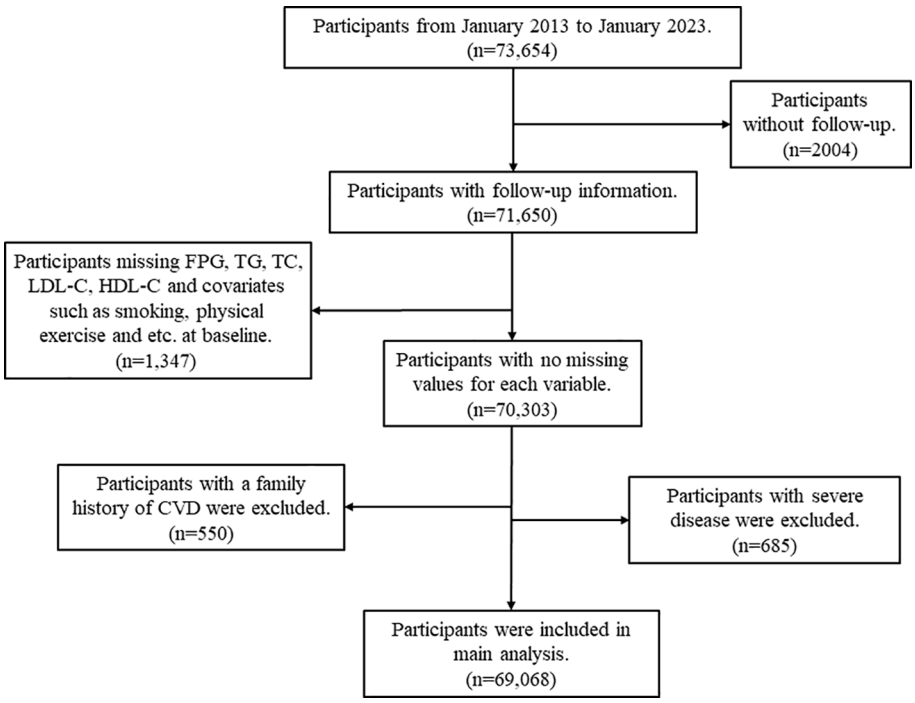

FIGURE 1
Flow chart of study participants.

lifestyle information at each health examination. Sociodemographic information included participants' age, gender (male/female), and marital status (married/unmarried/widowed/divorced); disease history information included hypertension (yes/no), T2DM (yes/no), CHD (yes/no), stroke (yes/no) and cancer (yes/no). Lifestyle information included smoking status (never/ever/current), drinking status (never/occasional/more than once a week/daily), and physical activity status (never/occasional/more than once a week/daily). Current smoking was defined as having smoked more than 100 cigarettes in a lifetime and currently smoking (22). Alcohol consumption is defined as drinking more than 30 grams of alcohol in a single sitting, and more than 30 gram of alcohol per day is considered to be alcohol consumption for the day (23). Regular exercise is defined as 30 minutes of moderate-intensity exercise or 20 minutes of vigorous-intensity exercise three or more times per week (24). Participants' height, weight, blood lipids, WC, FPG, systolic blood pressure (SBP), diastolic blood pressure (DBP), and resting heart rate (RHR) were measured by trained health professionals. Blood samples taken after participants fasted for 8 hours were used to measure FPG and blood lipids. Blood pressure (BP) was measured using an electronic sphygmomanometer (Omron HEM-7125, Kyoto, Japan). The subjects were instructed to rest quietly for five minutes in a standard supine position. Two measurements of SBP and DBP were then taken in the right brachial artery, with an interval of 30 minutes between each measurement. The average level was taken as the result of the BP measurements. Hypertension was defined as SBP ≥140 mmHg and DBP ≥90 mmHg or the use of antihypertensive medication (25). T2DM was defined as FPG ≥7.0 mmol/L or use of insulin or oral hypoglycemic agents, or a self-reported history of T2DM diagnosis (26). BMI was calculated as weight (kilograms) divided by the square of height (meters). A scoring scale consistent with Chinese body mass was used. The TyG index, calculated as TyG index = ln [Fasting TG (mg/dl) × FPG (mg/dl)]/2, is a composite indicator composed of TG and FPG levels (27). The diagnostic criteria for abnormal LDL-C is a level of greater than 130 mg/dl, and for HDL-C, a level of less than 40 mg/dl for men or less than 50 mg/dl for women is considered abnormal (28).

2.4 Outcomes

The outcome of interest was all-cause and CVD mortality. We defined CVD as a composite of CHD and stroke. Mortality causes were recorded using the international Classification of Diseases (ICD-10) codes. The study utilized ICD-10 codes I20-I25 for CHD and ICD-10 codes I60-I69 for stroke. All-cause mortality was defined as deaths resulting from any cause, while CVD mortality was defined as deaths resulting from either CHD or stroke.

2.5 Statistical analysis

Baseline characteristics of participants were presented based on their grouping by all-cause or CVD mortality, and the Kolmogorov-Smirnov test was used to verify the normal distribution of the data. Continuous variables that followed a normal distribution were described as mean (standard deviation), while non-normal variables were described as median (interquartile range). Descriptive variables were presented as frequencies and percentages. To compare baseline characteristics, categorical variables were analyzed using the Pearson chi-square test and continuous variables were analyzed using the Kruskal-Wallis H test.

Cox proportional risk regression models were used to estimate the hazard ratio (HR) and 95% confidence interval (CI) of the TyG index, LDL-C, and HDL-C for all-cause or CVD mortality. Model 1 was not adjusted, while model 2 was adjusted for age and gender at baseline. Finally, model 3 was adjusted for marital status, smoking, alcohol consumption, physical activity, SBP, DBP, BMI, WC, history of T2DM, and history of hypertension, based on model 2.

Restricted cubic spline plots were used to characterize the dose-response associations and to examine potential linear or non-linear associations between the TyG index, LDL-C, and HDL-C as continuous variables, and all-cause or CVD mortality. The three nodes of the cubic spline curve were set at the 10th, 50th, and 90th percentiles, respectively. The overall association was initially assessed for significance, and if significant, the results of the linear and non-linear tests were examined. A significance level of P <0.05 was reached for both the overall association test, which indicated that the overall association was significant, and a non-linear level of P <0.05, which indicated the presence of a non-linear association.

Thresholds were estimated by testing all possible values and selecting the threshold point with the highest likelihood. Additionally, a two-segment Cox proportional risk model was used to examine the relationship between TyG index, LDL-C or HDL-C, and the risk of all-cause or CVD mortality on both sides of the inflection point.

In subgroup analyses, participants were stratified based on gender (male/female), and age (<65/≥65) at baseline to test for differences in outcomes across subgroups. To test the robustness of the current study, we performed a sensitivity analysis. Participants with less than two years of follow-up were excluded from the principal component analysis.

Statistical analyses were conducted using R software, version 4.1.3. All P-values were 2-sided and a P < 0.05 was considered statistically significant unless otherwise stated.

3 Result

3.1 Baseline characteristics of study participants

Table 1 shows baseline characteristics for all participants. The baseline data were analyzed for 69,068 older participants (median age 65 years [interquartile range 61-71]). During the 400,094 person-year follow-up period (median follow-up time 5.8 years [interquartile range 3.0-9.12]), 13664 deaths were recorded, of which 7045 were due to CVD. During the follow-up period, individuals who died were more likely to be male, had no spouse, were less physically active, were former or current smokers, drank alcohol daily, had lower weight, WC, BMI, TyG index, TC, TG, LDL-C, and higher RHR, SBP,

10.3389/fendo.2024.1422086

TABLE 1 Baseline characteristics of the study population stratified by outcome.

Variables	All-cause mortality		*P* value	Cardiovascular disease mortality		*P* value
	No(n=55,547)	Yes(n=13,521)		No(n=23,569)	Yes(n=6,975)	
Age, years	65.61 (5.66)	73.29 (7.93)	< 0.001	66.70 (5.79)	73.11 (7.46)	< 0.001
Gender, %			< 0.001			< 0.001
Male	25781 (46.41)	7318 (54.12)		9643 (40.91)	3632 (52.07)	
Female	29766 (53.59)	6203 (45.88)		13926 (59.09)	3343 (47.93)	
Marital status, %			< 0.001			< 0.001
married	45274 (81.51)	8716 (64.46)		18428 (78.19)	4561 (65.39)	
unmarried	808 (1.45)	367 (2.71)		373 (1.22)	139 (1.99)	
widowed	9147 (16.47)	4340 (32.10)		7025 (23.00)	2236 (32.06)	
divorced	318 (0.57)	98 (0.72)		157 (0.51)	39 (0.56)	
Weight, kg	63.19 (10.10)	60.75 (10.64)	< 0.001	62.94 (10.33)	60.76 (10.76)	< 0.001
WC, cm	85.42 (9.72)	84.08 (10.36)	< 0.001	85.87 (10.05)	84.85 (10.50)	< 0.001
Physical exercise, %			< 0.001			0.033
Highly active	12479 (22.47)	2870 (21.23)		5879 (24.94)	1628 (23.34)	
Sufficiently active	2456 (4.42)	622 (4.60)		1069 (4.54)	319 (4.57)	
Insufficiently active	2828 (5.09)	841 (6.22)		1407 (5.97)	453 (6.49)	
Inactive	37784 (68.02)	9188 (67.95)		15214 (64.55)	4575 (65.59)	
Smoking, %			< 0.001			< 0.001
Never smoker	46042 (82.89)	11017 (81.48)		19677 (83.49)	5638 (80.83)	
Former smoker	1472 (2.65)	522 (3.86)		736 (3.12)	297 (4.26)	
Current smoker	8033 (14.46)	1982 (14.66)		3156 (13.39)	1040 (14.91)	
Drinking, %			< 0.001			0.02
Never	51019 (91.85)	12480 (92.30)		21675 (91.96)	6407 (91.86)	
Once in a while	2820 (5.08)	590 (4.36)		1128 (4.79)	323 (4.63)	
More than once a week	637 (1.15)	117 (0.87)		252 (1.07)	57 (0.82)	
Every day	1071 (1.93)	334 (2.47)		514 (2.18)	188 (2.70)	
RHR, beats/min	72.49 (10.65)	74.26 (13.56)	< 0.001	72.48 (9.83)	74.09 (13.20)	< 0.001
SBP, mmHg	134.06 (19.44)	137.18 (21.39)	< 0.001	135.43 (19.96)	138.26 (21.76)	< 0.001
DBP, mmHg	79.97 (10.78)	80.04 (11.38)	0.528	79.97 (11.00)	80.20 (11.66)	0.179
TC, mmol/L	4.71 [4.13, 5.35]	4.69 [4.10, 5.30]	< 0.001	4.80 [4.20, 5.43]	4.74 [4.14, 5.39]	0.001
TG, mmol/L	1.24 [0.89, 1.65]	1.20 [0.87, 1.55]	< 0.001	1.27 [0.91, 1.69]	1.22 [0.89, 1.60]	< 0.001
LDL-C, mmol/L	2.77 [2.26, 3.26]	2.70 [2.20, 3.20]	< 0.001	2.90 [2.33, 3.40]	2.62 [2.15, 3.10]	< 0.001
HDL-C, mmol/L	1.31 [1.10, 1.60]	1.32 [1.10, 1.63]	< 0.001	1.30 [1.08, 1.59]	1.31 [1.09, 1.62]	0.002
BMI, kg/m^2	24.79 (5.36)	24.08 (3.51)	< 0.001	24.95 (3.46)	24.25 (3.59)	< 0.001
TyG index	8.58 (0.61)	8.55 (0.62)	< 0.001	8.61 (0.61)	8.58 (0.62)	< 0.001
Hypertension, %	33021 (59.45)	8981 (66.42)	< 0.001	15910 (67.50)	4941 (70.84)	< 0.001
T2DM, %	12535 (22.57)	3467 (25.64)	< 0.001	6244 (26.49)	1948 (27.93)	0.018

Data are presented as number (percentage), mean (SD), or median [interquartile range].
BMI, body mass index; DBP, diastolic blood pressure; HDL-C, high-density lipoprotein cholesterol; LDL-C, low-density lipoprotein cholesterol; RHR, resting heart rate; SBP, systolic blood pressure; TC, total cholesterol; TG, triglyceride; TyG, triglyceride glucose; T2DM, type 2 diabetes mellitus; WC, Waist circumference.

DBP, HDL-C, and were more likely to have hypertension and T2DM. Similarly, individuals who died from CVD had similar baseline characteristics. In addition, according to the TyG index, LDL-C, and HDL-C, there were significant differences between the four groups in terms of age, gender, marital status, WC, BMI, smoking, alcohol consumption, physical activity, TC, TG, hypertension, and T2DM (Supplementary Tables S1-S3).

3.2 Association of TyG index and LDL-C or HDL-C with all-cause and CVD mortality

After adjusting for covariates such as age, gender, marital status, physical activity, smoking, alcohol consumption, BMI, WC, hypertension, and T2DM, Cox proportional risk analyses showed that the multivariate-adjusted HR (95% CI) for all-cause mortality in the first, third, and fourth quartiles of the TyG index compared with the second quartile were 1.03 (0.99,1.09), 1.05 (1.01,1.10), and 1.16 (1.12,1.22), and the multivariable-adjusted HR (95% CI) for CVD mortality was 1.13 (1.06,1.21), 1.02 (0.96,1.09), and 1.08 (1.01,1.16), respectively.

At the same time, the risk of all-cause and CVD mortality increased significantly with increasing quartiles of LDL-C and HDL-C. Compared with the third quartile of the LDL-C, the multivariable-adjusted HR (95% CI) for all-cause mortality in the first, second, and fourth quartiles of LDL-C was 0.96 (0.92,1.01), 0.99 (0.94,1.03), and 1.07 (1.02,1.12), and that for CVD mortality was were 0.94 (0.88,1.00), 0.96 (0.90,1.03), and 1.09 (1.01,1.17), respectively. Compared with the second quartile of the HDL-C, the multivariable-adjusted HR (95% CI) for all-cause mortality in the first, third, and fourth quartiles of HDL-C was 0.97 (0.93,1.02), 1.01 (0.97,1.06), and 1.10 (1.05,1.16), and that for CVD mortality was were 0.95 (0.89,1.01), 1.07 (1.01,1.15), and 1.11 (1.04,1.18), respectively. In models 2 and 3, LDL-C and HDL-C were associated with an increasing trend in all-cause and CVD mortality (Table 2, P for trend all <0.001).

Cox proportional risk regression models with restricted cubic spline were used to estimate the dose-response relationships of TyG index, LDL-C, and HDL-C with all-cause and CVD mortality. The three nodes of the cubic spline curve were set at the 10th, 50th, and 90th percentiles, respectively. The results showed non-linear associations between TyG index and all-cause (Figure 2A, $P_{\text{non-linear}}$ <0.001) and CVD mortality (Figure 2D, $P_{\text{non-linear}}$ <0.001) after adjusting for covariates in model 3. The study found J-shaped associations between both LDL-C and all-cause mortality (Figure 2B, $P_{\text{non-linear}}$ <0.05) and HDL-C and CVD mortality (Figure 2F, $P_{\text{non-linear}}$ <0.05). However, no non-linear associations were found between LDL-C and all-cause mortality, and HDL-C and CVD mortality (Figures 2C, E, all $P_{\text{non-linear}}$ >0.05). It is important to note that the TyG index and CVD mortality had a U-shaped association.

The inflection points of TyG index, LDL-C, or HDL-C for all-cause and CVD mortality were determined using a two-segment Cox proportional risk-based regression model (Table 3). After adjusting for covariates in model 3, both TyG index, LDL-C, and HDL-C were found to be significantly and positively associated with all-cause and CVD mortality when above the inflection point. It should be noted that CVD mortality decreased by 5% when the TyG index was below the inflection point (HR: 0.95, 95% CI: 0.92, 0.98). Additionally, when LDL-C was below the inflection point, all-cause mortality decreased by 22% (HR: 0.78, 95% CI: 0.64, 0.96).

To examine the relationship between the TyG index and LDL-C or HDL-C and the risk of all-cause and CVD mortality, we divided the participants into four subgroups based on their baseline TyG index levels and whether their LDL-C or HDL-C levels were within the normal range (Table 4). Compared to the low TyG index combined with LDL-C normal group, participants in the high TyG index combined with LDL-C abnormal group had a 14% (adjusted HR: 1.14, 95% CI: 1.08,1.20), and 13% (adjusted HR: 1.13, 95% CI: 1.04,1.22) increase in all-cause and CVD mortality, respectively. No significant interactive effects of TyG index and LDL-C on the risk of all-cause and CVD mortality. Participants in the high TyG index combined with the abnormal HDL-C group had an 11% increase in all-cause mortality compared to the low TyG index combined with the normal HDL-C group (adjusted HR: 1.11, 95% CI: 1.04,1.17). However, a high TyG index combined with HDL-C abnormality did not significantly increase CVD mortality. Similarly, there were no significant interactive effects of TyG index and HDL-C on the risk of all-cause and CVD mortality.

3.3 Subgroup analyses and sensitivity analyses

Subgroup analyses showed that TyG index and LDL-C or HDL-C were more consistently positively associated with all-cause mortality by gender, and age (Figure 3). Sensitivity analyses produced results consistent with the main analysis (Supplementary Table S4, Supplementary Figure S1).

4 Discussion

In this study, we found that after adjusting for various covariates, the TyG index had a non-linear association with the risk of all-cause and CVD mortality. LDL-C had a non-linear association with the risk of all-cause mortality and a linear with CVD mortality. HDL-C had a linear association with the risk of all-cause mortality and a non-linear with CVD mortality. Additionally, through threshold effect analysis, we have identified a turning point for the TyG index (8.56 for all-cause mortality and 8.74 for CVD mortality). At this point, a high TyG index combined with abnormal LDL-C significantly increases the risk of all-cause and CVD mortality. Furthermore, the combination of abnormal HDL-C significantly increases the risk of all-cause mortality only. It is noteworthy that the fourth quartile of the TyG index is associated with lower mortality than the third quartile. This finding is inconsistent with the j-shaped curve observed in the restricted cubic spline plot. This apparent incongruity may have arisen because the value of the vertical coordinate of the restricted cubic spline plot plotted under the survival analysis condition is the risk ratio, whereas the number of outcome events presented in the table

TABLE 2 Risk of all-cause and CVD mortality according to quartiles of TyG index, LDL-C and HDL-C.

Outcomes	Variables		No. of deaths	HR (95% CI)		
				Model 1	Model 2	Model 3
All-cause mortality	TyG index	Q1	3500	1.01 (0.96,1.06)	1.04 (0.99,1.09)	1.03 (0.99,1.09)
		Q2	3322	1.00 (ref)	1.00 (ref)	1.00 (ref)
		Q3	3558	1.01 (0.96,1.06)	1.06 (1.01,1.11)	1.05 (1.01,1.10)
		Q4	3141	1.01 (0.96,1.06)	1.17 (1.12,1.23)	1.16 (1.12,1.22)
	P for trend			0.99	< 0.001	< 0.001
	LDL-C	Q1	3347	1.07 (1.02,1.12)	0.95 (0.91,0.99)	0.96 (0.92,1.01)
		Q2	3696	1.00 (0.95,1.05)	0.98 (0.93,1.03)	0.99 (0.94,1.03)
		Q3	3462	1.00 (ref)	1.00 (ref)	1.00 (ref)
		Q4	3016	1.01 (0.96,1.06)	1.08 (1.03,1.14)	1.07 (1.02,1.12)
	P for trend			0.02	< 0.001	< 0.001
	HDL-C	Q1	3297	1.02 (0.97,1.07)	0.98 (0.94,1.03)	0.97 (0.93,1.02)
		Q2	3307	1.00 (ref)	1.00 (ref)	1.00 (ref)
		Q3	3330	1.00 (0.96,1.05)	1.01 (0.97,1.06)	1.01 (0.97,1.06)
		Q4	3587	1.08 (1.03,1.13)	1.10 (1.05,1.15)	1.10 (1.05,1.16)
	P for trend			0.003	< 0.001	< 0.001
Cardiovascular disease mortality	TyG index	Q1	1715	1.13 (1.06,1.21)	1.14 (1.07,1.22)	1.13 (1.06,1.21)
		Q2	1714	1.00 (ref)	1.00 (ref)	1.00 (ref)
		Q3	1783	0.96 (0.90,1.02)	1.03 (0.96,1.10)	1.02 (0.96,1.09)
		Q4	1763	0.98 (0.92,1.05)	1.07 (1.01,1.15)	1.08 (1.01,1.16)
	P for trend			< 0.001	< 0.001	< 0.001
	LDL-C	Q1	2088	1.01 (0.94,1.07)	0.94 (0.88,1.00)	0.94 (0.88,1.00)
		Q2	1845	0.99 (0.92,1.06)	0.96 (0.90,1.03)	0.96 (0.90,1.03)
		Q3	1642	1.00 (ref)	1.00 (ref)	1.00 (ref)
		Q4	1400	1.04 (0.97,1.12)	1.09 (1.02,1.18)	1.09 (1.01,1.17)
	P for trend			0.5	< 0.001	< 0.001
	HDL-C	Q1	1794	0.98 (0.91,1.04)	0.95 (0.89,1.01)	0.95 (0.89,1.01)
		Q2	1684	1.00 (ref)	1.00 (ref)	1.00 (ref)
		Q3	1705	1.08 (1.01,1.16)	1.07 (1.01,1.15)	1.07 (1.01,1.15)
		Q4	1792	1.14 (1.07,1.22)	1.11 (1.04,1.18)	1.11 (1.04,1.18)
	P for trend			< 0.001	< 0.001	< 0.001

TyG index: Q1 (3.19-8.19), Q2 (8.19-8.55), Q3 (8.55-8.90), Q4(8.90-13.51). LDL-C: Q1 (0.04-2.25), Q2 (2.25-2.76), Q3 (2.76-3.26), Q4(3.26-12.10). HDL-C: Q1 (0.02-1.10), Q2 (1.10-1.31), Q3 (1.31-1.61), Q4(1.61-11.68).
Model 1: Unadjusted.
Model 2: Adjusted for gender and age.
Model 3: Adjusted for gender, age, marital status, current smoking, alcohol consumption, T2DM, SBP, DBP, RHR, WC, and BMI.
HR, hazards ratio; CI, confidence interval.

represents only one of the two variables of the survival analysis, i.e., it is the survival outcome. However, in the context of survival analysis, it is essential to consider the survival time of the subjects. The data demonstrated that individuals who died in the fourth quartile of the TyG index survived for a significantly longer period than those who died in the other three quartiles. Although the risk ratio increased in the fourth quartile group, the magnitude was less pronounced, suggesting that fewer individuals died in the fourth quartile group than in the third quartile group.

Some aspects of our findings are consistent with previous studies that have shown a positive correlation between higher TyG index and higher all-cause and CVD mortality. For instance,

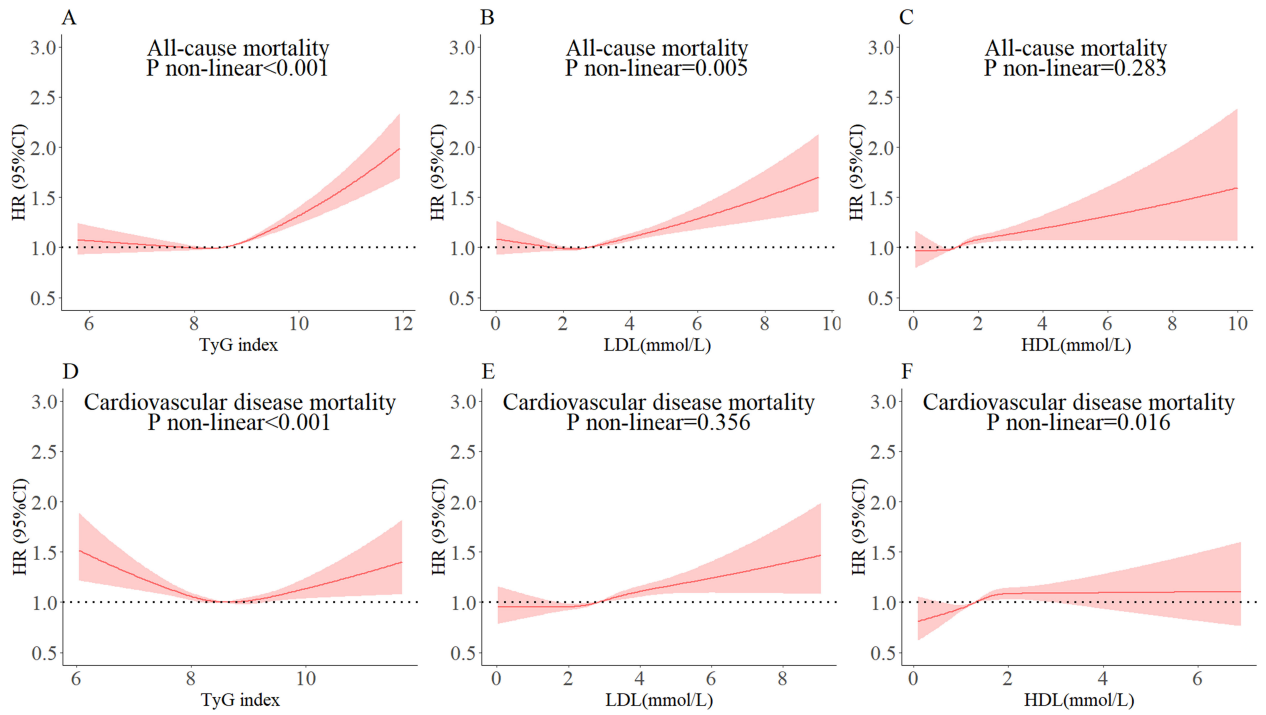

FIGURE 2
Dose-response relationships of TyG index, LDL-C, and HDL-C with all-cause and cardiovascular mortality. The cut-off levels for TyG index in all-cause and cardiovascular mortality were 8.56 **(A)** and 8.74 **(D)**, for LDL-C 1.66 **(B)** and 2.84 **(E)**, and for HDL-C 1.36 **(C)** and 1.30 **(F)**, respectively. The circles represent the points (5, 25, 50, 75, and 95 percentiles) where the nodes were placed. The region between the two dotted lines represents the 95% confidence interval (95% CI). The model was adjusted for gender, age, marital status, current smoking, alcohol consumption, T2DM, SBP, DBP, RHR, WC, and BMI.

a cohort study conducted by the National Health and Nutrition Examination Survey, which included 20,194 participants and had a follow-up period of 9.82 years, demonstrated a non-linear relationship between the TyG index and all-cause and CVD mortality in the general population. The study found that the lowest risk of all-cause or CVD mortality occurred when the TyG index was 9.36 or 9.52 (29). Another recent study, which only included adults 18 years of age and older, similarly demonstrated a non-linear association between the TyG index and all-cause and CVD mortality. However, this study found a shift from a non-linear association to a linear positive association between the TyG index and CVD mortality when focusing on study participants aged 45-64 years (30). One possible explanation for the association between age and the TyG index is that younger people are believed to be more susceptible to IR (31), which is closely linked to the TyG index (32). As a result, as the TyG index increases, this group is more likely to develop concomitant metabolic diseases that contribute to CVD mortality. Additionally, studies investigating the relationship between the TyG index and cardiovascular metabolic multimorbidity (CMM) have discovered U-shaped associations between the TyG index and all-cause and CVD mortality (33). However, conflicting results exist regarding the effect of the TyG index on all-cause and CVD mortality in older adults. A meta-analysis that included 12 cohort studies found no statistical correlation between the TyG index and all-cause and CVD mortality (34). This lack of correlation may be due to the small number of studies included in the analysis.

Previous studies have found a strong association between lower or higher elevations of FPG and CVD morbidity and mortality even in nondiabetic patients, with a J-shaped association between blood glucose levels and CVD mortality (35). A study of TG reported that elevated TG was associated with a reduced risk of CVD mortality (36). Low TG and blood glucose may represent individuals in a poorer nutritional state, and in addition, hypoglycemia-induced thrombosis contributes to increased CVD mortality (37). Therefore, we need to maintain normal TyG index levels.

A cohort study in Denmark found that higher LDL-C was associated with an increased risk of all-cause and CVD mortality (18). Similarly, a meta-analysis of 14 studies found that LDL-C is associated with a higher risk of CVD mortality (38). These findings support the view that LDL-C is the 'bad cholesterol' and that higher levels of LDL-C are associated with an increased risk of death (14). Our study is similar to these studies and similarly demonstrates the association of higher LDL-C with death from CVD. Also, the fact that LDL-C collection preceded and the outcome of death appeared later in the study population confirms the causal relationship between LDL-C and CVD mortality. Regarding the evidence for HDL-C, it was found that higher levels of HDL-C were associated with an increased risk of all-cause mortality (39). This is consistent with the findings of a cohort study conducted in Copenhagen, where HDL-C is known as an 'anti-atherogenic lipoprotein' that prevents atherosclerosis and slows the onset of CVD (40). However, our study found the opposite. Individuals who died of all-cause and cardiovascular disease during the follow-up period were, on

TABLE 3 Threshold effect analysis of TyG index, LDL-C, and HDL-C on all-cause and CVD mortality.

Outcome	Variables	Inflection point	HR (95% CI)	*P*-value
All-cause mortality	TyG index	8.56		
	<8.56		0.97 (0.92,1.04)	0.401
	≥8.56		1.21 (1.15,1.28)	< 0.001
	LDL-C	1.66		
	<1.66		0.78 (0.64,0.96)	0.016
	≥1.66		1.08 (1.05,1.11)	< 0.001
	HDL-C	1.36		
	<1.36		1.10 (0.97,1.25)	0.140
	≥1.36		1.07 (1.02,1.11)	0.002
Cardiovascular disease mortality	TyG index	8.74		
	<8.74		0.95 (0.92,0.98)	< 0.001
	≥8.74		1.05 (1.01,1.09)	0.02
	LDL-C	2.84		
	<2.84		1.01 (0.98,1.04)	0.458
	≥2.84		1.07 (1.03,1.11)	0.002
	HDL-C	1.30		
	<1.30		1.03 (0.99,1.06)	0.08
	≥1.30		1.03 (0.97,1.09)	0.336

The lowest point of the continuous variables TyG index, LDL-C, and HDL-C mortality risk ratios was taken as the cutoff value, and the mortality risk ratios for each variable on both sides were calculated at the cutoff value, respectively. Model was adjusted for gender, age, marital status, current smoking, alcohol consumption, T2DM, SBP, DBP, RHR, WC, and BMI. Abbreviations: HR, hazards ratio; CI, confidence interval.

average, approximately seven to eight years older than those who survived. However, individuals with lower high-density lipoprotein cholesterol (HDL-C) may have died during the 5.8-year follow-up period and therefore could not be included in the study. Due to the survival effect, high-density lipoprotein cholesterol (HDL-C) was observed to be higher in the deceased cohort than in the surviving cohort. Consequently, it is plausible that elevated HDL-C levels may be associated with an increased risk of all-cause mortality.

In this study, we analyzed the interaction between the TyG index and LDL-C or HDL-C about the risk of all-cause and CVD mortality. Our findings suggest that an elevated TyG index is more strongly associated with all-cause and CVD mortality in subjects with abnormal LDL-C, and with all-cause mortality in those with abnormal HDL-C. It is important to note that the TyG index and serum cholesterol level are two independent measurements. However, the TyG index is obtained from the combined

TABLE 4 HR of all-cause and CVD mortality by combined categories of TyG index, LDL-C, and HDL-C.

Outcomes	TyG index	LDL-C		*P*-interaction	HDL-C		*P*-interaction
		normal	abnormal		normal	abnormal	
All-cause mortality	TyG index < 8.56	1.00 (ref)	1.10 (1.05,1.17)	0.021	1.00 (ref)	1.09 (1.03,1.15)	0.036
	TyG index ≥ 8.56	1.09 (1.05,1.14)	1.14 (1.08,1.20)		1.10 (1.05,1.14)	1.11 (1.04,1.17)	
Cardiovascular disease mortality	TyG index< 8.74	1.00 (ref)	1.11 (1.04,1.19)	0.041	1.00 (ref)	0.96 (0.89,1.03)	0.129
	TyG index≥ 8.74	1.01 (0.95,1.07)	1.13 (1.04,1.22)		1.01 (0.95,1.07)	1.00 (0.91,1.09)	

The relationship between normal and abnormal LDL-C or HDL-C and the risk of mortality under these conditions was determined by calculating the interaction using the cutoff value of the TyG index as the cutoff value for categorization into high and low TyG index, respectively. Data are presented as hazard ratios, 95% confidence intervals. Model was adjusted for gender, age, marital status, current smoking, alcohol consumption, T2DM, SBP, DBP, RHR, WC, and BMI.

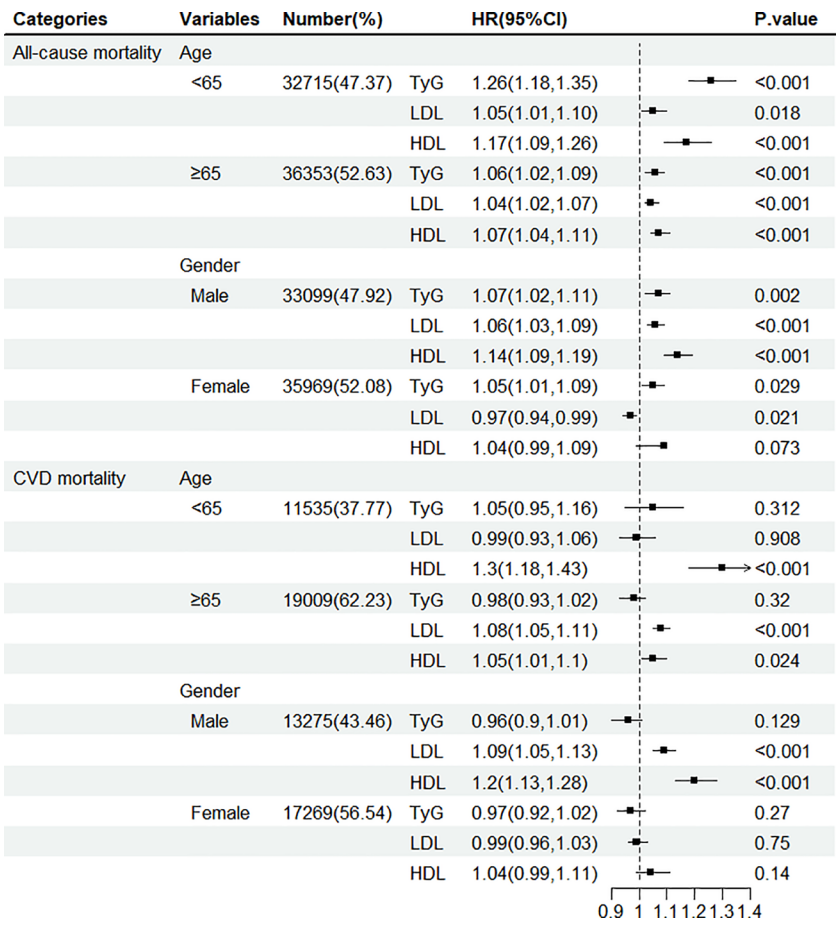

FIGURE 3
Hazard ratio (95% confidence interval) of all-cause and CVD mortality for per 1-SD increase in TyG index, LDL-C, and HDL-C according to gender and age.

measurement of TG and FPG. TG and LDL-C or HDL-C levels are often considered interrelated biomarkers of the underlying state of the circulatory and cardiovascular systems. Hypertension, hyperlipidemia, and hyperglycemia have been referred to as the 'three highs.' Studies have demonstrated that they interact with each other (41). It is worth mentioning that previous researchers have used the ratio of TG to HDL-C in combination with the TyG index to explore associations with the development of CVD (42). The potential biological mechanisms through which the TyG index and LDL-C or HDL-C are linked to all-cause mortality and CVD mortality, respectively, are outlined below. A reduction in NO results in impaired endothelial-dependent vasodilation. Moreover, impaired vasodilation is not a cause or risk of diabetes; on the contrary, endothelial dysfunction is a frequent consequence of diabetes (43, 44). Furthermore, evidence indicates that IR serves as a marker for cardiovascular metabolic diseases (CMD) and dyslipidemia (45). Elevated blood lipids have been demonstrated to promote the formation of atherosclerotic plaques (46). Furthermore, dyslipidemia is associated with an increased risk of thrombotic events and, consequently, mortality from cardiovascular causes (47). The aforementioned mechanisms may partially elucidate the potential correlation between the TyG index and lipids and the risk of mortality in patients with cardiovascular disease (48). There was no consistency found between the TyG index and LDL-C or HDL-C level to all-cause mortality across different age and sex groups. The effect of the TyG index and LDL-C or HDL-C level on all-cause mortality decreased with age among females. However, a positive correlation still reached a significant level even among those over 65 years of age, which is consistent with previous findings (49–51). It is worth noting that the risk of all-cause mortality was greater for each 1 SD increase in HDL-C in participants younger than 65 years of age compared with participants older than 65 years of age. This suggests that older adults, especially those in the early stages of aging, should pay particular attention to HDL-C metrics. The reason for this phenomenon may be related to the fact that the participants were in a degenerative stage of body functions when they first entered old age.

The study has several strengths. Firstly, the data were obtained from the records of annual health checkups in Xinzheng City, Henan Province, China, focusing on adults aged 60 years and older, which represents a large sample size. Secondly, instruments were used to measure participants' serum cholesterol levels rather than relying on self-reporting, reducing information bias. Additionally, our mortality data were obtained from the Centers for Disease Control and Prevention, and the causes of death were reviewed by at

least three clinical experts. Finally, no previous study has explored the interaction between the TyG index and serum cholesterol levels, and we explored whether there was an interaction between the two. However, this study has some limitations. Firstly, individuals who died of all-cause and CVD during the follow-up period were approximately 7 to 8 years older than those who did not die. However, during the follow-up time of 5.8 years, some of their peers with higher TyG index, LDL-C, and lower HDL-C may have died, and thus they could not be recruited into the study. Due to survival effects, the TyG index and LDL-C were lower in those who died than in those who did not die, and HDL-C was higher than in those who died. It is therefore possible that the data presented in the study may be biased. Secondly, the latent category trajectory model (LCGM) analysis highlights the importance of considering dynamic changes in participant measures during follow-up, regardless of baseline. Furthermore, the questionnaire did not include information on diet and cardiorespiratory fitness, which would have helped to eliminate the possibility of reverse causation and residual confounding. Additionally, the study focused on individuals aged 60 years and older, which may limit generalizability to the entire population.

5 Conclusion

In this study, we found that TyG index and LDL-C or HDL-C were significantly associated with an increased risk of all-cause and CVD mortality in a Chinese population of older adults. Furthermore, a high TyG index combined with abnormal LDL-C levels was also associated with an elevated risk. These findings suggest that routine monitoring and control of TyG index and lipids should be strengthened, and these indices should be included in risk assessment as risk factors for all-cause and CVD mortality.

Data availability statement

The original contributions presented in the study are included in the article/Supplementary Material. Further inquiries can be directed to the corresponding author.

Ethics statement

The studies involving humans were approved by Ethics Committee of Zhengzhou University (ID: ZZUIRB2019-019). The studies were conducted in accordance with the local legislation and institutional requirements. The participants provided their written informed consent to participate in this study.

Author contributions

DS: Writing – review & editing, Visualization, Methodology, Investigation, Formal analysis, Data curation, Conceptualization, Writing – original draft. ZA: Writing – review & editing, Conceptualization. LC: Writing – review & editing, Funding acquisition. XC: Writing – review & editing, Investigation. WW: Writing – review & editing, Data curation, Conceptualization. YFC: Writing – review & editing, Validation. YLC: Writing – review & editing, Resources. SS: Writing – review & editing, Resources.

Funding

The author(s) declare financial support was received for the research, authorship, and/or publication of this article. This study was supported by National Key Research and Development Program "Research on prevention and control of major chronic non-communicable diseases" of China (Grant No:2017YFC1307705).

Acknowledgments

The investigators are grateful to the dedicated participants and all research staff of the study.

Conflict of interest

The authors declare that the research was conducted in the absence of any commercial or financial relationships that could be construed as a potential conflict of interest.

Publisher's note

Supplementary material

The Supplementary Material for this article can be found online at: https://www.frontiersin.org/articles/10.3389/fendo.2024.1422086/full#supplementary-material

References

1. Zhou M, Wang H, Zhu J, Chen W, Wang L, Liu S, et al. Cause-specific mortality for 240 causes in China during 1990-2013: a systematic subnational analysis for the Global Burden of Disease Study 2013. *Lancet (London England).* (2016) 387:251–72. doi: 10.1016/s0140-6736(15)00551-6

2. Yang G, Wang Y, Zeng Y, Gao GF, Liang X, Zhou M, et al. Rapid health transition in China, 1990-2010: findings from the Global Burden of Disease Study 2010. *Lancet (London England)*. (2013) 381:1987–2015. doi: 10.1016/s0140-6736(13)61097-1

3. National Centre For Cardiovascular Diseases The Writing Committee of The Report on Cardiovascular Health And Diseases In China. The W: report on cardiovascular health and diseases in China 2022: an updated summary. *Biomed Environ sciences: BES*. (2023) 36:669–701. doi: 10.3967/bes2024.162

4. Roth GA, Mensah GA, Johnson CO, Addolorato G, Ammirati E, Baddour LM, et al. Global burden of cardiovascular diseases and risk factors, 1990-2019: update from the GBD 2019 study. *J Am Coll Cardiol*. (2020) 76:2982–3021. doi: 10.1016/j.jacc.2020.11.010

5. Lee SH, Park SY, Choi CS. Insulin resistance: from mechanisms to therapeutic strategies. *Diabetes Metab J*. (2022) 46:15–37. doi: 10.4093/dmj.2021.0280

6. Tangvarasittichai S. Oxidative stress, insulin resistance, dyslipidemia and type 2 diabetes mellitus. *World J Diabetes*. (2015) 6:456–80. doi: 10.4239/wjd.v6.i3.456

7. Htay T, Soe K, Lopez-Perez A, Doan AH, Romagosa MA, Aung K. Mortality and cardiovascular disease in type 1 and type 2 diabetes. *Curr Cardiol Rep*. (2019) 21:45. doi: 10.1007/s11886-019-1133-9

8. Sánchez-García A, Rodríguez-Gutiérrez R, Mancillas-Adame L, González-Nava V, Díaz González-Colmenero A, Solis RC, et al. Diagnostic accuracy of the triglyceride and glucose index for insulin resistance: A systematic review. *Int J Endocrinol*. (2020) 2020:4678526. doi: 10.1155/2020/4678526

9. Minh HV, Tien HA, Sinh CT, Thang DC, Chen CH, Tay JC, et al. Assessment of preferred methods to measure insulin resistance in Asian patients with hypertension. *J Clin hypertension (Greenwich Conn)*. (2021) 23:529–37. doi: 10.1111/jch.14155

10. Wang T, Li M, Zeng T, Hu R, Xu Y, Xu M, et al. Association between insulin resistance and cardiovascular disease risk varies according to glucose tolerance status: A nationwide prospective cohort study. *Diabetes Care*. (2022) 45:1863–72. doi: 10.2337/dc22-0202

11. Junren Z, Runlin G. Chinese guidelines for prevention and control of dyslipidemia in adults (2016 revision). *China Circ Mag*. (2016) 31.

12. Zhao M, Xiao M, Tan Q, Lu F. Triglyceride glucose index as a predictor of mortality in middle-aged and elderly patients with type 2 diabetes in the US. *Sci Rep*. (2023) 13:16478. doi: 10.1038/s41598-023-43512-0

13. Yu Y, Wang J, Ding L, Huang H, Cheng S, Deng Y, et al. Sex differences in the nonlinear association of triglyceride glucose index with all-cause and cardiovascular mortality in the general population. *Diabetol Metab Syndrome*. (2023) 15:136. doi: 10.1186/s13098-023-01117-7

14. Ference BA, Ginsberg HN, Graham I, Ray KK, Packard CJ, Bruckert E, et al. Low-density lipoproteins cause atherosclerotic cardiovascular disease. 1. Evidence from genetic, epidemiologic, and clinical studies. A consensus statement from the European Atherosclerosis Society Consensus Panel. *Eur Heart J*. (2017) 38:2459–72. doi: 10.1093/eurheartj/ehx144

15. Wilson PW, Abbott RD, Castelli WP. High density lipoprotein cholesterol and mortality. The Framingham Heart Study. *Arterioscler (Dallas Tex)*. (1988) 8:737–41. doi: 10.1161/01.atv.8.6.737

16. Liu C, Dhindsa D, Almuwaqqat Z, Ko YA, Mehta A, Alkhoder AA, et al. Association between high-density lipoprotein cholesterol levels and adverse cardiovascular outcomes in high-risk populations. *JAMA Cardiol*. (2022) 7:672–80. doi: 10.1001/jamacardio.2022.0912

17. Sung KC, Huh JH, Ryu S, Lee JY, Scorletti E, Byrne CD, et al. Low levels of low-density lipoprotein cholesterol and mortality outcomes in non-statin users. *J Clin Med*. (2019) 8. doi: 10.3390/jcm8101571

18. Johannesen CDL, Langsted A, Mortensen MB, Nordestgaard BG. Association between low density lipoprotein and all cause and cause specific mortality in Denmark: prospective cohort study. *BMJ (Clinical Res ed)*. (2020) 371:m4266. doi: 10.1136/bmj.m4266

19. Ke C, Shen Y. Letter by ke and shen regarding article, "Long-term association of low-density lipoprotein cholesterol with cardiovascular mortality in individuals at low 10-year risk of atherosclerotic cardiovascular disease: results from the cooper center longitudinal study. *Circulation*. (2019) 139:2190–1. doi: 10.1161/circulationaha.118.038328

20. Zhao D, Liu J, Wang M, Zhang X, Zhou M. Epidemiology of cardiovascular disease in China: current features and implications. *Nat Rev Cardiol*. (2019) 16:203–12. doi: 10.1038/s41569-018-0119-4

21. Evers IM, de Valk HW, Visser GHA. Risk of complications of pregnancy in women with type 1 diabetes: nationwide prospective study in the Netherlands. *Obstetrics Gynecol*. (2004) 104. doi: 10.1136/bmj.38043.583160.EE

22. Tomar SL, Asma S. Smoking-attributable periodontitis in the United States: findings from NHANES III. National Health and Nutrition Examination Survey. *J periodontol*. (2000) 71:743–51. doi: 10.1902/jop.2000.71.5.743

23. Choi YJ, Lee DH, Han KD, Kim HS, Yoon H, Shin CM, et al. The relationship between drinking alcohol and esophageal, gastric or colorectal cancer: A nationwide population-based cohort study of South Korea. *PloS One*. (2017) 12:e0185778. doi: 10.1371/journal.pone.0185778

24. Ainsworth BE, Haskell WL, Whitt MC, Irwin ML, Swartz AM, Strath SJ, et al. Compendium of physical activities: an update of activity codes and MET intensities. *Med Sci sports Exercise*. (2000) 32:S498–504. doi: 10.1097/00005768-200009001-00009

25. UN Centre for Human Settlements (Habitat) WHO. Global status report on non-communicable diseases 2010. (2011).

26. Jia W, Weng J, Zhu D, Ji L, Lu J, Zhou Z, et al. Standards of medical care for type 2 diabetes in China 2019. *Diabetes/metabol Res Rev*. (2019) 35:e3158. doi: 10.1002/dmrr.3158

27. Guerrero-Romero F, Simental-Mendía LE, González-Ortiz M, Martínez-Abundis E, Ramos-Zavala MG, Hernández-González SO, et al. The product of triglycerides and glucose, a simple measure of insulin sensitivity. Comparison with the euglycemic-hyperinsulinemic clamp. *J Clin Endocrinol Metab*. (2010) 95:3347–51. doi: 10.1210/jc.2010-0288

28. Alavi Tabatabaei G, Mohammadifard N, Rafiee H, Nouri F, Maghami Mehr A, Najafian J, et al. Association of the triglyceride glucose index with all-cause and cardiovascular mortality in a general population of Iranian adults. *Cardiovasc Diabetol*. (2024) 23:66. doi: 10.1186/s12933-024-02148-8

29. Liu XC, He GD, Lo K, Huang YQ, Feng YQ. The triglyceride-glucose index, an insulin resistance marker, was non-linear associated with all-cause and cardiovascular mortality in the general population. *Front Cardiovasc Med*. (2020) 7:628109. doi: 10.3389/fcvm.2020.628109

30. Chen J, Wu K, Lin Y, Huang M, Xie S. Association of triglyceride glucose index with all-cause and cardiovascular mortality in the general population. *Cardiovasc Diabetol*. (2023) 22:320. doi: 10.1186/s12933-023-02054-5

31. Sun M, Guo H, Wang Y, Ma D. Association of triglyceride glucose index with all-cause and cause-specific mortality among middle age and elderly US population. *BMC geriatrics*. (2022) 22:461. doi: 10.1186/s12877-022-03155-8

32. Liu R, Li L, Wang L, Zhang S. Triglyceride-glucose index predicts death in patients with stroke younger than 65. *Front Neurol*. (2023) 14:1198487. doi: 10.3389/fneur.2023.1198487

33. Liu Q, Zhang Y, Chen S, Xiang H, Ouyang J, Liu H, et al. Association of the triglyceride-glucose index with all-cause and cardiovascular mortality in patients with cardiometabolic syndrome: a national cohort study. *Cardiovasc Diabetol*. (2024) 23:80. doi: 10.1186/s12933-024-02152-y

34. Liu X, Tan Z, Huang Y, Zhao H, Liu M, Yu P, et al. Relationship between the triglyceride-glucose index and risk of cardiovascular diseases and mortality in the general population: a systematic review and meta-analysis. *Cardiovasc Diabetol*. (2022) 21:124. doi: 10.1186/s12933-022-01546-0

35. Lee JH, Han K, Huh JH. The sweet spot: fasting glucose, cardiovascular disease, and mortality in older adults with diabetes: a nationwide population-based study. *Cardiovasc Diabetol*. (2020) 19:44. doi: 10.1186/s12933-020-01021-8

36. Ambrosy AP, Yang J, Sung SH, Allen AR, Fitzpatrick JK, Rana JS, et al. Triglyceride levels and residual risk of atherosclerotic cardiovascular disease events and death in adults receiving statin therapy for primary or secondary prevention: insights from the KP REACH study. *J Am Heart Assoc*. (2021) 10:e020377. doi: 10.1161/jaha.120.020377

37. Li G, Zhong S, Wang X, Zhuge F. Association of hypoglycaemia with the risks of arrhythmia and mortality in individuals with diabetes - a systematic review and meta-analysis. *Front Endocrinol*. (2023) 14:1222409. doi: 10.3389/fendo.2023.1222409

38. Jung E, Kong SY, Ro YS, Ryu HH, Shin SD. Serum cholesterol levels and risk of cardiovascular death: A systematic review and a dose-response meta-analysis of prospective cohort studies. *Int J Environ Res Public Health*. (2022) 19. doi: 10.3390/ijerph19148272

39. Madsen CM, Varbo A, Nordestgaard BG. Extreme high high-density lipoprotein cholesterol is paradoxically associated with high mortality in men and women: two prospective cohort studies. *Eur Heart J*. (2017) 38:2478–86. doi: 10.1093/eurheartj/ehx163

40. Gordon T, Castelli WP, Hjortland MC, Kannel WB, Dawber TR. High density lipoprotein as a protective factor against coronary heart disease. *Framingham Study Am J Med*. (1977) 62:707–14. doi: 10.1016/0002-9343(77)90874-9

41. Zanchetti A. Hyperlipidemia in the hypertensive patient. *Am J Med*. (1994) 96:3s–8s. doi: 10.1016/0002-9343(94)90225-9

42. Mirshafiei H, Darroudi S, Ghayour-Mobarhan M, Esmaeili H, AkbariRad M, Mouhebati M, et al. Altered triglyceride glucose index and fasted serum triglyceride high-density lipoprotein cholesterol ratio predict incidence of cardiovascular disease in the Mashhad cohort study. *BioFactors (Oxford England)*. (2022) 48:643–50. doi: 10.1002/biof.1816

43. Molina MN, Ferder L, Manucha W. Emerging role of nitric oxide and heat shock proteins in insulin resistance. *Curr hypertension Rep*. (2016) 18:1. doi: 10.1007/s11906-015-0615-4

44. Trifunovic D, Stankovic S, Sobic-Saranovic D, Marinkovic J, Petrovic M, Orlic D, et al. Acute insulin resistance in ST-segment elevation myocardial infarction in non-diabetic patients is associated with incomplete myocardial reperfusion and impaired coronary microcirculatory function. *Cardiovasc Diabetol*. (2014) 13:73. doi: 10.1186/1475-2840-13-73

45. Hill MA, Yang Y, Zhang L, Sun Z, Jia G, Parrish AR, et al. Insulin resistance, cardiovascular stiffening and cardiovascular disease. *Metabol: Clin Exp*. (2021) 119:154766. doi: 10.1016/j.metabol.2021.154766

46. Ormazabal V, Nair S, Elfeky O, Aguayo C, Salomon C, Zuñiga FA. Association between insulin resistance and the development of cardiovascular disease. *Cardiovasc Diabetol*. (2018) 17:122. doi: 10.1186/s12933-018-0762-4

47. Zhao X, Wang Y, Chen R, Li J, Zhou J, Liu C, et al. Triglyceride glucose index combined with plaque characteristics as a novel biomarker for cardiovascular outcomes after percutaneous coronary intervention in ST-elevated myocardial infarction patients: an intravascular optical coherence tomography study. *Cardiovasc Diabetol*. (2021) 20:131. doi: 10.1186/s12933-021-01321-7

48. Adeva-Andany MM, Ameneiros-Rodríguez E, Fernández-Fernández C, Domínguez-Montero A, Funcasta-Calderón R. Insulin resistance is associated with subclinical vascular disease in humans. *World J Diabetes*. (2019) 10:63–77. doi: 10.4239/wjd.v10.i2.63

49. Cersosimo E, Solis-Herrera C, Trautmann ME, Malloy J, Triplitt CL. Assessment of pancreatic β-cell function: review of methods and clinical applications. *Curr Diabetes Rev*. (2014) 10:2–42. doi: 10.2174/1573399810666140214093600

50. Wu M, Liao S, Si J, Guo X, Kang L, Xu B, et al. Association of low-density lipoprotein-cholesterol with all-cause and cause-specific mortality. *Diabetes Metab syndrome*. (2023) 17:102784. doi: 10.1016/j.dsx.2023.102784

51. Hong S, Han K, Park CY. The triglyceride glucose index is a simple and low-cost marker associated with atherosclerotic cardiovascular disease: a population-based study. *BMC Med*. (2020) 18:361. doi: 10.1186/s12916-020-01824-2

frontiers | Frontiers in Medicine

TYPE Original Research
PUBLISHED 01 November 2024
DOI 10.3389/fmed.2024.1453502

OPEN ACCESS

EDITED BY
Prem Prakash Kushwaha,
Case Western Reserve University,
United States

REVIEWED BY
Pei Shang,
Mayo Clinic, United States
Robert Kiss,
McGill University, Canada

*CORRESPONDENCE
Min Liu
✉ rahosjoint@wmu.edu.com
Weili Wu
✉ weili896@163.com

†These authors have contributed equally to this work

RECEIVED 23 June 2024
ACCEPTED 15 October 2024
PUBLISHED 01 November 2024

CITATION
Leng P, Qiu Y, Zhou M, Zhu Y, Yin N, Zhou M, Wu W and Liu M (2024) Hypothyroidism correlates with osteoporosis: potential involvement of lipid mediators.
Front. Med. 11:1453502.
doi: 10.3389/fmed.2024.1453502

Hypothyroidism correlates with osteoporosis: potential involvement of lipid mediators

Pengyuan Leng[1†], Ying Qiu[2†], Mengxue Zhou[2], Yuhang Zhu[1], Na Yin[3], Mingming Zhou[4], Weili Wu[5*] and Min Liu[1*]

[1]Department of Orthopedics, The Third Affiliated Hospital of Wenzhou Medical University, Wenzhou, Zhejiang, China, [2]Postgraduate Training Base Alliance of Wenzhou Medical University (The Third Affiliated Hospital of Wenzhou Medical University), Ruian, Zhejiang, China, [3]College of Nursing, Hangzhou Normal University, Hangzhou, China, [4]Department of Anesthesiology, The Third Affiliated Hospital of Wenzhou Medical University, Wenzhou, Zhejiang, China, [5]Department of Thyroid and Breast Surgery, The Third Affiliated Hospital of Wenzhou Medical University, Wenzhou, Zhejiang, China

Background: Observational studies have demonstrated a correlation between thyroid dysfunction and osteoporosis (OP); however, the underlying causality has yet to be fully elucidated.

Methods: The necessary dataset was sourced from public databases. Initially, instrumental variables (IVs) were selected based on three primary hypotheses. Subsequently, Cochran's Q test was employed to exclude IVs exhibiting heterogeneity. The MR-PRESSO test and the leave-one-out sensitivity test were further applied to detect potential pleiotropy. Inverse variance was utilized for the analysis. This study primarily utilized the inverse variance weighted (IVW) model for Mendelian analysis. Since Type 1 diabetes mellitus can also contribute to the development of osteoporosis, this study additionally employed multivariate Mendelian analysis. Furthermore, 249 circulating metabolites were selected for mediation analysis in the Mendelian randomization framework.

Results: In this study, the two-sample Mendelian randomization (MR) analysis primarily employed the random-effects IVW model and demonstrated a causal relationship between hypothyroidism (OR = 1.092, 95% CI: 1.049–1.137, $p < 0.001$) and hyperthyroidism (OR = 1.080, 95% CI: 1.026–1.137, $p = 0.003$) with the risk of OP. No causal relationships were identified between FT3, FT4, TSH, and the risk of OP ($p > 0.05$). The results of the multivariate Mendelian randomization (MVMR) analysis indicated that hyperthyroidism was no longer a risk factor for OP (OR = 0.984, 95% CI: 0.918–1.055, $p = 0.657$), whereas hypothyroidism persisted as a risk factor (OR = 1.082, 95% CI: 1.021–1.147, $p = 0.008$). The mediated Mendelian randomization analysis revealed that hypothyroidism may exert an indirect effect on OP via triglycerides in large VLDL, mediating approximately 2.47% of the effect.

Conclusion: This study identifies a potential link between hypothyroidism and OP, possibly mediated indirectly via triglyceride levels in large VLDL. Further investigations are required to elucidate the direct or indirect causal mechanisms underlying this association.

KEYWORDS

circulating metabolites, Mendelian randomization, mediation analysis thyroid dysfunction, osteoporosis, thyroid-related hormones

1 Introduction

American scholars project that by 2025, more than 3 million fractures will occur among osteoporosis patients in the United States, with associated medical costs expected to reach $25.3 billion (1). Osteoporosis (OP), a hallmark of aging, is a systemic metabolic bone disease characterized by decreased bone mineral density and increased fracture susceptibility, and, from a cytological perspective, by an imbalance in the functions of osteoblasts, osteoclasts, and adipocytes (2, 3). Multiple factors contribute to the development of OP, including insufficient calcium intake, smoking, alcohol consumption, long-term use of certain medications, and the presence of specific diseases (4).

Hyperthyroidism and hypothyroidism are the most prevalent thyroid dysfunctions, each influencing various physiological functions. In the United States, hypothyroidism affects approximately 5% of the population, while hyperthyroidism affects nearly 1% (5). Numerous observational studies have demonstrated an association between thyroid dysfunction and OP (6); however, the causal relationships between hyperthyroidism, hypothyroidism, TSH, FT4, FT3, and OP remain unclear.

To elucidate the causal relationship, Mendelian randomization (MR) analysis was conducted in this study. MR analysis is a widely used method that evaluates potential causal relationships between exposure factors and outcomes using instrumental variables (IVs) and is less susceptible to confounders, thereby producing more reliable results (7). Therefore, this study employed MR analysis to investigate the potential causal relationship between thyroid dysfunction, thyroid function, and the risk of OP.

Patients with type 1 diabetes have a higher likelihood of developing thyroid dysfunction, and type 1 diabetes is also a known risk factor for OP. Therefore, this study incorporated type 1 diabetes into the multivariate Mendelian randomization (MVMR) analysis (8). This was done to explore the effect of adjusting for type 1 diabetes on OP, and subsequently to assess whether a causal relationship exists between thyroid dysfunction and OP.

Metabolomics is an emerging field of research that offers novel insights into how metabolites influence various physiological systems, particularly the endocrine system (9). The metabolome consists of metabolites and their associated metabolic pathways (10). A study analyzed plasma metabolites from 41 individuals with subclinical hypothyroidism, 45 hypothyroid patients, and 40 euthyroid individuals using metabolomics and machine learning algorithms. The findings revealed that the metabolic patterns of the hypothyroid and subclinical hypothyroid groups differed significantly from those of the euthyroid group. Specifically, primary bile acid biosynthesis, lysine degradation, tryptophan metabolism, steroid hormone biosynthesis, and purine metabolism were significantly impacted (11). However, few studies have focused on circulating metabolites in plasma.

Several observational studies have demonstrated an association between hypothyroidism and dyslipidemia, as well as a link between dyslipidemia and OP (12, 13). However, it remains unclear whether hypothyroidism influences the development of OP through circulating metabolites. Therefore, this study will explore this question using mediated Mendelian randomization analysis.

2 Methods and materials

2.1 Study design and data sources

Our data were sourced from the widely recognized IEU OpenGWAS database, the ThyroidOmics Consortium, and the FinnGen database (Table 1). As these databases were externally developed, ethical approval was not required. In this study, hyperthyroidism, hypothyroidism, TSH, FT4, and FT3 were used as exposure variables, with OP as the outcome variable. An MR analysis was conducted to investigate potential causal relationships between these factors (Figure 1).

2.2 Instrumental variables

In MR analysis, instrumental variables are genetic variants, often single nucleotide polymorphisms (SNPs), used to study the impact of genetic variation (14). The screening criteria were as follows: (1) instrumental variables must be strongly correlated with exposure variables. We set a significance threshold of $p < 5 \times 10\text{^-}8$ to identify SNPs with strong associations. (2) Instrumental variables must be independent, meaning they are not correlated with confounders (15). Linkage disequilibrium among SNPs was addressed by setting kb = 10,000 and $r^2 \leq 0.001$ (16). (3) Instrumental variables should affect the outcome exclusively through the exposure variables (17). The *F*-statistic assesses the strength of the correlation between instrumental variables and exposure factors. Thus, we calculated the *F*-statistic for each exposure-related SNP ($F = \beta^2/SE^2$) (18), where β represents the

TABLE 1 Sources and status of data.

Exposures/ outcome	Sample size	Data sources	Ancestry	GWAS ID	Total SNPs	Selected SNPs
Hyperthyroidism	46	IEU open database	European	ebi-a-GCST90018860	24,189,279	11
Hypothyroidism	405,357	IEU open database	European	ebi-a-GCST90013893	11,038,721	104
TSH	271,040	The ThyroidOmics Consortium database	European	–	–	161
FT3	59,061				–	6
FT4	119,120				–	60
Osteoporosis	399,054	Finn Biobank	European	R10_M13_ OSTEOPOROSIS	–	–

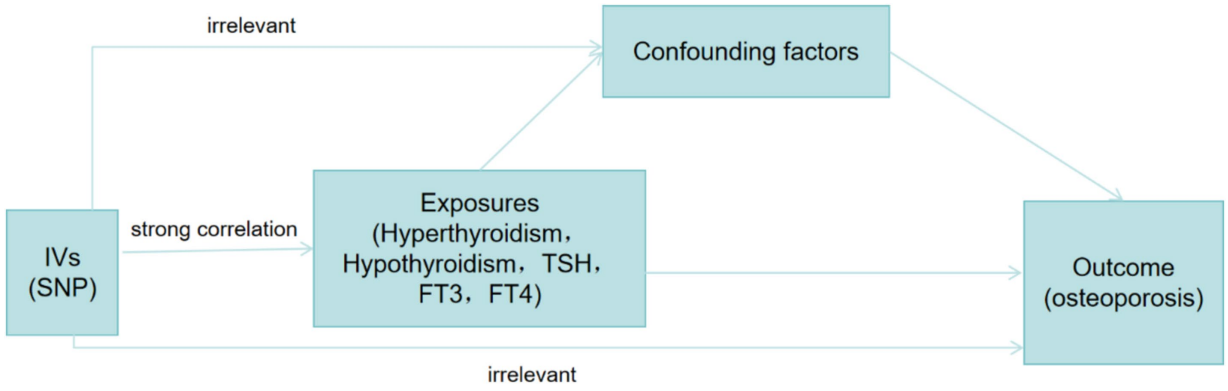

FIGURE 1
Diagram for this study. IVs, instrumental variable; SNP, single nucleotide polymorphism.

effect estimate of the exposure factor and SE is the standard error. We selected IVs with $F > 10$ to reduce bias from weak instruments (19). Subsequently, we identified SNPs where the exposure and outcome overlapped to remove palindromic SNPs and misaligned alleles.

2.3 MR analysis

To determine whether a causal relationship exists between genetic exposure and outcome, we employed several commonly used MR methods, including inverse-variance weighted (IVW), MR-Egger regression, weighted median (WM), weighted mode techniques, and MR-PRESSO. IVW is widely regarded as the primary statistical method in MR, and thus, this study adopts IVW as the main analysis approach. The fixed-effects IVW model operates under the assumption that all instrumental variables (IVs) are valid, whereas the random-effects IVW model assumes that not all IVs are valid (20). Therefore, we initially conducted a heterogeneity test using R. If heterogeneity was detected (i.e., $p < 0.05$), the random-effects model was applied (21). Subsequently, a pleiotropy test was conducted, and if $p > 0.05$, it indicated that the likelihood of pleiotropy was minimal or nonexistent and could be disregarded (22). Additionally, the intercept of the MR-Egger regression was not statistically significant, and the funnel plot was symmetric around zero, further confirming the absence of pleiotropy. A Cochran Q test was also conducted to assess SNP heterogeneity, which was statistically significant at $p < 0.05$ (23).In this study, we used the "TwoSampleMR," "MendelianRandomization," and "MR-PRESSO" packages in R (version 4.4.0) for MR analysis (24).

2.4 Mediator analysis link "hypothyroidism-blood-metabolites-OP"

Data on 249 circulating metabolites, collected and provided by Nightingale Health, were obtained from the IEU Open-GWAS Project public database (25). Circulating metabolites were used as mediators to decompose the direct and indirect effects of hypothyroidism on OP through a two-step Mendelian randomization (TSMR) approach. The total effect of hypothyroidism on OP was denoted as TE, the effect of hypothyroidism on circulating metabolites as β1, and the effect of circulating metabolites on OP as β2. The indirect effect (IE), representing the causal pathway through which hypothyroidism influences the occurrence of OP via the mediator, was estimated using the product of coefficients method ($\beta 1 \times \beta 2$). Accordingly, the proportion of the total effect mediated by the circulating metabolites was calculated as "indirect effect/total effect (IE/TE)," with the direct effect (DE) determined as TE - IE (26). Confidence intervals (CIs) for the mediated proportions were calculated using the delta method (27).

3 Results

3.1 Genetic variation selection

In this study, based on the selection criteria for instrumental variables, SNPs without a palindromic structure, no linkage disequilibrium, and an F-statistic >10 were selected. Specifically, 104, 11, 6, 60, and 161 SNPs were selected as valid instrumental variables (IVs) for hypothyroidism, hyperthyroidism, FT3, FT4, and TSH, respectively.

3.2 Causal effect of thyroid disease on OP

To investigate the effects of thyroid disease and thyroid function on OP, a TSMR analysis was conducted. Specifically, we examined the causal relationships between hypothyroidism, hyperthyroidism, FT3, FT4, TSH, and the risk of OP.

The results indicated a causal relationship between hypothyroidism and an increased risk of OP (IVW: OR = 1.092, 95% CI: 1.049–1.137, $p < 0.001$). A causal relationship was also found between hyperthyroidism and OP risk (IVW: OR = 1.080, 95% CI: 1.026–1.137, $p = 0.003$). However, no causal relationships were observed between FT3, FT4, TSH, and OP risk ($p > 0.05$) (Figure 2). The intercept of the MR-Egger regression was not statistically significant, and the symmetry of the funnel plot around zero suggested that the selected instrumental variables were minimally, affected by horizontal pleiotropy (Figure 3). A multiplicity test conducted using R software showed that all p-values were greater than 0.05, indicating negligible or no multiplicity effects among the instrumental variables. Leave-one-out sensitivity analysis revealed that all SNPs in the hyperthyroidism and hypothyroidism groups were on one side of the

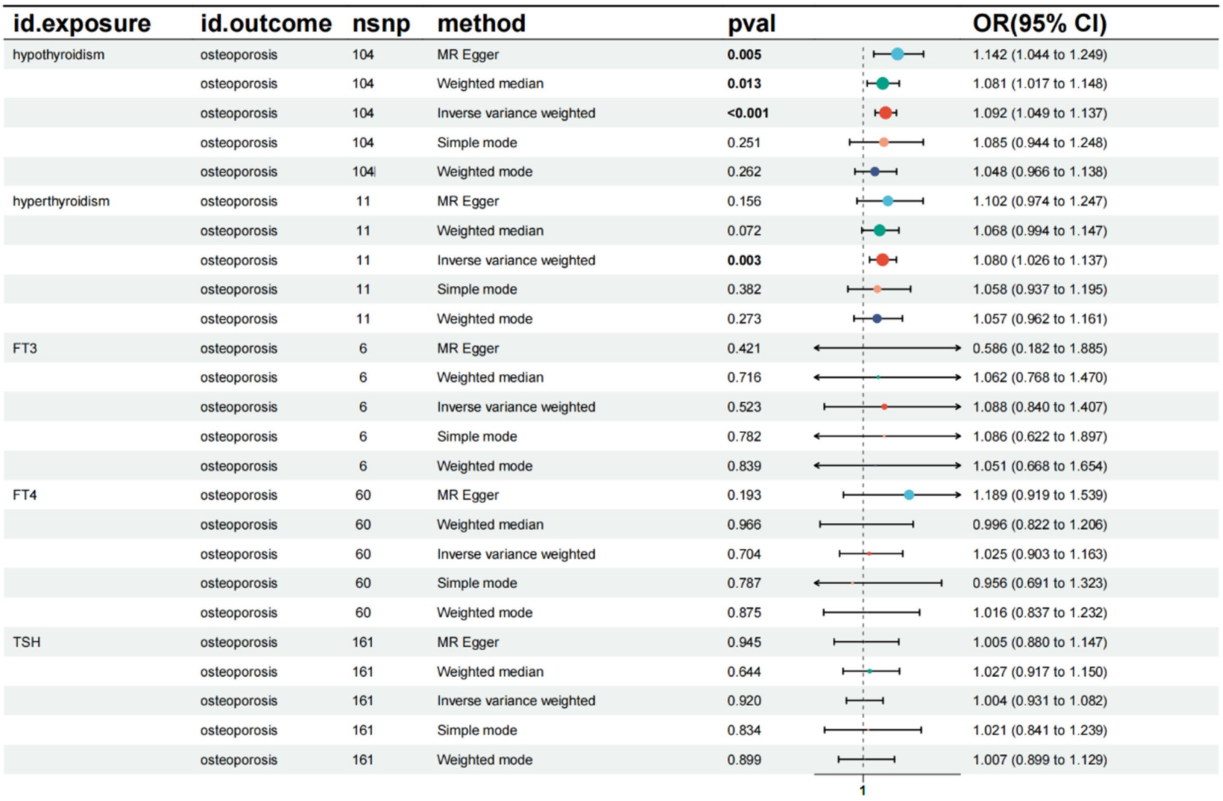

id.exposure	id.outcome	nsnp	method	pval	OR(95% CI)
hypothyroidism	osteoporosis	104	MR Egger	**0.005**	1.142 (1.044 to 1.249)
	osteoporosis	104	Weighted median	**0.013**	1.081 (1.017 to 1.148)
	osteoporosis	104	Inverse variance weighted	**<0.001**	1.092 (1.049 to 1.137)
	osteoporosis	104	Simple mode	0.251	1.085 (0.944 to 1.248)
	osteoporosis	104	Weighted mode	0.262	1.048 (0.966 to 1.138)
hyperthyroidism	osteoporosis	11	MR Egger	0.156	1.102 (0.974 to 1.247)
	osteoporosis	11	Weighted median	0.072	1.068 (0.994 to 1.147)
	osteoporosis	11	Inverse variance weighted	**0.003**	1.080 (1.026 to 1.137)
	osteoporosis	11	Simple mode	0.382	1.058 (0.937 to 1.195)
	osteoporosis	11	Weighted mode	0.273	1.057 (0.962 to 1.161)
FT3	osteoporosis	6	MR Egger	0.421	0.586 (0.182 to 1.885)
	osteoporosis	6	Weighted median	0.716	1.062 (0.768 to 1.470)
	osteoporosis	6	Inverse variance weighted	0.523	1.088 (0.840 to 1.407)
	osteoporosis	6	Simple mode	0.782	1.086 (0.622 to 1.897)
	osteoporosis	6	Weighted mode	0.839	1.051 (0.668 to 1.654)
FT4	osteoporosis	60	MR Egger	0.193	1.189 (0.919 to 1.539)
	osteoporosis	60	Weighted median	0.966	0.996 (0.822 to 1.206)
	osteoporosis	60	Inverse variance weighted	0.704	1.025 (0.903 to 1.163)
	osteoporosis	60	Simple mode	0.787	0.956 (0.691 to 1.323)
	osteoporosis	60	Weighted mode	0.875	1.016 (0.837 to 1.232)
TSH	osteoporosis	161	MR Egger	0.945	1.005 (0.880 to 1.147)
	osteoporosis	161	Weighted median	0.644	1.027 (0.917 to 1.150)
	osteoporosis	161	Inverse variance weighted	0.920	1.004 (0.931 to 1.082)
	osteoporosis	161	Simple mode	0.834	1.021 (0.841 to 1.239)
	osteoporosis	161	Weighted mode	0.899	1.007 (0.899 to 1.129)

FIGURE 2
Summary of the five Mendelian randomization analysis methods. CI, confidence interval; OR, odds ratio; TSH, Thyroid stimulating hormone.

distribution. The *p*-values from the heterogeneity test were greater than 0.05, indicating no biased SNPs (Figure 4).

3.3 Multivariate Mendelian analysis

Diabetes mellitus is a known risk factor for OP and fractures, with patients with type 1 diabetes mellitus having an elevated risk of developing OP (28). Therefore, type 1 diabetes was included in this study for MVMR analysis. The results indicated that hyperthyroidism was no longer a risk factor for OP (OR = 0.984, 95% CI: 0.918–1.055, $p = 0.657$). However, hypothyroidism remained a risk factor for OP (OR = 1.082, 95% CI: 1.021–1.147, $p = 0.008$), and type 1 diabetes also emerged as a risk factor for OP (OR = 1.049, 95% CI: 1.029–1.069, $p < 0.001$) (Figure 5).

3.4 Mediated Mendelian randomization analysis

We investigated the effect of hypothyroidism on circulating metabolites in 249 individuals and identified a significant correlation between hypothyroidism and 59 circulating metabolites after applying FDR correction ($p < 0.05$) (29). Hypothyroidism was found to be a risk factor for citrate (OR = 1.021, 95% CI: 1.001–1.032, $p = 0.005$) and creatinine (OR = 1.018, 95% CI: 1.006–1.030, $p = 0.017$). It was also inversely associated with ApoA1 (OR = 0.980, 95% CI: 0.966–0.995, $p = 0.038$), cholines (OR = 0.976, 95% CI: 0.962–0.990, $p = 0.011$), the concentration of large high-density lipoprotein particles (HDL) (OR = 0.975, 95% CI: 0.960–0.990, $p = 0.013$), large cholesteryl esters in LDL (OR = 0.981, 95% CI: 0.965–0.996, $p = 0.047$), cholesteryl esters in large very-low-density lipoproteins (VLDL) (OR = 0.983, 95% CI: 0.970–0.997, p = 0.047), triglycerides in large VLDL (OR = 0.982, 95% CI: 0.969–0.996, $p = 0.045$), linoleic acid (LA) (OR = 0.970, 95% CI: 0.951–0.990, $p = 0.018$), low-density lipoprotein cholesterol (LDL) (OR = 0.981, 95% CI: 0.966–0.994, $p = 0.032$), free cholesterol in medium VLDL (OR = 0.981, 95% CI: 0.968–0.996, $p = 0.039$), concentration of medium VLDL particles (OR = 0.980, 95% CI: 0.968–0.993, $p = 0.020$), and phospholipids in small HDL (OR = 0.971, 95% CI: 0.960–0.985, $p = 0.002$), along with other protective factors. None of the selected SNPs exhibited significant horizontal pleiotropy ($p > 0.05$) or heterogeneity ($p < 0.05$). A Mendelian randomization analysis was then conducted with these 59 circulating metabolites as exposure variables and OP as the outcome variable. A causal effect was found only for triglycerides in large VLDL (OR = 0.885, 95% CI: 0.787–0.995, $p = 0.042$). Subsequently, a mediated Mendelian randomization analysis was performed, revealing that hypothyroidism exerted an indirect effect on OP through triglycerides in large VLDL, mediating 2.47% of the total effect (Figure 6).

4 Discussion

In this study, we employed univariate and MVMR analyses, along with mediation analyses, to evaluate the relationships between hypothyroidism, circulating metabolites, and OP. Our findings

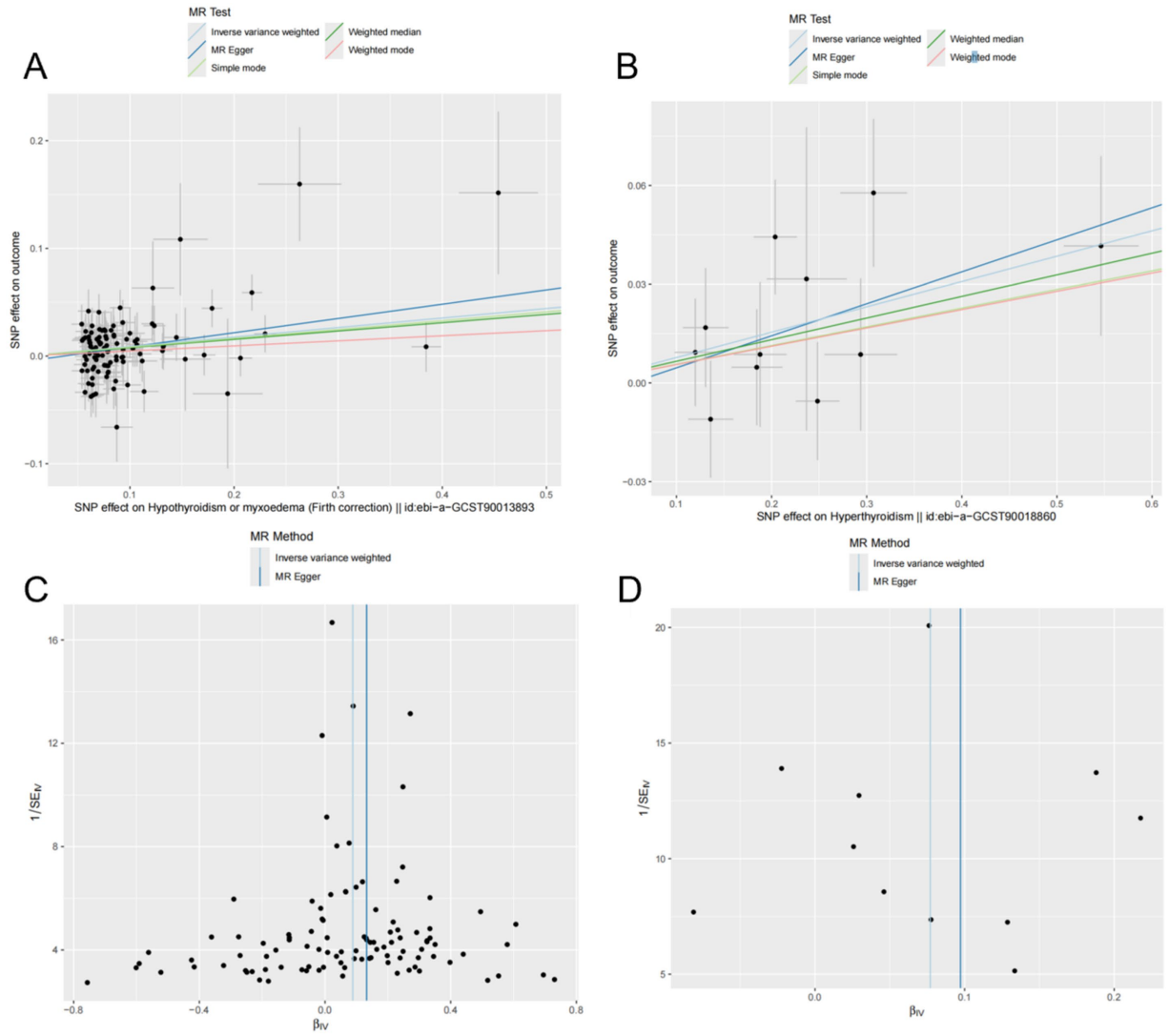

FIGURE 3
Mendelian randomization (MR) analyses of hyperthyroidism, hypothyroidism, and OP were conducted using multiple models. (A,B) Scatter plots depict the potential causal relationships between hypothyroidism (A), hyperthyroidism (B), and OP, where the slopes represent the estimated magnitude of causality. (C,D) Funnel plots present heterogeneity tests, highlighting causal effect estimates of hypothyroidism (C) and hyperthyroidism (D) on OP. The lines represent causal effect estimates derived from the inverse variance weighting and MR-Egger models.

demonstrated that hypothyroidism and hyperthyroidism acted as risk factors for OP in two-sample MR analyses. However, after adjusting for confounders, including diabetes mellitus, in MVMR models, hyperthyroidism was no longer a significant risk factor. Furthermore, hypothyroidism may elevate the risk of OP by altering blood metabolite levels, with triglycerides in large VLDL potentially playing a mediating role, contributing to approximately 2.7% of the overall association between hypothyroidism and OP risk.

Thyroid hormone promotes the growth of long bones, stimulates the growth and differentiation of osteoblasts, and increases osteoclast activity (30). Yang et al. investigated the relationship between thyroid autoimmune diseases and OP within the normal range of TSH. Their results indicated that thyroid peroxidase antibodies (TPO) levels were significantly higher in the serum of patients with OP compared to those without the condition ($p < 0.05$) (31). TPO is a key indicator for diagnosing thyroid autoimmune disorders, which are most commonly associated with hyperthyroidism and hypothyroidism. These findings suggest a relationship between hyperthyroidism, hypothyroidism, and OP, which is consistent with the genetic conclusions drawn in this study. We propose that hypothyroidism is a risk factor for OP, a viewpoint shared by other scholars (32). Some studies have found that higher serum concentrations of TSH are associated with increased bone density and a lower likelihood of developing OP. The proposed mechanism is that TSH promotes osteoblast differentiation and proliferation. Additionally, a correlation has been identified between elevated FT3 and FT4 levels and an increased risk of fractures and reduced bone density (33). Studies have also shown that in older adults with normal TSH levels, a positive correlation between TSH concentration and OP still exists (34). In this study, from a genetic perspective, we did not find a definitive causal relationship between TSH and OP. This may be due to population selection bias in the data used, indicating the need for further research. Some scholars analyzed

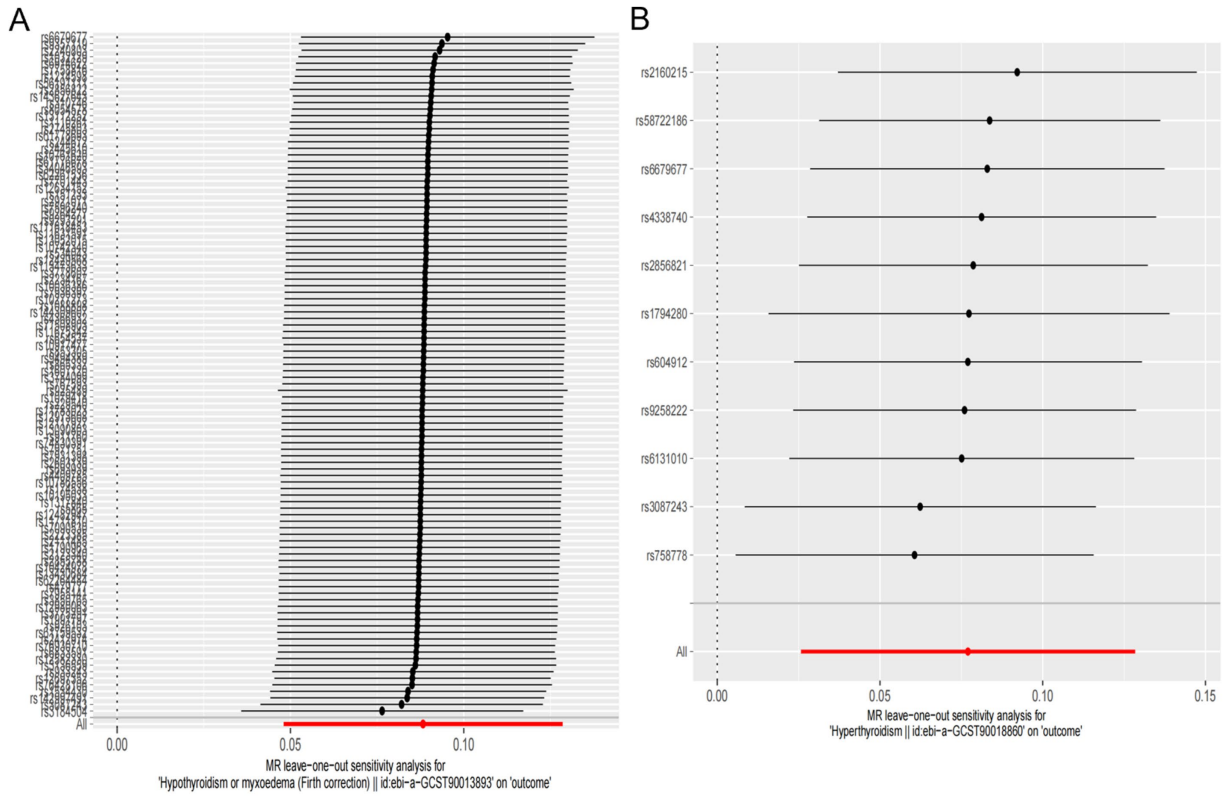

FIGURE 4
Plot of leave-one-out sensitivity analysis for hyperthyroidism and hypothyroidism.

id.exposure	id.outcome	nsnp	pval	OR(95% CI)
Hypothyroidism	osteoporosis	82	0.008	1.082 (1.021 to 1.147)
Type 1 diabetes	osteoporosis	52	<0.001	1.049 (1.029 to 1.069)
Hyperthyroidism	osteoporosis	7	0.657	0.984 (0.918 to 1.055)

FIGURE 5
Multivariate Mendelian randomization analysis. CI, confidence interval; OR, odds ratio.

3,338 men without thyroid or bone diseases and found no association between TSH, FT4, and either fracture or bone mineral density, which is consistent with our findings (35). In this study, we also included type 1 diabetes mellitus in the multivariate Mendelian analysis and found that both hypothyroidism and type 1 diabetes mellitus were risk factors for OP, though the underlying mechanism remains unclear. A possible explanation is a synergistic effect between hypothyroidism and type 1 diabetes.

Mediated MR approaches enable the investigation of potential causal pathways linking genetic risk factors to disease outcomes via specific biomarkers or metabolic pathways. In this study, we employed the genetic instrumental variable for hypothyroidism to evaluate its indirect influence on OP risk, mediated through circulating metabolites. We found that hypothyroidism may have an indirect effect on OP via triglycerides in large VLDL, though the underlying mechanism remains unknown. In a study involving patients in the early post-thyroidectomy phase, total cholesterol (TC), low-density lipoprotein cholesterol (LDL-C), triglycerides (TG), and the TC/HDL-C ratio were elevated in the thyroid hormone-naïve group compared to the control group (36). Cai et al. (37) analyzed 27 pregnant women with hypothyroidism and 28 healthy pregnant women, and found that plasma lipid levels in the hypothyroid group were significantly higher than in the healthy group. Zhang et al. (38) conducted a TSMR analysis and identified a causal relationship between dyslipidemia and OP, where VLDL was found to be a protective factor for OP

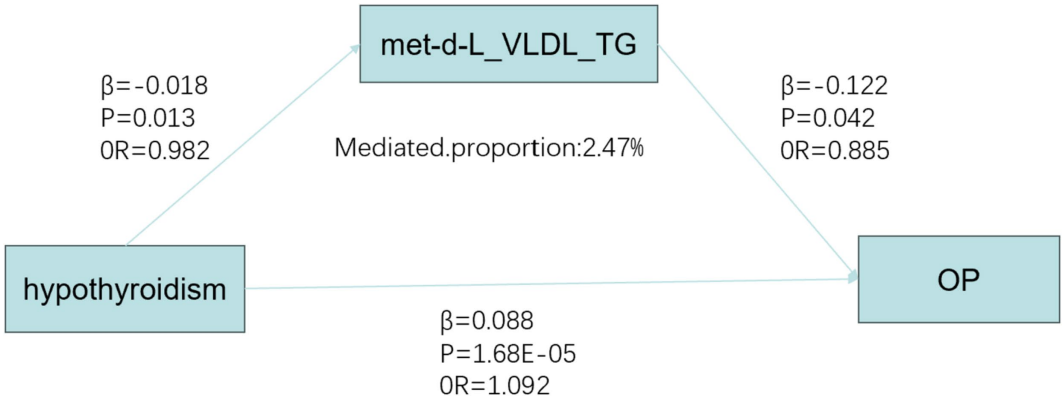

FIGURE 6
Mediated Mendelian analysis. OP, osteoporosis; OR, odds ratio; met-d-L_VLDL_TG, Triglycerides in large very low-density lipoprotein.

(OR = 0.948), consistent with our findings. They further suggested that this result might be related to abnormal methylation gene modifications. In a study investigating the relationship between triglyceride-glucose (TyG) index and bone mass, findings indicated a significant association between elevated TyG and an increased risk of OP (39). Elevated triglycerides (TG) in VLDL may disrupt the balance between bone formation and resorption, but further research is required to elucidate the precise role of these metabolites in bone health.

Our study has several strengths, including multiple data sources, a large sample size, and the use of heterogeneity, multiplicity, sensitivity analyses, and FDR correction to ensure the robustness of the findings. Notably, this study is the first to use circulating metabolites as mediators to investigate the indirect effect of hypothyroidism on OP, the first to explore the causal effect of FT3 on OP, and the first to examine the impact of MVMR analyses on type 1 diabetes mellitus and thyroid disease in relation to the causal effect on OP.

Limitations of this study include: first, the study population was European, which may not be representative of the global population. Second, the only intervening variable analyzed was type 1 diabetes mellitus, while many other factors contribute to the development of OP, suggesting that future studies should incorporate additional variables for multivariate analysis. Third, due to the lack of distinction between OP subtypes in publicly available GWAS data on functional outcomes in hypothyroidism, it is currently not feasible to evaluate functional outcomes across specific OP subtypes. Fourthly, we only used summary data and did not assess and analyze other factors such as different age and gender. Moreover, full-scale clinical trials are necessary to validate these clinical conclusions. Therefore, a more comprehensive GWAS database and further trials are needed to clarify the mechanisms by which thyroid disease influences OP through lipid metabolism.

5 Conclusion

In this study, we evaluated the causal relationships between hypothyroidism, hyperthyroidism, FT3, FT4, TSH, and OP using TSMR analysis. Our findings suggest that hypothyroidism is a risk factor for OP, while a causal relationship between FT3, FT4, TSH, and OP has not yet been supported, and whether hyperthyroidism is a risk factor for OP requires further investigation. We also conducted a mediation analysis and found that hypothyroidism may have an indirect effect on OP through triglycerides in large VLDL, with a mediation proportion of 2.47%. This study highlights the importance of reminding patients with thyroid disease, especially those with concomitant dyslipidemia, and clinicians that lipid control should be emphasized in the treatment of thyroid disorders. Additionally, proactive measures should be taken to prevent the development and progression of osteoporosis.

Data availability statement

The datasets presented in this study can be found in online repositories. The names of the repository/repositories and accession number (s) can be found in the article/Supplementary material.

Ethics statement

The study did not require ethical approval according to local legislation and institutional requirements, and no written informed consent was obtained from participants or their legal guardians/next of kin in accordance with these guidelines.

Author contributions

PL: Validation, Investigation, Formal analysis, Conceptualization, Writing – original draft, Methodology, Writing – review & editing, Data curation. YQ: Software, Resources, Methodology, Investigation, Formal analysis, Conceptualization, Writing – original draft, Writing – review & editing, Data curation. MeZ: Writing – original draft, Visualization, Validation, Supervision, Conceptualization, Writing – review & editing, Data curation. YZ: Writing – original draft, Visualization, Validation, Supervision, Methodology, Writing – review & editing, Data curation. NY: Writing – original draft, Visualization, Validation, Supervision,

Formal analysis, Data curation, Conceptualization, Writing – review & editing. MiZ: Methodology, Conceptualization, Writing – review & editing. WW: Visualization, Validation, Supervision, Project administration, Data curation, Writing – review & editing, Writing – original draft. ML: Visualization, Validation, Investigation, Formal analysis, Conceptualization, Writing – review & editing, Supervision, Project administration, Writing – original draft, Methodology, Data curation.

Funding

The author(s) declare that no financial support was received for the research, authorship, and/or publication of this article.

Acknowledgments

Appreciation is also due to the MRC IEU Open GWAS project and the FinnGen database for their valuable contributions in making data accessible to the public.

Conflict of interest

The authors declare that the research was conducted in the absence of any commercial or financial relationships that could be construed as a potential conflict of interest.

Publisher's note

Supplementary material

The Supplementary material for this article can be found online at: https://www.frontiersin.org/articles/10.3389/fmed.2024.1453502/full#supplementary-material

References

1. Burge R, Dawson-Hughes B, Solomon DH, Wong JB, King A, Tosteson A. Incidence and economic burden of osteoporosis-related fractures in the United States, 2005-2025. *J Bone Miner Res*. (2007) 22:465–75. doi: 10.1359/jbmr.061113

2. Letarouilly JG, Broux O, Clabaut A. New insights into the epigenetics of osteoporosis. *Genomics*. (2019) 111:793–8. doi: 10.1016/j.ygeno.2018.05.001

3. Aibar-Almazán A, Voltes-Martínez A, Castellote-Caballero Y, Afanador-Restrepo DF, Carcelén-Fraile MC, López-Ruiz E. Current status of the diagnosis and Management of Osteoporosis. *Int J Mol Sci*. (2022) 23:9465. doi: 10.3390/ijms23169465

4. Leboff MS, Greenspan SL, Insogna KL, Lewiecki EM, Saag KG, Singer AJ, et al. The clinician's guide to prevention and treatment of osteoporosis. *Osteoporos Int*. (2022) 33:2049–102. doi: 10.1007/s00198-021-05900-y

5. Vanderpump MP. The epidemiology of thyroid disease. *Br Med Bull*. (2011) 99:39–51. doi: 10.1093/bmb/ldr030

6. Lee K, Lim S, Park H, Woo HY, Chang Y, Sung E, et al. Subclinical thyroid dysfunction, bone mineral density, and osteoporosis in a middle-aged Korean population. *Osteoporos Int*. (2020) 31:547–55. doi: 10.1007/s00198-019-05205-1

7. Gao N, Kong M, Li X, Wei D, Zhu X, Hong Z, et al. Systemic lupus erythematosus and cardiovascular disease: a Mendelian randomization study. *Front Immunol*. (2022) 13:908831. doi: 10.3389/fimmu.2022.908831

8. Nederstigt C, Corssmit EP, De Koning EJ, Dekkers OM. Incidence and prevalence of thyroid dysfunction in type 1 diabetes. *J Diabetes Complicat*. (2016) 30:420–5. doi: 10.1016/j.jdiacomp.2015.12.027

9. Rinschen MM, Ivanisevic J, Giera M, Siuzdak G. Identification of bioactive metabolites using activity metabolomics. *Nat Rev Mol Cell Biol*. (2019) 20:353–67. doi: 10.1038/s41580-019-0108-4

10. Wishart DS. Metabolomics for investigating physiological and pathophysiological processes. *Physiol Rev*. (2019) 99:1819–75. doi: 10.1152/physrev.00035.2018

11. Shao F, Li R, Guo Q, Qin R, Su W, Yin H, et al. Plasma metabolomics reveals systemic metabolic alterations of subclinical and clinical hypothyroidism. *J Clin Endocrinol Metab*. (2022) 108:13–25. doi: 10.1210/clinem/dgac555

12. Wei X, Zhang Y, Sun C, Qi B, Huang X, Chen M, et al. Elucidating the relationship between dyslipidemia and osteoporosis: a multicenter, prospective cohort study protocol. *Front Cardiovasc Med*. (2022) 9:901786. doi: 10.3389/fcvm.2022.901786

13. Han Y, Wang C, Zhang L, Zhu J, Zhu M, Li Y, et al. Menopausal impact on the association between thyroid dysfunction and lipid profiles: a cross-sectional study. *Front Endocrinol*. (2022) 13:853889. doi: 10.3389/fendo.2022.853889

14. Larsson SC, Butterworth AS, Burgess S, Zhu J, Zhu M, Li Y. Mendelian randomization for cardiovascular diseases: principles and applications. *Eur Heart J*. (2023) 44:4913–24. doi: 10.1093/eurheartj/ehad736

15. Burgess S, Labrecque JA. Mendelian randomization with a binary exposure variable: interpretation and presentation of causal estimates. *Eur J Epidemiol*. (2018) 33:947–52. doi: 10.1007/s10654-018-0424-6

16. Myers TA, Chanock SJ, Machiela MJ. LdlinkR: an R package for rapidly calculating linkage disequilibrium statistics in diverse populations. *Front Genet*. (2020) 11:157. doi: 10.3389/fgene.2020.00157

17. Van Kippersluis H, Rietveld CA. Pleiotropy-robust Mendelian randomization. *Int J Epidemiol*. (2018) 47:1279–88. doi: 10.1093/ije/dyx002

18. Li H, Pan X, Zhang S, Shen X, Li W, Shang W, et al. Association of autoimmune diseases with the occurrence and 28-day mortality of sepsis: an observational and Mendelian randomization study. *Crit Care*. (2023) 27:476. doi: 10.1186/s13054-023-04763-5

19. Fang P, Liu X, Qiu Y, Wang Y, Wang D, Zhao J, et al. Exploring causal correlations between inflammatory cytokines and ankylosing spondylitis: a bidirectional mendelian-randomization study. *Front Immunol*. (2023) 14:1285106. doi: 10.3389/fimmu.2023.1285106

20. Lin Z, Deng Y, Pan W. Combining the strengths of inverse-variance weighting and egger regression in Mendelian randomization using a mixture of regressions model. *PLoS Genet*. (2021) 17:e1009922. doi: 10.1371/journal.pgen.1009922

21. Zhou J, Ye Z, Wei P, Yi F, Ouyang M, Xiong S, et al. Effect of basal metabolic rate on osteoporosis: a Mendelian randomization study. *Front Public Health*. (2023) 11:1096519. doi: 10.3389/fpubh.2023.1096519

22. Ding M, Zhang Z, Chen Z, Song J, Wang B, Jin F. Association between periodontitis and breast cancer: two-sample Mendelian randomization study. *Clin Oral Investig*. (2023) 27:2843–9. doi: 10.1007/s00784-023-04874-x

23. Nagayoshi M, Hishida A, Shimizu T, Kato Y, Kubo Y, Okada R, et al. Bmi and Cardiometabolic traits in Japanese: a Mendelian randomization study. *J Epidemiol*. (2024) 34:51–62. doi: 10.2188/jea.JE20220154

24. Hemani G, Zheng J, Elsworth B, Wade KH, Haberland V, Baird D, et al. The Mr-Base platform supports systematic causal inference across the human phenome. *elife*. (2018) 7:e34408. doi: 10.7554/eLife.34408

25. Ritchie SC, Surendran P, Karthikeyan S, Lambert SA, Bolton T, Pennells L, et al. Quality control and removal of technical variation of Nmr metabolic biomarker data in ~120,000 Uk biobank participants. *Sci Data*. (2023) 10:64. doi: 10.1038/s41597-023-01949-y

26. Carter AR, Sanderson E, Hammerton G, Richmond RC, Davey Smith G, Heron J, et al. Mendelian randomisation for mediation analysis: current methods and challenges for implementation. *Eur J Epidemiol*. (2021) 36:465–78. doi: 10.1007/s10654-021-00757-1

27. Mackinnon DP, Lockwood CM, Hoffman JM, West SG, Sheets V. A comparison of methods to test mediation and other intervening variable effects. *Psychol Methods*. (2002) 7:83–104. doi: 10.1037/1082-989X.7.1.83

28. Vilaca T, Eastell R. Antiresorptive versus anabolic therapy in managing osteoporosis in people with type 1 and type 2 diabetes. *Jbmr Plus*. (2023) 7:e10838. doi: 10.1002/jbm4.10838

29. Deng K, Shuai M, Zhang Z, Jiang Z, Fu Y, Shen L, et al. Temporal relationship among adiposity, gut microbiota, and insulin resistance in a longitudinal human cohort. *BMC Med*. (2022) 20:171. doi: 10.1186/s12916-022-02376-3

30. Kenkre JS, Bassett J. The bone remodelling cycle. *Ann Clin Biochem*. (2018) 55:308–27. doi: 10.1177/0004563218759371

31. Yang L, Wang H, Guo J, Zheng G, Wei D, Zhang T. Low Normal Tsh levels and thyroid autoimmunity are associated with an increased risk of osteoporosis in Euthyroid postmenopausal women. *Endocr Metab Immune Disord Drug Targets*. (2021) 21:859–65. doi: 10.2174/1871530320666200810144506

32. González-Rodríguez LA, Felici-Giovanini ME, Haddock L. Thyroid dysfunction in an adult female population: a population-based study of Latin American vertebral osteoporosis study (Lavos) - Puerto Rico site. *P R Health Sci J*. (2013) 32:57–62.

33. Deng T, Zhang W, Zhang Y, Zhang M, Huan Z, Yu C, et al. Thyroid-stimulating hormone decreases the risk of osteoporosis by regulating osteoblast proliferation and differentiation. *BMC Endocr Disord*. (2021) 21:49. doi: 10.1186/s12902-021-00715-8

34. Leader A, Ayzenfeld RH, Lishner M, Cohen E, Segev D, Hermoni D. Thyrotropin levels within the lower normal range are associated with an increased risk of hip fractures in euthyroid women, but not men, over the age of 65 years. *J Clin Endocrinol Metab*. (2014) 99:2665–73. doi: 10.1210/jc.2013-2474

35. Siru R, Alfonso H, Chubb SAP, Golledge J, Flicker L, Yeap BB. Subclinical thyroid dysfunction and circulating thyroid hormones are not associated with bone turnover markers or incident hip fracture in older men. *Clin Endocrinol*. (2018) 89:93–9. doi: 10.1111/cen.13615

36. Al-Janabi G, Hassan HN, Al-Fahham A. Biochemical changes in patients during hypothyroid phase after thyroidectomy. *J Med Life*. (2022) 15:104–8. doi: 10.25122/jml-2021-0297

37. Cai Y, Xu Y, Ban Y, Li J, Sun Z, Zhang M, et al. Plasma lipid profile and intestinal microflora in pregnancy women with hypothyroidism and their correlation with pregnancy outcomes [J]. *Front Endocrinol*. (2021) 12:792536. doi: 10.3389/fendo.2021.792536

38. Zhang Z, Duan Y, Huo J. Lipid metabolism, methylation aberrant, and osteoporosis: a multi-omics study based on Mendelian randomization. *Calcif Tissue Int*. (2024) 114:147–56. doi: 10.1007/s00223-023-01160-6

39. Zhuo M, Chen Z, Zhong ML, Lei F, Qin JJ, Liu S, et al. Association of insulin resistance with bone mineral density in a nationwide health check-up population in China. *Bone*. (2023) 170:116703. doi: 10.1016/j.bone.2023.116703

frontiers | Frontiers in Endocrinology

TYPE Original Research
PUBLISHED 04 February 2025
DOI 10.3389/fendo.2025.1514857

OPEN ACCESS

EDITED BY
Robert Kiss,
McGill University, Canada

REVIEWED BY
Oana Stanoiu-Pinzariu,
University of Medicine and Pharmacy Iuliu Hatieganu, Romania
Genco Görgü,
Ministry of Health, Türkiye

*CORRESPONDENCE
Xiang Li
ideal.li@163.com
Hua Wei
13829701168@163.com

†These authors have contributed equally to this work

RECEIVED 21 October 2024
ACCEPTED 16 January 2025
PUBLISHED 04 February 2025

CITATION
Yan M, Shi W, Gong P, Xie Y, Zhang K, Li X and Wei H (2025) A U-shaped non-linear association between serum uric acid levels and the risk of Hashimoto's thyroiditis: a cross-sectional study.
Front. Endocrinol. 16:1514857.
doi: 10.3389/fendo.2025.1514857

A U-shaped non-linear association between serum uric acid levels and the risk of Hashimoto's thyroiditis: a cross-sectional study

Manli Yan[1†], Wenhua Shi[1†], Ping Gong[1†], Yunsi Xie[1†], Kaiyuan Zhang[1], Xiang Li[2*] and Hua Wei[3,4*]

[1]Second Clinical Medical College, Guangzhou University of Chinese Medicine, Guangzhou, China, [2]Department of Orthopedics, Guangdong Provincial Hospital of Chinese Medicine, Guangzhou, China, [3]Department of Endocrinology, Guangdong Provincial Hospital of Chinese Medicine, Guangzhou, China, [4]State Key Laboratory of Dampness Syndrome of Chinese Medicine, The Second Affiliated Hospital of Guangzhou University of Chinese Medicine, Guangzhou, China

Objective: Previous studies have found that the relationship between metabolic indicators and Hashimoto's thyroiditis (HT) in non-diabetic adults remains unclear. This study aims to explore the association between metabolic indicators and HT, providing new theoretical insights for the clinical management of HT.

Methods: Clinical data were collected from 2,015 non-diabetic adults at Guangdong Provincial Hospital of Chinese Medicine. The relationship between metabolic indicators and HT was analyzed using SPSS 26.0, R (version 4.2.1), and Zstats.

Results: Among the 2,015 non-diabetic adult participants included in the study, 1,877 were in the non-HT group, while 138 were in the HT group. Significant differences were observed in metabolic indicators, including serum uric acid (SUA), serum creatinine (SCr), albumin (ALB) and high-density lipoprotein cholesterol (HDL-C), between the two groups, with statistical significance. A binary logistic regression model was established, revealing that SCr had a significant impact in both univariate and multivariate analyses. To further investigate the relationship between metabolic indicators and HT, we conducted a restricted cubic spline (RCS) analysis. The results demonstrated a clear non-linear relationship between SUA and HT, both before and after adjustment (All $P < 0.01$). Therefore, based on the inflection points derived from the RCS analysis, a segmented logistic regression analysis was performed. The findings indicated a significant association between both low and high levels of SUA and HT (Lower OR: 2.043; 95% CI: 1.405-3.019; $P < 0.001$; Higher OR: 2.369; 95% CI: 0.998-4.999; $P = 0.034$).

Conclusion: This study is the first to reveal a U-shaped association between SUA levels and the risk of HT, suggesting that maintaining SUA levels within the range

of 359.0-540.0 μmol/L may help reduce the risk of HT occurrence. This finding provides a new perspective for early intervention and long-term management of HT, particularly in terms of SUA regulation in HT patients, which holds potential clinical value.

KEYWORDS

Hashimoto's thyroiditis, non-diabetic adults, serum uric acid, RCS analysis, U-shaped curve

1 Introduction

Hashimoto's thyroiditis (HT), also known as chronic lymphocytic thyroiditis or autoimmune thyroiditis, is a chronic inflammatory disease of the thyroid with an etiology that remains incompletely understood. According to a meta-analysis (1), the global prevalence of HT among adults is 7.5%, with women being approximately four times more likely to be affected than men.

In HT, the immune system mistakenly targets the thyroid gland (2), producing antibodies such as anti-thyroid peroxidase antibody (TPOAb) and thyroid globulin antibody (TgAb), leading to persistent lymphocytic infiltration and chronic inflammation of the thyroid tissue, which results in specific thyroid dysfunction (3). As an autoimmune disease, the immune attack and antibody production are ongoing and often coexist with other autoimmune disorders (3), such as type 1 diabetes (3) and systemic lupus erythematosus (4).

Long-term immune activation may promote abnormal proliferation of lymphocytes, making HT a significant risk factor for primary thyroid lymphoma (5) and thyroid carcinoma (6), being associated with over 90% of thyroid lymphoma cases. Furthermore, persistent autoimmune responses can lead to severe central nervous system complications, such as Hashimoto's encephalopathy (7). If not treated promptly, these complications may result in irreversible neurological damage (8). Therefore, early treatment of HT plays a crucial role in preventing complications and improving patient outcomes.

The late-stage glycation end products (AGEs) formed under chronic hyperglycemic conditions are evaluated as potential new biomarkers of oxidative stress (9). Elevated levels of oxidative stress-mediated by AGEs can induce damage to thyroid follicular cells, trigger thyroid inflammation and ultimately promote the development of HT (10). Research indicates that (11) the expression of IL-23 in thyroid follicular cells of HT patients is increased, contributing to autophagy suppression and the accumulation of reactive oxygen species (ROS). Additionally, elevated levels of TPOAb (12) in HT patients are also believed to be associated with increased concentrations of interleukin-6 and tumor necrosis factor-alpha, which play significant roles in the pathogenesis of insulin resistance (13). Therefore, some researchers suggest that TPOAb may exacerbate insulin resistance by promoting chronic inflammation, thereby interfering with normal glucose metabolism.

HT patients often experience dyslipidemia (14). Liu et al. (15) found a significant positive correlation between TPOAb levels and total cholesterol, triglycerides, insulin resistance and high-sensitivity C-reactive protein concentrations. Several studies (16–18) also suggest that TPOAb may serve as a potential link between HT and dyslipidemia. Previous research (19, 20) indicates that both hypothyroid and hyperthyroid patients may have an increased risk of developing hyperuricemia(HUA). The relationship between HT and metabolic disorders extends beyond the direct effects of hypothyroidism (21); autoimmune responses and chronic inflammation may play a more active role in the metabolic disturbances observed in HT patients (22). There is growing evidence that (23) thyroid hormones and the immune system interact in a complex bidirectional manner. As modulators of immune responses, thyroid hormones may ultimately lead to functional abnormalities through immune-mediated mechanisms.

Diabetic patients are often accompanied by metabolic disorders, including dyslipidemia (24). In addition, a strong correlation between diabetes and its related complications with elevated uric acid levels has been well established (25). To further investigate the relationship between HT and metabolic disturbances, we decided to select a non-diabetic population as the study group. Previous studies have shown that the relationship between metabolic-related indicators and non-diabetic populations with HT remains unclear. This study aims to explore the relationship between HT and metabolic products, providing a stronger theoretical basis for the long-term management of HT patients.

2 Materials and methods

2.1 Data collection

The data used in this study were collected from adult participants who underwent health examinations at Guangdong Provincial Hospital of Chinese Medicine from January 2023 to December 2023, with complete datasets. After evaluating the availability of laboratory data,

including age, gender, glycated hemoglobin (HbA1c), fasting plasma glucose (FPG), lipid profiles (triglycerides (TG), total cholesterol (TC), high-density lipoprotein cholesterol (HDL-C), non-HDL cholesterol (nonHDL-C) and low-density lipoprotein cholesterol (LDL-C)), serum creatinine (SCr) and serum uric acid (SUA), participants meeting the screening criteria for non-diabetic adults were included (specifically, those aged over 18 years, with HbA1c levels below 6.0% and FPG below 6.1 mmol/L). A total of 2,015 participants were included in the study (1,164 males and 851 females).

According to the 2008 Guidelines for the Diagnosis and Treatment of Thyroid Diseases in China and the American Thyroid Association's handbook on Hashimoto's thyroiditis (26), participants with positive TPOAb and TgAb were defined as the Hashimoto's thyroiditis group (HT group). Participants with negative serum TPOAb and TgAb were defined as the non-Hashimoto's thyroiditis group (Non-HT group).

2.2 Statistical analysis

We employed univariate and multivariate logistic regression models to analyze the association between metabolic-related indicators and HT in a non-diabetic adult population. In evaluating the goodness of fit for the multivariable logistic regression model, we used the Hosmer-Lemeshow test. The results showed that the model fits well. To further assess the performance of the model, we introduced the concordance index as an evaluation metric. In this study, the concordance index of the constructed multivariable logistic regression model was 0.64 (95% confidence interval: 0.59-0.69). To further assess the impact of these indicators on the risk of HT, we constructed a multivariate logistic regression model based on restricted cubic splines (RCS). RCS is an effective strategy for analyzing the relationship between the risk of disease occurrence and independent variables, particularly suitable for exploring non-linear associations. Restricted cubic splines utilize smooth connections of polynomial functions to avoid assuming a linear relationship between covariates and the response variable. To avoid overfitting, the model was selected based on the minimum Akaike Information Criterion (AIC). The AIC value was smallest when the number of nodes was set to 4. Therefore, we used a restricted cubic spline function with 4 nodes at the 5th, 35th, 65th, and 95th percentiles to flexibly model the association between metabolic markers and HT. A P-value for non-linearity < 0.05 was defined as evidence of a non-linear relationship between the two. Additionally, the RCS model can identify risk inflection points (thresholds), defined as the values that minimize the odds ratio (OR). Once the thresholds were established, we conducted piecewise logistic regression analyses to explore the relationships between relevant indicators and HT across different intervals. The chi-squared test was used for categorical variables, while non-parametric tests were employed for continuous variables. All statistical tests were two-sided, with $P < 0.05$ considered statistically significant. All statistical analyses were performed using SPSS 26.0, R (version 4.2.1), and the "Zstats" package.

3 Results

3.1 Participant characteristics

A total of 2,015 non-diabetic adult participants were included. Among them, 138 participants were in the HT group, while 1,877 were in the Non-HT group. There were no significant differences in age and sex between the two groups. Notable differences with statistical significance were observed in metabolic-related indicators such as SUA, SCr, ALB and HDL-C between the two groups. In terms of thyroid-related indicators, the HT group showed significantly higher levels of TSH, TPOAb and TgAb compared to the Non-HT group, with these differences also being statistically significant (see Table 1).

3.2 Univariate and multivariate logistic regression analysis

We established a binary logistic regression model, incorporating variables with $P < 0.05$ into both univariate and multivariate logistic regression analyses (see Table 2). The influence of SCr was significant in both the univariate and multivariate analyses (univariate analysis: OR 0.976; 95% CI 0.965–0.987; multivariate analysis: OR 0.979; 95% CI 0.966–0.993; both $P < 0.01$). The impacts of SUA, ALB and HDL-C were not significant in the multivariate analysis ($P > 0.05$), indicating that their associations with the outcome diminished after controlling for other variables.

3.3 Restrictive cubic spline identification of uric acid ranges related to minimum risk

To further investigate the relationship between metabolic-related indicators and HT, we conducted a RCS analysis (see Figures 1, 2). The results showed that neither SCr, ALB, nor HDL-C demonstrated a significant non-linear relationship with HT in both univariate analyses and after adjusting for age and gender (all $P > 0.05$). In contrast, SUA exhibited a significant non-linear relationship with HT before and after adjustment (all $P < 0.01$). Therefore, based on the inflection points derived from the RCS, we further analyzed the "U" shaped relationship between SUA and HT. The reference range was set at 359.0-540.0 μmol/L, where the lower subgroup consisted of participants with SUA levels below 359.0 μmol/L, and the higher subgroup comprised those with SUA levels above 540.0 μmol/L. By establishing a segmented logistic regression model, we analyzed the relationship between SUA levels in different ranges and HT. Compared to the reference range, the adjusted logistic model indicated that both lower and higher SUA levels were significantly associated with HT (Lower OR: 2.043; 95% CI: 1.405-3.019; $P < 0.001$; Higher OR: 2.369; 95% CI: 0.998-4.999; $P = 0.034$) (see Table 3).

TABLE 1 Comparison of baseline characteristics in the non-diabetic population.

	Total (n=2015)	Non-HT group (n=1877)	HT group (n=138)	*P*-value
Age (median (IQR))	45.0 (38.0, 52.0)	45.0 (38.0, 52.0)	44.0 (38.0, 52.0)	0.519
Sex (%)				0.929
Male	57.8%	57.8%	57.2%	
Female	42.2%	42.2%	42.8%	
HbA1c (median (IQR))	5.50 (5.20, 5.70)	5.50 (5.20, 5.70)	5.40 (5.20, 5.70)	0.314
FPG (median (IQR))	5.04 (4.78, 5.33)	5.03 (4.78, 5.32)	5.12 (4.83, 5.41)	0.087
SUA (median (IQR))	359.00 (297.00, 429.50)	361.00 (299.00, 432.00)	325.50 (271.75, 414.50)	0.001
SCr (median (IQR))	72.00 (59.00, 84.00)	72.00 (59.00, 84.00)	62.00 (55.00, 76.75)	<0.001
ALB (median (IQR))	46.40 (44.80, 48.10)	46.40 (44.80, 48.10)	46.00 (44.40, 47.58)	0.013
TG (median (IQR))	1.19 (0.87, 1.75)	1.20 (0.87, 1.76)	1.12 (0.84, 1.65)	0.121
TC (median (IQR))	5.15 (4.55, 5.76)	5.14 (4.55, 5.74)	5.19 (4.50, 5.90)	0.482
HDL-C (median (IQR))	1.37 (1.16, 1.62)	1.36 (1.15, 1.62)	1.44 (1.23, 1.69)	0.003
nonHDL-C (median (IQR))	3.74 (3.12, 4.38)	3.75 (3.13, 4.38)	3.70 (3.10, 4.34)	0.927
LDL-C (median (IQR))	3.22 (2.67, 3.77)	3.22 (2.67, 3.76)	3.25 (2.73, 3.84)	0.686
FT3 (median (IQR))	5.39 (5.00, 5.76)	5.41 (5.02, 5.77)	5.13 (4.77, 5.54)	<0.001
FT4 (median (IQR))	15.44 (14.25, 16.80)	15.46 (14.28, 16.82)	15.10 (14.01, 16.43)	0.052
TSH (median (IQR))	1.84 (1.33, 2.51)	1.82 (1.33, 2.48)	2.24 (1.51, 3.11)	<0.001
TPOAB (median (IQR))	28.00 (28.00, 29.17)	28.00 (28.00, 28.00)	1,095.30 (319.47, 1,300.00)	<0.001
TGAB (median (IQR))	1.30 (1.30, 1.79)	1.30 (1.30, 1.30)	85.18 (26.63, 206.37)	<0.001

4 Discussion

To our knowledge, this is the first cross-sectional study investigating the relationship between metabolic-related indicators and HT in a non-diabetic population. Our findings reveal a significant non-linear U-shaped relationship between SUA and HT in this cohort.

UA (27) is primarily synthesized in the liver, intestines and vascular endothelium. It is produced endogenously through purine metabolism, catalyzed by enzymes, from damaged, dying and dead cells. Additionally, UA levels are influenced by the purine content in dietary intake (28).

TABLE 2 Binary logistic regression analysis of the relationship between metabolic-related indicators and HT in the non-diabetic population.

	Univariate analysis		Multivariate analysis	
	OR (95%CL)	*P*-value	OR (95%CL)	*P*-value
SUA	0.997 (0.996~0.999)	0.010	1.000 (0.998~1.003)	0.777
SCr	0.976 (0.965~0.987)	<0.001	0.979 (0.966~0.993)	0.004
ALB	0.916 (0.856~0.980)	0.011	0.944 (0.880~1.013)	0.108
HDL-C	1.799 (1.138~2.843)	0.012	1.359 (0.809~2.283)	0.246

The human body maintains homeostasis of UA concentration through a dynamic balance of production and excretion (29). However, when this balance is disrupted, it often results in elevated UA levels in the blood, leading to HUA.

UA is known to promote the elimination of reactive oxygen species (ROS), which contributes to its antioxidant properties (30). However, recent studies (31) have shown that the formation of UA is also accompanied by the generation of ROS. UA can stimulate the activity of NADPH oxidase while inhibiting the activity of endothelial nitric oxide synthase, consequently reducing the metabolism of nitric oxide (NO). Furthermore, UA enhances the affinity of arginase for L-arginine, which further promotes ROS production. Although ROS (32) plays a crucial role in regulating cellular signaling and physiological homeostasis, excessive production of ROS (32, 33) can lead to pathological states of oxidative stress. This overproduction has been shown to irreversibly alter cellular structure and function. Overall, the generation of ROS is vital for regulating appropriate immune responses.

The human gut (34) is the only site that continuously activates the immune system through direct contact with the microbiome. The production of ROS in the gut is considered a double-edged sword (34): it is an indispensable mechanism for defending against pathogens and facilitating mucosal healing, but excessive ROS production can adversely affect mucosal integrity and epithelial

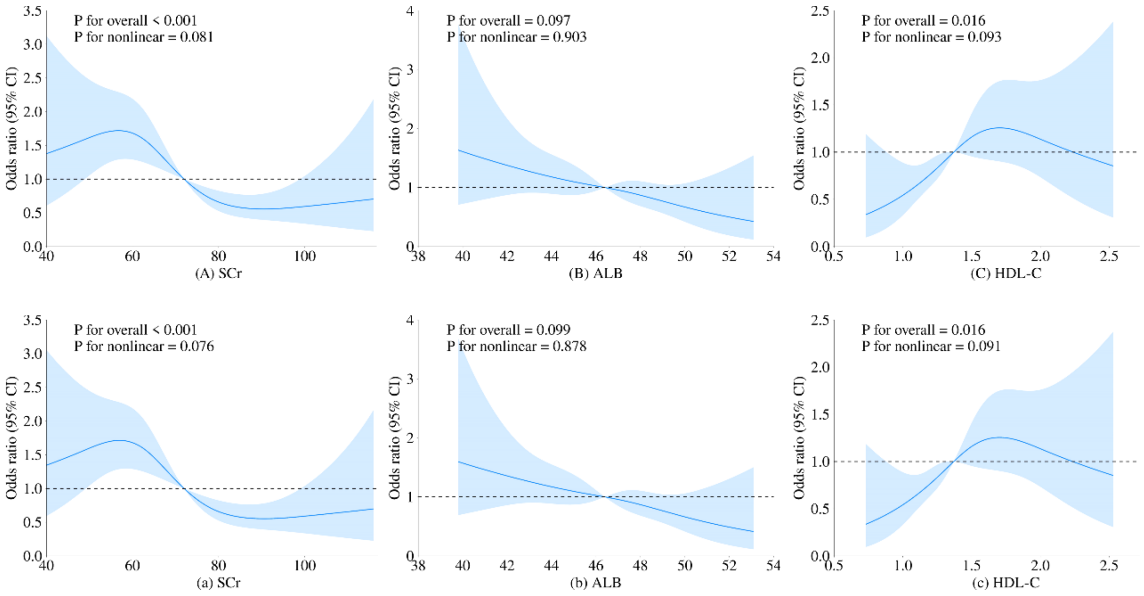

FIGURE 1
Restricted cubic spline regression analysis of the relationship between SCr, ALB, and HDL-C as continuous variables and HT. The blue solid line represents the estimated adjusted OR, while the shaded area indicates the 95% confidence interval. The dashed line represents an odds ratio or risk ratio of 1.0. Panels **(A–C)** show the spline curves for univariate regression, while subpanels (a-c) present the spline curves adjusted for age and gender.

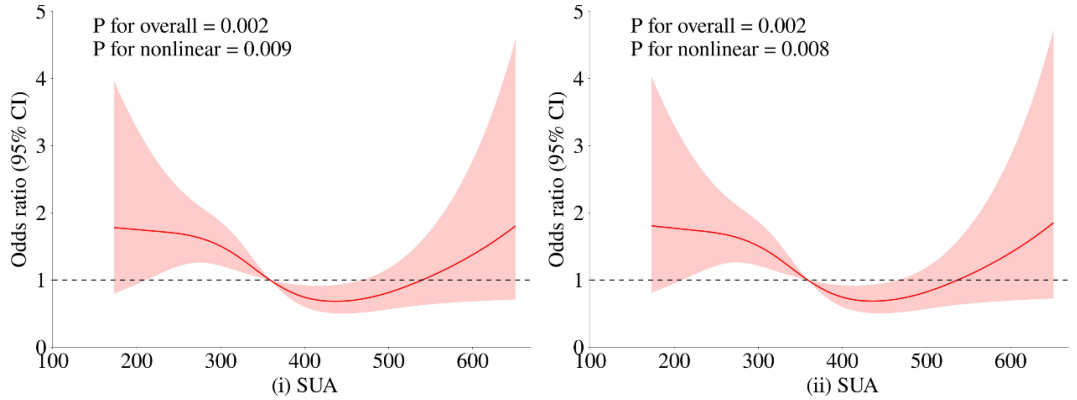

FIGURE 2
Restricted cubic spline regression analysis of the relationship between SUA as a continuous variable and HT. The red solid line represents the estimated adjusted OR, while the shaded area indicates the 95% confidence interval. The dashed line represents an odds ratio or risk ratio of 1.0. Panel (i) shows the spline curve for univariate regression, while panel (ii) presents the spline curve adjusted for age and gender.

TABLE 3 Threshold effect analysis of SUA and HT in the non-diabetic population.

Outcome	Adjusted OR (95% CI)	*P*-value
Model 1 Fitting by standard linear model	0.997 (0.996-0.999)	0.01
Model 2 Fitting by three-piecewise linear model		
Reference interval (359.0-540.0 μmol/L)	[Reference]	
Lower (< 359.0 μmol/L)	2.043 (1.405-3.019)	<0.001
Higher (> 540.0 μmol/L)	2.369 (0.998-4.999)	0.034
P for log-likelihood ratio	0.003	

Adjusted for age and sex.

barrier function, and is even closely associated with the occurrence and progression of multisystem diseases.

HT is characterized by the infiltration of inflammatory cells into the thyroid gland and the production of antibodies against thyroid-specific antigens, which triggers a persistent state of immune inflammation (26). Chronic inflammation leads to progressive destruction and fibrosis of follicular cells, ultimately resulting in hypothyroidism. Recent studies suggest (35) that oxidative stress is a primary molecular driver of tissue damage and has garnered significant attention in the pathogenesis of autoimmune and inflammatory diseases. Under the influence of environmental and genetic factors, lymphocytes (36) participate in the pathogenesis of autoimmune diseases by producing autoantibodies and ROS.

Research by Virili et al. (37) has indicated that in patients with HT, transmission electron microscopy reveals changes in microvillus thickness and increased spacing between adjacent microvilli, along with ultrastructural morphological changes in the epithelial cells of the distal duodenum. Several studies (37, 38) have also found a close relationship between gut microbiota and thyroid function, as well as the risk of HT.

Approximately 30-40% (39) of SUA is excreted via the gut. Recent studies have suggested that gut clearance defects (40) are one of the significant causes of HUA, highlighting the important role of gut microbiota (41) in regulating UA metabolism. Research by Li, Tianhe et al. (42) has confirmed the feasibility of alleviating endocrine diseases by improving gut microbiota to reduce gut oxidative stress. UA is closely related to nutrition, immune inflammation, oxidative stress and gut microbiota, and these critical biological characteristics position UA as a key player in the pathogenesis of various diseases (43, 44).

In our study, we observed that SUA levels within a specific range (359-540 μmol/L) were significantly associated with a lower risk of HT. Therefore, maintaining SUA levels within this reference range may help reduce the incidence of HT, which is potentially linked to mechanisms involving oxidative stress and gut microbiota. This finding could provide important clinical recommendations for the prevention and management of HT.

5 Limitations

This study is a large-sample, single-center cross-sectional investigation; however, it does have some limitations. For instance, the sample size is relatively small, and the study population is drawn from a specific region and ethnic group, which may limit the generalizability of the findings. Additionally, the study did not consider individual-specific disease-related information, which could introduce bias into the results. Another limitation is that thyroid function was not categorized or analyzed in detail, as we considered immune dysregulation to be the primary driver of metabolic abnormalities. However, thyroid dysfunction could potentially amplify the effects of immune factors, or abnormal thyroid function itself may serve as an indicator of immune factor severity. This is an important aspect worth further discussion, which could lead to a more comprehensive understanding of the relationship between thyroid function, immune factors and metabolic disturbances.

6 Conclusion

This study is the first to explore the relationship between metabolic-related indicators and HT in a non-diabetic population. We found a significant non-linear U-shaped relationship between UA levels and the risk of HT. Specifically, lower risk of HT was significantly associated with UA levels within the range of 359-540 μmol/L. Our results suggest that maintaining UA levels within the reference range may help reduce the incidence of HT, potentially linked to mechanisms involving oxidative stress and gut microbiota regulation.

Despite limitations such as the relatively small sample size and the specificity of the regional and ethnic population, these findings provide important clinical insights for the prevention and management of HT. They emphasize the potential role of SUA in endocrine diseases, warranting further research and validation.

Data availability statement

The original contributions presented in the study are included in the article/supplementary material. Further inquiries can be directed to the corresponding authors.

Ethics statement

The studies involving humans were approved by the Ethics Committee of Guangdong Provincial Hospital of Chinese Medicine (Approval No. ZE2024-411). The studies were conducted in accordance with the local legislation and institutional requirements. Written informed consent for participation was not required from the participants or the participants' legal guardians/next of kin in accordance with the national legislation and institutional requirements.

Author contributions

MY: Data curation, Writing – original draft, Writing – review & editing. WS: Data curation, Writing – original draft, Writing – review & editing. PG: Data curation, Writing – original draft, Writing – review & editing. YX: Data curation, Writing – original draft, Writing – review & editing. KZ: Data curation, Writing – original draft. XL: Writing – review & editing. HW: Writing – review & editing.

Funding

The author(s) declare that financial support was received for the research, authorship, and/or publication of this article. This study

was supported by grants from the Guangdong Famous Chinese Medicine Workshop: Shusen Li Workshop Foundation Program, the Guangdong Famous Chinese Medicine Workshop: Zhizheng Lu Workshop Foundation Program (E43710), State Key Laboratory of Dampness Syndrome of Chinese Medicine (SZ2021ZZ3203) and Lin Dingkun Guangdong Famous Traditional Chinese Medicine Inheritance Workshop (0103030912).

Conflict of interest

The authors declare that the research was conducted in the absence of any commercial or financial relationships that could be construed as a potential conflict of interest.

Generative AI statement

The author(s) declare that no Generative AI was used in the creation of this manuscript.

Publisher's note

All claims expressed in this article are solely those of the authors and do not necessarily represent those of their affiliated organizations, or those of the publisher, the editors and the reviewers. Any product that may be evaluated in this article, or claim that may be made by its manufacturer, is not guaranteed or endorsed by the publisher.

References

1. Hu X, Chen Y, Shen Y, Tian R, Sheng Y, Que H. Global prevalence and epidemiological trends of Hashimoto's thyroiditis in adults: A systematic review and meta-analysis. *Front Public Health*. (2022) 10. doi: 10.3389/fpubh.2022.1020709

2. Antonelli A, Ferrari SM, Corrado A, Di Domenicantonio A, Fallahi P. Autoimmune thyroid disorders. *Autoimmun Rev*. (2015) 14:174–80. doi: 10.1016/j.autrev.2014.10.016

3. Caturegli P, De Remigis A, Rose NR. Hashimoto thyroiditis: Clinical and diagnostic criteria. *Autoimmun Rev*. (2014) 13:391–7. doi: 10.1016/j.autrev.2014.01.007

4. Ralli M, Angeletti D, Fiore M, D'Aguanno V, Lambiase A, Artico M, et al. Hashimoto's thyroiditis: An update on pathogenic mechanisms, diagnostic protocols, therapeutic strategies, and potential Malignant transformation. *Autoimmun Rev*. (2020) 19. doi: 10.1016/j.autrev.2020.102649

5. Iskra I, Tomaš MI, Crnčić TB, Kukić E, Hadžisejdić I, Avirović M, et al. Two lymphoma histotypes and papillary thyroid carcinoma coexisting on Hashimoto ground: a case report and review of the literature. *Diagn Pathol*. (2024) 19. doi: 10.1186/s13000-024-01472-7

6. Klubo-Gwiezdzinska J, Wartofsky L. Hashimoto thyroiditis: an evidence-based guide: etiology, diagnosis and treatment. *Polish Arch Internal Med*. (2022) 132(3). doi: 10.20452/pamw.16222

7. Waliszewska-Prosół M, Ejma M. Hashimoto encephalopathy—Still more questions than answers. *Cells*. (2022) 11. doi: 10.3390/cells11182873

8. Payer J, Petrovic T, Lisy L, Langer P. Hashimoto encephalopathy: A rare intricate syndrome. *Int J Endocrinol Metab*. (2012) 10:506–14. doi: 10.5812/ijem.4174

9. Ruggeri RM, Vicchio TM, Cristani M, Certo R, Caccamo D, Alibrandi A, et al. Oxidative stress and advanced glycation end products in hashimoto's thyroiditis. *Thyroid*. (2016) 26:504–11. doi: 10.1089/thy.2015.0592

10. Burek CL, Rose NR. Autoimmune thyroiditis and ROS. *Autoimmun Rev*. (2008) 7:530–7. doi: 10.1016/j.autrev.2008.04.006

11. Zheng T, Xu C, Mao C, Mou X, Wu F, Wang X, et al. Increased interleukin-23 in hashimoto's thyroiditis disease induces autophagy suppression and reactive oxygen species accumulation. *Front Immunol*. (2018) 9. doi: 10.3389/fimmu.2018.00096

12. Rodríguez-Muñoz A, Vitales-Noyola M, Ramos-Levi A, Serrano-Somavilla A, González-Amaro R, Marazuela M. Levels of regulatory T cells CD69+NKG2D+IL-10+ are increased in patients with autoimmune thyroid disorders. *Endocrine*. (2015) 51:478–89. doi: 10.1007/s12020-015-0662-2

13. Duvnjak L, Blaslov K, Perković MN, Ćuća JK. Dipeptidyl peptidase-4 activity might be a link between tumour necrosis factor alpha and insulin resistance in type 1 diabetes. *Endocrine*. (2016) 53:453–8. doi: 10.1007/s12020-016-0899-4

14. Yetkin DO, Dogantekin B. The lipid parameters and lipoprotein(a) excess in hashimoto thyroiditis. *Int J Endocrinol*. (2015) 2015:1–6. doi: 10.1155/2015/952729

15. Liu J, Duan Y, Fu J, Wang G. Association between thyroid hormones, thyroid antibodies, and cardiometabolic factors in non-obese individuals with normal thyroid function. *Front Endocrinol*. (2018) 9. doi: 10.3389/fendo.2018.00130

16. Wu Y, Shi X, Tang X, Li Y, Tong N, Wang G, et al. The correlation between metabolic disorders and tpoab/tgab: A cross-sectional population-based study. *Endocrine Pract*. (2020) 26:869–82. doi: 10.4158/EP-2020-0008

17. Tamer GMM, Tamer I, Mesci B, Kilic D, Arik S. Effects of thyroid autoimmunity on abdominal obesity and hyperlipidaemia. *Endokrynol Pol*. (2011) 62:421–8.

18. Hu Y, Zheng J, Ye X, Song Y, Wu X. Association between elevated thyroid peroxidase antibody and abdominal fat distribution in patients with type 2 diabetes mellitus. *Diabetes Metab Syndr Obes*. (2022) 15:863–71. doi: 10.2147/DMSO.S345507

19. Lu Y, Wang J, An Y, Liu J, Wang Y, Wang G, et al. Impaired sensitivity to thyroid hormones is associated with hyperuricemia in a Chinese euthyroid population. *Front Endocrinol (Lausanne)*. (2023) 14:1132543. doi: 10.3389/fendo.2023.1132543

20. Wu Z, Jiang Y, Li P, Wang Y, Zhang H, Li Z, et al. Association of impaired sensitivity to thyroid hormones with hyperuricemia through obesity in the euthyroid population. *J Trans Med*. (2023) 21:436. doi: 10.1186/s12967-023-04276-3

21. Mikulska AA, Karaźniewicz-Łada M, Filipowicz D, Ruchała M, Główka FK. Metabolic characteristics of hashimoto's thyroiditis patients and the role of microelements and diet in the disease management—An overview. *Int J Mol Sci*. (2022) 23. doi: 10.3390/ijms23126580

22. Rajarajeswari R, Sumathi S, Asmathulla S, Ar S, Girija S, Maithilikarpagaselvi N. Association of anti-TPO antibodies with insulin resistance and dyslipidemia in hashimoto's thyroiditis: an observational study on South Indian population. *Int J Curr Res Rev*. (2021) 13:88–94. doi: 10.31782/IJCRR.2021.13933

23. Montesinos MDM, Pellizas CG. Thyroid hormone action on innate immunity. *Front Endocrinol (Lausanne)*. (2019) 10:350. doi: 10.3389/fendo.2019.00350

24. Tomkin GH, Owens D. Diabetes and dyslipidemia: characterizing lipoprotein metabolism. *Diabetes Metab syndrome obesity: Targets Ther*. (2017) 10:333–43. doi: 10.2147/DMSO.S115855

25. Xiong Q, Liu J, Xu Y. Effects of uric acid on diabetes mellitus and its chronic complications. *Int J Endocrinol*. (2019) 2019:9691345. doi: 10.1155/2019/9691345

26. Yan M, Wu H, Zhang K, Gong P, Wang Y, Wei H. Analysis of the correlation between Hashimoto's thyroiditis and food intolerance. *Front Nutr*. (2024) 11:1452371. doi: 10.3389/fnut.2024.1452371

27. Yanai H, Adachi H, Hakoshima M, Katsuyama H. Molecular biological and clinical understanding of the pathophysiology and treatments of hyperuricemia and its association with metabolic syndrome, cardiovascular diseases and chronic kidney disease. *Int J Mol Sci*. (2021) 22. doi: 10.3390/ijms22179221

28. Glantzounis GK, Tsimoyiannis EC, Kappas AM, Galaris DA. Uric acid and oxidative stress. *Curr Pharm design*. (2005) 11:4145–51. doi: 10.2174/138161205774913255

29. Dalbeth N, Gosling AL, Gaffo A, Abhishek A. Gout. *Lancet (London England)*. (2021) 397:1843–55. doi: 10.1016/S0140-6736(21)00569-9

30. Wang Z, Zhang Y, Huang S, Liao Z, Huang M, Lei W, et al. UA influences the progression of breast cancer via the AhR/p27(Kip1)/cyclin E pathway. *FASEB J*. (2024) 38:e70058. doi: 10.1096/fj.202400938R

31. Zhang S, Li D, Fan M, Yuan J, Xie C, Yuan H, et al. Mechanism of reactive oxygen species-guided immune responses in gouty arthritis and potential therapeutic targets. *Biomolecules*. (2024) 14. doi: 10.3390/biom14080978

32. Chen Z, Su Z, Pang W, Huang Y, Lin J, Ding Z, et al. Antioxidant status of serum bilirubin and uric acid in patients with polymyositis and dermatomyositis. *Int J Neurosci*. (2017) 127:617–23. doi: 10.1080/00207454.2016.1220380

33. Elhinnawi MA, Boushra MI, Hussien DM, Hussein FH, Abdelmawgood IA. Mitochondria's role in the maintenance of cancer stem cells in hepatocellular carcinoma. *Stem Cell Rev Rep*. (2024). doi: 10.1007/s12015-024-10797-1

34. Kunst C, Schmid S, Michalski M, Tümen D, Buttenschön J, Müller M, et al. The influence of gut microbiota on oxidative stress and the immune system. *Biomedicines*. (2023) 11(5):1388. doi: 10.3390/biomedicines11051388

35. Ates I, Arikan MF, Altay M, Yilmaz FM, Yilmaz N, Berker D, et al. The effect of oxidative stress on the progression of Hashimoto's thyroiditis. *Arch Physiol Biochem*. (2018) 124:351–6. doi: 10.1080/13813455.2017.1408660

36. Ates I, Yilmaz FM, Altay M, Yilmaz N, Berker D, Güler S. The relationship between oxidative stress and autoimmunity in Hashimoto's thyroiditis. *Eur J Endocrinol*. (2015) 173:791–9. doi: 10.1530/EJE-15-0617

37. Virili C, Fallahi P, Antonelli A, Benvenga S, Centanni M. Gut microbiota and Hashimoto's thyroiditis. *Rev endocrine Metab Disord*. (2018) 19:293–300. doi: 10.1007/s11154-018-9467-y

38. Knezevic J, Starchl C, Tmava Berisha A, Amrein K. Thyroid-gut-axis: how does the microbiota influence thyroid function? *Nutrients*. (2020) 12. doi: 10.3390/nu12061769

39. Lv Q, Xu D, Zhang X, Yang X, Zhao P, Cui X, et al. Association of hyperuricemia with immune disorders and intestinal barrier dysfunction. *Front Physiol*. (2020) 11:524236. doi: 10.3389/fphys.2020

40. Hosomi A, Nakanishi T, Fujita T, Tamai I. Extra-renal elimination of uric acid via intestinal efflux transporter BCRP/ABCG2. *PLoS One*. (2012) 7:e30456. doi: 10.1371/journal.pone.0030456

41. Wang H, Zheng Y, Yang M, Wang L, Xu Y, You S, et al. Gut microecology: effective targets for natural products to modulate uric acid metabolism. *Front Pharmacol*. (2024) 15:1446776. doi: 10.3389/fphar.2024.1446776

42. Li T, Zhang T, Gao H, Liu R, Gu M, Yang Y, et al. Tempol ameliorates polycystic ovary syndrome through attenuating intestinal oxidative stress and modulating of gut microbiota composition-serum metabolites interaction. *Redox Biol*. (2021) 41:101886. doi: 10.1016/j.redox.2021.101886

43. Dos Santos M, Veronese FV, Moresco RN. Uric acid and kidney damage in systemic lupus erythematosus. *Clinica chimica acta; Int J Clin Chem*. (2020) 508:197–205. doi: 10.1016/j.cca.2020.05.034

44. Liu T, Zuo R, Song J, Wang J, Zhu Z, Sun L, et al. Association of serum uric acid level with risk of abdominal aortic calcification: A large cross-sectional study. *J Inflammation Res*. (2023) 16:1825–36. doi: 10.2147/JIR.S404668

frontiers | Frontiers in Endocrinology

TYPE Original Research
PUBLISHED 13 February 2025
DOI 10.3389/fendo.2025.1522928

OPEN ACCESS

EDITED BY
Prem Prakash Kushwaha,
Case Western Reserve University,
United States

REVIEWED BY
Suman Bharti,
Washington University in St. Louis,
United States
Saurabh Mishra,
Cleveland Clinic, United States

*CORRESPONDENCE
Guangyao Song
sguangyao2@163.com

RECEIVED 05 November 2024
ACCEPTED 20 January 2025
PUBLISHED 13 February 2025

CITATION
Tian P, Zeng S, Hou Y, Liu D, Lu Y and Song G (2025) Postprandial triglyceride levels affecting postprandial thyroid stimulating hormone levels may be responsible for the increased postprandial thyroid stimulating hormone levels in people with reduced lipid tolerance.
Front. Endocrinol. 16:1522928.
doi: 10.3389/fendo.2025.1522928

Postprandial triglyceride levels affecting postprandial thyroid stimulating hormone levels may be responsible for the increased postprandial thyroid stimulating hormone levels in people with reduced lipid tolerance

Peipei Tian[1,2,3], Shaojing Zeng[4], Yilin Hou[1,2], Dandan Liu[1,2,5], Yamin Lu[6] and Guangyao Song[1,2]*

[1]Department of Internal Medicine, Hebei Medical University, Shijiazhuang, Hebei, China, [2]Hebei Key Laboratory of Metabolic Diseases, Hebei General Hospital, Shijiazhuang, Hebei, China, [3]Department of Endocrinology and Metabolism, Cangzhou Central Hospital, Cangzhou, Hebei, China, [4]Department of Endocrinology, Hebei General Hospital, Shijiazhuang, Hebei, China, [5]Department of Endocrinology, Baoding First Central Hospital, Baoding, Hebei, China, [6]Department of Nuclear Medicine, Hebei General Hospital, Shijiazhuang, Hebei, China

Objective: In this study, we aimed to explore the relationship between postprandial triglyceride (TG) and postprandial thyroid stimulating hormone (TSH) levels and compare the postprandial TSH levels in participants with normal lipid tolerance and reduced lipid tolerance.

Methods: A total of 81 eligible participants were enrolled and given a high-fat meal of 1500 kcal, and blood samples were collected at 2, 4, 6, and 8 hours. Fasting blood glucose, total cholesterol, high-density lipoprotein cholesterol, low-density lipoprotein cholesterol, and fasting and postprandial TG, triiodothyronine (T3), tetraiodothyronine (T4), and TSH levels were tested. Based on the postprandial serum TG level, participants were divided into the normal lipid tolerance group (NFT) and the decreased lipid tolerance group (IFT).

Results: Postprandial TG levels increased in both the NFT and IFT groups and then decreased over time. A higher and delayed peak of postprandial TG was observed in the IFT group, and there were statistically significant differences in TG levels at each time point in both groups. The area under the curve (TGAUC) was an independent influencing factor for the area under the curve (TSHAUC) of TSH. Postprandial TSH levels in both groups reached a trough at 2 h and peaked at 6 h, with a higher peak in the IFT group. Except for 2 h, TSH levels were significantly different at all other time points. There was no statistically significant difference in T3 or T4 levels between the two groups, with opposite trends for TSH.

Conclusion: After a high-fat meal is consumed, the postprandial TSH level is influenced by the postprandial TG level, which may be the reason for the decreased thyroid function in the population with reduced lipid tolerance.

Clinical Trial Registration: http://www.chictr.org.cn/index.aspx, identifier ChiCTR1800019514.

KEYWORDS

triglyceride, thyroid stimulating hormone, high-fat meal, oral fat tolerance test, normal fat tolerance, impaired fat tolerance

Introduction

Hypothyroidism is a common pathological state associated with thyroid hormone deficiency and includes subclinical hypothyroidism (SCH) and overt hypothyroidism. SCH is defined as elevated serum thyroid-stimulating hormone (TSH) and free thyroxine (FT4) levels within the lower limit of the normal range. Numerous studies have indicated that SCH is an independent risk factor for cardiovascular diseases (1–6). Some studies have indicated (7–9) that thyroid hormones are associated with various metabolic abnormalities, even at the lower end of the normal range, suggesting that it is crucial to identify the potential factors affecting thyroid function early. Although autoimmune diseases are commonly recognized causes of thyroid dysfunction, the risk factors that trigger hypothyroidism are not well understood. Therefore, further research on the etiology of SCH is warranted. Jankovic et al. (10) observed that obese patients with hypertriglyceridemia exhibit elevated TSH levels, which significantly decrease after serum triglyceride (TG) levels decrease following bariatric surgery. A previous study (11) showed a positive correlation between hyperlipidemia and the risk of SCH. In a prospective study, an exploratory analysis of the relationship between the components of metabolic syndrome and decreased thyroid function in participants with and without metabolic syndrome showed that metabolic syndrome increased the risk of developing SCH. An analysis of the individual components of metabolic syndrome revealed that high TG levels were associated with an increased risk of SCH (12). These studies suggest that thyroid function in patients with hypertriglyceridemia may be adversely affected by lipotoxicity. In populations with abnormal lipid metabolism, lipids have long-term effects, and exploring the relationship between abnormal lipid metabolism and the risk of developing SCH is crucial for the prevention and effective management of SCH. In recent years, many studies have shown that postprandial TG levels are closely associated with type 2 diabetes and cardiovascular disease (13–15). An increasing number of researchers are focusing on the importance of postprandial TG. However, previous studies have been based on the effect of fasting TG levels on thyroid function. Research has also indicated that, in normal individuals, TSH levels decrease 2 hours after a meal (16–18). It is unclear whether postprandial serum TG levels are related to postprandial serum TSH levels and whether postprandial TSH levels differ in different lipid tolerance populations. Therefore, this study aimed to observe the relationship between postprandial TG levels and postprandial TSH levels by performing a lipid tolerance test in volunteers with normal fasting TG and thyroid hormone levels. This study also aimed to compare postprandial TSH levels between participants with normal lipid tolerance and those with reduced lipid tolerance.

Abbreviations: TG, triglyceride; TSH, thyroid-stimulating hormone; TC, total cholesterol; HDL-C high density lipoprotein cholesterol; LDL-C, low density lipoprotein cholesterol; T3, triiodothyronine; T4, thyroxine; NFT, normal fat tolerance; IFT, impaired fat tolerance; OFTT, oral fat tolerance test; BMI, body mass index; SBP, systolic blood pressure; DBP, diastolic blood pressure; FBG, fasting blood glucose; 4Htg, 4-hour postprandial triglycerides; TGAUC, triglyceride area under the curve; TSHAUC, thyroid-stimulating hormone area under the curve; T3AUC, triiodothyronine area under the curve; T4AUC, thyroxine area under the curve.

Materials and methods

Study sample

This study included volunteers aged 25–70 years from the endocrinology outpatient department of Hebei General Hospital from May 2018 to December 2019. This study was approved by the Ethics Committee of Hebei General Hospital (Approval No.: 2018 No. 2, Date: February 26, 2018) and registered with the Chinese Clinical Trial Registration Center (Registration No.: ChiCTR1800019514). All volunteers signed informed consent forms and completed questionnaires as required.

Exclusion criteria

Vegetarians; individuals with hyperthyroidism and hypothyroidism, diabetes, heart disease, kidney disease, malignant tumours, acute or chronic blood diseases, and infectious diseases; those with a family history of endocrine-related diseases, such as familial hypercholesterolaemia; individuals currently taking

medications that affect glucose and lipid metabolism or inflammation (fish oil, contraceptives, hormones, beta-blockers, diuretics, hypoglycaemic drugs, and lipid-lowering drugs); and those who had experienced stroke, pregnancy, mental disorders, surgery, trauma, or weight changes >3 kg within the past 3 months.

Oral fat tolerance test

All participants were instructed to follow a normal diet for 1 week and abstain from foods high in fat and protein (a list of foods to avoid was provided to all participants 1 week before the test). The participants began fasting at 22:00 on the day before the oral fat tolerance test (OFTT) and continued until 08:00. Participants were asked to consume a high-fat meal within 10 minutes, and during the 8-hour test period, they were allowed to drink water freely but were prohibited from smoking, eating, or engaging in strenuous exercise. Blood samples were collected before the high-fat meal and 2, 4, 6, and 8 hours after the meal. The high-fat meal had a total caloric content of 1500 kcal, with fat accounting for 60% (900 kcal) (monounsaturated fatty acids, polyunsaturated fatty acids: saturated fatty acids ratio = 2:2:1), carbohydrates for 20% (300 kcal), and protein for 20% (300 kcal). The production of the high-fat meal was completed by the nutrition department of our hospital.

Laboratory assays

Body mass index (BMI), systolic blood pressure(SBP), and diastolic blood pressure(DBP) of the participants were uniformly measured by the same physician. The serum levels of fasting blood glucose (FBG), TG, total cholesterol (TC), high-density lipoprotein cholesterol (HDL-C), low-density lipoprotein cholesterol (LDL-C), triiodothyronine (T3), thyroxine (T4), TSH and the postprandial serum levels of TG, T3, T4 after a high-fat meal were measured by a fully automated biochemical analyser.

Definitions of clinical conditions

Definition of normal fasting TG level: According to the "Guidelines for the Prevention and Treatment of Dyslipidemia in Chinese Adults (Revised 2016)", a fasting TG level<1.7 mmol/L is defined as normal fasting triglycerides (19).

Definition of postprandial TG elevation: Based on the consensus recommendations of the 2011 Greek Conference, a TG level >2.5 mmol/L 4 hours after a high-fat meal load was defined as postprandial hypertriglyceridaemia (20).

Grouping of subjects

Participants were divided into two groups: normal fat tolerance group (NFT): (Fasting TG <1.7 mmol/L, postprandial 4-hour TG ≤2.5 mmol/L) and impaired fat tolerance group (IFT): (Fasting TG <1.7 mmol/L, postprandial 4-hour TG >2.5 mmol/L).

Statistical analysis

Statistical analysis was performed using SPSS 25.0 software. Normally distributed continuous data were expressed as mean ± standard deviation, and non-normally distributed continuous data were expressed as median (interquartile range). The trapezoidal rule was used to calculate the AUC. The change in TG (△TG) was defined as the difference between the postprandial 4-hour value and the fasting value, and the change in TSH (△TSH) was defined as the difference between the postprandial 6-hour value and the fasting value. Two-way multilevel repeated-measures analysis of variance was used to analyse the data between groups. One-way repeated-measures analysis of variance was used to analyse the data within each group. Between-group comparisons were performed using the t-test for normally distributed data with equal variance; otherwise, non-parametric tests were used. Pearson's correlation analysis was used to assess the strength of the association between normally distributed variables; otherwise, Spearman's correlation analysis was used. Statistical significance was set at $P < 0.05$. Multiple linear regression analysis of the relationship between TGAUC and TSHAUC. We used PASS 2021 (v21.0.3) software to test the sample size and analysis a power.

Results

Comparison of baseline data between two groups

A total of 81 volunteers met the inclusion criteria. There were 45 participants (21 men and 24 women) in the NFT group and 36 (14 men and 22 women) in the IFT group. We used PASS 2021 (v21.0.3) software with a significance level of α =0.05. The sample size of the NFT group was 45, and that of the IFT group was 36 (4 h, 6 h, and 8 h). The minimum difference between the values was input into the software for calculation. The results showed that the sample size of this study achieved a power of 91.40%, which is higher than the required 90%. Therefore, our sample size was sufficient.

BMI, SBP, DBP, FBG, TG, 4-hour postprandial triglycerides (4hTG), HDL-C and TSH levels were significant differences in two groups ($P < 0.05$). We did not observe any significant differences in age, sex, TC, LDL-C, T3, T4, triiodothyronine area under the curve (T3AUC), and thyroxine area under the curve (T4AUC) between the two groups ($P > 0.05$) (Table 1).

Comparison of the Serum TG levels between two groups during the OFTT

Postprandial TG levels in the NFT and IFT groups increased over time. The NFT group reached peak TG levels at 2 hours postprandially, while the IFT group reached peak TG levels at 4 hours postprandially. There were statistically significant differences in TG levels between the two groups at all time points ($P < 0.001$). The TGAUC were also significantly different between the two groups ($P < 0.001$). Repeated-measures analysis of variance

10.3389/fendo.2025.1522928

TABLE 1 Comparison of baseline data between two groups.

	Total (n=81)	NFT (n=45)	IFT (n=36)
Age (year)	38.00 (27.50,53.50)	32.00 (28.00,51.00)	45.50 (27.00,56.25)
Male,n (%)	35 (43.2%)	21 (46.7%)	14 (38.9%)
BMI (kg/m^2)	25.89 ± 3.77	23.61 ± 3.24	25.88 ± 3.77 *
SBP (mmHg)	126.31 ± 15.98	116.36 ± 14.34	126.31 ± 15.98 *
DBP (mmHg)	77.17 ± 8.59	73.11 ± 8.83	77.17 ± 8.59 *
FBG (mmol/L)	5.58 ± 0.85	5.16 ± 0.51	5.58 ± 0.85 *
TC (mmol/L)	4.63 ± 0.97	4.46 ± 0.91	4.63 ± 0.97
TG (mmol/L)	1.30 ± 0.25	0.90 ± 0.25	1.30 ± 0.25 **
4hTG (mmol/L)	3.34 ± 0.66	1.59 ± 0.45	3.34 ± 0.66 **
HDL-C (mmol/L)	1.18 ± 0.27	1.32 ± 0.27	1.18 ± 0.27 *
LDL-C (mmol/L)	2.99 ± 0.66	2.74 ± 0.69	2.99 ± 0.66
T3 (nmol/L)	1.64 ± 0.30	1.61 ± 0.23	1.64 ± 0.30
T4 (nmol/L)	89.09 ± 20.20	91.35 ± 16.00	89.09 ± 20.20
TSH (uIU/mL)	1.82 (1.38,2.34)	1.52 (0.99,2.02)	1.82 (1.38,2.34) *

*P<0.05, compared with NFT group. **P<0.001, compared with NFT group.

showed that the changes in postprandial TG levels over time were statistically different between the two groups (P < 0.001), and there were statistically significant differences between the two groups (P < 0.05). △TG and TGAUC in the IFT group were higher than those in the NFT group, with statistical significance (P < 0.001). Individuals with reduced fat tolerance exhibit a delayed peak time and higher peak values of postprandial TG after consuming a high-fat meal than those with normal fat tolerance (Table 2, Figure 1A).

Comparison of the Serum TSH levels between two groups during the OFTT

Postprandial TSH levels in both NFT and IFT groups initially decreased, reaching a nadir at 2 hours, and then increased, peaking at 6 hours, with the IFT group showing a higher peak. Compared with the NFT group, except for the 2-hour mark, there were statistically significant differences in TSH levels at all other time points in the IFT group (P < 0.05). △TSH and TSHAUC in the IFT group were higher than those in the NFT group, with statistical significance (P < 0.001). Repeated-measures analysis of variance indicated that the changes in postprandial TSH levels over time were statistically different between the two groups (P < 0.05), and there were statistically significant differences between the two groups (P < 0.05) (Table 3, Figure 1B).

Comparison of the Serum T3 and T4 levels between two groups during the OFTT

Postprandial T3 and T4 levels in both NFT and IFT groups initially increased, peaked at 2 hours, and then decreased, reaching a nadir at 6 hours. Repeated-measures analysis of variance showed that the changes in postprandial T3 and T4 over time were statistically different all the two groups (P < 0.05); however, there were no statistically significant differences in the comparison between two groups. There were also no differences in triiodothyronine area under the curve (T3AUC) and thyroxine area under the curve (T4AUC) between the two groups (P > 0.05) (Tables 4, 5, Figures 1C, D).

Relationship between TGAUC and TSHAUC

There was a positive correlation between TGAUC and TSHAUC in both groups (r = 0.386, P < 0.05). Univariate linear regression analysis showed that TGAUC was a influencing factor for TSHAUC (P < 0.01). After adjustment for age, sex, BMI, SBP, DBP, FBG and TC, multiple linear regression analysis showed that TGAUC was an independent influencing factor for TSHAUC(P < 0.001).

TABLE 2 Comparison of the Serum TG levels between two groups during the OFTT.

TG (mmol/L)	0h	2h	4h	6h	8h	△TG	TGAUC
NFT	0.90 ± 0.25	1.64 ± 0.50	1.59 ± 0.45	1.53 ± 0.51	1.36 ± 0.57	0.74 ± 0.44	11.78 ± 2.86
IFT	1.30 ± 0.25 **	2.51 ± 0.56 **	3.34 ± 0.66 **	3.09 ± 1.18 **	2.43 ± 1.14 **	2.04 ± 0.66**	21.60 ± 4.59 **

*P<0.05, compared with the NFT group at different time points, **P<0.001, compared with the NFT group at different time points.

10.3389/fendo.2025.1522928

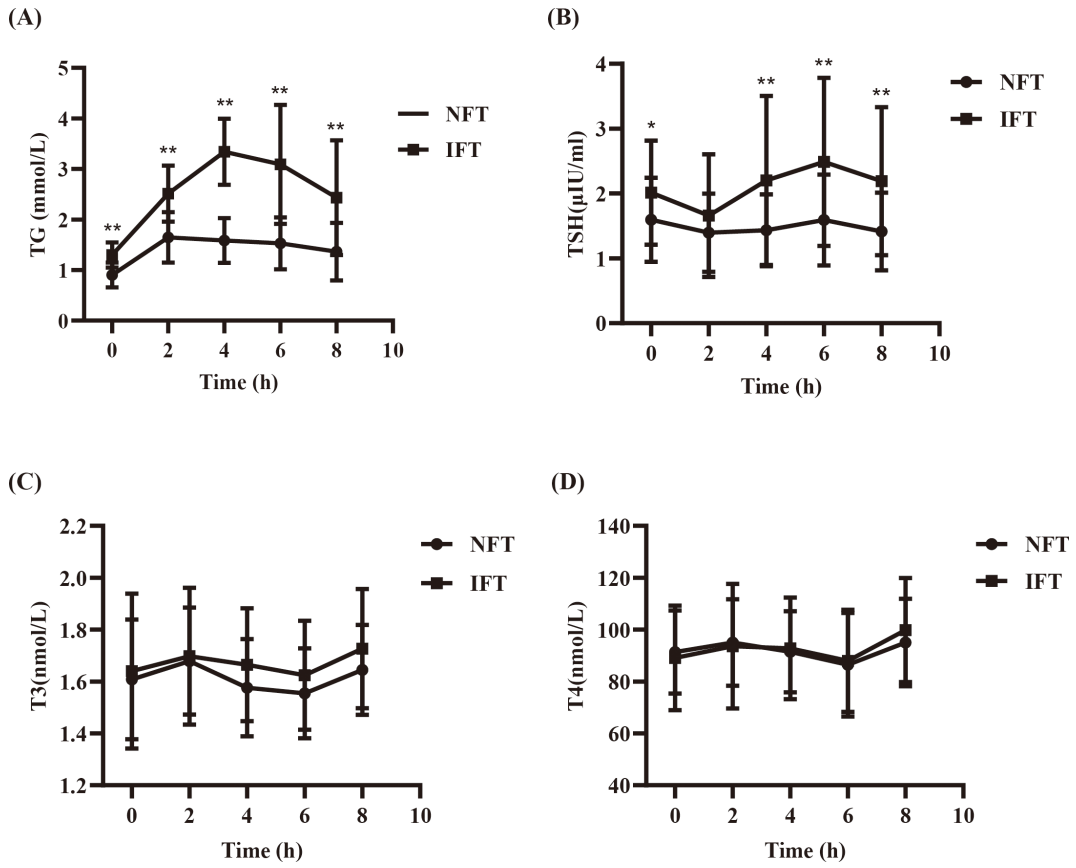

FIGURE 1
(A) Comparison of the Serum TG levels between two groups during the OFTT. **(B)** Comparison of the SerumTSH levels between two groups during the OFTT. **(C)** Comparison of the Serum T3 levels between two groups during the OFTT. **(D)** Comparison of the Serum T4 levels between two groups during the OFTT. *P<0.05, compared with the NFT group at different time points. **P<0.001, compared with the NFT group at different time points.

Discussion

With improvements in living standards, the prevalence of hyperlipidemia keeps increasing. Clinically, the lipid metabolism state of the human body is often determined by the fasting blood lipid level. However, during most of the day, the body is in the postprandial state, so the detection of fasting blood lipids does not reflect the overall picture of lipid metabolism. In recent years, many studies have shown that postprandial TG levels are closely associated with type 2 diabetes and cardiovascular disease (13–15). An increasing number of researchers are focused on the importance of postprandial TG. Based on the importance of postprandial TG, we used the oral fasting tolerance test to observe the changes in postprandial TG levels over time in participants with normal fasting TG levels after eating a high-fat meal to observe the overall lipid metabolism status.

TABLE 3 Comparison of the Serum TSH levels between two groups during the OFTT.

TSH (uIU/mL)	0h	2h	4h	6h	8h	△TSH	TSHAUC
NFT	1.52 (1.00,2.02)	1.31 (1.00,1.72)	1.39 (1.04,1.82)	1.36 (1.10,2.07)	1.37 (1.00,1.68)	-0.02 (-0.30,-0.21)	10.84 (8.36,14.39)
IFT	1.82 (1.38,2.34)*	1.36 (1.05,2.08)	1.85 (1.51,2.30)**	2.18 (1.72,2.93)**	1.94 (1.47,2.52)**	0.38 (0.12,0.85) **	16.25 (11.79,20.31)**

*P<0.05, compared with the NFT group at different time points, **P<0.001, compared with the NFT group at different time points.

TABLE 4 Comparison of the Serum T3 levels between two groups during the OFTT.

T3 (nmol/L)	0h	2h	4h	6h	8h
NFT	1.61 ± 0.23	1.68 ± 0.21	1.58 ± 0.19	1.55 ± 0.17	1.65 ± 0.17
IFT	1.64 ± 0.30	1.70 ± 0.26	1.67 ± 0.22	1.62 ± 0.21	1.73 ± 0.23

10.3389/fendo.2025.1522928

TABLE 5 Comparison of the SerumT4 levels between two groups during the OFTT.

T4 (nmol/L)	0h	2h	4h	6h	8h
NFT	91.35 ± 16.00	95.02 ± 16.64	91.47 ± 15.63	86.50 ± 20.01	95.07 ± 16.93
IFT	89.09 ± 20.20	93.59 ± 24.03	92.79 ± 19.55	87.99 ± 19.70	99.85 ± 20.10

The first important finding of our study was that TG levels were increased postprandially in participants in both groups. Compared with the NFT group, even though the fasting TG level in the ITF group was normal, the postprandial TG peak was higher and delayed. The △ TG and TG AUCs were also significantly higher than those of the NFT group. These findings suggest that a reduced lipid tolerance is hidden in individuals with normal fasting TG levels, which is an early stage of lipid metabolism disorder. Therefore, in our clinical work, attention should be paid to identifying patients with lipid metabolism disorders in the early stage, which has important guiding significance for the prevention and management of hyperlipidemia and its complications.

Previous clinical studies have shown that fasting TSH levels are also elevated in individuals with a high fasting TG-emia, compared with those with normal fasting TG levels (10–12). However, all previous studies were based on fasting TG levels, and no study has investigated the effect of postprandial TG on postprandial TSH levels. Based on the significance of postprandial TG, we observed the relationship between postprandial TG levels and postprandial TSH levels in individuals with normal fasting TG levels.

The second important finding of our study was that TGAUC was an independent influencing factor of TSHAUC and was positively correlated. There were statistically significant differences in BMI, SBP, DBP, and FBG between the two groups, and abnormalities in these indicators are often present in people with lipid metabolism disorders, which may be potential factors affecting TSH secretion. Therefore, after we further corrected for these potential confounders, we found that TGAUC remained an independent influencing factor for TSHAUC. This suggests that the postprandial TSH levels are influenced by the postprandial TG levels.

Some studies on organ damage caused by lipotoxicity have confirmed that excessive dietary fat intake triggers ectopic lipid deposition, leading to cellular function damage, also known as "lipotoxic damage." This interferes with the endocrine system and leads to the development of diseases, such as thyroid disease, especially hypothyroidism (21–23). Shao Shanshan et al. (24) found that when rats consumed a diet containing high-fat lard for some time, serum TSH level was significantly increased, serum T4 and FT4 levels were significantly decreased, and serum T4 level was negatively correlated with serum TG level. The team also found that the TG content in the thyroid was significantly increased, the morphology and ultrastructure of the thyroid were changed, and the protein expression level related to thyroid hormone synthesis decreased. These findings suggest that lipotoxicity may be involved in the development of thyroid dysfunction. MinHee Lee et al. (25) found that all three mice showed varying degrees of primary hypothyroidism after receiving a high-fat diet for some time. Lipid deposition and ultrastructural changes, including endoplasmic reticulum swelling and mitochondrial deformation of thyroid cells, were observed in thyroid tissue. These findings indicated that high-fat diet-induced lipotoxicity damages thyroid tissue and participates in the development of thyroid dysfunction. In a mechanistic study of high-fat diet-induced hypothyroidism in rats by Wang et al. (26), it was found that endoplasmic reticulum stress occurred in rat thyroid cells, which reduced the expression level of thyroglobulin, a key molecule of thyroid hormone synthesis. The research team also produced the same results using a palmitate-induced high-fat model of human primary thyrocytes. This evidence indicates that the high-fat diet-induced lipotoxicity can change the thyroid morphology, increase the endoplasmic reticulum stress, and promote a decline in thyroid function. These findings strongly support our results, and we further identified that the postprandial TG levels affect the postprandial TSH level based on previous studies. This study fills the gap in the effect of postprandial TG on postprandial TSH levels and further explores the effects of lipid metabolism disorders on thyroid function.

The third important finding of our study was that the postprandial TSH levels in both groups reached a trough at 2 h and peaked at 6 h, with the opposite trend of T3 and T4 levels and TSH. All the postprandial TSH levels reached a trough at 2 h, which is consistent with the findings of previous studies. TSH secretion primarily depends on two factors: thyrotropin-releasing hormone and somatostatin; the former stimulates TSH secretion, while the latter inhibits it (27). A study by Ehrenkranz et al. based on large-scale laboratory data showed significant diurnal rhythmic changes in circulating TSH levels. Despite the pulsatile secretion of TSH, the low amplitude of pulses and long half-life of TSH result in only minor fluctuations in blood TSH levels (28). One possible reason for the acute decline in TSH postprandially is the suppression of TSH secretion due to an increase in circulating somatostatin levels induced by food (29). After consuming a high-fat meal, the levels of lipoproteins rich in TG, such as chylomicrons and very-low-density lipoproteins, increase in the body; thyroid hormones can hydrolyze TG-rich lipoproteins by regulating the activity of lipoprotein lipase, thereby reducing circulating TG levels (30). Thyroid hormones also participate in the regulation of the rate-limiting enzyme CPT-1α in fatty acid β-oxidation by inducing the activation of Akt, thus reducing circulating levels of fatty acids and TG (31). Therefore, after a high-fat meal is consumed, the increase in TG-rich lipoproteins in the body prompts the thyroid to respond to the next step of fat metabolism, with the secretion of T3 and T4 increasing 2 h postprandially. This leads to a transient decrease in TSH levels through negative feedback regulation, which may be another important reason for the decrease in postprandial TSH levels. Surprisingly, we found that TSH levels peaked at 6 h after the meal, and T3 and T4 reached their lowest values. TGAUC is an

independent influencing factor of TSHAUC and is positively correlated, which indicates that the increase in postprandial TSH levels is influenced by increased postprandial TG levels. We speculate that after a high-fat meal, the circulating TG levels increase, and the demand for thyroid hormones involved in fat metabolism increases. Consequently, the consumption of T3 and T4 increases, causing their levels to reach their lowest values. This triggers negative feedback regulation, leading to increased TSH secretion, which explains the observed peak.

The fourth and most important finding of our study was that the postprandial peak TSH, △ TSH, and TSHAUC were significantly higher in the IFT group than in the NFT group. This indicates that participants in the IFT group had a trend towards hypothyroidism. Based on the conclusions of previous studies on the mechanism of lipotoxic damage to thyroid function and the conclusion of this study that postprandial TG levels affect postprandial TSH levels, it can be speculated that TG clearance is slowed down after high-fat meals are consumed. This continuous postprandial high TG state can aggravate the thyroid damage caused by lipotoxicity and lead to hypothyroidism. This suggests that we should not only focus on thyroid function in people with elevated fasting TG levels but also on thyroid function in people with early lipid metabolism disorders with normal fasting TG levels but elevated postprandial TG levels. The findings of our study provide an important clinical basis for the effective prevention and management of SCH.

With the improvement in living standards, the prevalence of hyperlipidemia is increasing. Previous studies have emphasized that people with elevated fasting TG are prone to hypothyroidism. Based on previous studies, we further found that in individuals with normal fasting TG levels, the hidden individuals with elevated postprandial TG levels are those with early lipid metabolism disorders, and their fasting and postprandial TSH levels are also higher than those of individuals with normal postprandial TG levels, who are prone to hypothyroidism. This prompts us to pay attention to identifying people with early lipid metabolism disorders and their thyroid function. This has important clinical implications for early detection and better management of lipid metabolism disorders and hypothyroidism.

Some limitations of this study need to be addressed. First, this study is our initial exploration of the effect of postprandial TG levels on postprandial thyroid function. Due to our limited experimental conditions and the sample size not being large enough, we will expand the sample size in the future to further validate this study's results. Second, there is no mechanistic study carried out in this study. The next step will consider animal and cell experiments for an in-depth analysis of the interaction relationship and the potential mechanisms.

In conclusion, our study shows that after a high-fat meal is consumed, postprandial TSH levels are influenced by postprandial TG levels. The decrease in lipid tolerance not only decreases TG clearance ability but also decreases thyroid function. This is the first study in which an oral fasting tolerance test was used to identify higher fat postprandial TG levels and higher postprandial TSH levels in people with early lipid metabolism disorders than in those with normal lipid metabolism. Our findings have important clinical implications for the effective prevention and management of lipid metabolism disorders and hypothyroidism.

Data availability statement

The original contributions presented in the study are included in the article/supplementary material. Further inquiries can be directed to the corresponding author.

Ethics statement

The studies involving humans were approved by Ethics Committee of Hebei General Hospital. The studies were conducted in accordance with the local legislation and institutional requirements. The participants provided their written informed consent to participate in this study.

Author contributions

PT: Writing – original draft, Formal analysis, Data curation, Methodology. SZ: Formal Analysis, Visualization, Writing – original draft. YH: Formal Analysis, Visualization, Writing – original draft. DL: Conceptualization, Supervision, Writing – original draft. YL: Methodology, Supervision, Writing – original draft. GS: Conceptualization, Methodology, Supervision, Project administration, Funding acquisition, Writing – review & editing.

Funding

The author(s) declare that financial support was received for the research, authorship, and/or publication of this article. This work was supported by the National Natural Science Foundation of China (82170878).

Acknowledgments

We sincerely thank the teachers of the Clinical Medical Research Centre of Hebei General Hospital for their help with the study.

Conflict of interest

The authors declare that the research was conducted in the absence of any commercial or financial relationships that could be construed as a potential conflict of interest.

Generative AI statement

The author(s) declare that no Generative AI was used in the creation of this manuscript.

Publisher's note

References

1. Razvi S, Weaver JU, Vanderpump MP, Pearce SH. The incidence of ischemic heart disease and mortality in people with subclinical hypothyroidism: reanalysis of the Whickham Survey cohort. *J Clin Endocrinol Metab*. (2010) 95:1734–40. doi: 10.1210/jc.2009-1749

2. Rodondi N, den Elzen WP, Bauer DC, Cappola AR, Razvi S, Walsh JP, et al. Subclinical hypothyroidism and the risk of coronary heart disease and mortality. *Jama*. (2010) 304:1365–74. doi: 10.1001/jama.2010.1361

3. Gencer B, Djousse L, Al-Ramady OT, Cook NR, Manson JE, Albert CM. Effect of long-term marine ω-3 fatty acids supplementation on the risk of atrial fibrillation in randomized controlled trials of cardiovascular outcomes: A systematic review and meta-analysis. *Circulation*. (2021) 144:1981–90. doi: 10.1161/CIRCULATIONAHA.121.055654

4. Inoue K, Ritz B, Brent GA, Ebrahimi R, Rhee CM, Leung AM. Association of subclinical hypothyroidism and cardiovascular disease with mortality. *JAMA Netw Open*. (2020) 3:e1920745. doi: 10.1001/jamanetworkopen.2019.20745

5. Sato Y, Yoshihisa A, Kimishima Y, Kiko T, Watanabe S, Kanno Y, et al. Subclinical hypothyroidism is associated with adverse prognosis in heart failure patients. *Can J Cardiol*. (2018) 34:80–7. doi: 10.1016/j.cjca.2017.10.021

6. Rhee CM, Curhan GC, Alexander EK, Bhan I, Brunelli SM. Subclinical hypothyroidism and survival: the effects of heart failure and race. *J Clin Endocrinol Metab*. (2013) 98:2326–36. doi: 10.1210/jc.2013-1039

7. Mehran L, Amouzegar A, Azizi F. Thyroid disease and the metabolic syndrome. *Curr Opin Endocrinol Diabetes Obes*. (2019) 26:256–65. doi: 10.1097/MED.0000000000000500

8. Laurberg P, Knudsen N, Andersen S, Carle A, Pedersen IB, Karmisholt J. Thyroid function and obesity. *Eur Thyroid J*. (2012) 1:159–67. doi: 10.1159/000342994

9. Kota SK, Meher LK, Krishna S, Modi K. Hypothyroidism in metabolic syndrome. *Indian J Endocrinol Metab*. (2012) 16:S332–33. doi: 10.4103/2230-8210.104079

10. Jankovic D, Wolf P, Anderwald CH, Winhofer Y, Promintzer-Schifferl M, Hofer A, et al. Prevalence of endocrine disorders in morbidly obese patients and the effects of bariatric surgery on endocrine and metabolic parameters. *Obes Surg*. (2012) 22:62–9. doi: 10.1007/s11695-011-0545-4

11. Zhao M, Tang X, Yang T, Zhang B, Guan Q, Shao S, et al. Lipotoxicity, a potential risk factor for the increasing prevalence of subclinical hypothyroidism? *J Clin Endocrinol Metab*. (2015) 100:1887–94. doi: 10.1210/jc.2014-3987

12. Chang CH, Yeh YC, Caffrey JL, Shih SR, Chuang LM, Tu YK. Metabolic syndrome is associated with an increased incidence of subclinical hypothyroidism - A Cohort Study. *Sci Rep*. (2017) 7:6754. doi: 10.1038/s41598-017-07004-2

13. Nordestgaard BG, Hilsted L, Stender S. Plasma lipids in non-fasting patients and signal values of laboratory results. *Ugeskr Laeger*. (2009) 171:1093. doi: 10.1016/j.jacc.2017.08.006

14. Miller M, Stone NJ, Ballantyne C, Bittner V, Criqui MH, Ginsberg HN, et al. Triglycerides and cardiovascular disease: a scientific statement from the American Heart Association. *Circulation*. (2011) 123:2292–333. doi: 10.1161/CIR.0b013e3182160726

15. Wierzbicki A, Ahmad R, Banks L, Clark L, Duerden M, Grey E. *2023 exceptional surveillance of cardiovascular disease: risk assessment and reduction, including lipid modification (NICE guideline CG181)*. London: National Institute for Health and Care Excellence (NICE (2023).

16. Nair R, Mahadevan S, Muralidharan RS, Madhavan S. Does fasting or postprandial state affect thyroid function testing? *Indian J Endocrinol Metab*. (2014) 18:705–07. doi: 10.4103/2230-8210.139237

17. Kamat V, Hecht WL, Rubin RT. Influence of meal composition on the postprandial response of the pituitary-thyroid axis. *Eur J Endocrinol*. (1995) 133:75–9. doi: 10.1530/eje.0.1330075

18. Bajana W, Aranda E, Arredondo ME, Brennan-Bourdon LM, Campelo MD, Espinoza E, et al. Impact of an Andean breakfast on biochemistry and immunochemistry laboratory tests: an evaluation on behalf COLABIOCLI WG-PRE-LATAM. *Biochem Med (Zagreb)*. (2019) 29:20702. doi: 10.11613/BM.2019.020702

19. Zengwu W, Jing L, Jianjun L, Naqiong W, Guoping L, Zhenyue C, et al. Guidelines on blood lipid management in China (2023). *China Circ Magazine*. (2023) 38:237–71. doi: 10.3969/j.issn.1000-3614.2023.03.001

20. Kolovou GD, Mikhailidis DP, Kovar J, Lairon D, Nordestgaard BG, Ooi TC, et al. Assessment and clinical relevance of non-fasting and postprandial triglycerides: an expert panel statement. *Curr Vasc Pharmacol*. (2011) 9:258–70. doi: 10.2174/157016111795495549

21. Shimano H. Novel qualitative aspects of tissue fatty acids related to metabolic regulation: lessons from Elovl6 knockout. *Prog Lipid Res*. (2012) 51:267–71. doi: 10.1016/j.plipres.2011.12.004

22. Chokshi A, Drosatos K, Cheema FH, Ji R, Khawaja T, Yu S, et al. Ventricular assist device implantation corrects myocardial lipotoxicity, reverses insulin resistance, and normalizes cardiac metabolism in patients with advanced heart failure. *Circulation*. (2012) 125:2844–53. doi: 10.1161/CIRCULATIONAHA.111.060889

23. Oakes ND, Cooney GJ, Camilleri S, Chisholm DJ, Kraegen EW. Mechanisms of liver and muscle insulin resistance induced by chronic high-fat feeding. *Diabetes*. (1997) 46:1768–74. doi: 10.2337/diab.46.11.1768

24. Shao SS, Zhao YF, Song YF, Xu C, Yang JM, Xuan SM, et al. Dietary high-fat lard intake induces thyroid dysfunction and abnormal morphology in rats. *Acta Pharmacol Sin*. (2014) 35:1411–20. doi: 10.1038/aps.2014.82

25. Lee MH, Lee JU, Joung KH, Kim YK, Ryu MJ, Lee SE, et al. Thyroid dysfunction associated with follicular cell steatosis in obese male mice and humans. *Endocrinology*. (2015) 156:1181–93. doi: 10.1210/en.2014-1670

26. Zhang X, Shao S, Zhao L, Yang R, Zhao M, Fang L, et al. ER stress contributes to high-fat diet-induced decrease of thyroglobulin and hypothyroidism. *Am J Physiol Endocrinol Metab*. (2019) 316:E510–18. doi: 10.1152/ajpendo.00194.2018

27. Scobbo RR, VonDohlen TW, Hassan M, Islam S. Serum TSH variability in normal individuals: the influence of time of sample collection. *W V Med J*. (2004) 100:138–42. doi: 10.1002/9781119707677.ch4

28. Ehrenkranz J, Bach PR, Snow GL, Schneider A, Lee JL, Ilstrup S, et al. Circadian and circannual rhythms in thyroid hormones: determining the TSH and free T4 reference intervals based upon time of day, age, and sex. *Thyroid*. (2015) 25:954–61. doi: 10.1089/thy.2014.0589

29. Arosio M, Porretti S, Epaminonda P, Giavoli C, Gebbia C, Penati C, et al. Elevated circulating somatostatin levels in acromegaly. *J Endocrinol Invest*. (2003) 26:499–502. doi: 10.1007/BF03345210

30. Martinez-Triguero ML, Hernandez-Mijares A, Nguyen TT, Munoz ML, Pena H, Morillas C, et al. Effect of thyroid hormone replacement on lipoprotein(a), lipids, and apolipoproteins in subjects with hypothyroidism. *Mayo Clin Proc*. (1998) 73:837–41. doi: 10.4065/73.9.837

31. de Lange P, Senese R, Cioffi F, Moreno M, Lombardi A, Silvestri E, et al. Rapid activation by 3,5,3'-L-triiodothyronine of adenosine 5'-monophosphate-activated protein kinase/acetyl-coenzyme a carboxylase and akt/protein kinase B signaling pathways: relation to changes in fuel metabolism and myosin heavy-chain protein content in rat gastrocnemius muscle in *vivo*. *Endocrinology*. (2008) 149:6462–70. doi: 10.1210/en.2008-0202

frontiers | Frontiers in Endocrinology

TYPE Original Research
PUBLISHED 17 February 2025
DOI 10.3389/fendo.2025.1433106

OPEN ACCESS

EDITED BY
Matthias Blüher,
Leipzig University, Germany

REVIEWED BY
Robert Kiss,
McGill University, Canada
Marika Alborghetti,
Sapienza University of Rome, Italy

*CORRESPONDENCE
Ting Li
li.ting@xjtu.edu.cn
Yue Wu
wu.yue@xjtu.edu.cn
Zuyi Yuan
zuyiyuan@mail.xjtu.edu.cn

†These authors have contributed equally to this work

RECEIVED 07 June 2024
ACCEPTED 23 January 2025
PUBLISHED 17 February 2025

CITATION
Ding N, Hua R, Guo H, Xu Y, Yuan Z, Wu Y and Li T (2025) Effect of thyroid stimulating hormone on the prognosis of coronary heart disease.
Front. Endocrinol. 16:1433106.
doi: 10.3389/fendo.2025.1433106

Effect of thyroid stimulating hormone on the prognosis of coronary heart disease

Ning Ding[1,2,3†], Rui Hua[1,2,3†], Hanqing Guo[4†], Yu Xu[1†], Zuyi Yuan[1,2,3*], Yue Wu[1,2,3*] and Ting Li[1,2,3*]

[1]Department of Cardiovascular Medicine, The First Affiliated Hospital, Xi'an Jiaotong University, Xi'an, Shaanxi, China, [2]Key Laboratory of Molecular Cardiology, Xi'an Jiaotong University, Xi'an, Shaanxi, China, [3]Key Laboratory of Environment and Genes Related to Diseases, Ministry of Education, Xi'an, Shaanxi, China, [4]Department of Gastroenterology, Xi'an Central Hospital, Xi'an Jiaotong University, Xi'an, Shaanxi, China

Introduction: Clinical studies have shown that thyroid stimulating hormone (TSH) is associated with increased cardiovascular disease risk and mortality. Even within normal ranges, elevated TSH levels have an impact on the cardiovascular system and have been associated with cardiac dysfunction. The aim of our study was to evaluate the predictive value of admission fasting serum TSH levels in patients with coronary heart disease in relation to long-term major adverse cardiovascular events (MACE) and all-cause mortality.

Method: A total of 3515 patients with coronary heart disease who met the inclusion criteria were divided into four groups according to the quantile of TSH levels: Group 1 (TSH, 0.34-1.02 mIU/L, n=878); Group 2 (TSH, 1.03-1.71 mIU/L, n=886); Group 3 (TSH, 1.72-2.84 mIU/L, n=880); and Group 4 (TSH, 2.86-5.50 mIU/L, n=873). MACE and all-cause mortality were also compared. TSH concentrations associated with the risk of MACE, all-cause mortality were assessed using continuous scales (restricted quartic splines) and Cox proportional hazards regression models.

Results: A total of 3515 patients with coronary heart disease were eligible for analysis. At a median follow-up of 70 months, patients in group 2 had a lower incidence of MACE compared to the other three groups. All-cause mortality was lower in the 3rd group. Restricted quartic spline analysis also revealed that TSH concentrations were associated with heart failure risk.

Discussion: TSH levels have predictive value for adverse cardiovascular events and heart failure in patients with coronary heart disease.

KEYWORDS

thyroid stimulating hormone, coronary-heart-disease, major adverse cardiovascular events, mortality, prognosis

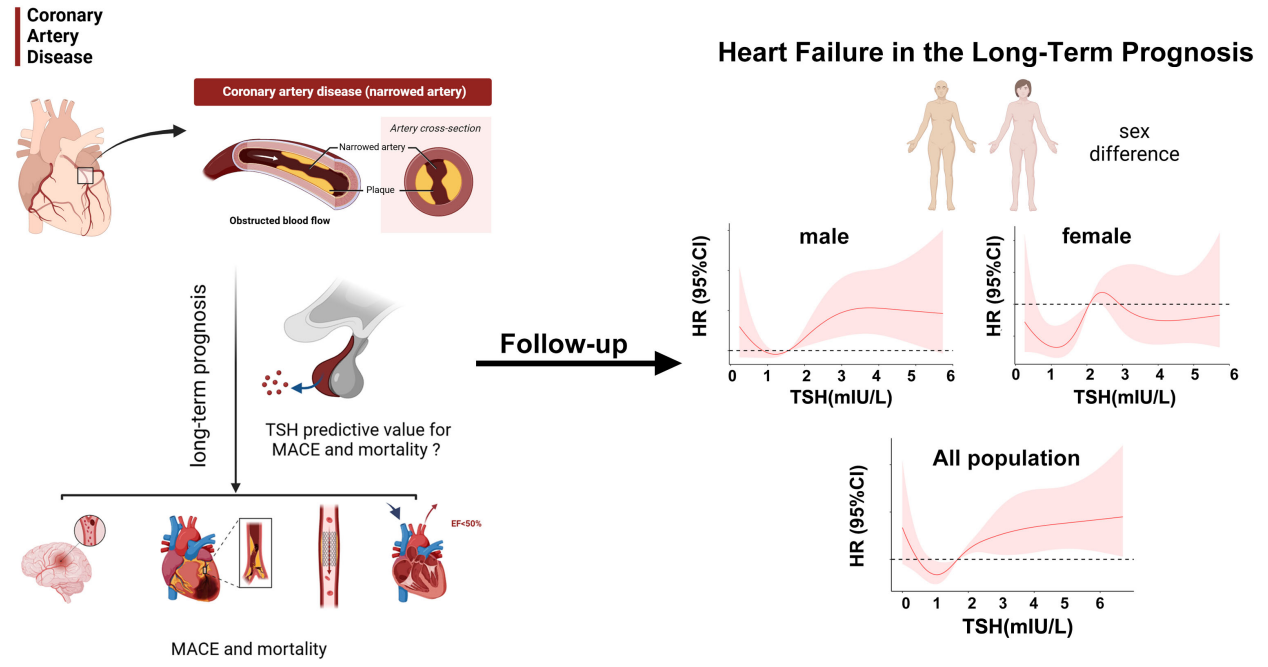

Introduction

Coronary heart disease (CHD), the main cause of ischemic heart disease, is one of the major cardiovascular diseases threatening the global human health. In 2019, heart disease was the top cause of disability-adjusted life year in the 50-year-and-older age group (1, 2). CHD progression is dynamic and unpredictable and can accidentally lead to major adverse cardiovascular events (MACE), such as myocardial infarction (MI), revascularization, heart failure, stroke and cardiovascular death. It is particularly concerning that patients remain at high risk of MACE despite revascularization and optimal secondary prevention according to the current guidelines (3–6). Thus, additional risk stratification models, including sensitive biomarkers and clinical indicators, are needed to identify high-risk patients for accurate secondary prevention of CHD.

The role of thyroid hormones in triggering and exacerbating potential cardiovascular disease has been increasingly recognized, and the use of thyroid function status as a new risk factor for cardiovascular events has attracted increasing attention (7–10). Previous studies have reported that minor fluctuations in thyroid hormone levels have a detrimental impact on the cardiovascular system (11–13). TSH levels are the most sensitive indicator of thyroid function. TSH levels are correlated with an increased risk of cardiovascular morbidity and mortality (14–18). Recent studies have also indicated that even TSH concentrations within normal range may have influence on cardiovascular outcomes. In particular, persistent hypothyroidism leads to increased endothelial dysfunction and decreased left ventricular function (19). In addition, TSH levels in the upper part of the reference range are related to a worse cardiovascular risk profile, including systolic and diastolic blood pressure, body mass index, coronary or carotid atherosclerosis, and a higher risk of mortality, MACE (HR, 1.06 per additional 1 mIU/L) and heart failure (9, 13, 20, 21). In animal models, cells in the vascular wall are directly influenced by thyroid hormones. A higher triiodothyronine concentration leads to the relaxation of vascular smooth muscle cells, upregulation of vascular resistance, dysfunction of endothelial cells, and increased cardiac contractility (22–24). These findings indicate that thyroid function status is a highly important risk factor for predicting cardiovascular events.

To date, it is unclear whether TSH levels within the reference range have predictive value for long-term prognosis in patients with chronic coronary heart disease. In this study, we aimed to investigate the association between normal TSH levels and the long-term incidence of MACE and all cause mortality in patients diagnosed with CHD.

Methods

Study population

From January 2013 to July 2020, 4016 consecutive coronary artery disease patients were admitted to the cardiology department of the First Affiliated Hospital of Xi'an Jiaotong University. Only patients with TSH levels within the reference range (0.34 to 5.50 mIU/L) were

eligible for analysis. Patients were divided into four groups according to the tertile of the TSH levels. The exclusion criteria consisted of 1) missing thyroid function test results (n = 59); 2) abnormal thyroid status and TSH above the reference range (n = 397); 3) prior or current thyroid disease (including prior history, surgery, or drug therapy for thyroid disease) (n = 132); and 4) receiving steroids and amiodarone before admission (n = 44).

The detailed demographic, clinical, drug, hematologic, and angiographic data were obtained from the medical records. The demographic variables included respondent age, sex, race/ethnicity, and education status. Smoking status; history of cancer, diabetes, hypertension, or dyslipidemia; and receipt of a statin prescription were self-reported. Weight and height were measured and used to calculate body mass index (BMI; calculated as weight in kilograms divided by height in meters squared).

Patients were treated according to standard clinical guidelines. Our study was conducted in accordance with the Declaration of Helsinki and was approved by the Ethics Committee of the First Affiliated Hospital of Xi'an Jiaotong University. Written informed consent was obtained from all study participants.

CHD was diagnosed on the basis of the presence of at least 50% coronary stenosis in at least one major coronary artery according to the CAG results assessed by at least two experienced interventional cardiologists.

Thyroid function

Blood samples were collected within 24 h of hospital admission. The thyroid function test included serum TSH, free triiodothyronine (FT3), and free thyroxine (FT4) levels. The normal ranges for TSH and FT4 were defined as 0.34 to 5.50 mIU/L and 0.6 to 1.6 ng/dL, respectively. 3515 Participants with serum TSH and FT4 concentrations within the normal range were considered to be euthyroid. Given the potential U-curve association between TSH and MACE, a total of 3515 patients with coronary heart disease who met the inclusion criteria were divided into four groups according to the quantile of TSH levels: Q1 (TSH, 0.34-1.02 mIU/L, n=878); Q2 (TSH, 1.03-1.71 mIU/L, n=886; Q3 (TSH, 1.72-2.84 mIU/L, n=880; and Q4 (TSH, 2.86-5.50 mIU/L, n=873) (Figure 1).

Outcome ascertainment

The primary endpoint was major cardiovascular adverse events (MACE), including all-cause death, myocardial infarction, revascularization, and heart failure. The secondary endpoints included all-cause death and stroke. A myocardial infarction event was defined as a nonfatal myocardial infarction or cardiac or muscle infarction-related death diagnosed by symptoms and signs; a revascularization event was defined as a secondary hospitalization or death after percutaneous or cutaneous coronary intervention or coronary artery bypass grafting; and a heart failure event was defined as any heart failure-related hospitalization or death. Stroke events were defined as hospitalization or death related to ischemic or nonischemic stroke. The time to event was calculated from the day of TSH measurement to the end of follow-up and the date of death and MACE.

Statistical analysis

The mean and standard deviation were calculated for continuous variables, and the proportion was calculated for categorical variables in each category according to the TSH concentration. Categorical variables are shown as frequencies and percentages. The Shapiro–Wilk normality test was performed to

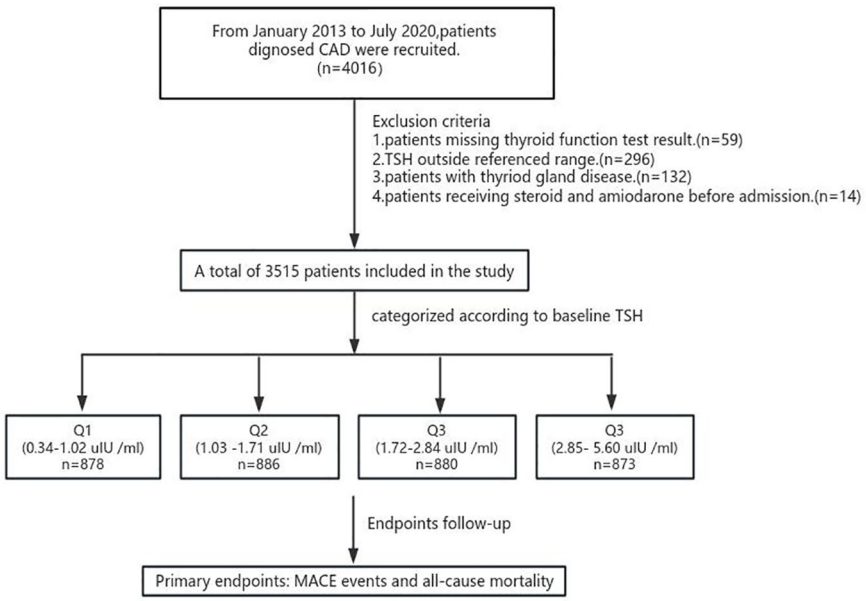

FIGURE 1
The study flowchart. CHD, coronary heart disease; TSH, thyroid-stimulating hormone(mIU/L=uIU/ml).

10.3389/fendo.2025.1433106

test the normality of the data. The means of continuous variables were compared using one-way analysis of the Kruskal–Wallis test. Analysis was performed using SPSS 26 statistical analysis software. ANOVA was used for comparisons between multiple groups, and the rank-sum test was used for comparisons of variables with uneven variance; categorical variables are expressed as frequencies (percentages), and the $\chi 2$ test or Fisher's exact test was used. Univariate and multivariate Cox regression models were used to analyze the risk of composite cardiovascular adverse events and all-cause death in patients with CHD with different thyroid function. The Kaplan-Meier method was used to construct patient survival curves and lines, and comparisons between groups were performed with the log-rank test. The associations between TSH concentration in the reference range and MACE events and all-cause mortality were evaluated on a continuous scale with restricted cubic spline curves based on Cox proportional hazards models with 4 nodes at the 5th, 35th, 65th and 95th percentiles of TSH (25); restricted cubic spline curves were rerestricted by sex stratification with 4 nodes at the 5th, 35th, 65th and 95th percentiles of TSH by the R package.

Results

Baseline data

A total of 3515 consecutive patients were enrolled and divided into four groups according to the quartile of TSH levels: Q1 (TSH, 0.34-1.02 mIU/L, n=878), Q2 (TSH, 1.03-1.71 mIU/L, n=886), Q3 (TSH, 1.72-2.84 mIU/L, n=880) and Q4 (TSH, 2.86-5.50 mIU/L, n=873)]. Age, sex ratio, current smoking status, hypertension proportion, systolic blood pressure, STEMI proportion, and thrombolysis proportion were significantly different among the patients in the four groups. There were no differences in BMI, history of diabetes, or history of any other diseases (Table 1).

Regarding laboratory tests, significant differences were found among the four groups in terms of triglyceride concentration, HGB, WBC, CK-MB, free thyroxine, CRP, and hs-cTnT. Except for the use of ACEIs, there was no significant difference in medication prescription among the four groups after hospitalization and discharge (Table 1).

TABLE 1 Comparison of baseline data among the four groups [patients (%)].

Characteristic	TSH quartile μmol/L				P value
	Q1 (<1.02)	Q2 (1.02≤ ≤1.71)	Q3 (1.71-2.84)	Q4 (≥2.84)	
N=	878	886	880	873	
Age at randomization, year	61.4 (10.7)	60.5 (10.4)	61.4 (9.8)	62.7 (9.9)	0.0012
Female,n (%)	173 (19.7)	184 (20.8)	259 (29.4)	325 (37.2)	<0.0001
Past medical history					
Current smoker,n (%)	398 (45.3)	374 (42.2)	356 (40.5)	423 (48.5)	0.0041
Hypertension, n (%)	463 (52.7)	507 (57.2)	513 (58.3)	550 (63.0)	0.0003
Diabetes mellitus, n (%)	242 (27.6)	226 (25.5)	250 (28.4)	216 (24.7)	0.264
BMI, median (IQR), kg/m2	24.3 (3.3)	24.39 (3.0)	24.43 (3.2)	24.29 (3.0)	0.7803
Previous stroke, n (%)	61 (6.9)	51 (5.8)	39 (4.4)	58 (6.6)	0.1115
Renal insufficiency	36 (4.1)	31 (3.5)	34 (3.9)	42 (4.8)	0.5585
Heart failure	45 (5.1)	36 (4.1)	40 (4.5)	43 (4.9)	0.7287
History of atrial fibrillation, n (%)	32 (3.6)	28 (3.1)	34 (3.9)	34 (3.9)	0.8331
PCI (%)	102 (11.6)	96 (10.1)	119 (13.5)	100 (11.5)	0.3333
CABG (%)	4 (0.46)	4 (0.45)	3 (0.34)	1 (0.11)	0.5779
Clinical feature					
Systolic blood pressure, mm Hg	128.1 (21.0)	130.7 (20.4)	130.9 (19.0)	134.6 (21.2)	<0.0001
Diastolic blood pressure, mm Hg	77.4 (13.1)	77.2 (11.4)	76.54 (11.3)	77.7 (11.4)	0.2853
Killip classification					
I (%)	601 (68.4)	493 (55.6)	474 (53.8)	446 (51.1)	<0.0001
II (%)	171 (19.5)	223 (25.1)	256 (29.1)	226 (25.9)	<0.0001
III (%)	16 (1.8)	20 (2.3)	28 (3.2)	32 (3.7)	<0.01
IV (%)	7 (0.8)	7 (0.8)	2 (0.2)	9 (1.0)	0.2256

(Continued)

10.3389/fendo.2025.1433106

TABLE 1 Continued

Characteristic	TSH quartile μmol/L				P value
	Q1 (<1.02)	Q2 (1.02≤ ≤1.71)	Q3 (1.71-2.84)	Q4 (≥2.84)	
N=	878	886	880	873	
Killip classification					
EF, % (SD)	52.98 (10.56)	51.93 (9.38)	52.91 (9.93)	52.35 (9.22)	0.6025
STEMI (%)	463 (52.7)	286 (32.3)	244 (27.7)	217 (24.9)	<0.0001
Thrombolysis (%)	133 (15.1)	82 (9.3)	85 (9.6)	80 (9.2)	<0.0001
Laboratory examination					
Fasting blood glucose, mmol/L (SD)	7.593 (3.4)	7.213 (3.4)	7.204 (3.5)	7.372 (3.8)	0.0691
Serum lipid					
Total cholesterol	3.916 (0.94)	3.804 (0.94)	3.815 (0.95)	3.958 (0.98)	0.3423
LDL cholesterol	2.313 (0.8)	2.216 (0.8)	2.221 (0.8)	2.332 (0.8)	0.6168
HDL cholesterol	0.9761 (0.2)	0.9656 (0.2)	0.9691 (0.2)	0.9909 (0.2)	0.185
Triglycerides	1.588 (1.1)	1.600 (1.0)	1.676 (1.1)	1.779 (1.3)	0.0002
HGB,g/L (SD)	138.6 (18.8)	139.9 (16.7)	137.8 (16.4)	135.4 (16.8)	<0.0001
WBC,10^9/L (SD)	8.547 (3.5)	7.156 (2.4)	6.964 (2.4)	6.849 (2.4)	<0.0001
CK-MB U/L (SD)	56.22 (98.4)	27.92 (53.4)	23.24 (42.7)	22.9 (51.9)	<0.0001
Scr umol/L (SD)	69.68 (31.0)	68.66 (42.3)	65.78 (26.0)	67 (20.2)	0.0195
Free thyroxine pmol/L, (SD)	4.406 (1.1)	4.606 (1.0)	4.6 (1.0)	4.608 (1.0)	0.0002
CRP,mg/L (SD)	4.99 (3.9)	3.31 (3.5)	3.17 (3.4)	3.17 (3.5)	<0.0001
hsTnT,ng/mL (SD)	0.8273 (1.72)	0.3443 (0.79)	0.3253 (0.83)	0.3444 (0.96)	<0.0001
Medication,n (%)					
Aspirin	792 (90.2)	820 (92.6)	806 (91.6)	793 (90.8)	0.3339
Plavix	615 (70.0)	637 (71.9)	621 (70.6)	611 (70.0)	0.8003
β-Blocker	650 (74.0)	666 (75.2)	651 (74.0)	654 (74.9)	0.9156
ACEI/ARB	643 (81.2)	710 (86.6)	699 (86.7)	689 (86.9)	0.0015
Statin	775 (88.3)	805 (90.9)	804 (91.4)	792 (90.1)	0.1235

Clinical outcome

The median follow-up time was 70 (interquartile range=60-82) months, and the follow-up rate was 96.7%. Clinical adverse events occurred in 910 (25.9%) patients. Interestingly, we found that both elevated and low TSH levels within the normal range were associated with increased mortality and incidence of MACE.

The lowest mortality, incidence of MACE and heart failure were evident in Q2 patients. Besides, elevated TSH levels were also found to be associated with a higher incidence of revascularization events. The cardiac mortality rate was significantly lower in Q3 than in the other three groups. There was no significant difference in the incidence of myocardial infarction or stroke among the four groups (Table 2).

K-M survival curve analysis revealed lower survival without composite adverse cardiovascular events in Q1, Q3, and Q4 patients than in Q2 patients. (log-rank test, Q2 *vs*. Q1: P.adj=0.0363, HR=0.815; Q2 *vs*. Q3: P.adj=0.034, HR=0.813; Q2 *vs*. Q4: P.adj<0.0001, HR=0.656) (Figure 2).

The TSH levels have independent predictive value for MACE in patients

Cox regression analysis of risk ratios for adverse cardiovascular events among patients in the four groups (Tables 3, 4): Cox multivariate regression models adjusted for other covariates (including age (<60, ≥60), male sex, hypertension, diabetes status, smoking status, and Killip class) showed that TSH in the upper part of the reference range was a significant predictor of the long-term occurrence of MACE. The highest TSH levels were associated with a greater risk of MACE than was the highest TSH levels (HR_{Q4} = 1.462, 95% CI=1.255-1.816, P=0.003). Moreover, patients with both a high TSH levels and a low TSH levels

10.3389/fendo.2025.1433106

TABLE 2 Comparison of clinical adverse events in the four groups during the 5-year follow-up.

Comparison of clinical adverse events in the four group after 5 years follow-up, patients(%)						
Endpoint events	Total (n=3517)	Q1 (n=878)	Q2 (n=886)	Q3 (n=880)	Q4 (n=873)	P
MACE (%)	910 (25.9)	230 (26.2)	194 (21.9)	227 (24.7)	269 (30.8)	0.0004
All-cause mortailty	252 (7.2)	81 (9.2)	60 (6.8)	46 (5.2)	65 (7.5)	0.0124
cardiac death	209 (5.9)	72 (8.2)	43 (4.9)	41 (4.7)	53 (6.1)	0.0872
Myocardial infarction	138 (3.9)	37 (4.2)	34 (3.8)	30 (3.4)	37 (4.2)	0.7864
Revascularization	332 (9.4)	68 (7.7)	78 (8.8)	79 (9.0)	107 (9.0)	0.0236
Heart failure	262 (7.4)	60 (6.8)	38 (4.3)	79 (9.0)	95 (10.9)	<0.0001
Stroke	134 (3.8)	29 (4.3)	30 (3.4)	40 (4.5)	35 (5.2)	0.4855

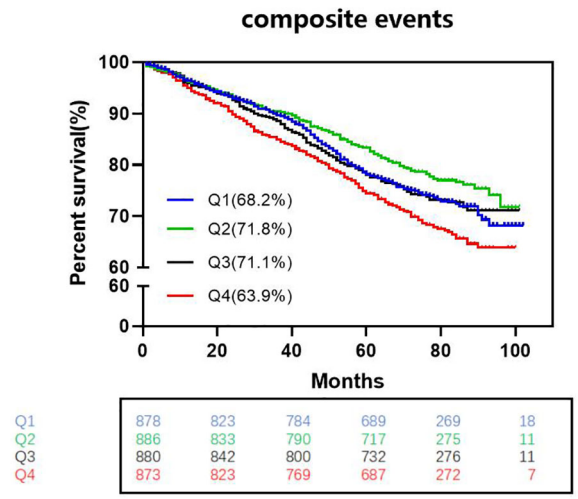

FIGURE 2
Kaplan-Meier survival curves without complex cardiovascular events among the four groups. (log-rank test, Q2 vs. Q1: Padj=0.0363, HR=0.815; Q2 vs. Q3: P.adj=0.034, HR=0.813; Q2 vs. Q4: P.adj<0.0001, HR=0.656) HR indicates hazard ratio (The p-values have already been adjusted using FDR).

had an increased risk of heart failure compared with Q2 individuals (HR_{Q1} = 1.654, 95% CI=1.066-1.792, P=0.014; HR_{Q3} = 2.019, 95% CI=1.303-3.127, P=0.002; HRQ4 = 2.556, 95% CI=1.671-3.909, P=0.001).

There are sex differences in TSH levels for predicting heart failure

We further utilized a restricted quartic spline to build a flexible model, visually illustrating the relationship between TSH concentrations within the reference range and MACE in patients with CHD (Figure 3A). Elevated TSH levels, regardless of gender, were strongly associated with an increased risk of MACE (Figures 4A, B).

A higher serum TSH concentration above the median was linked to an increase in all-cause mortality, and mortality continued to rise with increasing TSH levels (Figure 3B). Low TSH concentrations were also associated with higher mortality, though the differences between sexes were minimal (Figures 4C, D).

TSH levels in both the upper and lower regions of the reference range were connected to an increased risk of heart failure (Figure 3C). In females, lower TSH concentrations were negatively associated with the risk of heart failure, while in males,

TABLE 3 Univariate Cox regression analysis was used to analyze the hazard ratio (HR) of different TSH levels on adverse cardiovascular events.

Univariate Cox regression analysis was used to analyze the hazard ratio of different levels of TSH on adverse cardiovascular events							
Endpoint events	Q2 (n=886)	Q1 (n=878)		Q3 (n=886)		Q4 (n=873)	
		HR (95%CI)	P	HR (95%CI)	P	HR (95%CI)	P
MACE (%)	1	1.230 (1.016-2.164)	0.034	1.233 (1.018-1.494)	0.032	1.510 (1.255-1.816)	<0.0001
All-cause mortailty	1	1.379 (0.987-1.927)	0.059	0.772 (0.526-1.133)	0.186	1.109 (0.781-1.575)	0.564
cardiac death	1	1.20 (0.808-1.237)	0.361	0.649 (0.407-1.035)	0.069	1.001 (0.660-1.517)	0.998
Myocardial infarction	1	1.202 (0.732-1.972)	0.467	0.893 (0.546-1.459)	0.65	1.116 (0.701-1.778)	0.644
Revascularization	1	0.872 (0.630-1.208)	0.411	1.041 (0.762-1.422)	0.801	1.430 (1.068-1.915)	0.016
Heart failure	1	1.669 (1.112-2.506)	0.013	2.127 (1.445-3.133)	<0.001	2.678 (1.838-3.902)	<0.0001
Stroke	1	0.976 (0.586-1.626)	0.925	1.369 (0.853-2.197)	0.194	1.208 (0.742-1.967)	0.448

HR indicates hazard ratio (According to the formula for Bonferroni-corrected p-values, the original p-value must be less than 0.167 to achieve significance).

10.3389/fendo.2025.1433106

TABLE 4 Cox multivariate regression analysis was used to analyze the hazard ratios (HRs) of different TSH levels for adverse cardiovascular events (adjusted for age (<60, ≥60), male sex, hypertension, diabetes, smoking status, and Killip class (I and II, III and IV).

Univariate Cox regression analysis was used to analyze the hazard ratio of different levels of TSH on adverse cardiovascular events							
Endpoint events	Q2 (n=886)	Q1 (n=878)		Q3 (n=886)		Q4 (n=873)	
		HR (95%CI)	P	HR (95%CI)	P	HR (95%CI)	P
MACE (%)	1	1.198 (0.968-1.482)	0.097	1.230 (0.995-1.521)	0.056	1.462 (1.189-1.79)	0.003
All-cause mortailty	1	1.383 (0.956-2.002)	0.086	0.742 (0.481-1.145)	0.178	1.093 (0.739-1.617)	0.657
cardiac death	1	1.258 (0.811-1.961)	0.305	0.657 (0.309-1.105)	0.113	0.914 (0.569-1.468)	0.374
Myocardial infarction	1	1.081 (0.629-1.856)	0.779	0.989 (0.573-1.708)	0.97	1.253 (0.743-2.112)	0.398
Revascularization	1	0.756 (0.523-1.093)	0.137	1.100 (0.784-1.544)	0.581	1.390 (1.009-1.916)	0.044
Heart failure	1	1.654 (1.046-2.616)	0.031	2.019 (1.303-3.127)	0.002	2.556 (1.671-3.909)	0.001
Stroke	1	0.993 (0.578-1.705)	0.979	1.234 (0.739-2.058)	0.421	1.169 (0.683-2.00)	0.569

HR indicates hazard ratio. (According to the formula for Bonferroni-corrected p-values, the original p-value must be less than 0.167 to achieve significance).

both high and low TSH concentrations were positively associated with heart failure risk (Figures 4E, F).

Discussion

The present study assessed the impact of fasting serum TSH levels at admission in patients with coronary heart disease on long-term MACE and all-cause mortality (for a median follow-up of 70 months). The most important findings of the study can be summarized as follows: 1). There was an increased risk of all-cause mortality and MACE among patients in the higher TSH levels group compared to patients in the other groups. 2). TSH in the upper and lower regions of the reference range is an independent predictor of increased risk of heart failure. 3). TSH is a risk factor for MACE, and there are sex differences in HF.

This study revealed that a higher TSH levels were independent predictor of MACE for patients with CHD, which is consistent with the findings of several previous studies (21). Previous studies have also reported that subclinical hypothyroidism is associated with an

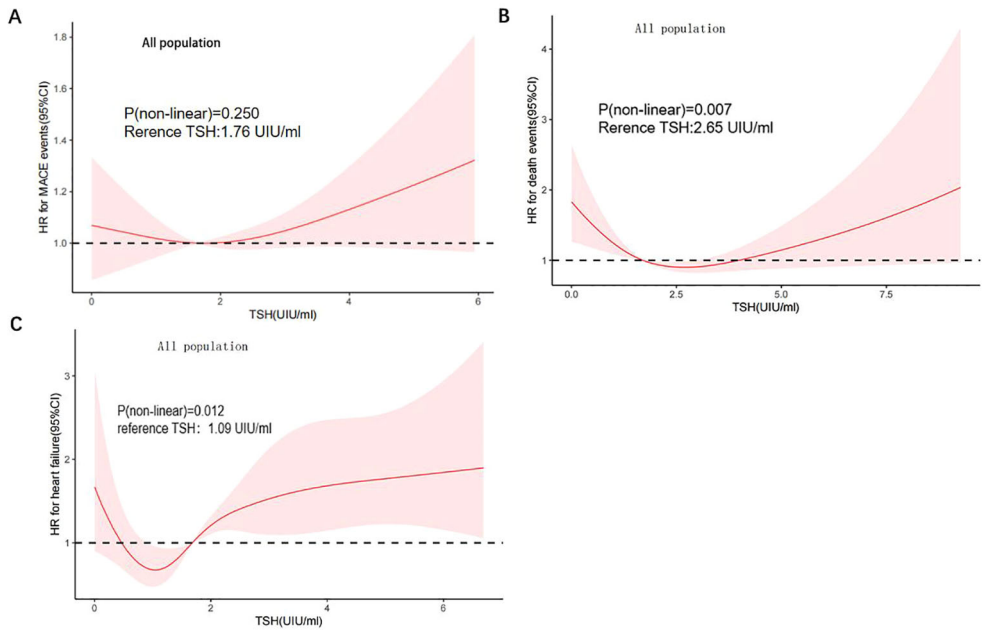

FIGURE 3
A restricted cubic spline regression model. **(A)** TSH with all-cause mortality; **(B)** TSH with MACE; **(C)** TSH with heart failure) The results were adjusted for age, smoking status, cancer history, and estimated glomerular filtration rate. A restricted cubic spline regression model was constructed with 4 nodes at the 5th, 35th, 65th and 95th percentiles of TSH. The dotted lines represent the 95% confidence intervals for the spline model. The range of TSH should be restricted to 0.34 to 6.5 mIU/L because predictions greater than 6.5 mIU/L (95th percentile) are based on too few data points. HR indicates hazard ratio.

10.3389/fendo.2025.1433106

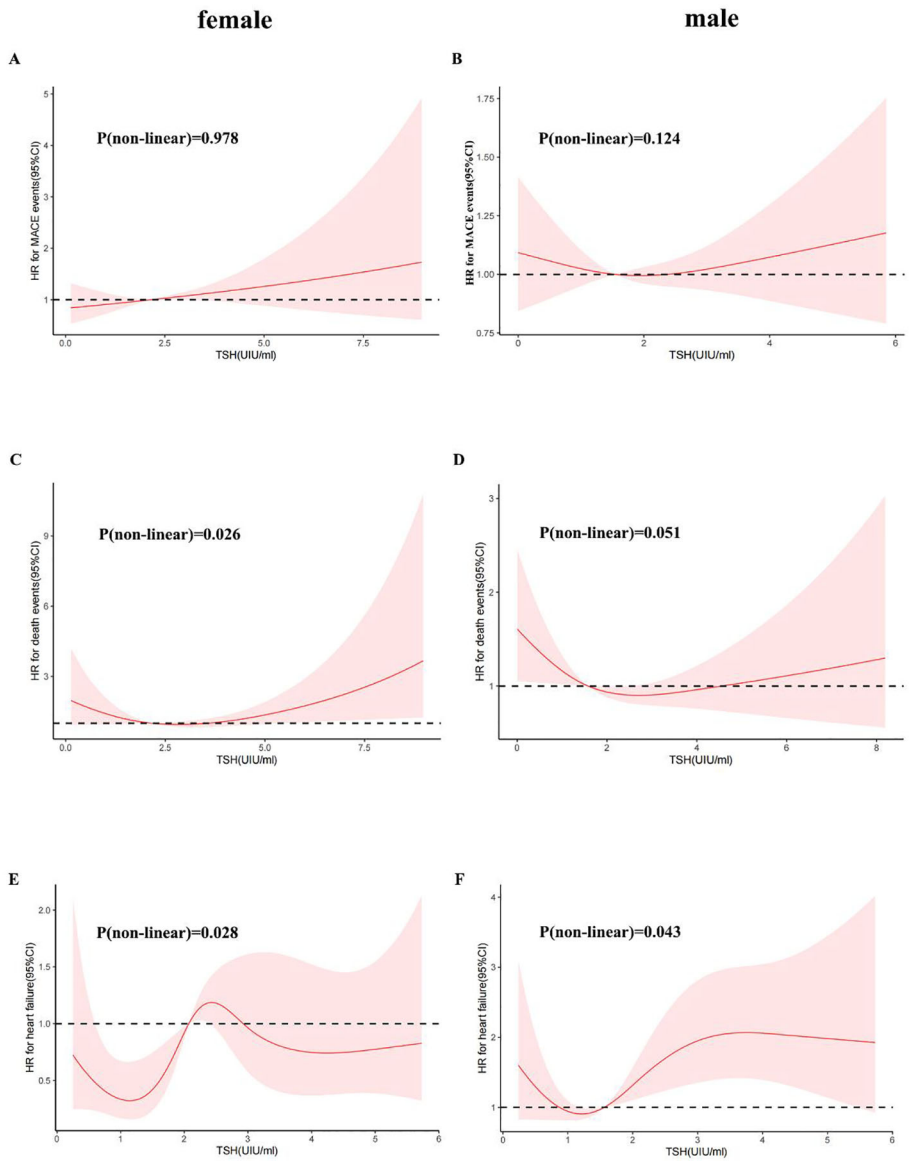

FIGURE 4
A restricted cubic spline regression model was used for sex. (Female: **(A)** TSH with all-cause mortality; **(C)** TSH with MACE events; **(E)** TSH with heart failure; Male: **(B)** TSH with all-cause mortality; **(D)** TSH with MACE events; **(F)** TSH with heart failure) The results were adjusted for age, smoking status, cancer history, and estimated glomerular filtration rate. A restricted cubic spline regression model was constructed with 4 nodes at the 5th, 35th, 65th and 95th percentiles of TSH. The dotted lines represent the 95% confidence intervals for the spline model. The range of TSH should be restricted to 0.34 to 6.5 mIU/L because predictions greater than 6.5 mIU/L (95th percentile) are based on too few data points. HR indicates hazard ratio.

increased risk of CHD events, CHD mortality and CHD severity in individuals with higher TSH levels (20, 26–28).Even in patients with CHD who underwent PCI, TSH levels in the upper part of the reference range was also associated with an increased risk of mortality after PCI (20). Some studies suggest that subclinical hyperthyroidism, as identified by a reduced TSH level, is an important risk factor for cardiac events, mortality, and the development of atrial fibrillation (29). However, our study revealed that there was no independent association between lower TSH levels and cardiac events or mortality. The incidence of STEMI and thrombolysis was greater in the baseline data of the lower TSH group than in those of the other groups, which may have affected the clinical prognosis of the patients. Thus, the correlation between lower TSH levels and MACE disappeared after correction for multivariate Cox analysis.

This study also revealed that the TSH levels within the upper and lower limits of the reference range is an independent predictor of an increased risk of heart failure. A population-based survey of 4,987 patients revealed that the elevated TSH levels were associated with heart failure (30). Individual participant data analyses of prospective cohort studies with 25390 participants from the International Thyroid Studies Collaboration showed that heart failure risk increased with both higher and lower TSH levels (13).This finding is consistent with our findings.

This study revealed that the TSH concentration is a risk factor for MACE. We used a restricted quartic spline to visualize the association between TSH concentration and MACE and all-cause death in CHD patients. For females, TSH concentrations were linearly positively associated with the risk of MACE. For males, with increasing TSH concentration, the hazard ratio (HR) first increased and then decreased (Figures 4A, B). TSH concentrations were within the reference range for heart failure and for CHD patients. For all populations above 1.09 mIU/L, the TSH concentration was positively associated with the risk of heart failure (Figure 3C). Although the HRs for men and women were similar to that for TSH, men with the same TSH levels had a significantly greater risk of heart failure (Figures 4E, F). Therefore, the TSH levels within the normal range are more predictive of long-term heart failure events in male CHD patients.

There are a few reasons for the prognostic influence of TSH levels in patients with CHD in this study. Previously, studies have demonstrated that the correlation between TSH and the cardiovascular system includes changes in arterial compliance, diastolic blood pressure, endothelial dysfunction, vascular resistance, and cardiac contractility (22–24, 31). Other cardiovascular effects include myocardial damage; pericardial effusion; and metabolic syndrome-related factors, including hypertension, increased dyslipidemia, and waist circumference (32, 33). The TSH levels were found to be independently correlated with both carotid plaque incidence and intima-media thickness, and TSH can contribute to atherogenesis directly by promoting macrophage inflammation in atherosclerotic (31, 34). In addition, TSH was found to be positively related to serum lipid concentration (35). High serum levels of TSH accelerate the production of inflammatory molecular and cardiovascular risk biomarkers, increasing the risk of cardiovascular diseases (36). An increase in inflammatory reactions accelerates atherosclerosis and heart failure. It is obvious that TSH directly affects many cardiovascular system physiological processes. However, further studies are needed to elucidate the mechanism by which different TSH levels independently predict adverse outcomes in the CHD population.

Therefore, TSH is not only a risk marker but also a risk target that should be considered to decrease adverse cardiovascular outcomes.

The strength of our study is that we continuously enrolled patients according to the seven-year CAG results. This method significantly decreases the potential misdiagnosis. In addition, this was a single-center study. Consistent detection methods for TSH and other clinical indicators can reduce errors caused by differences in methods and detection standards. This study has several limitations. First, this was a single-center study restricted to Chinese Shaanxi patients. Therefore, generalizing our findings to other ethnic groups requires further research on different ethnic groups to support our findings. Second, this study only examined a single TSH level during hospitalization, lacking dynamic TSH data. Third, patient information extracted from medical records was used, and its completeness and accuracy depended on the physician. Furthermore, this was an observational study. Therefore, the possibility of error cannot be ruled out. However, further prospective studies are needed to support our findings.

Conclusion

In patients with CHD, TSH levels in the upper and lower parts of the reference range are associated with an increased risk of long-term MACE and heart failure. TSH levels have independent predictive value for adverse cardiovascular events and heart failure in patients, especially male patients, with CHD. Additionally, screening TSH levels may help improve risk classification and treatment outcomes for CHD patients. Future studies are needed to clarify this relationship and explore whether treatments targeting TSH improvement can reduce the occurrence of adverse events.

Data availability statement

The raw data has been stripped of sensitive information and added to the supplementary materials, with full public access.

Ethics statement

Patients were treated according to standard clinical guidelines. Our study was conducted in accordance with the Declaration of Helsinki and was approved by the Ethics Committee of the First Affiliated Hospital of Xi'an Jiaotong University. Written informed consent was obtained from all study participants.

Author contributions

ND: Formal analysis, Methodology, Writing – original draft, Writing – review & editing. RH: Formal analysis, Writing – original draft. HG: Formal analysis, Writing – original draft. YX: Formal analysis, Writing – original draft. ZY: Funding acquisition, Writing – review & editing. YW: Funding acquisition, Writing – review & editing. TL: Funding acquisition, Writing – review & editing.

Funding

The author(s) declare financial support was received for the research, authorship, and/or publication of this article. This work was supported by the following fundings: the National Key R&D Program of China grant (2021YFA1301201 and 2021YFA0805403); The National Science Foundation of China (no. 82000474; no. 82370458); the Natural Science Foundation of Shaanxi Province of China (no. 2020JM-383); the Innovative Talents Promotion Plan of Shaanxi Province of China (no. 2021KJXX-04);the Xi'an Health Commission Cultivate Project (no. 2020MS01) and Funding of Xi'an Jiaotong University (no. xzy012019093); and the National Cancer Institute Intramural Research Program.

Conflict of interest

The authors declare that the research was conducted in the absence of any commercial or financial relationships that could be construed as a potential conflict of interest.

Publisher's note

All claims expressed in this article are solely those of the authors and do not necessarily represent those of their affiliated organizations, or those of the publisher, the editors and the reviewers. Any product that may be evaluated in this article, or claim that may be made by its manufacturer, is not guaranteed or endorsed by the publisher.

Supplementary material

The Supplementary Material for this article can be found online at: https://www.frontiersin.org/articles/10.3389/fendo.2025.1433106/full#supplementary-material

References

1. Stefanos T, Andy S, Varsha SK, Angela Y, Vegard S, Joseph LD, et al. Global, regional, and national burden of diseases and injuries for adults 70 years and older: systematic analysis for the Global Burden of Disease 2019 Study. *Bmj*. (2022) 376: e068208. doi: 10.1136/bmj-2021-068208

2. Theo V, Stephen S, Cristiana A, Kaja MA, Mohammad A, Mitra A, et al. Global burden of 369 diseases and injuries in 204 countries and territories, 1990-2019: a systematic analysis for the Global Burden of Disease Study 2019. *Lancet*. (2020) 396:1204–22. doi: 10.1016/s0140-6736(20)30925-9

3. Clayton TC, Lubsen J, Pocock SJ, Vokó Z, Kirwan BA, Fox KA, et al. Risk score for predicting death, myocardial infarction, and stroke in patients with stable angina, based on a large randomised trial cohort of patients. *Bmj*. (2005) 331:869. doi: 10.1136/bmj.38603.656076.63

4. Collet JP, Zeitouni M, Procopi N, Hulot JS, Silvain J, Kerneis M, et al. Long-term evolution of premature coronary artery disease. *J Am Coll Cardiol*. (2019) 74:1868–78. doi: 10.1016/j.jacc.2019.08.1002

5. Schuurman AS, Vroegindewey M, Kardys I, Oemrawsingh RM, Cheng JM, de Boer S, et al. Near-infrared spectroscopy-derived lipid core burden index predicts adverse cardiovascular outcome in patients with coronary artery disease during long-term follow-up. *Eur Heart J*. (2018) 39:295–302. doi: 10.1093/eurheartj/ehx247

6. Schuurman AS, Vroegindewey MM, Kardys I, Oemrawsingh RM, Garcia-Garcia HM, van Geuns RJ, et al. Prognostic value of intravascular ultrasound in patients with coronary artery disease. *J Am Coll Cardiol*. (2018) 72:2003–11. doi: 10.1016/j.jacc.2018.08.2140

7. Sun L, Xiao K, Miao Z, Zhang Y, Si J, Shi N, et al. Prognostic value of normal thyroid stimulating hormone in long-term mortality in patients with STEMI. *Front Endocrinol (Lausanne)*. (2022) 13:806997. doi: 10.3389/fendo.2022.806997

8. de Vries TI, de Valk HW, van der Graaf Y, de Borst GJ, Cramer MJM, Jaap Kappelle L, et al. Normal-range thyroid-stimulating hormone levels and cardiovascular events and mortality in type 2 diabetes. *Diabetes Res Clin Pract*. (2019) 157:107880. doi: 10.1016/j.diabres.2019.107880

9. Li W, Qiu D, Yin H, Wang Y, Chen Y, Liu Q, et al. The prognostic value of thyroid-stimulating hormone in patients with coronary artery disease and depression. *Int J Gen Med*. (2022) 15:4675–83. doi: 10.2147/ijgm.S364146

10. Müller P, Leow MK, Dietrich JW. Minor perturbations of thyroid homeostasis and major cardiovascular endpoints-Physiological mechanisms and clinical evidence. *Front Cardiovasc Med*. (2022) 9:942971. doi: 10.3389/fcvm.2022.942971

11. Takamura N, Hayashida N, Maeda T. Risk of coronary heart disease and mortality for adults with subclinical hypothyroidism. *Jama*. (2010) 304:2481–2. doi: 10.1001/jama.2010.1787

12. Baumgartner C, da Costa BR, Collet TH, Feller M, Floriani C, Bauer DC, et al. Thyroid function within the normal range, subclinical hypothyroidism, and the risk of atrial fibrillation. *Circulation*. (2017) 136:2100–16. doi: 10.1161/circulationaha.117.028753

13. Floriani C, Gencer B, Collet TH, Rodondi N. Subclinical thyroid dysfunction and cardiovascular diseases: 2016 update. *Eur Heart J*. (2018) 39:503–7. doi: 10.1093/eurheartj/ehx050

14. Kannan L, Shaw PA, Morley MP, Brandimarto J, Fang JC, Sweitzer NK, et al. Thyroid dysfunction in heart failure and cardiovascular outcomes. *Circ Heart Fail*. (2018) 11:e005266. doi: 10.1161/circheartfailure.118.005266

15. Jabbar A, Pingitore A, Pearce SH, Zaman A, Iervasi G, Razvi S. Thyroid hormones and cardiovascular disease. *Nat Rev Cardiol*. (2017) 14:39–55. doi: 10.1038/nrcardio.2016.174

16. Vargas-Uricoechea H, Bonelo-Perdomo A, Sierra-Torres CH. Effects of thyroid hormones on the heart. *Clin Investig Arterioscler*. (2014) 26:296–309. doi: 10.1016/j.arteri.2014.07.003

17. Bielecka-Dabrowa A, Godoy B, Suzuki T, Banach M, von Haehling S. Subclinical hypothyroidism and the development of heart failure: an overview of risk and effects on cardiac function. *Clin Res Cardiol*. (2019) 108:225–33. doi: 10.1007/s00392-018-1340-1

18. Ning Y, Cheng YJ, Liu LJ, Sara JD, Cao ZY, Zheng WP, et al. What is the association of hypothyroidism with risks of cardiovascular events and mortality? A meta-analysis of 55 cohort studies involving 1,898,314 participants. *BMC Med*. (2017) 15:21. doi: 10.1186/s12916-017-0777-9

19. Razvi S, Jabbar A, Pingitore A, Danzi S, Biondi B, Klein I, et al. Thyroid hormones and cardiovascular function and diseases. *J Am Coll Cardiol*. (2018) 71:1781–96. doi: 10.1016/j.jacc.2018.02.045

20. Ndrepepa G, Braun S, Mayer K, Cassese S, Fusaro M, Byrne RA, et al. Prognostic value of thyroid-stimulating hormone within reference range in patients with coronary artery disease. *Metabolism*. (2015) 64:1308–15. doi: 10.1016/j.metabol.2015.07.009

21. Cohen B, Bental T, Perl L, Vaknin Assa H, Codner P, Orvin K, et al. Hypothyroidism predicts worsened prognosis in patients undergoing percutaneous coronary intervention. *Front Cardiovasc Med*. (2022) 9:984952. doi: 10.3389/fcvm.2022.984952

22. Chen WJ, Lin KH, Lai YJ, Yang SH, Pang JH. Protective effect of propylthiouracil independent of its hypothyroid effect on atherogenesis in cholesterol-fed rabbits: PTEN induction and inhibition of vascular smooth muscle cell proliferation and migration. *Circulation*. (2004) 110:1313–9. doi: 10.1161/01.Cir.0000140764.15398.F3

23. Legallois D, Hardouin J, Agostini D, Milliez P, Manrique A. Coronary endothelial dysfunction demonstrated by means of (15)O-labeled water PET/CT in hypothyroid cardiomyopathy. *Clin Nucl Med*. (2013) 38:289–91. doi: 10.1097/RLU.0b013e3182817d13

24. Danzi S, Klein I. Thyroid disease and the cardiovascular system. *Endocrinol Metab Clin North Am*. (2014) 43:517–28. doi: 10.1016/j.ecl.2014.02.005

25. Desquilbet L, Mariotti F. Dose-response analyses using restricted cubic spline functions in public health research. *Stat Med*. (2010) 29:1037–57. doi: 10.1002/sim.3841

26. Biondi B, Cappola AR, Cooper DS. Subclinical hypothyroidism: A review. *Jama*. (2019) 322:153–60. doi: 10.1001/jama.2019.9052

27. Rodondi N, den Elzen WP, Bauer DC, Cappola AR, Razvi S, Walsh JP, et al. Subclinical hypothyroidism and the risk of coronary heart disease and mortality. *Jama*. (2010) 304:1365–74. doi: 10.1001/jama.2010.1361

28. Ortolani PD Jr., Romaldini JH, Guerra RA, Portes ES, Meireles GCX, Pimenta J. Association of serum thyrotropin levels with coronary artery disease documented by quantitative coronary angiography: a transversal study. *Arch Endocrinol Metab*. (2018) 62:410–5. doi: 10.20945/2359-3997000000054

29. Kim HJ, McLeod DSA. Subclinical hyperthyroidism and cardiovascular disease. *Thyroid*. (2024) 34:1335–45. doi: 10.1089/thy.2024.0291

30. Perez AC, Jhund PS, Stott DJ, Gullestad L, Cleland JG, van Veldhuisen DJ, et al. Thyroid-stimulating hormone and clinical outcomes: the CORONA trial (controlled rosuvastatin multinational study in heart failure). *JACC Heart Fail*. (2014) 2:35–40. doi: 10.1016/j.jchf.2013.07.008

31. Papadopoulou AM, Bakogiannis N, Skrapari I, Moris D, Bakoyiannis C. Thyroid dysfunction and atherosclerosis: A systematic review. *In Vivo*. (2020) 34:3127–36. doi: 10.21873/invivo.12147

32. Chaker L, Bianco AC, Jonklaas J, Peeters RP. Hypothyroidism. *Lancet*. (2017) 390:1550–62. doi: 10.1016/s0140-6736(17)30703-1

33. Chaker L, Razvi S, Bensenor IM, Azizi F, Pearce EN, Peeters RP. Hypothyroidism. *Nat Rev Dis Primers*. (2022) 8:30. doi: 10.1038/s41572-022-00357-7

34. Yang C, Lu M, Chen W, He Z, Hou X, Feng M, et al. Thyrotropin aggravates atherosclerosis by promoting macrophage inflammation in plaques. *J Exp Med*. (2019) 216:1182–98. doi: 10.1084/jem.20181473

35. Asvold BO, Vatten LJ, Nilsen TI, Bjøro T. The association between TSH within the reference range and serum lipid concentrations in a population-based study. The HUNT Study. *Eur J Endocrinol*. (2007) 156:181–6. doi: 10.1530/eje.1.02333

36. Gómez-Zamudio JH, Mendoza-Zubieta V, Ferreira-Hermosillo A, Molina-Ayala MA, Valladares-Sálgado A, Suárez-Sánchez F, et al. High thyroid-stimulating hormone levels increase proinflammatory and cardiovascular markers in patients with extreme obesity. *Arch Med Res*. (2016) 47:476–82. doi: 10.1016/j.arcmed.2016.10.007

frontiers | Frontiers in Endocrinology

TYPE Original Research
PUBLISHED 07 March 2025
DOI 10.3389/fendo.2025.1468737

OPEN ACCESS

EDITED BY
Robert Kiss,
McGill University, Canada

REVIEWED BY
Durai Sellegounder,
Buck Institute for Research on Aging, United States
Kirti Parwani,
Charotar University of Science and Technology, India

*CORRESPONDENCE
Yi Zhang
zy18356056506@163.com
Qiu Zhang
zhangqiu@ahmu.edu.cn

RECEIVED 22 July 2024
ACCEPTED 21 January 2025
PUBLISHED 07 March 2025

CITATION
Xue L, Zhang Y and Zhang Q (2025) The relationship between advanced glycation end products, metabolic metrics, HbA_{1c}, and diabetic nephropathy. *Front. Endocrinol.* 16:1468737. doi: 10.3389/fendo.2025.1468737

The relationship between advanced glycation end products, metabolic metrics, HbA_{1c}, and diabetic nephropathy

Liping Xue, Yi Zhang* and Qiu Zhang*

Department of Endocrinology, First Affiliated Hospital of Anhui Medical University, Hefei, China

Background: In this cross-sectional study, we aim to investigate the value of non-invasive advanced glycation end products (AGEs) detection in the early screening of diabetic nephropathy(DN) among individuals with type 2 diabetes mellitus and assess whether metabolic parameters and glycated hemoglobin A_{1c} (HbA_{1c}) can moderate this relationship.

Methods: A total of 912 T2DM patients were enrolled. The urinary albumin-to-creatinine ratio (UACR) was measured in morning urine samples to assess DN. AGEs were non-invasively measured through skin autofluorescence. Recognizing the role of age in both AGEs and DN, AGE_{age} was calculated as AGEs × age/100 for related analyses.

Results: The overall prevalence of DN in the present study was 37.2%. Elevated AGE_{age}(χ^2 = 61.06) was associated with a higher prevalence of DN. Multivariable linear regression demonstrated that AGE_{age} was positively associated with UACR levels(β = 0.154, 95% CI: 0.126, 0.306, P<0.001). In the moderation analysis, glycated hemoglobin A_{1c} (HbA_{1c}) affected the correlation between AGE_{age} and UACR. Body mass index (BMI) and triglyceride glucose-body mass index (TyG-BMI) also affect the correlation between AGE_{age} and UACR, there were significant interactions between AGE_{age}, HbA_{1c}, BMI, TyG-BMI, and UACR.

Conclusions: Complex associations and interactions were observed between AGEs, metabolic metrics, HbA_{1c}, and DN. Implementing comprehensive interventions can potentially benefit the prevention of DN in T2DM patients.

KEYWORDS

advanced glycation end products, BMI, diabetes, UACR, obesity, TyG-BMI

1 Introduction

Type 2 diabetes mellitus (T2DM) has escalated into a global health crisis, which stands as the 11th leading cause of death worldwide due to chronic complications (1). Among the myriad microvascular complications associated with T2DM, diabetic nephropathy (DN) emerges as one of the most prevalent and severe, often culminating in end-stage kidney disease (ESKD). Current evidence suggests that DN is detected in approximately 33.6% of diabetic patients (2). It is generally characterized by an initial elevation in microalbuminuria excretion, a substantial increase in albuminuria, and a decline in glomerular filtration rate (GFR) (3). Research has underscored that diabetic patients exhibiting albuminuria are at a heightened risk of cardiovascular disease, mortality, and renal deterioration (4). Therefore, albuminuria serves as an early indicator of DN. Once DN manifests, its progression is challenging to reverse. Importantly, identifying diabetic patients prone to developing albuminuria could significantly aid in preventing the onset of DN.

Advanced glycation end products (AGEs) arise from the nonenzymatic glycosylation of proteins and lipids (5). This glycosylation process is intricate and slow. However, in a prolonged state of elevated glucose levels, glycosylation rates significantly accelerate, increasing AGEs. Studies have demonstrated a clear correlation between AGE accumulation in tissues and blood glucose levels (6). Furthermore, even after correcting hyperglycemia, AGE levels in diabetic tissues often fail to return to normal, leading to the concept of "metabolic memory" (7). Unlike HbA_{1c}, AGEs are not merely byproducts of hyperglycemia but are also implicated in the development of diabetes (8). It is now understood that AGEs can crosslink with proteins, altering their structure, interfering with their functional properties, and binding to the receptor for advanced glycation end products (RAGE), thereby activating proinflammatory signaling pathways (9). These processes are also thought to contribute to the development of diabetic microvascular complications (10). Therefore, AGEs are gaining increasing attention, especially concerning their potential role as markers of DN. However, current methods for measuring AGEs are often complex and costly, making the need for cost-effective, portable, and stable measurement methods paramount. The non-invasive diabetes detector (DM scan), developed using optical detection technology for AGEs, offers the advantage of rapid, non-invasive measurements without the risk of cross-infection. Nevertheless, few studies have explored the relationship between DN and AGEs measured by skin autofluorescence.

While the significance of glycemic control in DN management has been established, it is imperative to consider other metabolism-associated risk factors. Obesity, a burgeoning global public health concern (11), has also been linked to kidney disease (12), with body mass index (BMI) serving as a common measure of obesity. A study in the UK revealed a positive correlation between higher BMI and an increased incidence of microalbuminuria, with this association particularly pronounced among individuals with higher BMI (13). Beyond BMI, various metabolic metrics are employed to assess their relationship with kidney disease. One such metric, the triglyceride-glucose-BMI (TyG-BMI) index, is a product of fasting blood glucose and triglyceride levels combined with BMI. It is currently used to evaluate the association with diabetes (14) and is considered an alternative surrogate marker for insulin resistance (IR), which itself is linked to kidney disease (15). However, few studies have investigated the association between TyG-BMI and DN.

As the prevalence of diabetes continues to surge, the burden of diabetes-associated nephropathy is also poised to increase. Accordingly, there is a pressing need for enhanced clinical prevention strategies to mitigate modifiable DN risk factors. Most existing studies have predominantly focused on the relationship between individual risk factors and DN, with few examining potential synergistic effects among these risk factors. Acknowledging the influence of glycemic management on DN, this study incorporates HbA_{1c} into the model. Accordingly, we put forth the following hypotheses: 1) AGEs are associated with DN, 2) Obesity can modulate this relationship, and 3) An interaction exists between AGEs, obesity, HbA_{1c}, and DN. The outcomes of this study are anticipated to provide vital insights for healthcare providers and decision-makers, facilitating informed clinical decisions in the realm of healthcare.

2 Materials and methods

2.1 Study design and participants

Given the complexity of DN and the absence of a genetic or proteomic marker for accurate DN prediction, we opted to assess the modifiable risk factors for DN, thereby enabling more practical approaches to DN prevention and risk management. Most DN prediction models include non-modifiable factors such as age and disease duration (16, 17). While these factors influence DN, they are beyond our control. Therefore, we focused on intervenable and manageable risk factors in this study.

This cross-sectional study employed comprehensive survey procedures to investigate the impact of metabolic factors on albuminuria. We collected data from inpatients diagnosed with T2DM admitted to the Department of Endocrinology at First Affiliated Hospital of Anhui Medical University from September 1, 2019 to September 30, 2020. Through the patient's hospitalization number, we were still able to identify individual participant information during or after data collection. The diagnosis of T2DM was based on the 1999 World Health Organization (WHO) criteria (18). The study received approval from the Ethics Committee of the First Affiliated Hospital of Anhui Medical University, and written informed consent was obtained from all participants (Ethics Committee approval number PJ2023-11-43).

Abbreviations: AGEs, Advanced glycation end products; DN, diabetic nephropathy; T2DM, type 2 diabetes mellitus; HbA_{1c}, glycated hemoglobin A_{1c}; UACR, urinary albumin-to-creatinine ratio; BMI, body mass index; TyG-BMI, triglyceride glucose-body mass index; SBP, higher systolic blood pressure; DBP, diastolic blood pressure; TG, triglyceride; TC, total cholesterol; ESKD, end-stage kidney disease; GFR, glomerular filtration rate; IR, insulin resistance; WHO, World Health Organization; FPG, fasting plasma glucose; Cr, creatinine; UA, uric acid; IQRs, interquartile ranges; CI, confidence interval; CML, carboxymethyllysine.

2.2 Sample size estimation

Based on previous research indicating a 33.6% incidence of DN among diabetic patients (2) and the desired level of relative precision of 0.15(ε), α=0.05, $Z_{1-\alpha/2}$ = 1.96, the minimum sample size was determined to be 172 using the following formula. Considering the design of diabetic nephropathy staging, ensuring that each group had a certain sample size for stratified analysis, we investigated 940 patients.

$$n = \frac{(1-p)Z_{1-\alpha/2}}{\varepsilon^2 p}$$

2.3 Inclusion and exclusion criteria

We included patients with T2DM between 18 and 80 years of age. Exclusion criteria encompassed: (1) acute illnesses; (2) known genetic renal diseases; and (3) acute renal failure attributed to factors such as drug use or contrast agents. Of the 940 patients initially considered, 28 were excluded due to missing potential confounding factors, ultimately leaving us with a total of 912 T2DM patients included in the study.

2.4 Exposure

All participants underwent a comprehensive medical history assessment and physical examination, including age, diabetes duration, current hypoglycemic regimen, past medical history, height, weight, and blood pressure. Body Mass Index (BMI) was calculated as weight (kg)/height^2(m^2). Fasting venous blood samples were collected for laboratory assays, including fasting plasma glucose (FPG), HbA1c, total cholesterol (TC), triglycerides (TG), creatinine (Cr), and uric acid (UA).

Hypertension was defined as SBP ≥ 140 mmHg or DBP ≥ 90 mmHg or current use of antihypertensive medication (19). Hyperlipidemia was defined as TC>5.69 mmol/L or TG>1.68 mmol/L or current lipid-lowering medication use. According to Chinese criteria, overweight was defined as BMI ≥ 24 kg/m^2 and < 28 kg/m2, while obesity was defined as BMI ≥28 kg/m2 (20). HbA1c levels exceeding 7.0% were considered elevated (21). The age limit was set at 65 years based on the literature (22). The maximum diabetes duration was 10 years (22). The study utilized two surrogate markers of IR: TyG (23) and TyG-BMI (24). The estimation of the glomerular filtration rate (eGFR) was conducted through calculation using the Chronic Kidney Disease Epidemiology Collaboration (CKD-EPI) equation (25).

2.5 Outcome

Morning urine samples were collected to measure urinary albumin-to-creatinine ratio (UACR) levels. Albuminuria was categorized as nonalbuminuria (<30 mg/g), microalbuminuria (30 to 300 mg/g), or macroalbuminuria (>300 mg/g) (26).

2.6 Assessment of AGEs

Skin AGEs were assessed using the DM Scan detection device (Anhui Yikangda Optoelectronics Technology Co., Ltd., Hefei, China). The device employed an excitation light source with a peak wavelength of 370 nm to illuminate approximately 0.1 cm^2 of skin, measuring emitted light with a spectrometer within the range of 420 - 600 nm. Skin autofluorescence was calculated from the ratio of emitted light to reflected light using DM Scan software version 1.02. All measurements were conducted by trained nurses in semi-dark, room-temperature settings. Emphasis was placed on taking measurements from normal skin sites devoid of visible vessels, scars, lichenization, or other skin irregularities. Each subject's skin AGEs were measured three times, and the mean was recorded. AGE_{age} was calculated as AGEs × age/100.

2.7 Sensitivity analysis

To assess the robustness of the model, we employed UACR as a categorical variable in the moderation analysis.

2.8 Statistical analysis

All data were subjected to statistical analysis using SPSS 23.0. Demographic and clinical characteristics of the participants were presented as either means with standard deviations or interquartile ranges (IQRs) for skewed data. Missing values were not filled in and were normally processed for analysis. The analysis proceeded through four distinct steps. Step 1 entailed the descriptive statistics, providing an overview of the general situation within the three albuminuria groups. Step 2 involved calculating Spearman's correlation coefficients to assess the relationships between UACR and other biomarkers. Moving to Step 3, we conducted a multivariable logistic regression analysis to unveil the associations between metabolic indicators and UACR. Finally, in Step 4, we undertook a moderating analysis using the PROCESS method to elucidate the intricate relationships between metabolic indicators and UACR. To establish the presence of a moderating effect, the following criteria needed to be met: (a) a significant direct effect of AGE_{age} on UACR, (b) a significant direct effect of the moderator (metabolic metrics) on UACR, and (c) a significant direct interaction effect (AGE_{age} × HbA_{1c} × metabolic metrics) on UACR. Within SPSS software, the interactive effect was automatically computed, and it also provided the proportion of variance explained by the moderating effect of BMI (indicated by an increase in R^2). A significant moderating effect was considered when the 95% confidence interval (CI) did not include zero.

3 Results

3.1 Characteristics of the study population

A total of 940 patients diagnosed with type 2 diabetes were initially enrolled in this study. After excluding those with missing

data, the final analysis included 912 patients with T2DM (470 men and 442 women). The clinical characteristics of the participants, categorized based on the degree of albuminuria, are presented in Table 1. Notably, 339 participants exhibited higher levels of UACR, resulting in an overall prevalence of 37.2%. Among the various factors analyzed, older age (χ^2 = 8.305), longer duration of diabetes (χ^2 = 35.284), higher systolic blood pressure (SBP) (χ^2 = 60.268), diastolic blood pressure (DBP) (χ^2 = 6.55),increased accumulation of AGEs (χ^2 = 31.66), higher AGE_{age} (χ^2 = 61.06), higher triglyceride (TG) levels (χ^2 = 8.716), higher total cholesterol (TC) levels (χ^2 = 14.362), Female gender (χ^2 = 23.135), higher TyG (χ^2 = 21.351), higher TyG-BMI (χ^2 = 18.62), and lower eGFR (χ^2 = 225.7) were significantly associated with a higher prevalence of albuminuria. Conversely, factors such as BMI(χ^2 = 3.164), HbA_{1c} (χ^2 = 2.484),did not exhibit significant correlations across the three groups.

3.2 Spearman correlation analysis between the risk factors and UACR

Next, spearman correlation analysis was utilized to assess the relationships between AGE_{age}, BMI, TyG-BMI, HbA_{1c}, and UACR. The results indicated that AGE_{age} exhibited a significant association with BMI (rs=-0.218, P<0.01), TyG-BMI (rs=-0.27, P<0.01), HbA_{1c} (rs=-0.103, P<0.01), and UACR (rs = 0.157, P<0.01). Additionally, BMI showed a significant correlation with TyG-BMI (rs=0.904, P<0.01) but did not exhibit statistically significant correlations with HbA_{1c} (rs = -0.03, P > 0.05) or UACR (rs=0.056, P>0.05). TyG-BMI demonstrated significant correlations with HbA_{1c} (rs=0.078, P<0.05) and UACR (rs=0.137, P < 0.01), while HbA_{1c} displayed a significant correlation with UACR (rs=0.094, P<0.01). The results are summarized in Table 2.

3.3 Multilevel linear regression between UACR and independent variables

In Table 3, the data indicated a dose-response relationship between AGE_{age} and UACR (β=0.154), There was a borderline dose-response relationship between HbA_{1c} and UACR (β=0.064). However, no dose-response relationship was observed between BMI, TyG-BMI, and UACR. After adjusting for gender and age, the relationship between AGE_{age}, HbA_{1c} and UACR remained statistically significant. Notably, there was a dose-response relationship between BMI, TyG-BMI, and UACR (BMI: β=0.05, TyG-BMI: β=0.086).

3.4 Moderation analysis

Moderation analyses were performed for AGE_{age}, HbA_{1c}, BMI, and UACR, as shown in Table 4. First, AGE_{age} significantly predicted the severity of UACR (P < 0.05). However, HbA_{1c} was not associated with UACR (P > 0.05), and BMI exhibited no significant correlation with UACR (P > 0.05). Second, the moderation analysis revealed that HbA_{1c} moderated the effect of AGE_{age} on UACR (P < 0.01). Similarly, BMI moderated the effect of AGE_{age} on UACR (P < 0.05), indicating that higher levels of both HbA_{1c} and BMI were associated with increased AGE_{age} and, subsequently, higher UACR levels. BMI did not moderate the effect of HbA_{1c} on UACR (P > 0.05). Finally, a significant three-way interaction among AGE_{age}, BMI, and HbA_{1c} was observed for UACR levels in the overall sample (P < 0.01).

Additional moderation analyses were conducted for AGE_{age}, HbA_{1c}, TyG-BMI, and UACR, as detailed in Table 5. The results revealed no significant correlation between UACR and AGE_{age} (P > 0.05), HbA_{1c} (P > 0.05), or TyG-BMI (P > 0.05). However, moderation analysis indicated that both HbA_{1c} and TyG-BMI moderated UACR as a result of AGE_{age} (P < 0.05), suggesting that elevated levels of HbA_{1c} and TyG-BMI were associated with increased AGE_{age} and subsequent elevations in UACR. Notably, TyG-BMI did not moderate the effect of HbA_{1c} on UACR (P > 0.05). Moreover, a significant three-way interaction among AGE_{age}, TyG-BMI, and HbA_{1c} was observed for UACR levels in the overall sample (P < 0.05).

3.5 Sensitivity analyses

An analysis using UACR as a three-level categorical variable was performed to further examine the interactions. The results, presented in Table 6 and Table 7, indicated a significant three-way interaction among AGE_{age}, BMI, and HbA_{1c} for UACR in the overall sample (P = 0.0563), along with a significant three-way interaction among AGE_{age}, TyG-BMI, and HbA_{1c} for UACR (P < 0.05).

4 Discussion

In this retrospective cross-sectional study, several key findings emerged. First, we observed a DN incidence of 37.2% among hospitalized T2DM patients, slightly higher than the rates reported in previous studies (2). Notably, among these DN patients, 58.4% had a BMI exceeding 24 kg/m², and only 11.5% had HbA_{1c} levels below 7%. This finding highlights the inadequacy of comprehensive T2DM management among this population. Second, our study revealed a significant correlation between AGEs and DN, with higher AGE levels indicating an increased risk of DN. Considering the influence of age on both AGEs and DN, we introduced the AGE_{age} index, which integrates AGEs and age. Lastly, we identified a three-way interaction among obesity, AGEs, and DN with HbA_{1c} in this regulatory relationship. These findings were supported by the results of sensitivity analyses, emphasizing their robustness.

Unlike diabetic macroangiopathy, diabetic microangiopathy is more closely associated with blood glucose, as evidenced in numerous large clinical studies (27, 28). Chronic hyperglycemia leads to increased oxidative stress, initiating the accumulation of AGEs in cells via activation through pathways such as the hexose pathway, polyol pathway, and protein kinase C, resulting in overexpression of RAGE and subsequent activation of various inflammatory cytokines (29). Studies on animals have indicated

10.3389/fendo.2025.1468737

TABLE 1 The prevalence characteristics of three groups of albuminuria.

		nonalbuminuria	microalbuminuria	macroalbuminurianormal	χ^2value	P
Age					8.305*	0.016
	<65	437(65.2%)	173(25.8%)	60(9%)		
	≥65	136(56.2%)	71(29.3%)	35(14.5%)		
BMI					3.164	0.531
	Normal	257(64.6%)	103(25.9%)	38(9.5%)		
	Overweight	221(63.5%)	90(25.9%)	37(10.6%)		
	Obesity	94(57%)	51(30.9%)	20(12.1%)		
durations					35.284**	<0.001
	<10	344(69.8%)	122(24.7%)	27(5.5%)		
	≥10	228(54.5%)	122(29.2%)	68(16.3%)		
HbA_{1c}					2.484	0.289
	<7	87(69%)	28(22.2%)	11(8.7%)		
	≥7	484(61.7%)	216(27.6%)	84(10.7%)		
DBP					6.55*	0.038
	Normal	461(64.7%)	177(24.8%)	75(10.5%)		
	Abnormal	111(56.1%)	67(33.8%)	20(10.1%)		
SBP					60.268**	<0.01
	Normal	404(72.1%)	122(21.8%)	34(6.1%)		
	Abnormal	168(47.9%)	122(34.8%)	61(17.4%)		
AGE					31.66**	<0.01
	≤P25	168(73%)	48(20.9%)	14(6.1%)		
	P25-P50	153(67.4%)	58(25.6%)	16(7%)		
	P50-P75	137(59.6%)	66(28.7%)	27(11.7%)		
	>P75	115(51.1%)	72(32%)	38(16.9%)		
AGE_{age}					61.06**	<0.01
	≤P25	160	56	12		
	P25-P50	154	50	24		
	P50-P75	103	68	57		
	>P75	51	134	43		
TG					8.716*	0.013
	Normal	317(67.2%)	109(23.1%)	46(9.7%)		
	Abnormal	253(57.9%)	135(30.9%)	49(11.2%)		
TC					14.362**	0.001
	Normal	507(64.3%)	210(26.6%)	71(9%)		
	Abnormal	63(52.1%)	34(28.1%)	24(19.8%)		
Gender					23.135**	<0.001
	Male	323(68.7%)	118(25.1%)	29(6.2%)		
	Female	250(56.6%)	126(28.5%)	66(14.9%)		

(Continued)

TABLE 1 Continued

		nonalbuminuria	microalbuminuria	macroalbuminurianormal	χ^2value	P
TyG index					21.351**	0.002
	≤P25	161(70%)	52(22.6%)	17(7.4%)		
	P25-P50	151(66.8%)	51(22.6%)	24(10.6%)		
	P50-P75	144(62.9%)	60(26.2%)	25(10.9%)		
	>75	114(50.9%)	81(36.2%)	29(12.9%)		
TyG-BMI					18.62**	0.005
	≤P25	160(70.2%)	55(24.1%)	13(5.7%)		
	P25-P50	152(67%)	50(22%)	25(11%)		
	P50-P75	135(59.5%)	64(28.2%)	28(12.3%)		
	>75	123(54.2%)	75(33%)	29(12.8%)		
eGFR	≥90	427(70.9%)	156(25.9%)	19(3.2%)	225.7**	<0.001
ml/(min·1.73m^2)	60-89	127(59.1%)	60(27.9%)	28(13.0%)		
	30-59	19(24.7%)	23(29.9%)	35(45.4%)		
	15-29	0	4(30.8%)	9(69.2%)		
	<15	0	1(20.0%)	4(80.0%)		

*P <0.05, **P <0.01.

that inhibiting carboxymethyllysine (CML) may protect against DN progression (30), while young diabetic rats treated with AGEs precursors exhibit renal lesions similar to those seen in aged diabetic rats (31). AGEs are, therefore, crucial in DN development, and AGEs-generated markers can be harnessed to assess DN risk.

Recent studies have shown that non-invasive devices measuring skin AGE fluorescence can be used for diabetes screening, offering a simple and rapid approach (32). However, previous research on the association between non-invasive skin AGEs and diabetic complications has primarily focused on Caucasian populations, showing significant positive correlations between AGEs and diabetic vascular complications (33). Given the impact of skin tone on skin AGE levels, research on the relationship between AGEs and DN in Chinese diabetic populations remains limited. In this study, we employed UACR as a marker for DN to investigate the AGE-DN relationship. Given the significance of age in both AGEs and DN, we introduced the AGE_{age} index. We found that AGE_{age} levels were significantly elevated in DN, and after adjusting for factors including age, sex, and HbA_{1c}, AGE_{age} remained positively correlated with UACR levels. This finding indicates that AGE_{age} influences UACR independently of HbA_{1c}, underlining its value in assessing DN.

One of the management strategies for T2DM is lifestyle modification, including weight loss. A longitudinal study involving 369,362 participants aged 2-15 years indicated that a high percentage of T2DM patients were obese (47.1%), with only

TABLE 2 The Spearman correlation matrices for AGE_{age}, HbA_{1c}, BMI, TyG-BMI, and UACR.

	AGE_{age}	BMI	TyG-BMI	HbA_{1c}	UACR
AGE_{age}	–	-0.218**	-0.27**	-0.103**	0.157**
BMI	-0.218**	–	0.904**	-0.03	0.056
TyG-BMI	-0.27**	0.904**	–	0.078*	0.137**
HbA_{1c}	-0.103**	-0.03	0.078*	–	0.094**
UACR	0.157**	0.056	0.137**	0.094**	–

*P <0.05, **P <0.01.

TABLE 3 The multilevel linear regression between independent variables and UACR.

UACR							
AGE_{age}	R^2	β	t	P	F	LLCI	ULCI
Model 1	0.024	0.154	4.705	<0.001	22.138	0.126	0.306
Model 2	0.049	0.325	4.909	<0.001	15.756	0.274	0.639
HbA_{1c}							
Model 1	0.004	0.064	1.918	0.055	3.678	-0.014	1.202
Model 2	0.03	0.076	2.305	<0.001	9.339	0.106	1.314
BMI							
Model 1	0.001	0.025	0.758	0.449	0.575	-0.235	0.531
Model 2	0.027	0.05	1.505	<0.001	8.278	-0.09	0.682
TyG-BMI							
Model 1	0.003	0.055	1.647	0.1	2.713	-0.005	0.059
Model 2	0.031	0.086	2.528	<0.05	9.793	0.009	0.075

Model 1: crude model; Model 2: Controlled for patients' gender and age.AGE_{age}, advanced glycation end products × age/100 index; HbA_{1c}, glycated hemoglobin A_{1c}; BMI, body mass index; TyG-BMI, triglyceride glucose-body mass index.

TABLE 4 Association between AGE_{age} and HbA_{1c}, BMI and UACR.

Variables	UACR(continuity variable)					
	coeff	*SE*	*t* value	*P* value	LLCI	ULCI
AGE_{age}	-3.0847	1.3348	-2.3109	0.0211	-5.7044	-0.4650
HbA_{1c}	-7.1257	6.8073	-1.0468	0.2955	-20.4857	6.2344
BMI	-3.9661	2.7027	-1.4674	0.1426	-9.2705	1.3383
Int_1	0.1560	0.0559	2.7904	0.0054	0.0463	0.2658
Int_2	0.3277	0.1361	2.4076	0.0163	0.0606	0.5948
Int_3	0.4126	0.2790	1.4790	0.1395	-0.1349	0.9601
Int_4	-0.0156	0.0058	-2.7080	0.0069	-0.0269	-0.0043

Int 1: AGE_{age} × HbA_{1c}; Int 2: AGE_{age} × BMI; Int 3: HbA_{1c} ×BMI; Int 4: AGE_{age} × HbA_{1c} × BMI; AGE_{age}, advanced glycation end products × age/100 index; HbA_{1c}, glycated hemoglobin A_{1c}; BMI, body mass index.

4.33% having a normal BMI (34). This underscores the strong link between obesity and diabetes. Moreover, studies have independently identified BMI as a risk factor for DN (16). Large population-based investigations have corroborated the increased risk of nephropathy in individuals with both diabetes and obesity, and this risk remains elevated even after stringent glycemic control (35). This highlights the role of obesity in DN development, independently of blood glucose control. Overall, our study findings confirm the association of BMI with DN, emphasizing the importance of BMI control in T2DM management.

The interaction between BMI and AGEs has become a research hotspot. AGEs typically accumulate slowly through glycation processes, with hyperglycemia and hyperlipidemia accelerating AGE accumulation *in vivo* (36). Given that both hyperglycemia and hyperlipidemia are prevalent in obese individuals, it is reasonable to speculate that AGE levels are higher in obese patients, as supported by previous research (37). Our study consistently validated the association between BMI and AGE_{age}. *In vitro* and animal experiments further supported this relationship, demonstrating that RAGE overexpression induces adipocyte hypertrophy (38) and that mice fed a high-fat high-AGE diet exhibit greater weight gain and more visceral fat compared with mice fed a high-fat low AGE diet for 6 weeks (39). Additionally, obese individuals often have less healthy dietary habits, consuming highly processed Western-style foods rich in exogenous AGEs, which can be absorbed into the bloodstream and accumulate in the body (40). Considering this interaction, we propose that AGEs interact with BMI to facilitate DN development. Our study validated this hypothesis, with moderating analysis showing that AGE_{age} interacts with BMI to increase the UACR. In contrast, HbA_{1c} and BMI did not exhibit a synergistic effect on DN risk, underscoring the greater importance of AGE_{age} in DN, with BMI exacerbating the condition. Although HbA_{1c} did not exert a moderating effect on BMI, we identified a three-way interaction between AGE_{age}, HbA_{1c}, BMI, and UACR, suggesting that patients with T2DM, especially those with higher AGEs, obesity, and HbA_{1c} levels, are at a heightened risk of urinary proteinuria. Effective management of HbA_{1c} and weight reduction can mitigate the impact of AGEs on UACR, emphasizing the importance of a comprehensive approach. On one hand, it involves strict blood glucose control to reduce HbA_{1c} levels and minimize endogenous AGE production. On the other hand, it necessitates dietary control to reduce the consumption of high-AGE foods, thereby decreasing the absorption of exogenous AGEs and lowering the risk of obesity.

While obesity is primarily linked to dietary factors, there are additional contributors to obesity, including IR. The development of

TABLE 5 Association between AGE_{age} and HbA_{1c}, TyG-BMI and UACR.

Variables	UACR(continuity variable)					
	coeff	*SE*	*t* value	*P* value	LLCI	ULCI
AGE_{age}	-1.5556	0.8933	-1.7414	0.0820	-3.3089	0.1976
HbA_{1c}	-4.2932	4.8096	-0.8926	0.3723	-13.7325	5.1461
TyG-BMI	-0.2624	0.2058	-1.2754	0.2025	-0.6663	0.1414
Int_1	0.0102	0.0041	2.4531	0.0143	0.0020	0.0183
Int_2	0.1867	0.930	2.0069	0.0451	0.0041	0.3693
Int_3	0.0315	0.0212	1.4810	0.1390	-0.0102	0.0732
Int_4	-0.0011	0.0004	-2.4215	0.0157	-0.0019	-0.0002

Int 1: AGE_{age} × HbA_{1c}; Int 2: AGE_{age} × TyG-BMI; Int 3: HbA_{1c} ×TyG-BMI; Int 4: AGE_{age} × HbA_{1c} × TyG-BMI. AGE_{age}, advanced glycation end products x age/100 index; HbA_{1c}, glycated hemoglobin A_{1c}; TyG-BMI, triglyceride glucose-body mass index.

TABLE 6 Association between AGE_{age} and HbA_{1c}, BMI among three groups of albuminuria.

Variables	UACR (classified variable)					
	coeff	*SE*	*t* value	*P* value	LLCI	ULCI
AGE_{age}	-0.0692	0.0434	-1.5959	0.1109	-0.1543	0.0159
HbA_{1c}	-0.2547	0.2211	-1.1516	0.2498	-0.6886	0.1793
BMI	-0.1076	0.0878	-1.2252	0.2208	-0.2799	0.0647
Int_1	0.0035	0.0018	1.9226	0.0548	-0.0001	0.0071
Int_2	0.0079	0.0044	1.7780	0.0757	-0.0008	0.0165
Int_3	0.0130	0.0091	1.4313	0.1527	-0.0048	0.0308
Int_4	-0.0004	0.0002	-1.9109	0.0563	-0.0007	0.0000

Int 1: $AGE_{age} \times HbA_{1c}$; Int 2: $AGE_{age} \times$ BMI; Int 3: $HbA_{1c} \times$ BMI; Int 4: $AGE_{age} \times HbA_{1c} \times$ BMI. AGE_{age}, advanced glycation end products x age/100 index; HbA_{1c}, glycated hemoglobin A_{1c}; BMI, body mass index.

IR is closely associated with obesity in a complex relationship, both being integral components of the metabolic syndrome. IR is a well-established risk factor for cardiovascular and cerebrovascular diseases and plays a significant role in DN. Animal studies have shown that mice fed a high-fat diet, resulting in obesity and IR, exhibit increased UACR levels and altered renal outcomes, indicating tubular dilation and interstitial vacuolation (41). Therefore, we examined another metabolic indicator, TyG-BMI, to represent IR. TyG-BMI, derived from the product of the TyG index and BMI, effectively reflects various metabolic processes in the body. Studies have previously established that elevated levels of TyG-BMI can heighten the risk of prediabetes, especially among non-obese individuals (42). Causality between TyG-BMI and the incidence of diabetes has been reported, particularly in non-obese populations (14). Nevertheless, the relationship between TyG-BMI and DN has received less attention. Our study provided hitherto undocumented evidence of a significant positive relationship between TyG-BMI and UACR, indicating that TyG-BMI is a potential risk factor for DN, possibly surpassing BMI's significance. As a moderating variable, TyG-BMI exerts a distinct influence on the relationship between AGEs and UACR levels. Concurrently, *in vitro* and animal experiments suggest that AGEs can influence cellular insulin sensitivity and insulin secretion capacity (43, 44). This implies that non-obese type 2 diabetes patients, despite seemingly meeting BMI standards, should consider other metabolic factors since BMI fails to capture fat distribution, and abdominal obesity is more strongly associated with IR.

Herein, we established a retrospective model to assess the correlation between these metabolic indicators and DN. We unveiled the intricate interaction among AGEs, obesity-related metabolic metrics, and HbA_{1c}, all associated with UACR levels. This underscores the significance of comprehensive diabetes management. Given that albuminuria in diabetic patients is largely preventable, effective management and treatment strategies should persist even after the onset of DN, aiming to retard disease progression. Comprehensive management awareness is imperative for diabetic patients, and early, timely interventions can substantially reduce the incidence of DN.

This study boasts several strengths, including its multilevel design and the inclusion of a substantial sample size. Furthermore, our study uniquely investigates DN by exploring the relationship between obesity and non-invasive AGEs, offering compelling insights into preventing proteinuria in type 2 diabetes mellitus. However, certain limitations should be acknowledged. First, in recent years, a subtype of DN has been proposed with low estimated glomerular filtration rate but without albuminuria,

TABLE 7 Association between AGE_{age} and HbA_{1c}, TyG-BMI among three groups of albuminuria.

Variables	UACR (classified variable)					
	coeff	*SE*	*t* value	*P* value	LLCI	ULCI
AGE_{age}	-0.0514	0.0287	-1.7883	0.0741	-0.1078	0.0050
HbA_{1c}	-0.2517	0.1547	-1.6275	0.1040	-0.5553	0.0518
TyG-BMI	-0.0106	0.0066	-1.6090	0.1080	-0.0236	0.0023
Int_1	0.0003	0.0001	2.2673	0.0236	0.0000	0.0006
Int_2	0.0062	0.0030	2.0666	0.0391	0.0003	0.0121
Int_3	0.0014	0.0007	1.9900	0.0469	0.0000	0.0027
Int_4	0.0000	0.0000	-2.2131	0.0271	-0.0001	0.0000

Int 1: $AGE_{age} \times HbA_{1c}$; Int 2: $AGE_{age} \times$ TyG-BMI; Int 3: $HbA_{1c} \times$TyG-BMI; Int 4: $AGE_{age} \times HbA_{1c} \times$ TyG-BMI; AGE_{age}, advanced glycation end products x age/100 index; HbA_{1c}, glycated hemoglobin A_{1c}; TyG-BMI, triglyceride glucose-body mass index.

accounting for about 10.1% of diabetes patients (45), thus this subtype therefore needs to be studied to adjust the management strategy. Second, the cross-sectional nature of this study makes it challenging to establish causal relationships or confirm long-term clinical outcomes.

In conclusion, our study highlights the higher incidence of DN within the hospitalized T2DM population. We propose multifaceted management strategies to prevent DN in T2DM patients. Additionally, we introduce AGE_{age}, a non-invasive measure of accumulated AGEs adjusted for age, as a promising approach for identifying patients at high risk of developing DN.

Data availability statement

The raw data supporting the conclusions of this article will be made available from the corresponding author on reasonable use.

Ethics statement

The studies involving humans were approved by The First Affiliated Hospital of Anhui Medical University. The studies were conducted in accordance with the local legislation and institutional requirements. The participants provided their written informed consent to participate in this study.

Author contributions

LX: Formal Analysis, Investigation, Methodology, Writing – original draft, Writing – review & editing. YZ: Data curation, Formal Analysis, Resources, Supervision, Writing – review & editing. QZ: Conceptualization, Formal Analysis, Funding acquisition, Project administration, Supervision, Writing – review & editing.

Funding

The author(s) declare financial support was received for the research, authorship, and/or publication of this article. This work was supported by the National Natural Science Foundation of China under Grant (number 82370836).

Acknowledgments

We would like to acknowledge our cooperators for assistance in data collection.

Conflict of interest

The authors declare that the research was conducted in the absence of any commercial or financial relationships that could be construed as a potential conflict of interest.

Publisher's note

All claims expressed in this article are solely those of the authors and do not necessarily represent those of their affiliated organizations, or those of the publisher, the editors and the reviewers. Any product that may be evaluated in this article, or claim that may be made by its manufacturer, is not guaranteed or endorsed by the publisher.Abbreviation

References

1. Nicholas JK, Arora M, Ryan MB, Zulfiqar AB, Brown J, Carter A, et al. Global, regional, and national disability-adjusted life-years (DALYs) for 315 diseases and injuries and healthy life expectancy (HALE), 1990-2015: a systematic analysis for the Global Burden of Disease Study 2015. *Lancet*. (2016) 388:1603–58. doi: 10.1016/S0140-6736(16)31460-X

2. Ma RCW. Correction to: Epidemiology of diabetes and diabetic complications in China. *Diabetologia*. (2018) 61:1491. doi: 10.1007/s00125-018-4616-0

3. Mogensen CE. Diabetic renal disease in patients with type 2 diabetes mellitus: new strategies for prevention and treatment. *Treat Endocrinol*. (2002) 1:3–11. doi: 10.2165/00024677-200201010-00001

4. Niu J, Zhang X, Li M, Wu S, Zheng R, Chen L, et al. Risk of cardiovascular disease, death, and renal progression in diabetes according to albuminuria and estimated glomerular filtration rate. *Diabetes Metab*. (2023) 49:101420. doi: 10.1016/j.diabet.2023.101420

5. Shamsi A, Shahwan M, Husain FM, Khan MS. Characterization of methylglyoxal induced advanced glycation end products and aggregates of human transferrin: Biophysical and microscopic insight. *Int J Biol Macromol*. (2019) 138:718–24. doi: 10.1016/j.ijbiomac.2019.07.140

6. Li Q, Wen Y, Wang L, Chen B, Chen J, Wang H, et al. Hyperglycemia-induced accumulation of advanced glycosylation end products in fibroblast-like synoviocytes promotes knee osteoarthritis. *Exp Mol Med*. (2021) 53:1735–47. doi: 10.1038/s12276-021-00697-6

7. Rajaobelina K, Cougnard-Gregoire A, Delcourt C, Gin H, Barberger-Gateau P, Rigalleau V. Autofluorescence of skin advanced glycation end products: marker of metabolic memory in elderly population. *J Gerontol A Biol Sci Med Sci*. (2015) 70:841–6. doi: 10.1093/gerona/glu243

8. Khalid M, Petroianu G, Adem A. Advanced glycation end products and diabetes mellitus: mechanisms and perspectives. *Biomolecules*. (2022) 12:542. doi: 10.3390/biom12040542

9. Nowotny K, Jung T, Höhn A, Weber D, Grune T. Advanced glycation end products and oxidative stress in type 2 diabetes mellitus. *Biomolecules*. (2015) 5:194–222. doi: 10.3390/biom5010194

10. Mengstie MA, Chekol Abebe E, Behaile Teklemariam A, Tilahun Mulu A, Agidew MM, Teshome Azezew M, et al. Endogenous advanced glycation end products in the pathogenesis of chronic diabetic complications. *Front Mol Biosci*. (2022) 9:1002710. doi: 10.3389/fmolb.2022.1002710

11. Perdomo CM, Cohen RV, Sumithran P, Clément K, Frühbeck G. Contemporary medical, device, and surgical therapies for obesity in adults. *Lancet*. (2023) 401:1116–30. doi: 10.1016/S0140-6736(22)02403-5

12. Kjaergaard AD, Teumer A, Witte DR, Stanzick KJ, Winkler TW, Burgess S, et al. Obesity and kidney function: A two-sample mendelian randomization study. *Clin Chem*. (2022) 68:461–72. doi: 10.1093/clinchem/hvab249

13. Kawar B, Bello AK, El Nahas AM. High prevalence of microalbuminuria in the overweight and obese population: data from a UK population screening programme. *Nephron Clin Pract*. (2009) 112:c205–12. doi: 10.1159/000218365

14. Wang X, Liu J, Cheng Z, Zhong Y, Chen X, Song W. Triglyceride glucose-body mass index and the risk of diabetes: a general population-based cohort study. *Lipids Health Dis*. (2021) 20:99. doi: 10.1186/s12944-021-01532-7

15. Parvathareddy VP, Wu J, Thomas SS. Insulin resistance and insulin handling in chronic kidney disease. *Compr Physiol*. (2023) 13:5069–76. doi: 10.1002/cphy.c220019

16. Jiang W, Wang J, Shen X, Lu W, Wang Y, Li W, et al. Establishment and validation of a risk prediction model for early diabetic kidney disease based on a systematic review and meta-analysis of 20 cohorts. *Diabetes Care*. (2020) 43:925–33. doi: 10.2337/dc19-1897

17. Ravizza S, Huschto T, Adamov A, Böhm L, Büsser A, Flöther FF, et al. Predicting the early risk of chronic kidney disease in patients with diabetes using real-world data. *Nat Med*. (2019) 25:57–9. doi: 10.1038/s41591-018-0239-8

18. Alberti KG, Zimmet PZ. Definition, diagnosis and classification of diabetes mellitus and its complications. Part 1: diagnosis and classification of diabetes mellitus provisional report of a WHO consultation. *Diabetes Med*. (1998) 15:539–53. doi: 10.1002/(SICI)1096-9136(199807)15:7<539::AID-DIA668>3.0.CO;2-S

19. Chalmers J, MacMahon S, Mancia G, Whitworth J, Beilin L, Hansson L, et al. 1999 World Health Organization-International Society of Hypertension Guidelines for the management of hypertension. Guidelines sub-committee of the World Health Organization. *Clin Exp Hypertens*. (1999) 21:1009–60. doi: 10.3109/10641969909061028

20. Chen K, Shen Z, Gu W, Lyu Z, Qi X, Mu Y, et al. Prevalence of obesity and associated complications in China: A cross-sectional, real-world study in 15.8 million adults. *Diabetes Obes Metab*. (2023) 25:3390–9. doi: 10.1111/dom.v25.11

21. Wang J, Zhang L, Bai Y, Wang X, Wang W, Li J, et al. The influence of shorter red blood cell lifespan on the rate of HbA_{1c} target achieved in type 2 diabetes patients with a HbA_{1c} detection value lower than 7. *J Diabetes*. (2023) 15:7–14. doi: 10.1111/1753-0407.13345

22. Kim KS, Park SW, Cho YW, Kim SK. Higher prevalence and progression rate of chronic kidney disease in elderly patients with type 2 diabetes mellitus. *Diabetes Metab J*. (2018) 42:224–32. doi: 10.4093/dmj.2017.0065

23. Zhang T, Liu Y, Ge Z, Tian D, Lin L, Zhao Z, et al. Predictive value of triglyceride-glucose index fo2021r in-hospital mortality in patients with severe fever with thrombocytopenia syndrome: A multi-center observational study. *Front Med (Lausanne)*. (2021) 8:768101. doi: 10.3389/fmed.2021.768101

24. Song B, Zhao X, Yao T, Lu W, Zhang H, Liu T, et al. Triglyceride glucose-body mass index and risk of incident type 2 diabetes mellitus in Japanese people with normal glycemic level: A population-based longitudinal cohort study. *Front Endocrinol (Lausanne)*. (2022) 13:907973. doi: 10.3389/fendo.2022.907973

25. Levey AS, Stevens LA, Schmid CH, Zhang LYP, Castro AF, Feldman HI, et al. A new equation to estimate glomerular filtration rate. *Ann Intern Med*. (2009) 150:604–12. doi: 10.7326/0003-4819-150-9-200905050-00006

26. Stevens PE, Levin A. Evaluation and management of chronic kidney disease: synopsis of the kidney disease: improving global outcomes 2012 clinical practice guideline. *Ann Intern Med*. (2013) 158:825–30. doi: 10.7326/0003-4819-158-11-201306040-00007

27. Diabetes control and complications trial (DCCT). Update. DCCT research group. *Diabetes Care*. (1990) 13:427–33. doi: 10.2337/diacare.13.4.427

28. Intensive blood-glucose control with sulphonylureas or insulin compared with conventional treatment and risk of complications in patients with type 2 diabetes (UKPDS 33). UK Prospective Diabetes Study (UKPDS) Group. *Lancet*. (1998) 352:837–53. doi: 10.1016/S0140-6736(98)07019-6

29. Peterson SB, Hart GW. New insights: A role for O-GlcNAcylation in diabetic complications. *Crit Rev Biochem Mol Biol*. (2016) 51:150–61. doi: 10.3109/10409238.2015.1135102

30. Yuan Y, Sun H, Sun Z. Advanced glycation end products (AGEs) increase renal lipid accumulation: a pathogenic factor of diabetic nephropathy (DN). *Lipids Health Dis*. (2017) 16:126. doi: 10.1186/s12944-017-0522-6

31. Rodrigues L, Matafome P, Crisóstomo J, Santos-Silva D, Sena C, Pereira P, et al. Advanced glycation end products and diabetic nephropathy: a comparative study using diabetic and normal rats with methylglyoxal-induced glycation. *J Physiol Biochem*. (2014) 70:173–84. doi: 10.1007/s13105-013-0291-2

32. Atzeni IM, van de Zande SC, Westra J, Zwerver J, Smit AJ, Mulder DJ. The AGE Reader: A non-invasive method to assess long-term tissue damage. *Methods*. (2022) 203:533–41. doi: 10.1016/j.ymeth.2021.02.016

33. Yozgatli K, Lefrandt JD, Noordzij MJ, Oomen PHN, Brouwer T, Jager J, et al. Accumulation of advanced glycation end products is associated with macrovascular events and glycaemic control with microvascular complications in Type 2 diabetes mellitus. *Diabetes Med*. (2018). doi: 10.1111/dme.2018.35.issue-9

34. Abbasi A, Juszczyk D, van Jaarsveld CHM, Gulliford MC. Body mass index and incident type 1 and type 2 diabetes in children and young adults: A retrospective cohort study. *J Endocr Soc*. (2017) 1:524–37. doi: 10.1210/js.2017-00044

35. Ejerblad E, Fored CM, Lindblad P, Fryzek J, McLaughlin JK, Nyrén O. Obesity and risk for chronic renal failure. *J Am Soc Nephrol*. (2006) 17:1695–702. doi: 10.1681/ASN.2005060638

36. Kajikawa M, Nakashima A, Fujimura N, Maruhashi T, Iwamoto Y, Iwamoto A, et al. Ratio of serum levels of AGEs to soluble form of RAGE is a predictor of endothelial function. *Diabetes Care*. (2015) 38:119–25. doi: 10.2337/dc14-1435

37. Uribarri J, Cai W, Woodward M, Tripp E, Goldberg L, Pyzik R, et al. Elevated serum advanced glycation endproducts in obese indicate risk for the metabolic syndrome: a link between healthy and unhealthy obesity? *J Clin Endocrinol Metab*. (2015) 100:1957–66. doi: 10.1210/jc.2014-3925

38. Monden M, Koyama H, Otsuka Y, Morioka T, Mori K, Shoji T, et al. Receptor for advanced glycation end products regulates adipocyte hypertrophy and insulin sensitivity in mice: involvement of Toll-like receptor 2. *Diabetes*. (2013) 62:478–89. doi: 10.2337/db11-1116

39. Sayej WN, Knight Iii PR, Guo WA, Mullan B, Ohtake PJ, Davidson BA, et al. Advanced glycation end products induce obesity and hepatosteatosis in CD-1 wild-type mice. *BioMed Res Int 2016*. (2016), 7867852. doi: 10.1155/2016/7867852

40. Uribarri J, Woodruff S, Goodman S, Cai W, Chen X, Pyzik R, et al. Advanced glycation end products in foods and a practical guide to their reduction in the diet. *J Am Diet Assoc*. (2010) 110:911–16.e12. doi: 10.1016/j.jada.2010.03.018

41. Glastras SJ, Chen H, Teh R, McGrath RT, Chen J, Pollock CA, et al. Mouse models of diabetes, obesity and related kidney disease. *PloS One*. (2016) 11:e0162131. doi: 10.1371/journal.pone.0162131

42. Jiang C, Yang R, Kuang M, Yu M, Zhong M, Zou Y. Triglyceride glucose-body mass index in identifying high-risk groups of pre-diabetes. *Lipids Health Dis*. (2021) 20:161. doi: 10.1186/s12944-021-01594-7

43. Riboulet-Chavey A, Pierron A, Durand I, Murdaca J, Giudicelli J, Van Obberghen E. Methylglyoxal impairs the insulin signaling pathways independently of the formation of intracellular reactive oxygen species. *Diabetes*. (2006) 55:1289–99. doi: 10.2337/db05-0857

44. Fiory F, Lombardi A, Miele C, Giudicelli J, Beguinot F, Van Obberghen E. Methylglyoxal impairs insulin signalling and insulin action on glucose-induced insulin secretion in the pancreatic beta cell line INS-1E. *Diabetologia*. (2011) 54:2941–52. doi: 10.1007/s00125-011-2280-8

45. Kramer H, Boucher RE, Leehey D, Fried L, Wei G, Greene T, et al. Increasing mortality in adults with diabetes and low estimated glomerular filtration rate in the absence of albuminuria. *Diabetes Care*. (2018) 41:775–81. doi: 10.2337/dc17-1954

frontiers | Frontiers in Endocrinology

TYPE Clinical Trial
PUBLISHED 10 March 2025
DOI 10.3389/fendo.2025.1522753

OPEN ACCESS

EDITED BY
Antonio C. Bianco,
University of Chicago Medicine, United States

REVIEWED BY
Matthew D. Ettleson,
University of Chicago Medicine, United States
Marco Medici,
Erasmus Medical Center, Netherlands

*CORRESPONDENCE
Francesco S. Celi
celi@uchc.edu

RECEIVED 04 November 2024
ACCEPTED 05 February 2025
PUBLISHED 10 March 2025

CITATION
Phan GQ, Yavuz S, Stamatouli AM, Madan R, Chen S, Grover AC, Nilubol N, Bedoya P, Trankle C, Markley R, Abbate A and Celi FS (2025) A feasibility double-blind trial of levothyroxine vs. levothyroxine-liothyronine in postsurgical hypothyroidism.
Front. Endocrinol. 16:1522753.
doi: 10.3389/fendo.2025.1522753

A feasibility double-blind trial of levothyroxine vs. levothyroxine-liothyronine in postsurgical hypothyroidism

Giao Q. Phan[1], Sahzene Yavuz[2], Angeliki M. Stamatouli[3], Ritu Madan[3], Shanshan Chen[3], Amelia C. Grover[4], Naris Nilubol[5], Pablo Bedoya[6], Cory Trankle[7], Roshanak Markley[7], Antonio Abbate[8] and Francesco S. Celi[9]*

[1]Division of Surgical Oncology, Neag Cancer Center, UConn Health, Farmington, CT, United States, [2]Department of Medicine, The Guthrie Clinic, Sayre, PA, United States, [3]Division of Endocrinology, Diabetes and Metabolism, Virginia Commonwealth University, Richmond, VA, United States, [4]Division of Surgical Oncology, Virginia Commonwealth University, Richmond, VA, United States, [5]Surgical Oncology Program, National Cancer Institute, National Institutes of Health, Bethesda, MD, United States, [6]Virginia Diabetes and Endocrinology, Richmond, VA, United States, [7]Division of Cardiology, Virginia Commonwealth University, Richmond, VA, United States, [8]Berne Cardiovascular Research Center, University of Virginia, Charlottesville, VA, United States, [9]Department of Medicine, UConn Health, Farmington, CT, United States

Context: Despite normalization of Thyrotropin (TSH), some patients with hypothyroidism treated with Levothyroxine (LT4) report residual symptoms which may be attributable to loss of endogenous triiodothyronine (T3).

Objective: Feasibility trial LT4/liothyronine (LT3) combination vs. LT4/placebo in post-surgical hypothyroidism.

Design: Double-blind, placebo-controlled, 24-week study.

Setting: Academic medical center

Patients: Individuals with indications for total thyroidectomy and replacement therapy.

Interventions: LT4/LT3 5 mcg (twice daily) vs. LT4/placebo (twice daily). LT4 was adjusted at 6- and 12-weeks with the goal of baseline TSH ± 0.5 mcIU/ml.

Main Outcome Measures: Changes in body weight, cholesterol, TSH, total T3, free tetraiodothyronine (T4). Cardiovascular function, energy expenditure, and quality of life (ThyPRO-39) were assessed in patients who completed at least the 3-month visit, last measure carried-forward.

Results: Twelve patients (10 women and 2 men), age 51 ± 13.8 years (7 LT4/placebo, 5 LT4/LT3), were analyzed. No significant differences were observed in TSH. Following thyroidectomy, LT4/placebo resulted in higher free T4 + 0.26 ± 0.15 $p<0.005$ and lower total T3 -18 ± 9.6 ng/dl $p<0.003$, respectively, not observed in the LT4/LT3 group. The LT4/placebo group had a non-significant increase in body weight, +1.7 ± 3.8 Kg, total- and LDL-cholesterol +43.1 ± 72.8

and +32.0 ± 64.4 mg/dl. Conversely the LT4/LT3 group changes were -0.6 ± 1.9 Kg, -28.8 ± 49.0 and -19.0 ± 28.3 mg/dl, respectively, all non-significant. Non-significant improvement were observed in ThyPRO-39 measures in both groups, while energy expenditure, and diastolic function increased in the LT4/LT3 group.

Conclusions: In this group of patients with post-surgical hypothyroidism LT4 replacement alone does not normalize free T4 and total T3 levels and is associated with non-significant increase in weight and cholesterol. LT4/LT3 combination therapy appears to prevent these changes.

Clinical Trial Registration: Clinicatrials.gov, identifier NCT05682482.

KEYWORDS

hypothyroidism, post-surgical hypothyroidism, combination therapy, clinical trial, levothyroxine, liothyronine

Introduction

The treatment of hypothyroidism is based on the substitution of synthetic T4, levothyroxine (LT4), for the loss of endogenous thyroid hormone (TH) production, and its efficacy is measured by the normalization of thyrotropin (TSH) (1). This strategy assumes that pituitary euthyroidism indicates restoration of hormonal signaling to all tissues targeted by TH action. While most patients do well on LT4 alone, a sizable minority, in excess of 40% in a study (2), reports residual symptoms consistent with hypothyroidism, which may be attributed to the loss of endogenous production of T3 not completely compensated by the peripheral conversion of exogenous T4 into T3 (3, 4). Studies conducted in animal models of hypothyroidism demonstrated that LT4 alone is not sufficient to restore T3 and T4 concentrations in all tissues, while the combination of LT4/liothyronine (synthetic T3, LT3) can (5–7). While a prospective study indicated that LT4 therapy is able to restore circulating levels of T3 (8), previous observations and large longitudinal studies reported that effective (*i.e.* resulting in TSH normalization) LT4 therapy is associated with decrease in T3 and increase in free T4 (9–11). Several trials were conducted to test the effects of T3-containing therapies (12–25). The results have been inconclusive because of a lack of statistical power, heterogeneous populations and treatment schemes (26). While professional organizations' guidelines do not support the use of T3-containing therapies on a routine basis (1, 27–29), they lament the lack of evidence and encourage the development of well-designed studies to assess the efficacy of these treatment options (30).

Patients undergoing total thyroidectomy are unique since they transition from a state of euthyroidism to complete dependence from exogenous administration of TH. To this end, these patients represent an ideal experimental model to assess the effects of different modalities of replacement therapy on circulating TH concentrations and end-organ effects of TH action.

Here we present a proof-of-concept/feasibility study of LT4/placebo vs. LT4/LT3 replacement therapy in patients undergoing total thyroidectomy. This study was designed to explore the changes in TH and in indices of hormonal action within, and between study groups, with the goal of obtaining point estimates of these measures to adequately power subsequent large trial(s).

Materials and methods

Study design

This was a double-blind, placebo-controlled, two active comparators (LT4/placebo vs. LT4/LT3) parallel, six-month study (Figure 1) in patients undergoing thyroidectomy designed to obtain point estimates of the effect size of each intervention. The study was approved by the Virginia Commonwealth University IRB, and all study participants provided written informed consent (Clinicaltrials.gov ID NCT04782856). The research was completed in accordance with the Declaration of Helsinki as revised in 2013.

Study participants, inclusion criteria, and randomization

Inclusion criteria were age>18 years, normal TSH, and clinical indication for total thyroidectomy. Exclusion criteria were indication for TSH suppression; history of hypothyroidism or thyrotoxicosis; congestive heart failure or unstable coronary artery disease (angina, coronary event, or revascularization within 6 months); atrial fibrillation; uncontrolled hypertension (>140/90 mmHg at screening); uncontrolled diabetes (HbA1c>8% at screening); pregnancy, breastfeeding, or planned pregnancy during the study; history of major depression or psychosis; use of drugs known to interfere with TH absorption or activity (e.g. antiacids, bile acid sequestrants, dopaminergic or dopamine antagonists, amiodarone) (31); conditions that in the opinion of the principal investigator may impede the successful completion of the study. Participants taking

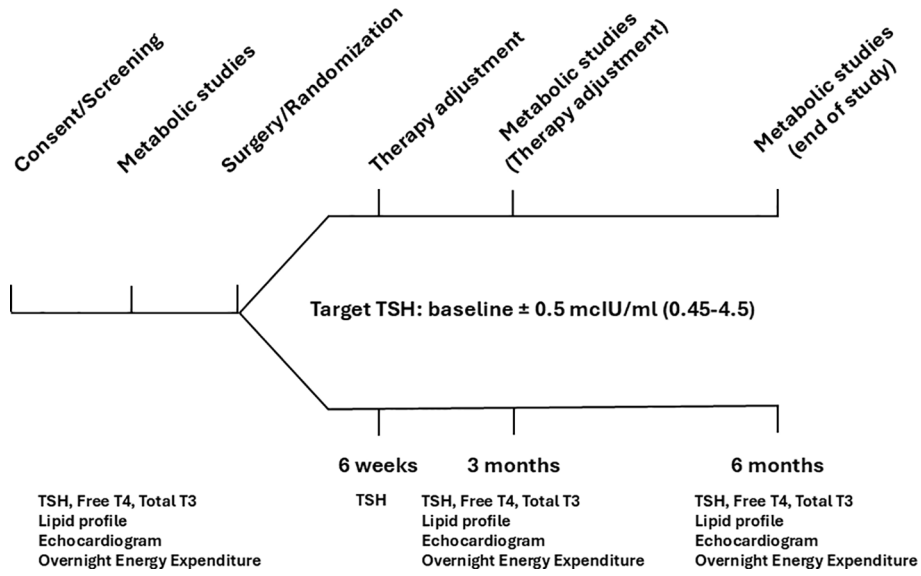

FIGURE 1
Study scheme and procedures.

lipid-lowering medications were instructed not to change their regimen during the trial. Following enrollment, the participants were randomized to the treatment groups by the investigational pharmacy.

Sample size

This feasibility study was designed to obtain point estimates of the effects of LT4/LT3 compared to LT4/placebo on weight, and LDL cholesterol. Based on prior observations (32, 33), with a sample size of 15 participants per arm, a difference of 2.2 Kg would provide 80% power at a significance of 0.05. Similarly, a difference in LDL cholesterol of 8% would provide 70% power at a significance of 0.05. These estimates were based on the assumption of 50% of the effect size observed in our prior crossover LT3 substitution trial (32) and an expected 40% increase in average serum total T3 following LT4/LT3 combination therapy compared to LT4 alone (33). Changes in quality of life (ThyPRO-39) (34), cardiovascular parameters and energy expenditure were considered exploratory endpoints. Due to the exploratory nature of the study the accrual target of the study was placed at 30 participants.

Screening visit

This encounter was conducted to verify inclusion and exclusion criteria, and to allow participants to provide informed consent.

Baseline visit

Study volunteers were admitted prior to surgery (usually the night before the procedure) for overnight energy expenditure recording in a whole-room indirect calorimeter (35, 36). The next morning, study participants underwent a standard transthoracic Doppler echocardiogram to measure left ventricular dimensions and diastolic/systolic function (37), including the myocardial performance (Tei index) obtained by subtracting the ejection time (ET) from the interval between cessation and onset of the mitral inflow velocity to give the sum of isovolumetric contraction time (ICT) and isovolumentric relaxation time (IRT) and calculated as (ICT+IRT)/ET, with smaller numbers reflecting better left ventricular diastolic and systolic function (38); Arterial elastance (Ea) was measured as left ventricular end-systolic pressure (LVESP), estimated as 0.9 x systolic blood pressure divided by LV stroke volume, and end-systolic elastance (EES) measured as LVESP divided by the left ventricular end-systolic volume, and expressing Ea/EES as a measure of ventricular-arterial coupling (39).

Following the echocardiogram, anthropometric measurements and quality of life assessment by ThyPRO-39 (34) were recorded, and fasting blood sampling for TSH, free T4, total T3, and lipid panel was collected. At the time of discharge from surgery (usually in the evening of the same day), study participants were given two study medications bottles, one "AM", containing LT4/placebo or LT4/LT3, and a second "PM" containing placebo or LT3 (*see study medications and therapy adjustments*).

Six-week visit

Six weeks following surgery, study participants were seen for therapy adjustment which consisted of a brief exam, and blood draw for TSH measurement. Study medications were then adjusted and delivered to the participants (*see below*).

10.3389/fendo.2025.1522753

Three- and six-month visits

Three- and six-months following surgery, study participants returned for an overnight visit. The procedures were identical to the baseline visit, apart from therapy adjustment at the three-month visit. Upon study completion, patients returned to the care of their endocrinologists.

Study medications

Patients were randomized to (a) LT4/placebo, starting at a dose of 1.6 mcg/Kg (32, 40), or (b) LT4/LT3 combination therapy. For the LT4/LT3 arm, the initial dose was calculated by decreasing the estimated dose LT4 by 25 mcg, and adding a fixed dose of LT3, 5 mcg twice daily according to our pharmacokinetics modeling (33). Study drugs were over-encapsulated in identical capsules as LT4/placebo or LT4/LT3 (AM), and placebo or LT3 (PM). The LT4 dose was adjusted at the six-week and three-month visits using the scheme reported in Table 1 by an unblinded physician (SY, AMS, RM) and delivered by courier; no changes were made to the LT3 dose throughout the study. Study participants were instructed to take the AM capsule in the morning, with an empty stomach, to wait at least 30 minutes before having breakfast or taking any other medications, and to take the PM dose at least 30 minutes before dinner. During the whole-room indirect calorimetry measurements, study volunteers were instructed to take their study medications following their regular schedule.

Statistical analysis

Two-tailed unpaired t test was used to compare data between treatment arms, while two-tailed paired t test was used to compare baseline vs. end-of-study results within the same treatment arm. Results are expressed as mean ± SD and median and interquartile ranges (IQR); $p < 0.05$ was considered the threshold for significance. Analyses were conducted using Prism version 5 (GraphPad, La Jolla, CA) and SPSS Version 29.0 (IBM, Chicago, IL) in participants who completed at least the three-month visit, with last measure carried forward. No adjustment for multiple comparisons was made.

TABLE 1 Levothyroxine adjustment scheme.

TSH (mcIU/ml)	Dose adjustment
Baseline ± 0.5	No change
Baseline > 0.5 -7.0	Increase by 10%
> 7.0	Increase by 20%
Baseline < 0.5 - 0.1	Decrease by 10%
< 0.1	Decrease by 20%

Dose adjustments were common to both treatments, therapy rounded to the closest available dose.

Results

Study participants

Thirteen participants (11 females, 2 males, age 51 ± 13.2 years) were randomized between 10/29/2020 and 10/26/2022; twelve participants who completed at least the three-month follow up visit were included in the analysis. Of them, five were allocated to LT4/LT3, and seven to LT4/placebo; their characteristics are reported in Table 2. Screening, randomization, drop-out and completion of the study data are reported in Figure 2. No patient-reported adverse event was recorded. A change in dosing outside the titration scheme (dose reduction) was deemed necessary because of sustained TSH suppression at month-3 in a LT4/LT3 group patient. This was attributed to oral GLP-1 analog therapy (41).

Study medications dose adjustments

The average initial LT4 dose in the LT4/placebo group was 119.3 ± 24.8 mcg (1.57 ± 0.0 mcg/Kg), while at end-of-study it was 107 ± 23.5 mcg (1.43 ± 0.4 mcg/Kg) (p=0.406). The LT4 dose was unchanged in one patient, increased in one, and decreased in four. In the LT4/LT3 group the initial average LT4 dose was 120.00 ± 41.1 mcg (1.31 ± 0.1 mcg/Kg), while at end-of-study it was 86.5 ± 10.1 mcg (1.03 ± 0.2 mcg/Kg) (p=0.023). The LT4 dose was increased in one patient and decreased in four. The data are ported in Table 2.

Thyroid hormone and TSH

Compared to baseline (pre-thyroidectomy) TSH, in the LT4/placebo group no differences were observed at end-of-study (1.64 ± 0.70 vs. 1.64 ± 1.09 mcIU/ml), while a non-significant decrease (1.57 ± 0.63 vs. 0.86 ± 1.46 mcIU/ml, p=0.265) was observed in the LT4/LT3 group. At end-of-study the free T4 concentrations were significantly increased in the LT4/placebo (0.91 ± 0.12 vs. 1.17 ± 0.26 ng/dl, p=0.005), while no significant changes (0.96 ± 0.13 vs. 1.02 ± 0.26 ng/dl, p=0.645) were observed in the LT4/LT3 group. The total T3 concentrations were significantly decreased in the LT4/placebo (98.7 ± 10.9 vs. 80.7 ± 14.6 ng/dl, p=0.003), while a non-significant increase (96.8 ± 15.7 vs. 121.4 ± 23.9 ng/dl, p=0.142) was observed in the LT4/LT3 group. Similarly, at end-of-study the total T3/free T4 ratio was significantly decreased in the LT4/placebo (110.0 ± 22.2 vs. 71.0 ± 16.6, p<0.001), while a non-significant increase (103.7 ± 25.9 vs. 121.5 ± 20.0, p=0.142) was observed in the LT4/LT3 group.

In between groups analyses, no significant differences were observed in TSH and free T4 at end-of-study (p=0.337 and p=0.135, respectively), while the differences in total T3 and total T3/free T4 were statistically significant (LT4/Placebo -18.0 ± 9.6 vs. LT4/LT3 20.5 ± 28.8 ng/dl, p=0.005 and LT4/Placebo -39.1 ± 12.1 vs. LT4/LT3 17.8 ± 27.5, p<0.001, respectively). The data are ported in Table 3.

10.3389/fendo.2025.1522753

TABLE 2 Baseline characteristics of study participants included in the analysis.

	All participants	LT4/LT3	LT4/placebo	Significance
Number (sex)	12 (10 f, 2 M)	5 (4F, 1M)	7 (6F, 1M)	n/a
Age (years)	51.7±13.8	50.0±13.8	53.0±13.6	P=0.728
Weight (Kg)	81.8±20.2	90. 0±23.8	76.0±16.7	P=0.257
Ethnicity	9 Caucasian, 3 Black	3 Caucasian, 2 Black	6 Caucasian, 1 Black	n/a
Multinodular goiter	6	3	3	n/a
Papillary thyroid cancer	5	1	4	n/a
Medullary thyroid cancer	1	1	0	n/a

Lipid parameters

In the LT4/placebo group, compared to baseline, a non-significant increase in total and LDL-cholesterol was observed at end-of-study (213.3 ± 69.2 vs. 256.4 ± 105.6 mg/dl p=0.168, and 131.6 ± 49.3 vs. 163.6 ± 84.1 mg/dl p=0.236, respectively). Conversely in the LT4/LT3 group a non-significant decrease in total and LDL-cholesterol was observed at end-of-study (214.4 ± 48.8 vs. 179.8 ± 20.0 mg/dl p=0.214, and 132.6 ± 37.6 vs. 109.8 ± 15.4 mg/dl p=0.163, respectively). With respect to HDL-cholesterol and triglycerides, in the LT4/placebo group, a non-significant increase in HDL-cholesterol and triglycerides was observed at end-of-study. In the LT4/LT3 group, when compared to baseline, non-significant increase in HDL-cholesterol, and decrease in triglycerides were observed at end-of-study. The data are ported in Table 4.

Weight and energy metabolism assessment

A non-significant increase in body weight was observed at end-of-study in the LT4/placebo group (76.0 ± 16.6 vs. 77.7 ± 17.8 Kg p=0.294), not seen in the LT4/LT3 group (90.0 ± 23.8 vs. 89.2 ± 23.5 Kg p=0.457). Conversely, compared to baseline, the LT4/placebo group had a non-significant decrease in energy expenditure (1,544.4 ± 241.3 vs. 1,504.9 ± 213.9 calorie/24hours p=0.215) while the LT4/LT3 group showed an opposite trend (1,655.8 ± 362.6 vs. 1,683.8 ± 388.9 mg/dl calorie/24hours p=0.147). When the pre-post changes in energy expenditure were analyzed between groups a significant (p=0.03) difference was observed. The data are ported in Table 4.

Cardiovascular parameters

No significant differences were observed in heart rate, blood pressure and ejection fraction between baseline and end-of-study in both groups. Statistically significant differences were observed between groups in Tei index, an indicator of diastolic function: compared to baseline, the LT4/placebo group showed an increase of +18.2 95% [IQR 3.8, 100], while the LT4/LT3 group showed a decrease of -12.7 95% [IQR -21.7, -8.5], p=0.005, with negative changes reflecting better function (38). The data are ported in Table 5.

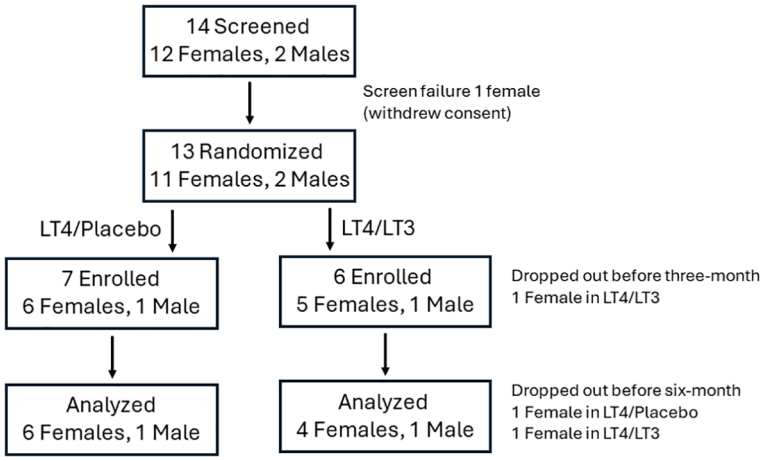

FIGURE 2
CONSORT chart. The analysis was conducted (last measure carried forward) on study participants who completed the three-month visit.

10.3389/fendo.2025.1522753

TABLE 3 Thyroid hormone, TSH, and study medications.

	LT4/LT3				LT4/placebo				
Parameter	Baseline	End of study	Delta	p	Baseline	End of study	Delta	p	p for Delta
TSH (mcIU/ml)	1.57±0.63	0.86±1.46	-0.59±1.14	0.265	1.64±0.70	1.64±1.09	0.00±1.19	0.998	0.337
FreeT4 (ng/dl)	0.96±0.13	1.02±0.26	0.05±0.24	0.645	0.91±0.12	1.17±0.26	0.26±0.15	**0.005**	0.135
T3 (ng/dl)	96.8±15.7	121.4±23.9	20.5±28.8	0.142	98.7±10.9	80.7±14.6	-18.0±9.6	**0.003**	**0.005**
T3/FreeT4	103.7±25.9	121.5±20.0	17.8±27.5	0.221	110.0±22.2	71.0±16.6	-39.1±12.1	**<0.001**	**<0.001**
LT4 dose (mcg)	120±41.1	86.5±10.1	-33.5±34.6	0.096	119.3±24.8	107.0±23.5	-12.3±22.8	0.406	n/a
LT4 dose (mcg/Kg)	1.31±0.14	1.03±0.22	-0.28±0.18	**0.023**	1.57±0.04	1.43±0.41	-0.14±0.41	0.406	n/a
LT3/LT4	1:9.0±1.4	1:6.8±1.2	-2.2±2.2	**0.003**	n/a	n/a	n/a	n/a	n/a

Bold font indicates statistical significance.

Quality of life

Overall, at end-of-study improvements were observed across the ThyPRO-39 domains both in the LT4/placebo and in the LT4/LT3 groups. No significant differences were observed between the two groups. The data are ported in Table 6.

Discussion

Since the seminal observations of Dr. Morreale d'Escobar (5, 6) demonstrating that in animal models of hypothyroidism only LT4/LT3 combination therapy could restore T3 and T4 concentrations in most tissues, several trials have attempted to assess whether humans would benefit from such a regimen (12–25). The results have been conflicting, although a plurality of participants preferred T3-containing therapy regimens, mostly driven by reported weight loss (12–16). Heterogeneity of the study populations, with the inclusion of participants requiring low-dose LT4, thus presumably with residual endogenous TH production was recognized as a major confounder (26). Our study was unique because we characterized patients prior to total thyroidectomy, enabling the comparison of the two thyroid replacement regimens against the baseline of endogenous euthyroidism. Prior studies have evaluated TH levels pre- and post-thyroidectomy (8, 42), but none has attempted to characterize in detail the metabolic profile of patients by performing dense phenotyping.

The LT4/placebo group data provide empirical confirmation that the initial LT4 dose of 1.6 mcg dose (1) is accurate, the minimal reduction in dose when compared to our original observation (32, 40) can be attributed to the trice daily regimen adopted in that study, which could have led to adherence problems. Conversely, most of the patients in the LT4/LT3 group required a significant decrease in their LT4 dose, suggesting that our estimation of the dose adjustment (33) was not sufficient.

Our study demonstrated clear differences in TH concentrations between the two regimens following thyroidectomy. The LT4/placebo group data demonstrated that LT4 alone does not normalize circulating TH concentrations (9), while LT4/LT3 combination therapy may. Of interest, our data appear in contrast with Dr. Jonklaas' report which did not demonstrate significant changes in T3 levels in patients undergoing thyroidectomy. It is worth noting that several patients with benign thyroid pathology underwent subtotal thyroidectomy, with the potential confounder of residual thyroid hormone production.

TABLE 4 Lipid parameters, weight and energy expenditure assessment.

	LT4/LT3				LT4/placebo				
Parameter	Baseline	End of study	Delta	p	Baseline	End of study	Delta	p	p for Delta
Total Cholesterol (mg/dl)	214.4±48.8	179.8±20.0	-28.8±49.0	0.214	213.3±69.2	256.4±105.6	43.1±72.8	0.168	0.070
LDL Cholesterol (mg/dl)	132.6± 37.6	109.8± 15.4	-19.0± 28.3	0.163	131.6±49.3	163.6±84.1	32.0±64.4	0.236	0.110
HDL Cholesterol (mg/dl)	53.2±11.2	56.8±16.3	3.0±6.5	0.322	58.4±19.8	63.0±18.6	4.6±12.5	0.373	0.880
Triglycerides (mg/dl)	151.8±135.1	100.0±50.3	-43.2±94.2	0.322	124.0±71.0	150.0±96.3	26.0±38.2	0.122	0.070
Weight (Kg)	90.0±23.8	89.2±23.5	-0.6±1.9	0.457	76.0±16.6	77.7±17.8	1.7±3.8	0.294	0.231
EE (Calorie/24 hour)	1,655.8±362.6	1,683.8±388.9	24.5±29.5	0.147	1,544.4± 241.3	1,504.9±213.9	-39.5±68.2	0.215	**0.03**
RQ	0.87± 0.02	0.88± 0.03	0.01±0.03	0.464	0.85± 0.03	0.89± 0.1	0.04± 0.08	0.327	0.125

Bold font indicates statistical significance.

10.3389/fendo.2025.1522753

TABLE 5 Cardiovascular parameters.

	LT4/LT3				LT4/placebo				
	Baseline	End of study	Delta	p	Baseline	End of study	Delta	p	p for Delta
SBP (mmHg)	125[119-131]	128 [120-140]	2.4 [0.4 – 6.5]	0.08	130 [127-137]	127 [171-136]	-8.5 [-10.7 - 0]	0.25	0.11
DBP (mmHg)	75 [63-83]	74 [58-85]	-2.4 [-10.1 – 3.8]	0.42	76 [70-89]	73 [62-84]	-11.4 [-15.8 – 15.2]	0.27	0.53
HR (bpm)	81 [61-100]	70 [61-82]	1.4 [-28.4 – 9.7]	0.69	81 [50-95]	81 [54-96]	1.1 [-2.0 – 16.0]	0.29	0.53
LVEDV (ml)	89 [68-108]	67 [64-108]	-4.0 [-24.9 – 15.5]	0.50	90 [82-98]	75 [75-90]	-5.6 [-23.0 - 0]	0.12	0.76
LVESV (ml)	37 [26-51]	27 [24-44]	-15.1 [-32.2 – 17.0]	0.35	35 [29-37]	29 [26-39]	-6.9 [-14.0 – 2.9]	0.20	0.43
LVEF (%)	59 [54-62]	59 [57-66]	8.0 [-5.7 – 14.6]	0.23	60 [54-70]	64 [57-65]	-3.7 [-7.9 – 5.6]	0.60	0.43
E (ms)	77 [54-85]	74 [51-84]	-1.2 [-12.6 – 7.5]	0.59	71 [56-76]	68 [57-79]	1.8 [-8.1 – 26-1]	0.61	0.64
A (ms)	57 [44-96]	66 [49-89]	0 [-7.0 – 18.4]	0.85	58 [42-93]	65 [55-76]	12.2 [-18.5 – 13.5]	0.74	0.76
E/A ratio	1.1 [0.9-1.3]	1.0 [0.9-1.2]	-2.4 [-19.1 – 6.5]	0.35	1.2 [0.8-1.2]	1.2 [0.9-1.3]	-3.1 [-19.0 – 2.9]	0.40	1
DT (ms)	210 [180-220]	227 [209-271]	8.1 [-2.4 – 50.4]	0.14	190 [155-208]	211 [183-239]	16.8 [-4.1 – 19.5]	0.06	1
E/DT ratio	0.34 [0.26-0.47]	0.30 [0.22-0.36]	-10.7 [-35.4 – 6.7]	0.23	0.39 [0.27-0.43]	0.31 [0.23-0.43]	-12.9 [-22.5 – 34.0]	0.61	1
AE (ms)	419 [370-482]	420 [381-451]	-3.9 [-14.3 – 14.8]	0.89	441 [339-495]	419 [398-478]	3.0 [-13.1 – 17.1]	0.61	0.88
ET (ms)	270 [266-325]	309 [262-324]	1.1 [-8.6 – 14.4]	0.69	348 [259 -353]	308 [264-318]	-0.8 [-10.2 – 12.0]	0.60	0.64
Tei Index	0.36 [0.32 – 0.68]	0.32 [0.29-0.55]	-12.7 [-21.7 - -8.5]	**0.04**	0.27 [0.25-0.40]	0.36 [0.33-0.55]	18.2 [3.8 - 100]	0.08	**0.005**
E' (cm/s)	8.1 [7.3-11.7]	6.9 [6.5-12.5]	-5.3 [19.9 – 10.8]	0.69	9.1 [9.0 – 9.8]	9.5 [7.6-10.0]	4.9 [-21.3 – 11.1]	1	0.88
E/E' (cm/s)	8.4 [5.3-11.0]	8.2 [6.1-10.4]	1.8 [-9.0 – 19.4]	0.89	7.2 [5.9-8.3]	7.5[6.1-9.2]	-3.4 [-16.7 – 22.9]	0.87	1
E'/DT	0.04 [0.03-0.06]	0.03 [0.03-0.05]	-15.2 [-39.1 – 5.0]	0.35	0.05 [0.04-0.06]	0.04 [0.03-0.05]	-9.9 [-28.6 – 2.0]	0.09	0.53
Ea	2.1 [2.0-2.9]	2.8 [1.9-2.9]	-1.9 [-12.5 – 30.8]	0.69	2.1 [1.8-2.7]	2.2 [1.8-2.7]	-2.2 [-12.1 – 26.5]	0.87	1
Ees	3.0 [2.4-4.5]	3.8 [2.9-4.9]	19.6 [-8.2 – 57.4]	0.35	3.6 [3.3-3.9]	3.7 [2.5-4.8]	-2.2 [-5.4 – 31.4]	0.61	0.53
Ea/Ees	0.70 [0.63-0.87]	0.67 [0.54-0.57]	-18.0 [-27.4 – 15.2]	0.35	0.70 [0.44-0.85]	0.57 [0.56-0.77]	2.7 [-15.5 – 29.3]	0.87	0.53

A, atrial contraction transmitral flow velocity at pulsed wave Doppler; AE, time between end of atrial contraction and mitral valve closure and mitral opening with initiation of early filling; DBP, diastolic blood pressure; DT, transmitral early flow velocity deceleration time; E, early transmitral velocity at pulsed wave Doppler; E', tissue Doppler velocity of the mitral annulus averaged between medial and lateral; Ea, arterial elastance; EES, end-systolic elastance; ET, ejection time; HR, heart rate; LVEDV, left ventricular end-diastolic volume; LVEF, left ventricular ejection fraction; LVESV, left ventricle end-systolic volume; SBP, systolic blood pressure. Data are presented as median and interquartile range.
Bold font indicates statistical significance.

Conversely, patients with malignant disease had lower TSH when compared to their pre-surgical baseline (8). These factors may have played a role in the apparent discrepancies between the observations. We did not measure trough total T3 levels, and most study participants underwent phlebotomy 1-3 hour following LT3 administration, which approximates the Tmax (33); hence the increase in serum total T3 observed at end-of-study in the LT4/LT3 group likely represents an overestimation.

Following thyroidectomy the LT4/placebo group experienced a non-significant weight gain whose effect size is consistent with the observations reported in a recent meta-analysis (43), while LT4/LT3 therapy appears to prevent it. Interestingly, the whole room indirect calorimetry data indicate divergent trends in energy expenditure between the LT4/placebo and the LT4/LT3 groups. Projected over one year, a decrease of 39.5 calorie/day observed in the LT4/placebo group would correspond to approximately 2 Kg of weight gain, which could be counterbalanced with the equivalent of ten days of fasting. These latter estimates are likely overstated since they do not take in account compensatory mechanisms (44).

Similar to the weight data, the LT4/placebo group experienced non-significant increase in total- and LDL-cholesterol which did not occur in the LT4/LT3 group, again consistent with the observation that LT4 alone does not restore euthyroidism.

The LT4/LT3 group had a small yet statistically significant improvement in Tei index, a measure cardiac performance (38). Interestingly, this is consistent with our LT3 vs. LT4 therapy trial where a marginal improvement in diastolic function was observed in the LT3-treated arm (32).

Overall, both groups showed a trend toward improvement in quality of life when compared to baseline (pre-surgery). It is possible that the anxiety associated with the upcoming surgery may have played a role. Indeed, the changes in "eye" domain which one would not expect be affected by the surgery (since Graves' disease and thyrotoxicosis were exclusion criteria) support this

TABLE 6 Quality of life (Thy-PRO-39).

	LT4/LT3				LT4/placebo				
Domain	Baseline	End of study	Delta	p	Baseline	End of study	Delta	p	p for Delta
Goiter	60.0±41.0	15.0±25.3	-45.0±38.0	0.057	23.8±36.8	0.0±0.0	-23.8±36.8	0.137	0.355
Hyperthyroid	25.0±20.7	10.0±19.0	-15.0±18.1	0.136	23.2±29.9	10.7±10.6	-12.5±20.4	0.156	0.829
Hypothyroid	36.2±34.3	26.2±27.4	-10.0±24.0	0.405	11.6±17.5	14.3±14.8	2.7±17.2	0.695	0.310
Eye	26.7±27.2	21.7±29.8	-5.0±12.6	0.426	16.7±17.3	3.6±17.3	-13.1±17.9	0.101	0.408
Tiredness	78.3±31.5	41.7±40.4	-36.7±45.1	0.143	45.8±28.9	34.5±16.3	-11.2±19.3	0.174	0.207
Cognitive	60.0±42.2	26.7±29.7	-33.3±45.3	0.175	23.8±15.6	9.5±8.9	-14.3±15.8	0.054	0.320
Anxiety	65.0±38.4	23.3±21.6	-41.7±45.3	0.109	19.1±15.7	4.8±6.6	-14.3±19.1	0.095	0.178
Depressivity	56.7±42.2	26.7±30.8	-30.0±42.7	0.192	16.6±12.7	14.3±6.3	-2.3±11.5	0.609	0.128
Emotional	61.7±32.0	21.7±20.9	-40.0±41.8	0.099	21.4±22.5	11.9±11.6	-9.5±19.0	0.231	0.116
Social life	25.0±34.3	0.0±0.0	-25.0±34.3	0.179	9.5±14.0	0.0±0.0	-9.5±14.0	0.121	0.301
Daily life	50.0±46.8	11.7±18.3	-38.3±51.2	0.211	9.5±14.0	2.4±4.0	-7.1±13.1	0.199	0.148
Appearance	50.0±47.1	11.7±16.2	-38.3±62.8	0.244	17.9±37.4	8.3±22.0	-9.5±47.2	0.613	0.384
Composite	65.0±37.9	20.0±27.4	-45.0±64.7	0.195	17.9±23.8	3.6±9.4	-14.3±28.3	0.231	0.285

ThyPRO-39 score: 0-100±SD, higher value worst outcome. No correction was made for multiple comparisons.

interpretation. This is consistent with the observations of Azaria and colleagues (45).

The study was conducted during the COVID-19 pandemic which hampered recruitment and retention, as many potential participants objected to the "clinically unnecessary" pre-surgical and subsequent overnight admissions for baseline energy expenditure recording and overnight follow up studies. This led to an unanticipated limited number of participants and a significant attrition rate, causing an underpowered study and the need to use suboptimal (last measure carried forward in individuals who did not complete the 6-months visit) statistical analysis. It should be noted that the primary goal of the study was to provide point estimates for the design of larger intervention studies (30). To this end, the trend and the consistency of the findings clearly provides an unequivocal "go" to proceed with larger studies. By applying the point estimates of this study in *post-hoc* analyses, 11 participants in each treatment arm would provide 80% power to demonstrate a difference in weight, while 16 participants would provide 80% power to demonstrate a difference in total cholesterol between groups similar to the ones we observed in our study.

Another limitation of the study is that by design the recruitment was limited to patients undergoing total thyroidectomy, thus resulting in hypothyroidism devoid of residual TH production. It is possible that the point estimates obtained in this population comparing LT4/LT3 therapy to LT4/placebo are larger than the effects in patients with hypothyroidism due to autoimmune thyroid disease who presumably have some degree of residual TH production (26).

Our study design did not allow for adjustment of LT3 dosing neither as ratio to LT4 nor to participants' weight. Within the LT4/LT3 treatment group the ratio LT3/LT4 ranged between 1:10 and 1:6, above the estimated endogenous T3 production from the thyroid gland (46). This is an obvious limitation driven by the practical need to use commercially available LT3 formulations which could then be utilized in larger studies. The trend toward a decrease in TSH, associated with decrease in weight and lipids observed in the LT4/LT3 group compared to baseline, suggests that the LT3 dosing employed in this study is supraphysiologic (pharmacologic). This is an important consideration which will need to be addressed by subsequent studies. Prior studies demonstrated that changes in TSH achieved by modulation of LT4 dose did not result in changes in indices of TH action (weight, cholesterol, energy expenditure) (47), thus the differences observed between groups are unlikely attributable to the non-significant differences in TSH at the end of the study. Of note, the "low" TSH in that particular study was higher than the average TSH observed in the LT4/LT3 group, hence one could speculate that the LT4 dose was not sufficient to exert a measurable metabolic effect. We did not measure additional indices of TH action such as sex hormone binding globulin or angiotensin converting enzyme (48). In the context of a feasibility study for a larger (effectiveness) trial these assays would have provided only limited additional information. Due to the limited number of patients, an assessment of the role of common polymorphisms in the type-2 deiodinase and TH transporter genes (49–51) on the response to therapy were not feasible.

Despite its limitations, this study has clearly demonstrated that LT4 alone, while normalizing TSH, does not restore euthyroidism when considering the circulating TH levels (9). Moreover, the lipid profile and weight data, which are clinically relevant indices of TH

action, suggest that "optimal" LT4 therapy (1) in individuals devoid of endogenous TH production not only results in measurable abnormalities in circulating TH homeostasis, but possibly in inability of restoring euthyroidism at important end-organ targets of the hormonal action. Conversely, the supplementation of LT3 appears to be able to prevent these changes. The consistency of trends across multiple indices of TH action does not support the interpretation that our findings are due to type II error.

In conclusion, this feasibility study provides supportive evidence to design adequately powered large studies to evaluate the efficacy and effectiveness of LT4/LT3 combination therapy for the treatment of hypothyroidism, at least in patients undergoing total thyroidectomy.

Data availability statement

The raw data supporting the conclusions of this article will be made available by the authors, without undue reservation.

Ethics statement

The studies involving humans were approved by Virginia Commonwealth University. The studies were conducted in accordance with the local legislation and institutional requirements. The participants provided their written informed consent to participate in this study.

Author contributions

GQP: Conceptualization, Investigation, Resources, Writing – original draft, Writing – review & editing. SY: Investigation, Writing – review & editing. AS: Investigation, Writing – review & editing. RiM: Investigation, Writing – review & editing. SC: Data curation, Formal analysis, Investigation, Resources, Writing – review & editing. AG: Investigation, Writing – review & editing. NN: Investigation, Writing – review & editing. PB: Investigation, Writing – review & editing. CT: Investigation, Writing – review & editing. RoM: Investigation, Writing – review & editing. AA: Formal analysis, Investigation, Writing – review & editing. FSC: Conceptualization, Formal analysis, Funding acquisition, Investigation, Methodology, Project administration, Supervision, Writing – original draft, Writing – review & editing.

Funding

The author(s) declare financial support was received for the research, authorship, and/or publication of this article. FSC: This study was supported by the NIDDK 1R21DK122310-01A and NIDDK 1R01DK140455-01 awards; role: Principal Investigator.

Acknowledgments

The authors gratefully acknowledge the support of Trang Le (Data Safety and Monitoring), Joyce Ruddley (study coordination), the VCU investigational Pharmacy (randomization, study drugs over-encapsulation and dispensing), and the personnel of the VCU Clinical Research Services Unit. This study could not have happened without the selfless participation of our patients that volunteered to participate during the COVID-19 pandemic.

Conflict of interest

FSC has served as consultant for IBSA Institut Biochimique and Alora pharmaceuticals. Both companies produce thyroid medication. None of these companies nor their products have been involved in this study.

The remaining authors declare that the research was conducted in the absence of any commercial or financial relationships that could be construed as a potential conflict of interest.

The author(s) declared that they were an editorial board member of Frontiers, at the time of submission. This had no impact on the peer review process and the final decision.

Generative AI statement

The author(s) declare that no Generative AI was used in the creation of this manuscript.

Publisher's note

References

1. Jonklaas J, Bianco AC, Bauer AJ, Burman KD, Cappola AR, Celi FS, et al. Guidelines for the treatment of hypothyroidism: prepared by the american thyroid association task force on thyroid hormone replacement. *Thyroid*. (2014) 24:1670–751. doi: 10.1089/thy.2014.0028

2. Saravanan P, Chau WF, Roberts N, Vedhara K, Greenwood R, Dayan CM. Psychological well-being in patients on 'adequate' doses of l-thyroxine: results of a large, controlled community-based questionnaire study. *Clin Endocrinol (Oxf)*. (2002) 57:577–85. doi: 10.1046/j.1365-2265.2002.01654.x

3. Ettleson MD, Prieto WH, Russo PST, de Sa J, Wan W, Laiteerapong N, et al. Serum thyrotropin and triiodothyronine levels in levothyroxine-treated patients. *J Clin Endocrinol Metab*. (2023) 108:e258–e66. doi: 10.1210/clinem/dgac725

4. Batistuzzo A, Salas-Lucia F, Gereben B, Ribeiro MO, Bianco AC. Sustained pituitary T3 production explains the T4-mediated TSH feedback mechanism. *Endocrinology*. (2023) 164. doi: 10.1210/endocr/bqad155

5. Escobar-Morreale HF, Obregon MJ, Escobar del Rey F, Morreale de Escobar G. Replacement therapy for hypothyroidism with thyroxine alone does not ensure euthyroidism in all tissues, as studied in thyroidectomized rats. *J Clin Invest*. (1995) 96:2828–38. doi: 10.1172/JCI118353

6. Escobar-Morreale HF, del Rey FE, Obregon MJ, de Escobar GM. Only the combined treatment with thyroxine and triiodothyronine ensures euthyroidism in all tissues of the thyroidectomized rat. *Endocrinology*. (1996) 137:2490–502. doi: 10.1210/endo.137.6.8641203

7. Werneck de Castro JP, Fonseca TL, Ueta CB, McAninch EA, Abdalla S, Wittmann G, et al. Differences in hypothalamic type 2 deiodinase ubiquitination explain localized sensitivity to thyroxine. *J Clin Invest*. (2015) 125:769–81. doi: 10.1172/JCI77588

8. Jonklaas J, Davidson B, Bhagat S, Soldin SJ. Triiodothyronine levels in athyreotic individuals during levothyroxine therapy. *JAMA*. (2008) 299:769–77. doi: 10.1001/jama.299.7.769

9. Gullo D, Latina A, Frasca F, Le Moli R, Pellegriti G, Vigneri R. Levothyroxine monotherapy cannot guarantee euthyroidism in all athyreotic patients. *PloS One*. (2011) 6:e22552. doi: 10.1371/journal.pone.0022552

10. Stock JM, Surks MI, Oppenheimer JH. Replacement dosage of L-thyroxine in hypothyroidism. A re-evaluation. *N Engl J Med*. (1974) 290:529–33. doi: 10.1056/NEJM197403072901001

11. Penna GC, Bensenor IM, Bianco AC, Ettleson MD. Thyroid hormone homeostasis in levothyroxine-treated patients: findings from ELSA-brasil. *J Clin Endocrinol Metab*. (2024) 109:2504–12. doi: 10.1210/clinem/dgae139

12. Bunevicius R, Kazanavicius G, Zalinkevicius R, Prange AJ Jr. Effects of thyroxine as compared with thyroxine plus triiodothyronine in patients with hypothyroidism. *N Engl J Med*. (1999) 340:424–9. doi: 10.1056/NEJM199902113400603

13. Escobar-Morreale HF, Botella-Carretero JI, Gomez-Bueno M, Galan JM, Barrios V, Sancho J. Thyroid hormone replacement therapy in primary hypothyroidism: a randomized trial comparing L-thyroxine plus liothyronine with L-thyroxine alone. *Ann Intern Med*. (2005) 142:412–24. doi: 10.7326/0003-4819-142-6-200503150-00007

14. Nygaard B, Jensen EW, Kvetny J, Jarlov A, Faber J. Effect of combination therapy with thyroxine (T4) and 3,5,3'-triiodothyronine versus T4 monotherapy in patients with hypothyroidism, a double-blind, randomised cross-over study. *Eur J Endocrinol*. (2009) 161:895–902. doi: 10.1530/EJE-09-0542

15. Bunevicius R, Jakuboniene N, Jurkevicius R, Cernicat J, Lasas L, Prange AJ Jr. Thyroxine vs thyroxine plus triiodothyronine in treatment of hypothyroidism after thyroidectomy for Graves' disease. *Endocrine*. (2002) 18:129–33. doi: 10.1385/ENDO:18:2:129

16. Shakir MKM, Brooks DI, McAninch EA, Fonseca TL, Mai VQ, Bianco AC, et al. Comparative effectiveness of levothyroxine, desiccated thyroid extract, and levothyroxine+Liothyronine in hypothyroidism. *J Clin Endocrinol Metab*. (2021) 106:e4400–e13. doi: 10.1210/clinem/dgab478

17. Rodriguez T, Lavis VR, Meininger JC, Kapadia AS, Stafford LF. Substitution of liothyronine at a 1:5 ratio for a portion of levothyroxine: effect on fatigue, symptoms of depression, and working memory versus treatment with levothyroxine alone. *Endocr Pract*. (2005) 11:223–33. doi: 10.4158/EP.11.4.223

18. Walsh JP, Shiels L, Lim EM, Bhagat CI, Ward LC, Stuckey BG, et al. Combined thyroxine/liothyronine treatment does not improve well-being, quality of life, or cognitive function compared to thyroxine alone: a randomized controlled trial in patients with primary hypothyroidism. *J Clin Endocrinol Metab*. (2003) 88:4543–50. doi: 10.1210/jc.2003-030249

19. Appelhof BC, Fliers E, Wekking EM, Schene AH, Huyser J, Tijssen JG, et al. Combined therapy with levothyroxine and liothyronine in two ratios, compared with levothyroxine monotherapy in primary hypothyroidism: a double-blind, randomized, controlled clinical trial. *J Clin Endocrinol Metab*. (2005) 90:2666–74. doi: 10.1210/jc.2004-2111

20. Sawka AM, Gerstein HC, Marriott MJ, MacQueen GM, Joffe RT. Does a combination regimen of thyroxine (T4) and 3,5,3'-triiodothyronine improve depressive symptoms better than T4 alone in patients with hypothyroidism? Results of a double-blind, randomized, controlled trial. *J Clin Endocrinol Metab*. (2003) 88:4551–5. doi: 10.1210/jc.2003-030139

21. Clyde PW, Harari AE, Getka EJ, Shakir KM. Combined levothyroxine plus liothyronine compared with levothyroxine alone in primary hypothyroidism: a randomized controlled trial. *JAMA*. (2003) 290:2952–8. doi: 10.1001/jama.290.22.2952

22. Fadeyev VV, Morgunova TB, Melnichenko GA, Dedov II. Combined therapy with L-thyroxine and L-triiodothyronine compared to L-thyroxine alone in the treatment of primary hypothyroidism. *Hormones (Athens)*. (2010) 9:245–52. doi: 10.14310/horm.2002.1274

23. Saravanan P, Simmons DJ, Greenwood R, Peters TJ, Dayan CM. Partial substitution of thyroxine (T4) with tri-iodothyronine in patients on T4 replacement therapy: results of a large community-based randomized controlled trial. *J Clin Endocrinol Metab*. (2005) 90:805–12. doi: 10.1210/jc.2004-1672

24. Siegmund W, Spieker K, Weike AI, Giessmann T, Modess C, Dabers T, et al. Replacement therapy with levothyroxine plus triiodothyronine (bioavailable molar ratio 14: 1) is not superior to thyroxine alone to improve well-being and cognitive performance in hypothyroidism. *Clin Endocrinol (Oxf)*. (2004) 60:750–7. doi: 10.1111/j.1365-2265.2004.02050.x

25. Valizadeh M, Seyyed-Majidi MR, Hajibeigloo H, Momtazi S, Musavinasab N, Hayatbakhsh MR. Efficacy of combined levothyroxine and liothyronine as compared with levothyroxine monotherapy in primary hypothyroidism: a randomized controlled trial. *Endocr Res*. (2009) 34:80–9. doi: 10.1080/07435800903156340

26. Madan R, Celi FS. Combination therapy for hypothyroidism: rationale, therapeutic goals, and design. *Front Endocrinol (Lausanne)*. (2020) 11:371. doi: 10.3389/fendo.2020.00371

27. Garber JR, Cobin RH, Gharib H, Hennessey JV, Klein I, Mechanick JI, et al. Clinical practice guidelines for hypothyroidism in adults: cosponsored by the American Association of Clinical Endocrinologists and the American Thyroid Association. *Thyroid*. (2012) 22:1200–35. doi: 10.1089/thy.2012.0205

28. Guglielmi R, Frasoldati A, Zini M, Grimaldi F, Gharib H, Garber JR, et al. Italian association of clinical endocrinologists statement-replacement therapy for primary hypothyroidism: A brief guide for clinical practice. *Endocr Pract*. (2016) 22:1319–26. doi: 10.4158/EP161308.OR

29. Brenta G, Vaisman M, Sgarbi JA, Bergoglio LM, Andrada NC, Bravo PP, et al. Clinical practice guidelines for the management of hypothyroidism. *Arq Bras Endocrinol Metabol*. (2013) 57:265–91. doi: 10.1590/S0004-27302013000400003

30. Jonklaas J, Bianco AC, Cappola AR, Celi FS, Fliers E, Heuer H, et al. Evidence-based use of levothyroxine/liothyronine combinations in treating hypothyroidism: A consensus document. *Thyroid*. (2021) 31:156–82. doi: 10.1089/thy.2020.0720

31. Burch HB. Drug effects on the thyroid. *N Engl J Med*. (2019) 381:749–61. doi: 10.1056/NEJMra1901214

32. Celi FS, Zemskova M, Linderman JD, Smith S, Drinkard B, Sachdev V, et al. Metabolic effects of liothyronine therapy in hypothyroidism: a randomized, double-blind, crossover trial of liothyronine versus levothyroxine. *J Clin Endocrinol Metab*. (2011) 96:3466–74. doi: 10.1210/jc.2011-1329

33. Van Tassell B, Wohlford G, Linderman JD, Smith S, Yavuz S, Pucino F, et al. Pharmacokinetics of L-triiodothyronine in patients undergoing thyroid hormone therapy withdrawal. *Thyroid*. (2019) 29:1371–9. doi: 10.1089/thy.2019.0101

34. Watt T, Bjorner JB, Groenvold M, Rasmussen AK, Bonnema SJ, Hegedus L, et al. Establishing construct validity for the thyroid-specific patient reported outcome measure (ThyPRO): an initial examination. *Qual Life Res*. (2009) 18:483–96. doi: 10.1007/s11136-009-9460-8

35. Chen S, Wohlers E, Ruud E, Moon J, Ni B, Celi FS. Improving temporal accuracy of human metabolic chambers for dynamic metabolic studies. *PloS One*. (2018) 13:e0193467. doi: 10.1371/journal.pone.0193467

36. Chen S, Scott C, Pearce JV, Farrar JS, Evans RK, Celi FS. An appraisal of whole-room indirect calorimeters and a metabolic cart for measuring resting and active metabolic rates. *Sci Rep*. (2020) 10:14343. doi: 10.1038/s41598-020-71001-1

37. Mitchell C, Rahko PS, Blauwet LA, Canaday B, Finstuen JA, Foster MC, et al. Guidelines for performing a comprehensive transthoracic echocardiographic examination in adults: recommendations from the American society of echocardiography. *J Am Soc Echocardiogr*. (2019) 32:1–64. doi: 10.1016/j.echo.2018.06.004

38. Tei C, Ling LH, Hodge DO, Bailey KR, Oh JK, Rodeheffer RJ, et al. New index of combined systolic and diastolic myocardial performance: a simple and reproducible measure of cardiac function–a study in normals and dilated cardiomyopathy. *J Cardiol*. (1995) 26:357–66.

39. Chantler PD, Lakatta EG, Najjar SS. Arterial-ventricular coupling: mechanistic insights into cardiovascular performance at rest and during exercise. *J Appl Physiol (1985)*. (2008) 105:1342–51. doi: 10.1152/japplphysiol.90600.2008

40. Celi FS, Zemskova M, Linderman JD, Babar NI, Skarulis MC, Csako G, et al. The pharmacodynamic equivalence of levothyroxine and liothyronine: a randomized, double blind, cross-over study in thyroidectomized patients. *Clin Endocrinol (Oxf)*. (2010) 72:709–15. doi: 10.1111/j.1365-2265.2009.03700.x

41. Hauge C, Breitschaft A, Hartoft-Nielsen ML, Jensen S, Baekdal TA. Effect of oral semaglutide on the pharmacokinetics of thyroxine after dosing of levothyroxine and the influence of co-administered tablets on the pharmacokinetics of oral semaglutide in healthy subjects: an open-label, one-sequence crossover, single-center, multiple-dose, two-part trial. *Expert Opin Drug Metab Toxicol*. (2021) 17:1139–48. doi: 10.1080/17425255.2021.1955856

42. Ito M, Miyauchi A, Hisakado M, Yoshioka W, Kudo T, Nishihara E, et al. Thyroid function related symptoms during levothyroxine monotherapy in athyreotic patients. *Endocr J*. (2019) 66:953–60. doi: 10.1507/endocrj.EJ19-0094

43. Huynh CN, Pearce JV, Kang L, Celi FS. Weight gain after thyroidectomy: A systematic review and meta-analysis. *J Clin Endocrinol Metab*. (2021) 106:282–91. doi: 10.1210/clinem/dgaa754

44. Hall KD, Sacks G, Chandramohan D, Chow CC, Wang YC, Gortmaker SL, et al. Quantification of the effect of energy imbalance on bodyweight. *Lancet*. (2011) 378:826–37. doi: 10.1016/S0140-6736(11)60812-X

45. Azaria S, Cherian AJ, Gowri M, Thomas S, Gaikwad P, Mj P, et al. Impact of thyroidectomy on quality of life in benign goitres: results from a prospective cohort study. *Langenbecks Arch Surg*. (2022) 407:1193–9. doi: 10.1007/s00423-021-02391-7

46. Pilo A, Iervasi G, Vitek F, Ferdeghini M, Cazzuola F, Bianchi R. Thyroidal and peripheral production of 3,5,3'-triiodothyronine in humans by multicompartmental analysis. *Am J Physiol*. (1990) 258:E715–26. doi: 10.1152/ajpendo.1990.258.4.E715

47. Samuels MH, Kolobova I, Niederhausen M, Purnell JQ, Schuff KG. Effects of altering levothyroxine dose on energy expenditure and body composition in subjects treated with LT4. *J Clin Endocrinol Metab*. (2018) 103:4163–75. doi: 10.1210/jc.2018-01203

48. Jansen HI, Bruinstroop E, Heijboer AC, Boelen A. Biomarkers indicating tissue thyroid hormone status: ready to be implemented yet? *J Endocrinol*. (2022) 253:R21–45. doi: 10.1530/JOE-21-0364

49. Mentuccia D, Proietti-Pannunzi L, Tanner K, Bacci V, Pollin TI, Poehlman ET, et al. Association between a novel variant of the human type 2 deiodinase gene Thr92Ala and insulin resistance: evidence of interaction with the Trp64Arg variant of the beta-3-adrenergic receptor. *Diabetes*. (2002) 51:880–3. doi: 10.2337/diabetes.51.3.880

50. Peeters RP, van den Beld AW, Attalki H, Toor H, de Rijke YB, Kuiper GG, et al. A new polymorphism in the type II deiodinase gene is associated with circulating thyroid hormone parameters. *Am J Physiol Endocrinol Metab*. (2005) 289:E75–81. doi: 10.1152/ajpendo.00571.2004

51. Sterenborg R, Galesloot TE, Teumer A, Netea-Maier RT, Speed D, Meima ME, et al. The effects of common genetic variation in 96 genes involved in thyroid hormone regulation on TSH and FT4 concentrations. *J Clin Endocrinol Metab*. (2022) 107:e2276–e83. doi: 10.1210/clinem/dgac136

frontiers | Frontiers in Endocrinology

TYPE Original Research
PUBLISHED 14 March 2025
DOI 10.3389/fendo.2025.1567573

OPEN ACCESS

EDITED BY
Ryusuke Takechi,
Curtin University, Australia

REVIEWED BY
Rose Willett,
National Center for Toxicological Research (FDA), United States
Xinlei Guo,
Texas A and M University, United States
Leidyanne Ferreira Gonçalves Hernandez,
Fluminense Federal University, Brazil

*CORRESPONDENCE
Antje Garten
antje.garten@medizin.uni-leipzig.de

†PRESENT ADDRESS
Ana Mendes Teixeira,
School of Applied Sciences,
University of Huddersfield,
Huddersfield, United Kingdom

RECEIVED 27 January 2025
ACCEPTED 25 February 2025
PUBLISHED 14 March 2025

CITATION
Meyer J, Teixeira AM, Richter S, Larner DP, Syed A, Klöting N, Matz-Soja M, Gaul S, Barnikol-Oettler A, Kiess W, Le Duc D, Penke M and Garten A (2025) Sex differences in diet-induced MASLD – are female mice naturally protected? *Front. Endocrinol.* 16:1567573. doi: 10.3389/fendo.2025.1567573

Sex differences in diet-induced MASLD – are female mice naturally protected?

Jana Meyer[1], Ana Mendes Teixeira[1†], Sandy Richter[1], Dean P. Larner[2], Asifuddin Syed[2], Nora Klöting[3], Madlen Matz-Soja[4], Susanne Gaul[1,5], Anja Barnikol-Oettler[1], Wieland Kiess[1], Diana Le Duc[6,7], Melanie Penke[1] and Antje Garten[1*]

[1]Center for Pediatric Research, University Hospital for Children and Adolescents, Leipzig University, Leipzig, Germany, [2]Department of Biosciences, School of Science and Technology, Nottingham Trent University, Nottingham, United Kingdom, [3]Helmholtz Institute for Metabolic, Obesity and Vascular Research (HI-MAG) belonging to Helmholtz Center Munich at the University and University Hospital, Leipzig, Germany, [4]Division of Hepatology, Clinic and Polyclinic for Oncology, Gastroenterology, Hepatology, and Pneumology, University Hospital Leipzig, Leipzig, Germany, [5]Klinik und Poliklinik für Kardiologie, University Hospital Leipzig, Leipzig University, Leipzig, Germany, [6]Institute of Human Genetics, University Medical Center Leipzig, Leipzig, Germany, [7]Department of Evolutionary Genetics, Max Planck Institute for Evolutionary Anthropology, Leipzig, Germany

Males suffer more often from profibrotic changes in liver than females. The underlying mechanism for this sex difference in the prevalence and manifestation of Metabolic dysfunction-associated Steatotic Liver Disease (MASLD) is not yet completely known. We studied male and female mice that were induced to develop MASLD by consuming a "fast food" diet (FFD) and assessed metabolic phenotype as well as liver histology and compared them with mice fed with a matched control diet (CD). Our aim was to check for sex-specific differences in MASLD development in a mouse model of diet-induced profibrotic changes in the liver. Our results demonstrate a clear difference in body weight, fat distribution and changes in liver tissue for male and female mice fed with FFD. We found that female mice stored lipids mainly in subcutaneous and visceral adipose tissue while males increased ectopic lipid accumulation in the liver which resulted in hepatomegaly and increased *transforming growth factor β 1* (*Tgfb1*) and *collagen I* (*Col1a1*) expression concomitant to fibrosis development. This was absent in female mice. Analysis of estrogen receptor -α *(Esr1)* and -β *(Esr2)* expression revealed an upregulation of *Esr2* in livers of male FFD-fed mice whereas in female liver tissue a higher expression in *Esr1* could be observed. This study supports *Esr1* and *Esr2* as potential targets to reverse negative effects of diet-induced profibrotic changes in the liver.

KEYWORDS

MAFLD, NAFLD, high fat diet, adipose tissue, fibrosis, estrogen, collagen I

1 Introduction

Metabolic dysfunction-associated Fatty Liver Disease (MAFLD) (1) or Metabolic dysfunction-associated Steatotic Liver Disease (MASLD) (2), previously named non-alcoholic fatty liver disease (NAFLD), is the major chronic liver disease worldwide (3).

MASLD denominates a spectrum of liver diseases ranging from simple accumulation of triglycerides in liver (steatosis) to inflammation (steatohepatitis, MASH) and fibrosis (4, 5). The disease is strongly correlated with obesity and insulin resistance (6).

Hepatic fibrosis is characterized by an excessive deposition of extracellular matrix (ECM) that could evolve to cirrhosis or hepatocellular carcinoma (7). Previously thought to be irreversible (8), a number of studies have shown a potential reversal of all stages of fibrosis (9, 10). For this reason, understanding the process of fibrogenesis allows the identification of markers of disease progression and offers a potential target for therapeutic intervention.

One possible target could be transforming growth factor beta (Tgf β), which is involved in all stages of MASLD progression. Tgf β plays a pivotal role in fibrosis development through inducing ECM protein production and activating hepatic stellate cells (HSC) (11). These liver injury activated HSCs have a key function in liver regeneration too, and are the key producers of collagen, the deposition of which is involved in the development of fibrosis and which is the most abundant component of ECM (6, 12, 13).

The incidence of MASLD is highest in obese children and adult men; however incidences also increase in menopausal and postmenopausal women (14–16). A groundbreaking study was published in 2000, supporting the notion that sexually dimorphic risk factors are associated with MASLD (17). Many studies suggest that estradiol (E_2) can be responsible for these sex differences and variable incidence ratios. The estrogen receptors (Er) α and β are the mediators of estrogen action and expressed in adipose tissue. The precise role of Er α and β in MASLD development is not clarified. Previous studies demonstrated that hepatic steatosis occurred in *Esr1* knockout mice (18) but not in *Esr2* deficient male mice (19). In addition, estrogen deficiency promotes MASH progression in high-fat and high-cholesterol fed mice (20). Moreover, it has been shown that high fat diet-fed rats develop fatty liver and hepatic insulin resistance after three days of feeding (21). Fast food diet-fed mice show also higher levels of aspartate aminotransferase (ASAT) as indicator of hepatocyte damage compared to control diet fed mice (22).

Using this mouse model of diet-induced fibrosis MASH (22) we aimed to identify sex-specific differences in MASLD development and ascertain factors involved, which could be targeted to prevent fibrotic changes in metabolic liver disease.

2 Materials and methods

2.1 Chemicals and Reagents

Unless otherwise stated, chemicals were bought from Sigma-Aldrich (St Louis, USA).

2.2 Animal experiments

Mouse experiments were performed in accordance with the guidelines approved by the local authorities of the State of Saxony, Germany, as recommended by the responsible local animal ethics review board (Landesdirektion Saxony, Leipzig, TVV43/14). C57BL/6NCrl mice (28 male, 28 female), 6 weeks old, were purchased from the Medical Experimental Center, Leipzig University and randomized according to fat mass into 4 groups per sex (n=7 each). Mice were housed in groups of 3-4 at 22 ± 2°C on a 12 h light/dark cycle with free access to feed and water, checked daily for signs of illness and weighed once a week.

Starting from an age of 8 weeks, mice of both sexes were fed either a control diet (CD88137, 5.1% crude fat, 23.2% sugar, no cholesterol) or the "fast food" diet, a modified Western diet (TD88137, Ssniff, Soest, Germany) containing 21.2% crude fat, 33.2% sugar and 2% cholesterol, providing 40% of energy as fat (milk fat, 12% saturated) for 16 or 24 weeks. This resulted in a total of 8 experimental groups, four per time point. Drinking water for both control and fast food diet groups was supplemented with 42 g/l sugar solution (55% fructose and 45% glucose). This dietary regimen has been described previously to recapitulate features of the metabolic syndrome and NASH with progressive fibrosis (22). Lean and fat mass were assessed by EchoMRI™ in week 8, 15 and 23. Intraperitoneal glucose tolerance tests (GTTs) were performed at the age of 16 and 24 weeks after an overnight fast of 12 h by injecting 2 g glucose per kg body weight. Blood samples for glucose measurements were taken from the tail vein after 0, 15, 30, 60, and 120 min and measured by using an automated glucose monitor (GlucoMen; Menarini Diagnostics, Wokingham, U.K.) as described previously (23). Mice were sacrificed by CO_2 asphyxiation, followed by cardiac puncture for blood collection and by organ collection. Blood was incubated at room temperature for 1h and centrifuged at 10 min, 2500 x *g* for serum collection to measure liver enzymes and glycated haemoglobin (HbA1c). Organs (liver, subcutaneous fat (SAT), epididymal [visceral] fat (VAT)) were harvested, weighed and processed for histological and biochemical analyses or snap frozen in liquid nitrogen.

2.3 Laboratory analyses

HbA1c and activities of alanine aminotransferase (ALAT) and aspartate aminotransferase (ASAT) in serum were measured spectrophotometrically as indicators of hepatocellular disintegration and necrosis using a Cobas C111 analyzer (Roche Diagnostics; Rotkreuz, Switzerland) according to the manufacturer's instructions.

2.4 Histological analyses

Adipose tissue histology, measurements of lipid droplet size and number and adipocyte size distributions analyses were performed as previously described (24). A liver lobe (*lobus hepatis sinister*) was

fixed in 4% paraformaldehyde for 3 days, paraffin-embedded and stained with hematoxylin and eosin for histological evaluation of the percentage of liver fat. Hepatic steatosis was quantified using ImageJ (25)from 100x magnified TIFF micrographs (n = 5-7 images per experimental group) and represented as the percentage of vacuoles as a proxy for lipid accumulation present in each section. Picrosirius red staining was used for fibrillar collagen detection and quantified using ImageJ analysis of 200x magnified TIFF micrographs (26) (n=6-7 images per experimental group). Another lobe (*lobus medialis dexter*) was cryo-embedded in Tissue-Tek and cryo-sectioned (6 µm), fixed in 4% formalin and stained with Oil-Red O for lipid droplet quantification with ImageJ (n=4-6 images per experimental group) as described previously (27). For visualization, an EVOS FL Auto 2 microscope (Thermo Scientific) was used.

2.5 Gene expression analysis

Total RNA of liver tissue was extracted using TRIzol® Reagent (Life Technologies) according to manufacturer's protocol. 1 µg of total RNA was transcribed into cDNA by M-MLV Reverse Transcriptase (#28025013, Invitrogen). Quantitative PCR analyses were performed using the Absolute qPCR SYBR Green Low ROX Mix (Thermo Scientific) or qPCR Master Mix Plus ROX (Eurogentec) and the Applied Biosystems QuantStudio 3 System (Thermo Scientific). Gene expression values are shown as fold changes respective to male CD fed mice. *Cyclophilin b* alternatively designated as *peptidylprolyl isomerase b* (*Ppib*) or *hypoxanthin-phosphoribosyltransferase* (*Hprt*) were used as housekeeping genes for normalization. The specific primer sequences are listed in Supplementary Table S1.

2.6 Statistical analysis

All statistical analyses were performed using GraphPad Prism version 10.2.3 for Windows, GraphPad Software, Boston, Massachusetts USA, www.graphpad.com. Analyses comparing male and female mice on CD or FFD (sex and diet as independent variables) were performed using two-way analyses of variance (ANOVA) with subsequent Tukey´s multiple comparisons *post hoc* test. Differences in gene expression fold changes were tested with one sample *t*-test. All data were presented as means ± SD. Statistical significance was defined as $p < 0.05$.

3 Results

3.1 Female FFD-fed mice stored more fat in adipose tissue depots than males

To determine the sex-specific impact of FFD, we measured body weight, fat and lean mass, the weight of adipose tissue depots and mean adipocyte size after 16 and 24 weeks on the respective diets. As expected, body weight of all mice, regardless of sex and diet, increased over the course of time (Figure 1A). Male FFD-fed mice gained weight faster and had a higher mean weight at the end of the 24-week period (47.0g ± 2.0g, n=7) than FFD females (38.7g, ± 1.9g, n=7) and CD male mice (35.8g ± 5.5g, n=7). Female mice on CD had the lowest body weight (31.0g ± 3.2, n=7, Figure 1B).

We compared fat mass, subcutaneous adipose tissue (SAT) and visceral adipose tissue (VAT) normalized to body weight at 16 weeks with 24 weeks. Fat mass was higher in both male and female FFD-fed mice compared to CD-fed mice at both 16 and 24 weeks, while there were no differences in fat mass between males and females on FFD at either time point (Figures 1C, D). Interestingly, at 16 weeks, fat mass of CD-fed mice was higher in males (10.9g ± 2.0g, n=6) compared to females (3.6g ± 1.0g, n=7; p<0.0001, Figure 1C), which was not the case anymore at 24 weeks (males 15.7 ± 3.1g, females 14.1 ± 2.8g, Figure 1D). Lean mass was not different between diets at any time point, but higher in males than in females on their respective diet at 24 weeks (Supplementary Figures S1A, B).

To examine sex-specific differences in fat deposition, we took a closer look at SAT and VAT weight. At 16 weeks, female mice on FFD had significantly more SAT relative to their body weight (3.4 ± 0.3, n=7) than FFD-fed males (2.4 ± 0.6, n=6, p=0.00332, Figure 1E) and CD females (1.4 ± 0.5, n=7, p<0.0001; Figure 1E). At 24 weeks, the difference between CD and FFD-fed mice was significant only for males (1.8 ± 1.0 vs. 2.8 ± 0.5, n=7, p=0.0296), while CD-fed females had accumulated more SAT/body weight than CD-fed males (2.8 ± 0.7 vs. 1.8 ± 1.0, n=7, p=0.0474). There was no more difference in SAT/body weight between CD and FFD-fed females at 24 weeks (Figure 1F).

For VAT/body weight, there was neither a difference between FFD-fed males and females or between FFD and CD-fed males at 16 weeks (Figure 1G), while CD-fed females had significantly less VAT/body weight than FFD-fed females (1.3 ± 0.4 vs. 4.2 ± 0.9, n=7, p<0.0001, Figure 1G) or CD-fed males (1.3 ± 0.4 vs. 3.6 ± 1.2, n=7, p=0.0003, Figure 1G). At 24 weeks, FFD-fed females has increased VAT/body weight, so that it was significantly more compared to FFD-fed males (5.8 ± 0.6 vs. 3.3 ± 0.6, n=7, p<0.0001, Figure 1H).

Absolute SAT (Supplementary Figures S1C, D) and VAT (Supplementary Figures S1E, F) masses were similar to the normalized masses. No significant differences in adipocyte size could be measured after 16 (data not shown) or 24 weeks for both adipose tissue depots (Supplementary Figures S1G, H).

Glucose tolerance at 16 weeks was similar in FFD-fed mice and CD-fed males, with CD-fed females having a smaller area under the curve (AUC, Supplementary Figures S2A, C; p=0.0008 comparing CD fed male mice and p<0.0001 comparing female FFD mice, n=6-7) than the other experimental groups. This difference vanished at 24 weeks with AUCs being similar in all groups (Supplementary Figures S2B, D). Fasting blood glucose was higher in FFD-fed compared to CD-fed mice of the respective sex (Supplementary Figures S2E, F). HbA1c was higher in male compared to female mice, but not different between CD and FFD-fed mice (Supplementary Figures S2G, H).

Collectively, we found sex-specific differences of body weight and fat distribution between male and female mice. Female FFD-fed

10.3389/fendo.2025.1567573

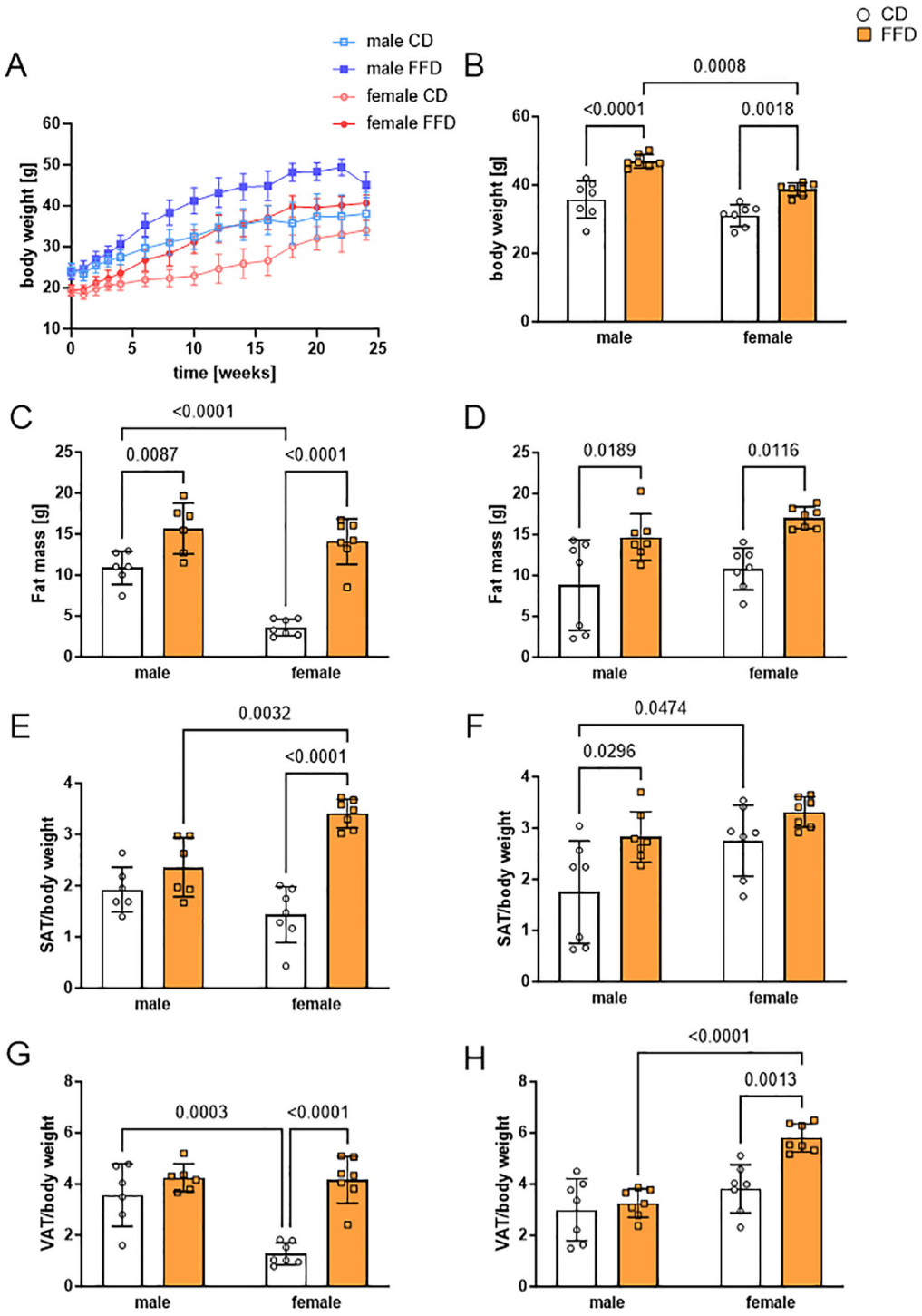

FIGURE 1
Fast food diet (FFD) fed mice showed sex-dependent differences in body weight, fat mass, and subcutaneous (SAT) or visceral (VAT) adipose tissue compared to control diet (CD) fed mice. **(A)** Body weight increase over the time course of the study (24 weeks). Male FFD mice in dark blue, male CD mice in light blue (both groups n = 13 until week 16, n = 7 until week 24), female FFD mice in dark red, female CD mice in light red (n = 14 until week 16, n = 7 until week 24). **(B)** At 24 weeks, male mice fed with FFD had a higher body weight compared to FFD-fed female (1.2fold, p=0.0008) and CD-fed male mice (1.3fold, p<0.0001). **(C)** At 16 weeks, fat mass of both FFD-fed groups was higher compared to CD-fed mice. CD-fed males had higher fat mass than CD-fed females (3fold, p<0.0001). **(D)** At 24 weeks, fat mass was increased in FFD-fed vs. CD-fed mice for both, males (1.7fold, p=0.0189) and females (1.6fold, p=0.0116). **(E)** At 16 weeks, SAT per body weight was higher in FFD female mice than in CD female mice (2.4fold, n=7 per group, p<0.0001) and FFD male mice (1.4fold, p=0.0032). **(F)** At 24 weeks, SAT per body weight was higher in FFD-fed compared to CD-fed male mice (1.6fold, p=0.0296). **(G)** At 16 weeks, VAT per body weight was higher in FFD-fed compared to CD-fed female mice (3.2fold, p<0.0001). Male CD-fed mice had higher VAT per body weight than female CD-fed mice (2.8fold, p=0.0003). **(H)** At 24 weeks, FFD-fed females had a higher VAT per body weight than both, CD-fed females (1.5fold, p=0.0013) and FFD-fed males (1.8fold, p<0.0001). Data are presented as mean ± SD, with points indicating 6-7 mice per group. Differences <0.05 were considered significant as determined by two-way analyses of variance (ANOVA) with subsequent Tukey´s multiple comparisons *post hoc* test.

mice had more SAT then CD-fed females already at 16 weeks and increased their VAT depot at 24 weeks, whereas male mice on FFD had similar amounts of SAT than CD males and showed increased SAT at 24 weeks. This points to a sex-dependent difference in the preferred fat storage depot in this animal model.

3.2 Fast food diet causes lipid accumulation mainly in livers of male mice

We next checked for sex-specific differences regarding fat storage in the liver. Liver per body weight of 16 week old mice was significantly higher in FFD-fed compared to CD-fed males (1.6fold, n=6, p<0.0001) and compared to female FFD-fed mice (1.3fold, n=6 males, 7 females, p=0.0055, Figure 2A). Similar differences in liver/body weight were seen at 24 weeks in males (CD male 4.1± 0.8, n=7, FFD male 7.1 ± 1.3, n=7, p<0.0001). In 24 week old females, the liver weight difference between FFD and CD-fed mice became significant (CD female 4.4 ± 0.8, n=7, FFD female 6.0 ± 1.1, n=7, p=0.0247; Supplementary Figure S3A). The macroscopic differences between livers of male FFD and CD mice were also obvious, with livers from FFD mice being considerably bigger and paler than from CD mice (Supplementary Figure S3B). Similarly, absolute liver weights were also higher in FFD males (2.9g ± 0.7g, n=6) compared to CD males (1.5g ± 0.3, n=6, p<0.0001) and to FFD females (1.8g ± 0.3, n=7, p=0.0004) after 16 weeks (Supplementary Figure S3C) and after 24 weeks (Supplementary Figure S3D). This suggests that the amount of liver fat in females increased between 16 and 24 weeks. Moreover, livers from male FFD-fed mice were heavier than the FFD-fed female ones.

Liver lipid accumulation was visible as vacuoles in both male and female mouse livers from FFD-fed mice after 16 (Figure 2B) and 24 (Supplementary Figure S4A) weeks, but was more pronounced in livers from male FFD-fed mice. Quantification showed a significantly higher percentage of steatosis in FFD-fed compared to CD-fed mice at 16 weeks (males: 3fold, n=,6, p=0.0157; females 4.8fold, n=5,6, p=0.0958, Figure 2C). At 24 weeks, there was no significant difference between male and female mice on either diet (Supplementary Figure S3E).

Hepatocellular ballooning as a sign for hepatocyte damage could be observed in some livers from FFD-fed mice, both at 16 and 24 weeks (Supplementary Figure S4B). In contrast, we did not observe any signs of immune cell infiltration, based on images from H&E stained tissue (Supplementary Figures S4A, B).

In order to examine markers for liver damage, we measured serum liver enzymes alanine aminotransferase (ALAT) and aspartate aminotransferase (ASAT). After 16 weeks, ALAT was significantly higher in male FFD-fed compared to CD-fed mice (p=0.0262; Figure 2D), implying more damage to hepatocytes in FFD males. This difference persisted at 24 weeks (Supplementary Figure S3F). ASAT measurements did not show significant differences (data not shown).

To assess histological changes, more specifically the incorporation of lipids into hepatocytes, we measured lipid droplet content by Oil Red O (ORO) staining (Figure 2E). We found that livers from male mice after FFD feeding presented more and bigger lipid droplets than the female ones, especially at 24 weeks. Already at 16 weeks, males on FFD showed a 4.1fold higher number of hepatic lipid droplets compared to CD males (n=4, p=0.026, Figure 2F). Although there were more hepatic lipid droplets also in female mice on FFD compared to CD, the difference was not significant (Figure 2F). After 24 weeks, males on FFD showed an 8.5fold higher hepatic lipid droplet number than CD males (n=5, p=0.025), while in females, hepatic lipid droplet number was similar between CD and FFD-fed mice (Supplementary Figure S3G).

The size of hepatic lipid droplets was not significantly different between CD-fed and FFD-fed mice after 16 weeks (Figure 2G). After 24 weeks, FFD-fed mice of both sexes showed larger hepatic lipid droplets (males 5.4 ± 0.5 µm compared to 3.1 ± 0.5 µm, n=5; p=0.0004, females 4.9 ± 1.0 µm compared to 3.2 ± 0.5 µm, n=6, p=0.0023) compared to the respective CD-fed mice (Supplementary Figure S3H).

3.3 FFD feeding promotes signs of fibrosis only in male mouse livers

Given the increased amount of hepatic lipids and significantly higher ALAT serum levels in male FFD-fed mice, we next examined the extent of collagen deposition as a measure for profibrotic changes at 16 and 24 weeks. We did not see picrosirius red (PSR) staining after 16 weeks (data not shown), but found more PSR positive areas in livers of male FFD-fed mice compared to CD-fed mice after 24 weeks. Quantification of staining suggested a higher amount of collagen deposition in livers of FFD-fed male mice compared to either FFD-fed females or CD-fed mice, however with a large phenotypic variation (FFD males: 2.1 ± 0.7, n=6, vs. FFD females: 0.2 ± 0.1, p<0.0001, Figure 3A). There were no obvious PSR positive areas in livers from female mice on either diet or CD fed mice (Figure 3B). This finding was supported by significantly increased hepatic *collagen I* (*Col1a1*) expression in male FFD-fed mice, which was detected already after 16 weeks compared to CD-fed males (5.2fold, n=6, p=0.0108, Figure 3C) and FFD-fed females (3.2fold, n=5, p=0.0438; Figure 3C). The same was seen at 24 weeks with livers of FFD-fed males showing a 7-fold higher *Col1a1* expression compared to CD-fed males (n=5-6, p=0.0050, Supplementary Figure S5A) and 2.9fold higher compared to FFD-fed females (n=5 - 6, p=0.0365, Supplementary Figure S5A).

We then asked what factors could contribute to increased collagen synthesis and measured the mRNA expression of *transforming growth factor beta 1 (Tgfb1)*, which we hypothesized to be higher in livers of FFD-fed mice. In fact, at 16 weeks FFD feeding was associated with an increase in *Tgfb1* expression in male mouse livers compared to male CD-fed mice (2.4fold, n=5-6, p=0.0095) and to female FFD-fed mice (2fold, n=5-6, p=0.0187, Figure 3D). At 24 weeks, livers of male FFD-fed mice showed the highest *Tgfb1* expression (4fold higher in comparison to male CD, n=6, p=0.0315, Supplementary Figure S4B), but no significant difference to FFD-fed females (Supplementary Figure S4B). It is interesting to note that hepatic *Tgfb1* expression in female mice hardly changed, regardless of diet or time point. Gene expression of

10.3389/fendo.2025.1567573

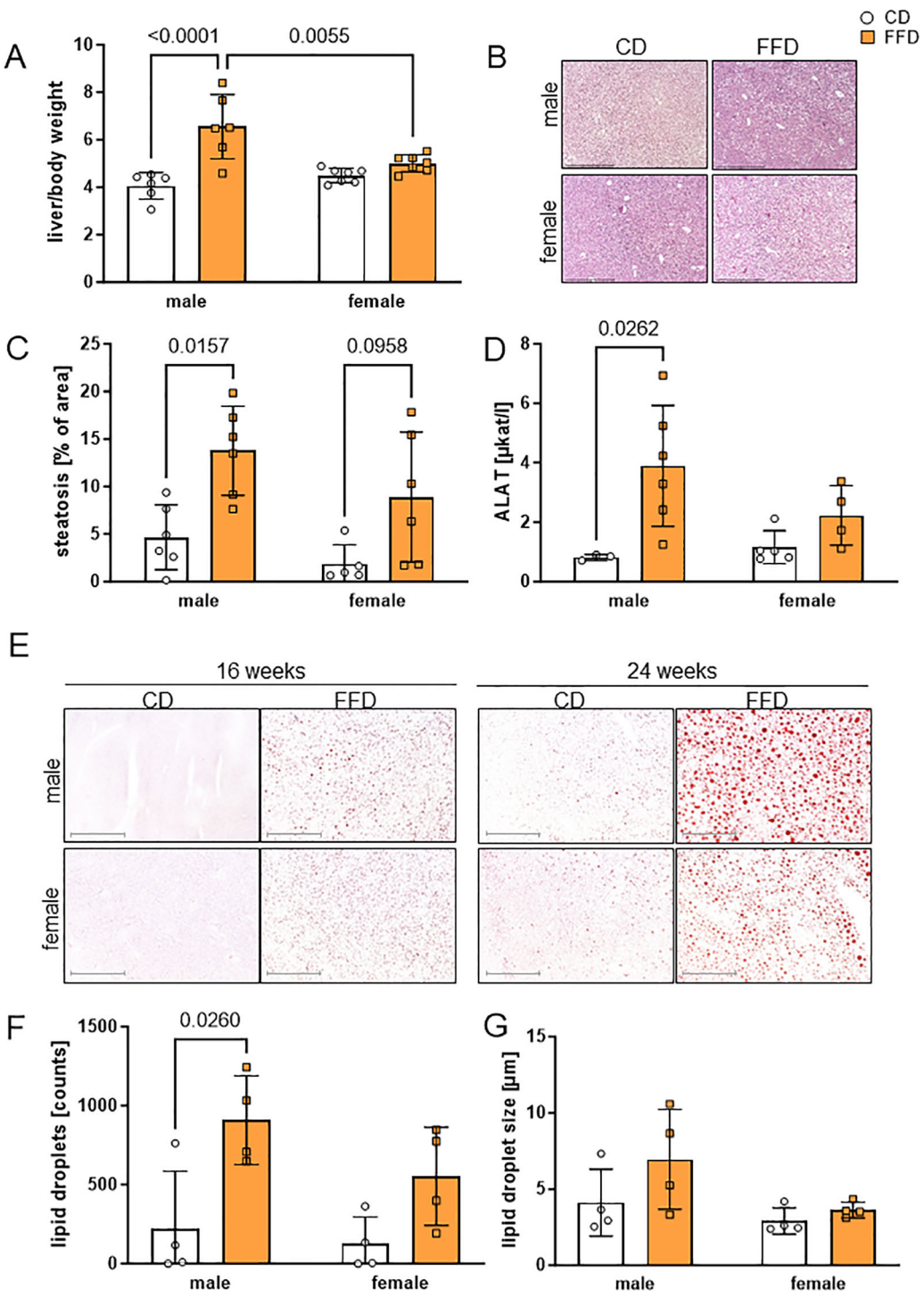

FIGURE 2
Fast food diet (FFD) was associated with progressive accumulation of lipids compared to control diet (CD) in male mouse livers. **(A)** At 16 weeks, weight of liver per body weight was higher for males on FFD compared to CD males (1.6fold, p<0.0001) and FFD females (1.3fold, p=0.0055). **(B)** Representative micrographs of male (upper) and female (lower) paraffin-embedded, hematoxylin/eosin stained mouse liver sections (100x magnification, scale bar 500 µm) at 16 weeks on CD (left) or FFD (right). **(C)** At 16 weeks, percentage of hepatic steatosis was higher in FFD males compared to CD males (3fold, p=0.0157) and showed a trend towards higher values in female livers (4.8fold, p=0.0958). **(D)** At 16 weeks, alanine aminotransferase (ALAT) was higher in male FFD compared to CD mice (4.7fold, p=0.0262). **(E)** Lipid droplet content in male and female mouse livers detected by Oil Red O staining at 16 and 24 weeks of CD or FFD feeding. Representative images for each time point, sex and diet are shown (magnification 100x, scale bar 500µm). Quantification of **(F)** lipid droplet number and **(G)** lipid droplet size after 16 weeks. Lipid droplet number was higher in livers from male FFD compared to CD mice (4.1fold, p=0.026). Data are presented as mean ± SD, points represent 3-7 mice per group, differences <0.05 were considered significant as determined by two-way analyses of variance (ANOVA) with subsequent Tukey´s multiple comparisons *post hoc* test.

10.3389/fendo.2025.1567573

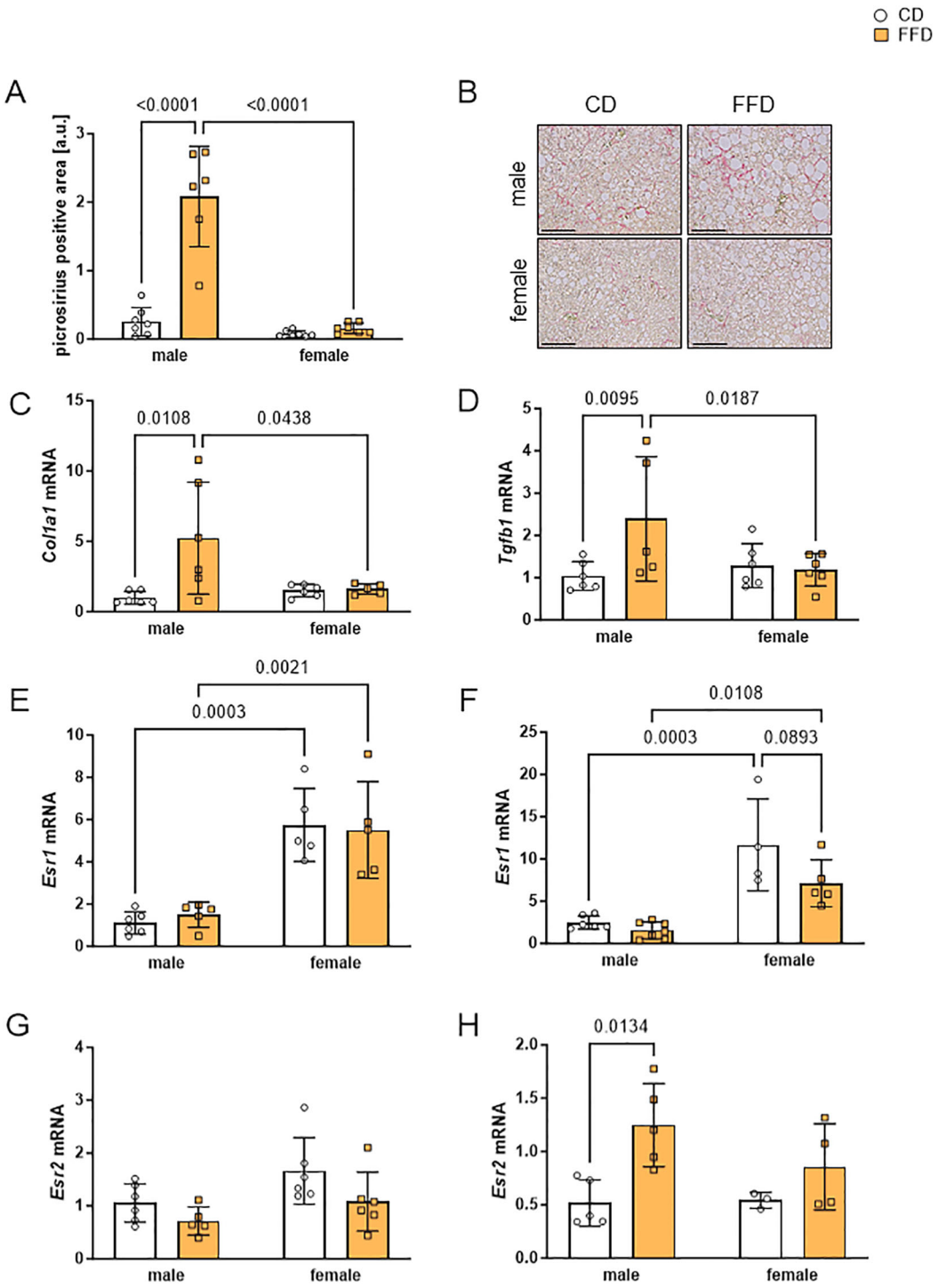

FIGURE 3
Livers from male fast food diet (FFD)-fed mice showed profibrotic changes and gene expression differences compared to FFD females and control diet (CD)-fed males. **(A)** Densitometric quantification of picrosirius red (PSR)-positive areas at 24 weeks showed more PSR-positive stained liver tissue in FFD males compared to CD males (8.1fold, p<0.0001) or to FFD females (13fold, p<0.0001). **(B)** Representative images of PSR- stained liver sections from male (upper) and female (lower) mice on CD (left) or FFD (right) for 24 weeks (magnification 200x, scale bar 200 µm). Hepatic gene expression was analyzed at 16 weeks on CD or FFD of **(C)** *collagen I* (*Col1a1)* and **(D)** *transforming growth factor beta 1* (*Tgfb1). Col1A1* and *Tgfb1* were increased in FFD males compared to CD males (*Col1A1*: 5.2fold, p=0.0108; *Tgfb1:*2.4fold, p=0.0095) and to FFD females (*Col1A1:* 3.2fold, p=0.0438; *Tgfb1:*2fold, p=0.0187). Gene expression of *estrogen receptor α* (*Esr1)* after **(E)** 16 and **(F)** 24 weeks. At 16 weeks, *Esr1* expression was 6fold higher in female mouse livers regardless of diet. At 24 weeks, *Esr1* expression in livers from female CD mice was 4.7fold (p=0.0003) and from female FFD mice 4.6fold (p=0.0108) increased compared to livers from male mice on the respective diet. Gene expression of *estrogen receptor β* (*Esr2)* after **(G)** 16 and **(H)** 24 weeks. Hepatic expression of *Esr2* was similar in all groups after 16 weeks. At 24 weeks, *Esr2* expression was higher in male FFD-fed compared to CD-fed mice (2.4fold, p=0.0134). Data are shown as mean fold changes ± SD related to expression values in CD male mice, with points indicating 4-7 mice per group. *Cyclophilin b (Ppib)* or *hypoxanthine phosphoribosyltransferase (Hprt)* were used as housekeeping genes. Statistical significance was defined as p<0.05 and tested by one sample *t*-test.

the gluconeogenic enzyme *phosphoenolpyruvate carboxykinase* (*Pepck*, Supplementary Figure S5C) and *glucose-6-phosphate dehydrogenase* (*G6pdh*, Supplementary Figure S5D), involved in the pentose phosphate pathway, was higher in livers of male FFD-fed compared to CD-fed male mice after 16 weeks, with a significant difference for *Pepck* expression (1.8fold, n=6, p=0.0128) and a trend towards significantly different *Pepck* expression compared to female FFD mice (Supplementary Figure S5C).

Because estradiol levels are obviously different between male and female mice and estradiol is known as a factor protecting from metabolic liver disease, we analyze *estrogen receptors alpha* (*Esr1*) and beta (*Esr2*) gene expression. *Esr1* and *Esr2* had different expression patterns (Figures 3E-H). At 16 weeks, female livers presented 4fold higher *Esr1* expression compared to male livers after CD (n=5-6, p=0.0003, Figure 3E) or FFD-feeding (n=5, p=0.0021, Figure 3E). At 24 weeks, hepatic *Esr1* expression in female mice was 4.7fold higher compared to males (CD, n=4-6, p=0.0003; FFD, n=5-6, p=0.0108; Figure 3F), but we saw a trend towards higher hepatic *Esr1* expression in female CD-fed mice compared to FFD-fed females (1.6fold higher in CD vs. FFD, n=4,5, p=0.0893). Hepatic *Esr2* expression was similar in all conditions at 16 weeks (Figure 3G). After 24 weeks, livers from male FFD mice demonstrated a higher *Esr2* expression compared to CD males (2.4fold, n=5, p=0.0134, Figure 3H).

4 Discussion

Both the prevalence and incidence of MASLD are increasing dramatically worldwide, reaching epidemic proportions with its onset occurring at younger ages in recent years (28–31). MASLD is now the second leading indication for liver transplantation (32) and accounts for an increasing proportion of hepatocellular carcinoma (33). The need to understand underlying pathomechanisms is therefore very considerable and medically significant.

According to the World Health Organization, the main reason for this dramatic trend in MASLD and Metabolic Dysfunction-associated Steatohepatitis (MASH) is the rising prevalence of obesity worldwide (34), which is partly due to increased food intake and a sedentary lifestyle (35). However, it should be noted that there are sex-specific differences. MASLD mainly and increasingly affects adult men (17, 36). Generally, women of fertile age have a lower risk of MASLD than men, while this protection is lost after menopause, when women have a MASLD prevalence comparable to men (14, 37). The underlying causes are still not fully understood. To learn more about this sexual dimorphism in diet-induced hepatic fibrosis development of MASLD we used a mouse model of metabolic liver disease induced by a “fast food diet” (FFD) high in saturated fat, fructose and cholesterol that was described to induce profibrotic changes and hepatocyte damage in murine liver (22). We compared the phenotype of male with that of female mice and found key differences in fat distribution, gene expression and fibrosis development. Of note, in the original study (22), both male and female mice were included in each experimental group without mentioning sex-dependent differences in phenotype.

As expected, both male and female mice on FFD gained more weight over the course of the study than mice on CD, with a bigger increase in male compared to female mice on FFD, as has previously been shown in other studies (14, 22, 38). Checking WAT depot mass at two time points during MASLD development, we could show that, in contrast to males, female mice on FFD primarily showed an increase in subcutaneous and, subsequently, visceral white adipose tissue (WAT) depots. Sex differences in fat deposition and mobilization in adipose tissue have previously been described in mice (39) and humans (40–42), with predominant lipid accumulation in subcutaneous WAT in females and visceral WAT in males. Interestingly, adipose tissue of the visceral WAT compartment contributes more to hepatic fatty acid uptake than subcutaneous WAT because of its anatomical position (43).

We also found sex-dependent differences in hepatic lipid accumulation, with male mice having bigger livers with a higher percentage of steatosis and more lipid droplets already after 16 weeks on FFD. While they did not quite reach the liver/body weight ratio reported by Charlton et al. (7.1 ± 1.3 vs. 8.5), male FFD-fed mice in our study also did not accumulate substantially more hepatic lipids at 24 (7.1 ± 1.3) than at 16 weeks (6.6 ± 1.4). In contrast, female FFD-fed mice reached a higher liver/body weight ratio than CD-fed only at 24 weeks, pointing to a delayed storage of lipids in the liver. This delay of adverse effects of FFD in females was also seen when checking serum levels of ALAT and number of lipid droplets. Large lipid droplets are a hallmark of steatosis (44, 45) There is evidence that the accumulation of lipids in the liver is linked to liver fibrosis, inflammation, apoptosis and cancer (11, 46). Blood glucose levels during GTT were strikingly lower in CD-fed female mice compared to the other groups at 16 weeks, pointing to a faster glucose metabolism and mirroring the lower overall fat mass as well as visceral fat per body weight in CD-fed females. This difference was lost completely at 24 weeks, when glucose tolerance was similar between all groups regardless of diet or sex. In contrast, Charlton et al. observed a significant higher blood glucose level after weeks on fast food vs. control diet or a high fat diet, indicating a bigger impact of fast food diet on glucose metabolism than in our study. Other differences included a higher level of ASAT and higher expression of myofibroblast activation marker anti-smooth muscle actin (ASMA, data not shown) (22), for both parameters we did not detect differences. There are several potential reasons for these differences in phenotype, such as different mouse strains (C57/B6J vs. C57/B6NCrl) and different animal facility (47), which was shown to exerts a mayor influence on mouse phenotypes (47, 48).

Tgf β has been recognized as a key molecular regulator in hepatic fibrosis. Its fibrogenic effects are mainly associated with hepatic stellate cell (HSC) activation and the production of extracellular matrix (ECM) protein, e.g. collagen (11). Moreover,

Tgf β signaling in hepatocytes under metabolic stress mediates hepatocyte death and lipid accumulation (49, 50), which are processes leading to the development of steatohepatitis (50).

Our study revealed that in contrast to fat accumulation, *Tgfb1* and *Col1a1* expression increased over time in male livers, suggesting that fibrosis was exacerbated with prolonged FFD feeding. This points to a sex difference in fibrosis development, as we did not observe these gene expression changes in the female mouse livers.

Previous studies have shown that estradiol prevented reactive oxygen species and *Tgfb1* production in cultured rat HSC (51). Interestingly, another study showed that the fibrogenic genes, *Tgfb1* and *Col1a1*, were upregulated in the livers of female ovariectomized and high-fat/high-cholesterol-fed mice (20). Estradiol and its derivatives were previously shown to be potent endogenous antioxidants that reduce lipid peroxide levels, are linked to fat metabolism in the liver (52, 53) and associated with sex-specific differences in fibrosis development (14, 36, 54).

Because hepatic estrogen receptors (Er) α and/or β mediate estrogen action (54), we asked whether the expression of these receptors shows sex-dependent differences in mouse livers, which could provide an explanation for the previously observed sex-specific differences in fibrosis development. A recent rodent study revealed that Er α, but not Er β, plays an essential role together with peroxisome proliferator-activated receptor-γ coactivator 1 α (Pgc1a). Expression of Pgc1a was shown to be inversely correlated with liver fat and MASLD severity. Er α partnering with Pgc1a is associated with a reduction of oxidative stress damage and impairs the transition from steatosis to severe steatohepatitis (55). Furthermore, *Esr1* knockout mice develop hepatic steatosis more often than their wild-type controls as a consequence of the increased expression of genes involved in *de novo* lipogenesis (18, 56). Similar protective effects of Er α were also found in other studies (57–59). In contrast to these studies, hepatic Er α was shown to be not required for the protection against FFD-induced hepatic steatosis in female mice and did not mediate sexual dimorphism in liver mitochondria function (60). Er β expression was found to be favorable in different animal models of liver injury (61, 62) mainly acting through suppression of hepatic stellate cell activation (63).

In our study, *Esr1* and *Esr2* mRNA levels encoding for Er α and β, respectively, were similar in livers from 16-week-old male mice, but differed in female livers, with a higher expression of *Esr1* in female mouse livers at 16 weeks, which was, however, not dependent on diet. High hepatic *Esr1* expression was also reported in other studies, where normal rat livers primarily express *Esr1* with low levels of *Esr2* (64). Interestingly, in our study, expression of *Esr2* was doubled in male livers from FFD-fed mice after 24 weeks, while there was a trend towards higher *Esr2* expression, but no significant changes in *Esr1* expression in female livers. This could suggest a compensatory upregulation of hepatic *Esr2* in males to prevent further damage after prolonged FFD.

In humans, the occurrence of MASLD was found to be higher in menopausal and postmenopausal than in premenopausal women (36). Besides, ovarian senescence, via hypo-estrogenemia, facilitates both the development of massive hepatic steatosis and the fibrotic progression of liver disease (65). The creation of novel medications based on the protective effects of estrogens could provide new therapeutic strategies for the treatment of MASLD (66). Our results support this proposed concept and additionally point specifically to Er β as potential target for novel MASLD treatment options.

In summary, we found that a diet high in fat, fructose and cholesterol led to an increased fat accumulation and an upregulation of profibrotic factors in livers of male mice, while female mice appeared to store excess fat mainly in subcutaneous and visceral adipose tissue depots. We also saw a diet- and time-associated change in expression patterns of estrogen receptors which was more pronounced in male mouse livers. Female mice seemed to be protected against these profibrotic changes.

Data availability statement

The raw data supporting the conclusions of this article will be made available by the authors, without undue reservation.

Ethics statement

The animal study was approved by Landesdirektion Saxony, Leipzig, TVV43/14. The study was conducted in accordance with the local legislation and institutional requirements.

Author contributions

JM: Formal analysis, Visualization, Writing – original draft, Writing – review & editing. AT: Investigation, Visualization, Writing – original draft. SR: Investigation, Writing – review & editing. DL: Formal analysis, Methodology, Writing – review & editing. AS: Methodology, Writing – review & editing. NK: Methodology, Resources, Supervision, Writing – review & editing. MM: Methodology, Resources, Writing – review & editing. SG: Conceptualization, Writing – review & editing. AB: Investigation, Writing – review & editing. WK: Supervision, Writing – review & editing. DD: Formal analysis, Methodology, Writing – review & editing. MP: Conceptualization, Funding acquisition, Investigation, Project administration, Supervision, Visualization, Writing – original draft, Writing – review & editing. AG: Conceptualization, Funding acquisition, Project administration, Supervision, Writing – original draft, Writing – review & editing.

Funding

The author(s) declare that financial support was received for the research and/or publication of this article. This work was funded by the EFSD Albert Renold Travel Fellowship Programme to MP, the German Research Foundation (DFG) through SFB 1052, project number 209933838, subproject B4 to NK and B10 to DLD and AG and grants 031L0313C and 031L0256C to MM. We acknowledge

support from the German Research Foundation (DFG) and Leipzig University within the program of Open Access Publishing. The funders had no role in the design of the study; in the collection, analyses, or interpretation of data; in the writing of the manuscript; or in the decision to publish the results. AMT was supported by the EU ERASMUS programme.

Acknowledgments

We thank the teams of the Medical Experimental Center (MEZ) Medical Faculty, Leipzig University, and of the Institute of Laboratory Medicine, Clinical Chemistry and Molecular Diagnostics, Leipzig University, for excellent technical support.

Conflict of interest

The authors declare that the research was conducted in the absence of any commercial or financial relationships that could be construed as a potential conflict of interest.

Generative AI statement

The author(s) declare that no Generative AI was used in the creation of this manuscript.

Publisher's note

Supplementary material

The Supplementary Material for this article can be found online at: https://www.frontiersin.org/articles/10.3389/fendo.2025.1567573/full#supplementary-material

References

1. Eslam M, Newsome PN, Sarin SK, Anstee QM, Targher G, Romero-Gomez M, et al. A new definition for metabolic dysfunction-associated fatty liver disease: An international expert consensus statement. *J Hepatol*. (2020) 73:202–9. doi: 10.1016/j.jhep.2020.03.039

2. Rinella ME, Lazarus JV, Ratziu V, Francque SM, Sanyal AJ, Kanwal F, et al. A multisociety Delphi consensus statement on new fatty liver disease nomenclature. *Hepatol (Baltimore Md)*. (2023) 78:1966–86. doi: 10.1097/HEP.0000000000000520

3. Younossi ZM, Koenig AB, Abdelatif D, Fazel Y, Henry L, Wymer M. Global epidemiology of nonalcoholic fatty liver disease-Meta-analytic assessment of prevalence, incidence, and outcomes. *Hepatol (Baltimore Md)*. (2016) 64:73–84. doi: 10.1002/hep.28431

4. Giorgio V, Prono F, Graziano F, Nobili V. Pediatric non alcoholic fatty liver disease: old and new concepts on development, progression, metabolic insight and potential treatment targets. *BMC Pediatr*. (2013) 13:40. doi: 10.1186/1471-2431-13-40

5. Penke M, Larsen PS, Schuster S, Dall M, Jensen BAH, Gorski T, et al. Hepatic NAD salvage pathway is enhanced in mice on a high-fat diet. *Mol Cell Endocrinol*. (2015) 412:65–72. doi: 10.1016/j.mce.2015.05.028

6. Cohen JC, Horton JD, Hobbs HH. Human fatty liver disease: old questions and new insights. *Sci (New York NY)*. (2011) 332:1519–23. doi: 10.1126/science.1204265

7. Huang J-L, Fu Y-P, Jing C-Y, Yi Y, Sun J, Gan W, et al. A novel and validated prognostic nomogram based on liver fibrosis and tumor burden for patients with hepatocellular carcinoma after curative resection. *J Surg Oncol*. (2018) 117:625–33. doi: 10.1002/jso.24895

8. Karanjia RN, Crossey MME, Cox IJ, Fye HKS, Njie R, Goldin RD, et al. Hepatic steatosis and fibrosis: Non-invasive assessment. *World J Gastroenterol*. (2016) 22:9880–97. doi: 10.3748/wjg.v22.i45.9880

9. Hammel P, Couvelard A, O'Toole D, Ratouis A, Sauvanet A, Fléjou JF, et al. Regression of liver fibrosis after biliary drainage in patients with chronic pancreatitis and stenosis of the common bile duct. *New Engl J Med*. (2001) 344:418–23. doi: 10.1056/NEJM200102083440604

10. Iredale JP, Benyon RC, Pickering J, McCullen M, Northrop M, Pawley S, et al. Mechanisms of spontaneous resolution of rat liver fibrosis. Hepatic stellate cell apoptosis and reduced hepatic expression of metalloproteinase inhibitors. *J Clin Invest*. (1998) 102:538–49. doi: 10.1172/JCI1018

11. Fabregat I, Moreno-Càceres J, Sánchez A, Dooley S, Dewidar B, Giannelli G, et al. TGF-β signalling and liver disease. *FEBS J*. (2016) 283:2219–32. doi: 10.1111/febs.13665

12. Friedman SL, Neuschwander-Tetri BA, Rinella M, Sanyal AJ. Mechanisms of NAFLD development and therapeutic strategies. *Nat Med*. (2018) 24:908–22. doi: 10.1038/s41591-018-0104-9

13. Huang J, Zhang L, Wan D, Zhou L, Zheng S, Lin S, et al. Extracellular matrix and its therapeutic potential for cancer treatment. *Signal Transduct Target Ther*. (2021) 6:153. doi: 10.1038/s41392-021-00544-0

14. Yang JD, Abdelmalek MF, Pang H, Guy CD, Smith AD, Diehl AM, et al. Gender and menopause impact severity of fibrosis among patients with nonalcoholic steatohepatitis. *Hepatol (Baltimore Md)*. (2014) 59:1406–14. doi: 10.1002/hep.26761

15. Kim MK, Ahn CW, Nam JS, Kang S, Park JS, Kim KR. Association between nonalcoholic fatty liver disease and coronary artery calcification in postmenopausal women. *Menopause (New York NY)*. (2015) 22:1323–7. doi: 10.1097/GME.0000000000000503

16. Zhang X, Wang Y, Liu P. Omic studies reveal the pathogenic lipid droplet proteins in non-alcoholic fatty liver disease. *Protein Cell*. (2017) 8:4–13. doi: 10.1007/s13238-016-0327-9

17. Lonardo A, Trande P. Are there any sex differences in fatty liver? A study of glucose metabolism and body fat distribution. *J Gastroenterol Hepatol*. (2000) 15:775–82. doi: 10.1046/j.1440-1746.2000.02226.x

18. Heine PA, Taylor JA, Iwamoto GA, Lubahn DB, Cooke PS. Increased adipose tissue in male and female estrogen receptor-α knockout mice. *Proc Natl Acad Sci U.S.A*. (2000) 23:12729–34.

19. Ohlsson C, Hellberg N, Parini P, Vidal O, Bohlooly-Y M, Rudling M, et al. Obesity and disturbed lipoprotein profile in estrogen receptor-alpha-deficient male mice. *Biochem Biophys Res Commun*. (2000) 278:640–5. doi: 10.1006/bbrc.2000.3827

20. Kamada Y, Kiso S, Yoshida Y, Chatani N, Kizu T, Hamano M, et al. Estrogen deficiency worsens steatohepatitis in mice fed high-fat and high-cholesterol diet. *Am J Physiol Gastrointest Liver Physiol*. (2011) 301:G1031–43. doi: 10.1152/ajpgi.00211.2011

21. Samuel VT, Liu Z-X, Qu X, Elder BD, Bilz S, Befroy D, et al. Mechanism of hepatic insulin resistance in non-alcoholic fatty liver disease. *J Biol Chem*. (2004) 279:32345–53. doi: 10.1074/jbc.M313478200

22. Charlton M, Krishnan A, Viker K, Sanderson S, Cazanave S, McConico A, et al. Fast food diet mouse: novel small animal model of NASH with ballooning, progressive fibrosis, and high physiological fidelity to the human condition. *Am J Physiol Gastrointest Liver Physiol*. (2011) 301:G825–34. doi: 10.1152/ajpgi.00145.2011

23. Klöting N, Koch L, Wunderlich T, Kern M, Ruschke K, Krone W, et al. Autocrine IGF-1 action in adipocytes controls systemic IGF-1 concentrations and growth. *Diabetes*. (2008) 57:2074–82. doi: 10.2337/db07-1538

24. Suchý T, Zieschang C, Popkova Y, Kaczmarek I, Weiner J, Liebing A-D, et al. The repertoire of Adhesion G protein-coupled receptors in adipocytes and their functional relevance. *Int J Obes*. (2020) 44:2124–36. doi: 10.1038/s41366-020-0570-2

25. Schindelin J, Arganda-Carreras I, Frise E, Kaynig V, Longair M, Pietzsch T, et al. Fiji: an open-source platform for biological-image analysis. *Nat Methods*. (2012) 9:676–82. doi: 10.1038/nmeth.2019

26. imagej.net. Quantifying stained liver tissue(2022). Available online at: https://imagej.net/ij/docs/examples/stained-sections/index.html (Accessed January 10, 2025).

27. Deutsch MJ, Schriever SC, Roscher AA, Ensenauer R. Digital image analysis approach for lipid droplet size quantitation of Oil Red O-stained cultured cells. *Anal Biochem*. (2014) 445:87–9. doi: 10.1016/j.ab.2013.10.001

28. Ching-Yeung-Yu B, Kwok D, Wong VW-S. Magnitude of nonalcoholic fatty liver disease: eastern perspective. *J Clin Exp Hepatol*. (2019) 9:491–6. doi: 10.1016/j.jceh.2019.01.007

29. Samji NS, Verma R, Satapathy SK. Magnitude of nonalcoholic fatty liver disease: western perspective. *J Clin Exp Hepatol*. (2019) 9:497–505. doi: 10.1016/j.jceh.2019.05.001

30. Zhang X, Wu M, Liu Z, Yuan H, Wu X, Shi T, et al. Increasing prevalence of NAFLD/NASH among children, adolescents and young adults from 1990 to 2017: a population-based observational study. *BMJ Open*. (2021) 11:e042843. doi: 10.1136/bmjopen-2020-042843

31. Younossi ZM, Kalligeros M, Henry L. Epidemiology of metabolic dysfunction-associated steatotic liver disease. *Clin Mol Hepatol*. (2025) 31(Suppl):S32-S50. doi: 10.3350/cmh.2024.0431

32. Wong RJ, Aguilar M, Cheung R, Perumpail RB, Harrison SA, Younossi ZM, et al. Nonalcoholic steatohepatitis is the second leading etiology of liver disease among adults awaiting liver transplantation in the United States. *Gastroenterology*. (2015) 148:547–55. doi: 10.1053/j.gastro.2014.11.039

33. Younossi ZM, Otgonsuren M, Henry L, Venkatesan C, Mishra A, Erario M, et al. Association of nonalcoholic fatty liver disease (NAFLD) with hepatocellular carcinoma (HCC) in the United States from 2004 to 2009. *Hepatol (Baltimore Md)*. (2015) 62:1723–30. doi: 10.1002/hep.28123

34. Finucane MM, Stevens GA, Cowan MJ, Danaei G, Lin JK, Paciorek CJ, et al. National, regional, and global trends in body-mass index since 1980: systematic analysis of health examination surveys and epidemiological studies with 960 country-years and 9·1 million participants. *Lancet (London England)*. (2011) 377:557–67. doi: 10.1016/S0140-6736(10)62037-5

35. Anstee QM, Targher G, Day CP. Progression of NAFLD to diabetes mellitus, cardiovascular disease or cirrhosis. *Nat Rev Gastroenterol Hepatol*. (2013) 10:330–44. doi: 10.1038/nrgastro.2013.41

36. Ballestri S, Nascimbeni F, Baldelli E, Marrazzo A, Romagnoli D, Lonardo A. NAFLD as a sexual dimorphic disease: role of gender and reproductive status in the development and progression of nonalcoholic fatty liver disease and inherent cardiovascular risk. *Adv Ther*. (2017) 34:1291–326. doi: 10.1007/s12325-017-0556-1

37. Balakrishnan M, Patel P, Dunn-Valadez S, Dao C, Khan V, Ali H, et al. Women Have a Lower Risk of Nonalcoholic Fatty Liver Disease but a Higher Risk of Progression vs Men: A Systematic Review and Meta-analysis. *Clin Gastroenterol Hepatol: Off Clin Pract J Am Gastroenterol Assoc*. (2021) 19:61–71.e15. doi: 10.1016/j.cgh.2020.04.067

38. Lau JKC, Zhang X, Yu J. Animal models of non-alcoholic fatty liver disease: current perspectives and recent advances. *J Pathol*. (2017) 241:36–44. doi: 10.1002/path.4829

39. Suchacki KJ, Thomas BJ, Ikushima YM, Chen K-C, Fyfe C, Tavares AAS, et al. The effects of caloric restriction on adipose tissue and metabolic health are sex- and age-dependent. *eLife*. (2023) 12. doi: 10.7554/eLife.88080

40. Palmer BF, Clegg DJ. The sexual dimorphism of obesity. *Mol Cell Endocrinol*. (2015) 402:113–9. doi: 10.1016/j.mce.2014.11.029

41. Tchernof A, Bélanger C, Morisset A-S, Richard C, Mailloux J, Laberge P, et al. Regional differences in adipose tissue metabolism in women: minor effect of obesity and body fat distribution. *Diabetes*. (2006) 55:1353–60. doi: 10.2337/db05-1439

42. Jensen MD, Cardin S, Edgerton D, Cherrington A. Splanchnic free fatty acid kinetics. *Am J Physiol Endocrinol Metab*. (2003) 284:E1140–8. doi: 10.1152/ajpendo.00268.2002

43. Nielsen S, Guo ZK, Johnson CM, Hensrud DD, Jensen MD. Splanchnic lipolysis in human obesity. *J Clin Invest*. (2004) 113:1582–8. doi: 10.1172/JCI21047

44. Onal G, Kutlu O, Gozuacik D, Dokmeci Emre S. Lipid droplets in health and disease. *Lipids Health Dis*. (2017) 16:128. doi: 10.1186/s12944-017-0521-7

45. Gluchowski NL, Becuwe M, Walther TC, Farese RV. Lipid droplets and liver disease: from basic biology to clinical implications. *Nat Rev Gastroenterol Hepatol*. (2017) 14:343–55. doi: 10.1038/nrgastro.2017.32

46. Dooley S, Dijke PT. TGF-β in progression of liver disease. *Cell Tissue Res*. (2012) 347:245–56. doi: 10.1007/s00441-011-1246-y

47. Corrigan JK, Ramachandran D, He Y, Palmer CJ, Jurczak MJ, Chen R, et al. A big-data approach to understanding metabolic rate and response to obesity in laboratory mice. *eLife*. (2020) 9. doi: 10.7554/eLife.53560

48. Jaric I, Voelkl B, Clerc M, Schmid MW, Novak J, Rosso M, et al. The rearing environment persistently modulates mouse phenotypes from the molecular to the behavioural level. *PloS Biol*. (2022) 20:e3001837. doi: 10.1371/journal.pbio.3001837

49. Sancho P, Mainez J, Crosas-Molist E, Roncero C, Fernández-Rodriguez CM, Pinedo F, et al. NADPH oxidase NOX4 mediates stellate cell activation and hepatocyte cell death during liver fibrosis development. *PloS One*. (2012) 7:e45285. doi: 10.1371/journal.pone.0045285

50. Yang L, Roh YS, Song J, Zhang B, Liu C, Loomba R, et al. Transforming growth factor beta signaling in hepatocytes participates in steatohepatitis through regulation of cell death and lipid metabolism in mice. *Hepatol (Baltimore Md)*. (2014) 59:483–95. doi: 10.1002/hep.26698

51. Itagaki T, Shimizu I, Cheng X, Yuan Y, Oshio A, Tamaki K, et al. Opposing effects of oestradiol and progesterone on intracellular pathways and activation processes in the oxidative stress induced activation of cultured rat hepatic stellate cells. *Gut*. (2005) 54:1782–9. doi: 10.1136/gut.2005.053278

52. Yoshino K, Komura S, Watanabe I, Nakawaga Y, Yagi K. Effect of estrogens on serum and liver lipid peroxide levels in mice. *J Clin Biochem Nutr*. (1987) 3):233–40. doi: 10.3164/jcbn.3.233

53. Della Torre S. Beyond the X factor: relevance of sex hormones in NAFLD pathophysiology. *Cells*. (2021) 10(9). doi: 10.3390/cells10092502

54. Shimizu I, Kohno N, Tamaki K, Shono M, Huang H-W, He J-H, et al. Female hepatology: Favorable role of estrogen in chronic liver disease with hepatitis B virus infection. *World J Gastroenterol*. (2007) 13:4295–305. doi: 10.3748/wjg.v13.i32.4295

55. Besse-Patin A, Léveillé M, Oropeza D, Nguyen BN, Prat A, Estall JL. Estrogen signals through peroxisome proliferator-activated receptor-γ Coactivator 1α to reduce oxidative damage associated with diet-induced fatty liver disease. *Gastroenterology*. (2017) 152:243–56. doi: 10.1053/j.gastro.2016.09.017

56. Lemieux C, Phaneuf D, Labrie F, Giguère V, Richard D, Deshaies Y. Estrogen receptor alpha-mediated adiposity-lowering and hypocholesterolemic actions of the selective estrogen receptor modulator acolbifene. *Int J Obes*. (2005) 29:1236–44. doi: 10.1038/sj.ijo.0803014

57. Della Torre S, Lolli F, Ciana P, Maggi A. Erratum to: sexual dimorphism and estrogen action in mouse liver. *Adv Exp Med Biol*. (2017) 1043:E1. doi: 10.1007/978-3-319-70178-3_28

58. Maggi A, Della Torre S. Sex, metabolism and health. *Mol Metab*. (2018) 15:3–7. doi: 10.1016/j.molmet.2018.02.012

59. Palmisano BT, Zhu L, Eckel RH, Stafford JM. Sex differences in lipid and lipoprotein metabolism. *Mol Metab*. (2018) 15:45–55. doi: 10.1016/j.molmet.2018.05.008

60. Fuller KNZ, Allen J, Kumari R, Akakpo JY, Ruebel M, Shankar K, et al. Pre- and post-sexual maturity liver-specific ERα Knockout does not impact hepatic mitochondrial function. *J Endocr Soc*. (2023) 7:bvad053. doi: 10.1210/jendso/bvad053

61. Mondal SA, Mann SN, van der Linden C, Sathiaseelan R, Kamal M, Das S, et al. Metabolic benefits of 17α-estradiol in liver are partially mediated by ERβ in male mice. *Sci Rep*. (2023) 13:9841. doi: 10.1038/s41598-023-37007-1

62. Zhou Y, Shimizu I, Lu G, Itonaga M, Okamura Y, Shono M, et al. Hepatic stellate cells contain the functional estrogen receptor beta but not the estrogen receptor alpha in male and female rats. *Biochem Biophys Res Commun*. (2001) 286:1059–65. doi: 10.1006/bbrc.2001.5479

63. Wang Y, Wu C, Zhou J, Fang H, Wang J. Overexpression of estrogen receptor β inhibits cellular functions of human hepatic stellate cells and promotes the anti-fibrosis effect of calycosin via inhibiting STAT3 phosphorylation. *BMC Pharmacol Toxicol*. (2022) 23:77. doi: 10.1186/s40360-022-00617-y

64. Zhang B, Zhang C-G, Ji L-H, Zhao G, Wu Z-Y. Estrogen receptor β selective agonist ameliorates liver cirrhosis in rats by inhibiting the activation and proliferation of hepatic stellate cells. *J Gastroenterol Hepatol*. (2018) 33:747–55. doi: 10.1111/jgh.13976

65. Turola E, Petta S, Vanni E, Milosa F, Valenti L, Critelli R, et al. Ovarian senescence increases liver fibrosis in humans and zebrafish with steatosis. *Dis Models Mech*. (2015) 8:1037–46. doi: 10.1242/dmm.019950

66. Morán-Costoya A, Proenza AM, Gianotti M, Lladó I, Valle A. Sex differences in nonalcoholic fatty liver disease: estrogen influence on the liver-adipose tissue crosstalk. *Antioxid Redox Signaling*. (2021) 35:753–74. doi: 10.1089/ars.2021.0044

frontiers | Frontiers in Medicine

TYPE Original Research
PUBLISHED 19 March 2025
DOI 10.3389/fmed.2025.1513375

OPEN ACCESS

EDITED BY
Dirk Müller-Wieland,
University Hospital RWTH Aachen, Germany

REVIEWED BY
Bin Chen,
Second Affiliated Hospital of Soochow University, China
Maryam Barancheshmeh,
Universal Scientific Education and Research Network (USERN), United States

*CORRESPONDENCE
Jianxian Luo
✉ 545044058@qq.com
Zhisheng Ji
✉ tzhishengji@jnu.edu.cn

†These authors have contributed equally to this work

RECEIVED 18 October 2024
ACCEPTED 25 February 2025
PUBLISHED 19 March 2025

CITATION
Pan H, Long X, Wu P, Xiao Y, Liao H, Wan L, Luo J and Ji Z (2025) The association between lipid accumulation product and osteoporosis in American adults: analysis from NHANES dataset.
Front. Med. 12:1513375.
doi: 10.3389/fmed.2025.1513375

The association between lipid accumulation product and osteoporosis in American adults: analysis from NHANES dataset

Huawen Pan[1,2†], Xiao Long[1†], Ping Wu[1], Yongchun Xiao[1], Huanran Liao[1], Li Wan[1], Jianxian Luo[1,3*] and Zhisheng Ji[1*]

[1]Department of Orthopedics, First Affiliated Hospital of Jinan University, Guangzhou, China, [2]Department of Spine Surgery, Maoming People's Hospital, Maoming, China, [3]Department of Orthopedics, First Affiliated Hospital of Guangdong Pharmaceutical University, Guangzhou, China

Background: The Lipid Accumulation Product (LAP), a novel indicator of fat accumulation, reflects the distribution and metabolic status of body fat. This study aims to evaluate the relationship between adult Americans' prevalence of osteoporosis and LAP.

Methods: This study used data from the NHANES cycles 2007–2010, 2013–2014, and 2017–2018, including 4,200 adults aged 50 and above. LAP was calculated using waist circumference and triglyceride levels, whereas osteoporosis was identified using information from dual-energy X-ray absorptiometry (DXA) assessments of bone mineral density (BMD). Restricted cubic spline (RCS) analysis was evaluated the relationship between LAP and osteoporosis. Additionally, subgroup analyses were conducted to assess the impact of demographic characteristics and health status on the relationship between LAP and osteoporosis.

Results: LAP and osteoporosis were shown to be significantly inversely correlated in the study. In the unadjusted model, the prevalence of osteoporosis and Log LAP showed a significant negative connection (OR = 0.62, 95% CI = 0.52–0.74). Osteoporosis prevalence decreased by 45% in the fully adjusted model for every unit rise in Log LAP (OR = 0.54, 95% CI = 0.44–0.66). RCS analysis revealed a nonlinear association between LAP and osteoporosis prevalence (*P*-nonlinear = 0.0025), showing an L-shaped negative correlation. Subgroup studies showed that, regardless of age, sex, ethnicity, or health condition, there was a constant negative connection between LAP and osteoporosis.

Conclusion: According to this study, there is a substantial negative relationship between adult prevalence of osteoporosis in America and LAP. LAP is an easy-to-use and practical indication that may be very helpful in osteoporosis prevention and early detection.

KEYWORDS

osteoporosis, lipid accumulation product, triglyceride, cross-sectional study, NHANES

1 Introduction

Decreased bone density and the breakdown of bone microarchitecture are the hallmarks of osteoporosis, a systemic skeletal disease that raises the risk of fractures dramatically and decreases bone mass (1–3). As the world's population ages more rapidly, osteoporosis is becoming a serious global public health problem (4, 5). Osteoporosis is particularly prevalent among postmenopausal elderly women, primarily due to estrogen deficiency (6, 7). The World Health Organization (WHO) estimates that 200 million men and women worldwide suffer from osteoporosis (8). In addition to severely lowering patients' quality of life, osteoporosis places a financial strain on healthcare systems (9, 10). The incidence of osteoporosis and fractures can be decreased by early identification and management.

Currently, dual-energy X-ray absorptiometry (DXA) is the gold standard for diagnosing osteoporosis. However, its application in large-scale screening is limited due to its high cost, equipment requirements, and low accessibility (11). Additionally, traditional risk assessment tools, such as the Fracture Risk Assessment Tool (FRAX), can predict fracture risk but remain controversial regarding their accuracy and applicability (12). Therefore, identifying an economical, convenient, and widely applicable biomarker for early screening and risk assessment of osteoporosis holds significant clinical value.

The Lipid Accumulation Product (LAP) is a novel indicator of fat accumulation that integrates waist circumference and serum triglyceride levels, providing a more accurate reflection of an individual's fat distribution and metabolic status (13–15). BMI and body fat percentage cannot differentiate the effects of different fat types on bone health (16). Previous studies have demonstrated a stronger association between visceral fat and bone metabolism. Moreover, LAP has been validated as a predictive marker for metabolic syndrome-related diseases, including diabetes, non-alcoholic fatty liver disease, and hypertension (17–20), suggesting its potential value in osteoporosis screening. However, systematic studies on the relationship between LAP and osteoporosis remain limited, particularly with regard to epidemiological evidence in the U.S. adult population.

This study utilizes data from the National Health and Nutrition Examination Survey (NHANES) to systematically assess the relationship between LAP and osteoporosis prevalence, aiming to explore the feasibility of LAP as a potential biomarker for early osteoporosis screening (21–23). Because hormones and cytokines secreted by visceral adipose tissue, such as leptin, may promote bone formation by stimulating osteoblasts (24), and a moderate increase in fat mass may enhance skeletal loading, thereby stimulating bone remodeling and increasing bone density (25). We hypothesize that LAP is significantly associated with bone mineral density (BMD), with higher LAP levels potentially correlating with a lower risk of osteoporosis. By further investigating this association, we aim to provide new theoretical insights for osteoporosis screening and prevention, as well as support future clinical practice and public health policies.

Abbreviations: BMD, Bone Mineral Density; BMI, Body Mass Index; CI, Confidence Interval; DXA, Dual-energy X-ray Absorptiometry; LAP, Lipid Accumulation Product; MET, Metabolic Equivalent; NHANES, National Health and Nutrition Examination Survey; OR, Odds Ratio; PIR, Poverty Income Ratio; RCS, Restricted Cubic Spline; TG, Triglycerides; WC, Waist Circumference.

2 Methods

2.1 Survey description

The National Health and Nutrition Examination Survey (NHANES), a cross-sectional survey, uses a complex, stratified, multistage sampling procedure to assess the overall health and nutritional status of the American population. Each participant provided signed, informed consent, and the trial was authorized by the Institutional Review Board.

2.2 Study population

Data from four NHANES cycles—2007–2010, 2013–2014, and 2017–2018—were used in this analysis. The absence of femoral bone density measurements led to the exclusion of data from the 2011–2012 and 2015–2016 cycles. The inclusion criteria were: (1) participants aged over 50; (2) participants with complete femoral bone density measurements; and (3) participants with complete waist circumference and triglyceride data.

2.3 Calculation of LAP

Using waist circumference (WC) and triglyceride (TG) values, the LAP index is computed using the formula presented in earlier research. This is the formula for calculation: The formula for calculating LAP is [WC (cm) - 65] × TG (mmol/l) for males and [WC (cm) - 58] for women. × TG in mol/l.

2.4 Definition of osteoporosis

Using mobile examination facilities, NHANES performed DXA scans on the proximal femur to collect data on bone mineral density (BMD) in the trochanter, femoral neck, whole hip, and intertrochanteric areas. In accordance with WHO recommendations, a T-score of less than −2.5 standard deviations in total hip BMD, femoral neck BMD, trochanter BMD, or intertrochanteric BMD indicates osteoporosis. The reference group is made up of white, non-Hispanic women between the ages of 20 and 29. The following formula is used to determine the T-score: T-Score is calculated as standard deviation / (individual BMD - mean normal BMD).

2.5 Covariates

This study considers demographic characteristics, lifestyle, health status, and laboratory tests as covariates. The poverty index ratio (PIR), age, sex, race, and educational attainment are examples of demographic characteristics. The PIR is categorized as <1, 1 to <3, and ≥ 3 based on the results. Lifestyle factors include smoking and physical activity. A smoker is defined as someone who has smoked more than 100 cigarettes in their lifetime. The following method is used to calculate physical activity in metabolic equivalent of task (MET) minutes per week based on data from the Global Physical Activity Questionnaire: MET (minutes/week) is calculated as follows:

MET value x weekly frequency × session time. A MET value less than 600 min/week is defined as inactive. Other health conditions are determined based on physician diagnosis records or self-reports, including diabetes, hypertension, and chronic kidney disease. Laboratory tests include blood uric acid, blood urea nitrogen, blood creatinine, alanine aminotransferase, aspartate aminotransferase, blood calcium, and blood phosphorus concentrations.

2.6 Statistical analysis

Analysis was based on NHANES data from 2007 to 2018, excluding the 2011–2012 and 2015–2016 cycles with missing femoral bone density data. Baseline data were displayed based on whether osteoporosis was present or absent using descriptive analysis. Categorical variables were displayed as percentages, while continuous variables were displayed as means and standard deviations. Supplementary Figure 5 revealed that the LAP data presented a left-skewed distribution. LAP was logarithmically transformed to correct the data skew and standardize the data. The corrected data are shown in Supplementary Figure 6. After controlling for confounders, the association between LAP and osteoporosis was examined using logistic regression. LAP was converted into a four-category variable to explore trends with osteoporosis at different levels and enhance result robustness. Saturation effect analysis was used to determine the critical point and restricted cubic spline (RCS) analysis was used to assess the dose–response relationship between LAP and osteoporosis. The possible effects of age, sex, race, smoking, physical activity, diabetes, chronic renal disease, and hypertension on the correlation between Log LAP and osteoporosis were examined using subgroup analysis. More study was done to look into the relationship between Log LAP and BMD in different femur locations using linear regression and RCS analysis in order to increase result robustness and consistency. $p < 0.05$ was used as the significance criterion, and all analyses were conducted using R software (version 4.2.3).

3 Results

3.1 Characteristics of study population

Data extracted from the NHANES database followed the inclusion process as shown in Figure 1, ultimately including 4,200 participants, with 3,826 classified as non-osteoporotic and 374 as osteoporotic. Supplementary Table 1 presents weighted baseline characteristics based on the osteoporosis categorization, whereas Table 1 presents participant characteristics. In contrast to the non-osteoporotic group, the osteoporotic individuals tended to be non-Hispanic white, more females than men, and older overall. Individuals with osteoporosis tended to lead more sedentary lives and had elevated blood phosphorus and blood urea nitrogen levels. It is noteworthy that osteoporotic participants had lower LAP levels, suggesting LAP may be a protective factor against osteoporosis.

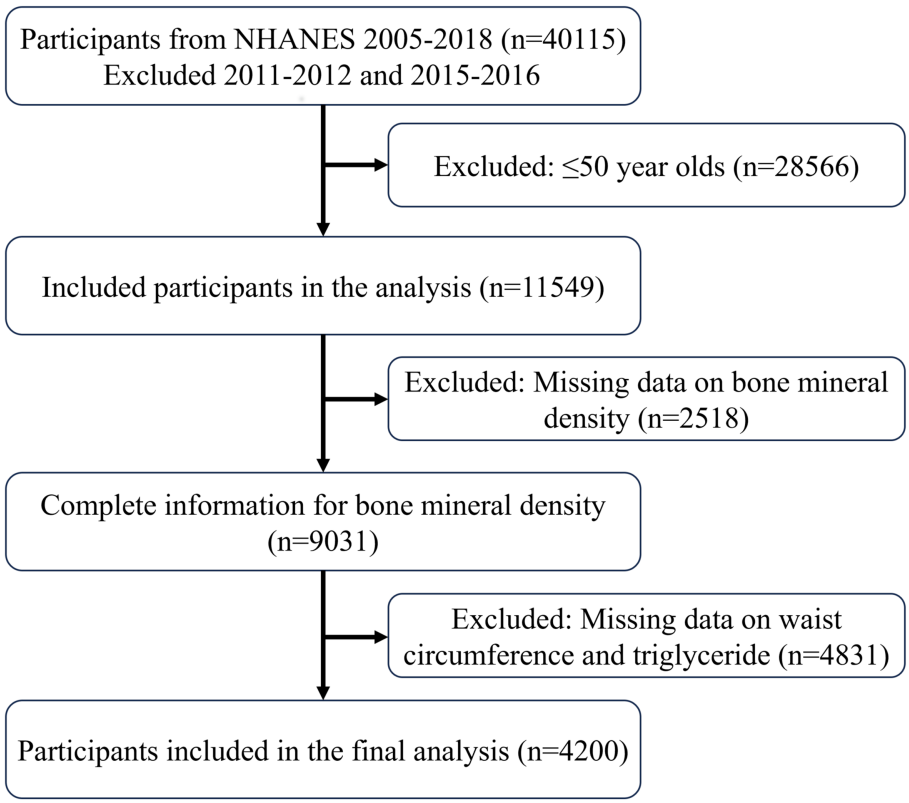

FIGURE 1
Include participants in the process.

TABLE 1 Baseline characteristics of the study population.

Characteristic	Overall	Non-osteoporosis	Osteoporosis	*p*-value
n	4,200	3,826	374	
Age (%)				<0.001
<65	2,315 (55.1)	2,213 (57.8)	102 (27.3)	
>65	1885 (44.9)	1,613 (42.2)	272 (72.7)	
Sex (%)				<0.001
Female	2068 (49.2)	1809 (47.3)	259 (69.3)	
Male	2,132 (50.8)	2017 (52.7)	115 (30.7)	
Race (%)				<0.001
Mexican American	554 (13.2)	515 (13.5)	39 (10.4)	
Non-Hispanic black	806 (19.2)	777 (20.3)	29 (7.8)	
Non-Hispanic white	2008 (47.8)	1774 (46.4)	234 (62.6)	
Others	832 (19.8)	760 (19.9)	72 (19.3)	
Education level (%)				<0.001
Under high school	1,186 (28.2)	1,056 (27.6)	130 (34.8)	
High school or equivalent	986 (23.5)	882 (23.1)	104 (27.8)	
Above high school	2021 (48.1)	1884 (49.2)	137 (36.6)	
PIR (%)				<0.001
<1	613 (16.3)	543 (15.9)	70 (20.5)	
1–3	1,670 (44.5)	1,490 (43.6)	180 (52.8)	
>3	1,474 (39.2)	1,383 (40.5)	91 (26.7)	
Activity status (%)				<0.001
Active	1766 (42.0)	1,656 (43.3)	110 (29.4)	
Inactive	2,434 (58.0)	2,170 (56.7)	264 (70.6)	
Smoke (%)				0.144
No	2094 (49.9)	1896 (49.6)	198 (52.9)	
Yes	2,103 (50.1)	1928 (50.4)	175 (46.8)	
Hypertension (%)				0.74
No	1919 (45.7)	1751 (45.8)	168 (44.9)	
Yes	2,276 (54.2)	2070 (54.1)	206 (55.1)	
CKD (%)				<0.001
No	4,007 (95.4)	3,668 (95.9)	339 (90.6)	
Yes	184 (4.4)	150 (3.9)	34 (9.1)	
Diabate (%)				0.146
No	3,236 (77.0)	2,934 (76.7)	302 (80.7)	
Yes	808 (19.2)	745 (19.5)	63 (16.8)	
Total femur BMD [mean (SD)] (gm/cm2)	0.92 (0.16)	0.95 (0.15)	0.66 (0.09)	<0.001
Femoral neck BMD [mean (SD)] (gm/cm2)	0.76 (0.14)	0.78 (0.13)	0.53 (0.05)	<0.001
Trochanter BMD [mean (SD)] (gm/cm2)	0.70 (0.14)	0.72 (0.13)	0.50 (0.08)	<0.001
Intertrochanter BMD [mean (SD)] (gm/cm2)	1.10 (0.19)	1.13 (0.17)	0.79 (0.12)	<0.001
BUN [mean (SD)] (mmol/L)	5.50 (2.31)	5.44 (2.24)	6.09 (2.86)	<0.001
ALT [mean (SD)] (IU/L)	23.79 (15.30)	24.10 (15.16)	20.59 (16.40)	<0.001
AST [mean (SD)] (U/L)	25.36 (13.18)	25.42 (13.37)	24.77 (11.12)	0.365
SCR [mean (SD)] (umol/L)	0.95 (0.47)	0.95 (0.46)	0.97 (0.51)	0.273
SUA [mean (SD)] (mg/dL)	5.70 (1.44)	5.73 (1.44)	5.35 (1.46)	<0.001

(Continued)

TABLE 1 (Continued)

Characteristic	Overall	Non-osteoporosis	Osteoporosis	*p*-value
Calcium [mean (SD)] (mmol/L)	2.35 (0.09)	2.35 (0.09)	2.34 (0.10)	0.122
Phosphorus [mean (SD)] (mmol/L)	1.17 (0.17)	1.17 (0.17)	1.21 (0.17)	<0.001
WC [mean (SD)] (cm)	100.29 (13.80)	101.05 (13.58)	92.51 (13.70)	<0.001
TG [mean (SD)] (mmol/L)	1.46 (1.10)	1.47 (1.14)	1.31 (0.66)	0.007
LAP [mean (SD)]	58.38 (52.46)	59.73 (53.80)	44.55 (32.93)	<0.001

Mean (SD) for continuous variables, % for categorical variables.
ALT, alanine aminotransferase; AST, aspartate aminotransferase; BUN, blood urea nitrogen; CKD, chronic kidney disease; LAP, lipid accumulation product; PIR, poverty income ratio; SCR, serum creatinine; SUA, serum uric acid; TG, triglyceride; WC, waist circumference.

TABLE 2 The relationship between log LAP and osteoporosis.

		Model 1 OR (95%CI) *P*-value	Model 2 OR (95%CI) *P*-value	Model 3 OR (95%CI) *P*-value
Osteoporosis	log LAP	0.62 (0.52, 0.74) <0.001	0.57 (0.47, 0.70) <0.001	0.54 (0.44, 0.67) <0.001
	Q1	[Reference]	[Reference]	[Reference]
	Q2	0.68 (0.49, 0.94) 0.020	0.65 (0.46, 0.93) 0.018	0.65 (0.44, 0.94) 0.025
	Q3	0.55 (0.37, 0.80) 0.002	0.46 (0.31, 0.69) <0.001	0.45 (0.28, 0.73) 0.002
	Q4	0.41 (0.26, 0.64) <0.001	0.39 (0.25, 0.59) <0.001	0.33 (0.20, 0.55) <0.001
	P for trend	<0.001	<0.001	<0.001

CI, confidence interval; LAP, lipid accumulation product; OR, odds ratio; Q, quartiles.
Model 1: No covariates adjusted.
Model 2: Adjusted for age, sex, and race.
Model 3: Adjusted for age, sex, race, educational level, PIR, calcium, phosphorus, smoke, hypertension, CKD, diabetes, SCR, BUN, SUA, AST, ALT.

3.2 Association between LAP and prevalence of osteoporosis

To correct the left-skewed data of LAP, we performed a logarithmic transformation (Log LAP) on LAP. The results of a logistic regression study that looked at the relationship between Osteoporosis Prevalence and Log LAP are shown in Table 2. Log LAP showed a significant negative correlation (OR = 0.62, 95% CI = 0.52–0.74) with the frequency of osteoporosis in the unadjusted model (Model 1). Once covariates were corrected for step-by-step, the completely adjusted model (Model 3) showed that for every unit increase in Log LAP, the prevalence of osteoporosis decreased by 45% (OR = 0.54, 95% CI = 0.44–0.66). Further analysis after converting LAP into a categorical variable revealed that as LAP levels increased, the prevalence of osteoporosis significantly decreased (P-trend <0.001). Even after adjusting for every other variable, there was still a significant negative correlation between the highest quartile of LAP levels and the prevalence of osteoporosis (OR = 0.33, 95% CI = 0.19–0.55).

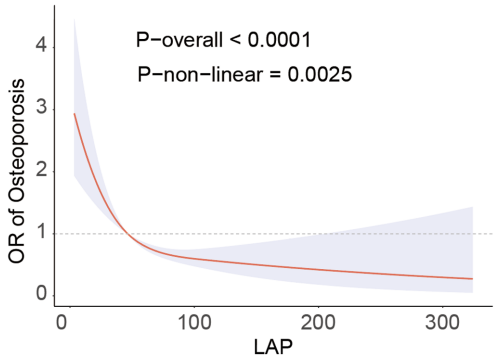

FIGURE 2
RCS analysis fitted the relationship between LAP and osteoporosis. Adjusted for age, sex, race, educational level, PIR, calcium, phosphorus, smoke, hypertension, CKD, diabetes, SCR, BUN, SUA, AST, ALT.

3.3 Nonlinear relationship and saturation effect analysis

The RCS analysis revealed a nonlinear association between LAP and the prevalence of osteoporosis (*P*-non-linear = 0.0025), presenting an L-shaped negative correlation (Figure 2). Through threshold effect analysis, we identified a turning point of LAP = 29 in the osteoporosis population. Segmental logistic regression analysis (Table 3) showed that when LAP <29, an increase in LAP was significantly associated with a reduced prevalence of osteoporosis (OR = 0.95, 95% CI = 0.93–0.97). However, when LAP >29, the effect of increasing LAP on osteoporosis prevalence gradually weakened (OR = 0.99, 95% CI = 0.99–1.00). These findings suggest a negative association with a saturation threshold between LAP and osteoporosis.

3.4 Subgroup analysis

We performed a subgroup analysis using Model 3 (Figure 3) in conjunction with stratification variables such age, gender, race, physical activity, smoking, diabetes, chronic kidney disease, and

hypertension to look into any possible associations between Log LAP and osteoporosis. The findings demonstrated that there was a persistent negative correlation between the prevalence of osteoporosis and Log LAP. Additionally, the interaction tests did not yield statistically significant results, suggesting that Log LAP may operate as a stand-alone protective factor against osteoporosis.

3.5 Additivity analysis

To verify the robustness and consistency of our findings, we conducted additional analyses. Supplementary Table 2 shows that Log LAP is positively and consistently associated with BMD in different regions of the femur, indicating that Log LAP is a favorable factor for BMD. Supplementary Figures 1–4 illustrate the RCS analyses of LAP and BMD in different regions of the femur, demonstrating nonlinear relationships and threshold saturation effects, thus supporting the robustness and consistency of our study results.

TABLE 3 Analysis of the LAP saturation effect and osteoporosis.

	LAP	OR (95%CI) *P*-value
Osteoporosis	Standard linear model	0.99 (0.98, 0.99) <0.001
	LAP <29	0.95 (0.93, 0.97) <0.001
	LAP >29	0.99 (0.99, 1.00) <0.001
	Log-likelihood ratio test	<0.001

LAP, lipid accumulation product; OR, odds ratio; CI, confidence interval.
Adjusted for age, sex, race, educational level, PIR, calcium, phosphorus, smoke, hypertension, CKD, diabetes, SCR, BUN, SUA, AST, ALT.

4 Discussion

This study used data from the NHANES database to examine the relationship between the prevalence of osteoporosis and LAP. The findings demonstrated a strong inverse relationship between osteoporosis and LAP. An increase in LAP considerably decreased the incidence of osteoporosis in the lower range of LAP; however, this protective impact progressively diminished when LAP above a certain threshold. These findings suggest that moderate fat distribution may positively impact bone health by increasing mechanical loading on bones and promoting the secretion of bone-forming factors.

LAP is an indicator of fat accumulation that combines waist circumference and triglyceride levels, effectively reflecting an individual's visceral fat level (26, 27). Compared to the traditional BMI, LAP has higher accuracy and sensitivity in assessing metabolic

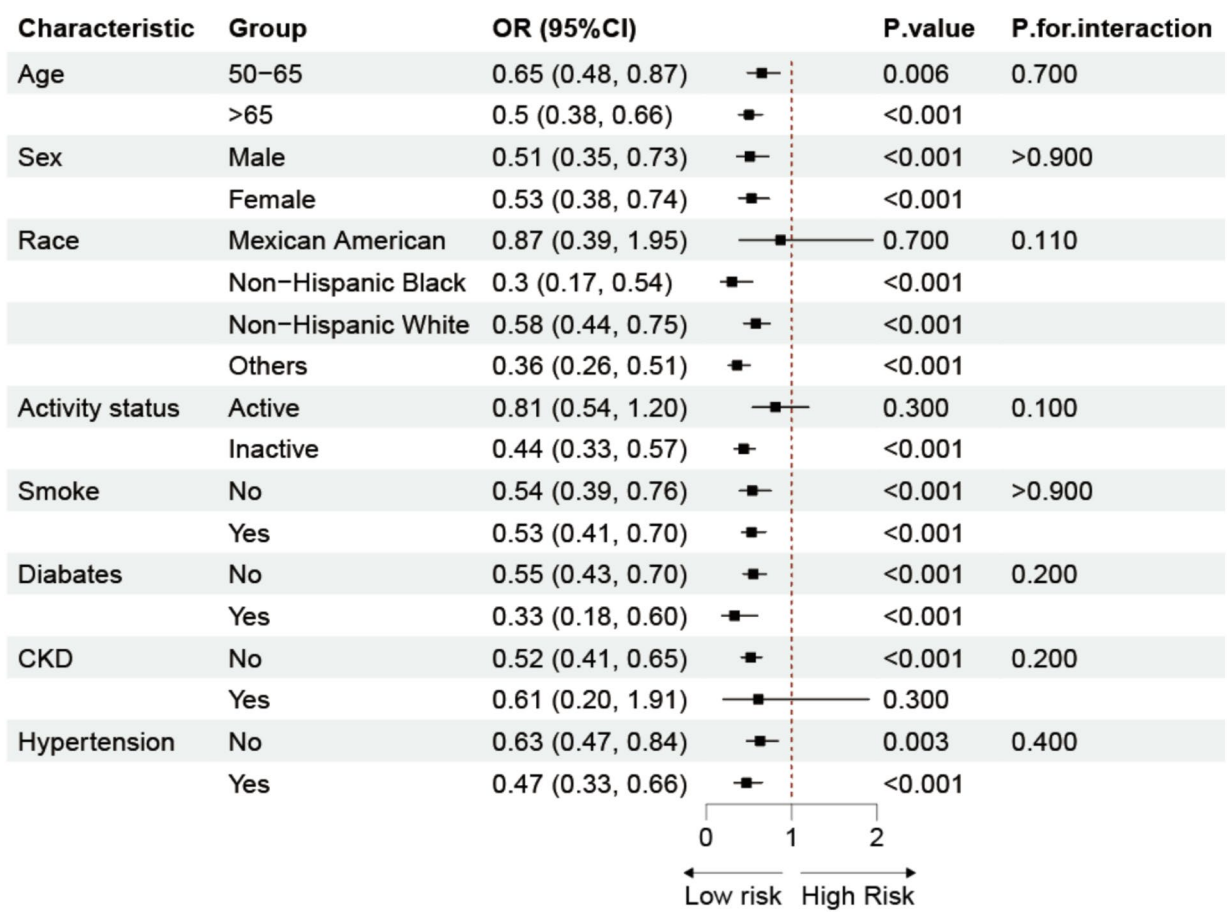

FIGURE 3
Subgroup analysis of the association between LAP and osteoporosis. Adjusted for age, sex, race, educational level, PIR, calcium, phosphorus, smoke, hypertension, CKD, diabetes, SCR, BUN, SUA, AST, ALT.

health and cardiovascular disease risk (28, 29). In line with certain other research findings, we discovered a strong negative connection between LAP and osteoporosis in our study. Similarly, in a study of the Visceral Adiposity Index (VAI) in adults over 20 years of age, those with high VAI scores also had high total femur BMD, suggesting that those with higher levels of visceral adiposity had a lower risk of fracture (30). Another study suggests that moderate weight gain protects bone density by increasing the mechanical load on bone through adipose tissue and by promoting bone formation through the secretion of several hormones and cytokines (31). In addition, the accumulation of visceral fat may have a positive effect on bone health by promoting the secretion of hormones such as leptin, which inhibits osteoclast activity (32, 33).

On the other hand, excessive fat buildup may be detrimental to bone health (34). High fat impaired bone mass and some trabecular microstructures in older mice in an experimental study of older mice (35). In another mechanistic study, the obesity-related adipose tissue secretes hormones and inflammatory substances such TNF-α and interleukin-6 (IL-6), which can raise the risk of osteoporosis by accelerating bone resorption and preventing the production of new bone (36–38). Excess fat may lead to adverse effects such as chronic inflammation, oxidative stress, and insulin resistance, ultimately accelerating bone loss (39). Particularly at higher LAP levels, these negative effects might outweigh the positive ones, leading to an increased risk of osteoporosis. Therefore, the nonlinear relationship between LAP and osteoporosis observed in this study suggests that the protective effect of fat accumulation on bone health diminishes or even disappears when fat accumulation reaches a certain level.

We carried out several more studies to confirm the consistency and robustness of our findings. First, we used restricted cubic spline (RCS) analysis to look at the dose–response relationship between LAP and osteoporosis (40, 41). The results showed that the risk of osteoporosis was significantly reduced for each unit increase in LAP when LAP <29 (OR = 0.95, 95% CI = 0.93–0.97, $p < 0.001$); however, this protective effect gradually diminished when LAP >29. Additionally, we conducted a subgroup analysis to explore the potential influence of variables such as age, sex, race, physical activity, smoking, diabetes, chronic kidney disease, and hypertension on the relationship between LAP and osteoporosis. The results indicated a consistent negative correlation between LAP and osteoporosis across different populations, suggesting that LAP may serve as an independent protective factor. This phenomenon may be attributed to the fact that LAP more directly reflects the metabolic status of visceral fat.

In assessing the connection between LAP and osteoporosis risk in adult Americans, this study identified LAP as a stand-alone protective factor against osteoporosis. The large sample size enhances the accuracy of our conclusions. Additionally, LAP outperforms traditional BMI in assessing individual fat distribution. Moreover, we adjusted for various confounding variables based on demographic characteristics and chronic diseases to minimize confounding bias, ensuring the broad applicability of the findings and enhancing both the internal and external validity of the study. In order to further understand the connection between LAP and osteoporosis in various groups, we lastly performed stratified subgroup analyses. These results highlight the necessity for more targeted osteoporosis preventive measures. There are many restrictions on this study. First of all, it is hard to establish a direct correlation between LAP and osteoporosis due to the cross-sectional nature of the study. Subsequent long-term investigations are required to confirm these results and investigate the possible utility of LAP in osteoporosis care and prevention. Secondly, this study used DXA to measure BMD and defined osteoporosis based on WHO criteria. Although DXA is considered the "gold standard" for osteoporosis diagnosis, it only assesses bone mineral density and does not evaluate bone quality or microarchitecture. Since fracture risk is also influenced by factors such as trabecular structure and cortical thickness, relying solely on BMD may underestimate the fracture risk in some patients. Due to the limitations of DXA, this study could not further explore the impact of LAP on bone microarchitecture. Future studies may integrate HR-pQCT or bone turnover markers to optimize osteoporosis risk assessment. Finally, as a novel body composition indicator, LAP requires further research to support its clinical application. This study found that LAP may be an independent protective factor against osteoporosis, as moderate fat distribution benefits bone health, while obesity may have adverse effects. LAP, being simple and practical, holds promise for osteoporosis prevention and early detection. Future studies should validate its applicability across different populations and its value in osteoporosis risk assessment.

5 Conclusion

According to this study, there is a substantial negative relationship between adult prevalence of osteoporosis in America and LAP. LAP is an easy-to-use and practical indication that may be very helpful in osteoporosis prevention and early detection.

Data availability statement

Publicly available datasets were analyzed in this study. This data can be found at: National Center for Health Statistics: www.cdc.gov/nchs/nhanes/.

Ethics statement

The studies involving humans were approved by The Research Ethics Review Board of the National Center for Health Statistics (NCHS). The studies were conducted in accordance with the local legislation and institutional requirements. Written informed consent for participation was not required from the participants or the participants' legal guardians/next of kin in accordance with the national legislation and institutional requirements.

Author contributions

HP: Data curation, Writing – original draft, Writing – review & editing, Formal analysis, Investigation. XL: Data curation, Writing – original draft, Writing – review & editing, Formal analysis, Software. PW: Writing – review & editing, Investigation. YX: Writing – review & editing, Resources. HL: Writing – review & editing, Project administration. LW: Writing – review & editing, Validation. JL: Writing – review & editing, Conceptualization, Methodology. ZJ: Methodology, Writing – review & editing, Supervision.

Funding

The author(s) declare that no financial support was received for the research and/or publication of this article.

Acknowledgments

We are appreciative that the National Center for Medical Research at the Institute of Prevention and Control of Disorders has made the National Health and Nutritional Evaluation Survey available to all citizens of the country. The authors acknowledge the use of ChatGPT for language refinement and coherence improvement in this manuscript.

Conflict of interest

The authors declare that the research was conducted in the absence of any commercial or financial relationships that could be construed as a potential conflict of interest.

Generative AI statement

The authors declare that no Gen AI was used in the creation of this manuscript.

Publisher's note

Supplementary material

The Supplementary material for this article can be found online at: https://www.frontiersin.org/articles/10.3389/fmed.2025.1513375/full#supplementary-material

References

1. Polito A, Barnaba L, Ciarapica D, Azzini E. Osteosarcopenia: a narrative review on clinical studies. *Int J Mol Sci*. (2022) 23:5591. doi: 10.3390/ijms23105591

2. Marcucci G, Domazetovic V, Nediani C, Ruzzolini J, Favre C, Brandi ML. Oxidative stress and natural antioxidants in osteoporosis: novel preventive and therapeutic approaches. *Antioxidants*. (2023) 12:373. doi: 10.3390/antiox12020373

3. Xiao Y, Xie X, Chen Z, Yin G, Kong W, Zhou J. Advances in the roles of ATF4 in osteoporosis. *Biomedicine Pharmacotherapy*. (2023) 169:115864. doi: 10.1016/j.biopha.2023.115864

4. Kirk B, Zanker J, Duque G. Osteosarcopenia: epidemiology, diagnosis, and treatment-facts and numbers. *J Cachexia Sarcopenia Muscle*. (2020) 11:609–18. doi: 10.1002/jcsm.12567

5. Thambiah SC, Yeap SS. Osteoporosis in south-east Asian countries. *Clinical Biochemist Reviews*. (2020) 41:29–40. doi: 10.33176/AACB-19-00034

6. Zhang L, Zheng YL, Wang R, Wang XQ, Zhang H. Exercise for osteoporosis: a literature review of pathology and mechanism. *Front Immunol*. (2022) 13:1005665. doi: 10.3389/fimmu.2022.1005665

7. Kushchayeva Y, Pestun I, Kushchayev S, Radzikhovska N, Lewiecki EM. Advancement in the treatment of osteoporosis and the effects on bone healing. *J Clin Med*. (2022) 11:7477. doi: 10.3390/jcm11247477

8. Noh JY, Yang Y, Jung H. Molecular mechanisms and emerging therapeutics for osteoporosis. *Int J Mol Sci*. (2020) 21:7623. doi: 10.3390/ijms21207623

9. Chen Y, Huang Y, Li J, Jiao T, Yang L. Enhancing osteoporosis treatment with engineered mesenchymal stem cell-derived extracellular vesicles: mechanisms and advances. *Cell Death Dis*. (2024) 15:119. doi: 10.1038/s41419-024-06508-w

10. Duan Y, Su YT, Ren J, Zhou Q, Tang M, Li J, et al. Kidney tonifying traditional Chinese medicine: potential implications for the prevention and treatment of osteoporosis. *Front Pharmacol*. (2022) 13:1063899. doi: 10.3389/fphar.2022.1063899

11. Williams S, Khan L, Licata AA. DXA and clinical challenges of fracture risk assessment in primary care. *Cleve Clin J Med*. (2021) 88:615–22. doi: 10.3949/ccjm.88a.20199

12. Kanis JA, Harvey NC, Johansson H, Liu E, Vandenput L, Lorentzon M, et al. A decade of FRAX: how has it changed the management of osteoporosis? *Aging Clin Exp Res*. (2020) 32:187–96. doi: 10.1007/s40520-019-01432-y

13. Khanmohammadi S, Tavolinejad H, Aminorroaya A, Rezaie Y, Ashraf H, Vasheghani-Farahani A. Association of lipid accumulation product with type 2 diabetes mellitus, hypertension, and mortality: a systematic review and meta-analysis. *J Diabetes Metab Disord*. (2022) 21:1943–73. doi: 10.1007/s40200-022-01114-z

14. Ebrahimi M, Seyedi SA, Nabipoorashrafi SA, Rabizadeh S, Sarzaeim M, Yadegar A, et al. Lipid accumulation product (LAP) index for the diagnosis of nonalcoholic fatty liver disease (NAFLD): a systematic review and meta-analysis. *Lipids Health Dis*. (2023) 22:41. doi: 10.1186/s12944-023-01802-6

15. Zhao S, Ren Z, Yu S, Chi C, Tang J, Maimaitiaili R, et al. Association between lipid accumulation product and target organ damage in elderly population: the northern Shanghai study. *Clin Interv Aging*. (2021) 16:1769–76. doi: 10.2147/CIA.S330313

16. Ayundini G, Astrella C, Tahapary D, Soewondo P. A systematic review on the association between lipid accumulation product index and type 2 diabetes mellitus. *J ASEAN Federation Endocrine Societies*. (2019) 34:16–20. doi: 10.15605/jafes.034.01.04

17. Baldini V, Mastropasqua M, Francucci CM, D'Erasmo E. Cardiovascular disease and osteoporosis. *J Endocrinol Investig*. (2005) 28:69–72.

18. Cavati G, Pirrotta F, Merlotti D, Ceccarelli E, Calabrese M, Gennari L, et al. Role of advanced glycation end-products and oxidative stress in Type-2-diabetes-induced bone fragility and implications on fracture risk stratification. *Antioxidants* (Basel). (2023) 12:928. doi: 10.3390/antiox12040928

19. Sirufo MM, De Pietro F, Bassino EM, Ginaldi L, De Martinis M. Osteoporosis in skin diseases. *Int J Mol Sci*. (2020) 21:4749. doi: 10.3390/ijms21134749

20. Im GI, Kim MK. The relationship between osteoarthritis and osteoporosis. *J Bone Miner Metab*. (2014) 32:101–9. doi: 10.1007/s00774-013-0531-0

21. Dillon CF, Hirsch R. The United States National Health and nutrition examination survey and the epidemiology of ankylosing spondylitis. *Am J Med Sci*. (2011) 341:281–3. doi: 10.1097/MAJ.0b013e31820f8c83

22. Ahluwalia N, Dwyer J, Terry A, Moshfegh A, Johnson C. Update on NHANES dietary data: focus on collection, release, analytical considerations, and uses to inform public policy. *Adv Nutr*. (2016) 7:121–34. doi: 10.3945/an.115.009258

23. Elnakib S, Vecino-Ortiz AI, Gibson DG, Agarwal S, Trujillo AJ, Zhu Y, et al. A novel score for mHealth apps to predict and prevent mortality: further validation and adaptation to the US population using the US National Health and nutrition examination survey data set. *J Med Internet Res*. (2022) 24:e36787. doi: 10.2196/36787

24. Mohammadi SM, Saniee N, Borzoo T, Radmanesh E. Osteoporosis and leptin: a systematic review. *Iran J Public Health*. (2024) 53:93–103. doi: 10.18502/ijph.v53i1.14686

25. Jiang GZ, Matsumoto H, Hori M, Gunji A, Hakozaki K, Akimoto Y, et al. Correlation among geometric, densitometric, and mechanical properties in mandible and femur of osteoporotic rats. *J Bone Miner Metab*. (2008) 26:130–7. doi: 10.1007/s00774-007-0811-7

26. Zhang X, Hong F, Liu L, Nie F, Du L, Guan H, et al. Lipid accumulation product is a reliable indicator for identifying metabolic syndrome: the China multi-ethnic cohort (CMEC) study. *QJM*. (2022) 115:140–7. doi: 10.1093/qjmed/hcaa325

27. Li H, Zhang Y, Luo H, Lin R. The lipid accumulation product is a powerful tool to diagnose metabolic dysfunction-associated fatty liver disease in the United States adults. *Front Endocrinol*. (2022) 13:977625. doi: 10.3389/fendo.2022.977625

28. Dong L, Lin M, Wang W, Ma D, Chen Y, Su W, et al. Lipid accumulation product (LAP) was independently associatedwith obstructive sleep apnea in patients with type 2 diabetes mellitus. *BMC Endocr Disord*. (2020) 20:179. doi: 10.1186/s12902-020-00661-x

29. Shao Q, Li J, Wu Y, Liu X, Wang N, Jiang Y, et al. Enhanced predictive value of lipid accumulation product for identifying metabolic syndrome in the general population of China. *Nutrients*. (2023) 15:3168. doi: 10.3390/nu15143168

30. Chen ZH, Zhou TF, Bu YT, Yang L. Bone mineral density saturation as influenced by the visceral adiposity index in adults older than 20 years: a population-based study. *Lipids Health Dis*. (2023) 22:170. doi: 10.1186/s12944-023-01931-y

31. Smith EL, Gilligan C. Dose-response relationship between physical loading and mechanical competence of bone. *Bone*. (1996) 18:455–505.

32. Sun A, Hu J, Wang S, Yin F, Liu Z. Association of the visceral adiposity index with femur bone mineral density and osteoporosis among the U.S. older adults from NHANES 2005-2020: a cross-sectional study. *Front Endocrinol*. (2023) 14:1231527. doi: 10.3389/fendo.2023.1231527

33. Wang H, Peng H, Zhang L, Gao W, Ye J. Novel insight into the relationship between muscle-fat and bone in type 2 diabetes ranging from Normal weight to obesity. *Diabetes Metabolic Syndrome Obesity*. (2022) 15:1473–84. doi: 10.2147/DMSO.S364112

34. Lopes KG, Rodrigues EL, da Silva Lopes MR, Do Nascimento VA, Pott A, Guimarães RCA, et al. Adiposity metabolic consequences for adolescent bone health. *Nutrients*. (2022) 14:3260. doi: 10.3390/nu14163260

35. Aikawa Y, Yamashita T, Nakai N, Higashida K. Low-carbohydrate, high-fat diet, and running exercise influence bone parameters in old mice. *J Applied Physiology*. (1985) 132:1204–12.

36. Herse F, Fain JN, Janke J, Engeli S, Kuhn C, Frey N, et al. Adipose tissue-derived soluble fms-like tyrosine kinase 1 is an obesity-relevant endogenous paracrine adipokine. *Hypertension*. (1979) 58:37–42.

37. Engeli S, Feldpausch M, Gorzelniak K, Hartwig F, Heintze U, Janke J, et al. Association between adiponectin and mediators of inflammation in obese women. *Diabetes*. (2003) 52:942–7. doi: 10.2337/diabetes.52.4.942

38. Eder K, Baffy N, Falus A, Fulop AK. The major inflammatory mediator interleukin-6 and obesity. *Inflammation Research*. (2009) 58:727–36. doi: 10.1007/s00011-009-0060-4

39. Puolakkainen T, Rummukainen P, Pihala-Nieminen V, Ritvos O, Savontaus E, Kiviranta R. Treatment with soluble Activin type IIB receptor ameliorates Ovariectomy-induced bone loss and fat gain in mice. *Calcif Tissue Int*. (2022) 110:504–17. doi: 10.1007/s00223-021-00934-0

40. Tan Y, Fu Y, Yao H, Wu X, Yang Z, Zeng H, et al. Relationship between phthalates exposures and hyperuricemia in U.S. general population, a multi-cycle study of NHANES 2007-2016. *Sci Total Environ*. (2023) 859:160208. doi: 10.1016/j.scitotenv.2022.160208

41. Wu C, Ren C, Song Y, Gao H, Pang X, Zhang L. Gender-specific effects of oxidative balance score on the prevalence of diabetes in the US population from NHANES. *Front Endocrinol*. (2023) 14:1148417. doi: 10.3389/fendo.2023.1148417

frontiers | Frontiers in Endocrinology

TYPE Original Research
PUBLISHED 21 March 2025
DOI 10.3389/fendo.2025.1528768

OPEN ACCESS

EDITED BY
Matthias Blüher,
Leipzig University, Germany

REVIEWED BY
Daniele Vergara,
University of Salento, Italy
Endre Károly Kristóf,
University of Debrecen, Hungary
Davide Gnocchi,
University of Bari Medical School, Italy

*CORRESPONDENCE
Hong-Mei Han
hanhm79@126.com
Lin-Hu Quan
lhquan@ybu.edu.cn

†These authors share first authorship

RECEIVED 15 November 2024
ACCEPTED 18 February 2025
PUBLISHED 21 March 2025

CITATION
Liu M, Song X-Z, Yang L, Fang Y-H, Lan L, Cui J-S, Lu X-C, Zhu H-Y, Quan L-H and Han H-M (2025) 1,25-dihydroxyvitamin D3 improves non-alcoholic steatohepatitis phenotype in a diet-induced rat model. *Front. Endocrinol.* 16:1528768. doi: 10.3389/fendo.2025.1528768

1,25-dihydroxyvitamin D3 improves non-alcoholic steatohepatitis phenotype in a diet-induced rat model

Mei Liu[1†], Xiang-Zhun Song[2†], Liu Yang[3†], Yu-Hui Fang[4], Liu Lan[5], Jing-Shu Cui[5], Xiao-Chen Lu[6], Hai-Yang Zhu[1], Lin-Hu Quan[7*] and Hong-Mei Han[1*]

[1]Department of Gastroenterology, Affiliated Hospital of Yanbian University, Yanji, Jilin, China, [2]Department of Gastroenterology, Jilin Provincial People's Hospital, Changchun, Jilin, China, [3]Department of Gastroenterology and Hepatology, Characteristic Medical Center of the Chinese People's Armed Police Force, Tianjin Key Laboratory of Hepatopancreatic Fibrosis and Molecular Diagnosis & Treatment, Tianjin, China, [4]Department of Dermatology, Fuyang People's Hospital of Anhui Medical University, Fuyang, Anhui, China, [5]Department of Pathology, Affiliated Hospital of Yanbian University, Yanji, Jilin, China, [6]Department of Gastroenterology, Jimo District People's Hospital, Qingdao, Shandong, China, [7]Department of College of Pharmacy, Yanbian University, Yanji, Jilin, China

We studied the potential protective effects of 1,25-dihydroxyvitamin D3 (1,25 VD3) supplementation on liver damage induced by a choline-deficient (CD) diet in rats, where impaired liver function leads to decreased 25-hydroxyvitamin D3 levels, the precursor for the active 1,25 VD3. The CD diet reduced serum 25 VD3 levels and increased liver enzymes, indicative of liver damage. Conversely, 1,25 VD3 supplementation alleviated liver damage, reducing liver enzymes and improving histopathological features characteristic of non-alcoholic steatohepatitis (NASH). Oxidative stress and inflammation were mitigated by 1,25 VD3, as evidenced by decreased malondialdehyde and nuclear factor kappa B (NF-κB) expression, and increased total antioxidant capacity (TAOC). 1,25 VD3 also enhanced fatty acid metabolism by increasing peroxisome proliferator-activated receptor alpha (PPARα) and carnitine palmitoyltransferase-1 (CPT-1) expression, promoting lipid transport and oxidation. Additionally, 1,25 VD3 supplementation modulated inflammation by increasing PPARγ expression, reducing NF-κB expression, and decreasing pro-inflammatory cytokines (TNF-α, IL-1β). Anti-inflammatory cytokines (IL-10, IL-4) were increased, and macrophage polarization was shifted towards an anti-inflammatory M2 phenotype. Moreover, 1,25 VD3 upregulated CYP2J3, a cytochrome P450 epoxygenase that converts arachidonic acid to anti-inflammatory epoxyeicosatrienoic acids (EETs) and decreased soluble epoxide hydrolase activity, likely contributing to increased EET levels. Correlation studies revealed positive associations between 1,25 VD3 supplementation, CYP2J3 expression, EETs, as well as negative correlations with NF-κB and TNF-α. PPARα expression

positively correlated with TAOC and CPT-1, while PPARγ expression negatively correlated with inflammatory markers. These findings demonstrate the therapeutic potential of 1,25 VD3 in alleviating NASH through regulation of fatty acid metabolism, inflammation, and oxidative stress.

KEYWORDS

vitamin D3, non-alcoholic steatohepatitis, CYP450, inflammation, macrophage

Introduction

Non-alcoholic fatty liver disease (NAFLD), proposed to be renamed metabolic (dysfunction)-associated fatty liver disease (MAFLD) (1) is a common chronic liver condition marked by excessive lipid accumulation in hepatocytes, independent of alcohol consumption or other toxic factors (2). It encompasses a spectrum of progressive stages, including simple non-alcoholic fatty liver, non-alcoholic steatohepatitis (NASH), liver cirrhosis, and hepatocellular carcinoma, highlighting its clinical significance and potential for progression to hepatocarcinogenesis. The pathogenesis of NASH is marked by hepatic lipid peroxidation and inflammation (3–5). Recently, active vitamin D3 (1,25-dihydroxyvitamin D3, (1,25 VD3) has emerged as a potential therapeutic agent, exhibiting antioxidant and anti-inflammatory properties. Notably, studies have shown that NASH patients have lower serum 1,25 VD3 levels compared to healthy controls (6, 7). Moreover, 1,25 VD3 supplementation has been found to improve insulin resistance and liver enzyme levels in NASH patients (6–10). Animal models have replicated NASH-like liver histopathology using a choline-deficient, amino acid-defined (CDAA) diet (11). Our previous research demonstrated that 1,25 VD3 improves lipid peroxidation and inflammation in NASH-induced rats in a dose-dependent manner (12). However, the specificity and mechanisms underlying this effect remain unclear, warranting further investigation. Recent research has highlighted the significance of the cytochrome P450 (CYP450) pathway in arachidonic acid (AA) metabolism in the development of non-alcoholic steatohepatitis (NASH) (13). Specifically, studies have identified substantial changes in CYP450 metabolites and AA metabolism in patients with NASH (14) and in animal models with NASH induced by high-fat diets (15, 16). The CYP450 pathway produces epoxide eicosatrienoic acids (EETs) as primary metabolites, comprising 5,6-EET, 8,9-EET, 11,12-EET, and 14,15-EET (17). Notably, EETs have been extensively shown to possess anti-lipid peroxidation and anti-inflammatory properties across various diseases (18–20). However, the beneficial effects of EETs are compromised upon hydrolysis by soluble epoxide hydrolase (sEH), converting them to dihydroxy eicosatrienoic acids (DHETs) (21). Interestingly, while EETs exhibit anti-inflammatory activities, the role of DHETs remains controversial.

The anti-inflammatory and antioxidant effects of EETs in the liver are primarily mediated through the peroxisome proliferator-activated receptor-alpha (PPARα) and nuclear factor-kappaB (NF-κB) pathways. As potent activators of PPARα (22), EETs regulate lipid homeostasis and mitigate lipid peroxidation in the liver (23–25). Studies employing mouse models of NAFLD induced by high-fat diets (HFD) have demonstrated the therapeutic potential of EETs. For instance, administering 14,15-EET to CYP450 2J2 (CYP2J2)-overexpressing mice reduced NF-κB expression, lipid peroxidation, and inflammation in the liver. *In vitro* experiments using palmitic acid-treated HepG2 cells further revealed that 14,15-EET inhibited the NF-κB/JNK signaling pathway, decreased malondialdehyde (MDA) levels, and enhanced antioxidant enzyme activities, including superoxide dismutase, catalase, and glutathione peroxidase (26). Consistent with these findings, other studies have shown that elevated EET levels alleviate liver inflammation in mice with NASH induced by HFD and methionine-choline-deficient (MCD) diets. Specifically, EETs suppressed the NF-κB pathway, leading to reduced liver inflammation (14, 15, 27). These studies collectively highlight the protective role of EETs in liver disease. To further explore the mechanisms underlying 1,25 VD3's therapeutic effects, we established a rat model of NASH using a choline-deficient, amino acid-defined (CDAA) diet and supplemented 1,25 VD3. We measured metabolic proteins, metabolites, and key enzymes of the liver CYP450 pathway to investigate whether 1,25 VD3 improves lipid peroxidation and inflammation through the CYP450 pathway.

Materials and methods

Materials

Standard chow diet (choline-sufficient, amino acid-defined, Cat # TP 1R810) and CDAA diet (Cat # TP 1R800) were procured from Trophic Animal Feed High-Tech Company, China. 1,25 VD3 from Sigma-Aldrich (CAS # 128723-16-0), BCA protein quantitation kit (Boster Bio, Cat # AR0146), RIPA lysis buffer (Boster Bio, Cat # 0105), protease inhibitor cocktails (Boster, Bio Cat # AR1182), phosphatase inhibitor (Boster Bio, Cat # AR1183), color pre-dyed protein marker (Boster Bio, Cat # AR1113), Western-specific primary and secondary antibody diluent (Boster Bio, Cat # AR1017), wash buffer TBS-T (Boster Bio, Cat # AR0195-10), ECL chemiluminiscent reagent (Boster Bio, Cat # AR1196), BSA TBS buffer system blocking solution (Boster Bio, Cat # AR0189), NF-κB

antibody (Boster Bio, Cat # A01228-1), β-actin antibody (Boster Bio, Cat # M01263), HRP-conjugated goat anti-rabbit IgG (Boster Bio, Cat # BA1054), CD163 antibody (Boster Bio, Cat # A00812-2), CD11c antibody (Boster Bio, Cat # A00357-3), CD68 antibody (Boster Bio, Cat # BA3638), fluorescent (DyLight 488) labelled goat anti-rabbit IgG (Boster Bio, Cat # BA1127), fluorescent (DyLight 594) labelled goat anti-rabbit IgG (Boster Bio, Cat # BA1142), rat TNF-α ELISA kit (Jiangsu Enzyme Immunoassay Co., Ltd., Cat # MM-0180R1), rat IL-1β ELISA kit (Boster Bio, Cat # EK0393), rat IL-4 ELISA kit (Jiangsu Enzyme Immunoassay Co., Ltd, Cat # MM-0191R1), rat IL-10 ELISA kit (Boster Bio, Cat # EK0418), 25 VD3 assay kit (Roche Diagnostics, Cat # 07028148190), TAOC assay kit (Nanjing Jiancheng, Cat # A015-3-1), MDA assay kit (Nanjing Jiancheng, Cat # A003-1-2), and free fatty acid kit (Kunchuang Biotechnology, Xian, China, Cat # SK125-2).

Animal study design and experimental procedures

The experimental procedures for this study complied with the ethical standards of the China Experimental Animal Management Association and were approved by the Ethics Committee of Yanbian University (approval number YD202309110024). Based on our previous research (12), we conducted a 12-week study using 6-week-old, specific-pathogen-free-grade Wistar rats purchased from Changchun Yisi Animal Co., Ltd.

Following an adaptation period, the rats were divided into four groups: 1. Control Group (CG): fed a normal rat chow diet; 2. Control plus 1,25 VD3 supplement Group (CVDG): fed a normal rat chow diet with 1,25 VD3 injection; 3. Choline-deficient Group (CDG): fed a CD diet that was amino acid sufficient; and 4. Choline-deficient plus 1,25 VD3 supplement Group (CDVDG): fed a CDAA diet with 1,25 VD3 injection. (Figure 1 presents the schematic diagram of the experimental design). We administered 5μg 1,25 VD3/kg body weight via intraperitoneal injection twice a week (12).

To prepare the 1,25 VD3 solution, 1mg 1,25 VD3 powder (Sigma Reagent Company) was dissolved in 20μL anhydrous ethanol and diluted in 0.9% sodium chloride to make a 5μg/mL solution. This solution was stored in a dark environment at 4°C and prepared every 2 weeks. Rats in the CDG received an equivalent volume of anhydrous ethanol in 0.9% sodium chloride (1mL/kg body weight) intraperitoneally. After 12 weeks of treatments, the rats were fasted for 2 h and euthanized by cervical dislocation. Body weight was measured, and blood was collected from the abdominal aorta. Serum was separated by centrifugation at 4°C (3000 rpm). The liver was removed, and its wet mass was recorded. A portion of the right lobe was fixed with 4% formaldehyde for histological analysis, while the remaining tissue was homogenized for further analysis.

Liver enzymes and blood lipids

Serum aspartate transaminase (AST) and alanine transaminase (ALT) activities were measured using a cobas c702 automatic biochemical analyzer (Roche Diagnostics GmbH). Serum triglyceride (TG), total cholesterol (TC), high-density lipoprotein-

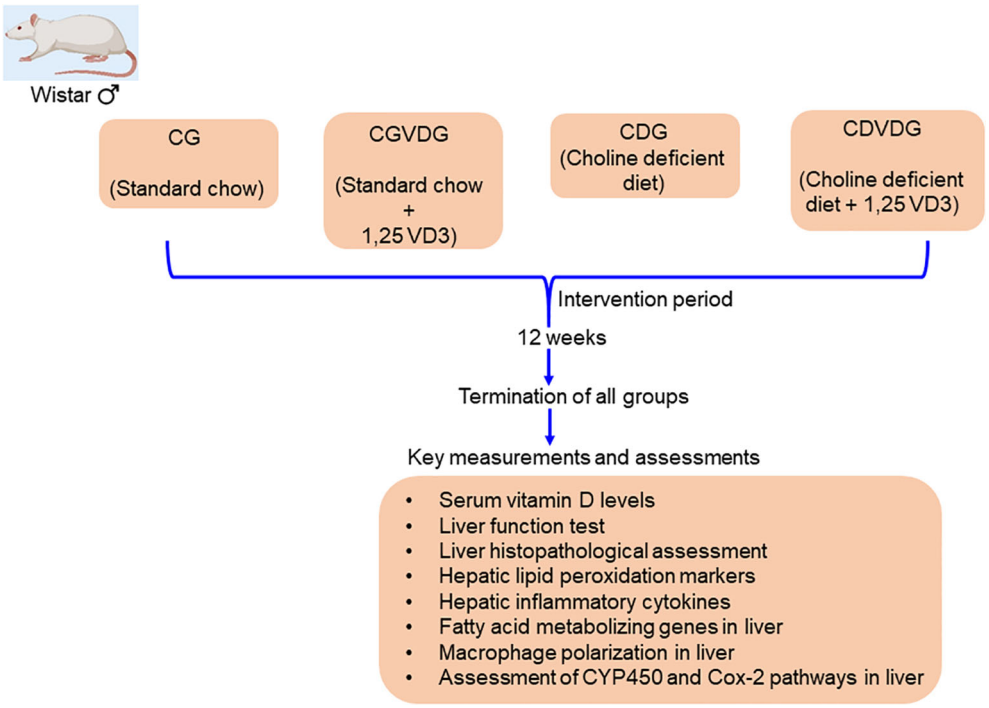

FIGURE 1
A schematic diagram representing study design.

cholesterol (HDL-C), and low-density lipoprotein-cholesterol (LDL-C) levels were determined using kits from Nanjing Jiancheng Bioengineering Institute, following the manufacturer's instructions.

Histopathological evaluation

Liver tissue from the right lobe was fixed with 4% formaldehyde, embedded in paraffin, and stained with haematoxylin and eosin (H&E). Steatosis, activity, and fibrosis (SAF) were scored by two pathologists blinded to the study design. Five visual fields from each section were magnified 200 times and averaged for statistical analysis. The SAF score was based on NASH Clinical Research Network criteria (22, 23) for grading steatosis and activity (Table 1). In this unweighted scoring system (28), the activity score is the sum of the lobular inflammation and hepatocellular ballooning scores, ranging from 0 to 5. A higher score indicates greater disease activity. A SAF score ≥3 was diagnosed as NASH.

Serum 25 VD3 measurement

Serum 25 VD3 levels were determined using the Roche electrochemiluminescence method on a Cobas 8000 automatic biochemical immunity analyzer (Roche Diagnostics GmbH).

TABLE 1 NASH scoring.

Steatosis		
Grade	Steatosis percentage (hepatocytes with fat droplets)	Description
0	<5%	No significant steatosis
1	5–33%	Mild steatosis
2	34–66%	Moderate steatosis
3	>66%	Severe steatosis
Lobular inflammation		
Score	Description	
0	No inflammatory foci	
1	<2 inflammatory foci per 200x field	
2	2–4 inflammatory foci per 200x field	
3	>4 inflammatory foci per 200x field	
Ballooning		
0	None	
1	Few ballooned cells	
2	Many ballooned cells or prominent ballooning	

Oxidation status

Liver lipid peroxidation was evaluated by measuring malondialdehyde (MDA) levels using a thiobarbituric acid kit, while total antioxidant capacity (TAOC) was assessed via the ferric reducing antioxidant power (FRAP) method, both performed according to the manufacturer's instructions (Nanjing Jiancheng Bioengineering Institute).

Detection of PPARα and CPT-1 by qPCR

PPARα regulates lipid homeostasis and liver lipid peroxidation (26, 27, 29). PPARα stimulates liver expression of carnitine palmitoyltransferase-1 (CPT-1), initiating mitochondrial fatty acid transport for β-oxidation (30). To investigate the expression of PPARα and CPT-1, we measured their mRNA levels in liver tissue using qPCR. Total RNA (20μg) was extracted from liver tissue using Trizol solution (Invitrogen). Reverse transcription was performed using RevertAid Reverse Transcriptase (Thermo Scientific). Quantitative PCR amplification was then carried out. qPCR data were processed using the ΔΔCT method. Primer sequences are listed in Table 2.

Inflammation and macrophage polarization analysis in liver tissue

To investigate inflammation and macrophage polarization, we measured: 1. NF-κB levels in liver tissue using Western blotting; 2. M1 (CD68+CD11c+) and M2 (CD68+CD163+) macrophage populations using double immunofluorescence labelling; 3. Pro-inflammatory (TNF-α and IL-1β) and anti-inflammatory (IL-10 and IL-4) factor levels using enzyme-linked immunosorbent assay (ELISA); and 4. PPARγ mRNA expression in liver tissue using qPCR.

For macrophage polarization study, we used the double immunofluorescence method. Liver tissue sections were dewaxed, rehydrated, and incubated with primary antibodies (anti-CD68,

TABLE 2 qPCR primers' sequence.

Gene	Sequence	Seq/RefSeq
PPARα(155bp)	F:CGGGTCATACTCGCAGGAAAG R:TGGCAGCAGTGGAAGAATCG	NM_013196.2
CTP-1(141bp)	F:CTGACGCCCGAGTTCCTG R:GCCTTCTGTCCTCTGTGTGG	NM_078622
PPARγ(141bp)	F:CCTTTACCACGGTTGATTTCTC R:CAGGCTCTACTTTGATCGCACT	NM_013124.3
CYP2J3(75bp)	F:TTCAGAATGTCCGTCACCAT R:TTCCTCTTCGACATCACAGC	NM_175766
GAPDH(114bp)	F:TTCAACGGCACAGTCAAGG R:CTCAGCACCAGCATCACC	NM_017008.4

1:100; anti-CD11c, 1:100; or anti-CD163, 1:200) followed by secondary antibodies labeled with fluorescein. DAPI staining and fluorescence microscopy were used to visualize and count macrophages. M1 macrophages were identified as CD68+CD11c+ cells, while M2 macrophages were identified as CD68+CD163+ cells. Nuclei were counterstained with DAPI (blue) for cell identification. The M1/M2 ratio was determined by counting CD68+CD11c+ (M1) cells and dividing it by the number of CD68+CD163+ (M2) cells in the same fields. Two pathologists randomly selected six regions with high positive staining rates from each group of double-stained liver tissue sections. The cell counts were averaged for each animal before calculating group means and conducting statistical analysis.

Western blotting

Liver tissue samples (100mg) were homogenized in RIPA buffer supplemented with protease and phosphatase inhibitors. The lysates were centrifuged at 14,000 × g for 15 minutes at 4°C to remove debris, and the supernatant was collected for protein quantification using the BCA assay. Equal amounts of protein (30 μg per lane) were loaded onto a 10% SDS-PAGE gel and electrophoresed at 100 V. Proteins were then transferred to a PVDF membrane at 300 mA for 1.5 hours in transfer buffer. The membrane was blocked in 5% non-fat milk in TBST for 1 hour at room temperature and then incubated overnight at 4°C with an antibody against NF-κB (1:1000 dilution). After washing, the membrane was incubated with an HRP-conjugated secondary antibody (1:2000 dilution) for 1 hour at room temperature. Signal detection was performed using ECL reagents (Boster Bio-Engineering Limited Company). Bands were visualized using a chemiluminescent imaging system. The membranes were stripped and reprobed with an antibody against β-actin (1:1000 dilution) as a loading control, followed by incubation with an HRP-conjugated secondary antibody (1:2000 dilution). Densitometry was performed using ImageJ software, and NF-κB expression was normalized to β-actin.

Analysis of CYP450 pathway

CYP2J3 expression was assessed for expression by qPCR following the protocol described above. To quantify the metabolites of the liver CYP450 pathway, specifically (EETs) and DHETs, we employed targeted liquid chromatography-tandem mass spectrometry (LC-MS/MS). Sample preparation was performed by adding PBS containing 0.1% butylated hydroxytoluene and an isotope internal standard to the sample. The mixture was then ground, incubated at 4°C for 1 hour, and centrifuged. The resulting supernatant was extracted and subsequently enriched with AA using an Oasis MAX SPE column (Waters, USA). Quantitative analysis of eicosanoids was performed after solid-phase extraction-enrichment in electrospray ionization mode using an Exion UPLC-QTRAP 6500 PLUS system (Sciex) (19, 20).

Statistical analysis

All experiments were repeated three times, with the average result taken for analysis. All data were analyzed by IBM SPSS Statistics 25.0 statistical software, and a two-way analysis of variance was used to explore the effects of 1,25 VD3 and NASH status. If statistical differences were detected, between-group comparisons were carried out using the Fisher's Least Significant Difference test. Pearson's correlation coefficient was used to analyze the correlation between parameters. Data are expressed as means and standard error of the mean (SEM); results were considered statistically significant when $p< 0.05$.

Results

1,25 VD3 improves liver function and alleviates histopathological features of CDAA-induced NASH

To investigate the impact of 1,25 VD3 supplementation on liver function in the CDAA-induced NASH model, we assessed key liver function markers by measuring serum ALT (Figure 2A) and AST (Figure 2B) activities. Compared to the CG, the CDG showed elevated serum AST ($p < 0.001$) and ALT ($p < 0.001$) levels, indicating impaired liver function. Conversely, CDVDG demonstrated reduced AST and ALT levels compared to CDG ($p < 0.001$), suggesting improved liver health. Notably, CDVDG and CGVDG groups exhibited similar AST and ALT levels. Increased 25 VD3 levels in CDVDG versus CDG indicate enhanced liver function, as the liver produces this precursor to active 1,25 VD3 (Figure 2C). These findings imply that 1,25 VD3 supplementation protects against CDAA-induced impairment in liver function.

The hallmark histopathological features of NASH, including steatosis, inflammation, and hepatocyte injury, were assessed using H&E staining (Figure 2D). Analyses of histopathological changes (Figure 2E) revealed that the CDG group had significantly increased steatosis, lobular inflammation, ballooning degeneration, activity score, and SAF score compared to the CG (all $p < 0.001$). The CDVDG demonstrated significantly reduced steatosis, lobular inflammation, ballooning degeneration, activity score, and SAF score compared to the CDG (all $p < 0.001$). These results suggest that 1,25 VD3 supplementation alleviates liver damage in CDAA diet-induced NASH rats, improving steatosis, inflammation, and histopathological scores.

1,25 VD3 attenuates oxidative stress and enhances fatty acid metabolism in CDAA-induced NASH

Liver MDA and TAOC levels were evaluated to investigate oxidative stress in NASH. While MDA levels remained higher in the CDVDG than in the CGVDG ($p < 0.001$), 1,25 VD3

10.3389/fendo.2025.1528768

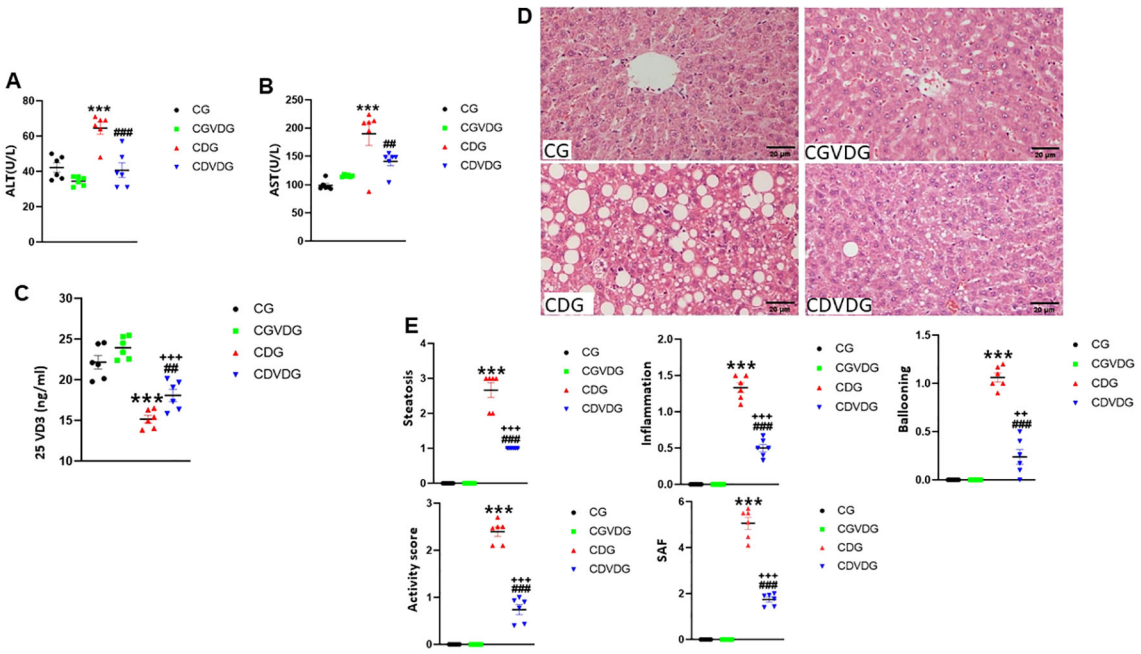

FIGURE 2
Effects of 1,25 VD3 supplementation on serum biomarkers and liver histopathology in a rat model of NASH. **(A)** Serum ALT and **(B)** AST activities were measured using Automatic Biochemical Analyzer. **(C)** 25VD_3 levels were measured using Roche Electrochemiluminescence method in the indicated groups. **(D)** Representative H&E-stained liver sections (5 μM) from the indicated groups. **(E)** Histopathological scores for steatosis, lobular inflammation, ballooning degeneration, activity, and SAF scores were determined following the protocol as described in Table 1. Data are presented as mean ± SEM, n=6. Statistical significance: A-C - ***p < 0.001 vs. CG; ##p < 0.01, ###p < 0.001 vs. CDG; +++p < 0.001 vs. CDVDG. D-E - ***p <0.001 vs. CG; ###p < 0.001 vs. CDG; ++p < 0.01, +++p < 0.001 vs. CDG. CG: Normal rat chow diet; CVDG: Normal diet + 1,25 VD3; CDG: Choline-deficient diet; CDVDG: Choline-deficient diet + 1,25 VD3.

supplementation reduced MDA levels in the CDVDG compared to the CDG ($p < 0.001$) (Figure 3A). CGVDG showed a modest yet significant increase in MDA levels compared to the CG. TAOC levels were significantly higher in the CDG and CDVDG compared to their respective controls (CG and CGVDG, $p < 0.001$). Notably, TAOC levels in the CDVDG surpassed those in the CDG ($p < 0.001$), while no difference was observed between the CGVDG and CG (Figure 3B).

Given that oxidative stress and inflammation are closely linked, we examined NF-κB expression, a key regulator of inflammatory pathways. The CDAA diet significantly increased NF-κB expression in the CDG compared to the CG rats ($p < 0.001$). The upregulation was observed as an increased intensity of the 65 kDa NF-κB band. Supplementation with 1,25 VD3 significantly mitigated the CDAA diet-induced increase in NF-κB expression observed in CDG rats ($p < 0.001$). In the CDVDG, NF-κB levels were restored to values comparable to the CG ($p < 0.001$) (Figure 3C).

NF-κB-driven inflammation in NASH can impact fatty acid metabolism, critically modulated by PPARα and CPT-1. PPARα regulates lipid homeostasis and liver lipid peroxidation (26, 27, 29), and also stimulates liver expression of CPT-1, initiating mitochondrial fatty acid transport for β-oxidation (30). PPARα and CTP-1 expression were significantly higher in the CDVDG compared to the CDG ($p < 0.001$ and $p < 0.01$, respectively). No significant changes in PPARα and CTP-1 expression were observed between the CGVDG and CG (Figures 3D, E).

These results demonstrate that the CDAA diet increases liver MDA and TAOC levels, while 1,25 VD3 supplementation enhances PPARα and CTP-1 expression, reduces MDA, and increases TAOC, indicating potential anti-lipid peroxidation and antioxidation activity.

1,25 VD3 favorably modulates KC polarization and upregulates PPARγ in NASH

KCs, including M1 and M2 macrophages, contribute to liver inflammation in NASH. An imbalance between pro-inflammatory M1 and anti-inflammatory M2 macrophages worsens inflammation. NF-κB upregulation favors M1 macrophage differentiation over M2, amplifying inflammatory responses in KCs. CD11c-positive, CD68-positive cells (yellow or orange in merged images) indicate a pro-inflammatory M1 phenotype (Figure 4A). CD68-positive, CD163-positive cells indicate an anti-inflammatory M2 phenotype (Figure 4B). The M1 (pro-inflammatory)/M2 (anti-inflammatory) ratio in the CDG was significantly higher than in the CG ($p< 0.001$), but the M1/M2 ratio in CDVDG was not significantly different from the CGVDG ($p> 0.05$). Compared with the CG, the M1/M2 ratio in the CGVDG was not significantly different, but was significantly lower in the CDG ($p< 0.001$) (Figure 4C).

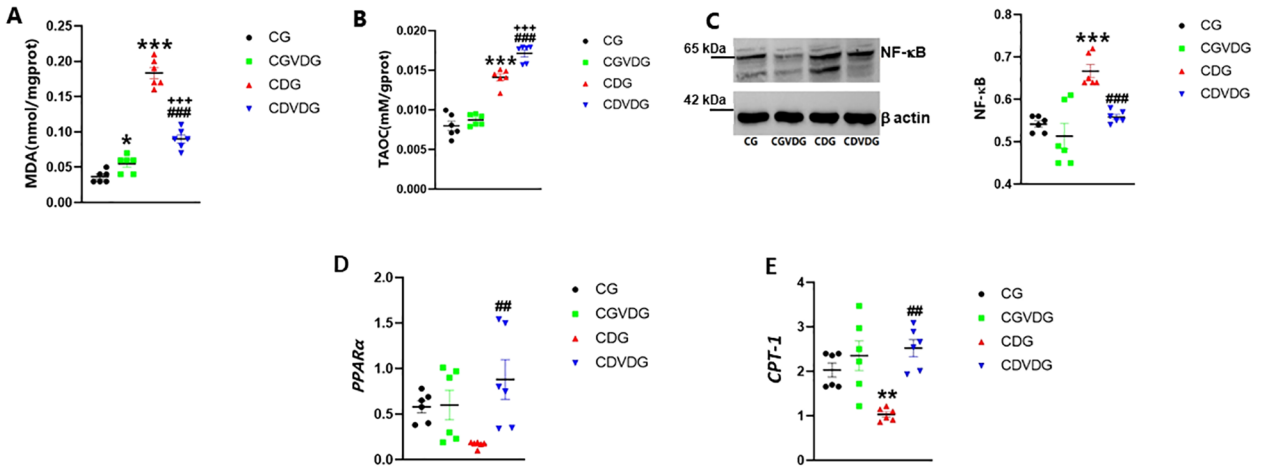

FIGURE 3
Effects of 1,25 VD3 supplementation on hepatic lipid peroxidation, inflammation and fatty acid metabolizing genes in NASH rats. To assess oxidative stress, hepatic **(A)** MDA was measured using a thiobarbituric acid kit and **(B)** TAOC levels measured using the FRAP method. **(C)** NF-κB expression in liver tissue, analyzed by Western blotting and normalized to β-actin (left panel showing representative blot and right panel showing quantification by densitometry of 65 kDa band). Antibodies used and their dilutions: primary antibodies against NF-κB (anti-rabbit, 1:1000) and β-actin (anti-rabbit, 1:1000), followed by HRP-conjugated secondary antibody (1:2000). **(D)** PPARα and **(E)** CPT-1 mRNA levels were quantified by qPCR in liver tissues of indicated groups, and expressed as relative mRNA levels following normalization to GAPDH mRNA levels. Data are presented as mean ± SEM, n=6. *p < 0.05, **p<0.01 and ***p < 0.001 vs CG; ##p < 0.01 and ###p < 0.001 vs CDG.

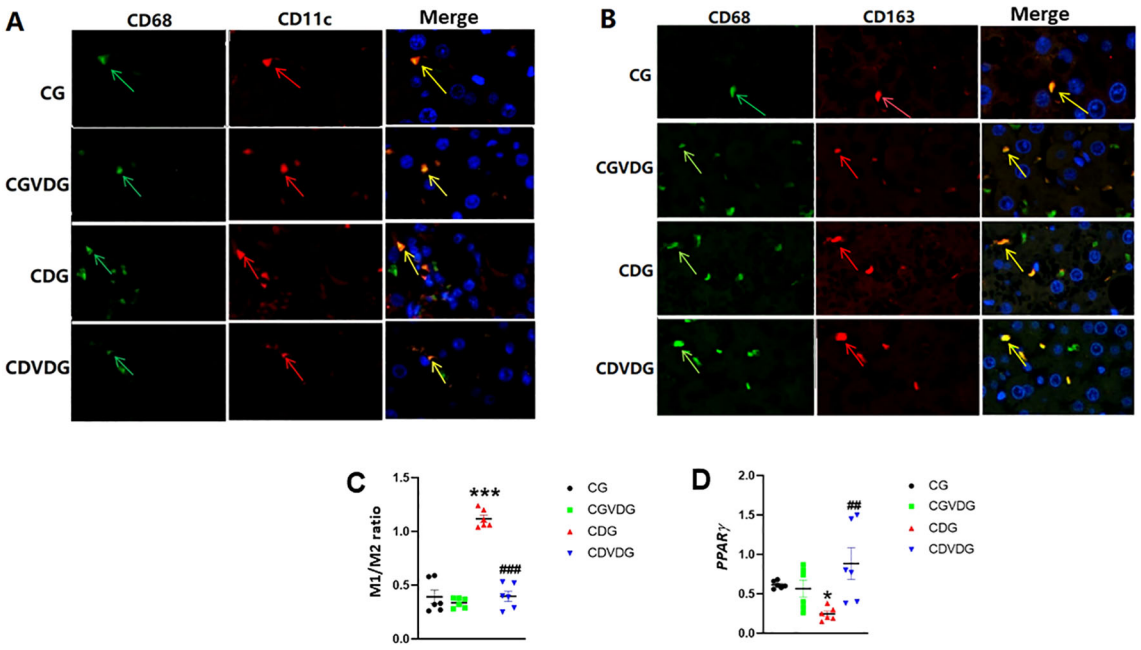

FIGURE 4
Effects of 1,25 VD3 supplementation on macrophage polarization and PPARγ expression in NASH rats. **(A)** M1-type KCs identified by double immunofluorescence staining; green arrows indicate CD68-positive cells, red arrows indicate CD11c-positive cells, and yellow arrows indicate CD11c/CD68 double-positive cells (M1KCs). **(B)** M2-type KCs identified by double immunofluorescence staining; green arrows indicate CD68-positive cells, red arrows indicate CD163-positive cells, and yellow arrows indicate CD163/CD68 double-positive cells (M2KCs). Antibodies were diluted as follows: anti-CD68 (1:100), anti-CD11c (1:100), and anti-CD163 (1:200). **(C)** The M1/M2 macrophage ratio was determined by quantifying the proportion of M1 and M2 KCs in liver tissue, as identified through double immunofluorescence staining. **(D)** PPARγ levels in liver tissue of the indicated groups were determined by qPCR and expressed as relative mRNA levels following normalization to GAPDH mRNA levels. Data are presented as mean ± SEM, n=6. *p < 0.05 and ***p < 0.001 vs CG; ##p < 0.01 and ###p < 0.001 vs CDG.

Since PPARγ activity negatively regulates M1/M2 ratio and liver inflammation (31), we evaluated its gene expression in liver. PPAR-γ expression was significantly downregulated in CDG ($p < 0.01$) but markedly upregulated in CDVDG, exceeding CG levels ($p < 0.01$) (Figure 4D).

1,25 VD3 restores cytokine balance by reducing pro-inflammatory and enhancing anti-inflammatory mediators in NASH

Given cytokine imbalance's role in NASH, we measured the levels of liver TNF-α, IL-1β, IL-4, and IL-10 to elucidate pro-inflammatory and anti-inflammatory mechanisms. Pro-inflammatory cytokines TNF-α (Figure 5A) and IL-1β (Figure 5B) were elevated in the CDG ($p < 0.001$), but 1,25 VD3 supplementation significantly decreased TNF-α in the CDVDG ($p < 0.05$) and IL-1β in both CDVDG and CGVDG ($p < 0.001$). Conversely, anti-inflammatory cytokines IL-10 (Figure 5C) and IL-4 (Figure 5D) were increased in the CDVDG compared to the CGVDG ($p < 0.001$) and CDG ($p < 0.001$). Notably, IL-4 was elevated in the CGVDG compared to the CG ($p < 0.001$), but reduced in the CDG ($p < 0.001$). These findings suggest that 1,25 VD3 supplementation exerts anti-inflammatory effects in liver tissue, mitigating the pro-inflammatory consequences of the CDAA diet.

1,25 VD3 enhances anti-inflammatory CYP2J3/EET pathway and reduces pro-inflammatory sEH/DHET activity in NASH

Liver-expressed CYP2J3, a key epoxygenase, and the CYP450 enzyme modulates inflammation by converting AA into anti-inflammatory EETs and pro-inflammatory HETEs (8, 17). CYP2J3 levels were significantly higher in the CDVDG compared to the CDG ($p < 0.01$) (Figure 6A). CYP2J3 converts AA to anti-inflammatory EETs, particularly 5,6-EET, which was detected in liver tissue. Interestingly, EET levels were elevated in the CDG compared to the CG ($p < 0.05$), and remarkably enhanced in the CDVDG compared to both CG and CDG groups (all $p < 0.001$) (Figure 6B).

However, sEH, a key enzyme in the CYP 450 pathway, metabolizes EETs to pro-inflammatory DHETs. Our results showed that sEH activity was significantly lower in the CDVDG compared to the CGVDG ($p < 0.01$), suggesting reduced EET metabolism (Figure 6C). Conversely, DHETs (5,6-DHET, 8,9-DHET, 11,12-DHET, and 14,15-DHET) were detected, with significantly higher levels in the CDVDG compared to both CGVDG and CDG (both $p < 0.001$). Additionally, DHET levels were higher in the CGVDG compared to the CG ($p < 0.05$) (Figure 6D).

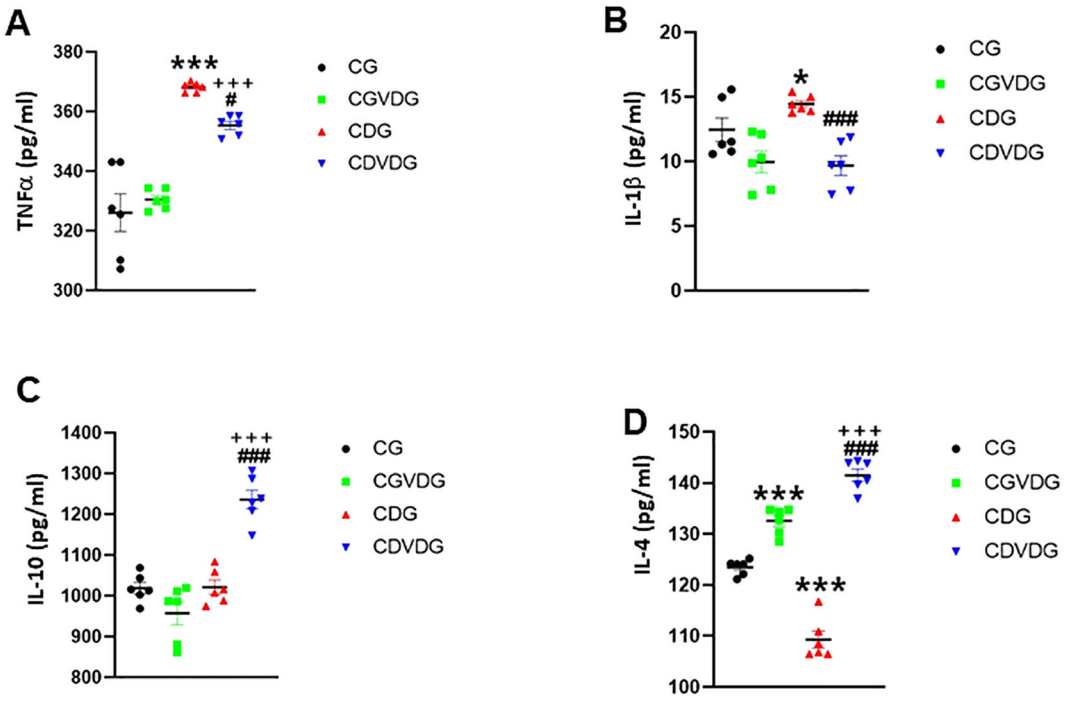

FIGURE 5
Effects of 1,25 VD3 supplementation on hepatic cytokine production in NASH rats. The proinflammatory, **(A)** TNF-α and **(B)** IL-1β levels, and the anti-inflammatory **(C)** IL-10 and **(D)** IL-4 levels in liver tissue lysates of indicated groups were measured using specific ELISA kits. Data are presented as mean ± SEM, n=6. *p,0.05 and ***$p < 0.001$ vs CG; #$p < 0.05$ and ###$p < 0.001$ vs CDG; +++$p < 0.001$ vs CG.

10.3389/fendo.2025.1528768

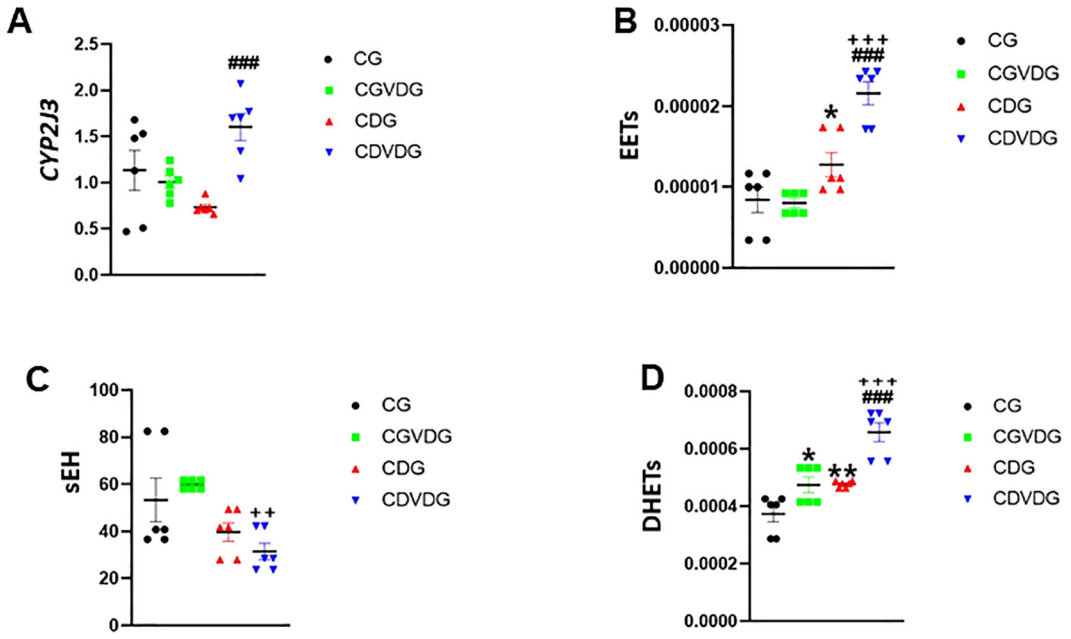

FIGURE 6
Effects of 1,25 VD3 supplementation on CYP450 and COX-2 pathways in liver of NASH rats. **(A)** CYP2J3 mRNA level was quantified by qPCR and expressed as relative mRNA levels following normalization to GAPDH mRNA levels. LC-MS/MS was used to measure **(B)** EETs, **(C)** sEH, and **(D)** DHETs levelss in livers of indicated groups. Data are presented as mean ± SEM, n=6. *p < 0.05 and **p < 0.01 vs CG; ###p < 0.001 vs CDG; ++p < 0.01.

Interactive effects of choline deficiency and 1,25 VD3 supplementation on liver function, oxidative stress, and inflammatory pathways in NASH

To explore the mechanisms behind NASH progression and the effects of 1,25 VD3 supplementation, we examined the interactive effects of the choline-deficient diet and 1,25 VD3 on liver and metabolic parameters (Table 3). A significant interaction indicates that the combined effects of the CDAA diet and 1,25 VD3 supplementation on liver and metabolic parameters were not simply the sum of their individual effects. Instead, the presence of one factor modified the influence of the other on the measured outcomes.

The interaction between the CDAA diet and 1,25 VD3 supplementation significantly affected various liver and metabolic parameters. 1,25 VD3 alone (CGVDG) did not affect liver enzyme levels, but its combination with the CDAA diet significantly altered both AST and ALT levels. Histopathological features such as steatosis, lobular inflammation, ballooning degeneration, activity score, and the SAF score were strongly influenced by both the CDAA diet and 1,25 VD3 supplementation, demonstrating a significant interaction between the two factors. The interaction between the CDAA diet and 1,25 VD3 supplementation significantly affected various liver and metabolic parameters. 1,25 VD3 alone (CGVDG) did not affect liver enzyme levels, but its combination with the CDAA diet significantly altered both AST and ALT levels. Histopathological features such as steatosis, lobular inflammation, ballooning degeneration, activity score, and the SAF score were strongly influenced by both the CDAA diet and 1,25 VD3 supplementation, demonstrating a significant interaction between the two factors.

Furthermore, markers of oxidative stress and antioxidant capacity, specifically MDA and TAOC, were significantly altered by the combined effects of both treatments. In terms of inflammatory markers, the interaction between the CDAA diet and 1,25 VD3 led to significant changes in NF-κB and TNF-α levels. Additionally, anti-inflammatory cytokines IL-4 and IL-10 were significantly influenced by this interaction, demonstrating significant enhancement in CDVDG group compared with CG. The M1/M2 macrophage ratio was significantly affected by both the CDAA diet and 1,25 VD3 supplementation, with the CDAA diet increasing the ratio (shifting toward M1) and 1,25 VD3 supplementation in the presence of the CDAA diet decreasing it (shifting toward M2), while 1,25 VD3 alone (CGVDG) had no effect, demonstrating a significant interaction between the CDAA diet and 1,25 VD3. Although the CDAA diet did not alter PPARγ expression, supplementation with 1,25 VD3 did, and the interaction between the two factors further influenced its expression. Moreover, both treatments affected the levels of EETs and DHETs, though no interaction was noted for sEH activity.

These findings underscore the complex interplay between choline deficiency and 1,25 VD3 supplementation, highlighting their combined effects on various liver functions, oxidative stress, inflammatory responses, and metabolic parameters.

10.3389/fendo.2025.1528768

TABLE 3 Two-way ANOVA showing individual effects of the CD diet and 1,25 VD3 supplementation, as well as their interactions, across various biochemical and histopathological parameters.

Parameter	CD Diet Effect	1,25 VD3 Supplementation Effect	Interaction Effect (CD x 1,25 VD3)
Serum AST	Significant ($p < 0.001$)	Not significant ($p > 0.05$)	Significant ($p < 0.001$)
Serum ALT	Significant ($p < 0.001$)	Significant ($p < 0.001$)	Significant ($p < 0.001$)
Steatosis	Significant ($p < 0.001$)	Significant ($p < 0.001$)	Significant ($p < 0.001$)
Lobular inflammation	Significant ($p < 0.001$)	Significant ($p < 0.001$)	Significant ($p < 0.001$)
Ballooning degeneration	Significant ($p < 0.001$)	Significant ($p < 0.001$)	Significant ($p < 0.001$)
Activity Score (Histopathology)	Significant ($p < 0.001$)	Significant ($p < 0.001$)	Significant ($p < 0.001$)
SAF Score	Significant ($p < 0.001$)	Significant ($p < 0.001$)	Significant ($p < 0.001$)
MDA (Malondialdehyde)	Significant ($p < 0.001$)	Significant ($p < 0.001$)	Significant ($p < 0.05$)
TAOC (Total Antioxidant Capacity)	Significant ($p < 0.001$)	Significant ($p < 0.001$)	Significant ($p < 0.001$)
PPARα expression	Not significant	Not significant	No significant interaction
CTP-1 expression	Not significant	Not significant	No significant interaction
NF-κB levels	Not reported	Not reported	Significant ($p < 0.05$)
TNF-α levels	Significant ($p < 0.001$)	Not significant	Significant ($p < 0.05$)
IL-1β levels	Not significant	Significant ($p < 0.001$)	Not significant
IL-4 levels	Significant ($p < 0.001$)	Significant ($p < 0.001$)	Significant ($p < 0.001$)
IL-10 levels	Significant ($p < 0.001$)	Significant ($p < 0.001$)	Significant ($p < 0.001$)
M1/M2 Ratio	Significant ($p < 0.001$)	Significant ($p < 0.001$)	Significant ($p < 0.001$)
PPARγ expression	Not significant	Significant ($p < 0.05$)	Significant ($p < 0.05$)
CYP2J3 levels	Not significant	Tends to increase ($p = 0.052$)	No significant interaction
EETs levels	Significant ($p < 0.01$)	Significant ($p < 0.01$)	Significant ($p < 0.01$)
DHETs levels	Significant ($p < 0.01$)	Significant ($p < 0.01$)	Significant ($p < 0.01$)
sEH activity	Not significant	Not significant	Not significant

Correlation analysis of liver markers and metabolic parameters in response to 1,25 VD3 supplementation and the CDAA diet in NASH

Correlation analysis revealed significant associations between liver tissue variables and their correlated markers in response to 1,25 VD3 supplementation and the CDAA diet (Table 4). 1,25 VD3 supplementation mitigated the CDAA diet's negative effects on liver, enhancing CYP2J3 expression and promoting positive correlations with EETs and DHETs. This supplementation also increased PPARγ expression, linked to anti-inflammatory effects, and reduced pro-inflammatory cytokines TNF-α and IL-1β. Elevated CYP2J3 levels correlated with lower EETs and MDA, suggesting potential benefits against oxidative stress. Conversely, PPARα expression positively correlated with TAOC and CTP-1, indicating enhanced antioxidant capacity and lipid transport. Both EETs and DHETs demonstrated positive correlations with IL-10, supporting their anti-inflammatory roles. In contrast, the CDAA diet elevated NF-κB and TNF-α levels, triggering in inflammatory responses. Importantly, DHETs' positive correlation with PPARα, combined with 1,25 VD3's benefits, underscores their critical role in counteracting the negative impacts of CDAA diet and regulating liver function and metabolic processes in NASH progression.

Discussion

In this study, we used a rat model of NASH induced by a CD diet to investigate the impact of 1,25 VD3. This active hormone improved liver function, enabling the liver to synthesize more 25 VD3, the precursor for 1,25 VD3. This suggests that alleviating liver dysfunction associated with the choline-deficient diet restores the liver's capacity to produce 25 VD3. 1,25 VD3 supplementation also significantly modulated CYP450 metabolism, increasing CYP2J3 expression and EETs production. Additionally, 1,25 VD3 enhanced

TABLE 4 Correlations between measured liver and metabolic variables and the effects of 1,25 VD3 and CDAA diet.

Measured Variable	Correlated Variable	Direction of Correlation	Effect of 1,25 VD3	Effect of CD Diet	r, p values
CYP2J3 expression	EETs	Negative	Increased	No effect	r=-0.790, p<0.01
CYP2J3 expression	MDA	Negative	Increased	No effect	r=-0.865, p<0.001
PPARα expression	TAOC	Positive	No effect	Increased	r=0.902, p<0.001; r=0.898, p<0.001
PPARα expression	CTP-1	Positive	No effect	Increased	r=0.908, p<0.001; r=0.854, p<0.001
NF-κB expression	MDA	Negative	Decreased	Increased	r=-0.748, p<0.01; r=-0.900, p<0.001
NF-κB expression	M1/M2 ratio	Negative	Decreased	Increased	r=-0.672, p<0.001; r=-0.826, p<0.01
TNF-α	MDA	Negative	Decreased	Increased	r=-0.727, p<0.01; r=-0.735, p<0.01
IL-1β	MDA	Negative	Decreased	No effect	r=-0.782, p<0.01; r=-0.629, p<0.05
PPARγ expression	IL-4	Positive	Increased	No effect	r=0.770, p<0.01; r=0.725, p<0.01
PPARγ expression	IL-10	Positive	Increased	No effect	r=0.585, p<0.05; r=0.585, p<0.01
EETs	IL-10	Positive	Increased	Increased	r=0.657, p<0.05
DHETs	MDA	Negative	Increased	Increased	r=-0.821, p<0.01
DHETs	NF-κB	Negative	Increased	Increased	r=-0.766, p<0.01
DHETs	TNF-α	Negative	Increased	Increased	r=-0.792, p<0.01
DHETs	M1/M2 ratio	Negative	Increased	Increased	r=-0.916, p<0.001
DHETs	TAOC	Positive	Increased	Increased	r=0.626, p<0.05
DHETs	PPARα	Positive	Increased	Increased	r=0.664, p<0.05
DHETs	CTP-1	Positive	Increased	Increased	r=0.627, p<0.05
sEH	TAOC	Negative	Increased	Increased	r=-0.707, p<0.01

- Measured variable: The primary variable measured in the study, related to liver function or metabolic processes.
- Correlated variable: Other variables found to correlate with the measured variable, based on statistical analysis.
- Direction of correlation: Indicates whether the correlation is positive or negative (e.g., an increase in one variable results in an increase or decrease in the other).
- Effect of 1,25 VD3: Whether 1,25 vitamin D3 supplementation had an effect on the measured variable.
- Effect of CDAA diet: Whether diet had an effect on the measured variable.
- r, p values: Statistical correlation (r) and significance (p) values indicating the strength and significance of the correlations between the measured and correlated variables.

PPARα and CTP-1 expression, reduced MDA levels, and increased TAOC, thereby improving lipid peroxidation and antioxidant defenses in NASH rat livers. Furthermore, 1,25 VD3 supplementation exhibited potent anti-inflammatory effects by downregulating NF-κB and upregulating PPARγ. This led to a phenotypic shift in macrophages from pro-inflammatory M1 to anti-inflammatory M2, increasing IL-4 and IL-10 secretion while decreasing TNF-α production.

Expanding on the modulation of liver function and metabolic pathways by 1,25 VD3 (13), we further investigated its effects on AA metabolism, which has an important role in liver lipid peroxidation and inflammation in NASH. We investigated AA metabolism in NASH, given its established link to liver lipid peroxidation and inflammation. Previous studies have shown altered AA metabolites in NASH patients, reduced CYP2J2 expression in high-fat diet (HFD)-induced NASH mice (26), decreased EETs (15), and increased sEH (32) in NASH mice. Additionally, EETs and DHETs are elevated in NAFLD patients and MCD diet-induced NAFLD animal models (14, 27). In our study, we found increased EETs and DHETs, decreased sEH activity, and unchanged CYP2J3 expression in CD diet-induced NASH rats. These findings suggest that 1,25 VD3 supplementation modulates AA metabolism in NASH, favoring anti-inflammatory pathways through increased EETs and decreased sEH activity, which may contribute to its protective effects against liver damage and inflammation in NASH.

The mechanisms by which 1,25 VD3 improves lipid metabolism and mitigates inflammation are through PPARα and PPARγ signaling (3–5, 33–38). We observed that 1,25 VD3 upregulated

PPARα and CPT-1, and shifted KC polarization. The shift in the composition of KCs from a pro-inflammatory phenotype (higher M1/M2 ratio) in the CDG group to a less inflammatory phenotype (lower M1/M2 ratio) in the CDVDG group likely contributed to the improved hepatic cytokine profile observed in the latter. This was reflected by reduced levels of pro-inflammatory cytokines (TNF-α and IL-1β) and increased levels of anti-inflammatory cytokines (IL-4 and IL-10) compared to the CDG group. Collectively, our results support the potential of 1,25 VD3 as an adjunct therapy for NASH, especially in individuals with vitamin D deficiency or insufficiency. However, further research is necessary to elucidate the optimal dosing regimens and long-term effects of 1,25 VD3 supplementation in NASH.

EETs, metabolites of the CYP450 pathway, have been shown to reduce liver lipid peroxidation and inflammation in NASH mice through PPARα and NF-κB signaling pathways (14, 15, 27, 39), highlighting their anti-inflammatory potential in various diseases (17–19). Our study extends these findings, demonstrating that 1,25 VD3 supplementation upregulates CYP2J3 expression, increases EETs and DHETs in rat liver tissue, and significantly interacts with NASH. This upregulation may contribute to anti-inflammatory effects, as CYP2J3 expression and EETs correlate with reduced lipid peroxidation markers (MDA, TAOC, PPARα, CTP-1) and inflammatory markers (NF-κB, M1/M2 ratio, TNF-α, IL-1β, IL-4, IL-10, PPARγ). Interestingly, DHETs exhibit anti-inflammatory activity, positively correlating with IL-10 and IL-4, which contrasts with previous reports of inactivity (40) or pro-inflammatory effects (20). However, recent studies reveal anti-inflammatory roles for DHETs in cystic pulmonary fibrosis (41) and pancreatic β-cell models (19), suggesting context-dependent effects. Furthermore, the context-dependent nature of DHETs' effects highlights the need for further research to elucidate the specific mechanisms and conditions under which these molecules exert their effects. Elucidating these relationships will be crucial in harnessing the therapeutic potential of 1,25 VD3 supplementation and EETs/DHETs in NASH and other diseases characterized by lipid peroxidation and inflammation.

Study of interactive effects of 1,25 VD3 supplementation and the CD diet revealed significant impacts on liver function and metabolic markers. 1,25 VD3 mitigated CD diet-induced liver impairment by enhancing CYP2J3 expression, which correlated with higher EETs, DHETs, and reduced oxidative stress (lower MDA). Further correlation studies linked increased PPARγ expression with anti-inflammatory cytokines (IL-10, IL-4) and reduced pro-inflammatory markers (TNF-α, IL-1β), while PPARα expression correlated with improved antioxidant capacity (TAOC) and lipid transport (CTP-1). These findings emphasize the interactive effects of 1,25 VD3 supplementation and choline deficiency in favorably modulating liver function and inflammation.

Our study has some limitations. Recent research highlights the role of circadian rhythms in NAFLD (42–45), with vitamin D identified as a modulator of circadian regulation (46, 47). However, we did not study circadian-related markers such as CLOCK, BMAL1, CRY, and PER1/2. Instead, we focused on metabolic proteins, metabolites, and CYP450 enzymes to investigate how 1,25 VD3 improves lipid peroxidation and inflammation via the CYP450 and AA pathways, which are critical in NASH progression. Secondly, liver weight and treatment-induced changes in cellular composition were not considered when interpreting cytokine levels. However, the shifts in KC composition likely influenced cytokine modulation and macrophage polarization, as discussed. Future studies could investigate the contributions of individual liver cell types to cytokine modulation. Thirdly, while we assessed NF-κB expression using Western blotting, we acknowledge that immunohistochemistry (IHC) could have been used to validate protein localization and spatial distribution. However, since the antibody detects additional bands besides the 65 kDa NF-κB, Western blotting allows for more accurate measurement of NF-κB expression than IHC.

Collectively, our study revealed novel mechanisms by which 1,25 VD3 supplementation may serve as a valuable adjunct therapy for NASH management, particularly in patients with vitamin D deficiency or insufficiency. Further research is necessary to elucidate the optimal dosing regimens and long-term effects of 1,25 VD3 supplementation in NASH.

Data availability statement

The original contributions presented in the study are included in the article/supplementary material. Further inquiries can be directed to the corresponding authors.

Ethics statement

The animal study was approved by the Ethics Committee of Yanbian University. The study was conducted in accordance with the local legislation and institutional requirements.

Author contributions

ML: Data curation, Writing – original draft. X-ZS: Data curation, Writing – original draft. LY: Data curation, Conceptualization, Writing – original draft. Y-HF: Data curation, Formal Analysis, Methodology, Writing – original draft. LL: Data curation, Methodology, Investigation, Writing – original draft. J-SC: Data curation, Methodology, Formal Analysis, Validation, Writing – original draft. X-CL: Data curation, Writing – original draft, Conceptualization. H-YZ: Methodology, Writing – original draft. L-HQ: Supervision, Validation, Writing – original draft, Writing – review & editing. H-MH: Supervision, Validation, Conceptualization, Funding acquisition, Investigation, Project administration, Resources, Software, Visualization, Writing – original draft, Writing – review & editing.

Funding

The author(s) declare that financial support was received for the research and/or publication of this article. This study was supported by grant from the National Natural Science Foundation, China (No. 81860110).

Conflict of interest

The authors declare that the research was conducted in the absence of any commercial or financial relationships that could be construed as a potential conflict of interest.

Generative AI statement

The author(s) declare that no Generative AI was used in the creation of this manuscript.

Publisher's note

All claims expressed in this article are solely those of the authors and do not necessarily represent those of their affiliated organizations, or those of the publisher, the editors and the reviewers. Any product that may be evaluated in this article, or claim that may be made by its manufacturer, is not guaranteed or endorsed by the publisher.

References

1. Eslam M, Sanyal AJ, George J, International Consensus P. Mafld: A consensus-driven proposed nomenclature for metabolic associated fatty liver disease. *Gastroenterology*. (2020) 158:1999–2014.e1. doi: 10.1053/j.gastro.2019.11.312

2. Sanders FW, Griffin JL. *De novo* lipogenesis in the liver in health and disease: more than just a shunting yard for glucose. *Biol Rev Camb Philos Soc*. (2016) 91:452–68. doi: 10.1111/brv.12178

3. Markiewicz A, Brozyna AA, Podgorska E, Elas M, Urbanska K, Jetten AM, et al. Vitamin D receptors (Vdr), hydroxylases cyp27b1 and cyp24a1 and retinoid-related orphan receptors (Ror) level in human uveal tract and ocular melanoma with different melanization levels. *Sci Rep*. (2019) 9:9142. doi: 10.1038/s41598-019-45161-8

4. Wei R, Christakos S. Mechanisms underlying the regulation of innate and adaptive immunity by vitamin D. *Nutrients*. (2015) 7:8251–60. doi: 10.3390/nu7105392

5. Lowry MB, Guo C, Borregaard N, Gombart AF. Regulation of the human cathelicidin antimicrobial peptide gene by 1alpha,25-dihydroxyvitamin D3 in primary immune cells. *J Steroid Biochem Mol Biol*. (2014) 143:183–91. doi: 10.1016/j.jsbmb.2014.02.004

6. Mahmoudi L, Asadi S, Al-Mousavi Z, Niknam R. A randomized controlled clinical trial comparing calcitriol versus cholecalciferol supplementation to reduce insulin resistance in patients with non-alcoholic fatty liver disease. *Clin Nutr*. (2021) 40:2999–3005. doi: 10.1016/j.clnu.2020.11.037

7. Gad AI, Elmedames MR, Abdelhai AR, Marei AM, Abdel-Ghani HA. Efficacy of vitamin D supplementation on adult patients with non-alcoholic fatty liver disease: A single-center experience. *Gastroenterol Hepatol Bed Bench*. (2021) 14:44–52.

8. Lukenda Zanko V, Domislovic V, Trkulja V, Krznaric-Zrnic I, Turk-Wensveen T, Krznaric Z, et al. Vitamin D for treatment of non-alcoholic fatty liver disease detected by transient elastography: A randomized, double-blind, placebo-controlled trial. *Diabetes Obes Metab*. (2020) 22:2097–106. doi: 10.1111/dom.14129

9. Namakin K, Hosseini M, Zardast M, Mohammadifard M. Vitamin D effect on ultrasonography and laboratory indices and biochemical indicators in the blood: an interventional study on 12 to 18-year-old children with fatty liver. *Pediatr Gastroenterol Hepatol Nutr*. (2021) 24:187–96. doi: 10.5223/pghn.2021.24.2.187

10. Kalveram L, Schunck WH, Rothe M, Rudolph B, Loddenkemper C, Holzhutter HG, et al. Regulation of the cytochrome P450 epoxyeicosanoid pathway is associated with distinct histologic features in pediatric non-alcoholic fatty liver disease. *Prostaglandins Leukot Essent Fatty Acids*. (2021) 164:102229. doi: 10.1016/j.plefa.2020.102229

11. Shojaei Zarghani S, Soraya H, Alizadeh M. Calcium and vitamin D(3) combinations improve fatty liver disease through ampk-independent mechanisms. *Eur J Nutr*. (2018) 57:731–40. doi: 10.1007/s00394-016-1360-4

12. Han H, Cui M, You X, Chen M, Piao X, Jin G. A role of 1,25(Oh)2d3 supplementation in rats with nonalcoholic steatohepatitis induced by choline-deficient diet. *Nutr Metab Cardiovasc Dis*. (2015) 25:556–61. doi: 10.1016/j.numecd.2015.02.011

13. Sztolsztener K, Chabowski A, Harasim-Symbor E, Bielawiec P, Konstantynowicz-Nowicka K. Arachidonic acid as an early indicator of inflammation during non-alcoholic fatty liver disease development. *Biomolecules*. (2020) 10. doi: 10.3390/biom10081133

14. Wells MA, Vendrov KC, Edin ML, Ferslew BC, Zha W, Nguyen BK, et al. Characterization of the cytochrome P450 epoxyeicosanoid pathway in non-alcoholic steatohepatitis. *Prostaglandins Other Lipid Mediat*. (2016) 125:19–29. doi: 10.1016/j.prostaglandins.2016.07.002

15. Gai Z, Visentin M, Gui T, Zhao L, Thasler WE, Hausler S, et al. Effects of farnesoid X receptor activation on arachidonic acid metabolism, nf-kb signaling, and hepatic inflammation. *Mol Pharmacol*. (2018) 94:802–11. doi: 10.1124/mol.117.111047

16. Schuck RN, Zha W, Edin ML, Gruzdev A, Vendrov KC, Miller TM, et al. The cytochrome P450 epoxygenase pathway regulates the hepatic inflammatory response in fatty liver disease. *PloS One*. (2014) 9:e110162. doi: 10.1371/journal.pone.0110162

17. Spector AA. Arachidonic acid cytochrome P450 epoxygenase pathway. *J Lipid Res*. (2009) 50:S52–6. doi: 10.1194/jlr.R800038-JLR200

18. Dai N, Yang C, Fan Q, Wang M, Liu X, Zhao H, et al. The anti-inflammatory effect of soluble epoxide hydrolase inhibitor and 14, 15-eet in kawasaki disease through ppargamma/stat1 signaling pathway. *Front Pediatr*. (2020) 8:451. doi: 10.3389/fped.2020.00451

19. Grimes D, Watson D. Epoxyeicosatrienoic acids protect pancreatic beta cells against pro-inflammatory cytokine toxicity. *Biochem Biophys Res Commun*. (2019) 520:231–6. doi: 10.1016/j.bbrc.2019.09.124

20. Bergmann CB, Hammock BD, Wan D, Gogolla F, Goetzman H, Caldwell CC, et al. Tppu treatment of burned mice dampens inflammation and generation of bioactive dhet which impairs neutrophil function. *Sci Rep*. (2021) 11:16555. doi: 10.1038/s41598-021-96014-2

21. Spector AA, Norris AW. Action of epoxyeicosatrienoic acids on cellular function. *Am J Physiol Cell Physiol*. (2007) 292:C996–1012. doi: 10.1152/ajpcell.00402.2006

22. Ng VY, Huang Y, Reddy LM, Falck JR, Lin ET, Kroetz DL. Cytochrome P450 eicosanoids are activators of peroxisome proliferator-activated receptor alpha. *Drug Metab Dispos*. (2007) 35:1126–34. doi: 10.1124/dmd.106.013839

23. Qin R, Zhang J, Li C, Zhang X, Xiong A, Huang F, et al. Protective effects of gypenosides against fatty liver disease induced by high fat and cholesterol diet and alcohol in rats. *Arch Pharm Res*. (2012) 35:1241–50. doi: 10.1007/s12272-012-0715-5

24. Tomkin GH, Owens D. Diabetes and dyslipidemia: characterizing lipoprotein metabolism. *Diabetes Metab Syndr Obes*. (2017) 10:333–43. doi: 10.2147/DMSO.S115855

25. Rakhshandehroo M, Knoch B, Muller M, Kersten S. Peroxisome proliferator-activated receptor alpha target genes. *PPAR Res*. (2010) 2010. doi: 10.1155/2010/612089

26. Chen G, Xu R, Zhang S, Wang Y, Wang P, Edin ML, et al. Cyp2j2 overexpression attenuates nonalcoholic fatty liver disease induced by high-fat diet in mice. *Am J Physiol Endocrinol Metab*. (2015) 308:E97–E110. doi: 10.1152/ajpendo.00366.2014

27. Wang X, Li L, Wang H, Xiao F, Ning Q. Epoxyeicosatrienoic acids alleviate methionine-choline-deficient diet-induced non-alcoholic steatohepatitis in mice. *Scand J Immunol*. (2019) 90:e12791. doi: 10.1111/sji.12791

28. Kleiner DE, Brunt EM, Van Natta M, Behling C, Contos MJ, Cummings OW, et al. Design and validation of a histological scoring system for nonalcoholic fatty liver disease. *Hepatology*. (2005) 41:1313–21. doi: 10.1002/hep.20701

29. Stark JM, Coquet JM, Tibbitt CA. The role of ppar-gamma in allergic disease. *Curr Allergy Asthma Rep*. (2021) 21:45. doi: 10.1007/s11882-021-01022-x

30. Song S, Attia RR, Connaughton S, Niesen MI, Ness GC, Elam MB, et al. Peroxisome proliferator activated receptor alpha (Pparalpha) and ppar gamma coactivator (Pgc-1alpha) induce carnitine palmitoyltransferase ia (Cpt-1a) via independent gene elements. *Mol Cell Endocrinol*. (2010) 325:54–63. doi: 10.1016/j.mce.2010.05.019

31. Luo W, Xu Q, Wang Q, Wu H, Hua J. Effect of modulation of ppar-gamma activity on kupffer cells M1/M2 polarization in the development of non-alcoholic fatty liver disease. *Sci Rep*. (2017) 7:44612. doi: 10.1038/srep44612

32. Liu Y, Dang H, Li D, Pang W, Hammock BD, Zhu Y. Inhibition of soluble epoxide hydrolase attenuates high-fat-diet-induced hepatic steatosis by reduced systemic inflammatory status in mice. *PloS One*. (2012) 7:e39165. doi: 10.1371/journal.pone.0039165

33. Jahn D, Dorbath D, Kircher S, Nier A, Bergheim I, Lenaerts K, et al. Beneficial effects of vitamin D treatment in an obese mouse model of non-alcoholic steatohepatitis. *Nutrients*. (2019) 11. doi: 10.3390/nu11010077

34. Su D, Nie Y, Zhu A, Chen Z, Wu P, Zhang L, et al. Vitamin D signaling through induction of paneth cell defensins maintains gut microbiota and improves metabolic disorders and hepatic steatosis in animal models. *Front Physiol*. (2016) 7:498. doi: 10.3389/fphys.2016.00498

35. Mu Y, Li J, Kang JH, Eto H, Zai K, Kishimura A, et al. A lipid-based nanocarrier containing active vitamin D(3) ameliorates nash in mice via direct and intestine-mediated effects on liver inflammation. *Biol Pharm Bull*. (2020) 43:1413–20. doi: 10.1248/bpb.b20-00432

36. El-Sherbiny M, Eldosoky M, El-Shafey M, Othman G, Elkattawy HA, Bedir T, et al. Vitamin D nanoemulsion enhances hepatoprotective effect of conventional vitamin D in rats fed with a high-fat diet. *Chem Biol Interact*. (2018) 288:65–75. doi: 10.1016/j.cbi.2018.04.010

37. Zhang X, Zhou M, Guo Y, Song Z, Liu B. 1,25-dihydroxyvitamin D(3) promotes high glucose-induced M1 macrophage switching to M2 via the vdr-ppargamma signaling pathway. *BioMed Res Int*. (2015) 2015:157834. doi: 10.1155/2015/157834

38. Das LM, Binko AM, Traylor ZP, Peng H, Lu KQ. Vitamin D improves sunburns by increasing autophagy in M2 macrophages. *Autophagy*. (2019) 15:813–26. doi: 10.1080/15548627.2019.1569298

39. Yao L, Cao B, Cheng Q, Cai W, Ye C, Liang J, et al. Inhibition of soluble epoxide hydrolase ameliorates hyperhomocysteinemia-induced hepatic steatosis by enhancing beta-oxidation of fatty acid in mice. *Am J Physiol Gastrointest Liver Physiol*. (2019) 316:G527–G38. doi: 10.1152/ajpgi.00148.2018

40. Morisseau C, Hammock BD. Impact of soluble epoxide hydrolase and epoxyeicosanoids on human health. *Annu Rev Pharmacol Toxicol*. (2013) 53:37–58. doi: 10.1146/annurev-pharmtox-011112-140244

41. Carnovale V, Castaldo A, Di Minno A, Gelzo M, Iacotucci P, Illiano A, et al. Oxylipin profile in saliva from patients with cystic fibrosis reveals a balance between pro-resolving and pro-inflammatory molecules. *Sci Rep*. (2022) 12:5838. doi: 10.1038/s41598-022-09618-7

42. Gnocchi D, Custodero C, Sabba C, Mazzocca A. Circadian rhythms: A possible new player in non-alcoholic fatty liver disease pathophysiology. *J Mol Med (Berl)*. (2019) 97:741–59. doi: 10.1007/s00109-019-01780-2

43. Jokl E, Llewellyn J, Simpson K, Adegboye O, Pritchett J, Zeef L, et al. Circadian disruption primes myofibroblasts for accelerated activation as a mechanism underpinning fibrotic progression in non-alcoholic fatty liver disease. *Cells*. (2023) 12. doi: 10.3390/cells12121582

44. Gnocchi D, Pedrelli M, Hurt-Camejo E, Parini P. Lipids around the clock: focus on circadian rhythms and lipid metabolism. *Biol (Basel)*. (2015) 4:104–32. doi: 10.3390/biology4010104

45. Gnocchi D, Bruscalupi G. Circadian rhythms and hormonal homeostasis: pathophysiological implications. *Biol (Basel)*. (2017) 6. doi: 10.3390/biology6010010

46. Arabi A, Nasrallah D, Mohsen S, Abugharbieh L, Al-Hashimi D, AlMass S, et al. Association between serum vitamin D status and circadian syndrome: A cross-sectional study. *Nutrients*. (2024) 16. doi: 10.3390/nu16132111

47. Gutierrez-Monreal MA, Cuevas-Diaz-Duran R, Moreno-Cuevas JE, Scott SP. A role for 1alpha,25-dihydroxyvitamin D3 in the expression of circadian genes. *J Biol Rhythms*. (2014) 29:384–8. doi: 10.1177/0748730414549239

frontiers | Frontiers in Medicine

TYPE Original Research
PUBLISHED 17 April 2025
DOI 10.3389/fmed.2025.1529074

OPEN ACCESS

EDITED BY
Prem Prakash Kushwaha,
Case Western Reserve University,
United States

REVIEWED BY
Zongmei Gao,
Columbia University, United States
Saurabh Mishra,
Cleveland Clinic, United States

*CORRESPONDENCE
Jiang-Lie Tu
✉ tujianglie123@163.com

RECEIVED 15 November 2024
ACCEPTED 31 March 2025
PUBLISHED 17 April 2025

CITATION
Tu J-L and Fang R-X (2025) Identification of fatty acid metabolism hub genes in endometriosis using integrative bioinformatics analysis.
Front. Med. 12:1529074.
doi: 10.3389/fmed.2025.1529074

Identification of fatty acid metabolism hub genes in endometriosis using integrative bioinformatics analysis

Jiang-Lie Tu[1]* and Rui-Xue Fang[2]

[1]Department of Obstetrics and Gynecology, The Affiliated Hospital of Guizhou Medical University, Guizhou Hospital of The First Affiliated Hospital, Sun Yat-sen University, Guiyang, Guizhou, China, [2]Department of Emergency, Yueqing Fifth People's Hospital, Wenzhou, Zhejiang, China

Background: Fatty acid metabolism plays a major role in several inflammatory diseases such as endometriosis. However, its specific mechanism in endometriosis remains unclear. Therefore, this study aimed to investigate the hub genes involved in endometriosis and fatty acid metabolism using bioinformatics analyses.

Methods: The R package sva was used to remove batch effects from the GSE120103 and GSE25628 datasets, resulting in the creation of a combined GEO dataset. Differential analysis of the combined GEO dataset was interposed with fatty acid metabolism-related genes. Differentially expressed genes associated with fatty acid metabolism (FAMRDEGs) were subsequently identified. Functional enrichment analyses were performed using the clusterProfiler package, whereas gene set enrichment analysis (GSEA) was used to identify significant pathways. Protein–protein interaction (PPI) networks were constructed using STRING and visualized using Cytoscape to identify hub genes. Moreover, regulatory networks involving transcription factors and microRNAs were constructed using ChIPBase and ENCORI databases, respectively. Hub genes were validated via expression comparison and receiver operating characteristic curve analysis.

Results: We identified 405 DEGs in the combined dataset, including 168 and 237 with upregulated and downregulated expression, respectively. Of these, 17 were FAMRDEGs. These genes were significantly involved in arachidonic acid and fatty acid metabolic processes. GSEA highlighted pathways such as Hamai_apoptosis_via_trail_dn for genes whose expression was downregulated, along with nuclear receptors in lipid metabolism and toxicity for genes with upregulated expression. The PPI network identified six hub genes: *PTGS2, CYP2C9, HSDL2, HSD17B3, ACSL4*, and *CYP2C18*. *ACSL4* showed the strongest positive correlation with immune cell effector memory CD8 T cells, whereas *HSDL2* showed the strongest negative correlation with immune cell-activated CD8 T cells.

Conclusion: The identified hub genes may be potential biomarkers of fatty acid metabolism in endometriosis. This reveals the potential molecular mechanisms underlying this metabolic process and identifies therapeutic targets for future interventions.

KEYWORDS

endometriosis, fatty acid metabolism, bioinformatic analysis, hub genes, PPI

1 Introduction

Endometriosis is an estrogen-dependent chronic inflammatory disease (1). According to the World Health Organization, approximately 10% of women of reproductive age are diagnosed with this condition worldwide (2). Despite the high prevalence of endometriosis, its pathogenesis remains unclear; this complicates both diagnosis and treatment. Current therapeutic approaches, including hormonal therapy and surgical interventions, often provide temporary relief. In addition, they often have side effects and are associated with a notably high recurrence rate post-surgery (3). Because the symptoms associated with endometriosis are frequently misattributed to dysmenorrhea, a condition commonly experienced by adolescent girls and young women, significant delays in diagnosis can occur (4). Therefore, further studies are required to better understand the underlying pathological mechanisms and develop new diagnostic and therapeutic strategies. Recent investigations have indicated that endometriosis should not be viewed solely as a localized condition; rather, it is associated with systemic alterations, including modifications in lipid metabolism.

Fatty acid metabolism plays an essential role in the pathophysiology of various inflammatory disorders (5). Notable alterations have been observed in the lipid profiles of women diagnosed with endometriosis, indicating a potential correlation between lipid metabolism and disease progression (6). In addition, genes related to A are involved in the regulation of inflammatory responses, which are pivotal for the development and maintenance of endometriotic lesions (7). These observations suggest that fatty acid metabolism-related genes (FAMRGs) are intricately associated with the onset and progression of endometriosis. However, a systematic investigation into the hub genes and potential regulatory mechanisms associated with fatty acid metabolism in the context of endometriosis remains to be conducted. Therefore, this study aimed to evaluate the differential expression of FAMRGs in endometriosis and explore the potential regulatory mechanisms involved.

Our findings highlight the potential application of fatty acid metabolism hub genes as diagnostic markers and therapeutic targets in endometriosis. This study further elucidates the molecular mechanisms underlying the pathogenesis of this disease and may provide valuable insights for developing new diagnostic markers and therapeutic targets.

Abbreviations: AUC, area under the curve; BP, biological process; DEGs, differentially expressed genes; EMs, endometriosis; FAMRDEGs, fatty acid metabolism-related differentially expressed genes; FAMRGs, fatty acid metabolism-related genes; GO, Gene Ontology; GSEA, gene set enrichment analysis; KEGG, Kyoto Encyclopedia of Genes and Genomes; MF, molecular function; miRNA, microRNA; PCA, principal component analysis; PPI, protein–protein interaction; ROC, receiver operating characteristic; ssGSEA, single-sample gene set enrichment analysis; TF, transcription factor.

2 Materials and methods

2.1 Data used

The endometriosis datasets GSE120103 and GSE25628 were downloaded from the GEO database[1] using the R package GEO query (Version 2.72.0). These datasets were extracted from human endometrial tissues. The chip platforms of GSE120103 and GSE25628 were GPL6480 and GPL571, respectively (Table 1). In total, 849 genes related to fatty acid metabolism were identified based on previous literature (8–10) after combination and deduplication (Supplementary Table S1).

2.2 Data preprocessing

The R package sva (version 3.52.0) was used to remove batch effects from the two datasets, resulting in the creation of a combined GEO dataset. The combined dataset included 33 endometriosis and 25 control samples. Finally, the R package limma (version 3.60.2) was used to standardize and normalize the integrated GEO dataset and annotate probes. Principal component analysis (PCA) was performed on the expression matrix, both before and after the removal of the batch effect, to assess the effectiveness of batch effect removal.

2.3 Identification of endometriosis-associated fatty acid metabolism-related differentially expressed genes

The data were divided into the Endometriosis and Control groups. The R package limma (version 3.60.2) was used to perform differential analysis of genes in the two groups. Genes with threshold values of $|\log FC| > 1$ and $p < 0.05$ were considered differentially expressed genes (DEGs). The R package ggplot2 (version 3.5.1) was used to plot the results of the differential analysis as volcano plots. The intersection of DEGs and FAMRGs was subsequently determined, and a Venn diagram was drawn to obtain FAMRDEGs. The R packages pheatmap (version 1.0.12) and RCircos (version 1.2.2) were used to draw a heatmap and a chromosome localization map, respectively.

2.4 Functional enrichment analysis

The R package clusterProfiler (version 4.12.0) was used to perform gene ontology (GO) and pathway (KEGG) enrichment analyses on FAMRDEGs. The entry screening criteria were adj. $p < 0.05$ and $q < 0.25$.

2.5 Gene set enrichment analysis (GSEA)

Genes in the combined GEO datasets were sorted according to their logFC values. GSEA was performed using the R package

1 https://www.ncbi.nlm.nih.gov/geo/

TABLE 1 GEO microarray chip information.

	GSE120103	GSE25628
Platform	GPL6480	GPL571
Species	*Homo sapiens*	*Homo sapiens*
Tissue	Endometriosis tissues	Endometriosis tissues
Samples in EMs group	18	16
Samples in control group	18	6
Reference	PMID: 30760267	PMID: 23460397

GEO, Gene Expression Omnibus; EMs, Endometriosis.

clusterProfiler (version 4.12.0) for all genes in the combined datasets. The c2 gene set was obtained using the R package msigdbr (version 7.5.1) before GSEA was performed. The screening criteria for GSEA were adj. $p < 0.05$ and $q < 0.25$.

2.6 Protein–protein interaction (PPI) network

The STRING database[2] was applied based on FAMRDEGs with a minimum interaction coefficient >0.4 to construct a PPI network related to these genes. The Cytoscape software was used to visualize the networks. The MCC algorithm in the CytoHubba plug-in of Cytoscape was used to calculate the scores of FAMRDEGs. Next, the top six FAMRDEGs were selected as related hub genes based on their scores. We predicted functionally similar hub genes using the GeneMANIA database[3] to construct a PPI network.

2.7 Construction of regulatory network

The ChIPBase database[4] was used to retrieve transcription factors (TFs). The regulatory function of TFs in hub genes was analyzed, and the mRNA-TF regulatory network was visualized using Cytoscape software. Hub genes associated with microRNAs (miRNAs) were retrieved from the ENCORI database[5] to evaluate the relationship between hub genes and miRNA. The mRNA-miRNA regulatory network was subsequently visualized using Cytoscape software.

2.8 Differential expression verification and receiver operating characteristic (ROC) curve analysis of hub genes

A comparative chart was constructed based on the expression levels of hub genes to further investigate the differential expression of the hub genes between the Endometriosis and Control groups within the integrated GEO datasets. Next, the R package pROC (version 1.18.5) was used to generate an ROC curve for the hub genes, thereby enabling the calculation of the area under the curve (AUC). This analysis assessed the diagnostic efficacy of hub gene expression in relation to the occurrence of endometriosis.

2.9 Single-sample GSEA (ssGSEA)

ssGSEA was used to quantify the relative abundance of each immune cell type. We then used the R package ggplot2 (version 3.5.0) to create comparative visualizations that depicted expression differences in immune cells between the Control and H groups within the combined GEO dataset. Immune cells that demonstrated significant differences between the two groups were selected for further analysis. We applied the Spearman correlation algorithm to assess the correlation between immune cell types. The R package pheatmap (version 1.0.12) was used to create a correlation heatmap. The correlation between hub genes and immune cells was subsequently calculated using Spearman's algorithm, and the results were retained at a p-value of <0.05. The R package ggplot2 (version 3.5.1) was used to draw a correlation bubble plot to show the correlation between hub genes and immune cells. Immune cells with TOP1-positive and TOP1-negative correlation with hub genes were identified, and a correlation scatter plot was drawn using ggplot2.

2.10 Statistical analyses

Statistical analyses were performed using the R statistical package (version 4.4.0; R Foundation for Statistical Computing, Vienna, Austria). The p-values were two-sided, and a p-value of <0.05 was considered statistically significant.

3 Results

3.1 Technology roadmap (Figure 1)

A flowchart illustrating the FAMRDEG analysis is shown in Figure 1.

3.2 Merging of endometriosis datasets

The endometriosis datasets GSE120103 and GSE25628 were processed using the R package sva to remove the batch effect and obtain a combined GEO dataset. The datasets before and after batch effects were compared using distribution box plots (Figures 2A,B) and PCA (Figures 2C,D). The batch effect in the dataset was successfully eliminated after batch processing.

3.3 DEGs related to endometriosis-associated fatty acid metabolism

The R package limma identified 405 DEGs in the combined dataset. Of these, the expression of 168 genes was upregulated, whereas that of 237 genes was downregulated. A volcano diagram for this dataset was drawn based on the results of differential analysis (Figure 3A). Moreover, a Venn diagram of all DEGs and FAMRGs was drawn to obtain FAMRDEGs (Figure 3B). In total, 17 FAMRDEGs

2 http://string-db.org
3 https://genemania.org/
4 http://rna.sysu.edu.cn/chipbase/
5 https://rnasysu.com/encori/

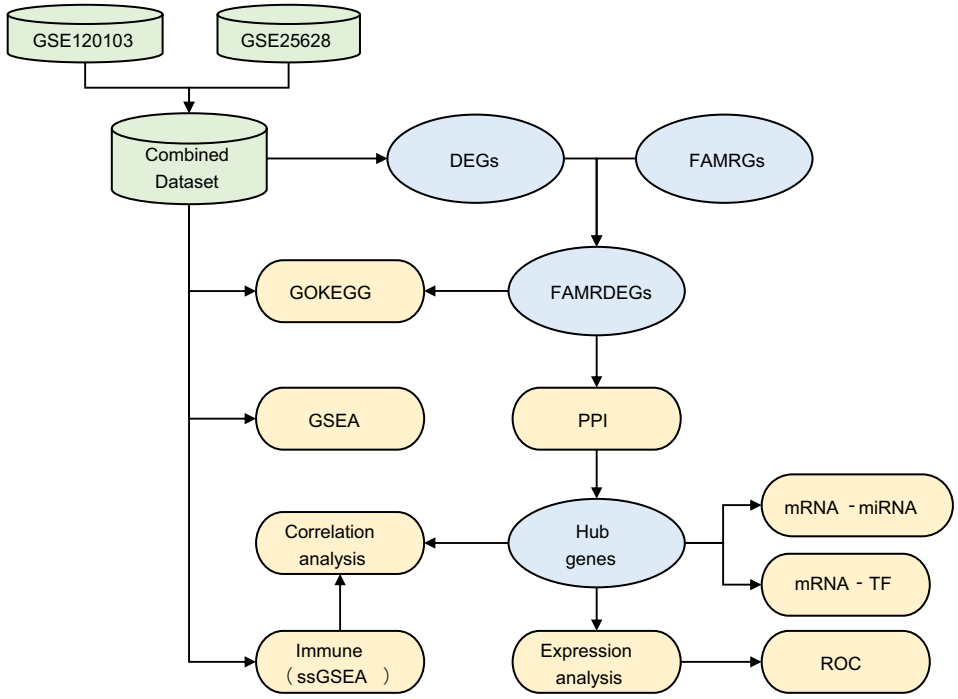

FIGURE 1
Flowchart for the comprehensive analysis of FAMRDEGs. EMs, endometriosis; DEGs, differentially expressed genes; FAMRGs, fatty acid metabolism-related genes; FAMRDEGs, fatty acid metabolism-related differentially expressed genes; GO, Gene Ontology; KEGG, Kyoto Encyclopedia of Genes and Genomes; GSEA, gene set enrichment analysis; PPI, protein–protein interaction; miRNA, MicroRNA; TF, transcription factor; ROC, receiver operating characteristic; ssGSEA, single-sample gene set enrichment analysis.

were obtained: *CRYL1, ASAH1, HSD17B3, DPEP3, PTGS2, PPFIA4, EIF6, DRD4, UROD, ETFB, CYP2C18, GIPR, CYP2C9, ACSL4, ERP29, HSDL2,* and *GPX1*. Differences in the expression of FAMRDEGs between sample groups in the combined GEO datasets were analyzed based on the intersection results. A heatmap of the analysis results is shown in Figure 3C. In addition, the chromosome localization map of the 17 FAMRDEGs is shown in Figure 3D. Chromosome mapping showed that FAMRDEGs were mostly located on chromosomes 1, 9, 10, and 19. *UROD, PTGS2,* and *PPFIA4* were located on chromosome 1; *HSDL2* and *HSD17B3* were located on chromosome 9; *CYP2C9* and *CYP2C18* were located on chromosome 10; and *GIPR* and *ETFB* were located on chromosome 19.

3.4 Functional enrichment analysis

The following GO and KEGG enrichment pathways were explored for the 17 FAMRGs: biological process (BP), cell component (CC), molecular function (MF), biological pathways (KEGG), and their relationship to endometriosis (EMs). The 17 FAMRDEGs used for GO and KEGG enrichment analyses are listed in Table 2. These genes were primarily enriched in arachidonic acid and fatty acid metabolic processes related to endometriosis. However, they were not enriched in the following pathways: BP, such as long-chain fatty acid and olefinic compound metabolic processes, regulation of protein transport, arachidonic acid epoxygenase activity, heme binding, oxidoreductase activity, acting on paired donors, and incorporation or reduction of molecular oxygen; MF, such as arachidonic acid monooxygenase and tetrapyrrole binding; or CC. In contrast, these genes were enriched in KEGG pathways including chemical carcinogenesis, DNA adducts, and serotonergic synapse. The results of the GO and KEGG enrichment analyses were visualized using bubble plots (Figure 4A). The network diagrams for BP, MF, and KEGG are shown in Figures 4B–D.

3.5 GSEA

The effect of all gene expression levels in the combined GEO datasets was evaluated. The GSEA results for genes involved in BP, CC, and MF are shown in Figure 5A and Table 3. Genes whose expression was downregulated in the combined datasets were significantly enriched in hamai apoptosis via TRAIL DN (Figure 5B), bilanges serum, as well as rapamycin sensitivity (Figure 5C) and other biologically relevant functions and signaling pathways. In contrast, genes whose expression was upregulated were significantly enriched in nuclear receptors in lipid metabolism and toxicity (Figure 5D), as well as srebf and mir33 in cholesterol and lipid homeostasis (Figure 5E) and other biologically related functions and signaling pathways.

3.6 Construction of the PPI network and screening of hub genes

The PPI network of 17 FAMRDEGs is shown in Figure 6A. In total, 12 FAMRDEGs were related: *UROD, ETFB, CRYL1, HSD17B3, CYP2C9, PTGS2, DRD4, ACSL4, ASAH1, CYP2C18, HSDL2,* and *DPEP3*. The scores of these genes were subsequently calculated, and the top six genes were screened based on these scores. The interaction

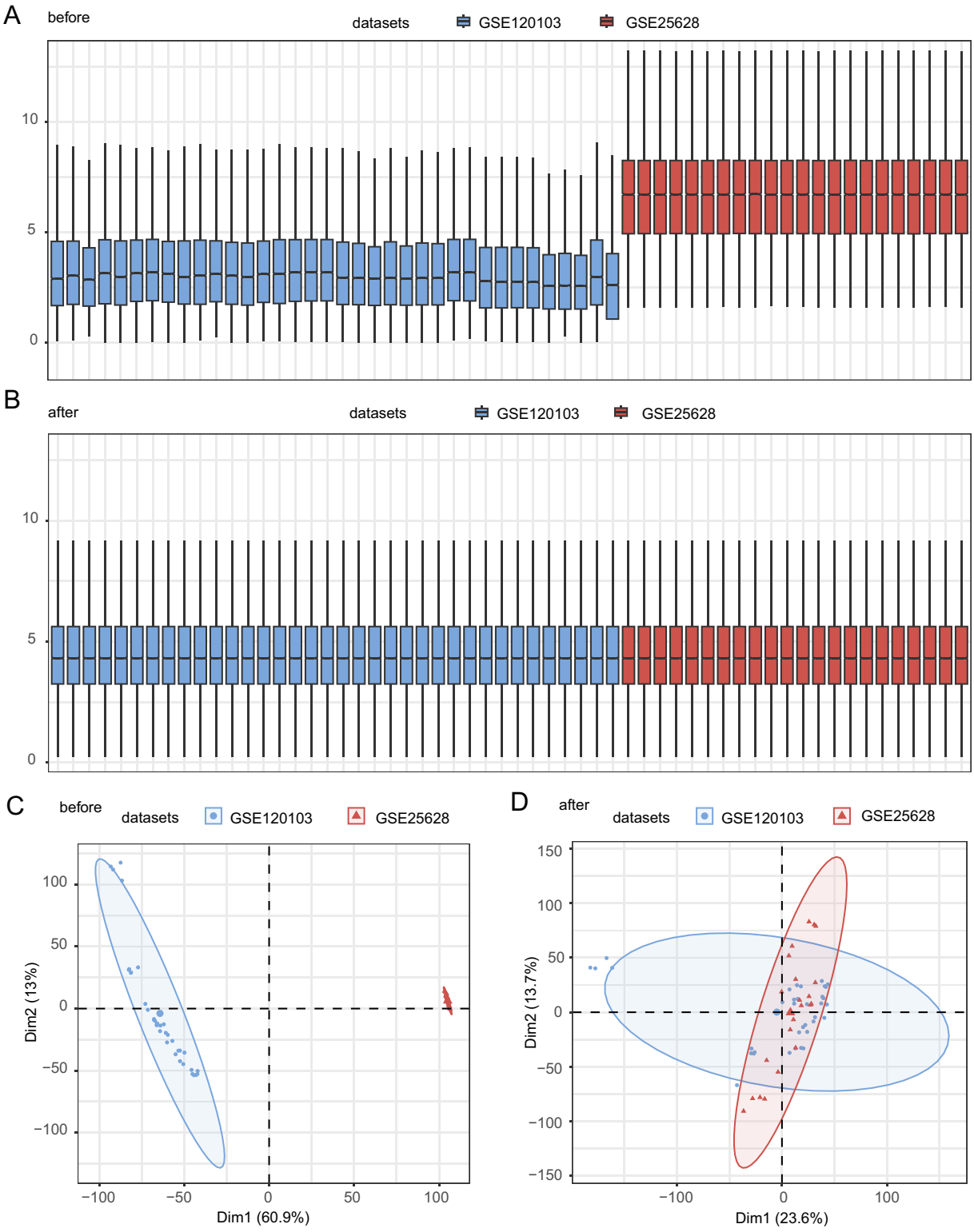

FIGURE 2
Batch effect removal for GSE73461 and GSE68004. **(A)** Boxplots showing the distribution of combined GEO datasets before batch removal. **(B)** Boxplots showing the distribution of post-batch integrated GEO datasets (combined datasets). **(C)** The PCA dataset before batch processing. **(D)** The PCA map of the combined GEO datasets after batch processing. Light red and blue represent the EMs datasets GSE25628 and GSE120103, respectively. PCA, principal component analysis; EMs, endometriosis.

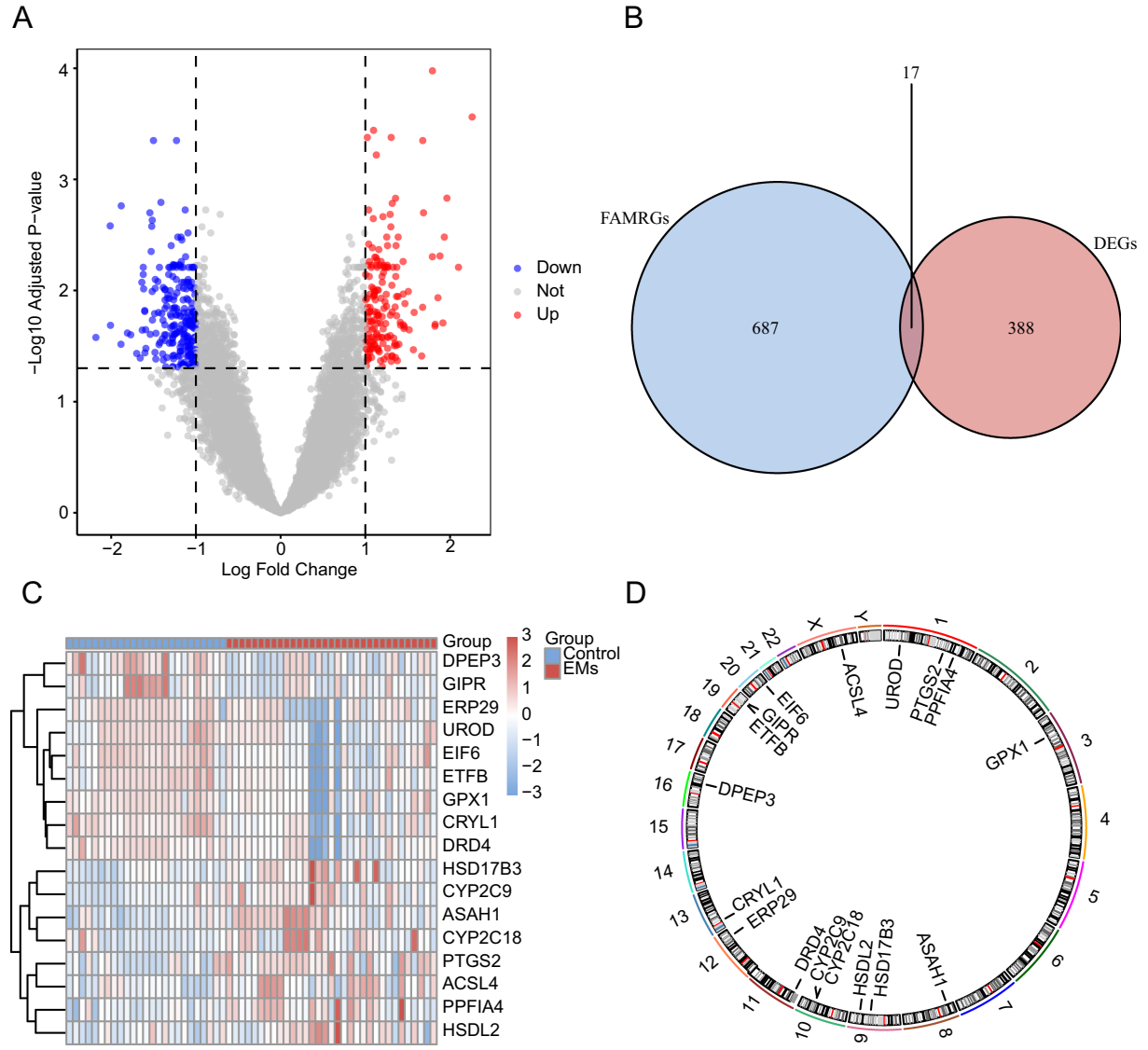

FIGURE 3
Differential gene expression analysis. **(A)** Volcano plot of DEG analysis between the EMs and control groups in the combined GEO datasets. **(B)** A Venn diagram of DEGs and FAMRGs in the integrated GEO datasets (combined datasets). **(C)** A heatmap of FAMRDEGs in the integrated GEO datasets (combined datasets). **(D)** Chromosomal mapping of FAMRDEGs. Light red and blue represent the EMs and Control groups, respectively. In the heatmap, red and blue represent high and low expressions, respectively. EMs, endometriosis; DEGs, differentially expressed genes; FAMRGs, fatty acid metabolism-related genes; FAMRDEGs, fatty acid metabolism-related differentially expressed genes.

network is shown in Figure 6B. Six hub genes were identified, namely, *PTGS2, CYP2C9, HSDL2, HSD17B3, ACSL4*, and *CYP2C18*.

Finally, the GeneMANIA website predicted an interaction network between the six hub genes and genes with similar functions (Figure 6C). Six hub genes and 20 functionally similar proteins were identified.

3.7 Construction of regulatory network

We used the ENCORI database to obtain microRNAs associated with the hub genes *PTGS2, CYP2C9, HSDL2, HSD17B3, ACSL4*, and *CYP2C18*. The constructed mRNA-miRNA regulatory network is shown in Figure 7A. Four hub genes and 28 miRNAs were identified (Table 4).

The ChIPBase database was used to construct the regulatory network of TFs in hub genes. The mRNA-TF regulatory network is shown in Figure 7B. Eight hub genes and 40 TFs were identified in this regulatory network (Table 5).

3.8 Validation of differentially expressed hub genes and ROC curve analysis

A grouping comparison chart was constructed to evaluate the differences in the expression of six hub genes between the Endometriosis and Control groups in the combined GEO datasets (Figure 8A). The analysis revealed statistically significant differences in the expression levels of high and low. Statistically significant differences were observed in the expression levels of six hub genes

TABLE 2 Results of GO and KEGG enrichment analysis for FAMRDEGs.

Ontology	ID	Description	Gene ratio	Bg ratio	*p* value	p adj	*q* value
BP	GO:0006631	fatty acid metabolic process	9/17	401/18888	1.68E-11	1.22E-08	6.97E-09
BP	GO:0001676	long-chain fatty acid metabolic process	5/17	109/18888	3.42E-08	1.24E-05	7.10E-06
BP	GO:0120254	olefinic compound metabolic process	5/17	162/18888	2.48E-07	4.52E-05	2.58E-05
BP	GO:0051223	regulation of protein transport	5/17	440/18888	3.29E-05	0.003424	0.001956
BP	GO:0019369	arachidonic acid metabolic process	4/17	58/18888	1.85E-07	4.49E-05	2.56E-05
MF	GO:0020037	heme binding	3/17	142/18522	0.000277	0.004808	0.001568
MF	GO:0046906	tetrapyrrole binding	3/17	152/18522	0.000339	0.004808	0.001568
MF	GO:0016705	oxidoreductase activity, acting on paired donors, with incorporation or reduction of molecular oxygen	3/17	179/18522	0.000546	0.006464	0.002108
MF	GO:0008392	arachidonic acid epoxygenase activity	2/17	16/18522	9.44E-05	0.00427	0.001393
MF	GO:0008391	arachidonic acid monooxygenase activity	2/17	18/18522	0.00012	0.00427	0.001393
KEGG	hsa05204	Chemical carcinogenesis – DNA adducts	3/13	71/8840	0.000134	0.006702	0.006209
KEGG	hsa04726	Serotonergic synapse	3/13	115/8840	0.000558	0.013944	0.012917
KEGG	hsa00590	Arachidonic acid metabolism	2/13	61/8840	0.003479	0.053821	0.049856
KEGG	hsa00830	Retinol metabolism	2/13	68/8840	0.004306	0.053821	0.049856
KEGG	hsa00061	Fatty acid biosynthesis	1/13	18/8840	0.026167	0.22962	0.212701

GO, Gene Ontology; BP, Biological Process; CC, Cellular Component; MF, Molecular Function; KEGG, Kyoto Encyclopedia of Genes and Genomes; FAMRDEGs, Fatty Acid Metabolism-Related Differentially Expressed Genes.

(*ACSL4, CYP2C18, CYP2C9, HSD17B3, HSDL2*, and *PTGS2*) between the Endometriosis and Control groups of the combined GEO datasets ($p < 0.001$). An ROC curve of expression levels of hub genes in the integrated GEO datasets is shown in Figures 8B–G. The expression levels of the six hub genes in the Endometriosis and Control groups were classified with high accuracy ($0.7 < AUC < 0.9$).

3.9 ssGSEA immune analysis

The abundance of 28 immune cell types was calculated using the ssGSEA algorithm. The group comparison diagram is shown in Figure 9A. Seven immune cells, namely, activated CD4 + T cells, gamma-delta T cells, CD56 dim natural killer cells, eosinophils, monocytes, natural killer T cells, and plasmacytoid dendritic cells, were significantly different between the Endometriosis and Control groups ($p < 0.05$). Correlation heatmaps of the immune infiltration of these cell types in the integrated GEO datasets are shown in Figure 9B. The association of six hub genes with these immune cells was analyzed using a correlation bubble chart (Figure 9C). The TOP1-positive and TOP1-negative correlation between hub genes and immune cells is shown in Figures 9D,E. *ACSL4* showed the strongest positive correlation with effector memory CD8 T cells ($r = 0.704$, $p < 0.05$) (Figure 9D), whereas *HSDL2* showed the strongest negative correlation with activated CD8 T cells ($r = -0.687$, $p < 0.05$) (Figure 9E).

4 Discussion

Endometriosis is a chronic gynecological disorder characterized by the presence of endometrial-like tissue outside the uterus; it results in inflammation, pain, and infertility (1). Despite the high prevalence of endometriosis, its pathogenesis remains unclear. This complicates both diagnosis and treatment. Current therapeutic approaches, including hormonal therapy and surgical interventions, often provide temporary relief. Furthermore, they have side effects and a notably high recurrence rate post-surgery (3). Because the symptoms associated with endometriosis are frequently misattributed to dysmenorrhea, a condition commonly experienced by adolescent girls and young women, significant delays in diagnosis can occur (4). This underscores the pressing need to elucidate the mechanisms underlying the pathogenesis of this disease and identify novel diagnostic markers. Endometriosis involves complex interactions between genetic, hormonal, and environmental factors (5). Recent studies have highlighted the role of metabolic dysregulation, particularly fatty acid metabolism, in the progression of this disease (7). However, the correlation between endometriosis and fatty acid metabolism remains largely understudied.

Endometriosis is a dynamic disease characterized by time-series changes in gene expression. Different stages of the disease involve distinct biological processes and molecular mechanisms, with fatty acid metabolism-related genes playing a key role (11). In the early stages, upregulation of fatty acid metabolism-related genes may help control local inflammatory responses and promote the repair of damaged tissue. For instance, these genes can increase the synthesis of anti-inflammatory substances and inhibit the production of pro-inflammatory factors, thereby reducing the inflammatory response. This mechanism is crucial for early response to disease progression. However, as the disease progresses, the expression of these genes may decline, leading to lipid metabolism imbalances and promoting the development of chronic inflammation and tissue remodeling.

Fluctuations in hormone levels significantly impact the regulation of fatty acid metabolism. In particular, estrogen and progesterone

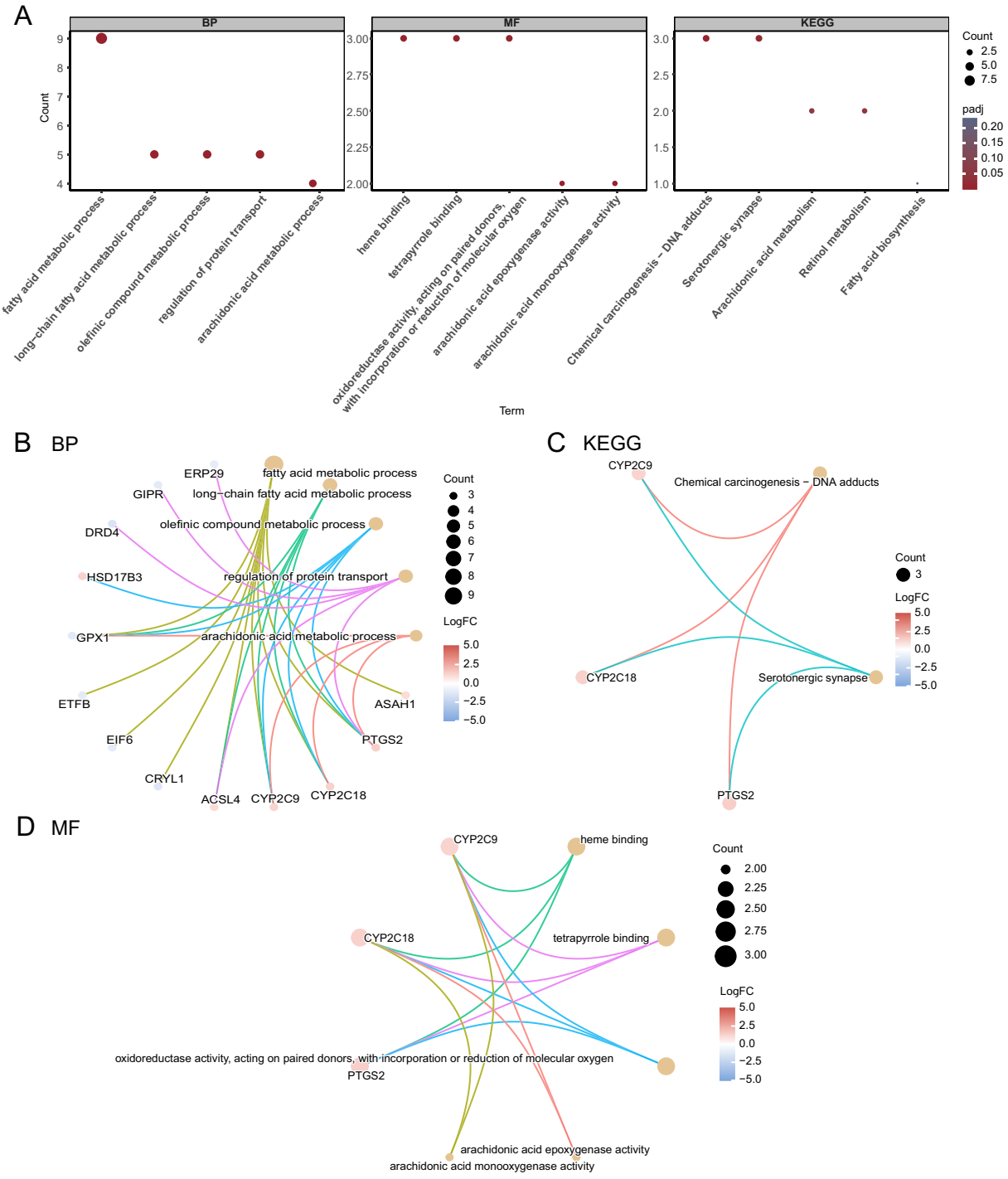

FIGURE 4
GO and KEGG enrichment analyses for FAMRDEGs. **(A)** A bubble plot of GO and KEGG enrichment analysis results for BP, MF, and biological pathway (KEGG) in FAMRDEG. GO and KEGG terms are shown on the abscissa. **(B–D)** GO and KEGG enrichment analysis results for the network diagram of FAMRDEGs showing BP **(B)**, KEGG **(C)**, and MF **(D)**. Lighter red and light brown nodes represent items, and nodes represent molecules. The attachment shows the genes and their corresponding access nodes. Larger pathway nodes indicate greater enrichment of the pathways in genes. The color of the gene node indicates its logFC. Red and blue represent upregulated and downregulated gene expression, respectively. The bubble size and color represent the number of genes and the size of the adj. *p*-value, respectively. A deeper red color indicates a smaller adj. *p*-value, whereas a bluer color indicates a larger adj. *p*-value. The screening criteria for GO and KEGG enrichment analyses were adj. $p < 0.05$ and FDR value $q < 0.25$, and the Benjamini–Hochberg *p*-value correction method was used. FAMRDEGs, fatty acid metabolism-related differentially expressed genes; GO, Gene Ontology; KEGG, Kyoto Encyclopedia of Genes and Genomes; BP, biological process; MF, molecular function.

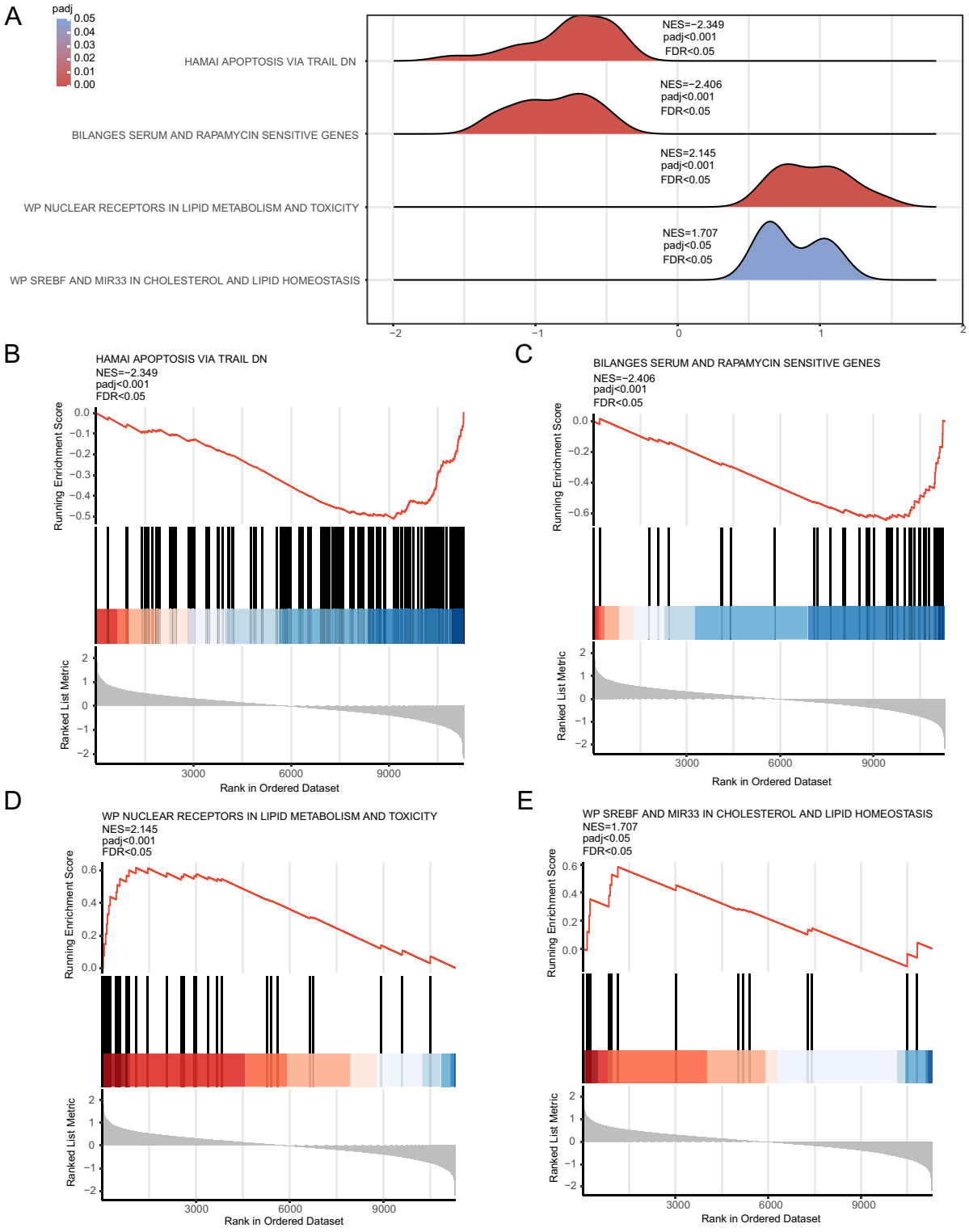

FIGURE 5
GSEA for the combined dataset. **(A)** Mountain map display of four biological functions from the GSEA of combined GEO datasets. **(B–E)** GSEA results for genes with downregulated **(B,C)** and upregulated **(D,E)** expression. The screening criteria for GSEA were adj. $p < 0.05$ and FDR value $q < 0.25$, and the Benjamini–Hochberg p-value correction method was used. GSEA, gene set enrichment analysis.

affect the synthesis, oxidation, and transportation of fatty acids. At different stages of the disease course, hormonal changes will directly affect the expression patterns of the genes, resulting in different clinical manifestations. For example, when hormone levels are elevated, the expression of related genes may promote an increase in fatty acid synthesis, which may be inhibited by a decrease in hormone levels. In addition, signaling pathways in cells are also closely related to changes in gene expression (12). For example, activation of

TABLE 3 Results of GSEA for combined datasets.

ID	Set size	Enrichment score	NES	*p* value	*p* adjust	*q* value
HSIAO HOUSEKEEPING GENES	326	−0.64948	−3.26751	1.00E-10	9.95E-09	7.43E-09
REACTOME EUKARYOTIC TRANSLATION ELONGATION	68	−0.77561	−3.16842	1.00E-10	9.95E-09	7.43E-09
REACTOME EUKARYOTIC TRANSLATION INITIATION	93	−0.72453	−3.14164	1.00E-10	9.95E-09	7.43E-09
WP CYTOPLASMIC RIBOSOMAL PROTEINS	67	−0.76639	−3.109	1.00E-10	9.95E-09	7.43E-09
KEGG RIBOSOME	65	−0.76707	−3.09318	1.00E-10	9.95E-09	7.43E-09
REACTOME RESPONSE OF EIF2AK4 GCN2 TO AMINO ACID DEFICIENCY	77	−0.73949	−3.0839	1.00E-10	9.95E-09	7.43E-09
REACTOME NONSENSE MEDIATED DECAY NMD	89	−0.70339	−3.02811	1.00E-10	9.95E-09	7.43E-09
REACTOME SRP DEPENDENT COTRANSLATIONAL PROTEIN TARGETING TO MEMBRANE	86	−0.70743	−3.00935	1.00E-10	9.95E-09	7.43E-09
REACTOME SELENOAMINO ACID METABOLISM	81	−0.712	−2.9979	1.00E-10	9.95E-09	7.43E-09
REACTOME INFLUENZA INFECTION	125	−0.65741	−2.97902	1.00E-10	9.95E-09	7.43E-09
REACTOME REGULATION OF EXPRESSION OF SLITS AND ROBOS	134	−0.63804	−2.91137	1.00E-10	9.95E-09	7.43E-09
REACTOME CELLULAR RESPONSE TO STARVATION	113	−0.65122	−2.89995	1.00E-10	9.95E-09	7.43E-09
REACTOME TRANSLATION	197	−0.60453	−2.89103	1.00E-10	9.95E-09	7.43E-09
REACTOME RRNA PROCESSING	145	−0.61885	−2.84159	1.00E-10	9.95E-09	7.43E-09
KIM ALL DISORDERS DURATION CORR DN	127	−0.61318	−2.78356	1.00E-10	9.95E-09	7.43E-09
PECE MAMMARY STEM CELL UP	98	−0.63343	−2.77538	1.00E-10	9.95E-09	7.43E-09
CHNG MULTIPLE MYELOMA HYPERPLOID UP	38	−0.77545	−2.7727	1.00E-10	9.95E-09	7.43E-09
REACTOME ACTIVATION OF THE MRNA UPON BINDING OF THE CAP BINDING COMPLEX AND EIFS AND SUBSEQUENT BINDING TO 43S	47	−0.72904	−2.74679	1.00E-10	9.95E-09	7.43E-09
REACTOME SIGNALING BY ROBO RECEPTORS	175	−0.5808	−2.73332	1.00E-10	9.95E-09	7.43E-09
YAO TEMPORAL RESPONSE TO PROGESTERONE CLUSTER 17	145	−0.58658	−2.69339	1.00E-10	9.95E-09	7.43E-09

GSEA, Gene Set Enrichment Analysis; NES, Controlized Enrichment Score.

inflammatory signaling pathways affects the expression of fatty acid metabolism-related genes, leading to changes in metabolites that may further promote disease progression. Together, these findings suggest that the pathological characteristics of endometriosis are closely linked to dynamic changes in gene expression, which may have distinct biological significance at different stages.

Seventeen FAMRDEGs were identified in the present study. These genes were significantly involved in arachidonic acid and fatty acid metabolic processes. GeneMANIA predicted a complex interaction network between six hub genes and 20 functionally similar proteins. The integration of gene expression data and functional analyses highlighted the potential application of hub genes related to fatty acid metabolism as diagnostic markers and therapeutic targets in endometriosis. This approach could improve the diagnosis and treatment of endometriosis, potentially leading to personalized and effective therapeutic interventions. Identifying the key regulatory genes and pathways involved in fatty acid metabolism could provide new insights into the pathogenesis of this disease. *PTGS2, CYP2C9, HSDL2, HSD17B3, ACSL4,* and *CYP2C18* were identified as hub genes in this study. Prostaglandin endoperoxidase synthase 2 (*PTGS2*) encodes COX-2 (13) that is overexpressed in the ectopic endometrium of women with endometriosis compared to that in the normal endometrium of women without the disease (14). *PTGS2* emerged as the central hub gene in the present study, exhibiting the highest score among the identified FAMRDEGs. This gene plays an important role in the inflammatory processes associated with endometriosis, contributing to the progression and physiological manifestation of the disease (15).

Prostaglandin lactone synthase (PTGS2) (16) is a hub gene with significantly upregulated expression in patients with endometriosis, driving prostaglandin synthesis. This process intensifies local inflammatory and pain, a hallmark of endometriosis. PTGS2 activity is closely linked to chronic inflammation, pain perception, and pathological changes, further promoting disease progression. In addition, our study also found that the two cytochrome P450 enzymes (17), namely, CYP2C9 and CYP2C18, play an important role in fatty acid metabolism. Their expression not only influences hormone metabolism but may also disrupt the biological function of the endometrium, highlighting their role in fatty acid metabolism disorders and associated pathophysiological states.

This overexpression was correlated with elevated levels of prostaglandins, which are potent mediators of inflammation and pain. Moreover, *PTGS2* is regulated by various factors, including hormonal therapy, which is a common treatment for endometriosis. Hormone therapy can enhance the expression of *PTGS2*, which may explain why it does not cure this disease (18). In addition, *PTGS2* polymorphisms are linked to an increased risk of endometriosis, with genetic susceptibility mediated by inflammatory pathways (19). Similarly, the

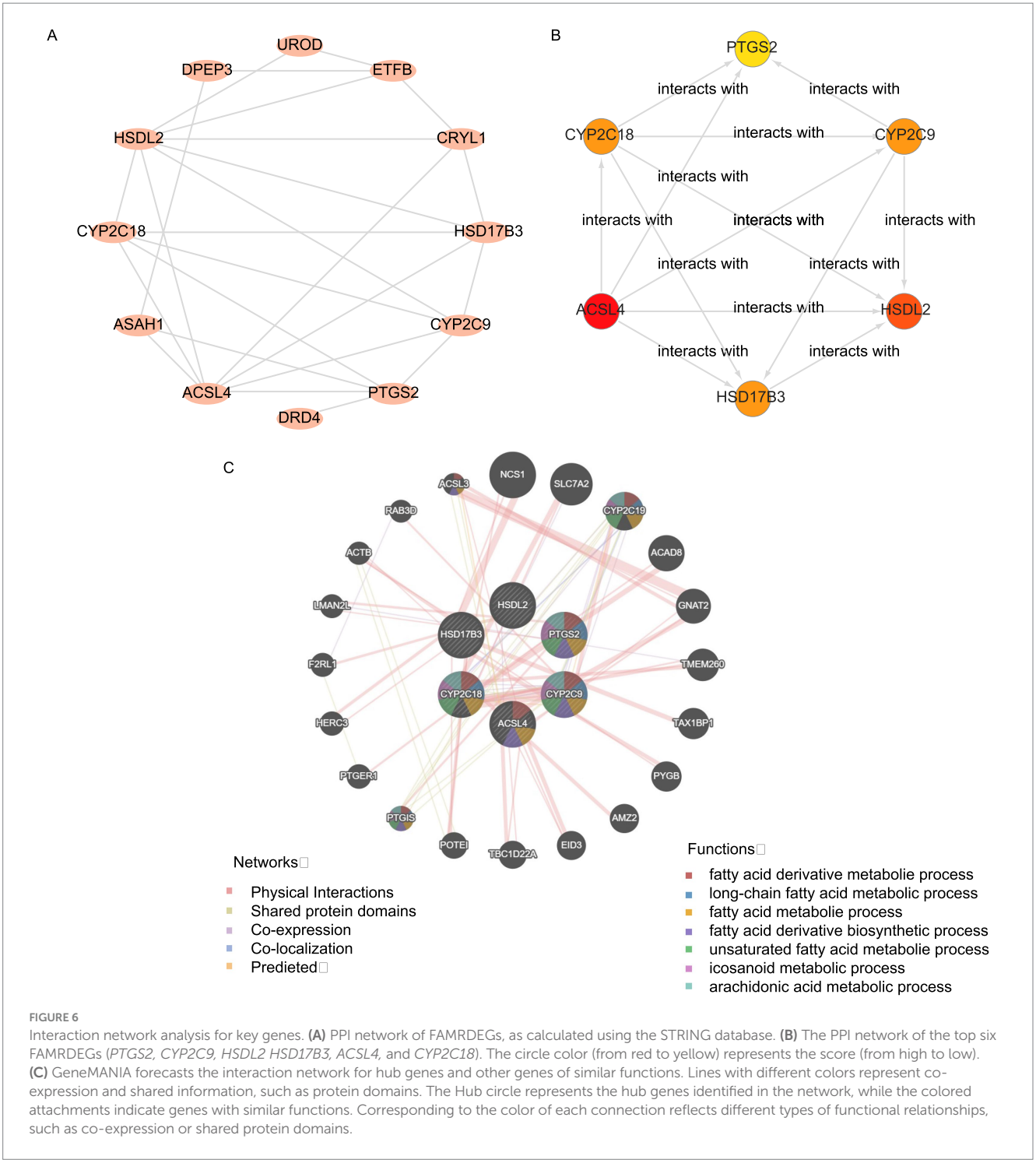

FIGURE 6
Interaction network analysis for key genes. **(A)** PPI network of FAMRDEGs, as calculated using the STRING database. **(B)** The PPI network of the top six FAMRDEGs (*PTGS2, CYP2C9, HSDL2 HSD17B3, ACSL4,* and *CYP2C18*). The circle color (from red to yellow) represents the score (from high to low). **(C)** GeneMANIA forecasts the interaction network for hub genes and other genes of similar functions. Lines with different colors represent co-expression and shared information, such as protein domains. The Hub circle represents the hub genes identified in the network, while the colored attachments indicate genes with similar functions. Corresponding to the color of each connection reflects different types of functional relationships, such as co-expression or shared protein domains.

upregulation of *HSD17B3* expression may increase the risk of endometriosis (20).

At the same time, acid alcohol esterase 1 (ASAH1) and lipase 2 (HSDL2) play crucial roles in fatty acid hydrolysis and metabolism. Changes in their expression directly impact intracellular energy metabolism, inflammatory response, and tissue remodeling, collectively influencing the biological characteristics and disease progression of endometriosis. The involvement of these central genes in regulating inflammation and fatty acid metabolism provides important clues for our understanding of the complex biology of endometriosis and may become key targets for future research and treatment. Therefore, elucidating their roles in inflammation and tissue remodeling could enhance our understanding of disease mechanisms and provide potential strategies for personalized treatment.

Our study identified several biological pathways closely linked to endometriosis through GO and KEGG enrichment analysis, offering key insights into the disease's pathogenesis. Pathways associated with fatty acid metabolism, including long-chain fatty acid metabolism and arachidonic acid metabolism, revealed the effects of lipid metabolism

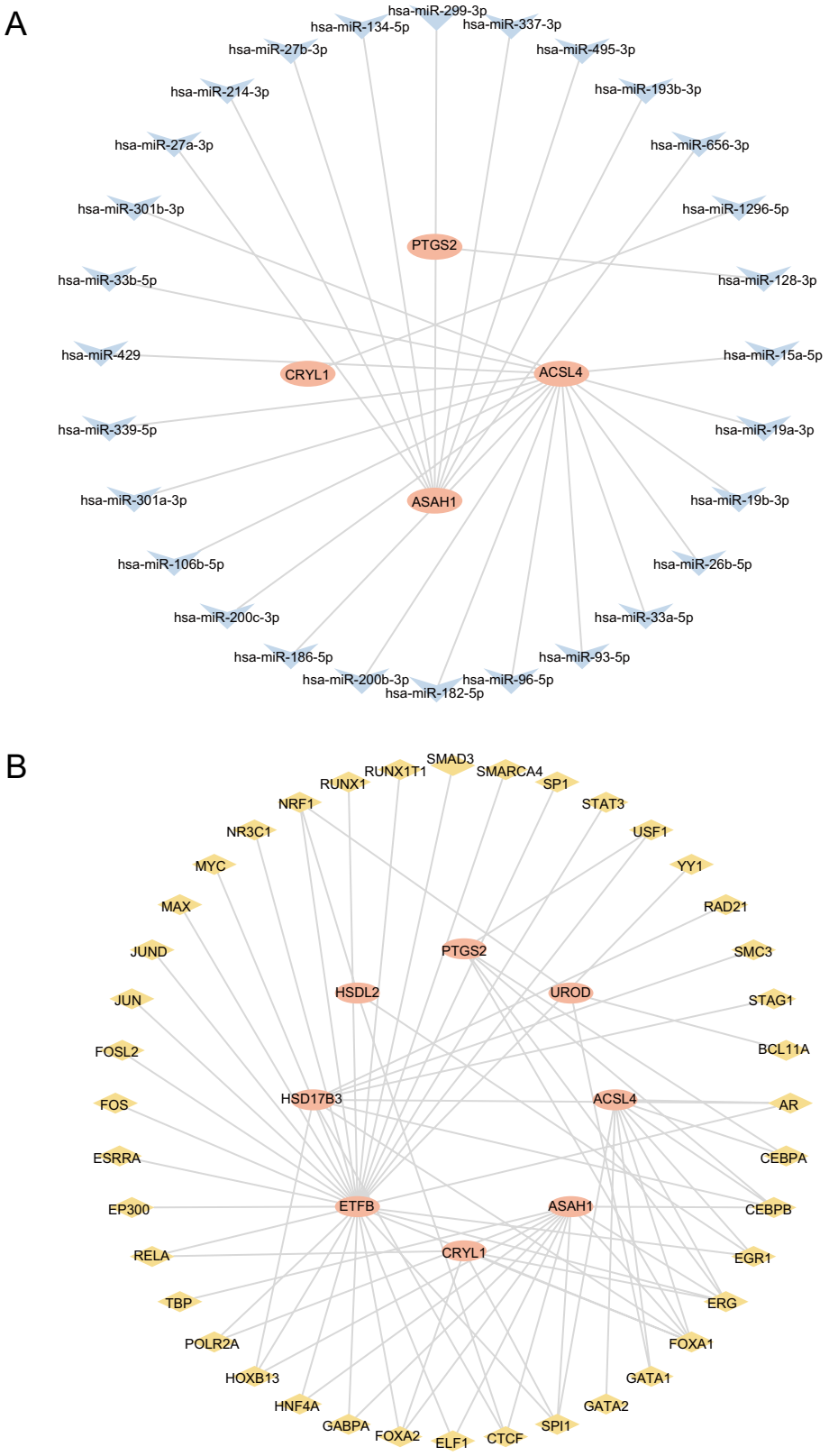

FIGURE 7
Construction of the regulatory network of FAMRDEGs. The mRNA-miRNA **(A)** and mRNA-TF **(B)** regulatory networks of FAMRDEGs. Orange, light blue, and pale yellow represent mRNA, miRNA, and TF, respectively. FAMRDEGs, fatty acid metabolism-related differentially expressed genes; miRNA, MicroRNA; TF, transcription factor.

TABLE 4 mRNA-miRNA interaction of key genes.

mRNA	miRNA
ACSL4	hsa-miR-15a-5p
ACSL4	hsa-miR-19a-3p
ACSL4	hsa-miR-19b-3p
ACSL4	hsa-miR-26b-5p
ACSL4	hsa-miR-33a-5p
ACSL4	hsa-miR-93-5p
ACSL4	hsa-miR-96-5p
ACSL4	hsa-miR-182-5p
ACSL4	hsa-miR-200b-3p
ACSL4	hsa-miR-186-5p
ACSL4	hsa-miR-200c-3p
ACSL4	hsa-miR-106b-5p
ACSL4	hsa-miR-301a-3p
ACSL4	hsa-miR-339-5p
ACSL4	hsa-miR-429
ACSL4	hsa-miR-33b-5p
ACSL4	hsa-miR-301b-3p
ASAH1	hsa-miR-27a-3p
ASAH1	hsa-miR-214-3p
ASAH1	hsa-miR-27b-3p
ASAH1	hsa-miR-134-5p
ASAH1	hsa-miR-299-3p
ASAH1	hsa-miR-337-3p
ASAH1	hsa-miR-495-3p
ASAH1	hsa-miR-193b-3p
ASAH1	hsa-miR-656-3p
CRYL1	hsa-miR-1296-5p
PTGS2	hsa-miR-128-3p

miRNA, MicroRNA.

on inflammatory responses. The activation of these pathways may elevate intracellular fatty acid levels, thereby intensifying the local inflammatory environment. Notably, fatty acid metabolites such as prostaglandins play a crucial role in modulating immune responses and promoting endometrial growth, potentially exacerbating the pathological status of endometriosis. This observation aligns with previous studies that underscore the fundamental role of arachidonic acid metabolism in the inflammatory processes associated with endometriosis. Jiang et al. (21) demonstrated that arachidonic acid metabolism is the most significantly enriched pathway among the common DEGs identified across various subtypes of endometriosis. This suggests the essential role of this metabolic process in the inflammatory pathogenesis of the disease. Upregulation of the expression of genes involved in the arachidonic acid pathway indicates a heightened inflammatory response, which is a hallmark of endometriosis. In addition, the role of fatty acid metabolism in endometriosis has been corroborated by metabolomic studies. Ortiz et al. (22) reviewed the metabolomic profiles of patients with endometriosis and identified significant alterations in lipid metabolism,

TABLE 5 mRNA-TF interaction of key genes.

mRNA	TF
ACSL4	AR
ACSL4	CEBPA
ACSL4	CEBPB
ACSL4	EGR1
ACSL4	ERG
ACSL4	FOXA1
ACSL4	GATA1
ACSL4	GATA2
ACSL4	SPI1
ASAH1	CEBPB
ASAH1	CTCF
ASAH1	ELF1
ASAH1	ERG
ASAH1	FOXA1
ASAH1	FOXA2
ASAH1	GABPA
ASAH1	HNF4A
ASAH1	HOXB13
ASAH1	POLR2A
ASAH1	SPI1
ASAH1	TBP
CRYL1	SPI1
CRYL1	ERG
CRYL1	FOXA1
CRYL1	FOXA2
CRYL1	RELA
ETFB	AR
ETFB	EGR1
ETFB	ELF1
ETFB	EP300
ETFB	ERG
ETFB	ESRRA
ETFB	FOS
ETFB	FOSL2
ETFB	FOXA1
ETFB	FOXA2
ETFB	GABPA
ETFB	HNF4A
ETFB	HOXB13
ETFB	JUN
ETFB	JUND
ETFB	MAX
ETFB	MYC
ETFB	NR3C1

(Continued)

TABLE 5 (Continued)

mRNA	TF
ETFB	NRF1
ETFB	POLR2A
ETFB	RELA
ETFB	RUNX1
ETFB	RUNX1T1
ETFB	SMAD3
ETFB	SMARCA4
ETFB	SP1
ETFB	SPI1
ETFB	STAT3
ETFB	USF1
ETFB	YY1
HSD17B3	AR
HSD17B3	CEBPB
HSD17B3	CTCF
HSD17B3	FOXA1
HSD17B3	HOXB13
HSD17B3	RAD21
HSD17B3	SMC3
HSD17B3	STAG1
HSDL2	CTCF
HSDL2	EGR1
HSDL2	NRF1
PTGS2	FOXA1
PTGS2	USF1
PTGS2	CEBPA
PTGS2	CEBPB
PTGS2	ERG
UROD	GATA1
UROD	NRF1
UROD	BCL11A

TF, Transcription factors.

including those of fatty acids. These metabolic changes demonstrate the impact of the disease on cellular processes, such as energy production, oxidative stress, and inflammation. The identification of specific metabolites could reveal non-invasive biomarkers for early diagnosis and further elucidate the pathophysiology of endometriosis.

At the same time, the enrichment results indicate that abnormal activity in key signaling pathways is directly linked to cell proliferation and survival, potentially dysregulating the cell cycle, thereby promoting disordered proliferation and migration of endometrial cells and increasing the formation of abnormal endometrial tissue. Meanwhile, signaling pathways associated with apoptosis, such as enrichment of apoptosis signaling pathways, indicate changes in cell survival mechanisms in the disease. The activation of pro-inflammatory cytokines may suppress normal apoptosis, thereby enhancing the survival and persistence of endometrial cells.

In this study, we focused on identifying genetic and molecular factors associated with fatty acid metabolism in endometriosis. However, external influences such as diet, hormone fluctuations, and lifestyle factors are crucial in disease occurrence and progression. These factors may have profound effects on fatty acid metabolism and play a crucial role in the occurrence and development of the disease. Studies have shown that eating habits (23) significantly affect lipid metabolism. A diet rich in omega-3 fatty acids (such as fish and nuts) can reduce chronic inflammation, which is often associated with the pathological processes of endometriosis. By inhibiting the synthesis of inflammatory mediators, omega-3 fatty acids may help alleviate symptoms and slow disease progression.

Antioxidant intake may improve lipid metabolism by reducing oxidative stress, which could influence the risk of developing endometriosis. Hormone levels, especially estrogen and progesterone (24), play a crucial role in regulating fatty acid metabolism. Estrogen can enhance the synthesis and transport of fatty acids by activating genes related to fat metabolism, thereby changing the function of fat cells (hormone fluctuations not only affect metabolism but also affect the expression of identified genes, thereby further interfering with the progress of the disease).

Lifestyle factors such as physical activity and environmental exposure can also affect fatty acid metabolism and disease severity. Lack of exercise is often associated with obesity, which may induce inflammatory responses and aggravate the symptoms of endometriosis. In addition, endocrine disruptors in the environment may affect hormone balance and further change metabolic pathways.

GSEA results indicate upregulation of lipid metabolism and toxicity-related pathways, a finding that has important clinical and therapeutic implications, especially in the management and intervention of endometriosis. Upregulation of lipid metabolism suggests that in a pathological state, the accumulation of fatty acids and related metabolites may lead to intensification of the inflammatory response, which is considered a key factor in promoting the development of endometriosis. Therefore, therapeutic strategies for lipid metabolism may help relieve local inflammation, thereby reducing patient symptoms and improving quality of life.

On the other hand, upregulation of toxic pathways suggests that apoptosis and stress responses may be imbalanced. In endometriosis, ectopic cells may be in a state of persistent stress, resulting in changes in cell physiological function. Recognizing the interaction of these toxic pathways can provide clues to novel therapeutic strategies, such as the use of antioxidants to combat cellular oxidative stress, or the use of small molecules to target specific toxic signaling pathways to restore normal cell function and slow disease progression.

The immune landscape of endometriosis is intricate and encompasses various immune cell types that considerably affect disease pathogenesis. In our study, ssGSEA revealed a correlation between endometriosis and several immune cell types, including activated CD4 + T cells, gamma-delta T cells, CD56 dim natural killer cells, eosinophils, monocytes, natural killer T cells, and plasmacytoid dendritic cells. The peritoneal fluid of women with endometriosis has a higher concentration of activated CD4 + T cells than that of healthy controls, suggesting an altered immune response in these patients. Furthermore, the peritoneal fluid of women with endometriosis displays increased levels of immunosuppressive cytokines, such as IL-10 and IL-12, which may inhibit the activity of activated CD4 + T cells and contribute to immune evasion by endometriotic lesions (25).

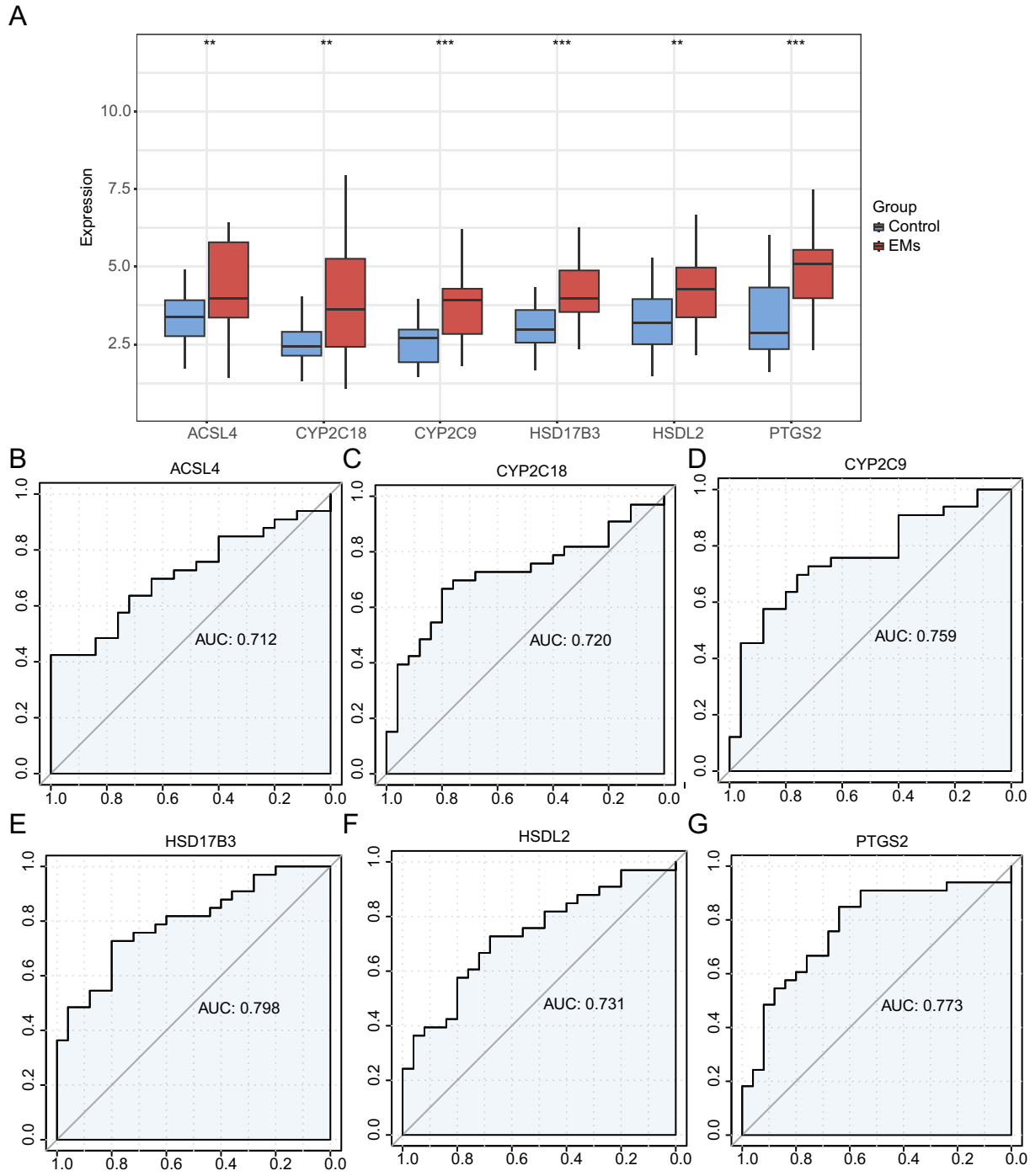

FIGURE 8
Validation of differential expression and ROC curve analysis. **(A)** Group comparison plot of hub genes in the EMs and control groups in the combined GEO datasets. **(B–G)** ROC curves of six hub genes in the integrated GEO Datasets: *ACSL4* **(B)**, *CYP2C18* **(C)**, *CYP2C9* **(D)**, *HSD17B3* **(E)**, *HSDL2* **(F)**, and *PTGS2* **(G)**. $^{**}p < 0.01$, $^{***}p < 0.001$. EMs, endometriosis; ROC, receiver operating characteristic; AUC, area under the curve; TPR, true positive rate; FPR, false positive rate. Red and blue represent the Endometriosis and Control groups, respectively.

The presence of these cytokines correlated with a reduction in peritoneal lymphocytes, particularly within the HLA-DR + CD4 + T cell subpopulation, further indicating an impaired immune response (26). In addition, the interactions between T cells and extracellular matrix (ECM) proteins are modified during endometriosis. Activated T cells from women with endometriosis show increased adhesion to ECM proteins, such as collagen IV and fibronectin. This suggests that these interactions might contribute to the pathogenesis of the disease by facilitating the implantation and survival of ectopic endometrial tissue. This enhanced adhesion could be a result of the altered expression of surface antigens on T cells. However, no significant differences in these antigens were observed between patients with endometriosis and healthy controls (27). These results indicate a close correlation between activated CD4 + T cells and endometriosis, which

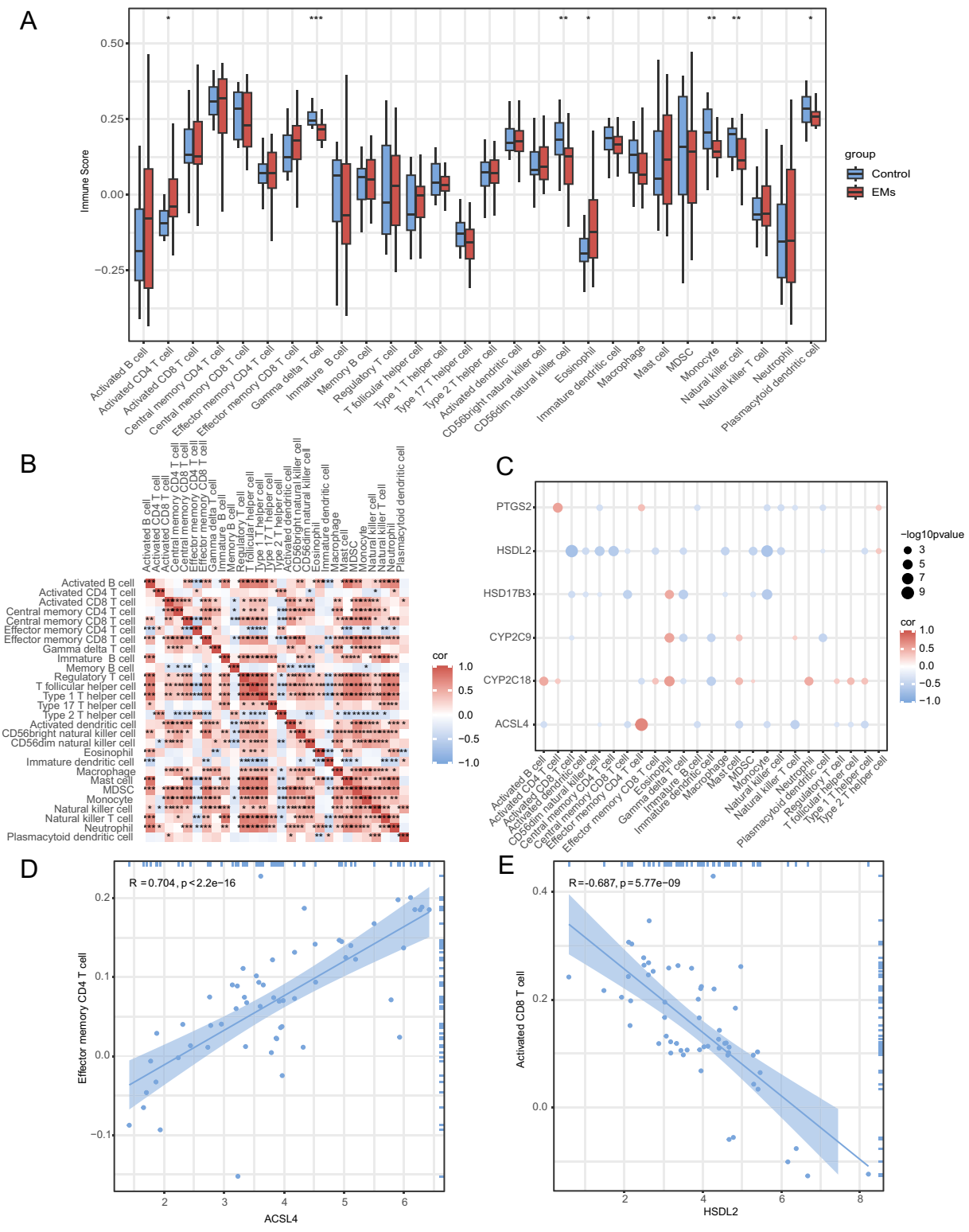

FIGURE 9
Immune infiltration analysis by ssGSEA algorithm. **(A)** Group comparison plot of immune cell infiltration in the Endometriosis and Control groups in combined GEO datasets. **(B)** A correlation heatmap of immune cell abundance. **(C)** A bubble plot showing the correlation between hub genes and immune cell infiltration in combined GEO datasets. **(D)** A scatter plot showing TOP1-positive correlation between hub genes and immune cells. **(E)** A scatter plot showing TOP1-negative correlation between hub genes and immune cells. ns represents $p \geq 0.05$; *$p < 0.05$; **$p < 0.01$; and ***$p < 0.001$. $r < 0.3$, $r = 0.3–0.5$, $r = 0.5–0.8$, and $r > 0.8$ were considered weak or irrelevant, weak, moderate, and strong correlation, respectively. Light red and light blue represent the Endometriosis and Control groups, respectively. Red indicates a positive correlation, whereas blue indicates negative correlation. The depth of the color represents the strength of the correlation. ssGSEA, single-sample gene set enrichment analysis; EMs, endometriosis.

is consistent with our results. In the present study, *ACSL4* had the strongest positive correlation with effector memory CD4 + T cells. In contrast, *HSDL2* showed the strongest negative correlation with activated CD8 + T cells. These results indicate that hub genes (*ACSL4* or *HSDL2*) are promising therapeutic targets for endometriosis.

Endometriosis (EMs) is a disease characterized by chronic inflammation and immune imbalances; a growing number of studies have revealed the key role of immune cells, especially T cell subsets (28), in the occurrence and development of the disease. In this study, we observed a potential correlation of effector memory CD8 + T cells in endometriosis tissues, suggesting that it may be an important factor affecting the immune microenvironment.

Effector memory CD8 + T cells (Tem) are a long-term survival subpopulation of T cells that are highly specific and can quickly recognize and respond to specific antigens. Typically, these cells quickly activate immune responses when the body is re-exposed to the same antigen, enhancing the body's defense. However, in the context of endometriosis, these cells may be continuously activated by prolonged exposure to antigens in ectopic endometrial tissue. Effector memory CD8 + T cells are able to secrete pro-inflammatory cytokines (29) such as interferon-γ (IFN-γ) and tumor necrosis factor-α (TNF-α), thereby mediating local inflammatory responses and increasing tissue damage. This inflammatory environment may not only promote the development of ectopic lesions but may also be closely related to the pain symptoms of the disease, as inflammatory mediators can directly or indirectly activate pain-related neural pathways.

Fatty acid synthase 4 (ACSL4) plays a crucial role in fatty acid metabolism and is closely linked to immune cell infiltration in endometriosis, mainly because ACSL4 plays a key role in fatty acid metabolism. ACSL4 influences the polarization of immune cells, especially in macrophages and T cells (30). Specifically, ACSL4 promotes the enhancement of anti-inflammatory response by promoting the synthesis of specific fatty acids (such as arachidonic acid), affecting the polarization process of macrophages, causing them to polarize to M2. This suggests that ACSL4 is not only involved in regulating fatty acid metabolism but also directly affects the function and infiltration patterns of immune cells, making them play a more effective role in the microenvironment of endometriosis. At the same time, ACSL4 further regulates the response of immune cells by changing the lipid composition of the cell membrane (31), which can significantly affect the migration, proliferation, and activation of immune cells, which is directly related to local inflammatory responses. In endometriosis, the expression of ACSL4 may be closely related to the synthesis of pro-inflammatory cytokines, which will lead to increased infiltration of immune cells in ectopic tissues, aggravating local inflammatory responses and corresponding symptoms. Therefore, understanding the specific mechanisms of ACSL4 in immune cell infiltration will help uncover the pathological mechanisms of endometriosis and provide new targets for future therapeutic strategies. Follow-up studies can further explore the improvement of clinical symptoms in patients with endometriosis by regulating ACSL4 expression activities, which will be a potential therapeutic development direction.

Despite our comprehensive analyses, this study has some limitations. First, this study did not combine wet laboratory validation. Rather, it relied only on bioinformatics analyses. Therefore, further experimental validation is needed to confirm our findings. Second, the sample size was small. Therefore, more samples are needed for validation. In addition, there was a lack of clinical validation analyses to ensure that the findings have practical applications.

In our study, key molecular features associated with endometriosis were identified through bioinformatics analysis and computational tools using publicly available gene expression dataset. Specifically, we downloaded endometriosis-related datasets (GSE120103 and GSE25628) from the GEO database, and batch processing was performed using the R package SVA to obtain the integrated gene expression dataset. Subsequently, differential analysis was performed using the R package limma to identify 405 differentially expressed genes. At the same time, six hub genes were screened from the differential genes through the MCC algorithm of the CytoHubba plug-in of the Cytoscape software. These six hub genes present a certain accuracy in the verification model, with an average AUC > 0.7. This suggests that they have high accuracy in the region of patients with endometriosis and healthy individuals. Therefore, our research not only reveals potential biomarkers but also provides a theoretical basis for future clinical applications.

However, owing to time and resource limitations, we have not yet carried out laboratory verification work. We plan to add relevant experiments to future studies to verify the function and mechanism of identified hub genes through *in vitro* and *in vivo* experiments; this will further enhance the application value of our research results and facilitate future research and treatment of endometriosis.

In this study, we aimed to explore the molecular mechanisms of endometriosis by analyzing the GSE120103 and GSE25628 datasets. Endometriosis is a complex gynecological disease with unclear pathogenesis, and so understanding its molecular basis is crucial to developing effective diagnostic and therapeutic methods. Our core analytical steps included identifying and screening differentially expressed genes (DEGs). By comparing the expression profiles of healthy tissues and lesion tissues, a series of genes that were significantly differentially expressed in endometriosis were successfully screened. Subsequently, the CytoHubba plug-in of the Cytoscape software was used along with the MCC algorithm to screen six hub genes from differential genes. These genes have important centrality in the network and likely play a key role in the development of endometriosis.

To verify the clinical application value of these hub genes, we constructed a validation model; the results showed that the average AUC of these genes was >0.7 in patients with endometriosis and healthy individuals, indicating that they have good predictive capabilities and potential biomarker effects.

A larger sample size would better represent genetic diversity and variability in a wider patient population. However, owing to time and resource constraints, we are currently unable to obtain a larger volume of sample data. Future research will consider incorporating more samples in a bid to further explore the complex heterogeneity and potential therapeutic targets of endometriosis. Moreover, we plan to include samples from patients of different ethnicities to more comprehensively explore the heterogeneity of endometriosis.

In conclusion, we systematically integrated and analyzed two GEO datasets and identified 17 DEGs related to fatty acid metabolism using a series of bioinformatics methods. The PPI network identified six hub genes: *PTGS2, CYP2C9, HSDL2, HSD17B3, ACSL4,* and *CYP2C18*. Moreover, ssGSEA immune infiltration analysis revealed that *ACSL4* showed the strongest positive correlation with effector memory CD8 T cells, whereas *HSDL2* showed the strongest negative correlation with activated CD8 T cells. These findings not only enrich our understanding

of the molecular mechanisms of the disease but also provide valuable insights for the development of new diagnostic markers and therapeutic targets in the future. We are committed to further experimental validations and clinical application transformations in future studies.

Data availability statement

The original contributions presented in the study are included in the article/Supplementary material, further inquiries can be directed to the corresponding author.

Author contributions

J-LT: Writing – original draft, Writing – review & editing. R-XF: Writing – review & editing.

Funding

The author(s) declare that no financial support was received for the research and/or publication of this article.

Acknowledgments

We thank all colleagues involved in the study for their contributions.

Conflict of interest

The authors declare that the research was conducted in the absence of any commercial or financial relationships that could be construed as a potential conflict of interest.

Generative AI statement

The authors declare that no Gen AI was used in the creation of this manuscript.

Publisher's note

Supplementary material

The Supplementary material for this article can be found online at: https://www.frontiersin.org/articles/10.3389/fmed.2025.1529074/full#supplementary-material

References

1. Macer ML, Taylor HS. Endometriosis and infertility: a review of the pathogenesis and treatment of endometriosis-associated infertility. *Obstet Gynecol Clin N Am*. (2012) 39:535–49. doi: 10.1016/j.ogc.2012.10.002

2. Smolarz B, Szyłło K, Romanowicz H. Endometriosis: epidemiology, classification, pathogenesis, treatment and genetics (review of literature). *Int J Mol Sci*. (2021) 22:10554. doi: 10.3390/ijms221910554

3. Chapron C, Marcellin L, Borghese B, Santulli P. Rethinking mechanisms, diagnosis and management of endometriosis. *Nat Rev Endocrinol*. (2019) 15:666–82. doi: 10.1038/s41574-019-0245-z

4. Ahn SH, Singh V, Tayade C. Biomarkers in endometriosis: challenges and opportunities. *Fertil Steril*. (2017) 107:523–32. doi: 10.1016/j.fertnstert.2017.01.009

5. Taylor HS, Kotlyar AM, Flores VA. Endometriosis is a chronic systemic disease: clinical challenges and novel innovations. *Lancet*. (2021) 397:839–52. doi: 10.1016/S0140-6736(21)00389-5

6. Matalliotakis IM, Arici A, Cakmak H, Goumenou AG, Koumantakis G, Mahutte NG. Familial aggregation of endometriosis in the Yale series. *Arch Gynecol Obstet*. (2008) 278:507–11. doi: 10.1007/s00404-008-0644-1

7. Varga J, Reviczká A, Háková H, Švajdler P, Rabajdová M, Ostró A. Predictive factors of endometriosis progression into ovarian cancer. *J Ovarian Res*. (2022) 15:5. doi: 10.1186/s13048-021-00940-8

8. Lang X, Huang C, Cui H. Prognosis analysis and validation of fatty acid metabolism-related lnc RNAs and tumor immune microenvironment in cervical Cancer. *J Immunol Res*. (2022) 2022:4954457.

9. Lyu Y, Guo C, Zhang H. Fatty acid metabolism-related genes in bronchoalveolar lavage fluid unveil prognostic and immune infiltration in idiopathic pulmonary fibrosis. *Front Endocrinol*. (2022) 13:1001563. doi: 10.3389/fendo.2022.1001563

10. Wang S, Chen A, Zhu W, Feng D, Wei J, Li Q, et al. Characterization of fatty acid metabolism in lung adenocarcinoma. *Front Genet*. (2022) 13:905508. doi: 10.3389/fgene.2022.905508

11. Bedrick BS, Courtright L, Zhang J, Snow M, Sampaio Amendola IL, Nylander E, et al. A systematic review of epigenetics of endometriosis. *F S Rev*. (2024) 5:100070. doi: 10.1016/j.xfnr.2024.01.003

12. Dai Y, Lin X, Liu N, Shi L, Zhuo F, Huang Q, et al. Integrative analysis of transcriptomic and metabolomic profiles reveals abnormal phosphatidylinositol metabolism in follicles from endometriosis-associated infertility patients. *J Pathol*. (2023) 260:248–60. doi: 10.1002/path.6079

13. Tanabe T, Tohnai N. Cyclooxygenase isozymes and their gene structures and expression. *Prostaglandins Other Lipid Mediat*. (2002) 68-69:95–114. doi: 10.1016/S0090-6980(02)00024-2

14. Dai S, Zhu M, Wu R, Lin D, Huang Z, Ren L, et al. Lipoxin a (4) suppresses IL-1β-induced cyclooxygenase-2 expression through inhibition of p 38 MAPK activation in endometriosis. *Reprod Sci*. (2019) 26:1640–9. doi: 10.1177/1933719119828115

15. Santulli P, Borghese B, Noël JC, Fayt I, Anaf V, de Ziegler D, et al. Hormonal therapy deregulates prostaglandin-endoperoxidase synthase 2 (PTGS2) expression in endometriotic tissues. *J Clin Endocrinol Metab*. (2014) 99:881–90. doi: 10.1210/jc.2013-2950

16. Sacco K, Portelli M, Pollacco J, Schembri-Wismayer P, Calleja-Agius J. The role of prostaglandin E2 in endometriosis. *Gynecol Endocrinol*. (2012) 28:134–8. doi: 10.3109/09513590.2011.588753

17. Piccinato CA, Neme RM, Torres N, Silvério R, Pazzini VB, Rosa E Silva JC, et al. Is cytochrome P450 3A4 regulated by menstrual cycle hormones in control endometrium and endometriosis? *Mol Cell Biochem*. (2017) 427:81–9. doi: 10.1007/s11010-016-2899-3

18. da Luz CM, da Broi MG, Donabela FC, Paro de Paz CC, Meola J, Navarro PA. PTGS2 down-regulation in cumulus cells of infertile women with endometriosis. *Reprod Biomed Online*. (2017) 35:379–86. doi: 10.1016/j.rbmo.2017.06.021

19. Calixto da Silva M, Escorsim Machado D, Vilarinho Cardoso J, Freitas-Alves DR, Tostes Berardo P, Vianna-Jorge R, et al. The-1195A>G polymorphism in Cyclooxygenase-2 gene is associated with lower risk of endometriosis. *Eur J Obstet Gynecol Reprod Biol*. (2020) 253:232–7. doi: 10.1016/j.ejogrb.2020.08.012

20. Wang HS, Wu HM, Cheng BH, Yen CF, Chang PY, Chao A, et al. Functional analyses of endometriosis-related polymorphisms in the estrogen synthesis and metabolism-related genes. *PLoS One*. (2012) 7:e47374. doi: 10.1371/journal.pone.0047374

21. Jiang L, Zhang M, Wang S, Han Y, Fang X. Common and specific gene signatures among three different endometriosis subtypes. *Peer J*. (2020) 8:e8730. doi: 10.7717/peerj.8730

22. Ortiz CN, Torres-Reverón A, Appleyard CB. Metabolomics in endometriosis: challenges and perspectives for future studies. *Reprod Fertil*. (2021) 2:R35–r50. doi: 10.1530/RAF-20-0047

23. Calderón-Pérez L, Companys J, Solà R, Pedret A, Valls RM. The effects of fatty acid-based dietary interventions on circulating bioactive lipid levels as intermediate biomarkers of health, cardiovascular disease, and cardiovascular disease risk factors: a systematic review and meta-analysis of randomized clinical trials. *Nutr Rev*. (2023) 81:988–1033. doi: 10.1093/nutrit/nuac101

24. Zhang D, Wei Y, Huang Q, Chen Y, Zeng K, Yang W, et al. Important hormones regulating lipid metabolism. *Molecules*. (2022) 27:7052. doi: 10.3390/molecules27207052

25. Gallinelli A, Chiossi G, Giannella L, Marsella T, Genazzani AD, Volpe A. Different concentrations of interleukins in the peritoneal fluid of women with endometriosis: relationships with lymphocyte subsets. *Gynecol Endocrinol*. (2004) 18:144–51. doi: 10.1080/09513590310001653044

26. Ho HN, Wu MY, Chao KH, Chen CD, Chen SU, Yang YS. Peritoneal interleukin-10 increases with decrease in activated CD4+ T lymphocytes in women with endometriosis. *Hum Reprod*. (1997) 12:2528–33.

27. Jerzak M, Baranowski W, Rechberger T, Górski A. Enhanced T cells interactions with extracellular matrix proteins in infertile women with endometriosis. *Immunol Lett*. (2002) 81:65–70. doi: 10.1016/S0165-2478(01)00337-6

28. Izumi G, Koga K, Takamura M, Makabe T, Satake E, Takeuchi A, et al. Involvement of immune cells in the pathogenesis of endometriosis. *J Obstet Gynaecol Res*. (2018) 44:191–8. doi: 10.1111/jog.13559

29. Kisovar A, Becker CM, Granne I, Southcombe JH. The role of CD8+ T cells in endometriosis: a systematic review. *Front Immunol*. (2023) 14:1225639. doi: 10.3389/fimmu.2023.1225639

30. Zhou X, Zhu X, Zeng H. Fatty acid metabolism in adaptive immunity. *FEBS J*. (2023) 290:584–99. doi: 10.1111/febs.16296

31. Fritsche KL. The science of fatty acids and inflammation. *Adv Nutr*. (2015) 6:293S–301S. doi: 10.3945/an.114.006940

frontiers | Frontiers in Endocrinology

TYPE Mini Review
PUBLISHED 17 April 2025
DOI 10.3389/fendo.2025.1562653

OPEN ACCESS

EDITED BY
Prem Prakash Kushwaha,
Case Western Reserve University,
United States

REVIEWED BY
Ankit Kushwaha,
Stanford University, United States
Saurabh Mishra,
Cleveland Clinic, United States

*CORRESPONDENCE
Penghua Fang
hlcollegesci@sina.cn
Yi Zhang
fsyy02043@njucm.edu.cn

RECEIVED 17 January 2025
ACCEPTED 31 March 2025
PUBLISHED 17 April 2025

CITATION
Zong X, Wang Y, Chen Y, Fang P and Zhang Y (2025) Role of lactoferrin and its derived peptides in metabolic syndrome treatment. *Front. Endocrinol.* 16:1562653. doi: 10.3389/fendo.2025.1562653

Role of lactoferrin and its derived peptides in metabolic syndrome treatment

Xicui Zong[1], Yajing Wang[2], Yuqing Chen[3], Penghua Fang[4]* and Yi Zhang[3]*

[1]Laboratory Training Center, Nanjing University of Chinese Medicine Hanlin College, Taizhou, Jiangsu, China, [2]Department of Endocrinology, Clinical Medical College, Yangzhou University, Yangzhou, China, [3]School of Life Sciences, Nanjing Normal University, Nanjing, Jiangsu, China, [4]The First School of Clinical Medicine, Nanjing University of Chinese Medicine, Nanjing, Jiangsu, China

The prevalence of metabolic syndrome is increasing globally year by year, which has prompted researchers to actively seek and develop natural biotherapeutics to address this challenge. Lactoferrin (LF), as a multifunctional iron-binding natural transferrin, has garnered significant attention due to its potential role in regulating metabolism and the immune system. Recent studies show lactoferrin may influence lipid metabolism and glucose-insulin balance, and its levels are linked to body measurements. We systematically summarized the phenotypic and genotypic changes of LF in patients with metabolic syndrome, and the effect of exogenous LF on the treatment of metabolic syndrome. We also recapitulate LF can alleviate insulin resistance by inhibiting the NF-κB inflammatory pathway, activating the IRS/PI3K/Akt/Glut signaling pathway, and inhibiting the renin-angiotensin system to reduce the blood pressure, therefore improving the metabolic syndrome. This provides an important theoretical basis for the clinical application of LF in metabolic syndrome.

KEYWORDS

lactoferrin, bioactive peptide, metabolic syndrome, insulin resistance, hypotension

1 Introduction

Metabolic syndrome (MS) is a worldwide healthcare issue of increasing magnitude, with the number of cases projected to reach approximately 2.568 billion by 2040 (1). MS is defined by metabolic abnormalities, including insulin resistance, central obesity, hyperlipidemia, hyperglycemia, and hypertension, and is also critically involved in the pathogenesis of cardiovascular diseases, strokes, and tumors (2). MS is a condition marked by insulin resistance that can lead to type 2 diabetes mellitus (T2DM). It has been well-documented that insulin resistance results in elevated levels of inflammatory factor markers, such as C-reactive protein (CRP) and cytokine interleukin 6 (IL-6) (3, 4), and promotes adverse outcomes of atherothrombosis through an acceleration of the premature atherosclerosis process (5, 6). Although it is commonly believed that obesity induces the onset of insulin resistance, hepatic insulin resistance is an early step in peripheral insulin

resistance, so insulin resistance actually precedes the onset of obesity (7). The accumulation of visceral fat, a typical symptom of obesity, leads to the production of adipokines such as leptin (8), lipocalin (9), C1q tumor necrosis factor-related protein 9 (10), chemerin (11), and retinol-binding protein 4 (12), which are involved in a variety of metabolic processes such as glucose uptake, insulin signaling, and fatty acid oxidation, and are highly correlated with T2DM and cardiovascular and microvascular complications are highly relevant (13, 14).

In addition to active intervention and improvement of the patient's lifestyle, the clinical treatment of MS focuses on individual or combined drug therapy for specific pathologic features to achieve reduction of insulin resistance, restoration of normal blood glucose, improvement of lipid metabolism disorders, and lowering of blood pressure. However, most of these drugs may cause more side effects, such as rimonabant and sibutramine having psychiatric or cardiovascular risks, respectively, and the pancreatic lipase inhibitors orlistat and metformin can cause gastrointestinal adverse effects (15). Although Chinese medicines with fewer side effects represented by polyphenols, polysaccharides, saponins, and alkaloids can also reduce MS symptoms better, there are still fewer clinical studies, insufficient sample size, and difficulty in extracting and identifying bioactive components (16). In view of these many problems, it is urgent to seek and develop novel natural biological drugs to prevent and treat MS.

In recent years, it has been found that LF is closely related to the development of MS and has the potential to treat MS (17, 18). LF was first found in cow's milk, and human LF, consisting of 710 amino acids, has a molecular weight of about 80 kDa. It is structurally similar to serum transferrin and can bind to ferric ions, and therefore is categorized as a member of the transferrin family. In addition to being present in most milk secretions, LF is also distributed in mucosal secretions and granules of neutrophils. It is now often used as a food additive and pharmaceutical adjuvant, playing the roles of antioxidant, bacterial inhibition, enhancement of drug efficacy and reduction of drug resistance. LF has been found to have the potential to be used as an antioxidant, drug enhancer, and drug mitigator in MS (18). Studies have reported that it is also involved in the regulation of glucose and lipid uptake, improvement of insulin production and signaling, inhibition of adipogenesis, reduction of inflammation, and oxidative stress associated with metabolic syndrome, among other processes.

2 Lactoferrin effective in improving metabolic syndrome

Clinical studies have shown a practical correlation between fluctuations in endogenous LF levels and metabolic disorders, and LF may regulate glucose metabolism, insulin homeostasis and lipid metabolism. Lactoferrin levels were significantly reduced in patients with gestational diabetes, which was linked to hyperglycemic indicators and iron homeostasis disorders, and may serve as a biomarker for detecting different stages of gestational diabetes (19). The concentration of LF in the saliva of healthy individuals was about 40% higher than that of patients with decompensated T2DM, and the release of LF from neutrophils was correspondingly reduced in insulin-resistant subjects (20). Lactoferrin could also enhance insulin signaling and inhibit the activity of RB1 and AMPK, promoting fat production in human adipocytes (21). The expression level of the LF gene was significantly lower in obese patients and negatively correlates with the expression level of inflammatory markers, with fasting triglyceride (TG), body mass index (BMI), and fasting glucose, and with plasma high-density lipoprotein cholesterol (HDL-C) levels, and there was also a significant correlation with the risk of hypertension (22). In severely obese patients, LF concentrations were negatively correlated with postprandial lipemia, oxidative stress parameters (e.g., catalase and glutathione peroxidase), and CRP, suggesting that endogenous LF was elevated and subjects had an improved response to fat load (23).

LF and LF receptor gene variants are associated with the prevalence of disorders of glucolipid metabolism. In subjects with altered glucose tolerance, two LF gene polymorphisms (LF rs1126477 and rs1126478) were associated with HDL-C and TG levels (18). Whereas in metabolically healthy obese patients, there was a significant difference in low-density lipoprotein cholesterol (LDL-C) levels between LTF rs1126477 gene variants, and LDL-C levels were significantly different (18), serum LF concentrations were also negatively correlated with HDL-C levels (24). Polymorphisms in the LF receptor gene (LRP1 rs4759277) have also been associated with fasting insulin levels and homeostatic modeling assessment of insulin resistance in patients with metabolic syndrome (25).

Exogenous supplementation of LF could also improve energy metabolism (26, 27). Three months of oral administration of camel LF capsules to pediatric patients with T2DM resulted in a significant increase in insulin expression and a decrease in serum glucose, suggesting a potential hypoglycemic effect of camel LF (28). Subjects supplemented with LF showed a significant reduction in total and visceral fat accumulation, leading to a decrease in body weight and BMI (29) as well as a decrease in intestinal absorption of TG (30).

3 Mechanisms of lactoferrin alleviating the metabolic syndrome

3.1 Anti-inflammatory effects of lactoferrin improve insulin resistance

Inflammation is an important cause of the development of insulin resistance (31). LF may significantly affect insulin signaling and related functions by reducing inflammation (26). Animal experiments have shown that LF improves the behavioral manifestation of pain in rats with chronic compression injury models and inhibits inflammatory responses by down-regulating the levels of inflammatory cytokines IL-6 and tumor necrosis factor-α (TNF-α), thus exerting analgesic effects (Figure 1) (32). Down-regulation of TNF-α and IL-6 mRNA expression in the pancreas of diabetic mice modulates pancreatic inflammatory state

10.3389/fendo.2025.1562653

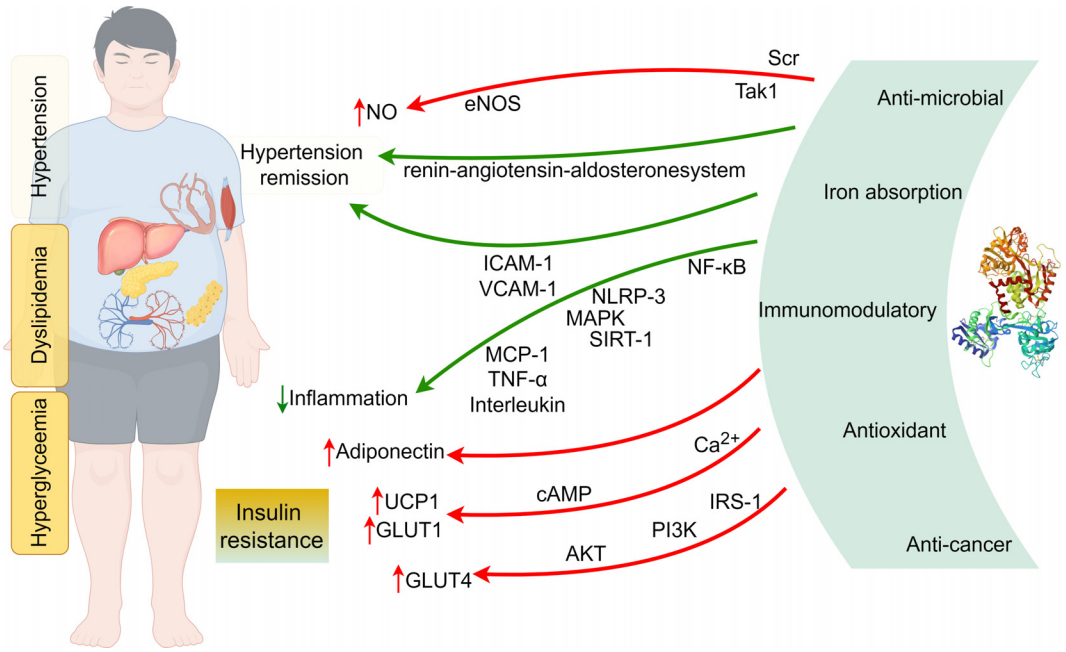

FIGURE 1
The mechanisms of lactoferrin alleviating the metabolic syndrome (By Figdraw).

to improve pancreatic dysfunction (30). Diabetic LF knockout mice are more susceptible to periodontal disease with increased secretion of pro-inflammatory cytokines compared to diabetic wild-type mice (33). LF inhibits the release of IL-1β in the liver (34), suppresses the expression of monocytes chemochemin-1 (MCP-1) in the liver and adipose tissue of epididymis in obese mice (35), decreases the levels of intercellular cell adhesion molecule-1 (ICAM-1) and vascular cell adhesion molecule-1 (VCAM-1) in mice fed a high-fat diet (22), and reduces the expression modulate the lipopolysaccharide (LPS)-mediated inflammatory cascade (36), mainly by inhibiting LPS-induced secretion of IL-6 by human monocyte cell lines (37), down-regulating LPS-stimulated secretion of IL-10 by macrophages (38), and inhibiting the expression of pro-inflammatory cytokines including TNF-α, IL-1, IL-6 and IL-8 (39), and upregulates lipocalin expression (18).

In T2DM mice, LF ameliorates pancreatic dysfunction by reducing inflammatory responses through regulating the PI3K/AKT signaling pathway. LF reduces serum glycated protein and fasting insulin concentrations and improves hepatic insulin sensitivity (30), and also reduces serum or hepatic levels of TNF-α, IL-6, and IL-1β, reversing abnormal inflammatory responses in diabetic mice (17). In addition, LF can maintain intestinal barrier integrity and alleviate LPS-induced inflammatory responses by attenuating the NF-κB/MAPK pathway (40), and regulate the expression of cytokines, such as TNF-α, IL-6, and IL-1, to exert the protective effect of the intestinal immune barrier (41), rebalance the disorders of glucose-lipid metabolism, and restore inflammatory parameters (42). The effect of lactoferricin bovine (LfcinB) in rats with enteritis led to a decrease in the mRNA expression of pro-inflammatory factors IL-6, IL-1β, and TNF-α in colonic tissues, which mainly inhibited the occurrence and development of inflammation through the NF-κB/NLRP3 signaling pathway and thus achieved the protection of the intestinal mucosal barrier function. MT10, the main product produced after gastric digestion, can prevent inflammatory damage of intestinal organoids by TNF-α and maintain stable growth of intestinal organoid cells (43).

The role of LF as an anti-inflammatory agent has also been validated in *in vitro* cellular-level experiments. In studies on the human hepatocellular carcinoma cell line HepG2 as well as the undifferentiated and pre-differentiated fibroblastic mouse cell line 3T3-L1 under non-inflammatory and inflammatory conditions, it was found that the hypoglycemic activity of LF may be related to the improvement of insulin resistance by regulating the expression of glycoprotein genes and thus exerting the anti-inflammatory mechanism of its activity (44, 45). LF down-regulated the expression of transforming growth factor-β-activated kinase 1 and IL-18, restored the level of AKT (Ser 473) phosphorylation in 3T3-L1 cells, and reduced the expression levels of IL-8, IL-6 and MCP-1 genes in subcutaneous and visceral adipocytes (22).

LF exerts insulin-sensitizing and anti-inflammatory effects by inhibiting the TLR-4/NF-kB/SIRT-1 signaling cascade and correspondingly decreases the expression of serum pro-inflammatory cytokines IL-1β, IL-6, lipocalin 2, and TNF-α, thereby reducing diabetes-related inflammation (28). It directly promotes glucose transport to small intestinal epithelial cells via sodium-dependent glucose transporter 1 through down-regulation of Ca^{2+} and cAMP signaling pathways (46) and leads to increased energy expenditure by promoting uncoupling protein 1 gene expression in brown adipocytes through the cAMP-PKA signaling pathway (47).

3.2 Lactoferrin activates IRS-1/PI3K/AKT to improve insulin resistance

Studies have shown that LF upregulates insulin receptor (IR), insulin receptor substrate-1 (IRS-1), glucose transporter 4 (GLUT4), PI3K and AKT in liver protein expression (30), increases peroxisome proliferator-activated receptor γ and regulatory protein SIRT-1 expression (28), and is negatively correlated with chronic inflammation-induced metabolic disorders of insulin resistance, hyperglycemia, and obesity, and positively correlated with insulin sensitivity (48). Huang (49) observed that the PI3K/AKT pathway was blocked in the T2DM state. Lactoferrin can activate the IRS-1/PI3K/AKT pathway by facilitating insulin binding to IR. AKT activation leads to phosphorylation of AS160, which contributes to the translocation of GLUT4 from intracellular vesicles to the cell membrane, thereby improving glucose uptake (30, 34). In addition, the protective effects of LF can be realized through its ability to bind glucose and its anti-inflammatory activity (50). During differentiation of HepG2 and 3T3-L1 cells, lactoferrin increases insulin-induced phosphorylation of AKT (Ser 473), leading to an increase in AMPK (pThr 172) and a decrease in adipogenesis (51). The LF effect of p-AKT has also been found in other diseases, with Alzheimer's disease patients having reduced levels of PI3K and p-AKT in peripheral blood lymphocyte solution, and significant improvements in all of these metrics with LF (52).

The bioactive peptides that were obtained through modification and alteration were also more successful in mitigating the effect of insulin resistance. The suggested peptide, which has the sequence RER-EtBn, has the ability to stimulate the phosphorylation of its major target, AKT serine, inhibit the phosphorylation of Gsk-3β, and then promote the translocation of the GLUT4 protein to the cell membrane's surface to promote glucose translocation, all of which have a positive impact on the state of insulin-resistant glucose metabolism (53).

It is evident that LF ameliorates hepatic insulin resistance and pancreatic dysfunction in T2DM mice by regulating the PI3K/AKT signaling pathway. In addition, it has been shown that whey protein can stimulate the translocation of GLUT4 to the plasma membrane of muscle tissue independently of insulin secretion (54), while LF itself can reverse the GLUT4 downregulation triggered by a high-fat diet (30). This may be another potential hypoglycemic mode of action of LF, and its specific mechanism needs to be further investigated.

3.3 Lactoferrin inhibits the renin-angiotensin system to regulate blood pressure

Hypertension, as a chronic disease, is the causative agent of a wide range of clinical disorders and often requires long-term medication. The regulatory effects of LF on blood pressure have also received attention, and its antihypertensive effects may be exerted by affecting nitric oxide (NO) synthesis and endothelium-dependent vasodilation. LF treatment significantly down-regulated the high-salt and high-fat-induced renal NLRP3 inflammatory vesicles and protein expression levels of inflammatory factors and regulated the expression levels of mRNAs related to the renin-angiotensin-aldosterone system pathway, which can prevent 8% NaCl diet-induced hypertension and renal injury in mice (55). LF reduces systolic blood pressure, serum adhesion molecules (ICAM-1 and VCAM-1) and aortic reactive oxygen species levels, and improves the endothelium-dependent diastolic function in mice fed a high-fat diet. In addition, LF down-regulated the Tak1/IL-18/eNOS pathway between perivascular adipose tissue and the aorta and promoted NO production in high-fat diet mice, which in turn ameliorated hypertension (22). Dexamethasone-induced systolic blood pressure elevation was lessened by LF administration (56), which also boosted NO generation in bovine aortic endothelial cells (57) and phosphorylated more eNOS in human aortic endothelial cells via a Scr/Akt/eNOS-dependent pathway (22).

Hypotensive peptides derived from lactoferrin have also been identified, and the angiotensin-converting enzyme-inhibiting tripeptide low-density lipoprotein receptor related protein (LRP) derived from bovine lactoferrin, has antihypertensive effects (58). RPYL, identified from the lactoferrin B-derived peptide LfcinB20-25 (RRWQWR), has antihypertensive activity comparable to valsartan (59). The antihypertensive effects of the heptapeptides found in lactoferrin pepsin LF hydrolysate and yeast protein hydrolysate (DPYKLRP) were observed in spontaneously hypertensive rats. The antihypertensive effects were comparable in magnitude and duration to those of the antihypertensive medication captopril (60). Long-term oral treatment of spontaneously hypertensive rats resulted in a considerable reduction in systolic blood pressure as well as a decrease in serum levels of aldosterone, angiotensin II, and the enzyme angiotensin converting enzyme; however, it had no antihypertensive impact on normotensive rats (61). In addition, data suggests that LfcinB20-25, LfcinB17-31, and LfcinB17-22 have a 10-fold *in vitro* antihypertensive effect. RPYL and LIWKL have similar inhibitory effects on angiotensin converting enzyme (ACE)-dependent vasoconstriction. LF hydrolysates, The antihypertensive effects of LfcinB20-25, RPYL and LIWKL may be due to ACE inhibition and induced reduction of vascular tone *in vivo*. The above ex vivo experiments showed that LF-derived peptides have higher ACE inhibitory capacity in ex vivo (62). It has been shown that LF-derived peptides' mechanisms of hypotensive action involve not only the inhibition of ACE but also interactions with the renin-angiotensin system, the endothelin system, and regulation of gene expression encoding proteins involved in the NO pathway and prostaglandin synthesis (61).

4 Conclusions

In summary, the mechanism of LF in human metabolism involves multiple processes, including regulation of glucose and lipid uptake, improvement of insulin production and signal transduction, inhibition of adipogenesis, elevation of HDL cholesterol and reduction of oxidized LDL cholesterol forms, and reduction of inflammation and oxidative stress associated with the metabolic syndrome. Therefore, LF may be an effective therapeutic target for metabolic disorders and is significant for the study of the occurrence and development of various diseases. Simultaneously,

LF is a nutritional additive that has received approval from regulatory agencies, with no significant potential side effects identified. Its safety has been corroborated through studies for the treatment of other conditions, including iron-deficiency anemia (63–65). However, LF is in reality degraded in the gastrointestinal tract, so its biological effects may derive mainly from its digestion products rather than from the intact LF molecule. It has been shown that exogenous LF is hydrolyzed by proteases and mainly exists in the form of peptides, which have small molecular masses, are well digested and absorbed, and even exhibit higher biological activities (66). Therefore, further investigation is needed to find out whether LF autocrine is consistent with the effect of exogenously added LF.

Author contributions

XZ: Data curation, Investigation, Methodology, Writing – original draft, Writing – review & editing. YW: Investigation, Writing – review & editing. YC: Conceptualization, Supervision, Writing – review & editing. PF: Conceptualization, Supervision, Writing – review & editing. YZ: Conceptualization, Writing – review & editing.

Funding

The author(s) declare that financial support was received for the research and/or publication of this article. This study was supported by the National Natural Science Foundation of China (grant numbers 81573337) and the Jiangsu Province natural science Foundation project (BK20171319) and Taizhou Science and technology support plan (social development) project(SSF20230019).

Conflict of interest

The authors declare that the research was conducted in the absence of any commercial or financial relationships that could be construed as a potential conflict of interest.

Generative AI statement

The author(s) declare that no Generative AI was used in the creation of this manuscript.

Publisher's note

References

1. Saklayen MG. The global epidemic of the metabolic syndrome. *Curr Hypertens Rep*. (2018) 20:12.

2. Xue JQ, Ni GH, Liu YP, Wan ZW, Sun P. Screening value and relevance of body measurements for metabolic syndrome in the 2018-2020 Chengdu physical examination population. *Health Res*. (2024) 53:21–9.

3. Liu Y-q, Lian M-z, Zhao S-j. Correlation between lipid ratio, β cell function index, hypersensitive C-reactive protein and insulin resistance in type 2 diabetes mellitus. *China J Modern Med*. (2023) 33:67–75.

4. Jiang YZ. *Study on the correlation between visceral fat content andInterleukin-6, insulin resistance and chronic complicationsof diabetes in type 2 diabetic patients*. Nanchang, China: Nanchang Univ. (2022).

5. Zhao Y. Research progress of overweight/obesity and atherogenesis. *Public Health Prev Med*. (2024) 35:129–32.

6. Sun JP, Xu CY, Gou L, Ji ZS, Jin AM, Pan YS. Correlation between insulin resistance and craniocervical vasculopathy. *Chin J Clin Health Care*. (2022) 25:614–8.

7. Qin W, Weng J. Hepatocyte NLRP3 interacts with PKCε to drive hepatic insulin resistance and steatosis. *Sci Bulletin*. (2023) 68:1413–29. doi: 10.1016/j.scib.2023.06.003

8. Rahmani A, Toloueitabar Y, Mohsenzadeh Y, Hemmati R, Sayehmiri K, Asadollahi K. Association between plasma leptin/adiponectin ratios with the extent and severity of coronary artery disease. *BMC Cardiovasc Disord*. (2020) 20:474. doi: 10.1186/s12872-020-01723-7

9. Li S, Zhu QS. Study on the effect of exogenous lipocalin on non-alcoholic fatty liver disease in rats. *J Xinjiang Med University*. (2017) 40:1322–1325 + 1329.

10. Ahmed SF, Shabayek MI, Ghany MEA, El-Hefnawy MH, El-Mesallamy HO. Role of CTRP3, CTRP9 and MCP-1 for the evaluation of T2DM associated coronary artery disease in Egyptian postmenopausal females. *PloS One*. (2018) 13:e0208038. doi: 10.1371/journal.pone.0208038

11. Ebert T, Gebhardt C, Scholz M, Wohland T, Schleinitz D, Fasshauer M, et al. Relationship between 12 adipocytokines and distinct components of the metabolic syndrome. *J Clin Endocrinol Metab*. (2018) 103:1015–23. doi: 10.1210/jc.2017-02085

12. Hu LP, Cai H, Li QJ, Tang L. Study on the pathogenesis of metabolism-related fatty liver disease. *Med Information*. (2023) 36:174–9.

13. Jaganathan R, Ravindran R, Dhanasekaran S. Emerging role of adipocytokines in type 2 diabetes as mediators of insulin resistance and cardiovascular disease. *Can J Diabetes*. (2018) 42:446–456.e1. doi: 10.1016/j.jcjd.2017.10.040

14. Nishimura M, Morioka T, Hayashi M, Kakutani Y, Yamazaki Y, Kurajoh M, et al. Plasma omentin levels are inversely associated with atherosclerosis in type 2 diabetes patients with increased plasma adiponectin levels: a cross-sectional study. *Cardiovasc Diabetology*. (2019) 18:167.

15. Yuxin H, Cuiping J, Wen T, Jieyuzhen Q, Xiaoming T, Qin G, et al. Comparison of gastrointestinal adverse events with different doses of metformin in the treatment of elderly people with type 2 diabetes. *J Clin Pharm Ther*. (2020) 45:470–6.

16. Mao ZY, Lin ZY, Duan ZW, Hong ZQ, Ji YH, Shen HX, et al. Research progress on the intervention of metabolic syndrome by medicinal food and traditional Chinese medicine. *Chin J Traditional Chin Med*. (2023) 38:4271–7.

17. Guo C, Xue H, Guo T, Zhang W, Xuan WQ, Ren YT, et al. Recombinant human lactoferrin attenuates the progression of hepatosteatosis and hepatocellular death by regulating iron and lipid homeostasis in ob/ob mice. *Food Funct*. (2020) 11:7183–96.

18. Jamka M, Kaczmarek N, Mądry E, Krzyżanowska-Jankowska P, Bajerska J, Kręgielska-Narożna M, et al. Metabolic health in obese subjects—Is there a link to lactoferrin and lactoferrin receptor-related gene polymorphisms? *Nutrients*. (2020) 12:2843.

19. Mohandas S, Milan KL, Anuradha M, Ramkumar KM. Exploring Lactoferrin as a novel marker for disease pathology and ferroptosis regulation in gestational diabetes. *J Reprod Immunol*. (2024) 161:104182.

20. Chorzewski M, Orywal K, Sierpinska T, Golebiewska M. Salivary protective factors in patients suffering from decompensated type 2 diabetes. *Adv Med Sci*. (2017) 62:211–5.

21. Moreno-Navarrete JM, Ortega F, Sabater M, Ricart W, Fernández-Real JM. Proadipogenic effects of lactoferrin in human subcutaneous and visceral preadipocytes. *J Nutr Biochem*. (2011) 22:1143–9.

22. Chen C, Yan Y, Wu Y, Lu M, Xing Y, Bai Y, et al. Lactoferrin ameliorated obesity-induced endothelial dysfunction by inhibiting the Tak1/IL-18/eNOS pathway between PVAT and vascular endothelium. *Free Radical Biol Med*. (2024) 212:309–21.

23. Jańczuk A, Brodziak A, Czernecki T, Król J. Lactoferrin—The health-promoting properties and contemporary application with genetic aspects. *Foods*. (2023) 12:70.

24. Jamka M, Krzyżanowska-Jankowska P, Mądry E, Lisowska A, Bogdański P, Walkowiak J. No difference in lactoferrin levels between metabolically healthy and unhealthy obese women. *Nutrients*. (2019) 11:1976.

25. Delgado-Lista J, Perez-Martinez P, Solivera J, Garcia-Rios A, Perez-Caballero AI, Lovegrove JA, et al. Top single nucleotide polymorphisms affecting carbohydrate metabolism in metabolic syndrome: from the LIPGENE study. *J Clin Endocrinol Metab*. (2014) 99:E384–9.

26. Artym J, Zimecki M, Kruzel ML. Lactoferrin for prevention and treatment of anemia and inflammation in pregnant women: A comprehensive review. *Biomedicines*. (2021) 9:898.

27. Artym J. A remedy against obesity? The role of lactoferrin in the metabolism of glucose and lipids. *Postepy Hig Med Dosw (Online)*. (2012) 66:937–53.

28. Mohamed WA, Schaalan MF. Antidiabetic efficacy of lactoferrin in type 2 diabetic pediatrics; controlling impact on PPAR-γ, SIRT-1, and TLR4 downstream signaling pathway. *Diabetol Metab Syndrome*. (2018) 10:89.

29. Ono T, Murakoshi M, Suzuki N, Iida N, Ohdera M, Iigo M, et al. Potent anti-obesity effect of enteric-coated lactoferrin: decrease in visceral fat accumulation in Japanese men and women with abdominal obesity after 8-week administration of enteric-coated lactoferrin tablets. *Br J Nutr*. (2010) 104:1688–95.

30. Du Y, Li D, Chen J, Li YH, Zhang Z, Hidayat K, et al. Lactoferrin improves hepatic insulin resistance and pancreatic dysfunction in high-fat diet and streptozotocin-induced diabetic mice. *Nutr Res*. (2022) 103:47–58.

31. Li H, Meng Y, He S, Tan X, Zhang Y, Zhang X, et al. Macrophages, chronic inflammation, and insulin resistance. *Cells*. (2022) 11:3001.

32. Li X, Li JS, Liu XJ, Zhang P. Effect of lactoferrin on pain threshold and inflammatory cytokines in rats with neuropathic pain. *J Clin Pharmacol*. (2020) 36:1549–1551 + 1558.

33. Alabdulmohsen W, Rozario SD, Markowitz K, Fine DH, Velliyagounder K. Diabetic lactoferrin deficient mice demonstrates greater susceptibility to experimental periodontal disease. *J Oral Biol (Northborough)*. (2015) 2:6.

34. Du YF. *Effects of lactoferrin on obesity and diabetes mellitus in mice induced by high-fat diet and study of the mechanism*. Suzhou, China: Soochow Univ. (2024).

35. Xiong L, Ren F, Lv J, Zhang H, Guo H. Lactoferrin attenuates high-fat diet-induced hepatic steatosis and lipid metabolic dysfunctions by suppressing hepatic lipogenesis and down-regulating inflammation in C57BL/6J mice. *Food Funct*. (2018) 9:4328–39.

36. Amiri M. Lactoferrin suppresses LPS-induced expression of HMGB1, microRNA 155, 146, and TLR4/MyD88/NF-κB pathway in RAW264.7 cells. *Immunopharmacol Immunotoxicol*. (2021) 43:153–9.

37. El Amrousy D, El-Afify D, Elsawy A, Elsheikh M, Donia A, Nassar M. Lactoferrin for iron-deficiency anemia in children with inflammatory bowel disease: a clinical trial. *Pediatr Res*. (2022) 92:762–6. doi: 10.1038/s41390-022-02136-2

38. Widjaja NA, Hamidah A, Purnomo MT, Ardianah E. Effect of lactoferrin in oral nutrition supplement (ONS) towards IL-6 and IL-10 in failure to thrive children with infection. *F1000Res*. (2023) 12:897. doi: 10.12688/f1000research

39. Wright SW, Lovelace-Macon L, Ducken D, Tandhavanant S, Teparrukkul P, Hantrakun V, et al. Lactoferrin is a dynamic protein in human melioidosis and is a TLR4-dependent driver of TNF-α release in Burkholderia Thailandensis infection in *vitro*. *PloS Negl Trop Dis*. (2020) 14:e0008495. doi: 10.1371/journal.pntd.0008495

40. Hu P, Zhao F, Wang J, Zhu W. Lactoferrin attenuates lipopolysaccharide-stimulated inflammatory responses and barrier impairment through the modulation of NF-κB/MAPK/Nrf2 pathways in IPEC-J2 cells. *Food Funct*. (2020) 11:8516–26. doi: 10.1039/D0FO01570A

41. Gao S, Zhou WJ, Meng QF, Chi HY, Li AL, Shao H. Research progress on the effect of milk protein on intestinal flora. *China Dairy Industry*. (2023) 51:45–49 + 64.

42. Li L, Ma C, Hurilebagen , Yuan H, Hu R, Wang W, et al. Effects of lactoferrin on intestinal flora of metabolic disorder mice. *BMC Microbiol*. (2022) 22:181. doi: 10.1186/s12866-022-02588-w

43. Peng LY. *Research on the protective effect of bovine milk ferritin peptide on intestinal mucosal barrier and its mechanism*. Hangzhou, China: Zhejiang Gongshang Univ. (2020).

44. Maekawa Y, Sugiyama A, Takeuchi T. Lactoferrin ameliorates corticosterone-related acute stress and hyperglycemia in rats. *J Vet Med Sci*. (2017) 79:412–7. doi: 10.1292/jvms.16-0498

45. Maekawa Y, Sugiyama A, Takeuchi T. Lactoferrin potentially facilitates glucose regulation and enhances the incretin effect. *Biochem Cell Biol*. (2017) 95:155–61. doi: 10.1139/bcb-2016-0082

46. Talukder JR, Griffin A, Jaima A, Boyd B, Wright J. Lactoferrin ameliorates prostaglandin E2-mediated inhibition of Na+-glucose cotransport in enterocytes. *Can J Physiol Pharmacol*. (2014) 92:9–20. doi: 10.1139/cjpp-2013-0211

47. Nakamura K, Kishida T, Ejima A, Tateyama R, Morishita S, Ono T, et al. Bovine lactoferrin promotes energy expenditure via the cAMP-PKA signaling pathway in human reprogrammed brown adipocytes. *Biometals*. (2018) 31:415–24.

48. Min QQ, Qin LQ, Sun ZZ, Zuo WT, Zhao L, Xu JY. Effects of metformin combined with lactoferrin on lipid accumulation and metabolism in mice fed with high-fat diet. *Nutrients*. (2018) 10:1628.

49. Huang X, Liu G, Guo J, Su Z. The PI3K/AKT pathway in obesity and type 2 diabetes. *Int J Biol Sci*. (2018) 14:1483–96.

50. Ianiro G, Niro A, Rosa L, Valenti P, Musci G, Cutone A. To boost or to reset: the role of lactoferrin in energy metabolism. *Int J Mol Sci*. (2023) 24:15925.

51. Moreno-Navarrete JM, Ortega FJ, Ricart W, Fernandez-Real JM. Lactoferrin increases 172ThrAMPK phosphorylation and insulin-induced p473SerAKT while impairing adipocyte differentiation. *Int J Obes*. (2009) 33:991–1000.

52. Mohamed WA, Salama RM, Schaalan MF. A pilot study on the effect of lactoferrin on Alzheimer's disease pathological sequelae: Impact of the p-Akt/PTEN pathway. *Biomedicine Pharmacotherapy*. (2019) 111:714–23.

53. Zhang BN. *Preliminary study on the effect of LFcinB peptide derivatives to improve insulin resistance and related mechanisms*. Chongqing, China: Chongqing University of Technology (2018).

54. Morato PN, Lollo PCB, Moura CS, Batista TM, Camargo RL, Carneiro EM, et al. Whey protein hydrolysate increases translocation of GLUT-4 to the plasma membrane independent of insulin in wistar rats. *PloS One*. (2013) 8:e71134.

55. Lu ML. Protective effect of lactoferrin on renal injury induced by high-fat and high-salt diet. *M.S. thesis*. Suzhou, China: Soochow Univ. (2024).

56. Safaeian L, Zabolian H. Antioxidant effects of bovine lactoferrin on dexamethasone-induced hypertension in rat. *ISRN Pharmacol*. (2014) 2014:943523.

57. Nii T, Islam MZ, Kake S, Shiraishi M, Takeuchi T, Kuwata H, et al. Direct evidence of nitric oxide production induced by lactoferrin and its enhancement by magnesium ions in cultured endothelial cells. *J Veterinary Med Science*. (2022) 84:1499–501.

58. Gu Y, Wu J. Bovine lactoferrin-derived ACE inhibitory tripeptide LRP also shows antioxidative and anti-inflammatory activities in endothelial cells. *J Funct Foods*. (2016) 25:375–84.

59. Fernández-Musoles R, Castelló-Ruiz M, Arce C, Manzanares P, Ivorra MD, Salom JB. Antihypertensive mechanism of lactoferrin-derived peptides: angiotensin receptor blocking effect. *J Agric Food Chem*. (2014) 62:173–81.

60. García-Tejedor A, Sánchez-Rivera L, Castelló-Ruiz M, Recio I, Salom JB, Manzanares P. Novel antihypertensive lactoferrin-derived peptides produced by kluyveromyces marxianus: gastrointestinal stability profile and *in vivo* angiotensin I-converting enzyme (ACE) inhibition. *J Agric Food Chem*. (2014) 62:1609–16.

61. García-Tejedor A, Manzanares P, Castelló-Ruiz M, Moscardó A, Marcos JF, Salom JB. Vasoactive properties of antihypertensive lactoferrin-derived peptides in resistance vessels: Effects in small mesenteric arteries from SHR rats. *Life Sci*. (2017) 186:118–24.

62. Manzanares P, Salom JB, García-Tejedor A, Fernández-Musoles R, Ruiz-Giménez P, Gimeno-Alcañiz JV. Unraveling the mechanisms of action of lactoferrin-derived antihypertensive peptides: ACE inhibition and beyond. *Food Funct*. (2015) 6:2440–52.

63. Paesano R, Berlutti F, Pietropaoli M, Goolsbee W, Pacifici E, Valenti P. Lactoferrin efficacy versus ferrous sulfate in curing iron disorders in pregnant and non-pregnant women. *Int J Immunopathol Pharmacol*. (2010) 23:577–87.

64. Mahmoud RMA, Mohammed A. Lactoferrin: A promising new player in treatment of iron deficiency anemia in patients on regular hemodialysis: a randomized controlled trial. *Saudi J Kidney Dis Transplantation*. (2023) 34:235.

65. Koikawa N, Nagaoka I, Yamaguchi M, Hamano H, Yamauchi K, Sawaki K. Preventive effect of lactoferrin intake on anemia in female long distance runners. *Bioscience Biotechnology Biochem*. (2008) 72:931–5.

66. Shi PJ, Xu SQ, Wang ZY, Wu C, Lu WH, Du M. Advances in biological activity and functional mechanism of peptides from lactoferrin. *Food Sci*. (2021) 42:267–74.

frontiers | Frontiers in Endocrinology

TYPE Original Research
PUBLISHED 08 May 2025
DOI 10.3389/fendo.2025.1423040

OPEN ACCESS

EDITED BY
Prem Prakash Kushwaha,
Case Western Reserve University,
United States

REVIEWED BY
Istvan Szokodi,
University of Pécs, Hungary
Robert Kiss,
McGill University, Canada

*CORRESPONDENCE
Jianjun Lan
pzhzxyyxnkljj@sina.com
Shiyang Li
lishiyangzyy@163.com

RECEIVED 25 April 2024
ACCEPTED 14 April 2025
PUBLISHED 08 May 2025

CITATION
Zeng X, Zhang Y, Xie X, Lan J and Li S (2025) Triglyceride-glucose index predicts ventricular aneurysm formation in acute ST-segment elevation myocardial infarction. *Front. Endocrinol.* 16:1423040. doi: 10.3389/fendo.2025.1423040

Triglyceride-glucose index predicts ventricular aneurysm formation in acute ST-segment elevation myocardial infarction

Xiaobin Zeng[1], Yanyu Zhang[2], Xiaoshuang Xie[1], Jianjun Lan[1]* and Shiyang Li[3,4]*

[1]Division of Cardiology, Panzhihua Central Hospital, Panzhihua, China, [2]Clinical Laboratory, Panzhihua Central Hospital, Panzhihua, China, [3]Department of Geriatrics, Panzhihua Central Hospital, Panzhihua, China, [4]Department of Geriatrics, Panzhihua Central Hospital Affiliated to Dali University, Dali, China

Background: The triglyceride–glucose (TyG) index has been confirmed to be a predictor of cardiovascular diseases. The present study aimed to assess the predictive value of TyG index for left ventricular aneurysm (LVA) formation and prognosis in patients with acute ST-segment elevation myocardial infarction (STEMI) who underwent primary percutaneous coronary intervention (PCI).

Methods: This prospective study included 991 patients with acute STEMI who underwent primary PCI. Multivariable logistic regression and receiver operating characteristic (ROC) curve analysis were used to assess the predictive value of TyG index for LVA formation. Prognosis analysis was performed with cox proportional hazard regression.

Results: The prevalence of LVA was 14.4%. A higher TyG index was associated with a greater incidence of LVA (23.1% vs. 11.8%, P< 0.001). The TyG index was also higher in the LVA group than in the non-LVA group (9.4 ± 0.9 vs. 9.0 ± 0.8, P<0.001). Multivariable logistic regression analysis revealed that the TyG index was independently associated with the risk of LVA [odds ratio (OR)= 2.4, 95% confidence interval (CI)= 1.51-3.82, P< 0.001]. The predictive value of the TyG index remained significant even after cross-validation by dividing the study population into a training set (OR= 2.32, 95% CI= 1.24-4.35, P= 0.009) and validation set (OR= 3.19, 95% CI= 1.42-7.19, P= 0.005). Higher TyG index was correlated with increased risk of cardiac death (HR= 2.17, P= 0.04). The maximal length and width of LVA were significantly increased in patients with TyG index ≥ 9.68 compared with < 9.68 (P< 0.001). The discriminant power of TyG index for LVA was 0.742, which was superior to both triglyceride (C statistic= 0.666) and fasting blood glucose (C statistic= 0.613). The combination of TyG index, left ventricular ejection fraction, gensini score, and left anterior descending artery as the culprit vessel could significantly improve the predictive ability (C statistic= 0.908).

Conclusions: A higher TyG index was an independent predictor for LVA formation and increased risk of cardiac death in patients with STEMI who underwent primary PCI.

KEYWORDS

triglyceride-glucose index, acute ST-segment elevation myocardial infarction, primary percutaneous coronary intervention, left ventricular aneurysm, predictive

Introduction

ST-segment elevation myocardial infarction (STEMI) is the most dramatic manifestation of acute myocardial infarction (AMI) associated with increased short- and long-term cardiac death (1). Left ventricular aneurysm (LVA) is a common and severe complication of AMI, characterized by the outward expansion of the infarcted myocardium during both systole and diastole (2). Patients with AMI and LVA have a six-fold higher cardiac death rate compared to those without LVA, primarily due to the higher incidence of arrhythmias, thromboembolic phenomena, congestive heart failure, and cardiac rupture (3, 4). Given the high incidence rate (10%-38% of patients with AMI) (5) and poor prognosis associated with LVA, it is crucial to identify risk factors that contribute to its formation for effective prophylactic treatment.

The triglyceride-glucose (TyG) index, which is calculated using fasting triglyceride and blood glucose level data, has been identified as a reliable biomarker for evaluating insulin resistance (IR) (6). Additionally, numerous studies have indicated an association between TyG index and cardiovascular diseases. In a prospective cohort study involving 823 patients, a high TyG index was found to be correlated with an increased risk for cardiac death and rehospitalization in patients with heart failure with preserved ejection fraction (7). Furthermore, Chen. et al. reported that the TyG index was associated with recurrent revascularization in patients with type 2 diabetes mellitus after percutaneous coronary intervention (8). Moreover, the TyG index has been demonstrated to be an effective prognostic factor and for risk stratification in patients with acute coronary syndrome (ACS) (9–13). More importantly, the molecular mechanisms of TyG index as a marker for predicting cardiovascular diseases have also been studied, and included metabolic fexibility, endothelial dysfunction, coagulation disorders, and smooth muscle cell dysfunction (9). However, no study has investigated the association between TyG index and the risk of LVA formation. As such, the purpose of the present study was to assess the predictive value of the TyG index for the risk of LVA formation in patients with acute STEMI in a sample of the Chinese population.

Methods

Study design and participants

This study was approved by the Review Board of Panzhihua central hospital (Sichuan, Panzhihua, China) and adhered to the principles of the Declaration of Helsinki. Written informed consents were obtained from all participants. A total of 1201 consecutive patients with acute STEMI, who underwent primary PCI at the Cardiology Division of Panzhihua Central Hospital between March 2018 and June 2023, were recruited. Acute STEMI was diagnosed based on the fourth universal definition of myocardial infarction (14), which includes the following criteria: typical chest pain lasting > 30 minutes, with new ST-segment elevation at the J point in at least two contiguous leads of > 2 mm (0.2 mV) in males or > 1.5 mm (0.15 mV) in females on admission electrocardiogram, and an increase in cardiac enzyme levels > 99th percentile cut-off point for cardiac troponin I (cTnI). The exclusion criteria consisted of non-ischemic cardiomyopathy (including hypertrophic and dilated cardiomyopathy), congenital heart disease, renal or liver failure, active infection, malignant tumors or a life expectancy < 1 year, thrombolytic therapy before admission, or loss to follow-up. Ultimately, a total of 991 patients were included in the association analysis.

PCI procedure and definitions

Before primary PCI, all patients were administered aspirin (300 mg loading dose followed by 100 mg daily), clopidogrel (of 600 mg loading dose followed by 75 mg daily), or ticagrelor (180 mg loading dose followed by 90 mg twice daily). In addition, a bolus of unfractionated heparin (UFH) was administered intravenously at a dose of 70 U/kg of body weight. The primary PCI procedure was performed using either the standard radial or femoral approach, in accordance with current guidelines. A stent was deployed in the culprit artery of all patients. During the PCI procedure, the operator had the discretion to decide whether to use balloon pre-dilatation or post-dilatation, type of stents (bare metal or drug-eluting), and the application of thrombus aspiration. The glycoprotein IIb/IIIa receptor inhibitor tirofiban was initiated during the PCI procedure, at the operator's discretion, with a 10 μg/kg intracoronary bolus followed by a 0.15 μg/kg/min intravenous infusion. A technically successful stent implantation was defined as residual postprocedural stenosis < 10% in the culprit lesion. Two independent experts assessed and confirmed the results of coronary angiograms, as well as the extent and degree of stenosis in each major coronary artery vessel. On discharge, medical therapy was prescribed based on individual patient condition and guideline recommendations for secondary prevention.

Clinical follow-up and data collection

In this study, we conducted follow-up every 3 months through outpatient interview or by telephone contact. The primary endpoint

was defined as development of LVA. The secondary endpoint was defined as cardiac deaths. Trained physicians blinded to the study's purpose were charged with collecting information regarding patient demographics and clinical characteristics, including age, sex, hypertension, diabetes, smoking status, and medication used at discharge from the electronic medical recording system. Venous blood samples for laboratory investigations were collected from all patients on admission to the emergency room before primary PCI, as well as 8–12 h after PCI. To determine the peak value of cardiac enzyme levels, blood samples for troponin I (TnI) and lactate dehydrogenase (LDH) were obtained from a peripheral vein, after admission to the intensive coronary care unit, every 12 h during the first 48 h and every 24 h during the remainder of the stay in the intensive coronary care unit. Fasting blood-glucose (FBG) and lipid levels were measured after PCI. The TyG index was calculated using the following equation (9): In (fasting triglyceride [mg/dl] × FBG [mg/dl])/2.

Definitions

The diagnosis of left ventricular aneurysm (LVA) was performed in accordance with the protocol outlined in the Coronary Artery Surgery Study (CASS) (15). The criteria for diagnosing LVA included the following: (I) bulging of the left ventricular wall during both diastole and systole, exhibiting either akinesia or dyskinesia; (II) clear demarcation of the infarcted segment; and (III) absence of trabeculation in the affected segment. After admission, two-dimensional transthoracic echocardiography (TTE) was performed within 3 days, and at 1 and 6 months during the follow-up period. LVA was diagnosed using TTE at the 6-month follow-up. Additionally, hypertension was defined as treatment for hypertension before admission or a blood pressure > 140/90 mmHg. Diabetes mellitus was defined as a fasting plasma glucose level > 7.0 mmol/L, a postprandial blood glucose level > 11.1 mmol/L, a hemoglobin A1c level > 6.5%, or treatment for diabetes mellitus. Smoking history was defined as having smoked > 2 pack-years and/or having smoked within the past year.

The Gensini score was calculated using the method developed by Celebi et al. (16). In summary, a severity score was assigned to each coronary stenosis based on the degree of narrowing (in %), as follows: ≤ 25% (1 point); 26% to 50% (2 points); 51% to 75% (4 points); 76% to 90% (8 points); 91% to 99% (16 points); and total occlusion (32 points). Additionally, each coronary stenosis score was multiplied by a factor that considered the importance of the lesion's position in the coronary circulation: 5 for the left main coronary artery; 2.5 for the proximal segment of the left anterior descending coronary artery (LAD); 2.5 for the proximal segment of the circumflex artery; 1.5 for the mid-segment of the LAD; 1.0 for the right coronary artery, the distal segment of LAD, the posterolateral artery, or the obtuse marginal artery; and 0.5 for the other segments. The sum of the scores for each coronary segment yielded the Gensini score.

Statistical analysis

Statistical analyses were performed using SPSS 26 (IBM Corporation Armonk, NY, USA). Descriptive statistics were expressed as number (percent) for categorical variables and as median and interquartile range (IQR) or mean and standard deviation (SD) for continuous variables. The best cut-off value of TyG index to stratify patients into two groups was determined to be 8.98 according to the receiver operating characteristic (ROC) curve analysis. Differences among groups were assessed using appropriate statistical tests, including the chi-squared, independent-sample *t*, or Mann–Whitney U tests. Univariate logistic regression analysis was used to examine the association between different variables and the risk for LVA formation. Variables with $P< 0.05$ in the univariate analysis were included in the multivariate logistic regression analysis. Cox proportional hazard regression models were performed to calculate the hazard ratio (HR) and 95% confidence intervals (95% CIs) for the associations between the TyG index and the prognosis of patients. All comparisons were two-sided, and differences with $P< 0.05$ were considered to be statistically significant.

Results

Patient characteristics

A flow-diagram depicting the overall workflow of the study is presented in Figure 1. Baseline characteristics of the cohort (n = 991) are summarized in Table 1. The mean (± SD) age of the study cohort (78.4% male) was 61.1 ± 12.8 years. Throughout the follow-up period for TTE, a total of 143 LVA incidents (14.4%) were observed.

Subsequently, baseline demographics and clinical characteristics of the patients in groups with and without LVA formation were compared. As shown in Table 1, patients in the LVA group were older, more likely to be female, and exhibited higher levels of diastolic blood pressure (DBP), heart rate, creatinine (Cr), total cholesterol (TC), low-density lipoprotein cholesterol (LDL-C), LDH, Peak cTnI, fasting blood glucose (FBG), TyG index, gensini score, and a higher proportion of thiazide or loop diuretic use, and LAD as the culprit vessel ($P< 0.05$) compared with those in the non-LVA group. Conversely, the proportion of patients who smoked and used β-blockers, the level of left ventricular ejection fraction (LVEF), hemoglobin, and triglycerides (TG) were lower in patients with LVA formation compared to those without LVA ($P< 0.05$).

According to the maximum Youden Index criterion and ROC curve analysis, the optimal cut-off value for the TyG index to stratify patients into two groups was determined to be < 8.98 and ≥ 8.98. As shown in Table 2, patients in the TyG≥ 8.98 group were younger, more likely to be female, and had higher systolic pressure (SBP), DBP, red blood cell count, hemoglobin, HbA1c, TC, TG, LDL-C, and FBG, as well as a higher prevalence of diabetes and LVA formation. In contrast, patients with TyG≥ 8.98 had lower levels of AST, high-density lipoprotein cholesterol (HDL-C), and Peak cTnI compared to those with TyG< 8.98.

10.3389/fendo.2025.1423040

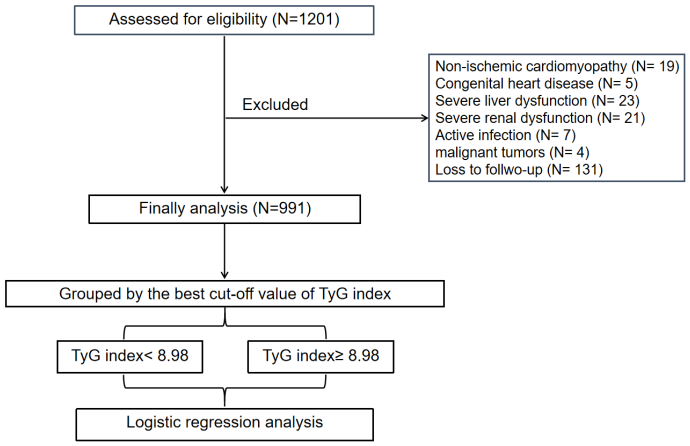

FIGURE 1
The overall workflow of methodology in the present study. TyG, triglyceride-glucose.

TABLE 1 Baseline characteristics and laboratory findings of study population according to the presence of center ventricular aneurysmus.

Demographics	Total population (N= 991)	Non-LVA patients (N= 848)	LVA patients (N= 143)	P-value
Age, years	61.1 ± 12.8	60.2 ± 12.7	66.5 ± 11.9	<0.001
Male, n (%)	777 (78.4)	678 (80.0)	99 (69.2)	0.004
Hypertension, n (%)	553 (55.8)	464 (54.7)	89 (62.2)	0.094
Diabetes, n (%)	299 (30.2)	249 (29.4)	50 (35.0)	0.177
Smoking, n (%)	521 (52.6)	460 (54.2)	61 (42.7)	0.01
LVEF, %	56 (50–60)	57 (53–60)	43 (37–50)	<0.001
SBP, mmHg	129.3 ± 20.8	129.3 ± 21.0	128.9 ± 19.7	0.81
DBP, mmHg	80.8 ± 14.3	80.2 ± 14.6	83.9 ± 11.7	0.001
Heart rate, beats/min	83.3 ± 16.0	82.3 ± 15.6	89.1 ± 16.9	<0.001
Laboratory tests				
White blood cell count, 109/L	9.8 (7.7-12.0)	9.8 (7.7-11.9)	9.7 (7.5-12.4)	0.71
Red blood cell count, 109/L	4.5 ± 0.6	4.5 ± 0.6	4.4 ± 0.7	0.14
Neutrophil count, 109/L	7.6 (5.7-9.6)	7.4 (5.7-9.5)	7.9 (5.9-10.2)	0.262
Platelet count, 109/L	223.6 ± 68.5	224.7 ± 70.2	217.1 ± 57.1	0.22
Hemoglobin, g/L	138.2 ± 20.3	139.0 ± 20.1	133.8 ± 21.1	0.005
ALT, U/L	27.2 (17.6-48.4)	27.1 (17.8-48.2)	28.1 (17.2-51)	0.865
AST, U/L	55.7 (24.7-160)	55.6 (24.8-152)	62.7 (24.6-226.8)	0.202
HbA1c, %	6 (5.6-6.9)	6 (5.6-6.8)	6.1 (5.7-7.1)	0.083
Cr, umol/L	72.2 (62.1-87.2)	71.6 (62-87.1)	78.3 (66.5-90.3)	0.007
TC, mmol/L	4.7 ± 1.2	4.7 ± 1.2	4.9 ± 1.2	0.04
TG, mmol/L	1.4 (1.0-2.1)	1.5 (1.0-2.2)	1.3 (0.8-1.7)	<0.001
HDL-C, mmol/L	1.0 ± 0.3	1.0 ± 0.3	1.0 ± 0.3	0.63
LDL-C, mmol/L	3.1 ± 1.1	3.1 ± 1.1	3.4 ± 1.3	0.006
LDH, U/L	311 (202-556)	283 (199-533)	472 (235-712)	<0.001

(Continued)

10.3389/fendo.2025.1423040

TABLE 1 Continued

Demographics	Total population (N= 991)	Non-LVA patients (N= 848)	LVA patients (N= 143)	P-value
Laboratory tests				
Peak cTnI, ng/mL	19.3 (3.5-50)	15.1 (3.5-47.7)	26.8 (4.9-50)	<0.001
FBG, mg/dl	7.1 (5.9-9.6)	7.0 (5.8-9.3)	7.7 (6.4-12.1)	<0.001
TyG index	9.1 ± 0.8	9.1 ± 0.8	9.4 ± 0.8	<0.001
Medication at hospital discharge				
Aspirin	1583 (100.0)	1360 (100.0)	223 (100.0)	>0.999
Clopidogrel/Ticagrelor	1583 (100.0)	1360 (100.0)	223 (100.0)	>0.999
Statin, n (%)	984 (99.3)	844 (99.5)	140 (97.9)	0.108
β-blockers, n (%)	715 (72.1)	622 (73.3)	93 (65.0)	0.04
ACE inhibitors or ARB, n (%)	516 (52.1)	446 (52.6)	70 (49.0)	0.42
Aldosterone receptor blockers, n (%)	331 (33.4)	275 (32.4)	56 (39.2)	0.114
Thiazide or loop diuretic, n (%)	370 (37.3)	306 (36.1)	64 (44.8)	0.047
Coronary artery disease				
Gensini Score	71 (46-92)	66 (44-90)	88 (67-104)	<0.001
Culprit vessel-LAD, n (%)	492 (49.6)	380 (44.8)	112 (78.3)	<0.001

LVEF, center ventricular ejection fraction; SBP, Systolic pressure; DBP, Diastolic pressure; ALT, Alanine aminotransferase; AST, Aspartate aminotransferase; HbA1c, glycated hemoglobin; Cr, Creatinine; TC, total cholesterol; TG, triglyceride; HDL-C, high-density lipoprotein cholesterol; LDL-C, low-density lipoprotein cholesterol; LDH, Lactate dehydrogenase; FBG, fasting blood glucose; TyG, triglyceride-glucose; ACE, Angiotensin converting enzyme; ARB, angiotensin receptor blocker; LAD, center anterior descending artery.

TyG index and the incidence of LVA in patients who underwent primary PCI

As depicted in Figure 2A, the incidence of LVA formation increased with the rise in TyG index (9.4% vs. 18.4%, P< 0.001). Additionally, the LVA group exhibited a significantly higher TyG index than the non-LVA group (9.4 ± 0.8 vs. 9.1 ± 0.8, P < 0.001) (Figure 2B).

Furthermore, subgroup analysis was performed to assess the association between the TyG index and the incidence of LVA. The prevalence of LVA increased with the rise in TyG index in both males (8.7% vs 16.4%, P= 0.027) and females (12.3% vs 24.8%, P= 0.002), age < 65 years (7.3% vs 15.9%, P= 0.002) and ≥ 65 years (11.9% vs 22.3%, P= 0.005), non-hypertension (6.8% vs 17.2%, P= 0.001) and hypertension (11.7% vs 19.3%, P= 0.017), non-diabetes (9.1% vs 15.4%, P= 0.011), non-smoking (12.6% vs 19.6%, P= 0.04) and smoking (6.3% vs 17.3%, P< 0.001), LVEF < 50% (30.5% vs 47.4%, P= 0.011) and LVEF ≥ 50% (3.5% vs 9.2%, P= 0.002) (Figures 3A–F). Simultaneously, the TyG index between the non-LVA and LVA groups in these subgroups was also compared. The results revealed that the TyG index was significantly higher in the LVA group compared to the non-LVA group in all subgroups except for female, patients with non-smoking and LVEF < 50% (Figures 4A–F).

Predictors of LVA formation

Logistic regression analysis was used to evaluate the predictive value of variables for the risk for LVA formation in patients with acute STEMI patients who underwent PCI. Twenty variables were found to be associated with LVA formation in univariate logistic regression analysis (Table 3). These variables included age, sex, smoking, LVEF, DBP, heart rate, hemoglobin, AST, HbA1c, TC, TG, LDL-C, LDH, Peak cTnI, FBG, β-blockers use, thiazide or loop diuretic use, gensini score, LAD as the culprit vessel, and TyG index. Subsequently, these 20 variables were included in a multivariate logistic regression analysis, which revealed that only age (OR= 1.04, 95% CI= 1.02-1.07, P= 0.002), LVEF (OR= 0.82, 95% CI= 0.79-0.85, P< 0.001), LDL-C (OR= 2.31, 95% CI= 1.24-4.31, P= 0.008), gensini score (OR= 1.01, 95% CI= 1.01-1.02, P= 0.038), LAD as the culprit vessel (OR= 4.41, 95% CI= 2.42-8.04, P< 0.001), and TyG index (OR= 2.46, 95% CI= 1.64-3.68, P< 0.001) remained significantly associated with the risk for LVA formation.

Additionally, the study population was randomly divided into a training set (495 patients) and a validation set (496 patients). Multivariate logistic regression analysis demonstrated that the TyG index was significantly and independently associated with the risk for LVA formation in both the training (OR= 2.33, 95% CI= 1.35-4.02, P= 0.002) and validation (OR= 2.68, 95% CI= 1.46-4.92, P= 0.002) set (Tables 4, 5).

Prognostic analysis

During the follow-up period, a total of 41 cardiac death occurred. The number of cardiac death in the non-LVA group, the LVA group, the TyG< 8.98 group, and TyG≥ 8.98 group were 25 (2.9%), 16 (11.2%), 11 (2.5%), and 30 (5.4%), respectively. Cox

10.3389/fendo.2025.1423040

TABLE 2 Comparison of the baseline characteristics and laboratory findings grouped by TyG index.

Demographics	TyG< 8.98 (N= 436)	TyG≥ 8.98 (N= 555)	P-value
Age, years	63.0 ± 11.7	59.6 ± 13.5	<0.001
Male, n (%)	355 (81.4)	422 (76.0)	0.041
Hypertension, n (%)	231 (53.0)	322 (58.0)	0.113
Diabetes, n (%)	62 (14.2)	237 (42.7)	<0.001
Smoking, n (%)	221 (50.7)	300 (54.1)	0.292
LVEF, %	56 (50-60)	56 (50-60)	0.669
SBP, mmHg	126.6 ± 18.5	131.4 ± 22.3	<0.001
DBP, mmHg	78.7 ± 12.9	82.4 ± 15.0	<0.001
Heart rate, beats/min	82.4 ± 17.0	84.0 ± 15.0	0.138
Laboratory tests			
White blood cell count, 109/L	9.6 (7.6-12.0)	9.9 (7.8-12.0)	0.397
Red blood cell count, 109/L	4.4 ± 0.6	4.6 ± 0.7	<0.001
Neutrophil count, 109/L	7.7 (5.5-10.0)	7.4 (5.8-9.2)	0.267
Platelet count, 109/L	219.1 ± 69.6	227.1 ± 67.5	0.068
Hemoglobin, g/L	135.4 ± 18.5	140.4 ± 21.5	<0.001
ALT, U/L	27.2 (15.8-46)	27.3 (18.8-49.9)	0.14
AST, U/L	68.5 (25.9-183.9)	50.4 (24.1-136.5)	<0.001
HbA1c, %	5.8 (5.5-6.2)	6.3 (5.8-7.9)	<0.001
Cr, umol/L	72 (61.8-88.8)	72.4 (62.2-86.4)	0.973
TC, mmol/L	4.3 ± 1.1	5.1 ± 1.3	<0.001
TG, mmol/L	0.9 (0.7-1.2)	2.0 (1.5-2.9)	<0.001
HDL-C, mmol/L	1.1 ± 0.3	1.0 ± 0.3	<0.001
LDL-C, mmol/L	2.9 ± 1.0	3.3 ± 1.2	<0.001
LDH, U/L	331 (207-592)	284 (197-532)	0.116
Peak cTnI, ng/mL	23.5 (4.9-50)	12.7 (2.5-50)	0.005
FBG, mmol/L	6.2 (5.5-7.3)	8.2 (6.7-11.6)	<0.001
TyG index	8.4 ± 0.5	9.6 ± 0.6	<0.001
LVA, %	41 (9.4)	102 (18.4)	<0.001
Medication at hospital discharge			
Aspirin	1262 (100.0)	321 (100.0)	>0.999
Clopidogrel/Ticagrelor	1262 (100.0)	321 (100.0)	>0.999
Statin, n (%)	434 (99.5)	550 (99.1)	0.658
β-blockers, n (%)	311 (71.3)	404 (72.8)	0.61
ACE inhibitors or ARB, n (%)	237 (54.4)	279 (50.3)	0.201
Medication at hospital discharge			
Aldosterone receptor blockers, n (%)	137 (31.4)	194 (35.0)	0.242
Thiazide or loop diuretic, n (%)	156 (35.8)	214 (38.6)	0.369
Coronary artery disease			
Gensini Score	69 (46-93)	71 (47-92)	0.859
Culprit vessel-LAD, n (%)	216 (49.5)	276 (49.7)	0.953

LVEF, center ventricular ejection fraction; SBP, Systolic pressure; DBP, Diastolic pressure; ALT, Alanine aminotransferase; AST, Aspartate aminotransferase; HbA1c, glycated hemoglobin; Cr, Creatinine; TC, total cholesterol; TG, triglyceride; HDL-C, high-density lipoprotein cholesterol; LDL-C, low-density lipoprotein cholesterol; LDH, Lactate dehydrogenase; FBG, fasting blood glucose; TyG, triglyceride-glucose; LVA, center ventricular aneurysm; ACE, Angiotensin converting enzyme; ARB, angiotensin receptor blocker; LAD, center anterior descending artery.

proportional hazard regression analysis indicated that patients with LVA had an increased cardiac death risk compared to those without LVA (HR= 3.94, 95% CI= 2.11-7.39; P < 0.001) (Table 6, Figure 5A). Furthermore, patients with TyG≥ 8.98 was associated with worse prognosis compared to those with TyG< 8.98 (HR= 2.17, 95% CI= 1.09-4.33; P= 0.04) (Table 6, Figure 5B). These statistical significances remained even after adjustments for sex, age, hypertension, diabetes, smoking state, and β-blocker use (Table 6).

Association between TyG index and clinical parameters of LVA

The study aimed to investigate the relationship between the TyG index and the size of LVA by comparing the maximal length and width of LVA in patients with TyG< 8.98 and TyG≥ 8.98. Both maximal length and width were significantly greater in patients with TyG ≥ 8.98 compared to those with TyG < 8.98 (maximal length, 3.04 ± 0.96 vs. 3.55 ± 1.15; maximal width, 1.89 ± 0.70 vs. 2.34 ± 0.86) (Figures 6A, B).

ROC curve analysis

ROC curve analysis was used to assess and compare the predictive abilities of TG, FBG, TyG index, and the composite variable (TyG index combined with LVEF and LAD as the culprit vessel). As shown in Figure 7A and Table 7, the average area under the ROC curve (AUC) for TG, FBG, TyG index, and the composite variable were 0.666 (95% CI = 0.641 - 0.690), 0.613 (95% CI = 0.587 - 0.638), 0.742 (95% CI= 0.719 - 0.764), and 0.908 (95% CI = 0.892 - 0.922), respectively. Furthermore, the TyG index demonstrated significantly higher AUCs for predicting the risk for LVA

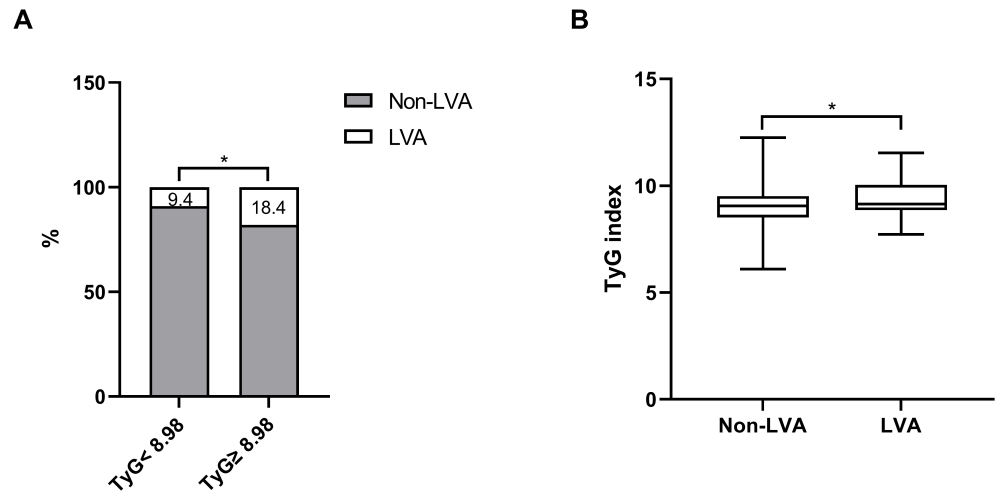

FIGURE 2
The association between the TyG index and the prevalence of LVA **(A)** and comparison of the TyG index level between the LVA and non-LVA groups **(B)**. TyG, triglyceride-glucose; LVA, left ventricular aneurysm; * P<0.05.

formation compared with TG (P < 0.001) and FBG (P < 0.001). Additionally, the composite variable exhibited the highest predictive value (P < 0.001). To avoid overfitting, cross-validation was conducted by randomly dividing the population into the training and the validation sets. As shown in Figure 6B, C and Table 6, the TyG index displayed superior discriminative power compared with both TG and FBG in both the training and validation sets (training set: P= 0.041 for TyG index vs. TG; P < 0.001 for TyG index vs. FBG; validation set: P= 0.002 for TyG index vs. TG; P < 0.001 for TyG index vs. FBG). Clearly, the composite variable demonstrated the highest predictive value in both the training and validation sets.

Additionally, we evaluated the predictive capabilities of LDH, LDL-C, and the TyG index concerning the risk of LVA formation. As illustrated in Supplementary Table 1, the TyG index exhibited superior predictive performance compared to both LDH (P < 0.001) and LDL-C (P < 0.001) in assessing the risk of LVA formation. Furthermore, the TyG index could improve the discriminatory capability of the composite of LVEF and LAD as a culprit vessel for identifying the development of LVA (Supplementary Table 2) (P< 0.001).

Subgroup analyses

Additional analyses were performed on several subgroups to evaluate the independent predictive value of the TyG index for LVA formation. The independent predictive effect of the TyG index on LVA formation was primarily represented in the subgroups of age< 65 and ≥65 years, male and female, with and without hypertension, without diabetes, with and without smoking, LVEF< 50% and LVEF≥ 50%, HbA1c≥ 6%, hemoglobin< 120g/L and ≥ 120g/L, LDL-C< 3.37mmol/L, TG <1.7mmol/L and ≥1.7 mmol/L, FBG <6.1 mmol/L and ≥6.1 mmol/L (Figure 8). The association between the TyG index and LVA formation showed no statistically significance in subgroup analysis of patients with diabetes, HbA1c< 6%, and LDL-C≥3.37mmol/L.

Discussion

In the present study, we investigated the predictive value of TyG index for LVA formation and prognosis in patients with STEMI. The results indicated that a higher TyG index independently predicted LVA formation. The predictive value remained significant in both the training and validation sets. Besides, higher TyG index was correlated with increased cardiac death risk. Among patients with LVA, those with a TyG index≥ 8.98 exhibited significantly larger maximal length and width compared to those with a TyG index < 8.98. The relationship between the TyG index and LVA formation was generally consistent across subgroups, except for patients with diabetes, HbA1c< 6%, and LDL≥3.37mmol/L. Additionally, the TyG index exhibited greater predictive power for LVA formation than both TG and FBG. However, the composite variable exhibited the best predictive value.

As a hallmark of type 2 diabetes mellitus, insulin resistance (IR) refers to a state of reduced sensitivity and responsiveness to the action of insulin (17). Multiply studies have demonstrated that IR was associated with the progression of cardiovascular diseases and could predict cardiovascular outcomes (18–21). The euglycemic insulin clamp and intravenous glucose tolerance testing are the gold standards for IR (22). However, they are not suitable for clinical practice due to invasiveness and high cost. Currently, the homeostasis model assessment-estimated insulin resistance (HOMA-IR) index is widely used for assessing β-cell function and IR. Nevertheless, its complexity and time-consuming nature limit its application in practical clinical settings and large-scale studies (23).

The TyG index has emerged as a reliable marker of IR and has been shown to be superior to HOMA-IR in assessing metabolic

10.3389/fendo.2025.1423040

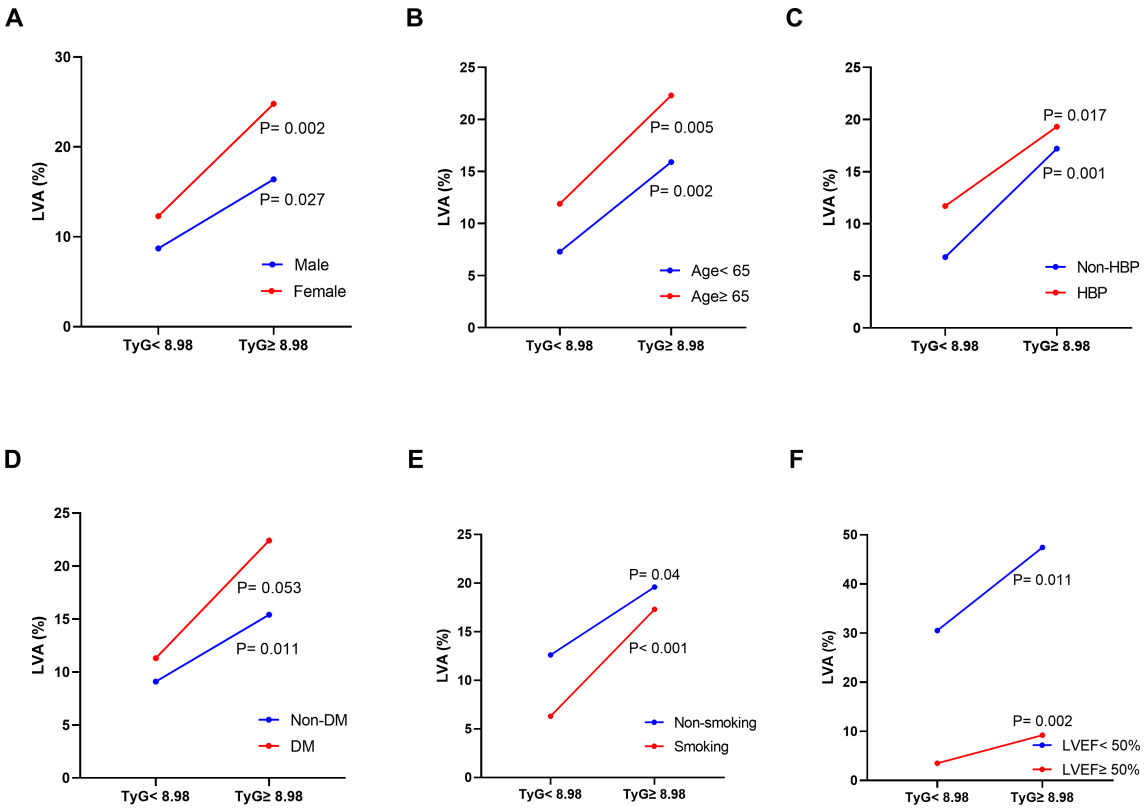

FIGURE 3
The impact of the TyG index on the prevalence of LVA across subgroups of gender **(A)**, age **(B)**, HBP status **(C)**, DM status **(D)**, current smoking status **(E)**, and LVEF **(F)**. TyG, triglyceride-glucose; LVA, left ventricular aneurysm; HBP, hypertension; DM, diabetes mellitus; LVEF, left ventricular ejection fraction.

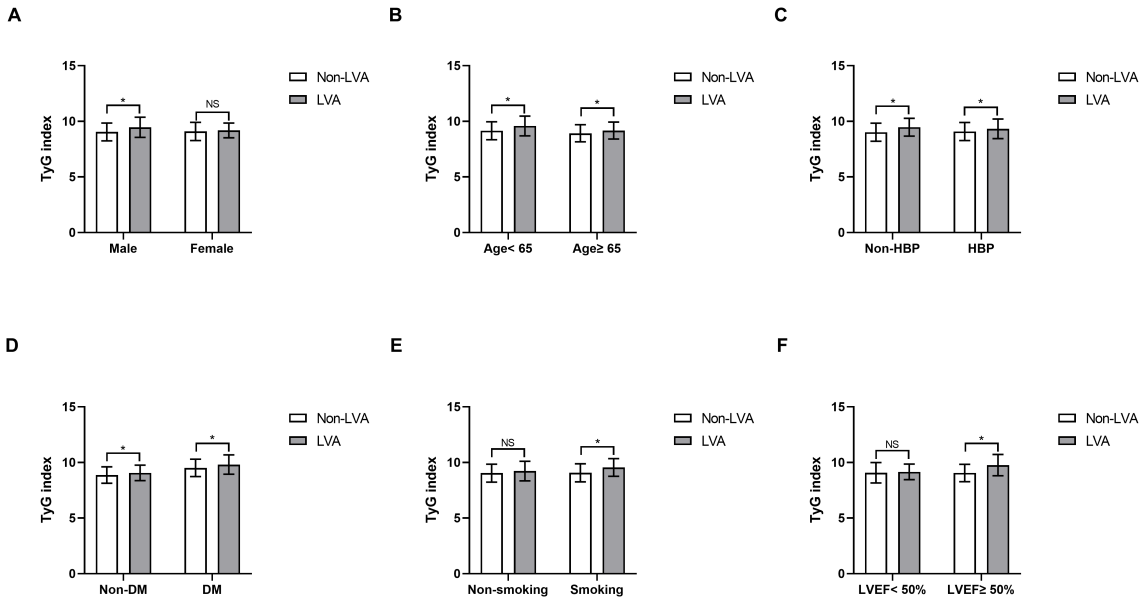

FIGURE 4
Comparison of the TyG index between non-LVA and LVA groups in the subgroups of gender **(A)**, age **(B)**, HBP status **(C)**, DM status **(D)**, current smoking status **(E)**, and LVEF **(F)**. TyG, triglyceride-glucose; LVA, left ventricular aneurysm; HBP, hypertension; DM, diabetes mellitus; LVEF, left ventricular ejection fraction.

10.3389/fendo.2025.1423040

TABLE 3 Effects of variables on center ventricular aneurysm formation after ST-segment elevation myocardial infarction.

Demographics	Univariate logistic regression analysis			Multivariate logistic regression analysis		
	OR	95% CI	P-value	OR	95% CI	P-value
Age, years	1.04	1.03-1.06	<0.001	1.04	1.02-1.07	0.002
Male, n (%)	1.77	1.20-2.63	0.004			
Hypertension, n (%)	1.36	0.95-1.96	0.095			
Diabetes, n (%)	1.29	0.89-1.88	0.178			
Smoking, n (%)	0.63	0.44-0.90	0.011			
LVEF, %	0.82	0.80-0.85	<0.001	0.82	0.79-0.85	<0.001
SBP, mmHg	1.00	0.99-1.01	0.806			
DBP, mmHg	1.02	1.01-1.03	0.005			
Heart rate, beats/min	1.03	1.02-1.04	<0.001			
White blood cell count, 10^9/L	1.03	0.98-1.08	0.256			
Red blood cell count, 10^9/L	0.82	0.62-1.07	0.143			
Neutrophil count, 10^9/L	1.04	0.99-1.10	0.116			
Platelet count, 10^9/L	1.00	1.00-1.00	0.222			
Hemoglobin, g/L	0.99	0.98-1.00	0.005			
ALT, U/L	1.00	1.00-1.01	0.721			
AST, U/L	1.00	1.00-1.00	0.028			
HbA1c, %	1.17	1.07-1.29	<0.001			
Cr, umol/L	1.00	0.99-1.00	0.227			
TC, mmol/L	1.15	1.00-1.31	0.044			
TG, mmol/L	0.73	0.61-0.88	<0.001			
HDL-C, mmol/L	1.17	0.61-2.24	0.632			
LDL-C, mmol/L	1.21	1.06-1.39	0.006	2.31	1.24-4.31	0.008
LDH, U/L	1.00	1.00-1.00	<0.001			
Peak cTnI, ng/mL	1.02	1.01-1.02	<0.001			
FBG, mmol/L	1.06	1.02-1.10	0.002			
TyG index	2.17	1.47-3.19	<0.001	2.46	1.64-3.68	<0.001
Statin, n (%)	0.22	0.05-1.00	0.05			
β-blockers, n (%)	0.68	0.46-0.98	0.041			
ACE inhibitors or ARB, n (%)	0.86	0.61-1.23	0.42			
Aldosterone receptor blockers, n (%)	1.34	0.93-1.93	0.115			
Thiazide or loop diuretic, n (%)	1.44	1.00-2.05	0.048			
Gensini Score	1.01	1.01-1.02	<0.001	1.01	1.01-1.02	0.038
Culprit vessel-LAD, n (%)	4.45	2.92-6.77	<0.001	4.41	2.42-8.04	<0.001

LVEF, center ventricular ejection fraction; SBP, Systolic pressure; DBP, Diastolic pressure; ALT, Alanine aminotransferase; AST, Aspartate aminotransferase; HbA1c, glycated hemoglobin; Cr, Creatinine; TC, total cholesterol; TG, triglyceride; HDL-C, high-density lipoprotein cholesterol; LDL-C, low-density lipoprotein cholesterol; LDH, Lactate dehydrogenase; FBG, fasting blood glucose; TyG, triglyceride-glucose; ACE, Angiotensin converting enzyme; ARB, angiotensin receptor blocker; LAD, center anterior descending artery.

syndrome (24, 25). TyG is a simple, convenient and low-cost clinical index that can easily be obtained for large-scale study. Numerous studies have demonstrated the association between TyG index and the cardiovascular diseases (8, 11, 26, 27). In a prospective study including 1574 patients with acute coronary syndrome (ACS), Zhu et al. found that an elevated TyG index was independently and positively associated with in-stent restenosis after drug-eluting stent (28). A study by Wang et al. investigated 2531 consecutive patients

10.3389/fendo.2025.1423040

TABLE 4 Effects of variables on center ventricular aneurysm formation after ST-segment elevation myocardial infarction in the training set.

Demographics	Univariate logistic regression analysis			Multivariate logistic regression analysis		
	OR	95% CI	P-value	OR	95% CI	P-value
Age, years	1.05	1.03-1.07	<0.001	1.05	1.02-1.09	0.003
Male, n (%)	1.46	0.83-2.57	0.185			
Hypertension, n (%)	1.88	1.13-3.13	0.016			
Diabetes, n (%)	1.30	0.79-2.14	0.3			
Smoking, n (%)	0.64	0.40-1.04	0.074			
LVEF, %	0.82	0.79-0.86	<0.001	0.84	0.80-0.88	<0.001
SBP, mmHg	1.01	1.00-1.02	0.198			
DBP, mmHg	1.02	1.01-1.04	0.006	1.03	1.00-1.06	0.026
Heart rate, beats/min	1.02	1.01-1.04	0.001			
White blood cell count, 109/L	1.03	0.97-1.10	0.369			
Red blood cell count, 109/L	0.82	0.58-1.17	0.282			
Neutrophil count, 109/L	1.05	0.98-1.12	0.161			
Platelet count, 109/L	1.00	1.00-1.00	0.965			
Hemoglobin, g/L	0.99	0.98-1.00	0.014			
ALT, U/L	1.00	0.99-1.00	0.251			
AST, U/L	1.00	1.00-1.00	0.348			
HbA1c, %	1.14	1.01-1.29	0.03			
Cr, umol/L	1.00	1.00-1.01	0.31			
TC, mmol/L	1.13	0.93-1.36	0.22			
TG, mmol/L	0.60	0.44-0.80	0.001			
HDL-C, mmol/L	1.35	0.56-3.23	0.503			
LDL-C, mmol/L	1.26	1.04-1.53	0.021			
LDH, U/L	1.00	1.00-1.00	0.06			
Peak cTnI, ng/mL	1.02	1.01-1.03	0.001			
FBG, mmol/L	1.02	0.96-1.09	0.446			
TyG index	2.03	1.21-3.40	0.007	2.33	1.35-4.02	0.002
Statin, n (%)	0.58	0.06-5.60	0.634			
β-blockers, n (%)	0.66	0.40-1.09	0.104			
ACE inhibitors or ARB, n (%)	0.81	0.50-1.31	0.388			
Aldosterone receptor blockers, n (%)	1.28	0.77-2.11	0.342			
Thiazide or loop diuretic, n (%)	1.58	0.98-2.56	0.062			
Gensini Score	1.01	1.01-1.02	<0.001			
Culprit vessel-LAD, n (%)	3.84	2.23-6.60	<0.001	3.41	1.58-7.39	0.002

LVEF, center ventricular ejection fraction; SBP, Systolic pressure; DBP, Diastolic pressure; ALT, Alanine aminotransferase; AST, Aspartate aminotransferase; HbA1c, glycated hemoglobin; Cr, Creatinine; TC, total cholesterol; TG, triglyceride; HDL-C, high-density lipoprotein cholesterol; LDL-C, low-density lipoprotein cholesterol; LDH, Lactate dehydrogenase; FBG, fasting blood glucose; TyG, triglyceride-glucose; ACE, Angiotensin converting enzyme; ARB, angiotensin receptor blocker; LAD, center anterior descending artery.

with diabetes who underwent coronary angiography for ACS and demonstrated TyG index to be an independent predictor for the major adverse cardiovascular events (10). Furthermore, a higher TyG index was found associated with the presence of a higher coronary anatomical complexity in ACS patients (29). However, no study has investigated the association among the TyG index, LVA formation, and the prognosis of patients with STEMI. In the present study, we demonstrated for the first time that TyG index≥ 8.98 was significantly

10.3389/fendo.2025.1423040

TABLE 5 Effects of variables on center ventricular aneurysm formation after ST-segment elevation myocardial infarction in the validation set.

Demographics	Univariate logistic regression analysis			Multivariate logistic regression analysis		
	OR	95% CI	P-value	OR	95% CI	P-value
Age, years	1.03	1.01-1.06	0.006			
Male, n (%)	2.25	1.29-3.93	0.004			
Hypertension, n (%)	0.94	0.56-1.60	0.83			
Diabetes, n (%)	1.24	0.70-2.20	0.458			
Smoking, n (%)	0.60	0.35-1.03	0.065			
LVEF, %	0.82	0.78-0.86	<0.001	0.81	0.76-0.86	<0.001
SBP, mmHg	0.99	0.98-1.00	0.091			
DBP, mmHg	1.01	0.99-1.03	0.248			
Heart rate, beats/min	1.03	1.01-1.05	0.001			
White blood cell count, 10^9/L	1.03	0.95-1.11	0.494			
Red blood cell count, 10^9/L	0.78	0.51-1.19	0.255			
Neutrophil count, 10^9/L	1.03	0.95-1.12	0.453			
Platelet count, 10^9/L	1.00	0.99-1.00	0.066			
Hemoglobin, g/L	0.99	0.98-1.00	0.123			
ALT, U/L	1.00	1.00-1.01	0.116			
AST, U/L	1.00	1.00-1.00	0.027			
HbA1c, %	1.21	1.04-1.41	0.012			
Cr, umol/L	1.00	1.00-1.01	0.56			
TC, mmol/L	1.18	0.98-1.42	0.078			
TG, mmol/L	0.87	0.70-1.09	0.216			
HDL-C, mmol/L	1.00	0.38-2.65	0.996			
LDL-C, mmol/L	1.19	0.97-1.45	0.093			
LDH, U/L	1.00	1.00-1.00	0.001			
Peak cTnI, ng/mL	1.02	1.00-1.03	0.007			
FBG, mmol/L	1.10	1.04-1.15	<0.001			
TyG index	2.37	1.32-4.26	0.004	2.68	1.46-4.92	0.002
Statin, n (%)	0.07	0.01-0.79	0.031			
β-blockers, n (%)	0.71	0.40-1.24	0.228			
ACE inhibitors or ARB, n (%)	0.94	0.55-1.59	0.809			
Aldosterone receptor blockers, n (%)	1.46	0.85-2.50	0.168			
Thiazide or loop diuretic, n (%)	1.26	0.74-2.16	0.400			
Gensini Score	1.01	1.01-1.02	0.001			
Culprit vessel-LAD, n (%)	5.61	2.85-11.05	<0.001	8.3	3.07-22.46	<0.001

LVEF, center ventricular ejection fraction; SBP, Systolic pressure; DBP, Diastolic pressure; ALT, Alanine aminotransferase; AST, Aspartate aminotransferase; HbA1c, glycated hemoglobin; Cr, Creatinine; TC, total cholesterol; TG, triglyceride; HDL-C, high-density lipoprotein cholesterol; LDL-C, low-density lipoprotein cholesterol; LDH, Lactate dehydrogenase; FBG, fasting blood glucose; TyG, triglyceride-glucose; ACE, Angiotensin converting enzyme; ARB, angiotensin receptor blocker; LAD, center anterior descending artery.

associated with increased LVA formation and cardiac death risk compared to TyG index < 8.98. Importantly, the risk for LVA formation in patients with TyG index≥ 8.98 exceeded 2-fold compared to those with TyG index< 8.98.

As a common and severe complication of AMI, LVA is characterized by the outward expansion of the infarcted myocardium during systole and diastole (30). Recently, the incidence of LVA after acute STEMI has decreased from 10-30%

10.3389/fendo.2025.1423040

TABLE 6 Prognosis analysis using cox proportional hazard regression model.

Model	Non-LVA vs. LVA		TyG< 8.98 vs. TyG≥ 8.98	
	HR (95% CI)	P-value	HR (95% CI)	P-value
Unadjusted	3.94 (2.11-7.39)	<0.001	2.17 (1.09-4.33)	0.04
Adjusted	3.16 (1.67-5.98)	<0.001	2.39 (1.09-5.23)	0.03

Hazard Ratio (HR) and 95% confidence intervals (95% CI) were obtained by cox proportional hazard regression, without and with adjustment for sex, age, hypertension,diabetes, smoking status and β-blocker use. LVA, center ventricular aneurysm.

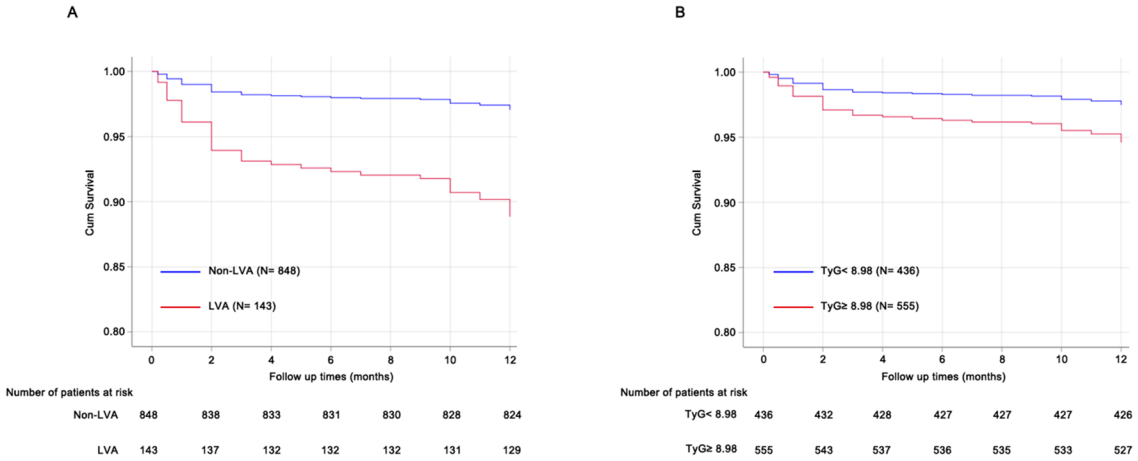

FIGURE 5
Prognosis analysis using Cox proportional hazard regression models. **(A)** patients with LVA was associated with poorer prognosis compared to those without LVA. **(B)**, patients with TyG≥ 8.98 showed increased cardiac death risk compared to those with TyG< 8.98. TyG, triglyceride-glucose; LVA, left ventricular aneurysm.

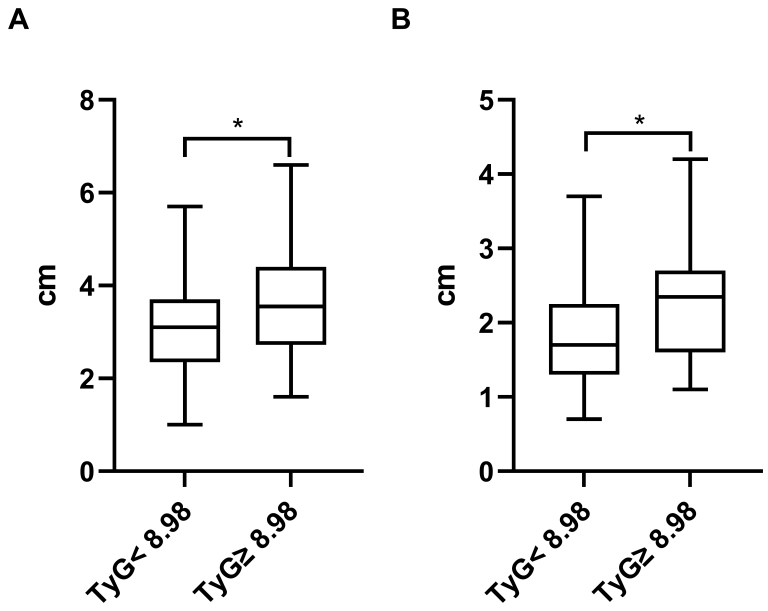

FIGURE 6
Comparison of the maximal length **(A)** and width **(B)** of LVA between patients grouped by TyG index. TyG, triglyceride-glucose; *P<0.05.

10.3389/fendo.2025.1423040

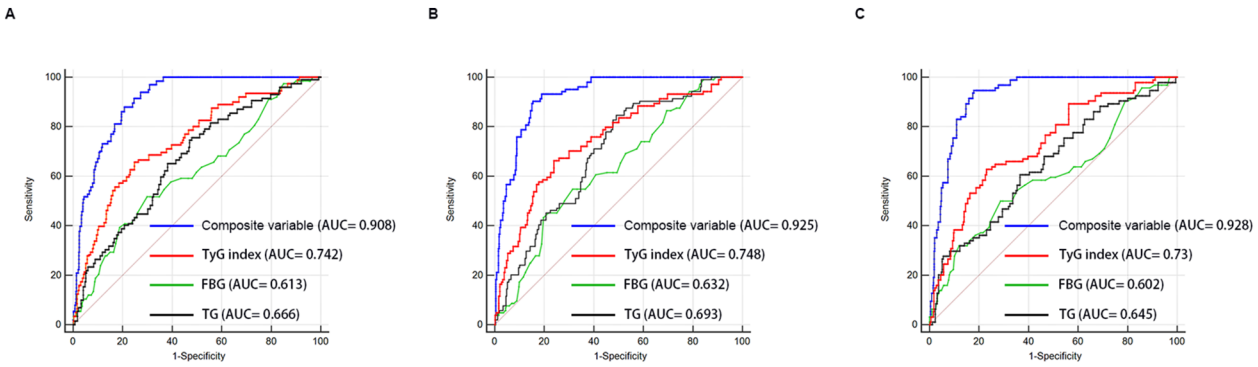

FIGURE 7
Receiver-operating characteristic curves for prediction of LVA formation in the whole cohort **(A)**, the training set **(B)**, and the validation set **(C)**. AUC, area under the curve; TyG, triglyceride-glucose; FBG, fasting blood glucose; TG, triglyceride.

to 8-15% due to advancements in the treatment for AMI (16). In our study, the incidence of LVA in acute STEMI patients who underwent primary PCI was approximately 14.4%, which aligns with previous reports (3, 5). In fact, numerous studies have aimed to identify predictors for LVA after AMI. Feng et al. found that single-vessel disease, decreased GFR and abnormal ferritin could independently predict the LVA formation (31). In a retrospective study involving 1823 STEMI patients, Zhang et al. found that female sex, peak NT-pro BNP, the time between the onset of pain and balloon time, presence of QS-waves on initial electrocardiogram were the independent predictors of early-onset LVA (32). In a prospective cohort study including 1519 patients with STEMI, Savas et al. found that plasma N- Terminal pro B type natriuretic peptide level at admission, among other variables, provided valuable predictive information regarding the development of LVA (16). Additionally, a cohort study by Zhang et al. identified the blood urea nitrogen-to-albumin ratio as an independent predictor for LVA formation in STEMI patients with primary PCI (33). However, disagreement persists concerning these risk factors among different cohort studies. Moreover, these studies primarily focused on single variables, most of which had only modest or small effects on LVA prediction. In the present study, we introduced the TyG index, for the first time, to predict LVA formation in patients with STEMI. The OR for LVA formation in patients with TyG index≥ 8.98 reached up to 2.46. Patients with a TyG index ≥ 8.98 exhibited a significant increase in maximal length and width compared to those with a TyG index < 8.98, which demonstrated the critical predictive role of TyG index in myocardial injury. In addition, LVEF was also identified as the independent predictor for LVA formation, which is consistent with the previous study (5). Furthermore, the TyG index proved to be a more potent predictor for LVA formation than both TG and FBG, with the composite variable yielding the highest predictive value.

TABLE 7 Analysis of the ROC curve for predictive power of center ventricular aneurysm formation.

Cohort	Variables	AUC	SE	95% CI
Whole cohort	FBG	0.613	0.022	0.587 - 0.638
	TG	0.666	0.02	0.641 - 0.690
	TyG index	0.742	0.019	0.719 - 0.764
	Composite variable	0.908	0.008	0.892 - 0.922
Training set	FBG	0.632	0.028	0.596 - 0.668
	TG	0.693	0.026	0.658 - 0.727
	TyG index	0.748	0.027	0.715 - 0.779
	Composite variable	0.925	0.011	0.903 - 0.943
Validation set	FBG	0.602	0.034	0.565 - 0.638
	TG	0.645	0.031	0.608 - 0.680
	TyG index	0.73	0.028	0.696 - 0.763
	Composite variable	0.928	0.01	0.906 - 0.946

ROC, receiver operating characteristic; FBG, fasting blood glucose; TG, triglyceride; TyG, triglyceride-glucose; AUC, area under curve; SE, standard error; CI, Confidence interval.

The precise mechanisms underlying the relationship between the TyG index and LVA formation remain incompletely elucidated. Firstly, the TyG index exhibits positive correlations with TC, LDL-C, and C-reactive protein, while showing a negative correlation with HDL-C. This suggests that the presence of cardiometabolic risk factors may partially account for this association. Secondly, the TyG index serves as a reliable indicator of insulin resistance (IR). Prior research has indicated that IR can lead to inflammation, oxidative stress, and cardiomyocyte apoptosis (34, 35), potentially elevating the risk of LVA. Thirdly, an elevated TyG index has been associated with increased arterial stiffness and coronary artery calcification (13, 36), which may represent another significant mechanism.

The association between the TyG index and LVA formation was not observed in patients with diabetes, those with HbA1c HbA1c< 6%, or those with LDL-C≥ 3.37mmol/L. The limited sample size of diabetic patients (N=299) may account for the lack of significant association between the TyG index and LVA. Patients with HbA1c < 6% demonstrated a lower incidence of LVA compared to those with HbA1c ≥ 6% (11.2% vs. 17.3%, P<0.001), potentially diminishing the impact of the TyG index on LVA risk in this

10.3389/fendo.2025.1423040

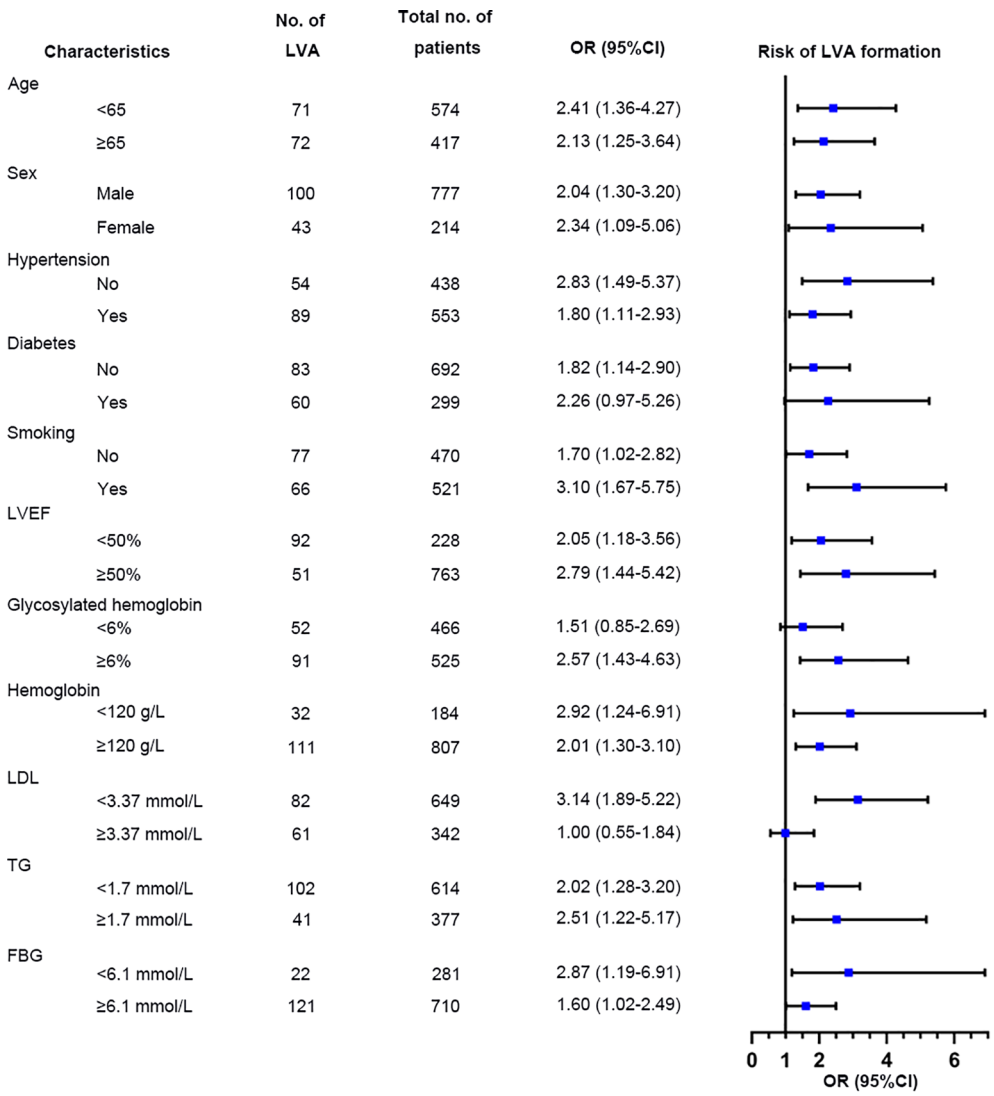

FIGURE 8
Forest plots for subgroup analysis of the relationship between TyG index and the risk for LVA formation. TyG, triglyceride-glucose; LVA, left ventricular aneurysm; LVEF, left ventricular ejection fraction; LDL-C, low-density lipoprotein cholesterol; TG, triglyceride; FBG, fasting blood glucose; OR, Odds Ratio.

subgroup. Additionally, the number of patients with LDL-C≥ 3.37mmol/L was significantly smaller than those with LDL-C< 3.37mmol/L. Furthermore, patients with LDL-C≥ 3.37mmol/L were younger than those with lower LDL-C levels (59.7 ± 13.3 vs. 61.9 ± 12.5, P=0.01) in our study. These factors collectively attenuate the relationship between the TyG index and LVA.

The primary strength of the present study is its novelty as the first investigation addressing the relationship between TyG index and the risk for LVA formation in patients with acute STEMI who underwent primary PCI. However, several limitations should be noted. First, our study failed to compare the predictive values of HOMA-IR and the TyG index due to the lack of routine insulin level measurements in these patients. Second, despite the large sample size in this study, our focus was solely on baseline serum TG and FBG levels, neglecting the dynamic changes in the TyG index, which could have provided valuable insight into the underlying mechanism. Third, the nature of observational study prevented the establishment of a causal association between the TyG index and LVA formation. Additionally, unmeasured or residual confounding effects may have impacted our findings. Finally, while our results indicated a significant association between the TyG index and the risk for LVA formation, its practical clinical application value requires confirmation in future prospective studies.

Conclusions

In conclusion, our study demonstrated that the TyG index was significantly associated with increased risk of LVA formation and cardiac death in patients with acute STEMI who underwent primary PCI. Additionally, the TyG index alone demonstrated excellent

discriminatory ability for LVA formation, and the composite variable including the TyG index, LVEF, and LAD as the culprit vessel significantly improved the discriminatory power. Our findings suggest the potential use of the TyG index in clinical practice as a preferable predictor for LVA formation in patients with acute STEMI who underwent primary PCI.

Data availability statement

The raw data supporting the conclusions of this article will be made available by the authors, without undue reservation.

Ethics statement

The studies involving humans were approved by the Review Board of Panzhihua central hospital (Number: 20200016). The studies were conducted in accordance with the local legislation and institutional requirements. The participants provided their written informed consent to participate in this study.

Author contributions

SL: Conceptualization, Investigation, Methodology, Writing – original draft, Writing – review & editing, Formal Analysis, Funding acquisition, Validation. XZ: Conceptualization, Data curation, Formal Analysis, Investigation, Software, Writing – original draft. YZ: Formal Analysis, Validation, Visualization, Writing – review & editing. XX: Formal Analysis, Resources, Software, Writing – original draft. JL: Formal Analysis, Investigation, Methodology, Project administration, Writing – review & editing.

Funding

The author(s) declare that financial support was received for the research and/or publication of this article. This work was supported by the project from Panzhihua Science and Technology Bureau (Nos.2020ZD-S-26), the Sichuan Medical Association Program (Nos.S20020), the Sichuan Province key clinical specialty construction Project, and Joint project of local universities in Yunnan Province (202101BA070001-104).

Conflict of interest

The authors declare that the research was conducted in the absence of any commercial or financial relationships that could be construed as a potential conflict of interest.

Publisher's note

All claims expressed in this article are solely those of the authors and do not necessarily represent those of their affiliated organizations, or those of the publisher, the editors and the reviewers. Any product that may be evaluated in this article, or claim that may be made by its manufacturer, is not guaranteed or endorsed by the publisher.

Supplementary material

The Supplementary Material for this article can be found online at: https://www.frontiersin.org/articles/10.3389/fendo.2025.1423040/full#supplementary-material

References

1. Karamasis GV, Varlamos C, Benetou D-R, Kalogeropoulos AS, Keeble TR, Tsigkas G, et al. The usefulness of intracoronary imaging in patients with ST-segment elevation myocardial infarction. *J Clin Med*. (2023) 12(18):5892. doi: 10.1016/j.jcin.2020.03.053

2. Mori M, Sakakura K, Wada H, Ikeda N, Jinnouchi H, Sugawara Y, et al. Left ventricular apical aneurysm following primary percutaneous coronary intervention. *Heart vessels*. (2013) 28:677–83. doi: 10.1007/s00380-012-0301-2

3. You J, Gao L, Shen Y, Guo W, Wang X, Wan Q, et al. Predictors and long-term prognosis of left ventricular aneurysm in patients with acute anterior myocardial infarction treated with primary percutaneous coronary intervention in the contemporary era. *J thoracic Dis*. (2021) 13:1706–16. doi: 10.1002/ccd.28712

4. Bai W, Tang H. Left ventricular pseudoaneurysm following acute myocardial infarction. *Anatolian J Cardiol*. (2018) 20:E10–1. doi: 10.14744/AnatolJCardiol.2018.39001

5. Wang Z, Ren L, Liu N, Peng J. The relationship between post-procedural platelet count and left ventricular aneurysm in patients with acute anterior ST-segment elevation myocardial infarction following primary percutaneous coronary intervention. *Kardiologia polska*. (2018) 76:899–907. doi: 10.5603/KP.2018.0008

6. Song Y, Cui K, Yang M, Song C, Yin D, Dong Q, et al. High triglyceride-glucose index and stress hyperglycemia ratio as predictors of adverse cardiac events in patients with coronary chronic total occlusion: A large-scale prospective cohort study. *Cardiovasc Diabetol*. (2023) 22:180. doi: 10.3390/jcm10030440

7. Zhou Q, Yang J, Tang H, Guo Z, Dong W, Wang Y, et al. High triglyceride-glucose (TyG) index is associated with poor prognosis of heart failure with preserved ejection fraction. *Cardiovasc Diabetol*. (2023) 22:263. doi: 10.1113/JP276747

8. Chen Q, Xiong S, Zhang Z, Yu X, Chen Y, Ye T, et al. Triglyceride-glucose index is associated with recurrent revascularization in patients with type 2 diabetes mellitus after percutaneous coronary intervention. *Cardiovasc Diabetol*. (2023) 22:284. doi: 10.1001/jama.299.13.1561

9. Tao L-C, Xu J-N, Wang T-T, Hua F, Li J-J. Triglyceride-glucose index as a marker in cardiovascular diseases: Landscape and limitations. *Cardiovasc Diabetol*. (2022) 21:68. doi: 10.2337/dc18-1920

10. Wang L, Cong H-L, Zhang J-X, Hu Y-C, Wei A, Zhang Y-Y, et al. Triglyceride-glucose index predicts adverse cardiovascular events in patients with diabetes and acute coronary syndrome. *Cardiovasc Diabetol*. (2020) 19:80. doi: 10.1186/s12933-020-01054-z

11. Akbar MR, Pranata R, Wibowo A, Irvan, Sihite TA, Martha JW. The association between triglyceride-glucose index and major adverse cardiovascular events in patients with acute coronary syndrome - dose-response meta-analysis. *Nutrition metabolism Cardiovasc Dis NMCD*. (2021) 31:3024–30. doi: 10.1016/j.numecd.2021.08.026

12. Jiao Y, Su Y, Shen J, Hou X, Li Y, Wang J, et al. Evaluation of the long-term prognostic ability of triglyceride-glucose index for elderly acute coronary syndrome patients: A cohort study. *Cardiovasc Diabetol*. (2022) 21:3. doi: 10.1161/CIRCRESAHA.117.311586

13. Wang J, Huang X, Fu C, Sheng Q, Liu P. Association between triglyceride glucose index, coronary artery calcification and multivessel coronary disease in Chinese patients with acute coronary syndrome. *Cardiovasc Diabetol*. (2022) 21:187. doi: 10.1186/s12944-020-1187-0

14. Thygesen K, Alpert JS, Jaffe AS, Chaitman BR, Bax JJ, Morrow DA, et al. Fourth universal definition of myocardial infarction (2018). *J Am Coll Cardiol*. (2018) 72:2231–64. doi: 10.1016/j.jacc.2018.08.1038

15. Bourassa MG, Fisher LD, Campeau L, Gillespie MJ, McConney M, Lespérance J. Long-term fate of bypass grafts: The Coronary Artery Surgery Study (CASS) and Montreal Heart Institute experiences. *Circulation*. (1985) 72:V71–8.

16. Celebi S, Celebi OO, Cetin S, Cetin HO, Tek M, Gokaslan S, et al. The usefulness of admission plasma NT-pro BNP level to predict left ventricular aneurysm formation after acute ST-segment elevation myocardial infarction. *Arquivos brasileiros cardiologia*. (2019) 113:1129–37. doi: 10.5935/abc.20190226

17. Zhou Y, Wang C, Che H, Cheng L, Zhu D, Rao C, et al. Association between the triglyceride-glucose index and the risk of mortality among patients with chronic heart failure: Results from a retrospective cohort study in China. *Cardiovasc Diabetol*. (2023) 22:171. doi: 10.1016/j.jchf.2017.06.013

18. Hill MA, Yang Y, Zhang L, Sun Z, Jia G, Parrish AR, et al. Insulin resistance, cardiovascular stiffening and cardiovascular disease. *Metabolism: Clin Exp*. (2021) 119:154766. doi: 10.1016/j.metabol.2021.154766

19. Mancusi C, de Simone G, Best LG, Wang W, Zhang Y, Roman MJ, et al. Myocardial mechano-energetic efficiency and insulin resistance in non-diabetic members of the Strong Heart Study cohort. *Cardiovasc Diabetol*. (2019) 18:56. doi: 10.1186/s12944-018-0914-2

20. Xie E, Ye Z, Wu Y, Zhao X, Li Y, Shen N, et al. The triglyceride-glucose index predicts 1-year major adverse cardiovascular events in end-stage renal disease patients with coronary artery disease. *Cardiovasc Diabetol*. (2023) 22:292. doi: 10.1186/s12933-022-01582-w

21. Zhang Q, Xiao S, Jiao X, Shen Y. The triglyceride-glucose index is a predictor for cardiovascular and all-cause mortality in CVD patients with diabetes or pre-diabetes: Evidence from NHANES 2001-2018. *Cardiovasc Diabetol*. (2023) 22:279. doi: 10.1212/WNL.0000000000007454

22. van Minh H, Tien HA, Sinh CT, Thang DC, Chen C-H, Tay JC, et al. Assessment of preferred methods to measure insulin resistance in Asian patients with hypertension. *J Clin hypertension (Greenwich Conn.)*. (2021) 23:529–37. doi: 10.1371/journal.pone.0149731

23. Muniyappa R, Lee S, Chen H, Quon MJ. Current approaches for assessing insulin sensitivity and resistance *in vivo*: Advantages, limitations, and appropriate usage. *Am J Physiol Endocrinol Metab*. (2008) 294:E15–26. doi: 10.1152/ajpendo.00645.2007

24. Son D-H, Lee HS, Lee Y-J, Lee J-H, Han J-H. Comparison of triglyceride-glucose index and HOMA-IR for predicting prevalence and incidence of metabolic syndrome. *Nutrition metabolism Cardiovasc Dis NMCD*. (2022) 32:596–604. doi: 10.1016/j.numecd.2021.11.017

25. Kim B, Kim G-M, Huh U, Lee J, Kim E. Association of HOMA-IR versus tyG index with diabetes in individuals without underweight or obesity. *Healthcare (Basel Switzerland)*. (2024) 12. doi: 10.1016/j.amjmed.2008.06.037

26. Hao Q, Yuanyuan Z, Lijuan C. The prognostic value of the triglyceride glucose index in patients with acute myocardial infarction. *J Cardiovasc Pharmacol Ther*. (2023) 28:10742484231181846. doi: 10.1177/10742484231181846

27. Wang M, Zhou L, Su W, Dang W, Li H, Chen H. Independent and joint associations between the triglyceride-glucose index and NT-proBNP with the risk of adverse cardiovascular events in patients with diabetes and acute coronary syndrome: A prospective cohort study. *Cardiovasc Diabetol*. (2023) 22:149. doi: 10.1136/bmj.k1497

28. Zhu Y, Liu K, Chen M, Liu Y, Gao A, Hu C, et al. Triglyceride-glucose index is associated with in-stent restenosis in patients with acute coronary syndrome after percutaneous coronary intervention with drug-eluting stents. *Cardiovasc Diabetol*. (2021) 20:137. doi: 10.1016/j.cmet.2011.07.015

29. Xiong S, Chen Q, Long Y, Su H, Luo Y, Liu H, et al. Association of the triglyceride-glucose index with coronary artery disease complexity in patients with acute coronary syndrome. *Cardiovasc Diabetol*. (2023) 22:56. doi: 10.1016/j.jacc.2021.03.314

30. Engel J, Brady WJ, Mattu A, Perron AD. Electrocardiographic ST segment elevation: Left ventricular aneurysm. *Am J Emergency Med*. (2002) 20:238–42. doi: 10.1053/ajem.2002.32634

31. Feng Y, Wang Q, Chen G, Ye D, Xu W. Impaired renal function and abnormal level of ferritin are independent risk factors of left ventricular aneurysm after acute myocardial infarction: A hospital-based case-control study. *Medicine*. (2018) 97:e12109. doi: 10.1097/MD.0000000000012109

32. Zhang Z, Guo J. Predictive risk factors of early onset left ventricular aneurysm formation in patients with acute ST-elevation myocardial infarction. *Heart Lung J Crit Care*. (2020) 49:80–5. doi: 10.1016/j.hrtlng.2019.09.005

33. Zhang K, Yang L, Wu X, Zheng X, Zhao Y. Urea nitrogen-to-albumin ratio predicts ventricular aneurysm formation in ST-segment elevation myocardial infarction. *ESC Heart failure*. (2024) 11(2):974–85. doi: 10.1002/ehf2.14620

34. Yang T, Li G, Wang C, Xu G, Li Q, Yang Y, et al. Insulin resistance and coronary inflammation in patients with coronary artery disease: A cross-sectional study. *Cardiovasc Diabetol*. (2024) 23:79. doi: 10.1007/s00330-020-07069-0

35. Wu H, Ballantyne CM. Skeletal muscle inflammation and insulin resistance in obesity. *J Clin Invest*. (2017) 127:43–54. doi: 10.2337/db08-0943

36. Wu S, Xu L, Wu M, Chen S, Wang Y, Tian Y. Association between triglyceride-glucose index and risk of arterial stiffness: A cohort study. *Cardiovasc Diabetol*. (2021) 20:146. doi: 10.1186/s12933-021-01342-2

frontiers | Frontiers in Endocrinology

TYPE Original Research
PUBLISHED 15 May 2025
DOI 10.3389/fendo.2025.1552484

OPEN ACCESS

EDITED BY
Matthias Blüher,
Leipzig University, Germany

REVIEWED BY
Anthony Martin Gerdes,
New York Institute of Technology, United States
Davide Gnocchi,
University of Bari Medical School, Italy
Mostafa Vaghari-Tabari,
Tabriz University of Medical Sciences, Iran

*CORRESPONDENCE
Zengyao Li
wxlzy23@163.com
Ye Zhang
zhangyekkw_color@126.com

RECEIVED 28 December 2024
ACCEPTED 22 April 2025
PUBLISHED 15 May 2025

CITATION
Zhou X, Zhang Y and Li Z (2025) Impaired sensitivity to thyroid hormones is positively associated to metabolic syndrome severity in euthyroid Chinese adults as revealed by a cross-sectional study.
Front. Endocrinol. 16:1552484.
doi: 10.3389/fendo.2025.1552484

Impaired sensitivity to thyroid hormones is positively associated to metabolic syndrome severity in euthyroid Chinese adults as revealed by a cross-sectional study

Xiong Zhou, Ye Zhang* and Zengyao Li*

Department of Minimally Invasive Laparoscopy, The Affiliated Wuxi People's Hospital of Nanjing Medical University, Wuxi People's Hospital, Wuxi Medical Center, Nanjing Medical University, Wuxi, China

Objective: Thyroid hormones (THs) play a pivotal role in regulating metabolism, and their sensitivity may influence the risk of metabolic syndrome (MetS). This study aimed to investigate the association of impaired sensitivity to THs with MetS and MetS severity score (MetSSS) in Chinese euthyroid adults.

Methods: A cross-sectional analysis was conducted involving 17,272 health check-up participants. THs sensitivity indices, including Thyroid Feedback Quantile-Based Index (TFQI), Parametric Thyroid Feedback Quantile-Based Index (PTFQI), TSH Index (TSHI), Thyrotropin Thyroxine Resistance Index (TT4RI), and free triiodothyronine/free thyroxine (FT3/FT4) ratio were assessed. Multivariable regression and restricted spline cubic analyses were conducted to explore the association between THs sensitivity indices and MetS and MetSSS. Subgroup analysis was also performed to examine this association stratified by sex and age.

Results: Multivariable logistic regression analysis indicated that MetS risk was positively associated with all impaired THs sensitivity indices (per SD increase) (TFQI: OR=1.20, 95%CI: 1.15-1.25); PTFQI: OR=1.28, 95%CI: 1.23-1.33; TSHI: OR=1.35, 95%CI: 1.29-1.42; TT4RI: OR=1.57, 95%CI: 1.47-1.67; FT3/FT4: OR=1.17, 95%CI: 1.12-1.23)(all P-value<0.001). After adjusting for confounders, compared with the lowest group of MetSSS, individuals in the highest group of MetSSS were positively associated with all impaired THs sensitivity indices (per SD increase) (TFQI: OR=1.16, 95%CI: 1.07-1.21 PTFQI: OR=1.12, 95%CI: 1.06-1.17; TSHI: OR=1.13, 95%CI: 1.06-1.19; TT4RI: OR=1.25, 95%CI: 1.15-1.35; FT3/FT4: OR=1.82, 95%CI: 1.72-1.93). Nonlinear associations were found between THs sensitivity indicators and MetS (P for non-linear<0.001). Subgroup analysis indicated that all thyroid hormones sensitivity indices were positively associated with MetS by gender (male/female) and age (<60 years/≥60 years).

Conclusion: Impaired sensitivity to THs is associated with an increased risk of MetS and MetSSS in Chinese euthyroid adults. Future research should consider thyroid hormones sensitivity indices in the assessment of MetS risk.

KEYWORDS

thyroid hormones sensitivity, metabolic syndrome, severity, euthyroid, Chinese adults

Introduction

Metabolic syndrome (MetS) is a complex metabolic disorder characterized by the presence of central obesity, high blood sugar levels, abnormal lipid levels, and high blood pressure (1). Central obesity, with excess visceral fat, affects insulin sensitivity and vascular health. Elevated blood sugar indicates insulin resistance, leading to atherosclerosis and microvascular damage. Dyslipidemia increases plaque formation risk, while hypertension, tied to insulin resistance and obesity, worsens vascular issues. Collectively, these components boost the risk of cardiovascular diseases and type 2 diabetes (2). The prevalence of MetS has become a major global health concern, with the International Diabetes Federation estimating that one in four people worldwide are affected (2, 3). In China, the situation is equally troubling, as there has been a noticeable rise in the prevalence of MetS in recent years, highlighting the need for further research in this area (4).

Thyroid hormones (THs) are crucial for regulating development, metabolism, homeostasis in multiple organ systems and various physiological functions including energy balance. The two primary thyroid hormones are thyroxine (T4) and triiodothyronine (T3). T4, mainly secreted by the thyroid, acts as a prohormone, while T3, generated via tissue-specific deiodination of T4, is the biologically active form that binds to nuclear thyroid hormone receptors (TRs) to regulate gene transcription (genomic effects) (5).

Emerging evidence highlights the significance of thyroid hormone metabolites, which were once considered inactive byproducts. These metabolites include reverse T3 (rT3), tetraiodothyroacetic acid (Tetrac), triiodothyroacetic acid (Triac), diiodothyronines (e.g., 3,5-T2 and 3,3'-T2), and thyronamines (e.g., 3-T1AM). They exhibit distinct biological activities, particularly through non-genomic pathways. For example, 3,5-T2 modulates mitochondrial energy expenditure and lipid metabolism, while 3-T1AM influences thermoregulation and neuronal signaling. These metabolites often function independently of classical TR-mediated mechanisms, playing roles in fine-tuning physiological processes such as metabolic rate, cardiovascular function, and central nervous system activity (6). Both hypothyroidism and hyperthyroidism can result in insulin resistance and have a detrimental impact on glucose and lipid metabolism, thereby being associated with the development of MetS (7, 8). Understanding the diversity and functional interplay of thyroid hormones and their metabolites is essential for elucidating their contributions to health and disease, particularly in metabolic disorders where traditional TH signaling may be dysregulated.

The study's biochemical basis is the complex link between thyroid hormones and metabolism. Thyroid hormones are key to energy balance, glucose and lipid metabolism, and cardiovascular function, with both genomic and non-genomic effects (9). Genomically, they bind to nuclear receptors, affecting genes related to glucose and lipid metabolism, which impacts insulin sensitivity and lipid profiles (10). For example, they boost insulin secretion and receptor expression. Non-genomically, thyroid hormones interact with cell membranes and cytoplasmic proteins, rapidly modulating ion channels and enzymes involved in energy and glucose metabolism (11). They also stimulate mitochondrial biogenesis and uncoupling proteins, influencing energy use and lipid oxidation. Moreover, thyroid hormones interact with other hormones like insulin and adrenaline, affecting metabolic regulation. The hypothalamus-pituitary-thyroid feedback loop controls thyroid hormone levels, and its disruption can cause metabolic issues (12).

Previous research has shown conflicting results when it comes to the relationship between thyroid function and MetS. Some studies have suggested a connection between normal levels of thyroid-stimulating hormone (TSH) and the presence of MetS (13, 14). while others have not found any association or have pointed to FT4 instead (15, 16). These discrepancies could be due to differences in study populations, methodologies, and the failure to consider potential confounding factors like gender, which has been shown to impact the prevalence of MetS components and their correlation with THs (17–19). Additionally, simply measuring TSH, FT3, and FT4 levels in individuals with normal thyroid function may not be enough to accurately assess thyroid function status. It is important to recognize that thyroid hormone balance may not be stable even if these markers fall within the normal range.

Recently, there has been a growing interest in the idea that reduced sensitivity to THs in the general population could play a role in metabolic disorders (20). This concept of THs sensitivity considers both FT4 and TSH levels. In cases of THs resistance syndrome, elevated levels of both FT4 and TSH are present, indicating issues with energy regulation. Normally, there is a negative correlation between THs and TSH due to the feedback loop of the hypothalamic-pituitary-thyroid axis (21, 22). However, individuals with mild resistance to THs may have high levels of both

hormones. Researchers have developed various indices, such as the thyroid feedback quantile-based index (TFQI), parametric thyroid feedback quantile-based index (PTFQI) (20), thyrotrophic thyroxine resistance index (TT4RI) (23), and thyroid-stimulating hormone index (TSHI) (24), to quantify the relationship between thyroid function and metabolic factors. These indices help to clarify conflicting findings regarding the link between THs and MetS.

Previous studies have demonstrated a direct link between sensitivity to THs and certain health issues like prediabetes, decreased kidney function, and higher risk of cardiovascular disease (25–27). Yet, there has been a lack of investigation into the relationship between THs sensitivity and MetS in individuals with normal thyroid function. This cross-sectional study seeks to investigate the link between sensitivity to THs and MetS, as well as its severity score, in a sizable group of Chinese euthyroid adults. Through the evaluation of various THs sensitivity indices, we aim to gain a more detailed understanding of the association between sensitivity to THs and MetS in euthyroid Chinese adults. The results could shed light on potential risk factors for MetS and aid in the creation of personalized prevention and treatment plans for Chinese adults.

Materials and methods

Study population and design

The study included adults over 18 years old who had undergone annual health examinations at the health check-up center of People's Hospital in Wuxi city, affiliated with Nanjing Medical University. Initially, a total of 25,360 individuals were part of this retrospective study. Participants were excluded if they had incomplete medical information, lacked blood parameters for thyroid function tests, had a history of thyroid surgery or were taking thyroid medication, were not euthyroid, or had oncology, severe liver, or kidney dysfunction. After excluding these individuals, the study included 17,272 participants, comprising 10,442 males and 6,830 females aged 18 to 89 years. This retrospective study was approved by the Health Examination Center of People's Hospital in Wuxi city (approval number: not applicable), affiliated with Nanjing Medical University, following the principles of the Declaration of Helsinki. Patient data was anonymized to ensure confidentiality, and statistical analysis was conducted securely for scientific research purposes. Therefore, informed consent was waived.

Data collection

We used a standard questionnaire to gather information on participants' age, gender, and use of cigarettes and alcohol. Smoking was defined as consuming three or more cigarettes daily for a year, while alcohol consumption was defined as drinking at least three times a week for twelve months. Participants provided fasting venous blood samples after a 12-hour overnight fast. Levels of fasting plasma glucose (FPG), triglycerides (TG), total cholesterol (TC), high-density lipoprotein cholesterol (HDL-C), low-density lipoprotein cholesterol (LDL-C), neutrophils (NE), and lymphocytes (LY) were measured using an automatic hematology analyzer. The neutrophil to lymphocyte ratio (NLR) was calculated. Strict quality control procedures were followed in the laboratory.

In addition, we gathered information on individuals' health, such as whether they had been previously diagnosed with hypertension or diabetes, and if they were currently taking any medications. Diabetes was defined as having fasting blood glucose levels of 7.0 mmol/L or higher, being prescribed insulin or oral hypoglycemic agents, or self-reporting a history of the condition (28). Hypertension was determined by having a systolic blood pressure of 140 mmHg or higher, or a diastolic blood pressure of 90 mmHg or higher, and currently using antihypertensive medications (29). We used the electrochemiluminescence immunoassay method to measure the concentrations of thyroid-stimulating hormone (TSH), free triiodothyronine (FT3), and free thyroxine (FT4). The reference ranges for FT3, FT4, and TSH were 3.10 to 6.80 pmol/L, 12.00 to 22.00 pmol/L, and 0.27 to 4.20 mIU/L, respectively. Euthyroid was defined as having serum TSH and FT4 levels within the normal ranges and not using thyroid hormone medication.

The physical examination included measuring height (in centimeters), weight (in kilograms), waist circumference (in centimeters), and blood pressure (in mmHg). BMI was calculated by dividing weight in kilograms by height in meters squared. Systolic and diastolic blood pressure were measured on the right arm using a sphygmomanometer after at least 5 minutes of rest, and the average of two readings was recorded.

Metabolic syndrome and MetS severity score

Metabolic syndrome (MetS) is defined according to the 2009 guidelines of the International Diabetes Federation (IDF) and the American Heart Association/National Heart, Lung, and Blood Institute (AHA/NHLBI) (30, 31). It includes three of the following five criteria: 1) elevated waist circumference, with specific measurements for men (≥90 cm) and women (≥80 cm); 2) elevated triglycerides (≥150 mg/dl) or use of medication for high triglyceride levels; 3) low HDL cholesterol (<40 mg/dl in men and <50 mg/dl in women) or use of medication for low HDL levels; 4) high blood pressure (systolic ≥130 mmHg and/or diastolic ≥85 mmHg) or use of antihypertensive medication; and 5) elevated fasting glucose (≥100 mg/dl) or use of medication for high glucose levels. Additionally, a Metabolic Syndrome Severity Score (MetSSS) is calculated based on specific equations for age, sex, and ethnicity (Table 1) (32).

Indices of thyroid hormone sensitivity

The participants' central sensitivity to THs was assessed using Thyroid Feedback Quartile-Based index (TFQI), parametric thyroid

10.3389/fendo.2025.1552484

TABLE 1 Age-sex-ethnicity-specific MetSSS equations.

Groups	MetSSS equations
Male	
<60 years	-2.9092 + 0.0262*WC +0.3098*TG-0.944*HDL-C+ 0.0097*MAP+0.0745*FBG
≥60 years	-2.3741 + 0.0264*WC+0.4933*TG-0.999*HDL-C+ 0.0054*MAP+0.0821*FBG
Female	
<60 years	-2.4981 + 0.0199*WC+0.5218*TG-0.8616*HDL-C+ 0.0110*MAP+0.1074*FBG
≥60 years	-0.5682 + 0.0153*WC+0.4587*TG-1.3567*HDL-C+ 0.0036*MAP+0.0688*FBG

feedback quantile-based index (PTFQI), TSH index (TSHI), and Thyrotroph T4 Resistance Index (TT4RI). Higher values of TFQI, PTFQI, TSHI, and TT4RI indicate lower central sensitivity to thyroid hormones. Peripheral THs sensitivity was evaluated using the FT3 to FT4 ratio (FT3/FT4), where higher values suggest higher sensitivity. The equations for calculation are provided with the following formulas (16, 19, 20): TFQI = cdf FT4 − (1 − cdf TSH); cdf: cumulative distribution function. PTFQI = φ((FT4-μFT4)/σFT4) - (1-φ ((ln TSH-μln TSH)/σlnTSH)), where μfT4 = 15.70, σfT4 = 1.80, μln TSH=0.62, and σln TSH=0.45 for the Chinese population. TSHI = ln TSH (mIU/L) + 0.1345 × FT4 (pmol/L). TT4RI = FT4 (pmol/L) × TSH (mIU/L). FT3/FT4 = FT3 (pmol/L)/FT4 (pmol/L).

Statistical analyses

The statistical analyses were conducted using SPSS 26.0 (Chicago, IL, USA) and R software (version 4.1). The normality of the variables was assessed using the Kolmogorov–Smirnov test. Normally distributed variables are presented as mean (standard deviation), skewed variables as median [interquartile range], and categorical variables as frequencies (proportions). One-way ANOVA test or Kruskal-Wallis H test were used to compare continuous variables, while the chi-square test was used for categorical variables. Multivariable logistic regression analysis was performed to assess the associations between MetS risk and thyroid hormone sensitivity indices, adjusting for potential confounding factors. Two models were used for adjustment: Model 1 included sex and age, while Model 2 included variables from Model 1 as well as smoking, drinking, BMI, and NLR. The relationship between thyroid hormone sensitivity indices and the risk of MetS and MetSSS in all euthyroid participants was examined using restricted cubic spline analysis. The model incorporated 4 knots placed at the 5th, 35th, 65th, and 95th percentiles of SII, with the p-value indicating the nonlinearity of the smooth curve fitting. Subgroup analysis was conducted to explore the correlation between thyroid hormone sensitivity indices and the risk of MetS and its components among different subgroups based on sex (males/females) and age (≥60 years/<60 years). A significance level of $P < 0.05$ (2-tailed) was considered statistically significant.

Results

Baseline characteristics

Table 2 presents the baseline characteristics of all participants categorized by quartiles of MetSSS. A total of 17,272 participants were included in the analysis, with 10,442 males (60.5%) and 6,830 females (39.5%) (Figure 1). There were significant differences in all baseline characteristics among the four quartiles of MetSSS (all P-values < 0.001). Individuals in the higher quartiles of MetSSS were more likely to be older, male, smokers, drinkers, and had higher rates of hypertension and diabetes (P for trend < 0.001). There were notable increases in BMI, WC, FBG, SBP, DBP, TG, TC, LDL-C, NLR, FT3, and FT4 across the quartiles of MetSSS, while HDLC decreased. Furthermore, participants in the higher quartiles of MetSSS exhibited higher levels of TFQI, PTFQI, TSHI, TT4RI, and FT3/FT4 (P for trend < 0.001).

Adjusted odds ratios for sensitivity to THs and risk of MetS and its components

Table 3 displays the adjusted odds ratios (ORs) and 95% confidence intervals (CIs) for the relationship between sensitivity to THs and the risk of MetS and its components. The analysis involved three models, including a crude model and two adjusted models controlling for various confounding factors. After adjusting for potential confounders such as age, sex, smoking, drinking, BMI, and NLR, the risk of MetS was found to be positively correlated with all sensitivity to THs [TFQI (+ 1 SD): OR=1.20, 95%CI: 1.15-1.25; PTFQI (+ 1 SD): OR=1.28, 95%CI: 1.23-1.33; TSHI (+ 1 SD): OR=1.35, 95% CI: 1.29-1.42; TT4RI (+ 1 SD): OR=1.57, 95%CI: 1.47-1.67; FT3/FT4 (+ 1 SD): OR=1.17, 95%CI: 1.12-1.23] (all P-value <0.001). Regarding MetS components, elevated waist circumference (WC) and low high-density lipoprotein cholesterol (HDL-C) did not show a significant association with thyroid sensitivity indices in the adjusted models. However, elevated blood pressure (BP), elevated triglycerides (TG), and elevated fasting plasma glucose (FPG) were positively associated with thyroid hormones sensitivity indices, with the strongest associations observed for FT3/FT4.

Association of sensitivity to THs and MetSSS quartiles

Table 4 shows the relationship between thyroid hormone sensitivity (per SD increase) and quartiles of MetSSS. The odds ratios for each quartile with 95% confidence intervals, adjusted for age, sex, smoking, drinking, BMI, and NLR, are presented. A significant positive trend was observed across MetSSS quartiles for TSHI and TT4RI (per SD increase), with the strongest association seen in the highest quartile (P for trend < 0.001). TFQI and PTFQI also demonstrated a positive trend, although less pronounced for the second quartile. The FT3/FT4 ratio showed a consistent and significant positive association across all quartiles, suggesting that higher peripheral thyroid hormone sensitivity

10.3389/fendo.2025.1552484

TABLE 2 Baseline characteristics of all participants.

Characteristic	MetSSS quartile					P-value	P for trend
	Overall N = 17,272	Q1 N = 4,347	Q2 N = 4,341	Q3 N = 4,327	Q4 N = 4,257		
Age, years	50.64 ± 10.03	47.06 ± 10.55	50.26 ± 9.67	52.08 ± 9.12	53.21 ± 9.63	<0.001	<0.001
Male, n (%)	10,442 (60.5%)	1,532 (35.2%)	2,529 (58.3%)	3,086 (71.3%)	3,295 (77.4%)	<0.001	<0.001
Smoking, n (%)	4,892 (28.3%)	538 (12.4%)	1,033 (23.8%)	1,493 (34.5%)	1,828 (42.9%)	<0.001	<0.001
Drinking, n (%)	3,008 (17.4%)	381 (8.8%)	690 (15.9%)	884 (20.4%)	1,053 (24.7%)	<0.001	<0.001
BMI, kg/m2	24.5 ± 3.2	21.8 ± 2.3	23.9 ± 2.3	25.4 ± 2.5	27.1 ± 3.2	<0.001	<0.001
WC, cm	82.64 ± 9.74	73.61 ± 6.84	80.78 ± 7.02	85.76 ± 7.21	90.60 ± 8.60	<0.001	<0.001
FBG, mmol/L	5.52 ± 1.15	5.02 ± 0.48	5.30 ± 0.67	5.54 ± 0.93	6.22 ± 1.74	<0.001	<0.001
SBP, mmHg	121.73 ± 16.30	111.69 ± 14.04	119.32 ± 14.18	125.03 ± 14.64	131.08 ± 15.70	<0.001	<0.001
DBP, mmHg	73.78 ± 10.68	67.23 ± 8.86	72.25 ± 9.24	76.00 ± 9.73	79.76 ± 10.62	<0.001	<0.001
TG, mmol/L	1.27 (0.90, 1.87)	0.78 (0.64, 0.96)	1.10 (0.89, 1.35)	1.50 (1.21, 1.84)	2.39 (1.82, 3.24)	<0.001	<0.001
TC, mmol/L	4.86 (4.28, 5.46)	4.85 (4.30, 5.44)	4.80 (4.23, 5.38)	4.85 (4.26, 5.45)	4.94 (4.36, 5.61)	<0.001	<0.001
LDLC, mmol/L	3.14 (2.61, 3.68)	2.95 (2.49, 3.46)	3.17 (2.66, 3.71)	3.29 (2.76, 3.80)	3.16 (2.54, 3.72)	<0.001	<0.001
HDLC, mmol/L	1.28 (1.06, 1.54)	1.71 (1.53, 1.93)	1.35 (1.22, 1.51)	1.16 (1.04, 1.30)	1.00 (0.88, 1.13)	<0.001	<0.001
Diabetes, n (%)	1,221 (7.1%)	31 (0.7%)	128 (2.9%)	254 (5.9%)	808 (19.0%)	<0.001	<0.001
Hypertension, n (%)	2,201 (12.7%)	138 (3.2%)	333 (7.7%)	623 (14.4%)	1,107 (26.0%)	<0.001	<0.001
NLR	1.53 (1.21, 1.93)	1.44 (1.14, 1.85)	1.55 (1.21, 1.92)	1.55 (1.23, 1.95)	1.58 (1.27, 1.98)	<0.001	<0.001
FT3, pmol/L	4.70 (4.34, 5.08)	4.44 (4.12, 4.79)	4.69 (4.34, 5.03)	4.82 (4.47, 5.17)	4.86 (4.50, 5.22)	<0.001	<0.001
FT4, pmol/L	15.50 (14.40, 16.80)	15.30 (14.30, 16.30)	15.53 (14.50, 16.90)	15.57 (14.60, 17.00)	15.60 (14.40, 16.90)	<0.001	<0.001
TSH, mIU/L	1.92 (1.40, 2.58)	1.93 (1.40, 2.60)	1.89 (1.38, 2.57)	1.89 (1.38, 2.55)	1.96 (1.44, 2.63)	<0.001	0.154
TSHI	2.75 (2.43, 3.07)	2.73 (2.40, 3.04)	2.75 (2.42, 3.07)	2.75 (2.43, 3.06)	2.79 (2.46, 3.08)	<0.001	<0.001
TT4RI	30 (22, 40)	29 (21, 40)	29 (22, 38)	30 (22, 40)	32 (22, 41)	<0.001	0.001
PTFQI	-0.03 (-0.25, 0.18)	-0.06 (-0.28, 0.14)	-0.03 (-0.26, 0.18)	-0.02 (-0.25, 0.19)	0.00 (-0.22, 0.22)	<0.001	<0.001
TFQI	-0.07 (-0.27, 0.15)	-0.10 (-0.29, 0.10)	-0.06 (-0.26, 0.16)	-0.05 (-0.25, 0.16)	-0.05 (-0.26, 0.17)	<0.001	<0.001
FT3/FT4	0.30 ± 0.04	0.29 ± 0.04	0.30 ± 0.04	0.32 ± 0.03	0.34 ± 0.04	<0.001	<0.001

Continuous variables are presented as mean ± standard deviation or median (interquartile) with number (proportion, %) for categorical variables. P values among groups are calculated by one-way ANOVA or Kruskal-Wallis H tests for continuous variables, Chi-square test for categorical variables.
BMI, body mass index; WC, waist circumference; SBP, systolic blood pressure; DBP, diastolic blood pressure; FPG, fasting plasma glucose; TG, triglycerides; TC, total cholesterol; HDL-C, high-density lipoprotein cholesterol; LDL-C, low-density lipoprotein cholesterol; NLR, neutrophil to lymphocyte ratio; FT3, free triiodothyronine; FT4, free thyroxine; TSH, thyroid-stimulating hormone; TFQI, thyroid feedback quantile-based index; PTFQI, parametric thyroid feedback quantile-based index; TSHI, TSH index; TT4RI, thyrotropin thyroxine resistance index; FT3/FT4, free triiodothyronine to free thyroxine ratio.

may be related to a more severe MetS. Individuals in the highest quartile of MetSSS were more likely to have impaired THs sensitivity indices compared to those in the lowest quartile (TFQI: OR=1.16, 95% CI: 1.07-1.21; PTFQI: OR=1.12, 95%CI: 1.06-1.17; TSHI: OR=1.13, 95%CI: 1.06-1.19; TT4RI: OR=1.25, 95%CI: 1.15-1.35; FT3/FT4: OR=1.82, 95%CI: 1.72-1.93).

Exploration of nonlinear relationships

Based on the results of regression analysis, we conducted a restricted cubic spline analysis to investigate the dose-response relationship between indicators of THs sensitivity and MetS (Figure 2). After adjusting for potential confounders such as age, sex, smoking, drinking, and NLR, we found a significant association between sensitivity to thyroid hormones indices and MetS in all euthyroid participants (overall P<0.001). Non-linear relationships were observed between all indicators of thyroid hormone sensitivity and MetS (P for nonlinearity<0.001). Furthermore, both central and peripheral sensitivity to thyroid hormones were positively correlated with MetSSS) (overall P<0.05 (Figure 3). TSHI, TT4RI, TFQI, and PTFQI showed a linear association with MetSSS (P for nonlinearity>0.05), while FT3/FT4 exhibited a non-linear relationship with MetSSS (P for nonlinearity=0.001).

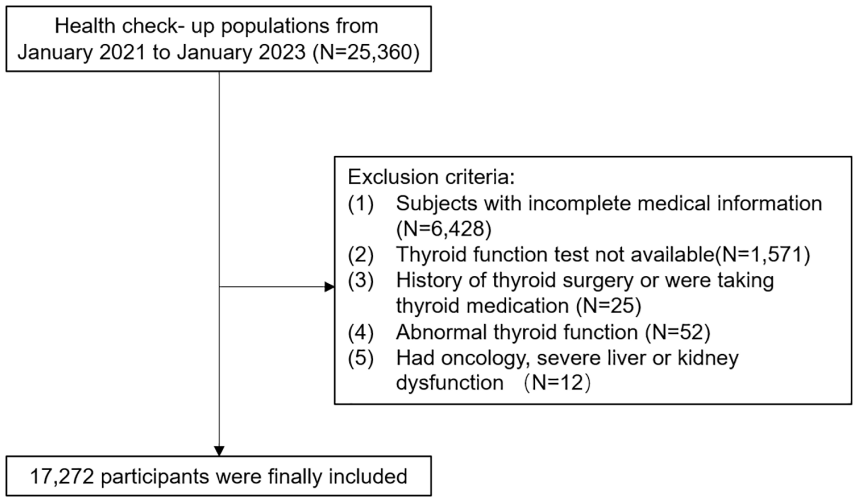

FIGURE 1
Study design flowchart.

Subgroup analysis

As shown in Figure 4, after adjusting for potential confounders, the odds ratios (ORs) for the risk of MetS were found to increase with every 1 standard deviation increase in TFQI, PTFQI, TSHI, TT4RI, and FT3/FT4 ratio. These associations were observed in individuals under 60 years old and those over 60 years old, as well as in males and females. specifically, the ORs for MetS risk were 1.19 to 1.61 among individuals under 60 years old, 1.21 to 1.37 among those over 60 years old, 1.13 to 1.44 in males, and 1.44 to 2.03 in females. Additionally, the FT3/FT4 ratio was positively associated with all MetS components risk in all subgroups. however, most central sensitivities to THs were not significantly associated with elevated WC and low HDL-C. They were positively associated with elevated blood pressure (BP) and triglycerides (TG) in females and individuals under 60 years old, and all sensitivity to THs were positively associated with elevated FPG in subjects under 60 years old.

Discussion

To the best of our knowledge, this is the first large-sample cross-sectional study to evaluate the association between central and peripheral thyroid hormones sensitivity and risk of MetS and MetSSS in euthyroid Chinese adults. The results provide evidence that both decreased central sensitivity to THs (elevated TFQI, PTFQI, TSHI, and TT4RI) and increased peripheral sensitivity to THs (elevated FT3/FT4) were associated with an increased risk of MetS and MetSSS in euthyroid Chinese adults. Additionally, subgroup analysis showed that these relationships remain stable regardless of sex and age. This analysis goes beyond simply examining the absolute levels of FT3, FT4, and TSH, and provides insight into the resistance of THs within MetS and MetSSS.

THs have been found to play a significant role in all aspects of MetS through various mechanisms. These hormones can impact metabolic rate, appetite control, and sympathetic activity, which in turn affects adiposity (33). The stimulation of the sympathetic nervous system by THs also influences glucose and lipid metabolism, as well as cardiovascular regulation (34). However, fluctuations in THs levels within both normal and abnormal ranges have been linked to metabolic disorders. Previous studies have shown that levels of TSH or THs alone may not fully explain the relationship between the thyroid system and metabolic dysfunction (35). Therefore, comprehensive indices that reflect THs homeostasis may provide a more accurate understanding of this relationship. Laclaustra et al. have proposed the use of TFQI and PTFQI to quantify the relationship between thyroid function and metabolic indices (16). This approach, based on the theory of THs resistance, aims to explain contradictory findings in research and has opened up new avenues for studying the connection between thyroid function and metabolic disorders.

Numerous studies have investigated the relationship between sensitivity to THs and metabolic disorders. A recent study involving 31,678 patients with coronary heart disease found that impaired sensitivity to THs was significantly linked to dyslipidemia, regardless of gender, glucose levels, and blood pressure (35). Another recent cross-sectional study also showed a positive correlation between TFQI and FT3/FT4 levels with lipid levels (36). Our study revealed that all measures of THs sensitivity were positively linked to low HDL-C and high TG levels in euthyroid individuals. Research has demonstrated that TSH directly influences the expression of HMG-CoA reductase in the liver, leading to increased cholesterol synthesis (37, 38). TSH binds to its receptor and regulates protein kinase activation through the cyclic adenosine monophosphate/protein kinase A pathway, altering its inhibitory effect on the peroxisome proliferator-activated receptor-γ signaling pathway. This, in

10.3389/fendo.2025.1552484

TABLE 3 Adjusted odds ratio (95% confidence interval) of sensitivity to THs and risk of MetS and its components.

	Crude model			Model 1			Model 2		
	OR	95%CI	P-value	OR	95%CI	P-value	OR	95%CI	P-value
MetS									
TFQI (+1 SD)	1.34	1.29, 1.40	<0.001	1.21	1.16, 1.26	<0.001	1.20	1.15, 1.25	<0.001
PTFQI (+1 SD)	1.35	1.30, 1.41	<0.001	1.26	1.21, 1.31	<0.001	1.28	1.23, 1.33	<0.001
TSHI (+1 SD)	1.37	1.30, 1.43	<0.001	1.34	1.27, 1.40	<0.001	1.35	1.29, 1.42	<0.001
TT4RI (+1 SD)	1.44	1.36, 1.53	<0.001	1.52	1.43, 1.62	<0.001	1.57	1.47, 1.67	<0.001
FT3/FT4 (+1 SD)	1.28	1.23, 1.34	<0.001	1.17	1.12, 1.22	<0.001	1.17	1.12, 1.23	<0.001
Elevated WC									
TFQI (+1 SD)	1.08	1.04, 1.11	<0.001	0.99	0.96, 1.03	0.710	0.99	0.95, 1.02	0.481
PTFQI (+1 SD)	1.07	1.04, 1.11	<0.001	1.03	0.99, 1.06	0.107	1.03	1.00, 1.07	0.059
TSHI (+1 SD)	1.05	1.01, 1.09	0.016	1.02	0.98, 1.06	0.319	1.02	0.98, 1.07	0.269
TT4RI (+1 SD)	1.05	0.99, 1.11	0.083	1.06	1.01, 1.12	0.045	1.07	1.01, 1.13	0.024
FT3/FT4 (+1 SD)	1.30	1.25, 1.35	<0.001	1.30	1.25, 1.36	<0.001	1.31	1.26, 1.36	<0.001
Elevated BP									
TFQI (+1 SD)	1.25	1.20, 1.29	<0.001	1.11	1.07, 1.15	<0.001	1.11	1.07, 1.15	<0.001
PTFQI (+1 SD)	1.13	1.10, 1.17	<0.001	1.06	1.02, 1.10	0.003	1.06	1.02, 1.10	0.002
TSHI (+1 SD)	1.15	1.10, 1.20	<0.001	1.11	1.06, 1.16	<0.001	1.11	1.07, 1.16	<0.001
TT4RI (+1 SD)	1.08	1.02, 1.14	0.005	1.11	1.05, 1.17	<0.001	1.12	1.05, 1.18	<0.001
FT3/FT4 (+1 SD)	1.26	1.21, 1.31	<0.001	1.20	1.15, 1.25	<0.001	1.20	1.15, 1.25	<0.001
Low HDL-C									
TFQI (+1 SD)	1.03	0.98, 1.09	0.269	1.12	1.04, 1.18	<0.001	1.15	1.08, 1.21	<0.001
PTFQI (+1 SD)	1.14	1.08, 1.20	<0.001	1.03	0.98, 1.09	0.213	1.06	1.01, 1.11	0.049
TSHI (+1 SD)	1.03	0.96, 1.09	0.418	0.99	0.93, 1.06	0.822	1.11	1.02, 1.16	<0.001
TT4RI (+1 SD)	1.00	0.92, 1.09	0.934	1.05	0.96, 1.14	0.288	1.10	1.01, 1.20	0.042
FT3/FT4 (+1 SD)	1.45	1.37, 1.53	<0.001	1.22	1.15, 1.29	<0.001	1.21	1.14, 1.29	<0.001
Elevated TG									
TFQI (+1 SD)	1.08	1.05, 1.12	<0.001	0.97	0.94, 1.01	0.098	1.12	1.04,1.18	<0.001
PTFQI (+1 SD)	1.16	1.12, 1.20	<0.001	1.07	1.03, 1.11	<0.001	1.08	1.04, 1.12	<0.001
TSHI (+1 SD)	1.10	1.06, 1.15	<0.001	1.08	1.03, 1.13	<0.001	1.09	1.04, 1.13	<0.001
TT4RI (+1 SD)	1.11	1.05, 1.17	<0.001	1.17	1.10, 1.23	<0.001	1.19	1.12, 1.26	<0.001
FT3/FT4 (+1 SD)	1.47	1.41, 1.53	<0.001	1.27	1.21, 1.32	<0.001	1.27	1.22, 1.33	<0.001
Elevated FPG									
TFQI (+1 SD)	1.25	1.21, 1.30	<0.001	1.11	1.07, 1.15	<0.001	1.10	1.06, 1.15	<0.001
PTFQI (+1 SD)	1.09	1.06, 1.13	<0.001	1.01	0.98, 1.05	0.492	1.09	1.03, 1.15	<0.001
TSHI (+1 SD)	1.12	1.07, 1.16	<0.001	1.07	1.03, 1.12	0.002	1.08	1.03, 1.13	<0.001
TT4RI (+1 SD)	1.04	0.98, 1.10	0.221	1.05	0.99, 1.12	0.092	1.07	1.01, 1.14	0.027
FT3/FT4 (+1 SD)	1.07	1.03, 1.11	<0.001	1.02	0.98, 1.07	0.266	1.03	0.99, 1.07	0.158

Model 1: adjusted for age and sex.
Model 2: adjusted for age, sex, smoking, drinking, BMI and NLR.

10.3389/fendo.2025.1552484

TABLE 4 Association of sensitivity to thyroid hormones and MetSSS quartiles.

	MetSSS quartiles							P for trend
	Q1	Q2		Q3		Q4		
		OR (95% CI)	P-value	OR (95% CI)	P-value	OR (95% CI)	P-value	
TSHI (+1 SD)	Ref.	1.07 (1.01~1.13)	0.016	1.06 (1.01~1.12)	0.032	1.13 (1.06~1.19)	<0.001	<0.001
TT4RI (+1 SD)	Ref.	1.07 (0.99~1.15)	0.071	1.10 (1.02~1.19)	0.013	1.25 (1.15~1.35)	<0.001	<0.001
TFQI (+1 SD)	Ref.	1.05 (1.00~1.10)	0.053	1.00 (0.96~1.05)	0.935	1.16 (1.07~1.21)	<0.001	<0.001
PTFQI (+1 SD)	Ref.	1.03 (0.98~1.08)	0.231	1.04 (1.00~1.09)	0.082	1.12 (1.06~1.17)	<0.001	<0.001
FT3/FT4 (+1 SD)	Ref.	1.31 (1.24~1.39)	<0.001	1.62 (1.53~1.71)	<0.001	1.82 (1.72~1.93)	<0.001	<0.001

turn, triggers the activity of sterol regulatory element-binding protein (SREBP) 1c in the liver, promoting the expression of genes related to fat formation (39). SREBP is a transcription factor that positively regulates the expression of LDLR and cholesterol synthesis, with T3 mediating cholesterol synthesis through SREBP-1 and SREBP-2 (40, 41). These established mechanisms illustrate the close connection between THs sensitivity and dyslipidemia. Another study conducted on a cross-sectional basis found that the TFQI was linked to a higher prevalence of diabetes in both 2296 euthyroid adults in America and 8319 euthyroid adults in China (42). It has been noted that TSH can stimulate the secretion of leptin in human adipose tissue, which in turn reduces insulin secretion and synthesis in pancreatic β-cells. Therefore, the combined index TFQI, which takes into account both TSH and FT3, may offer a more accurate indication of the risk of developing diabetes compared to individual indices in individuals with normal TSH, FT3, and FT4 levels.

Furthermore, several studies have suggested that THs can directly and indirectly influence blood pressure. Insensitivity to THs can result in a decrease in the dilation of arterial smooth muscle, availability of nitric oxide, and endothelium-dependent vasodilation (43–45). A recent study also found a positive association between decreased central sensitivity to THs and visceral adipose tissue (46), which aligns with our findings. Disorders in THs sensitivity can disrupt the body's metabolic balance, affecting the functioning of adipose tissue. While THs typically stimulate both brown and white adipose tissue, promoting thermogenesis and energy expenditure, impaired thyroid hormone sensitivity can lead to reduced activity in brown adipose tissue and impaired browning of white adipose tissue, resulting in decreased

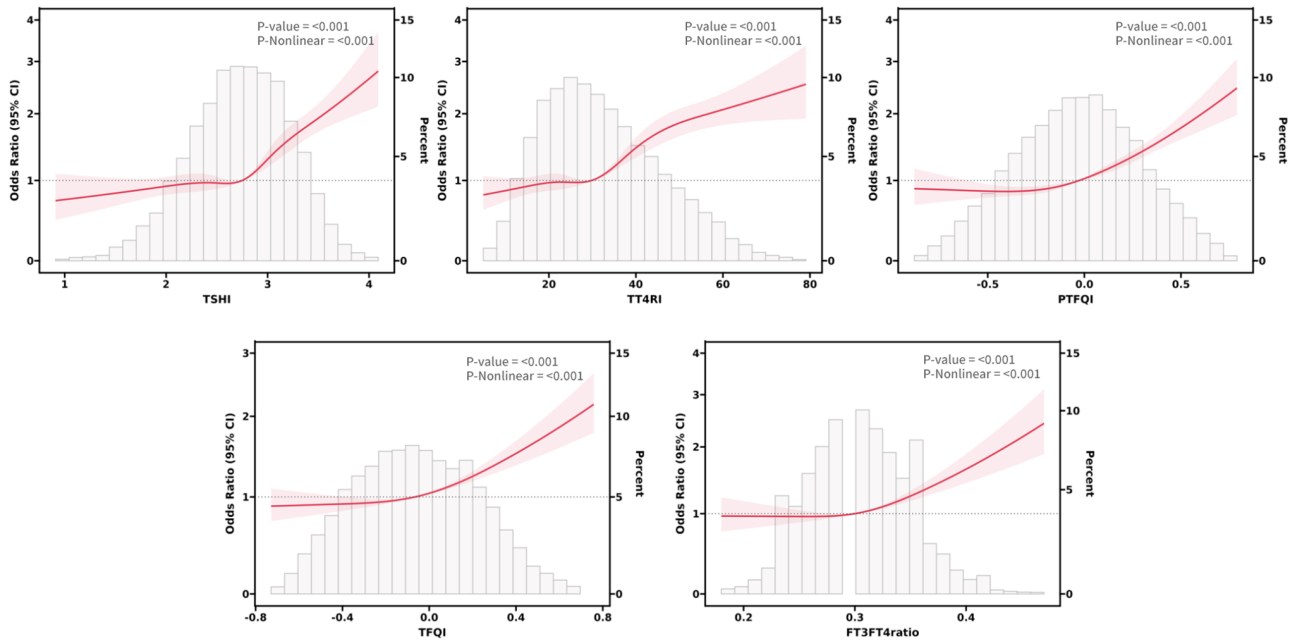

FIGURE 2
The smooth curve fitting between sensitivity to THs indicators and MetS. Solid red lines and red areas on both sides represent ORs and their 95%CI.

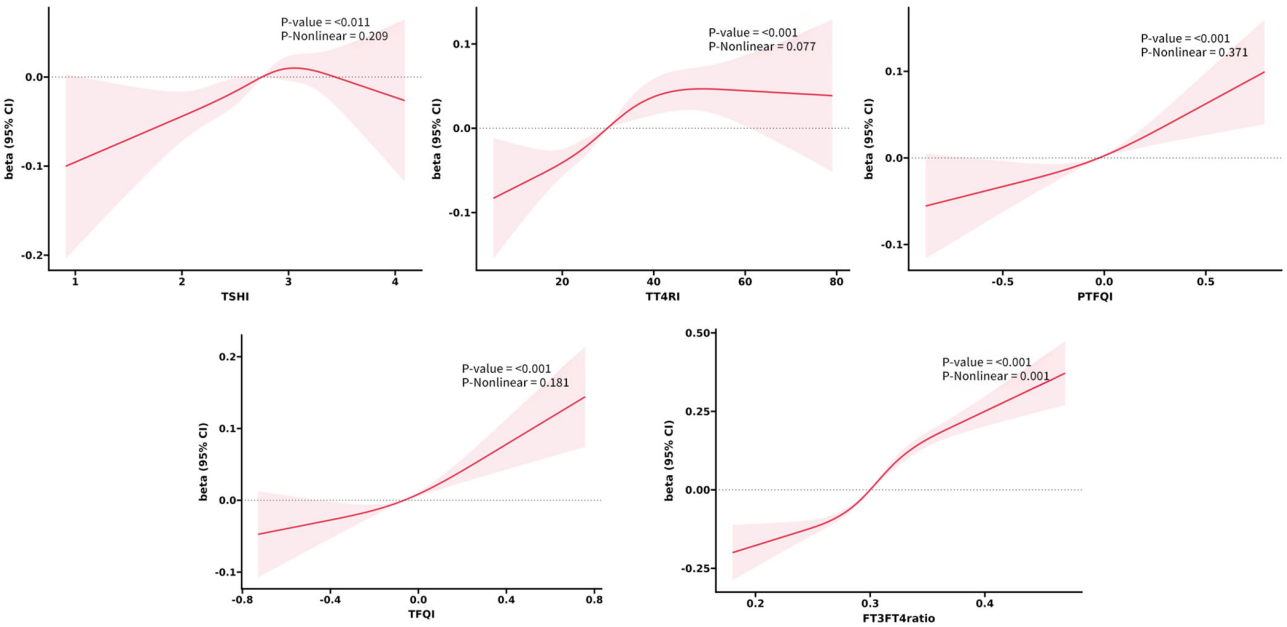

FIGURE 3
The smooth curve fitting between sensitivity to THs indicators and MetSSS. Solid red lines and red areas on both sides represent the estimated regression coefficient Beta and its 95% confidence interval.

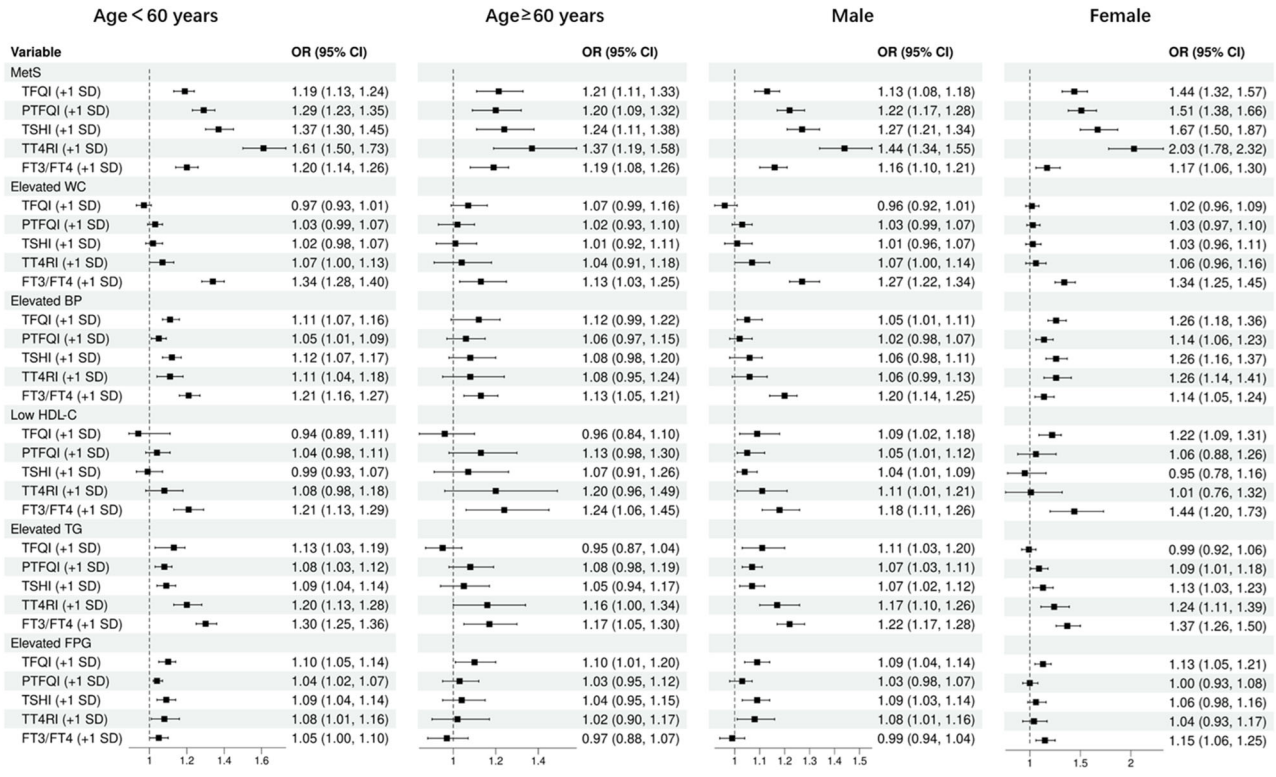

FIGURE 4
Subgroup analysis by age and gender.

energy expenditure and a tendency for fat accumulation, particularly in the abdominal region (47, 48).

Previous studies examining the relationship between the FT3/FT4 ratio and MetS have produced conflicting results. A recent cross-sectional study found that lower FT3/FT4 levels were linked to MetS components,[42] contradicting our findings. Greet et al. discovered a positive association between FT3, FT4, and the FT3/FT4 ratio with MetS components (49). Shon et al. observed a negative correlation between FT4 levels within the normal range and BMI (50). Roos et al. reported associations between low normal FT4 levels and increased insulin resistance and an unfavorable lipid profile in euthyroid adults (51). In a study involving 3,148 subjects, it was found that higher levels of FT4 were associated with higher levels of HDL cholesterol and lower levels of waist circumference, insulin resistance, and insulin (52). Additionally, previous studies have shown that higher levels of fT3 are linked to increased body fat mass and various metabolic parameters. A higher ratio of fT3 to fT4 has been associated with a less favorable metabolic profile and increased placental growth in pregnant women (53). Research has suggested that individuals with higher fat mass and/or less favorable metabolic profiles may have increased activity of deiodinase (DIO) 1 and/or 2, leading to higher conversion of fT4 to fT3 (54). This enhanced sensitivity to thyroid hormones can impact metabolic rate, glucose absorption and utilization, and lipid metabolism, potentially leading to fluctuations in blood sugar and lipid levels (55). It may also worsen insulin resistance, affect insulin signaling pathways, and increase cardiovascular activity, all of which are characteristics of metabolic syndrome. Essentially, an excessive response to normal thyroid hormone levels may increase the risk of developing metabolic abnormalities associated with MetS.

To further elaborate on the intricate relationship between thyroid function and metabolic regulation, it is essential to consider the role of circadian rhythms. Emerging evidence underscores the bidirectional interplay between thyroid hormones and circadian clocks (56). The hypothalamus-pituitary-thyroid axis demonstrates circadian oscillation, with thyroid hormone secretion orchestrated by both central and peripheral clocks. In turn, thyroid hormones modulate clock gene rhythmicity. Notably, triiodothyronine (T3) acts as a temporal cue for the central circadian clock by enhancing Bmal1 promoter activity, ensuring optimal metabolic regulation (57). Conversely, circadian disruptions, such as those in hypothyroidism, alter suprachiasmatic nucleus clock gene expression and impact metabolic parameters like oxygen consumption and body temperature, potentially contributing to metabolic syndrome (58). Importantly, aligning circadian rhythms through strategies like time-restricted feeding can restore metabolic health and enhance thyroid hormone signaling, underscoring the importance of circadian integrity in thyroid-metabolism axis regulation (59, 60). This interplay between circadian rhythms and thyroid function provides a more comprehensive framework for understanding metabolic regulation and suggests potential therapeutic avenues for addressing metabolic disorders.

The clinical importance of our study's results lies in its potential to improve the understanding and management of MetS in euthyroid individuals. By identifying the association between thyroid hormone sensitivity and MetS risk, clinicians can consider evaluating thyroid function more comprehensively using indices like TFQI and FT3/FT4 ratio, rather than relying solely on traditional markers such as TSH, FT3, and FT4. This approach may allow for earlier identification of individuals at risk of MetS, enabling timely interventions to prevent or delay the onset of metabolic complications. Additionally, the findings highlight the need for further research into the therapeutic potential of modulating thyroid hormone sensitivity as a strategy for MetS management.

There were several limitations that should be acknowledged. Firstly, the cross-sectional design restricts the ability to establish a cause-and-effect relationship between thyroid hormone sensitivity indices and MetS. Additionally, the generalizability of the findings may be limited as the study was conducted in a Chinese population and may not be applicable to other ethnicities or regions. Lastly, the study did not consider all potential confounding factors, such as diet patterns or physical activity levels, that could impact the relationship between TH sensitivity and MetS.

Conclusion

In summary, this study presents evidence of a significant correlation between impaired thyroid hormone sensitivity and MetS, along with its severity, in euthyroid adults. The relationships with waist circumference, dyslipidemia, hyperglycemia, and hypertension emphasize the possible involvement of thyroid hormones in the pathogenesis of MetS. Future investigations should take into account thyroid hormone sensitivity indices when assessing MetS risk and further explore the mechanisms that drive these associations.

Data availability statement

The raw data supporting the conclusions of this article will be made available by the authors, without undue reservation.

Ethics statement

The studies involving humans were approved by ethics committee of Health Examination Center of Wuxi people's hospital. The studies were conducted in accordance with the local legislation and institutional requirements. The ethics committee/institutional review board waived the requirement of written informed consent for participation from the participants or the participants' legal guardians/next of kin because this study is retrospectively designed.

Author contributions

XZ: Formal Analysis, Software, Validation, Writing – original draft. YZ: Funding acquisition, Resources, Writing – review & editing. ZL: Conceptualization, Methodology, Software, Visualization, Writing – review & editing.

Funding

The author(s) declare that financial support was received for the research and/or publication of this article. This research was supported by the "The role and mechanism of Brix 1 in colorectal cancer" program (No. BJRC-9) from the city's "double hundred" top plan.

Acknowledgments

We also thank all staff involved in this study for their painstaking efforts in conducting the data collection.

Conflict of interest

The authors declare that the research was conducted in the absence of any commercial or financial relationships that could be construed as a potential conflict of interest.

Generative AI statement

The author(s) declare that no Generative AI was used in the creation of this manuscript.

Publisher's note

References

1. Alberti KG, Eckel RH, Grundy SM, Zimmet PZ, Cleeman JI, Donato KA, et al. Harmonizing the metabolic syndrome: a joint interim statement of the International Diabetes Federation Task Force on Epidemiology and Prevention; National Heart, Lung, and Blood Institute; American Heart Association; World Heart Federation; International Atherosclerosis Society; and International Association for the Study of Obesity. *Circulation*. (2009) 120:1640–5. doi: 10.1161/CIRCULATIONAHA.109.192644

2. Ford ES, Li C, Zhao G, Pearson WS, Mokdad AH. Prevalence of the metabolic syndrome among U.S. adolescents using the definition from the International Diabetes Federation. *Diabetes Care*. (2008) 31:587–9. doi: 10.2337/dc07-1030

3. Castaneda G, Bhuket T, Liu B, Wong RJ. Low serum high density lipoprotein is associated with the greatest risk of metabolic syndrome among U.S. adults. *Diabetes Metab Syndr*. (2018) 12:5–8. doi: 10.1016/j.dsx.2017.08.002

4. Li W, Song F, Wang X, Wang L, Wang D, Yin X, et al. Prevalence of metabolic syndrome among middle-aged and elderly adults in China: current status and temporal trends. *Ann Med*. (2018) 50:345–53. doi: 10.1080/07853890.2018.1464202

5. Sinha RA, Yen PM. Metabolic messengers: thyroid hormones. *Nat Metab*. (2024) 6:639–50. doi: 10.1038/s42255-024-00986-0

6. Gnocchi D, Steffensen KR, Bruscalupi G, Parini P. Emerging role of thyroid hormone metabolites. *Acta Physiol (Oxf)*. (2016) 217:184–216. doi: 10.1111/apha.12648

7. Mehran L, Amouzegar A, Azizi F. Thyroid disease and the metabolic syndrome. *Curr Opin Endocrinol Diabetes Obes*. (2019) 26:256–65. doi: 10.1097/MED.0000000000000500

8. Iwen KA, Schroder E, Brabant G. Thyroid hormones and the metabolic syndrome. *Eur Thyroid J*. (2013) 2:83–92. doi: 10.1159/000351249

9. Mullur R, Liu YY, Brent GA. Thyroid hormone regulation of metabolism. *Physiol Rev*. (2014) 94:355–82. doi: 10.1152/physrev.00030.2013

10. Cheng SY, Leonard JL, Davis PJ. Molecular aspects of thyroid hormone actions. *Endocr. Rev*. (2010) 31:139–70. doi: 10.1210/er.2009-0007

11. Ortiga-Carvalho TM, Sidhaye AR, Wondisford FE. Thyroid hormone receptors and resistance to thyroid hormone disorders. *Nat Rev Endocrinol*. (2014) 10:582–91. doi: 10.1038/nrendo.2014.143

12. Duntas LH, Brenta G. A renewed focus on the association between thyroid hormones and lipid metabolism. *Front Endocrinol (Lausanne)*. (2018) 9:511. doi: 10.3389/fendo.2018.00511

13. Chang YC, Hua SC, Chang CH, Kao WY, Lee HL, Chuang LM, et al. High TSH level within normal range is associated with obesity, dyslipidemia, hypertension, inflammation, hypercoagulability, and the metabolic syndrome: A novel cardiometabolic marker. *J Clin Med*. (2019) 8(6):1–15. doi: 10.3390/jcm8060817

14. Ruhla S, Weickert MO, Arafat AM, Osterhoff M, Isken F, Spranger J, et al. A high normal TSH is associated with the metabolic syndrome. *Clin Endocrinol (Oxf)*. (2010) 72:696–701. doi: 10.1111/j.1365-2265.2009.03698.x

15. Mehran L, Delbari N, Amouzegar A, Hasheminia Tohidi M, Azizi MF. Reduced sensitivity to thyroid hormone is associated with diabetes and hypertension. *J Clin Endocrinol Metab*. (2022) 107:167–76. doi: 10.1210/clinem/dgab646

16. Kim BJ, Kim TY, Koh JM, Kim HK, Park JY, Lee KU, et al. Relationship between serum free T4 (FT4) levels and metabolic syndrome (MS) and its components in healthy euthyroid subjects. *Clin Endocrinol (Oxf)*. (2009) 70:152–60. doi: 10.1111/j.1365-2265.2008.03304.x

17. Asvold BO, Bjoro T, Vatten LJ. Association of serum TSH with high body mass differs between smokers and never-smokers. *J Clin Endocrinol Metab*. (2009) 94:5023–7. doi: 10.1210/jc.2009-1180

18. Nam JS, Cho M, Park JS, Ahn CW, Cha BS, Lee EJ, et al. Triiodothyronine level predicts visceral obesity and atherosclerosis in euthyroid, overweight and obese subjects: T3 and visceral obesity. *Obes Res Clin Pract*. (2010) 4:e247–342. doi: 10.1016/j.orcp.2010.08.003

19. Friedrich N, Rosskopf D, Brabant G, Volzke H, Nauck M, Wallaschofski H. Associations of anthropometric parameters with serum TSH, prolactin, IGF-I, and testosterone levels: results of the study of health in Pomerania (SHIP). *Exp Clin Endocrinol Diabetes*. (2010) 118:266–73. doi: 10.1055/s-0029-1225616

20. Laclaustra M, Moreno-Franco B, Lou-Bonafonte JM, Mateo-Gallego R, Casasnovas JA, Guallar-Castillon P, et al. Impaired sensitivity to thyroid hormones is associated with diabetes and metabolic syndrome. *Diabetes Care*. (2019) 42:303–10. doi: 10.2337/dc18-1410

21. Alkemade A. Central and peripheral effects of thyroid hormone signalling in the control of energy metabolism. *J Neuroendocrinol*. (2010) 22:56–63. doi: 10.1111/j.1365-2826.2009.01932.x

22. Bianco AC, Dumitrescu A, Gereben B, Ribeiro MO, Fonseca TL, Fernandes GW, et al. Paradigms of dynamic control of thyroid hormone signaling. *Endocr Rev*. (2019) 40:1000–47. doi: 10.1210/er.2018-00275

23. Yagi H, Pohlenz J, Hayashi Y, Sakurai A, Refetoff S. Resistance to thyroid hormone caused by two mutant thyroid hormone receptors beta, R243Q and R243W, with marked impairment of function that cannot be explained by altered *in vitro* 3,5,3'-triiodothyroinine binding affinity. *J Clin Endocrinol Metab*. (1997) 82:1608–14. doi: 10.1210/jcem.82.5.3945

24. Jostel A, Ryder WD, Shalet SM. The use of thyroid function tests in the diagnosis of hypopituitarism: definition and evaluation of the TSH Index. *Clin Endocrinol (Oxf)*. (2009) 71:529–34. doi: 10.1111/j.1365-2265.2009.03534.x

25. Liu B, Wang Z, Fu J, Guan H, Lyu Z, Wang W. Sensitivity to thyroid hormones and risk of prediabetes: A cross-sectional study. *Front Endocrinol (Lausanne)*. (2021) 12:657114. doi: 10.3389/fendo.2021.657114

26. Di Bonito P, Corica D, Marzuillo P, Di Sessa A, Licenziati MR, Faienza MF, et al. Sensitivity to thyroid hormones and reduced glomerular filtration in children and

adolescents with overweight or obesity. *Horm Res Paediatr*. (2024) 97(4):383–7. doi: 10.1159/000534472

27. Sun Y, Teng D, Zhao L, Shi X, Li Y, Shan Z, et al. Impaired sensitivity to thyroid hormones is associated with hyperuricemia, obesity, and cardiovascular disease risk in subjects with subclinical hypothyroidism. *Thyroid*. (2022) 32:376–84. doi: 10.1089/thy.2021.0500

28. Wang L, Peng W, Zhao Z, Zhang M, Shi Z, Song Z, et al. Prevalence and treatment of diabetes in China, 2013-2018. *JAMA*. (2021) 326:2498–506. doi: 10.1001/jama.2021.22208

29. Wang JG, Zhang W, Li Y, Liu L. Hypertension in China: epidemiology and treatment initiatives. *Nat Rev Cardiol*. (2023) 20:531–45. doi: 10.1038/s41569-022-00829-z

30. Bahar A, Kashi Z, Kheradmand M, Hedayatizadeh-Omran A, Moradinazar M, Ramezani F, et al. Prevalence of metabolic syndrome using international diabetes federation, National Cholesterol Education Panel- Adult Treatment Panel III and Iranian criteria: results of Tabari cohort study. *J Diabetes Metab Disord*. (2020) 19:205–11. doi: 10.1007/s40200-020-00492-6

31. de la Iglesia R, Lopez-Legarrea P, Abete I, Bondia-Pons I, Navas-Carretero S, Forga L, et al. A new dietary strategy for long-term treatment of the metabolic syndrome is compared with the American Heart Association (AHA) guidelines: the MEtabolic Syndrome REduction in NAvarra (RESMENA) project. *Br J Nutr*. (2014) 111:643–52. doi: 10.1017/S0007114513002778

32. Yang S, Yu B, Yu W, Dai S, Feng C, Shao Y, et al. Development and validation of an age-sex-ethnicity-specific metabolic syndrome score in the Chinese adults. *Nat Commun*. (2023) 14:6988. doi: 10.1038/s41467-023-42423-y

33. Mavromati M, Jornayvaz FR. Hypothyroidism-associated dyslipidemia: potential molecular mechanisms leading to NAFLD. *Int J Mol Sci*. (2021) 22(23):1–14. doi: 10.3390/ijms222312797

34. Koppeschaar HP, Meinders AE, Schwarz F. Metabolic responses during modified fasting and refeeding. The role of sympathetic nervous system activity and thyroid hormones. *Hum Nutr Clin Nutr*. (1985) 39:17–28.

35. Liu Y, Ma M, Li L, Liu F, Li Z, Yu L, et al. Association between sensitivity to thyroid hormones and dyslipidemia in patients with coronary heart disease. *Endocrine*. (2023) 79:459–68. doi: 10.1007/s12020-022-03254-x

36. Sun H, Zhu W, Liu J, An Y, Wang Y, Wang G. Reduced sensitivity to thyroid hormones is associated with high remnant cholesterol levels in chinese euthyroid adults. *J Clin Endocrinol Metab*. (2022) 108:166–74. doi: 10.1210/clinem/dgac523

37. Yuan C, Sun X, Liu Y, Wu J. The thyroid hormone levels and glucose and lipid metabolism in children with type 1 diabetes: a correlation analysis. *Transl Pediatr*. (2021) 10:276–82. doi: 10.21037/tp-20-204

38. Lei Y, Yang J, Li H, Zhong H, Wan Q. Changes in glucose-lipid metabolism, insulin resistance, and inflammatory factors in patients with autoimmune thyroid disease. *J Clin Lab Anal*. (2019) 33:e22929. doi: 10.1002/jcla.22929

39. Delitala AP, Delitala G, Sioni P, Fanciulli G. Thyroid hormone analogs for the treatment of dyslipidemia: past, present, and future. *Curr Med Res Opin*. (2017) 33:1985–93. doi: 10.1080/03007995.2017.1330259

40. Cho S, Lee HJ, Shim JS, Song BM, Kim HC. Associations between age and dyslipidemia are differed by education level: The Cardiovascular and Metabolic Diseases Etiology Research Center (CMERC) cohort. *Lipids Health Dis*. (2020) 19:12. doi: 10.1186/s12944-020-1189-y

41. Tognini S, Polini A, Pasqualetti G, Ursino S, Caraccio N, Ferdeghini M, et al. Age and gender substantially influence the relationship between thyroid status and the lipoprotein profile: results from a large cross-sectional study. *Thyroid*. (2012) 22:1096–103. doi: 10.1089/thy.2012.0013

42. Wan H, Yu G, He Y, Liu S, Chen X, Jiang Y, et al. Associations of thyroid feedback quantile-based index with diabetes in euthyroid adults in the United States and China. *Ann Med*. (2024) 56:2318418. doi: 10.1080/07853890.2024.2318418

43. Fernandez-Real JM, Lopez-Bermejo A, Castro A, Casamitjana R, Ricart W. Thyroid function is intrinsically linked to insulin sensitivity and endothelium-dependent vasodilation in healthy euthyroid subjects. *J Clin Endocrinol Metab*. (2006) 91:3337–43. doi: 10.1210/jc.2006-0841

44. Gu Y, Zheng L, Zhang Q, Liu L, Meng G, Yao Z, et al. Relationship between thyroid function and elevated blood pressure in euthyroid adults. *J Clin Hypertens (Greenwich)*. (2018) 20:1541–9. doi: 10.1111/jch.13369

45. Mehran L, Delbari N, Amouzegar A, Hasheminia M, Tohidi M, Azizi F. Reduced sensitivity to thyroid hormone is associated with diabetes and hypertension. *J Clin Endocrinol Metab*. (2022) 107:167–76. doi: 10.1210/clinem/dgab646

46. Lv F, Cai X, Li Y, Zhang X, Zhou X, Han X, et al. Sensitivity to thyroid hormone and risk of components of metabolic syndrome in a Chinese euthyroid population. *J Diabetes*. (2023) 15:900–10. doi: 10.1111/1753-0407.13441

47. Petito G, Cioffi F, Magnacca N, de Lange P, Senese R, Lanni A. Adipose tissue remodeling in obesity: an overview of the actions of thyroid hormones and their derivatives. *Pharmaceuticals (Basel)*. (2023) 16(4):1–17. doi: 10.3390/ph16040572

48. Volke L, Krause K. Effect of thyroid hormones on adipose tissue flexibility. *Eur Thyroid J*. (2021) 10:1–9. doi: 10.1159/000508483

49. Roef GL, Rietzschel ER, Van Daele CM, Taes YE, De Buyzere ML, Gillebert TC, et al. Triiodothyronine and free thyroxine levels are differentially associated with metabolic profile and adiposity-related cardiovascular risk markers in euthyroid middle-aged subjects. *Thyroid*. (2014) 24:223–31. doi: 10.1089/thy.2013.0314

50. Shon HS, Jung ED, Kim SH, Lee JH. Free T4 is negatively correlated with body mass index in euthyroid women. *Korean J Intern Med*. (2008) 23:53–7. doi: 10.3904/kjim.2008.23.2.53

51. Roos A, Bakker SJ, Links TP, Gans RO, Wolffenbuttel BH. Thyroid function is associated with components of the metabolic syndrome in euthyroid subjects. *J Clin Endocrinol Metab*. (2007) 92:491–6. doi: 10.1210/jc.2006-1718

52. Garduno-Garcia J, Alvirde-Garcia U, Lopez-Carrasco G, Padilla MM, Mehta R, Arellano-Campos O, et al. TSH and free thyroxine concentrations are associated with differing metabolic markers in euthyroid subjects. *Eur J Endocrinol*. (2010) 163:273–8. doi: 10.1530/EJE-10-0312

53. Bassols J, Prats-Puig A, Soriano-Rodriguez P, Garcia-Gonzalez MM, Reid J, Martinez-Pascual M, et al. Lower free thyroxin associates with a less favorable metabolic phenotype in healthy pregnant women. *J Clin Endocrinol Metab*. (2011) 96:3717–23. doi: 10.1210/jc.2011-1784

54. Yang L, Sun X, Tao H, Zhao Y. The association between thyroid homeostasis parameters and obesity in subjects with euthyroidism. *J Physiol Pharmacol*. (2023) 74(1):69–75. doi: 10.26402/jpp.2023.1.07

55. Corica D, Licenziati MR, Calcaterra V, Curro M, Di Mento C, Curatola S, et al. Central and peripheral sensitivity to thyroid hormones and glucose metabolism in prepubertal children with obesity: pilot multicenter evaluation. *Endocrine*. (2023) 80:308–11. doi: 10.1007/s12020-022-03276-5

56. Gnocchi D, Bruscalupi G. Circadian rhythms and hormonal homeostasis: pathophysiological implications. *Biol (Basel)*. (2017) 6(1):1–20. doi: 10.3390/biology6010010

57. Gnocchi D, Custodero C, Sabba C, Mazzocca A. Circadian rhythms: a possible new player in non-alcoholic fatty liver disease pathophysiology. *J Mol Med (Berl)*. (2019) 97:741–59. doi: 10.1007/s00109-019-01780-2

58. Emrich F, Gomes BH, Selvatici-Tolentino L, Lopes RA, Secio-Silva A, Carvalho-Moreira JP, et al. Hypothyroidism alters the rhythmicity of the central clock, body temperature and metabolism: evidence of Bmal1 transcriptional regulation by T3. *J Physiol*. (2024) 602:4865–87. doi: 10.1113/JP286449

59. Helbling JC, Ginieis R, Mortessagne P, Ruiz-Gayo M, Bakoyiannis I, Ducourneau EG, et al. Time-restricted feeding prevents memory impairments induced by obesogenic diet consumption, via hippocampal thyroid hormone signaling. *Mol Metab*. (2024) 90:102061. doi: 10.1016/j.molmet.2024.102061

60. Lincoln K, Zhou J, Oster H, de Assis L. Circadian gating of thyroid hormone action in hepatocytes. *Cells*. (2024) 13(12):1–13. doi: 10.3390/cells13121038

frontiers | Frontiers in Endocrinology

TYPE Perspective
PUBLISHED 29 May 2025
DOI 10.3389/fendo.2025.1576419

OPEN ACCESS

EDITED BY
Prem Prakash Kushwaha,
Case Western Reserve University,
United States

REVIEWED BY
Saurabh Mishra,
Cleveland Clinic, United States

*CORRESPONDENCE
Wojciech Łukowski
Wlukowski@gmail.com

RECEIVED 13 February 2025
ACCEPTED 28 April 2025
PUBLISHED 29 May 2025

CITATION
Łukowski W (2025) Reframing type 1 diabetes through the endocannabinoidome-microbiota axis: a systems biology perspective. *Front. Endocrinol.* 16:1576419. doi: 10.3389/fendo.2025.1576419

Reframing type 1 diabetes through the endocannabinoidome-microbiota axis: a systems biology perspective

Wojciech Łukowski*

CARE FOR T1D, Bydgoszcz, Poland

Type 1 diabetes (T1D) has long been recognized as a T-cell-driven autoimmune disease. However, growing evidence highlights the involvement of metabolic, inflammatory, and gut microbiota-related factors in its progression. The endocannabinoid system (ECS), a key regulator of immune and metabolic homeostasis, has been increasingly implicated in autoimmune pathophysiology, particularly through its interactions with gut-derived metabolites. This hypothesis article underscores the need to reframe T1D pathophysiology by integrating ECS dysfunction, gut dysbiosis, and metabolic imbalances into a systems biology framework. The proposed Endocannabinoidome-Microbiota (ECBoM) model highlights a shared hallmark of autoimmunity—SCFA depletion, increased intestinal permeability, and ECS dysregulation—as key drivers of chronic inflammation and immune dysfunction. These disturbances, observed in T1D as well as in celiac disease, Hashimoto's thyroiditis, rheumatoid arthritis, and multiple sclerosis, suggest a common immune-metabolic axis across autoimmune disorders. Recognizing ECS dysregulation as a systemic feature of autoimmunity opens avenues for novel therapeutic interventions, including ECS-targeted treatments, microbiota modulation, and phytocannabinoid-based therapies. This article highlights the necessity of conducting large-scale, multi-omics studies to establish disease-specific ECS signatures, linking endocannabinoid profiling, microbiota composition, and metabolic biomarkers to disease progression. By advocating for a paradigm shift in T1D research, this article emphasizes the importance of exploring new mechanistic references to develop targeted, immune-metabolic interventions that could reshape treatment strategies and improve clinical outcomes in T1D and related autoimmune diseases.

KEYWORDS

type 1 diabetes (T1D), endocannabinoid system (ECS), gut microbiota, autoimmune diseases, intestinal permeability, metabolic dysregulation, short-chain fatty acids, TRPV

Introduction

Type 1 diabetes (T1D) is a multifactorial autoimmune disease arising from a complex interplay between genetic susceptibility, environmental factors, and immune dysregulation (1). While considerable progress has been made in elucidating the genetic and immunological underpinnings of T1D, current models fail to fully explain the mechanisms initiating the breakdown of tolerance toward pancreatic β-cells (1, 2). In recent years, growing attention has focused on the endocannabinoid system (ECS) and gut microbiota as two dynamic, interconnected regulators of immune and metabolic homeostasis (3, 4).

The ECS is an evolutionarily conserved lipid-based signaling system composed of endocannabinoids such as anandamide (AEA) and 2-arachidonoylglycerol (2-AG), their receptors (CB1, CB2, TRPV1), and associated metabolic enzymes (FAAH, MAGL, DAGL) (5, 6). Unlike classical neurotransmitters or hormones, endocannabinoids are synthesized on demand, locally, in response to cellular stress or inflammatory stimuli (7). This system acts as a local buffer, fine-tuning immune responses, intestinal barrier integrity, and cellular stress adaptation (8, 9).

Emerging evidence indicates a bidirectional relationship between ECS signaling and gut microbiota composition, forming a regulatory axis known as the endocannabinoidome–microbiota axis (ECBoM) (3, 4). Gut dysbiosis has been shown to disrupt ECS tone through reduced production of short-chain fatty acids (SCFAs) and increased translocation of microbial-derived lipopolysaccharides (LPS), leading to chronic ECS overstimulation (10–12). This dysregulation, in turn, impairs intestinal barrier integrity, promotes systemic inflammation, and affects immune tolerance (9, 11, 13).

In this work, we propose a novel sequential model of T1D pathogenesis, grounded in molecular ECS-microbiota interactions, that links gut dysbiosis to β-cell autoimmunity, as pictured in the Figure 1. This model outlines a stepwise cascade:

Gut dysbiosis → SCFA depletion (4, 10)→ compensatory 2-AG overproduction → ECS overstimulation (3, 14)→ CB2 and TRPV1 receptor desensitization (15–18) → increased intestinal permeability ("leaky gut") (11, 13)→ systemic inflammation (19)→ immune ECS dysregulation due to excess 2-AG → disruption of the blood–pancreas barrier by ECS dysregulation → infiltration of inflammatory mediators into pancreatic islets → ECS dysregulation in pancreatic β-cells → closure of GDDC and VDCC calcium channels → impaired calcium influx into β-cells → suppression of insulin secretion → activation of β-cell apoptotic pathways → autoimmune targeting and destruction of β-cells (1, 20, 21).

This mechanistic framework integrates existing findings on ECS and microbiota into a coherent, testable hypothesis that may explain the early molecular events triggering T1D in genetically predisposed individuals. Furthermore, it highlights new therapeutic and preventive avenues by targeting ECS-microbiota balance to maintain immunometabolic homeostasis.

Endocannabinoid system and microbiota interactions

The endocannabinoid system (ECS) is an evolutionarily conserved lipid-signaling system extensively involved in maintaining homeostasis across multiple physiological processes, including metabolism, inflammation, immunity, and gut function (5, 22). Unlike classical neurotransmitters or circulating hormones, endocannabinoids such as anandamide (AEA) and 2-arachidonoylglycerol (2-AG) are synthesized *on demand* at the site of need, in response to local cellular stress, inflammatory stimuli, or membrane depolarization (7, 14). This localized and transient mode of synthesis underscores their role as fine-tuned regulators of homeostasis rather than long-range systemic signals. The ECS comprises endocannabinoids (primarily anandamide [AEA] and 2-arachidonoylglycerol [2-AG]), their associated receptors (CB1, CB2, TRPV1, GPR55), and metabolic enzymes such as fatty acid amide hydrolase (FAAH), monoacylglycerol lipase (MAGL), and diacylglycerol lipase (DAGL) (6, 22). Recent studies suggest that ECS signaling intricately interacts with gut microbiota, forming a critical axis termed the endocannabinoidome-microbiota axis (ECBoM). This interaction modulates gut barrier integrity, intestinal inflammation, immune responses, and systemic metabolic homeostasis, positioning ECBoM dysregulation as a potential pivotal event in autoimmune disorders, notably type 1 diabetes (T1D) (1, 20).

Building on these observations, we propose a sequential model of pathogenesis that mechanistically links gut dysbiosis to autoimmune β-cell destruction in T1D through progressive disruption of ECS-mediated homeostasis: This dysregulation is hypothesized to follow a specific, sequential cascade (1, 3, 7):

intestinal dysbiosis (3)→ reduction in SCFA production (3)→ compensatory overproduction of 2-AG (14) → chronic (often subclinical) intestinal inflammation (9)→ ECS dysregulation in the gut (12)→ tight junction (TJ) downregulation → leaky gut (13)→ translocation of pro-inflammatory mediators into systemic circulation (19)→ generalized systemic inflammation (1) → immune system–driven overproduction of 2-AG (15, 16)→ ECS dysregulation in immune cells (8) → 2-AG-induced dysfunction of the blood–pancreas barrier (depending on ECS-related genetic susceptibility) (23)→ penetration of inflammatory cytokines into pancreatic tissue (24)→ ECS dysregulation within pancreatic islets (20) → mitochondrial dysfunction and β-cell apoptosis signaling (25)→ immune recognition and targeting of β-cells (1)→ clinical onset of type 1 diabetes.

The human gut microbiota consists of trillions of microorganisms collectively contributing to essential host functions such as digestion, metabolism of dietary components, synthesis of critical nutrients, and modulation of immune function (10, 26). Dysbiosis, defined as a perturbation in the composition and diversity of gut microbiota, is increasingly recognized as a major factor contributing to autoimmune and inflammatory disorders, including T1D (2, 27, 28). Notably, dysbiotic conditions frequently correlate with altered ECS activity and expression, suggesting a complex bidirectional interaction between ECS and microbiota (3, 4, 12).

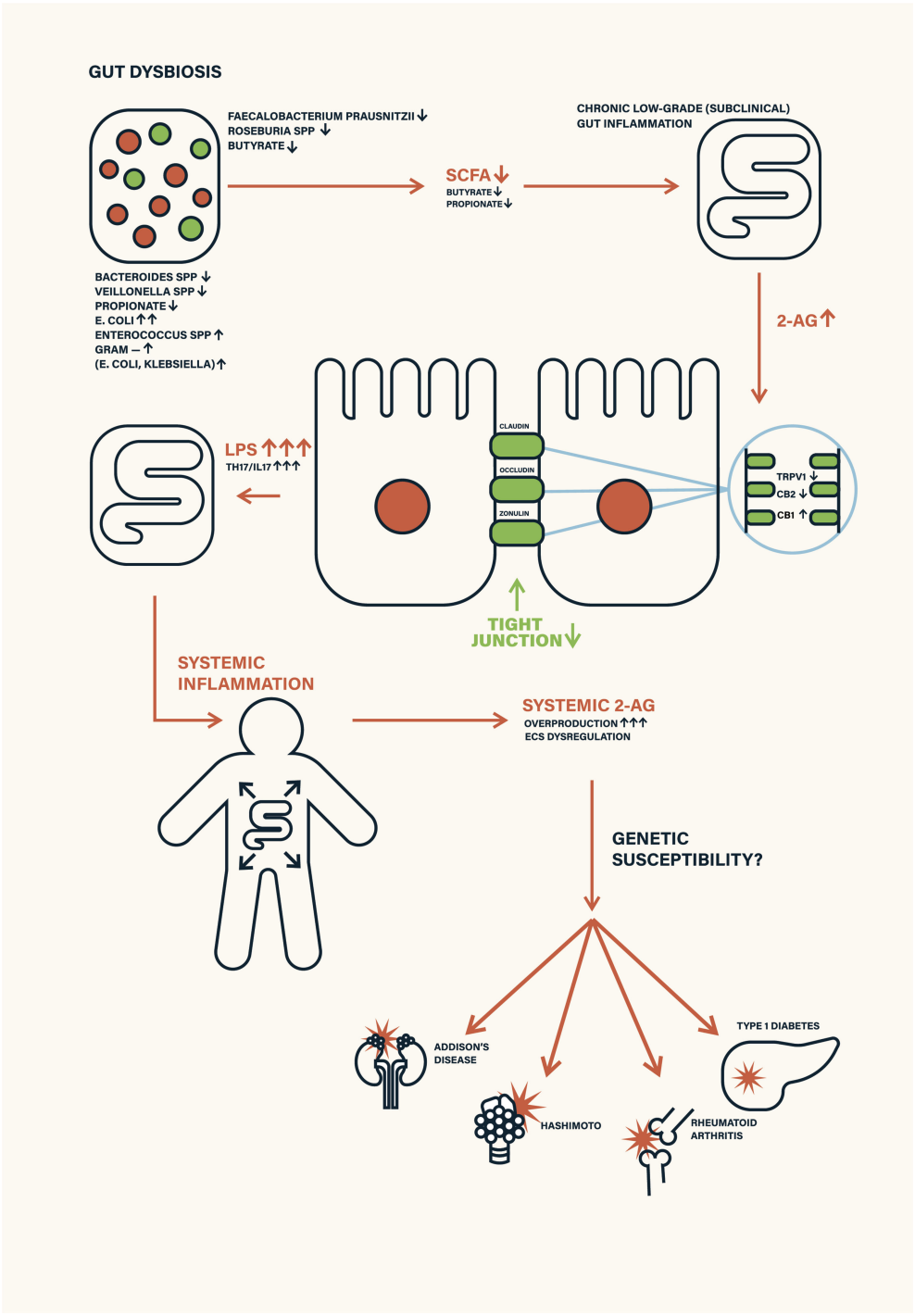

FIGURE 1
Schematic depiction of environmental triggers—such as antibiotic exposure, poor diet, infant formula feeding, and stress—disrupting gut microbiota and endocannabinoid system (ECS) homeostasis. This leads to ECS receptor desensitization, increased intestinal permeability (leaky gut), and systemic inflammation, ultimately contributing to autoimmune disease manifestation.

Beyond the classical endocannabinoids anandamide (AEA) and 2-arachidonoylglycerol (2-AG), the ECS also encompasses a broader family of lipid mediators often referred to as "endocannabinoid-like compounds", including oleoylethanolamide (OEA) and palmitoylethanolamide (PEA). These molecules do not bind strongly to CB1 or CB2 receptors but exert profound anti-inflammatory and immunoregulatory effects via activation of PPAR-α (14, 22). Notably, PEA has demonstrated protective effects in models of neuroinflammation and mast cell regulation (29), while OEA contributes to metabolic homeostasis, satiety regulation, and gut signaling (3). Their actions complement canonical ECS pathways, adding another layer of complexity to ECS–microbiota–immune

interactions, and their inclusion in future studies may provide a more comprehensive understanding of endocannabinoid tone in T1D pathogenesis.

Importantly, the ECBoM axis cannot be fully understood without considering the enzymatic regulation of endocannabinoid tone. Diacylglycerol lipase (DAGL), responsible for 2-AG synthesis, and monoacylglycerol lipase (MAGL), responsible for its degradation, are dynamically regulated by both inflammatory cytokines and microbial metabolites. For example, lipopolysaccharides (LPS) can upregulate DAGL expression in immune cells, enhancing 2-AG synthesis and promoting ECS overstimulation (3, 4). Simultaneously, SCFAs like butyrate may downregulate DAGL activity and support MAGL function, thus restoring ECS balance (10). These reciprocal interactions suggest that microbiota-derived signals may fine-tune ECS activity not only via receptor modulation but also through enzymatic control of endocannabinoid turnover. This enzymatic layer represents a critical regulatory node that warrants further exploration in future studies.

Gut microbiota directly influence ECS signaling through several distinct molecular mechanisms. A central mediator of this interaction is the production of short-chain fatty acids (SCFAs), primarily acetate, propionate, and butyrate, synthesized through bacterial fermentation of dietary fibers. SCFAs actively regulate ECS signaling by modulating the expression of ECS components in gut epithelial and immune cells. In particular, SCFAs have been shown to upregulate CB2 receptor expression on intestinal epithelial cells and immune cells, reinforcing intestinal barrier function and promoting anti-inflammatory responses (3, 25). Simultaneously, SCFAs enhance epithelial tight junction proteins, thereby decreasing gut permeability and limiting translocation of inflammatory mediators, pathogens, or bacterial components such as lipopolysaccharide (LPS) into systemic circulation (10, 11).

Conversely, a dysbiotic microbiome characterized by a reduction of beneficial SCFA-producing bacteria (e.g., *Faecalibacterium prausnitzii*, *Roseburia intestinalis*) is associated with decreased SCFA levels, impaired intestinal epithelial integrity, increased gut permeability, and consequent systemic inflammation (10, 28). Under dysbiotic conditions, elevated intestinal permeability allows increased translocation of microbial-derived LPS, which in turn activates toll-like receptor 4 (TLR4) signaling pathways on immune cells, leading to sustained ECS activation (3, 9). Specifically, increased systemic LPS directly elevates 2-AG levels via induction of DAGL activity, subsequently overstimulating ECS receptors, primarily CB1 and TRPV1 (6, 12, 18). Importantly, it is the resulting dysregulation of intestinal ECS – marked by CB2/TRPV1 desensitization and CB1 overactivation – that directly weakens tight junction integrity and leads to the structural collapse of the epithelial barrier (17, 25).

Prolonged ECS receptor overstimulation due to persistent dysbiotic signals (notably elevated LPS and diminished SCFAs) leads to receptor desensitization, particularly within TRPV1-rich tissues such as intestinal epithelia and pancreatic β-cells (17, 18, 25). Chronic 2-AG elevation results in TRPV1 channel desensitization, profoundly disturbing intracellular calcium homeostasis, mitochondrial functions, and cellular survival signaling pathways, thereby predisposing cells to inflammatory damage and apoptosis (15, 16). Thus, gut microbiota dysbiosis indirectly contributes to tissue-specific vulnerability through ECS receptor dysregulation, further amplifying systemic inflammation and immune dysregulation (1, 8).

Moreover, dysbiosis-induced changes in intestinal permeability and ECS signaling dramatically affect intestinal immune cell populations. The gut mucosal immune system, a primary site for immune tolerance and inflammatory control, expresses abundant ECS receptors, predominantly CB2, that regulate local inflammatory responses and T-cell differentiation (8, 25). CB2 signaling notably promotes the generation and maintenance of regulatory T-cells (Tregs) while suppressing inflammatory Th17 cell responses (29). Under healthy microbiota conditions, robust CB2 receptor signaling induced by SCFA-rich environments favors immune tolerance and intestinal barrier integrity (3, 4). Dysbiotic conditions disrupt this regulatory axis, leading to diminished CB2 expression, reduced Treg generation, and increased Th17-driven inflammatory responses, profoundly shifting intestinal immune homeostasis toward a pro-inflammatory phenotype, which systemically predisposes to autoimmunity (1, 12).

The ECS reciprocally modulates microbiota composition, demonstrating bidirectional interaction. ECS signaling pathways directly regulate intestinal motility, secretion, barrier function, and antimicrobial peptide production, significantly shaping microbial populations in the gut (3, 4). Animal model studies demonstrate that genetic deletion or pharmacological blockade of CB1 receptors alters intestinal motility and secretory functions, resulting in significant shifts in microbiota composition characterized by increased pro-inflammatory bacteria and reduced SCFA-producing populations (9, 12). Similarly, CB2 receptor knockout mice exhibit increased gut inflammation and altered microbiota profiles, reflecting ECS's essential role in maintaining intestinal immunological and microbial homeostasis (8, 25).

Clinical and preclinical observations highlight that conditions characterized by ECS dysregulation, such as obesity, inflammatory bowel disease, or metabolic syndrome, consistently associate with microbiota dysbiosis, supporting ECBoM's central role in human disease (4, 9, 22). Importantly, emerging clinical data from T1D patients reveal notable alterations in ECS tone, particularly elevated circulating 2-AG levels accompanied by intestinal microbiota shifts indicative of reduced SCFA-producing bacteria and increased LPS-bearing Gram-negative bacteria (10, 30). These observations suggest that ECBoM axis dysregulation might actively contribute to T1D pathogenesis rather than merely being secondary to the autoimmune disease process (1).

Given ECBoM's critical immunometabolic regulatory roles, therapeutic modulation of ECS signaling or gut microbiota represents an intriguing strategy for T1D management (1, 3). Potential interventions include probiotics enriched with SCFA-producing bacteria, dietary strategies aiming at microbiota restoration, and pharmacological ECS modulation (e.g., CB2 agonists, selective TRPV1 modulators, inhibitors of 2-AG metabolism), or phytocannabinoids (7, 25, 31, 32). Although promising, these approaches require rigorous clinical validation and consideration of individualized microbiota profiles and ECS states, emphasizing the complexity of clinical translation (3, 10).

Future research directions should prioritize detailed characterization of ECBoM interactions through multi-omics approaches, including metagenomics, metabolomics, transcriptomics, and proteomics, to comprehensively define microbiota-driven ECS alterations and their consequences for immune homeostasis and metabolic regulation (3, 4, 12). Additionally, longitudinal clinical studies of genetically predisposed individuals may reveal ECBoM biomarkers predictive of T1D onset, enabling early preventive interventions targeting ECS restoration and microbiota rebalancing (33–35).

In conclusion, ECS and gut microbiota interactions constitute a critical homeostatic regulatory axis whose dysregulation significantly contributes to T1D pathogenesis (1, 3). Detailed understanding of ECBoM's molecular interactions and pathophysiological mechanisms provides a compelling framework for novel preventive and therapeutic strategies, marking a potential paradigm shift in the management of autoimmune diabetes (4, 12, 31).

Genetic susceptibility: ECS-related genes and interactions

Type 1 diabetes (T1D) is widely recognized as a genetically complex autoimmune disease, with a strong influence exerted by the human leukocyte antigen (HLA) system within the major histocompatibility complex (MHC) on chromosome 6. The specific HLA haplotypes, notably DR3-DQ2 and DR4-DQ8, significantly increase T1D susceptibility, collectively accounting for approximately half of the genetic risk associated with disease development (19). These HLA molecules play pivotal roles in antigen presentation and T-cell activation, fueling autoimmune responses targeting pancreatic β-cells. Beyond HLA, numerous non-HLA genes, including PTPN22, CTLA4, IL2RA, FOXP3, and INS, further modulate immune responses, influencing T-cell activation, immune tolerance, and cytokine regulation, contributing cumulatively to genetic predisposition (33, 34). Yet, these known genetic loci explain only a fraction of the observed T1D heritability, underscoring the existence of additional susceptibility genes involved in metabolic and inflammatory regulation, particularly within newly explored regulatory systems, such as the endocannabinoid system (ECS) (1, 3).

The ECS consists of endocannabinoids (e.g., anandamide and 2-arachidonoylglycerol [2-AG]), cannabinoid receptors (CB1, CB2), transient receptor potential vanilloid channels (TRPV1), and enzymes responsible for endocannabinoid metabolism (FAAH, MAGL, DAGL). Recent evidence indicates that genetic variations in ECS components may profoundly influence susceptibility to autoimmune conditions, including T1D (1, 3, 25). ECS genes harbor functional polymorphisms that can critically modulate receptor expression levels, ligand availability, downstream signaling efficiency, and overall immunoregulatory capacities, thus significantly impacting autoimmune disease susceptibility (16, 36).

Genetic variations in the CB2 receptor gene (CNR2) hold particular relevance due to CB2's essential immunoregulatory functions. CB2 receptors, primarily expressed on immune cells, control inflammatory processes by suppressing pro-inflammatory cytokine release and promoting regulatory T-cell (Treg) stability. Polymorphisms such as rs35761398 and rs2501432 in CNR2 markedly reduce receptor expression and signaling efficacy (36), diminishing CB2's anti-inflammatory capabilities. The resultant immunoregulatory impairment predisposes carriers of these variants to increased inflammation and autoimmunity, notably by compromising Treg-mediated peripheral tolerance (16). Consequently, individuals harboring CNR2 risk alleles face an elevated risk of autoimmune destruction of pancreatic β-cells, which may accelerate T1D onset and severity (1).

Similarly, genetic variants in the CB1 receptor gene (CNR1), exemplified by rs1049353, modulate receptor activity and alter metabolic and inflammatory signaling cascades (6, 22). Dysregulated CB1 signaling contributes significantly to metabolic inflammation, insulin resistance, and cytokine dysregulation, thereby creating a persistent inflammatory milieu conducive to autoimmune activation (31). Overactivation of inflammatory pathways through abnormal CB1 signaling promotes autoreactive T-cell activation and β-cell stress, thereby increasing the susceptibility to T1D progression, especially in genetically predisposed individuals (1).

Moreover, polymorphisms within TRPV1 gene channels further compound genetic susceptibility. TRPV1 channels are critical calcium-permeable cation channels abundantly expressed in pancreatic β-cells, intestinal epithelial cells, and immune cells (17, 18, 37). Specific variants, such as rs8065080, alter TRPV1 receptor sensitivity and channel gating properties, profoundly affecting cellular calcium homeostasis (17, 18). Disturbed calcium influx resulting from TRPV1 dysfunction enhances endoplasmic reticulum stress, mitochondrial dysfunction, and apoptosis in pancreatic β-cells, undermining cellular integrity and increasing vulnerability to autoimmune destruction (15, 24). Furthermore, impaired TRPV1 activity in intestinal epithelial cells compromises barrier integrity, amplifying intestinal permeability and exacerbating systemic inflammation, thus connecting genetic susceptibility directly to dysregulated ECS-mediated barrier functions and immune dysregulation (17, 18).

Enzymatic components of the ECS, such as FAAH and MAGL, also harbor influential genetic polymorphisms that significantly modify endocannabinoid tone by regulating anandamide and 2-AG metabolism. For instance, FAAH polymorphism rs324420 (C385A) results in reduced enzymatic activity, elevating systemic anandamide levels and disturbing immune homeostasis (14, 38). Elevated endocannabinoid levels disrupt normal immune regulatory networks, skew cytokine production toward pro-inflammatory phenotypes, and impair Treg differentiation, thereby heightening autoimmune susceptibility in genetically predisposed individuals (16).

Importantly, ECS-related gene polymorphisms do not act in isolation; rather, they intricately interact epistatically with classical autoimmune genetic factors, amplifying autoimmune susceptibility. Notably, interactions between CB2 receptor variants (CNR2) and the FOXP3 gene, critical for Treg cell differentiation and stability, have significant consequences (16, 25). Impaired CB2 signaling

coupled with FOXP3 risk variants synergistically reduces Treg-mediated immune regulation, dramatically lowering thresholds required for autoimmune disease initiation. Similarly, epistatic interactions between CB1 receptor polymorphisms (CNR1) and PTPN22, a gene influencing T-cell receptor signaling, exacerbate autoreactive T-cell activation, inflammatory cytokine release, and metabolic dysregulation (1), further enhancing autoimmune vulnerability. TRPV1 variants interacting with polymorphisms in the IL2RA gene disrupt IL-2 signaling crucial for Treg stability and function, tipping immune balance toward pro-inflammatory Th17 dominance, thereby intensifying autoimmune pathology and pancreatic β-cell destruction (16, 17).

Collectively, ECS gene polymorphisms appear to modulate autoimmune susceptibility by acting as genetic integrators or "shock absorbers," buffering genetic predispositions to autoimmunity under normal physiological conditions (25, 39). Healthy ECS functionality preserves immune homeostasis, reduces inflammation, and maintains metabolic stability, counteracting genetic predispositions toward autoimmune responses (1). However, sustained environmental triggers, notably gut dysbiosis (3, 16) and chronic inflammation, overwhelm ECS protective capacities, causing receptor desensitization and ECS dysfunction. This critical transition point removes ECS-mediated protective buffering, fully unveiling autoimmune genetic predispositions and precipitating clinical autoimmune diabetes (36).

The ECS thus represents a vital integrative genetic node, bridging classical autoimmune susceptibility genes with metabolic and inflammatory regulation (22, 31). Therapeutically targeting ECS signaling through pharmacological modulation of receptor activity or endocannabinoid metabolism could potentially restore ECS functionality, thus reestablishing immune homeostasis and significantly reducing autoimmune disease risk in genetically susceptible populations (40, 41). Further research elucidating precise molecular mechanisms underlying these genetic interactions and ECS functionality is critical for developing effective preventive strategies and targeted interventions in T1D and other autoimmune diseases (29, 36).

While ECS-related genetic polymorphisms alone may not be sufficient to initiate autoimmunity, they appear to function as amplifiers of risk in the context of environmental or microbial challenges (12, 35). For instance, carriers of both CNR2 and TRPV1 variants who experience early-life dysbiosis or chronic low-grade inflammation may cross a biological threshold of ECS dysfunction more rapidly than non-carriers (29, 36). This combinatorial effect between genotype and environment aligns with the "two-hit hypothesis" (19) and suggests that ECS polymorphisms may serve as predictive markers for personalized risk stratification in T1D and related autoimmune diseases (42).

Environmental triggers, gut dysbiosis, and ECS dysfunction

Despite a significant genetic predisposition underlying type 1 diabetes (T1D), environmental factors are essential in triggering the manifestation of clinical autoimmunity, effectively translating latent genetic risk into overt disease (34, 43). The interplay between genetic susceptibility and environmental stimuli is particularly evident within the proposed endocannabinoidome-microbiota (ECBoM) framework (3, 4). Environmental triggers operate primarily by perturbing gut microbiota composition and diversity, initiating a cascade of microbial imbalance termed dysbiosis (2, 28). Gut dysbiosis subsequently disrupts endocannabinoid system (ECS) homeostasis, facilitating autoimmune activation through receptor overstimulation, chronic inflammation, barrier dysfunction, and impaired immune regulation (8, 12, 42).

The human gut microbiome is a dynamic and delicately balanced ecosystem sensitive to external perturbations. Factors pervasive in modern lifestyles—such as inappropriate antibiotic usage, chronic psychological stress, dietary patterns high in processed foods and refined sugars, cesarean deliveries, and early-life exposure to infant formulas—profoundly alter gut microbiota structure and function (28, 33). Antibiotics, especially during critical developmental windows, significantly reduce microbial diversity, selectively eliminating beneficial SCFA-producing bacterial species (e.g., *Faecalibacterium prausnitzii*, *Roseburia intestinalis*) and facilitating the proliferation of opportunistic pathogens (30, 44). Such disturbances limit the production of protective metabolites like short-chain fatty acids (SCFAs), crucial mediators of intestinal barrier integrity, immune tolerance, and ECS regulation (3, 4, 10).

Similarly, dietary factors typical of Western diets—characterized by excessive intake of saturated fats, refined carbohydrates, and artificial additives—promote microbial shifts toward pro-inflammatory bacterial populations (4, 10). These dietary habits enhance intestinal permeability ("leaky gut") by downregulating epithelial tight junction proteins via reduced SCFA levels and increased inflammatory mediators (11, 13). Consequently, disrupted intestinal barriers permit translocation of microbial-derived endotoxins (lipopolysaccharides, LPS), dietary antigens, and other immunostimulatory compounds into systemic circulation, initiating sustained low-grade systemic inflammation (43, 45). Furthermore, early-life nutritional exposures, particularly the replacement of human breast milk with artificial infant formulas, profoundly influence gut microbiome colonization. Breast milk provides bioactive components, including human milk oligosaccharides (HMOs), immunoglobulins, and essential fatty acids, that promote microbiota maturation and ECS homeostasis (19, 34). Formula feeding, devoid of these natural microbiota-regulating components, predisposes infants to gut dysbiosis, potentially heightening autoimmune risk later in life (28, 30).

Chronic psychological stress, increasingly prevalent in modern society, also significantly modulates gut microbiota composition and diversity through neuroendocrine pathways, particularly the hypothalamic-pituitary-adrenal (HPA) axis (13). Stress-induced cortisol elevations directly influence gut microbial populations, reducing beneficial species and promoting inflammatory microbiota profiles (10, 11). Consequently, chronic stress results in microbiota-driven ECS dysregulation, amplifying intestinal permeability, inflammation, and autoimmune susceptibility (3, 4). Notably, modern societal lifestyles characterized by high stress, poor dietary habits, and frequent antibiotic use converge to

systematically erode microbiome resilience, creating a milieu highly conducive to ECS dysregulation and subsequent autoimmune disease initiation in genetically predisposed individuals (30, 34).

These microbiome disruptions directly influence ECS signaling, initiating a maladaptive cycle of chronic ECS overstimulation, particularly through elevated 2-arachidonoylglycerol (2-AG) levels (3). Increased systemic exposure to microbial-derived endotoxins, such as LPS, induces ECS hyperactivity primarily via the enhanced expression and activity of diacylglycerol lipase (DAGL), responsible for 2-AG synthesis (4, 23). Sustained elevation of 2-AG leads to profound ECS receptor overstimulation, notably of TRPV1 and CB1, triggering receptor desensitization and reduced signaling efficacy (6, 17, 18). As previously detailed, rapid TRPV1 desensitization critically disrupts calcium homeostasis, mitochondrial function, and cellular integrity within tissues highly relevant to T1D pathogenesis, such as pancreatic β-cells and intestinal epithelium (15, 17, 24).

This receptor-level dysfunction, secondary to persistent environmental triggers, removes the protective buffering capacity normally conferred by ECS signaling (46). Under healthy conditions, ECS effectively mitigates inflammatory stressors, preserves intestinal barrier integrity, and maintains immune tolerance, thus preventing genetic susceptibility from translating into clinical disease (7, 8, 42). However, persistent ECS dysfunction resulting from chronic microbiota dysbiosis undermines these protective capacities, leading to sustained immune activation and loss of peripheral tolerance, thereby precipitating overt autoimmune diabetes (3, 45).

Crucially, the interaction between environmental triggers, gut dysbiosis, and ECS dysfunction exemplifies the concept of gene-environment interaction within the ECBoM framework (3, 4). Individuals genetically predisposed to T1D—particularly carriers of HLA risk alleles and ECS-related genetic variants (e.g., CNR2, TRPV1)—are inherently more vulnerable to environmental-induced microbiota perturbations and subsequent ECS dysfunction (29, 36). For these individuals, relatively modest environmental insults, commonplace in modern lifestyles, may suffice to initiate dysbiosis, ECS dysregulation, and progression toward clinical autoimmunity. Conversely, in genetically resilient individuals, identical environmental exposures might not elicit ECS dysfunction or overt autoimmune manifestations, highlighting the critical integrative role played by ECS genetics and microbiota composition in determining individual autoimmune susceptibility (3, 45).

Given this integrative framework, preventive strategies focused on minimizing environmental triggers and restoring microbiota-ECS homeostasis are emerging as attractive interventions to mitigate autoimmune risk (3, 4). Interventions such as dietary modifications emphasizing microbiota-supportive nutrients (e.g., prebiotics, probiotics, dietary fibers, omega-3 fatty acids) (10), phytocannabinoids (46), reduction in unnecessary antibiotic prescriptions (28), stress management techniques, and promotion of breastfeeding (44) could significantly reduce microbiota dysbiosis, ECS overstimulation, and subsequent autoimmune risk (26). These approaches, though intuitive and scientifically grounded, demand extensive clinical validation (3). A comparative overview of microbiota alterations, SCFA depletion, and barrier dysfunction across autoimmune diseases is provided in (Table 1). Nonetheless, the inherent plasticity of gut microbiota and ECS signaling pathways provides hope that proactive lifestyle interventions, particularly during early life and in genetically at-risk populations, could markedly alter autoimmune trajectories (45).

Future research must emphasize longitudinal studies and multi-omics analyses designed to elucidate precise molecular mechanisms linking specific environmental exposures, microbiota changes, and ECS dysfunction (3, 10). Comprehensive characterization of microbial metabolite profiles, ECS receptor expression patterns, and systemic inflammatory markers in at-risk populations could yield predictive biomarkers identifying individuals progressing toward autoimmune disease (33, 35). Furthermore, developing targeted therapeutic strategies aimed explicitly at preventing ECS receptor desensitization (6) or reversing dysbiosis-induced ECS dysfunction (4, 12) holds substantial promise for autoimmune disease prevention and management.

In conclusion, environmental factors play an indispensable role in manifesting latent genetic susceptibility to T1D through mechanisms centered around gut dysbiosis and ECS dysfunction (3, 13). The ECBoM framework provides an integrative perspective illustrating how pervasive environmental influences, commonplace in modern lifestyles, systematically degrade gut microbiome resilience and ECS homeostasis, facilitating autoimmune disease initiation and progression (4, 19). Effective interventions targeting gut microbiota restoration and ECS stabilization represent critical opportunities for reducing autoimmune risk, particularly in genetically susceptible individuals, marking a promising frontier in autoimmune disease prevention and management (28, 30).

ECS dysfunction across key tissues in T1D pathogenesis

The endocannabinoid system (ECS) functions as a critical regulator of physiological homeostasis across multiple tissues implicated in type 1 diabetes (T1D) pathogenesis, including pancreatic β-cells, intestinal epithelium, vascular endothelium, and immune tissues (1, 25). Chronic ECS dysregulation, induced primarily by persistent environmental triggers and gut dysbiosis, profoundly compromises the physiological functions of these tissues, promoting autoimmune activation and accelerating disease progression (3, 8). Understanding tissue-specific ECS dysfunction mechanisms is fundamental to fully appreciating the integrative pathology proposed by the ECBoM hypothesis. Table 2 summarizes ECS-related receptor expression patterns and calcium disturbances across tissues affected in autoimmune diseases.

Pancreatic β-cells are central to T1D pathogenesis due to their unique susceptibility to autoimmune destruction. These insulin-producing cells express functional ECS receptors, notably CB1, CB2, and prominently TRPV1 channels, that modulate cellular metabolism, insulin secretion, inflammation, and survival signaling (1, 15). Under normal physiological conditions, ECS signaling, especially via CB2 and TRPV1, provides essential regulatory input that maintains β-cell viability, mitigates inflammatory stress, and

TABLE 1 Alterations in gut microbiota and SCFA production across autoimmune diseases.

Disease	SCFA Levels (Butyrate, Acetate, Propionate)	SCFA-Producing Bacteria (Faecalibacterium, Roseburia, Bifidobacterium, Lactobacillus)	Pro-Inflammatory Bacteria (Proteobacteria, Escherichia-Shigella, Bacteroides)	Tight Junction Proteins (Claudins & Occludins)	Zonulin (Gut Permeability Marker)
Type 1 Diabetes (T1D) (34, 43)	↓ Reduced	↓ Reduced	↑ Increased	↓ Reduced	↑ Elevated
Celiac Disease (44, 47–49)	↓ Reduced	↓ Reduced	↑ Increased	↓ Reduced	↑ Elevated
Hashimoto's Thyroiditis (50, 51)	↓ Reduced	↓ Reduced	↑ Increased	↓ Reduced	↑ Elevated
Rheumatoid Arthritis (RA) (52–54)	↓ Reduced	↓ Reduced	↑ Increased	↓ Reduced	↑ Elevated
Multiple Sclerosis (MS) (52)	↓ Reduced	↓ Reduced	↑ Increased	↓ Reduced	↑ Elevated
Systemic Lupus Erythematosus (SLE) (55)	↓ Reduced	↓ Reduced	↑ Increased	↓ Reduced	↑ Elevated
Addison's Disease (13)	↓ Reduced	↓ Reduced	↑ Increased	↓ Reduced	↑ Elevated

This table summarizes the impact of gut microbiota composition, SCFA metabolism, and intestinal barrier integrity in autoimmune diseases. SCFA levels (butyrate, acetate, propionate) are consistently reduced across all listed diseases, reflecting a decrease in beneficial bacteria such as Faecalibacterium, Roseburia, Bifidobacterium, and Lactobacillus. In contrast, pro-inflammatory bacterial taxa (Proteobacteria, Escherichia-Shigella, Bacteroides) are elevated, which may contribute to chronic inflammation and immune dysregulation.
Tight junction proteins (claudins & occludins) are significantly reduced, indicating increased intestinal permeability ("leaky gut"), while zonulin levels are elevated, further supporting the presence of compromised gut barrier function. These findings are particularly pronounced in T1D, celiac disease, and Hashimoto's thyroiditis, where barrier dysfunction plays a key role in disease pathogenesis. Similar patterns are observed in RA, MS, SLE, and Addison's disease, underscoring gut permeability as a common factor in autoimmunity.
These data are derived from a combination of human clinical studies, animal models, and *in vitro* research. Further large-scale studies integrating microbiota profiling with functional markers of gut permeability and inflammation are necessary to better understand the systemic effects of gut dysbiosis in autoimmune diseases.

stabilizes mitochondrial functions (32). However, chronic elevation of 2-arachidonoylglycerol (2-AG), resulting from dysbiosis-induced ECS hyperactivation, profoundly disrupts these protective regulatory pathways (3). Persistent TRPV1 overstimulation rapidly induces receptor desensitization, impairing critical calcium influx necessary for insulin secretion and mitochondrial integrity (17, 24). Dysfunctional calcium signaling destabilizes mitochondrial membranes, induces reactive oxygen species (ROS) generation, and promotes endoplasmic reticulum (ER) stress, activating apoptotic pathways within β-cells. Concomitantly, reduced CB2 receptor responsiveness due to receptor internalization exacerbates inflammation and diminishes anti-inflammatory cytokine release (notably IL-10), rendering β-cells vulnerable to autoimmune-mediated destruction (16, 25). Thus, chronic ECS dysregulation directly amplifies β-cell stress, dysfunction, and susceptibility to autoimmunity, critically accelerating T1D progression.

ECS dysfunction similarly affects intestinal epithelial cells, essential regulators of gut permeability, immune tolerance, and systemic inflammation. Intestinal epithelia abundantly express CB2 and TRPV1 receptors, whose activation tightly controls intestinal barrier integrity, epithelial regeneration, mucus secretion, and antimicrobial peptide production (8, 17). Physiologically, ECS signaling strengthens epithelial tight junction proteins, thereby preserving barrier function and limiting systemic exposure to luminal inflammatory stimuli (3). Dysbiotic microbiota perturbations, however, elevate intestinal 2-AG levels, inducing chronic ECS receptor desensitization, predominantly TRPV1 (3, 25). Impaired TRPV1 signaling disrupts calcium homeostasis, directly compromising epithelial tight junction stability and reducing mucus barrier functionality, significantly enhancing intestinal permeability (17). Elevated intestinal permeability (leaky gut) facilitates translocation of microbial components such as lipopolysaccharides (LPS) and dietary antigens into systemic circulation, triggering systemic inflammation and immune dysregulation (11, 13). Additionally, ECS dysfunction reduces epithelial regenerative capacity by limiting proliferation signaling, impairing intestinal resilience, and exacerbating mucosal inflammation (3, 22). These barrier disruptions perpetuate systemic inflammation, directly linking gut ECS dysfunction to autoimmune pathogenesis.

The vascular endothelium represents another critical tissue profoundly impacted by ECS dysfunction. Endothelial cells express abundant TRPV1 and cannabinoid receptors (especially CB2), which regulate endothelial barrier permeability, leukocyte extravasation, inflammatory signaling, and vascular homeostasis (3, 23). Under

TABLE 2 ECS-related disturbances across autoimmune diseases.

Disease	Tissue of Analysis	AEA	2-AG	FAAH (Fatty Acid Amide Hydrolase)	MAGL (Monoacylglycerol Lipase)	CB1 Expression	CB2 Expression	TRPV1 Expression	TRPV2 Expression	Calcium Level (Blood)
Type 1 Diabetes (T1D) (15, 16)	Plasma, pancreas, immune cells	↓ Lowered	↑ Elevated	↓ Lowered (Pancreas, Gut)	↑ Increased (Pancreas, Gut)	↑ Increased (Brain, Pancreas)	↓ Lowered (Pancreas, Immune Cells)	↓ Lowered (Pancreas, Gut, Thyroid)	↓ Lowered (Pancreas, Gut, Thyroid)	↓ Lowered
Hashimoto's Thyroiditis (51)	Thyroid, plasma	↓ Lowered	↑ Elevated	↓ Lowered (Thyroid)	↑ Increased (Thyroid)	↑ Increased (Thyroid)	↑ Increased (Thyroid)	↓ Lowered (Thyroid)	↓ Lowered (Thyroid)	↓ Lowered
Celiac Disease (29)	Small intestine, plasma	↓ Lowered	↑ Elevated	↓ Lowered (Gut Mucosa)	↑ Increased (Gut Mucosa)	↑ Increased (Gut Mucosa)	↑ Increased (Gut Mucosa)	↓ Lowered (Gut Mucosa)	↓ Lowered (Gut Mucosa)	↓ Lowered
Rheumatoid Arthritis (RA) (56)	Synovial tissue, plasma	↓ Lowered	↑ Elevated	↓ Lowered (Synovium)	↑ Increased (Synovium)	↑ Increased (Synovium)	↑ Increased (Synovium)	↓ Lowered (Joints, Synovium)	↓ Lowered (Joints, Synovium)	↓ Lowered
Multiple Sclerosis (MS) (57)	Brain, spinal cord, plasma	↑ Elevated	↑ Elevated	No Change (Brain, Spinal Cord)	No Change (Brain, Spinal Cord)	↑ Increased (Brain, Spinal Cord)	↑ Increased (Brain, Spinal Cord)	↓ Lowered (Brain, Spinal Cord)	↓ Lowered (Brain, Spinal Cord)	↓ Lowered
Systemic Lupus Erythematosus (SLE) (36)	Plasma, immune cells	No Change	↑ Elevated	↑ Increased (Kidney, Skin)	No Change (Kidney, Skin)	↑ Increased (Kidney, Skin)	↑ Increased (Kidney, Skin)	↓ Lowered (Kidney, Skin)	↓ Lowered (Kidney, Skin)	↓ Lowered
Addison's Disease (13, 16)	Adrenal gland, plasma	↓ Lowered	↓ Lowered	↓ Lowered (Adrenal Gland)	↓ Lowered (Adrenal Gland)	↑ Increased (Adrenal Gland)	↓ Lowered (Adrenal Gland)	↓ Lowered (Adrenal Gland)	↓ Lowered (Adrenal Gland)	↓ Lowered

This table summarizes ECS-related biomarker alterations in autoimmune diseases, based on findings from human studies, animal models, and *in vitro* experiments. Across conditions, disruptions in AEA, 2-AG, and receptor expression suggest a widespread role for ECS in immune regulation and metabolic homeostasis.

In type 1 diabetes (T1D), elevated 2-AG and reduced AEA levels coincide with increased CB1 expression in the brain and pancreas, along with decreased CB2 in immune and pancreatic tissues, potentially contributing to β-cell dysfunction. Similar trends in ECS dysregulation appear in celiac disease and Hashimoto's thyroiditis, where altered endocannabinoid levels and receptor expression may influence gut permeability and thyroid autoimmunity.

Rheumatoid arthritis (RA) and multiple sclerosis (MS) exhibit ECS disturbances in inflamed joints and the central nervous system, respectively, with increased CB1 expression and reduced TRPV1/2, pointing to a role in chronic inflammation. In systemic lupus erythematosus (SLE), elevated 2-AG and altered CB1/CB2 expression suggest a complex interplay between ECS and systemic immune dysregulation. Addison's disease, primarily affecting adrenal function, shows reduced endocannabinoid levels and CB2 expression, implicating ECS in steroidogenesis and immune modulation.

Disruptions in calcium homeostasis across these conditions indicate a potential link between ECS dysfunction and broader metabolic disturbances. While animal models provide valuable insights, further human studies are needed to clarify ECS's role in autoimmunity and its potential as a therapeutic target.

10.3389/fendo.2025.1576419

physiological conditions, ECS signaling via CB2 and TRPV1 maintains endothelial integrity by stabilizing intercellular junctions, limiting inflammatory mediator expression, and restricting leukocyte trafficking (23). Persistent ECS overstimulation induced by chronic microbial dysbiosis significantly impairs endothelial receptor signaling, notably via TRPV1 receptor desensitization (17, 25). This receptor-level dysfunction compromises calcium-dependent endothelial barrier functions, increasing endothelial permeability and facilitating immune cell infiltration into pancreatic islets and intestinal tissues (23). Dysfunctional endothelial cells further amplify local inflammatory responses by secreting chemokines (e.g., MCP-1) and adhesion molecules (ICAM-1, VCAM-1), actively recruiting autoreactive T-cells and macrophages into target tissues (23). Consequently, vascular ECS dysfunction critically exacerbates autoimmune inflammatory infiltration, significantly accelerating β-cell destruction and overall disease progression.

Immune tissues and cells are similarly vulnerable to chronic ECS dysfunction, profoundly affecting immune regulation and autoimmune tolerance. Regulatory T-cells (Tregs), essential suppressors of autoimmunity, depend heavily on ECS signaling, especially CB2 activation, for their differentiation, stability, and functional integrity (8, 25). Physiological ECS stimulation promotes Treg induction through enhanced FOXP3 expression, stabilizes immunosuppressive cytokine profiles (IL-10, TGF-β), and restricts inflammatory Th17 cell differentiation (25, 29). However, persistent ECS receptor overstimulation caused by chronic microbiota-driven ECS hyperactivity induces receptor desensitization (notably CB2), diminishing Treg differentiation, stability, and function (16). The resultant depletion of functional Tregs directly compromises immune tolerance, enabling uncontrolled autoreactive T-cell activation and pro-inflammatory cytokine release (IL-17, IL-23), critically fueling autoimmune processes (16). Additionally, ECS dysfunction alters macrophage polarization toward pro-inflammatory (M1) phenotypes, exacerbating systemic inflammatory responses and further amplifying tissue-specific autoimmune damage (8, 16, 29).

Importantly, ECS dysfunction across these tissues does not occur in isolation; instead, it represents an interconnected pathogenic cascade driven by chronic environmental and microbial perturbations. For example, dysbiosis-induced gut ECS dysfunction increases systemic inflammation and intestinal permeability (3, 4, 12), exacerbating endothelial ECS impairment (23, 42) and promoting immune infiltration into pancreatic islets (1, 15, 20). Concurrently, β-cell ECS dysregulation amplifies local inflammatory responses (16, 58), increasing antigen exposure and immune activation (8, 25). This self-sustaining, tissue-spanning inflammatory cascade underscores ECS dysfunction as a central integrative pathology within T1D.

Therapeutically targeting tissue-specific ECS dysfunction thus offers compelling potential for interrupting disease progression. Pharmacological interventions designed to prevent ECS receptor desensitization (e.g., selective TRPV1 modulators or CB2 agonists) could restore ECS signaling, preserving β-cell viability (15, 58), intestinal barrier integrity (3, 42), endothelial function (23), and immune tolerance (8, 16). Additionally, strategies targeting endocannabinoid metabolism enzymes (DAGL, MAGL) to regulate systemic 2-AG levels (14, 22) may prevent chronic ECS overstimulation, thereby interrupting pathogenic inflammatory cascades (1, 4). Given ECS's integrative regulatory capacity, these targeted therapeutic interventions hold significant promise for mitigating tissue-specific autoimmune damage, preserving immune tolerance, and ultimately preventing or delaying clinical diabetes manifestation.

In conclusion, ECS dysfunction across pancreatic β-cells, intestinal epithelial cells, vascular endothelial cells, and immune tissues constitutes a critical, integrative molecular pathology underpinning T1D progression within the ECBoM hypothesis framework (1, 3). Chronic ECS receptor desensitization—driven by microbiota dysbiosis-induced ECS overstimulation—critically impairs tissue-specific functions (4, 9), exacerbating inflammatory, metabolic, and autoimmune pathologies (8, 42, 58). Elucidating tissue-specific ECS dysregulation mechanisms provides compelling insights into autoimmune diabetes pathogenesis and identifies novel therapeutic targets aimed at preserving ECS functionality and preventing T1D progression (15, 16).

Molecular pathology of ECS dysfunction: receptor desensitization and TRPV1 susceptibility

The prolonged elevation of endocannabinoid levels, particularly 2-arachidonoylglycerol (2-AG), contributes significantly to the pathogenesis of type 1 diabetes (T1D) through mechanisms involving desensitization of key receptors within the endocannabinoid system (ECS) (22, 23). ECS receptors, including cannabinoid receptor type 1 (CB1), cannabinoid receptor type 2 (CB2), and the transient receptor potential vanilloid type-1 (TRPV1) channel, orchestrate complex cellular signaling pathways essential for immune regulation, inflammatory control, and metabolic homeostasis (5, 6). Under physiological conditions, ECS receptor activation is transient, followed rapidly by mechanisms such as receptor phosphorylation, internalization, and recycling, processes designed to prevent overstimulation and cellular dysfunction (59). However, continuous receptor stimulation through persistently elevated 2-AG levels (7) induces chronic receptor desensitization (7, 9, 60). This maladaptive phenomenon involves receptor phosphorylation mediated by intracellular kinases, notably G protein-coupled receptor kinases (GRKs), protein kinase C (PKC), and protein kinase A (PKA), followed by β-arrestin binding, internalization, and eventual receptor degradation or recycling impairment (16). As a result, chronic receptor desensitization substantially reduces ECS signaling efficacy, compromising the critical immunoregulatory and anti-inflammatory actions exerted by these receptors (8). Although CB1, CB2, and TRPV1 all respond to elevated 2-AG levels, experimental studies consistently demonstrate that TRPV1 is the most susceptible to rapid desensitization, followed by CB1 and CB2 in descending order of sensitivity (15–17).

Significantly, ECS receptors exhibit marked differences in their vulnerability to prolonged agonist exposure. Among these, the TRPV1 receptor displays the highest susceptibility and the fastest kinetics of desensitization when persistently activated by elevated 2-AG (17). TRPV1, unlike CB1 and CB2, is a calcium-permeable cation channel rather than a classical G protein-coupled receptor (15). Upon activation, TRPV1 channels induce immediate calcium influx, triggering intracellular kinase cascades and subsequent receptor phosphorylation, rapidly reducing channel responsiveness (16). Experimental evidence consistently demonstrates that prolonged exposure to elevated 2-AG concentrations causes a swift decline in TRPV1 activity, profoundly disrupting calcium homeostasis and subsequent intracellular signaling pathways (15, 17).

The distinct sensitivity of TRPV1 to desensitization becomes critically significant due to the receptor's unique expression profile. TRPV1 channels are abundantly expressed in several tissues central to the ECBoM hypothesis of T1D pathogenesis, such as pancreatic β-cells, intestinal epithelial cells, vascular endothelial cells, and immune cell subsets (15, 17). Pancreatic β-cells, in particular, depend extensively on finely tuned calcium signaling for their metabolic function, insulin secretion, mitochondrial integrity, and cellular survival (24). Chronic TRPV1 desensitization in these cells disrupts essential calcium signaling, precipitating mitochondrial dysfunction, endoplasmic reticulum stress, and enhanced apoptotic susceptibility (16). This cellular vulnerability amplifies β-cell susceptibility to inflammatory cytokines and autoimmune attack, accelerating autoimmune destruction and progression toward overt T1D (15).

Furthermore, intestinal epithelial cells, another tissue type prominently expressing TRPV1, rely heavily on calcium-mediated signaling for barrier maintenance and immunoregulatory functions (17). Persistent desensitization of TRPV1 channels in intestinal epithelia impairs calcium-dependent tight junction stability, compromising intestinal barrier integrity (3). Such impairment facilitates increased intestinal permeability, allowing the translocation of bacterial antigens, lipopolysaccharides, and inflammatory mediators into systemic circulation, further exacerbating systemic inflammation and immune dysregulation (11, 17, 19). Thus, the rapid desensitization of TRPV1 in the gut represents a critical nexus linking gut dysbiosis-induced ECS dysfunction with systemic autoimmune and inflammatory responses central to T1D development.

In addition to TRPV1-mediated disruptions, accumulating evidence highlights the pivotal role of mitochondrial cannabinoid receptors (mtCB1 and mtCB2) in mediating intracellular stress responses and metabolic reprogramming in target cells (6, 22). Endocannabinoids, particularly 2-AG, readily diffuse across cellular and organelle membranes due to their lipophilic nature, accumulating in mitochondrial membranes (7). mtCB1 receptors, expressed predominantly on the outer mitochondrial membrane (OMM) and potentially also on the inner membrane (IMM), modulate mitochondrial respiration, membrane potential ($\Delta\Psi m$), and reactive oxygen species (ROS) generation (22). Persistent stimulation of mtCB1 by elevated 2-AG impairs mitochondrial oxidative phosphorylation, reduces ATP production, and promotes mitochondrial dysfunction—a pathological cascade especially detrimental to pancreatic β-cells and immune cells reliant on oxidative metabolism (15, 58). In β-cells, mtCB1 overstimulation compromises mitochondrial integrity and calcium handling, synergizing with TRPV1 desensitization to intensify apoptotic vulnerability and impair insulin secretion (58). In immune cells, ECS-mediated mitochondrial reprogramming shifts cellular metabolism toward glycolysis, inhibiting Treg stability and favoring pro-inflammatory phenotypes (e.g., Th17 and M1 macrophages), thereby exacerbating immune imbalance (8, 25). Similarly, mtCB2 receptors may influence mitochondrial survival pathways and ROS buffering in macrophages and dendritic cells, with dysfunctional mtCB2 signaling contributing to impaired M2 polarization and excessive pro-inflammatory activation (25). These findings underscore the role of ECS-driven mitochondrial dysfunction as a central mechanism coupling chronic endocannabinoid elevation with immune and metabolic dysregulation in T1D pathogenesis.

Similar mechanisms pertain to vascular endothelial cells, which prominently express TRPV1 channels and utilize calcium influx to regulate vascular permeability, endothelial cell survival, and leukocyte trafficking (23, 61). Chronic TRPV1 desensitization within endothelial cells compromises endothelial integrity, enhancing leukocyte extravasation into target tissues, notably pancreatic islets. Such augmented immune cell infiltration substantially increases local inflammation, promoting autoimmune activation and pancreatic β-cell destruction, thus actively contributing to the autoimmune pathogenesis of T1D (23, 62).

In the face of chronic TRPV1 desensitization, the ECS attempts to maintain physiological homeostasis through compensatory adjustments involving cannabinoid receptors CB1 and CB2 (25, 40). Initially, CB2 receptors exert significant anti-inflammatory and immunosuppressive effects, supporting regulatory T-cell stability and limiting pro-inflammatory cytokine release (8, 25). However, persistent ECS overstimulation eventually leads to compensatory CB2 receptor desensitization and functional impairment, diminishing this anti-inflammatory response (56). Concurrently, CB1 receptor activity becomes dysregulated, amplifying metabolic dysfunction and inflammatory signaling (22). Ultimately, this progressive receptor dysfunction erodes ECS buffering capacity, tipping immunological equilibrium from regulated tolerance toward autoimmunity and overt inflammation (46).

Recognizing the central role of receptor desensitization—especially the particular vulnerability of TRPV1—offers compelling therapeutic implications. Therapeutic strategies aimed at stabilizing TRPV1 receptor responsiveness without provoking chronic desensitization could prevent the downstream cellular and physiological consequences described above (16, 17). For instance, selective TRPV1 modulators, including partial agonists or antagonists designed to stabilize receptor function, may represent novel therapeutic interventions (17). Additionally, targeted modulation of endocannabinoid metabolism—specifically, inhibiting enzymes such as diacylglycerol lipase (DAGL) or monoacylglycerol lipase (MAGL)—to reduce chronic 2-AG

elevation could represent another promising strategy to prevent receptor overstimulation and subsequent desensitization (14, 46).

Future research should prioritize detailed elucidation of TRPV1 desensitization dynamics, intracellular molecular cascades, receptor recycling pathways, and strategies to pharmacologically modulate receptor activity effectively (14, 17). Longitudinal studies employing advanced multi-omics approaches to profile ECS receptor expression and function in genetically predisposed or high-risk populations may identify early markers predictive of T1D progression (3, 36). Integration of these findings into clinical practice could facilitate targeted early interventions designed to stabilize ECS signaling, delay or prevent autoimmune progression, and ultimately improve clinical outcomes in genetically susceptible individuals (7, 25).

In conclusion, ECS receptor desensitization—highlighted by the unique sensitivity of TRPV1 to chronic 2-AG overstimulation—represents a pivotal molecular pathology within the ECBoM model of T1D pathogenesis (14, 17). Addressing this receptor-specific desensitization therapeutically could provide powerful strategies for restoring ECS homeostasis, preserving immune-metabolic regulation, and ultimately preventing or delaying the clinical manifestation of autoimmune diabetes (3, 7, 25).

Immunological escalation & loss of tolerance

Autoimmune diabetes emerges through a progressive escalation of immune dysregulation characterized by compromised peripheral tolerance, aberrant immune cell activation, and chronic inflammatory cascades targeting pancreatic β-cells (63, 64). Central to this pathological progression is the chronic dysregulation of the endocannabinoid system (ECS), critically modulated by gut microbiota-derived short-chain fatty acids (SCFAs), particularly butyrate, and endocannabinoids, notably 2-arachidonoylglycerol (2-AG) (3, 65). The dysbiotic gut environment, featuring marked reductions in beneficial butyrate-producing bacterial species, results in diminished SCFA availability and consequent intestinal ECS dysregulation, laying the foundation for sustained systemic inflammation and profound immunological disturbances integral to autoimmune escalation and loss of immune tolerance (66).

Under physiological conditions, SCFAs—particularly butyrate—derived from beneficial gut microbial metabolism exert potent immunomodulatory effects within intestinal mucosa, enhancing regulatory T-cell (Treg) differentiation and stability, promoting anti-inflammatory cytokine production (IL-10, TGF-β), and supporting epithelial barrier integrity (67, 68). These effects are critically mediated through activation of peroxisome proliferator-activated receptors (PPARs), primarily PPARγ, expressed in immune cells, intestinal epithelia, and vascular endothelial cells (69, 70). PPARγ signaling enhances Treg induction via transcriptional upregulation of FOXP3, mitigates inflammatory cytokine expression, and fortifies epithelial tight junctions (70). Butyrate and other SCFAs thus represent pivotal microbiota-derived mediators linking microbiota composition directly to systemic immune homeostasis (70).

Chronic microbiota dysbiosis, however, characterized by substantial depletion of butyrate-producing bacteria (such as *Faecalibacterium prausnitzii*, *Roseburia intestinalis*) drastically diminishes SCFA availability, critically reducing PPARγ signaling, Treg differentiation, and epithelial barrier integrity (71, 72). Reduced SCFA levels directly exacerbate intestinal permeability, increasing the systemic translocation of luminal antigens and microbial endotoxins, particularly lipopolysaccharide (LPS), thus significantly amplifying inflammatory signaling via toll-like receptors (TLR4) and nuclear factor-kappa B (NF-κB) pathways (70, 73). Concurrently, decreased PPARγ signaling impairs immune regulatory networks, facilitating a shift from protective Treg-dominated responses toward pathogenic Th17 cell responses, intensifying systemic inflammation and autoimmunity (70).

Critically, reduced SCFA levels and heightened systemic LPS influx result in ECS dysregulation, primarily through profound alterations in intestinal and systemic endocannabinoid profiles, notably elevated 2-AG levels (12, 74). Elevated LPS robustly induces diacylglycerol lipase (DAGL) activity, enhancing 2-AG synthesis, contributing to persistent ECS receptor overstimulation (particularly TRPV1 and CB1) (14, 75). As previously discussed, chronic ECS receptor overstimulation leads to receptor desensitization and impaired downstream signaling in intestinal epithelial cells and immune cells, exacerbating gut barrier dysfunction, immune cell activation, and pro-inflammatory cytokine production (76).

Moreover, chronic inflammation within immune compartments further amplifies 2-AG overproduction. Monocytes, macrophages, and dendritic cells exposed to persistent inflammatory stimuli—particularly LPS—upregulate DAGL-β, the enzyme primarily responsible for peripheral 2-AG synthesis (7, 8). This leads to sustained paracrine and autocrine 2-AG signaling in immune microenvironments. Although CB2 activation by 2-AG typically exerts anti-inflammatory effects (25, 40), chronic overexposure may paradoxically impair CB2 receptor responsiveness, disrupt Treg differentiation, and favor Th1/Th17 skewing (8, 29), thus undermining immune regulation and accelerating autoimmunity. This feedback loop of inflammatory ECS amplification represents a crucial, yet underrecognized, axis of immune escalation and tolerance breakdown in T1D (1, 16).

The resultant ECS dysfunction significantly impairs local intestinal immune homeostasis, particularly compromising Treg induction, stability, and suppressive functionality (8, 25). Reduced CB2 receptor responsiveness critically diminishes Treg differentiation by limiting FOXP3 transcriptional activation and anti-inflammatory cytokine secretion, impairing peripheral tolerance (29, 40). Furthermore, ECS dysfunction disrupts macrophage polarization, skewing macrophage profiles toward pro-inflammatory (M1) phenotypes characterized by elevated secretion of TNF-α, IL-1β, and IL-6, thereby intensifying local and systemic inflammatory responses (1, 46). Simultaneously, impaired ECS signaling shifts dendritic cells (DCs) toward immunostimulatory phenotypes, enhancing their antigen-presenting capacity and promoting autoreactive T-cell activation,

particularly pathogenic Th17 cells producing IL-17 and IL-23 (25, 56). This pro-inflammatory shift critically weakens mucosal tolerance mechanisms, facilitating systemic autoimmunity (8, 22).

Concurrently, ECS dysregulation profoundly impacts vascular endothelial cells in intestinal mucosa, impairing endothelial barrier functions and exacerbating leukocyte trafficking into peripheral tissues (1, 23). Endothelial dysfunction mediated through TRPV1 desensitization critically amplifies leukocyte extravasation by upregulating endothelial adhesion molecules (ICAM-1, VCAM-1) and inflammatory chemokines (e.g., MCP-1), thus actively recruiting autoreactive lymphocytes and macrophages to pancreatic islets and intestinal tissues (17, 62). Enhanced leukocyte infiltration triggers local inflammatory cascades characterized by cytokine production (IFN-γ, IL-17, TNF-α), cytotoxic T-cell activation, and tissue-specific autoimmune responses targeting insulin-producing β-cells (1, 8).

Ultimately, sustained inflammatory cascades driven by impaired ECS and diminished SCFA-PPARγ signaling culminate in the progressive loss of immune tolerance (3, 10). Initial tolerance breakdown manifests through diminished Treg activity, followed by escalated autoreactive T-cell activation and clonal expansion (8, 25). Chronic inflammatory stimuli further amplify autoreactive lymphocyte populations, intensifying autoimmune responses and irreversibly damaging pancreatic β-cells (1, 31). This immunological escalation rapidly surpasses ECS's remaining compensatory capacities, firmly transitioning from latent autoimmune processes to overt clinical autoimmune diabetes (4, 43).

Therapeutically, targeting critical nodes within this immunological escalation pathway—such as enhancing SCFA availability, augmenting PPARγ activation, or pharmacologically restoring ECS receptor responsiveness—represents promising strategies to restore immune homeostasis and peripheral tolerance (3, 10). Dietary and probiotic interventions specifically designed to replenish SCFA-producing microbiota populations could significantly bolster mucosal Treg induction and reinforce epithelial barrier integrity (27, 28). Similarly, pharmacological agents directly activating PPARγ signaling, or selective ECS modulators aimed at stabilizing receptor responsiveness (e.g., CB2 agonists, TRPV1 partial modulators, inhibitors of 2-AG synthesis enzymes), could effectively restore local ECS signaling, reducing inflammation, preserving mucosal immune homeostasis, and preventing autoimmune progression (1, 25, 40).

Future studies should emphasize detailed mechanistic characterization of SCFA-PPARγ-ECS interactions in genetically predisposed or at-risk populations, employing advanced multi-omics approaches (3, 10). Longitudinal profiling of SCFA levels, ECS receptor activity, immune cell differentiation, and cytokine responses may identify predictive biomarkers capable of distinguishing individuals progressing toward overt autoimmune diabetes (25, 33). Integration of these predictive biomarkers into clinical practice could enable early, targeted preventive interventions aimed explicitly at restoring ECS and immune homeostasis, ultimately improving clinical outcomes in genetically susceptible populations (4, 28).

In conclusion, immunological escalation and loss of peripheral tolerance in T1D fundamentally involve chronic microbiota-driven depletion of beneficial SCFA-producing bacterial populations, reduced PPARγ signaling, subsequent ECS dysregulation, and sustained inflammatory cascades (3, 8, 10). Addressing SCFA-ECS-immune interactions thus represents a compelling therapeutic approach for restoring immunological balance, preventing autoimmune escalation, and delaying or even reversing the progression of clinical autoimmune diabetes (1, 4, 25).

Parallels to other autoimmune disorders

Type 1 diabetes (T1D) frequently coexists with a well-established cluster of autoimmune conditions, notably celiac disease (CD), Hashimoto's thyroiditis (HT), Addison's disease (AAD), and rheumatoid arthritis (RA). While each disease presents unique clinical manifestations and targets distinct tissues, accumulating evidence underscores shared molecular disturbances involving the endocannabinoid system (ECS), particularly alterations in transient receptor potential vanilloid channels (TRPV1 and TRPV2), cannabinoid receptor type 2 (CB2), and underlying genetic susceptibility (29, 42, 56). Identifying common ECS-mediated mechanisms and genetic predispositions elucidates critical integrative pathways that potentially drive autoimmune processes across these conditions, reinforcing the plausibility of the ECBoM hypothesis in T1D pathogenesis (25, 40).

Among these shared molecular mechanisms, the prominence of TRPV channels, particularly TRPV1 and TRPV2, is striking. TRPV1 and TRPV2 are calcium-permeable, nonselective cation channels abundantly expressed in endocrine and exocrine tissues, where regulated calcium influx is essential for proper cellular function, survival, and secretion (17, 24). Crucially, sustained elevations in endocannabinoid levels, notably 2-arachidonoylglycerol (2-AG), common in dysbiotic and inflammatory states, render these channels vulnerable to rapid receptor desensitization (22, 46). Chronic TRPV1/2 desensitization disrupts calcium homeostasis, mitochondrial integrity, endoplasmic reticulum function, and cellular survival pathways, thereby critically compromising the viability of hormone-producing and barrier-regulating cells within affected tissues (29, 42).

Celiac disease, frequently co-occurring with T1D, exemplifies this phenomenon. CD is characterized by autoimmune-mediated intestinal epithelial damage driven by gluten exposure, substantially impairing gut barrier function (47, 48). Significantly, intestinal epithelial cells in CD exhibit high TRPV1 expression, rendering them particularly sensitive to chronic ECS overstimulation and rapid receptor desensitization upon elevated 2-AG exposure (42, 46). TRPV1 dysfunction within intestinal epithelial cells impairs calcium-dependent regulation of tight junction proteins, mucus secretion, and epithelial regenerative capacity, exacerbating intestinal permeability and systemic inflammation (9, 29). Concurrently, reduced CB2 receptor expression in CD further

compounds immunological dysregulation, limiting anti-inflammatory and regulatory T-cell induction crucial for mucosal tolerance (42, 56). These ECS disturbances align precisely with mechanisms proposed for T1D, emphasizing shared ECS-mediated vulnerabilities between CD and T1D (49).

Hashimoto's thyroiditis, another common autoimmune disorder co-occurring with T1D, further highlights shared ECS dysfunction involving TRPV1/2 and CB2 receptors. The thyroid gland exhibits abundant expression of TRPV1 and TRPV2 channels, critical for calcium-regulated thyroid hormone synthesis, secretion, and epithelial cell survival (17, 61). Chronic inflammation observed in HT corresponds with significantly elevated 2-AG levels and subsequent TRPV1 receptor overstimulation, leading to rapid receptor desensitization, disrupted calcium homeostasis, mitochondrial dysfunction, and thyroid follicular cell apoptosis (1, 17). Genetic analyses in HT populations have identified polymorphisms in the TRPV1 gene (e.g., rs8065080), potentially linking impaired receptor function to increased thyroid autoimmunity risk (17, 50). Concurrent CB2 receptor dysregulation reduces anti-inflammatory signaling within thyroid tissue, perpetuating inflammatory processes (25, 56). Thus, thyroid ECS dysregulation parallels mechanisms seen in pancreatic β-cells in T1D, supporting a shared pathogenic ECS model.

Similarly, autoimmune Addison's disease, characterized by autoimmune-mediated destruction of adrenal cortical tissue, provides further compelling evidence of shared ECS-related autoimmune vulnerabilities. Adrenal cortical cells critically rely on TRPV1 and TRPV2 channels for regulated calcium influx, essential for steroidogenesis and mitochondrial energy production (17, 61). Chronic systemic inflammation and elevated endocannabinoid levels in AAD patients contribute significantly to rapid TRPV receptor desensitization and impaired calcium signaling (1, 46). Dysfunctional calcium homeostasis within adrenal cortical cells triggers mitochondrial dysfunction, ROS accumulation, and apoptosis, accelerating autoimmune-mediated adrenal damage. Genetic susceptibility studies in autoimmune adrenalitis patients have also highlighted polymorphisms in ECS-related genes, including CNR2 and TRPV1, suggesting shared ECS-driven genetic predispositions among these autoimmune disorders, further aligning with T1D susceptibility profiles (25, 50, 56).

Rheumatoid arthritis, although less commonly associated with T1D, demonstrates significant ECS dysregulation, particularly involving TRPV1/2 and CB2 receptors within synovial tissues. Synovial fibroblasts and inflammatory infiltrating immune cells abundantly express TRPV channels, whose chronic desensitization due to elevated 2-AG significantly disrupts calcium signaling, cellular proliferation, apoptosis regulation, and inflammatory mediator production (17, 22). Synovial inflammation and joint destruction in RA directly correlate with ECS dysregulation and diminished CB2 receptor responsiveness, exacerbating inflammatory cytokine release (IL-17, IL-6, TNF-α), leukocyte recruitment, and chronic tissue damage (16, 56). Genetic predisposition studies in RA have similarly identified variants in ECS-related genes (e.g., FAAH, TRPV1), further supporting the integrative role of ECS genetics in autoimmune vulnerability (12, 17).

These examples clearly demonstrate ECS dysregulation, particularly chronic TRPV1/2 receptor desensitization, calcium signaling disruption, and impaired CB2-mediated immune regulation as common pathological features among T1D and coexisting autoimmune disorders (16, 17, 56). Additionally, the consistent observation of gut microbiota dysbiosis—characterized by reduced SCFA/butyrate-producing populations, increased intestinal permeability, and elevated systemic inflammation—further reinforces ECS dysfunction across these diseases (10, 27, 43). Reduced intestinal SCFA availability critically diminishes peroxisome proliferator-activated receptor gamma (PPARγ)-mediated immunoregulatory pathways, enhancing ECS dysfunction and systemic autoimmune responses (3, 8, 12).

From a genetic perspective, autoimmune polyendocrine syndrome type 2 (APS-2), characterized by coexistence of T1D, AAD, and HT, strongly implicates shared genetic susceptibility loci involving ECS-related genes. Genome-wide association studies (GWAS) have identified overlapping susceptibility regions in these conditions, notably within HLA regions but increasingly involving non-HLA genes linked to immune regulation, calcium signaling, and ECS pathways (CNR2, TRPV1 (17, 25, 56)). Polymorphisms in the TRPV1 gene, such as rs8065080, have emerged as potential shared susceptibility factors, critically modulating receptor function and autoimmune vulnerability (16, 17). Epistatic interactions between ECS-related polymorphisms (CNR2, TRPV1) and classical autoimmune susceptibility loci (PTPN22, CTLA4, FOXP3) further amplify autoimmune risk by synergistically impairing immune tolerance and ECS functionality (3, 8).

In addition to the genetic and ECS-related receptor vulnerabilities identified within affected endocrine and epithelial tissues, autoimmune disorders such as T1D, celiac disease, Hashimoto's thyroiditis, Addison's disease, and rheumatoid arthritis share well-defined immunological predispositions involving critical alterations in immune cell populations and inflammatory signaling pathways. These common immunological disturbances include compromised regulatory T-cell (Treg) differentiation and function, heightened pro-inflammatory T-helper 17 (Th17) responses (77), dysregulated macrophage polarization, and increased antigen-presenting cell (APC) activation (8, 29). Significantly, these immunological abnormalities demonstrate profound interactions with ECS signaling, reflected by altered endocannabinoid levels, specifically increased 2-arachidonoylglycerol (2-AG) and reduced anandamide (AEA), along with distinct receptor expression patterns of CB1, CB2, TRPV1, and TRPV2 within immune cells (16, 22, 25, 40).

A central shared immunological dysfunction across these autoimmune diseases involves impaired induction and stability of regulatory T-cells (Tregs). Tregs, crucial for maintaining peripheral immune tolerance and preventing autoimmune reactions, rely substantially on ECS signaling, particularly via CB2 receptor activation. CB2 receptor stimulation by AEA and, under physiological conditions, balanced 2-AG levels significantly promotes FOXP3 expression, enhances Treg differentiation, and reinforces immunosuppressive cytokine secretion (IL-10, TGF-β) (8, 25). Chronic ECS dysregulation characterized by sustained

elevations of 2-AG results in profound CB2 receptor desensitization, diminishing Treg induction, suppressive function, and survival (16, 40). These immunological consequences are evident across T1D, CD, HT, AAD, and RA, where circulating Treg numbers and functionality are consistently compromised, correlating with increased autoimmune severity (29, 46).

Simultaneously, ECS dysfunction, especially CB2 receptor impairment due to chronic overstimulation, exacerbates pro-inflammatory T-helper 17 (Th17) cell responses, another critical autoimmune mediator common among these conditions. Reduced CB2-mediated signaling fails to restrain IL-17, IL-22, and IL-23 production, favoring Th17 cell differentiation, proliferation, and pathogenic activity (8, 25). Elevated Th17 cell populations and increased serum IL-17 and IL-23 concentrations are well-documented across autoimmune disorders such as T1D, CD, HT, AAD, and RA, highlighting a common ECS-mediated immunological imbalance potentiated by chronic 2-AG elevation and reduced CB2 signaling (16, 29, 46).

Further compounding these shared immunological predispositions is dysregulated macrophage polarization toward pro-inflammatory (M1) phenotypes driven by ECS dysfunction. Under physiological conditions, CB2 receptor activation by balanced endocannabinoid signaling promotes anti-inflammatory macrophage (M2) polarization (25, 40). Chronic 2-AG-driven receptor desensitization significantly disrupts this immunoregulatory function, increasing M1 polarization characterized by excessive secretion of TNF-α, IL-1β, and IL-6, intensifying tissue inflammation and autoimmune pathology (8, 29). Elevated pro-inflammatory macrophage populations and inflammatory cytokine profiles consistently accompany T1D, CD, HT, AAD, and RA, reflecting shared ECS-mediated immunological disturbances (16, 46).

Moreover, TRPV1 and TRPV2 receptor expression within immune cells, including macrophages, dendritic cells, and T-lymphocytes, represents an additional shared immunological vulnerability across these autoimmune diseases. TRPV channels mediate calcium-dependent immune cell activation, cytokine secretion, and apoptosis regulation (17, 24). Chronic receptor overstimulation, subsequent desensitization, and impaired calcium signaling due to elevated 2-AG contribute directly to dysregulated immune responses, APC hyperactivation, heightened pro-inflammatory cytokine production, and defective immune cell apoptosis, further amplifying autoimmune processes (22, 29). TRPV receptor dysfunction has been documented within immune cell populations in RA, HT, and CD (42, 50, 56), strongly suggesting similar mechanisms occur within T1D and AAD (25, 56, 59).

Finally, genetic susceptibility studies in autoimmune polyendocrine syndromes, particularly APS-2, consistently highlight polymorphisms in genes affecting ECS receptor function (CNR2, TRPV1) and immune regulatory genes (FOXP3, IL2RA, PTPN22) (22, 29, 42). Epistatic interactions between ECS-related polymorphisms and classical autoimmune susceptibility genes collectively exacerbate autoimmune vulnerability by synergistically impairing ECS-mediated immune regulation.

Taken together, these shared immunological disturbances—impaired Treg differentiation, heightened Th17 activity, dysregulated macrophage polarization, APC hyperactivation, and ECS receptor dysfunction—strongly support a unified ECS-mediated pathogenic mechanism underlying autoimmune vulnerability across T1D, CD, HT, AAD, and RA (8, 25, 29, 42, 56). This integrated immunological perspective further substantiates the ECBoM hypothesis, highlighting ECS restoration and microbiota-targeted interventions as promising therapeutic avenues for autoimmune diseases collectively (4, 22, 46).

Therefore, ECS dysfunction—exemplified by rapid TRPV1/2 receptor desensitization, compromised calcium signaling, and impaired CB2 immune regulation—represents a robust integrative pathogenic node consistently shared among T1D and frequently coexisting autoimmune disorders (8, 25, 29, 42, 56). Recognition of these common ECS-related vulnerabilities provides compelling evidence supporting the ECBoM hypothesis, suggesting that ECS dysfunction critically contributes to autoimmune pathogenesis across multiple disease contexts (22, 46).

Therapeutically, targeting ECS stabilization, microbiota restoration, and SCFA-mediated immunoregulation could offer substantial broad-spectrum benefits across these autoimmune conditions. Interventions such as selective TRPV modulators, CB2 receptor agonists, probiotics, dietary SCFA enrichment, and PPARγ activators could effectively interrupt autoimmune progression, preserving ECS functionality and restoring immune homeostasis (3, 8, 10, 25, 29, 40).

In summary, parallels in ECS dysfunction, TRPV receptor expression, calcium signaling disturbances, microbiota dysbiosis, and shared genetic susceptibility across T1D and commonly coexisting autoimmune disorders (CD, HT, AAD, RA) strongly substantiate the integrative ECBoM model. These findings underscore ECS's central role in autoimmune pathogenesis, providing novel insights and potential therapeutic targets for managing autoimmune diseases collectively (8, 25, 29, 42, 56). However, it is important to note that much of the current evidence is derived from animal models and observational studies. While strong mechanistic overlaps exist, the extrapolation of these findings across disease contexts must be approached with caution. ECS dysfunction in T1D may exhibit unique characteristics not fully shared with other autoimmune diseases. Therefore, further targeted research is essential to validate the ECBoM hypothesis, confirm tissue-specific ECS alterations, and establish causality in human cohorts.

Therapeutic potential: challenges & opportunities

The endocannabinoid system (ECS), acting as a dynamic interface between immune, metabolic, and neuronal networks, presents a compelling therapeutic target in the context of type 1 diabetes (T1D). As evidenced by the ECBoM model, ECS dysregulation—exemplified by chronic 2-arachidonoylglycerol (2-AG) elevation, receptor desensitization (especially of TRPV1), and downstream immune-metabolic dysfunction—constitutes a critical axis in T1D pathogenesis (1, 8, 17, 40). However, therapeutic manipulation of this complex system is fraught with both unique challenges and transformative opportunities (22, 25).

A primary challenge lies in the ligand promiscuity and bidirectional nature of endocannabinoid signaling. While CB2 activation confers robust anti-inflammatory and tolerogenic effects, CB1 stimulation—especially under chronic 2-AG excess—can exacerbate metabolic and inflammatory disturbances (7, 22). TRPV1, although protective under physiological stimulation, rapidly desensitizes under persistent activation, leading to loss of barrier integrity and mitochondrial dysfunction (17, 59). Moreover, ECS receptors are expressed not only on plasma membranes but also on mitochondrial membranes (mtCB1 and mtCB2), where they directly influence mitochondrial bioenergetics, apoptosis regulation, and reactive oxygen species (ROS) production (25, 40). This intracellular dimension of ECS signaling introduces further complexity, as chronic 2-AG diffusion into the inner mitochondrial membrane (IMM) can disrupt mitochondrial dynamics and compromise β-cell viability and immune homeostasis (1, 58).

Another promising direction lies in the use of dietary fatty acid precursors and lifestyle interventions to indirectly modulate ECS tone. Omega-3 fatty acids, for instance, can serve as precursors for endocannabinoid-like mediators (e.g., DHEA, EPEA) with anti-inflammatory properties and reduced receptor desensitization risk (4, 46). Preliminary data suggest these mediators may activate PPAR pathways without overstimulating CB1 or TRPV1 (22, 63). This opens the door to "nutritional ECS modulation," particularly in individuals where pharmacological targeting may be premature or contraindicated. Combining these interventions with microbiota-supportive dietary patterns may yield synergistic effects, stabilizing both ECS and gut-derived immunoregulation (10, 11).

Despite these challenges, several therapeutic entry points emerge. One strategy involves rebalancing endocannabinoid tone by selectively inhibiting 2-AG biosynthesis or degradation pathways. For example, inhibition of diacylglycerol lipase (DAGL), the primary enzyme responsible for 2-AG synthesis, may attenuate receptor overstimulation and preserve CB2 and TRPV1 responsiveness (7, 14). Conversely, monoacylglycerol lipase (MAGL) inhibition, though anti-inflammatory in certain contexts, risks exacerbating 2-AG overload if not precisely titrated —highlighting the need for tissue-specific and temporally controlled interventions (7, 46).

Another avenue focuses on receptor-specific pharmacological modulation. CB2-selective agonists may restore peripheral immune tolerance, enhance regulatory T-cell (Treg) stability, and suppress pro-inflammatory cytokine release without inducing psychoactive effects (8, 25, 40). Simultaneously, partial TRPV1 agonists may stabilize channel function and prevent rapid desensitization, preserving epithelial barrier integrity and mitochondrial calcium signaling (17, 61). Additionally, novel ligands targeting mtCB1/2 receptors could regulate mitochondrial function in immune and β-cells, opening new frontiers in intracellular immunometabolic modulation (9, 23).

A complementary and potentially synergistic approach involves dietary and microbiota-directed strategies. Restoring short-chain fatty acid (SCFA) production—particularly butyrate—through prebiotic supplementation, fecal microbiota transplantation (FMT), or colonization with next-generation probiotics (e.g., *Faecalibacterium prausnitzii*) can significantly enhance PPARγ activation (4, 10, 78). This, in turn, strengthens Treg differentiation, tight junction integrity, and anti-inflammatory cytokine profiles, indirectly stabilizing ECS signaling via the gut–immune–endocannabinoid axis (3, 8). Enhancing SCFA–PPARγ–ECS crosstalk may prove especially beneficial in early-stage or pre-symptomatic individuals with elevated genetic risk (33, 34).

Nevertheless, personalized ECS-targeted therapy remains a formidable challenge. The ECS exhibits high interindividual variability, influenced by genetic polymorphisms in ECS-related enzymes and receptors, microbiota composition, and environmental factors (35, 36, 41). Thus, successful therapeutic intervention will likely require precision medicine frameworks, integrating genetic, microbial, metabolomic, and ECS receptor expression profiles to tailor intervention strategies (3, 46).

Furthermore, the psychoactivity of CB1 ligands and the systemic immunomodulatory effects of ECS-targeted therapies raise regulatory and ethical concerns, particularly in pediatric populations (7, 40). Strategies to bypass these concerns include developing non-psychoactive ECS modulators, optimizing targeted delivery systems (e.g., nanoparticle-based gut-restricted formulations), or focusing on peripheral CB2- and TRPV1-centric pathways (17, 25, 29).

In conclusion, while ECS dysregulation presents considerable therapeutic challenges in the context of T1D, it simultaneously unveils unprecedented opportunities for targeted immune and metabolic reprogramming (1, 46). Future research must strive to refine ECS-targeted interventions, prioritize safety and tissue specificity, and integrate ECS-modulating strategies with microbiota restoration and immunometabolic suport (3, 4). Through this integrative approach, it may become possible not only to delay or halt autoimmune progression but also to restore a measure of immune tolerance and metabolic stability in individuals at risk for, or already diagnosed with, type 1 diabetes.

Future directions and experimental validation

In light of the central role played by the endocannabinoid system (ECS) in immune homeostasis, gut permeability, and inflammatory regulation (4, 8), further studies are warranted to investigate whether distinct biochemical signatures involving endocannabinoids and their associated immunometabolic markers can serve as predictors or modulators of autoimmune progression in Type 1 Diabetes (T1D) (3, 28). This design will also allow us to test the hypothesis that ECS dysregulation precedes measurable metabolic dysfunction, acting as an early indicator rather than a downstream consequence of β-cell loss (1, 20).

We propose a structured pilot study focused on the simultaneous quantification of circulating endocannabinoids—namely anandamide (AEA) and 2-arachidonoylglycerol (2-AG)—alongside key immunometabolic and gastrointestinal biomarkers in individuals with established T1D and in a comparative group of at-

risk individuals, such as first-degree relatives of patients who test positive for diabetes-related autoantibodies (1). The aim is to explore whether dysregulation in ECS components correlates with measures of glycemic control (HbA1c, C-peptide), systemic inflammation (e.g., IL-6, TNF-α, IL-10, CRP) (8, 25), gut barrier integrity (zonulin, claudin-1, occludin), ionomic balance (Na^+, K^+, Ca^{2+}, Mg^{2+}, Cl^-), and lipid metabolism (HDL, LDL, triglycerides, total cholesterol) (22, 26).

Given the mounting evidence linking intestinal dysbiosis and short-chain fatty acid (SCFA) depletion with ECS dysfunction, fecal samples will be analyzed for SCFA profiles, particularly levels of butyrate, propionate, and acetate, to establish potential associations between microbial metabolites and systemic ECS status (3, 10, 26). Moreover, assessment of zonulin and related markers of tight junction integrity will allow for the correlation of gut permeability with circulating inflammatory mediators and endocannabinoid tone (11, 13, 47).

As exploratory endpoints, the expression of CB1 and CB2 receptors at the mRNA level in peripheral blood mononuclear cells may be investigated, offering insights into receptor regulation under chronic inflammatory stress (23, 25, 56). This would allow the identification of receptor expression profiles potentially predictive of disease stage or progression.

To elucidate the temporal dynamics of ECS breakdown, longitudinal cohort studies are necessary, particularly in individuals at elevated risk for T1D but not yet diagnosed. Serial assessments of endocannabinoid levels, inflammatory cytokines, SCFA concentrations, and gut permeability markers over time would help determine whether specific ECS-related alterations precede the clinical onset of autoimmunity (4, 12, 19, 27). Likewise, follow-up studies in long-duration T1D patients may provide valuable information about ECS compensatory exhaustion, helping to delineate the tipping point beyond which immunometabolic resilience is lost (7, 46). Identifying this "immunological breaking point" may prove essential for designing timely and individualized preventive interventions.

The proposed pilot design includes cross-sectional profiling in a total of 70 individuals (50 with T1D and 20 at-risk), using multi-analyte platforms such as LC-MS/MS for endocannabinoid quantification and multiplex ELISA or Luminex for cytokine profiling (23, 25). Stool samples will be analyzed via gas chromatography for SCFA quantification, and RT-qPCR may be employed to assess cannabinoid receptor gene expression (8, 42). Blood samples will be collected in accordance with safe clinical limits for non-therapeutic studies, ensuring participant safety while allowing for the robust measurement of proposed biomarkers.

We envision that integrating ECS-specific biomarkers—such as 2-AG and AEA levels—with immunological and gut-derived parameters will not only refine our understanding of ECS involvement in T1D pathogenesis but may also unveil predictive signatures useful for early identification of at-risk individuals (8, 22, 28). Furthermore, the results from this pilot study could lay the foundation for the development of a broader ECS biomarker panel (ECBoM) capable of informing future preventive or therapeutic strategies targeting immunometabolic regulation in autoimmune diabetes (23, 25).

Ultimately, by focusing on non-interventional biomarker profiling in well-defined and longitudinally monitored cohorts, this research aims to bridge the translational gap between molecular ECS dysfunction and clinical T1D progression (3, 4, 25), opening new avenues for risk stratification, preventive screening, and personalized immunometabolic assessment (12, 28).

Conclusions

The model presented here positions the endocannabinoidome–microbiota axis (ECBoM) as a central integrative node in the pathogenesis of type 1 diabetes (T1D). It proposes a stepwise mechanistic cascade in which gut dysbiosis initiates ECS hyperactivation, leading to receptor desensitization—particularly of TRPV1—and subsequent failure of key immunoregulatory and metabolic processes across intestinal, endothelial, and pancreatic tissues (4, 12, 25, 28).

This hypothesis synthesizes current insights from immunology, microbiology, and cannabinoid signaling into a unifying pathophysiological sequence. The ECS emerges not only as a modulator of immune responses but also as a buffering system whose failure may be decisive in triggering the autoimmune attack on pancreatic β-cells (8, 46). Notably, the desensitization of ECS receptors, especially TRPV1, under chronic 2-AG exposure appears to be a critical inflection point, stripping the host of essential protective mechanisms (17, 22, 25).

Importantly, models of ECS or microbiota dysfunction already exist independently, but the integration of both into a single coherent cascade opens entirely new perspectives on T1D pathogenesis (3, 4, 12). However, validating this model requires ambitious, multidimensional studies that combine multi-omics profiling, endocannabinoid quantification, inflammatory and barrier markers, and longitudinal follow-up of genetically at-risk individuals (30, 33, 34). These investigations are complex and resource-intensive, but they offer a paradigm shift in how we conceptualize autoimmune diabetes.

Ultimately, better understanding of ECS-microbiota crosstalk may enable the development of predictive biomarkers, early interventions, and novel immunometabolic therapies tailored to ECS tone and microbiota status (3, 12, 26). By shifting the focus from downstream immune destruction to upstream homeostatic failure, this approach provides a fresh therapeutic outlook on a disease long considered irreversible and unpreventable (8, 31).

Data availability statement

The original contributions presented in the study are included in the article/Supplementary Material. Further inquiries can be directed to the corresponding author.

Author contributions

WL: Conceptualization, Data curation, Formal Analysis, Funding acquisition, Investigation, Methodology, Project

administration, Resources, Software, Supervision, Validation, Visualization, Writing – original draft, Writing – review & editing.

Funding

The author(s) declare that no financial support was received for the research and/or publication of this article.

Conflict of interest

The author declares that the research was conducted in the absence of any commercial or financial relationships that could be construed as a potential conflict of interest.

Generative AI statement

The author(s) declare that Generative AI was used in the creation of this manuscript. Artificial Intelligence tools were utilized to enhance the linguistic clarity, coherence, and overall flow of the manuscript. The conceptualization, analysis, and interpretation of the content remain the sole responsibility of the author.

Publisher's note

Supplementary material

The Supplementary Material for this article can be found online at: https://www.frontiersin.org/articles/10.3389/fendo.2025.1576419/full#supplementary-material

References

1. Gruden G, Barutta F, Kunos G, Pacher P. Role of the endocannabinoid system in diabetes and diabetic complications. *Br J Pharmacol*. (2016) 173:1116–27. doi: 10.1111/bph.v173.7

2. Alkanani AK, Hara N, Gottlieb PA, Ir D, Robertson CE, Wagner BD, et al. Alterations in intestinal microbiota correlate with susceptibility to type 1 diabetes. *Diabetes*. (2015) 64:3510–20. doi: 10.2337/db14-1847

3. Silvestri C, Di Marzo V. The gut microbiome–endocannabinoidome axis: A new way of controlling metabolism, inflammation, and behavior. *Funct (Oxf)*. (2023) 4: zqad003. doi: 10.1093/function/zqad003

4. Cani PD, Plovier H, Van Hul M, Geurts L, Delzenne NM, Druart C, et al. Endocannabinoids–at the crossroads between the gut microbiota and host metabolism. *Nat Rev Endocrinol*. (2016) 12:133–43. doi: 10.1038/nrendo.2015.211

5. Pertwee RG. The pharmacology of cannabinoid receptors and their ligands: an overview. *Int J Obes (Lond)*. (2006) 30 Suppl 1:S13–18. doi: 10.1038/sj.ijo.0803272

6. Zou S, Kumar U. Cannabinoid receptors and the endocannabinoid system: signaling and function in the central nervous system. *Int J Mol Sci*. (2018) 19:833. doi: 10.3390/ijms19030833

7. Pacher P, Bátkai S, Kunos G. The endocannabinoid system as an emerging target of pharmacotherapy. *Pharmacol Rev*. (2006) 58:389–462. doi: 10.1124/pr.58.3.2

8. Acharya N, Penukonda S, Shcheglova T, Hagymasi AT, Basu S, Srivastava PK. Endocannabinoid system acts as a regulator of immune homeostasis in the gut. *Proc Natl Acad Sci U S A*. (2017) 114:5005–10. doi: 10.1073/pnas.1612177114

9. Marzo VD, Izzo AA. Endocannabinoid overactivity and intestinal inflammation. *Gut*. (2006) 55:1373–6. doi: 10.1136/gut.2005.090472

10. Palmnäs-Bédard MSA, Costabile G, Vetrani C, Åberg S, Hjalmarsson Y, Dicksved J, et al. The human gut microbiota and glucose metabolism: a scoping review of key bacteria and the potential role of SCFAs. *Am J Clin Nutr*. (2022) 116:862–74. doi: 10.1093/ajcn/nqac217

11. Di Vincenzo F, Del Gaudio A, Petito V, Lopetuso LR, Scaldaferri F. Gut microbiota, intestinal permeability, and systemic inflammation: a narrative review. *Intern Emerg Med*. (2024) 19:275–93. doi: 10.1007/s11739-023-03374-w

12. Muccioli GG, Naslain D, Bäckhed F, Reigstad CS, Lambert DM, Delzenne NM, et al. The endocannabinoid system links gut microbiota to adipogenesis. *Mol Syst Biol*. (2010) 6:392. doi: 10.1038/msb.2010.46

13. Mu Q, Kirby J, Reilly CM, Luo XM. Leaky gut as a danger signal for autoimmune diseases. *Front Immunol*. (2017) 8:598/full. doi: 10.3389/fimmu.2017.00598/full

14. Marzo VD, Maccarrone M. FAAH and anandamide: is 2-AG really the odd one out? *Trends Pharmacol Sci*. (2008) 29:229–33.

15. Díaz-Asensio C, Setién R, Echevarría E, Casis L, Casis E, Garrido A, et al. Type 1 diabetes alters brain cannabinoid receptor expression and phosphorylation status in rats. *Hormone Metab Res*. (2008) 40:454–8. doi: 10.1055/s-2008-1065323

16. Sido JM, Nagarkatti PS, Nagarkatti M. Role of endocannabinoid activation of peripheral CB1 receptors in the regulation of autoimmune disease. *Int Rev Immunol*. (2015) 34:403–14. doi: 10.3109/08830185.2014.921165

17. Chen J, Sun W, Zhu Y, Zhao F, Deng S, Tian M, et al. TRPV1: The key bridge in neuroimmune interactions. *J Intensive Med*. (2024) 4:442–52. doi: 10.1016/j.jointm.2024.01.008

18. Yin M, Zhang Y, Liu S, Huang J, Li X. Gene expression signatures reveal common virus infection pathways in target tissues of type 1 diabetes, hashimoto's thyroiditis, and celiac disease. *Front Immunol*. (2022) 13:891698/full. doi: 10.3389/fimmu.2022.891698/full

19. Vaarala O, Atkinson MA, Neu J. The 'perfect storm' for type 1 diabetes: the complex interplay between intestinal microbiota, gut permeability, and mucosal immunity. *Diabetes*. (2008) 57:2555–62. doi: 10.2337/db08-0331

20. Aseer KR, Egan JM. An autonomous cannabinoid system in islets of langerhans. *Front Endocrinol (Lausanne)*. (2021) 12:699661. doi: 10.3389/fendo.2021.699661

21. Aseer KR, Mazucanti CH, O'Connell JF, González-Mariscal I, Verma A, Yao Q, et al. Beta cell specific cannabinoid 1 receptor deletion counteracts progression to hyperglycemia in non-obese diabetic mice. *Mol Metab*. (2024) 82:101906. doi: 10.1016/j.molmet.2024.101906

22. Silvestri C, Di Marzo V. The endocannabinoid system in energy homeostasis and the etiopathology of metabolic disorders. *Cell Metab*. (2013) 17:475–90. doi: 10.1016/j.cmet.2013.03.001

23. Gasperi V, Evangelista D, Chiurchiù V, Florenzano F, Savini I, Oddi S, et al. 2-Arachidonoylglycerol modulates human endothelial cell/leukocyte interactions by controlling selectin expression through CB1 and CB2 receptors. *Int J Biochem Cell Biol*. (2014) 51:79–88. doi: 10.1016/j.biocel.2014.03.028

24. Hisanaga. Regulation of Calcium-Permeable TRPV2 Channel by Insulin in Pancreatic β-Cells | Diabetes | American Diabetes Association (2009). Available online at: https://diabetesjournals.org/diabetes/article/58/1/174/13657/Regulation-of-Calcium-Permeable-TRPV2-Channel-by.

25. Liu QR, Aseer KR, Yao Q, Zhong X, Ghosh P, O'Connell JF, et al. Anti-inflammatory and pro-autophagy effects of the cannabinoid receptor CB2R: possibility of modulation in type 1 diabetes. *Front Pharmacol*. (2021) 12:809965. doi: 10.3389/fphar.2021.809965

26. Cani PD, Geurts L, Matamoros S, Plovier H, Duparc T. Glucose metabolism: focus on gut microbiota, the endocannabinoid system and beyond. *Diabetes Metab*. (2014) 40:246–57. doi: 10.1016/j.diabet.2014.02.004

27. Jamshidi P, Hasanzadeh S, Tahvildari A, Farsi Y, Arbabi M, Mota JF, et al. Is there any association between gut microbiota and type 1 diabetes? A systematic review. *Gut Pathog*. (2019) 11:49. doi: 10.1186/s13099-019-0332-7

28. Giongo A, Gano KA, Crabb DB, Mukherjee N, Novelo LL, Casella G, et al. Toward defining the autoimmune microbiome for type 1 diabetes. *ISME J*. (2011) 5:82–91. doi: 10.1038/ismej.2010.92

29. Argenziano M, Tortora C, Bellini G, Di Paola A, Punzo F, Rossi F. The endocannabinoid system in pediatric inflammatory and immune diseases. *Int J Mol Sci*. (2019) 20:5875. doi: 10.3390/ijms20235875

30. Shilo S, Godneva A, Rachmiel M, Korem T, Bussi Y, Kolobkov D, et al. The gut microbiome of adults with type 1 diabetes and its association with the host glycemic control. *Diabetes Care*. (2022) 45:555–63. https://diabetesjournals.org/care/article/45/3/555/140931/The-Gut-Microbiome-of-Adults-With-Type-1-Diabetes.

31. Di Marzo V, Piscitelli F, Mechoulam R. Cannabinoids and endocannabinoids in metabolic disorders with focus on diabetes. In: Schwanstecher M, editor. *Diabetes - Perspectives in Drug Therapy*. Springer, Berlin, Heidelberg (2011). p. 75–104. doi: 10.1007/978-3-642-17214-4_4

32. Sido JM, Jackson AR, Nagarkatti PS, Nagarkatti M. Marijuana-derived Δ-9-tetrahydrocannabinol suppresses Th1/Th17 cell-mediated delayed-type hypersensitivity through microRNA regulation. *J Mol Med (Berl)*. (2016) 94:1039–51. doi: 10.1007/s00109-016-1404-5

33. Vatanen T, Franzosa EA, Schwager R, Tripathi S, Arthur TD, Vehik K, et al. The human gut microbiome in early-onset type 1 diabetes from the TEDDY study. *Nature*. (2018) 562:589–94. doi: 10.1038/s41586-018-0620-2

34. Kostic AD, Gevers D, Siljander H, Vatanen T, Hyötyläinen T, Hämäläinen AM, et al. The dynamics of the human infant gut microbiome in development and in progression toward type 1 diabetes. *Cell Host Microbe*. (2015) 17:260–73. doi: 10.1016/j.chom.2015.01.001

35. Groot HE, van de Vegte YJ, Verweij N, Lipsic E, Karper JC, van der Harst P. Human genetic determinants of the gut microbiome and their associations with health and disease: a phenome-wide association study. *Sci Rep*. (2020) 10:14771. doi: 10.1038/s41598-020-70724-5

36. Navarini L, Bisogno T, Mozetic P, Piscitelli F, Margiotta DPE, Basta F, et al. Endocannabinoid system in systemic lupus erythematosus: First evidence for a deranged 2-arachidonoylglycerol metabolism. *Int J Biochem Cell Biol*. (2018) 99:161–8. doi: 10.1016/j.biocel.2018.04.010

37. Zhai K, Liskova A, Kubatka P, Büsselberg D. Calcium entry through TRPV1: A potential target for the regulation of proliferation and apoptosis in cancerous and healthy cells. *Int J Mol Sci*. (2020) 21:4177. doi: 10.3390/ijms21114177

38. De Petrocellis L, Ligresti A, Moriello AS, Allarà M, Bisogno T, Petrosino S, et al. Effects of cannabinoids and cannabinoid-enriched Cannabis extracts on TRP channels and endocannabinoid metabolic enzymes. *Br J Pharmacol*. (2011) 163:1479–94. doi: 10.1111/j.1476-5381.2010.01166.x

39. Pacher P, Kunos G. Modulating the endocannabinoid system in human health and disease – successes and failures. *FEBS J*. (2013) 280:1918–43. doi: 10.1111/febs.12260

40. Pacher P, Mechoulam R. Is lipid signaling through cannabinoid 2 receptors part of a protective system? *Prog Lipid Res*. (2011) 50:193–211.

41. Nouh RA, Kamal A, Abdelnaser A. Cannabinoids and multiple sclerosis: A critical analysis of therapeutic potentials and safety concerns. *Pharmaceutics*. (2023) 15:1151. doi: 10.3390/pharmaceutics15041151

42. Battista N, Di Sabatino A, Di Tommaso M, Biancheri P, Rapino C, Giuffrida P, et al. Altered expression of type-1 and type-2 cannabinoid receptors in celiac disease. *PloS One*. (2013) 8:e62078. doi: 10.1371/journal.pone.0062078

43. Vaarala O. Is the origin of type 1 diabetes in the gut? *Immunol Cell Biol*. (2012) 90:271–6. doi: 10.1038/icb.2011.115

44. De Palma G, Nadal I, Medina M, Donat E, Ribes-Koninckx C, Calabuig M, et al. Intestinal dysbiosis and reduced immunoglobulin-coated bacteria associated with coeliac disease in children. *BMC Microbiol*. (2010) 10:63. doi: 10.1186/1471-2180-10-63

45. Fu X, Ren X, Zhao M, Li L, Zhou Y, Lu Y, et al. Disruption of intestinal barrier and dysbiosis of gut microbiota in an experimental rhesus macaque model with 6-year diabetes mellitus. *Exp Anim*. (2025) 9:223-31. doi: 10.1538/expanim.24-0125

46. Di Marzo V, Piscitelli F. The endocannabinoid system and its modulation by phytocannabinoids. *Neurotherapeutics*. (2015) 12:692–8. doi: 10.1007/s13311-015-0374-6

47. Sapone A, Lammers KM, Casolaro V, Cammarota M, Giuliano MT, De Rosa M, et al. Divergence of gut permeability and mucosal immune gene expression in two gluten-associated conditions: celiac disease and gluten sensitivity. *BMC Med*. (2011) 9:23. doi: 10.1186/1741-7015-9-23

48. Nistal E, Caminero A, Herrán AR, Arias L, Vivas S, de Morales JMR, et al. Differences of small intestinal bacteria populations in adults and children with/without celiac disease: effect of age, gluten diet, and disease. *Inflamm Bowel Dis*. (2012) 18:649–56. doi: 10.1002/ibd.21830

49. Torun A, Hupalowska A, Trzonkowski P, Kierkus J, Pyrzynska B. Intestinal microbiota in common chronic inflammatory disorders affecting children. *Front Immunol*. (2021) 12:642166/full. doi: 10.3389/fimmu.2021.642166/full

50. Tzelepi VN, Tsamandas AC, Vlotinou HD, Vagianos CE, Scopa CD. Tight junctions in thyroid carcinogenesis: diverse expression of claudin-1, claudin-4, claudin-7 and occludin in thyroid neoplasms. *Mod Pathol*. (2008) 21:22–30. doi: 10.1038/modpathol.3800959

51. Virili C, Fallahi P, Antonelli A, Benvenga S, Centanni M. Gut microbiota and Hashimoto's thyroiditis. *Rev Endocr Metab Disord*. (2018) 19:293–300. doi: 10.1007/s11154-018-9467-y

52. Chen J, Wright K, Davis JM, Jeraldo P, Marietta EV, Murray J, et al. An expansion of rare lineage intestinal microbes characterizes rheumatoid arthritis. *Genome Med*. (2016) 8:43. doi: 10.1186/s13073-016-0299-7

53. Scher JU, Abramson SB. The microbiome and rheumatoid arthritis. *Nat Rev Rheumatol*. (2011) 7:569–78. doi: 10.1038/nrrheum.2011.121

54. Audo R, Sanchez P, Rivière B, Mielle J, Tan J, Lukas C, et al. Rheumatoid arthritis is associated with increased gut permeability and bacterial translocation which are reversed by inflammation control. *Rheumatol (Oxford)*. (2022), keac454.

55. Lu R, Luo XM. The role of gut microbiota in different murine models of systemic lupus erythematosus. *Autoimmunity*. (2024) 57:2378876. doi: 10.1080/08916934.2024.2378876

56. Richardson D, Pearson RG, Kurian N, Latif ML, Garle MJ, Barrett DA, et al. Characterisation of the cannabinoid receptor system in synovial tissue and fluid in patients with osteoarthritis and rheumatoid arthritis. *Arthritis Res Ther*. (2008) 10:R43. doi: 10.1186/ar2401

57. Centonze D, Bari M, Rossi S, Prosperetti C, Furlan R, Fezza F, et al. The endocannabinoid system is dysregulated in multiple sclerosis and in experimental autoimmune encephalomyelitis. *Brain*. (2007) 130:2543–53. doi: 10.1093/brain/awm160

58. Malenczyk K, Keimpema E, Piscitelli F, Calvigioni D, Björklund P, Mackie K, et al. Fetal endocannabinoids orchestrate the organization of pancreatic islet microarchitecture. *Proc Natl Acad Sci U S A*. (2015) 112:E6185–94. doi: 10.1073/pnas.1519040112

59. De Petrocellis L, Di Marzo V. An introduction to the endocannabinoid system: from the early to the latest concepts. *Best Pract Res Clin Endocrinol Metab*. (2009) 23:1–15. doi: 10.1016/j.beem.2008.10.013

60. Iannotti FA, Di Marzo V. The gut microbiome, endocannabinoids and metabolic disorders. *J Endocrinol*. (2021) 248:R83–97. doi: 10.1530/JOE-20-0444

61. Kojima T, Yamaguchi H, Ito T, Kyuno D, Kono T, Konno T, et al. Tight junctions in human pancreatic duct epithelial cells. *Tissue Barriers*. (2013) 1:e24894. doi: 10.4161/tisb.24894

62. Steffens S, Veillard NR, Arnaud C, Pelli G, Burger F, Staub C, et al. Low dose oral cannabinoid therapy reduces progression of atherosclerosis in mice. *Nature*. (2005) 434:782–6. doi: 10.1038/nature03389

63. Li X, Atkinson MA. The role for gut permeability in the pathogenesis of type 1 diabetes – A solid or leaky concept? *Pediatr Diabetes*. (2015) 16:485–92.

64. Ortiz-Alvarez L, Xu H, Di X, Kohler I, Osuna-Prieto FJ, Acosta FM, et al. Plasma levels of endocannabinoids and their analogues are related to specific fecal bacterial genera in young adults: role in gut barrier integrity. *Nutrients*. (2022) 14:2143. doi: 10.3390/nu14102143

65. Cani PD, Osto M, Geurts L, Everard A. Involvement of gut microbiota in the development of low-grade inflammation and type 2 diabetes associated with obesity. *Gut Microbes*. (2012) 3:279–88. doi: 10.4161/gmic.19625

66. Ratajczak W, Rył A, Mizerski A, Walczakiewicz K, Sipak O, Laszczyńska M. Immunomodulatory potential of gut microbiome-derived short-chain fatty acids (SCFAs). *Acta Biochim Pol*. (2019) 66:1–12. doi: 10.18388/abp.2018_2648

67. Furusawa Y, Obata Y, Fukuda S, Endo TA, Nakato G, Takahashi D, et al. Commensal microbe-derived butyrate induces the differentiation of colonic regulatory T cells. *Nature*. (2013) 504:446–50. doi: 10.1038/nature12721

68. Arpaia N, Campbell C, Fan X, Dikiy S, van der Veeken J, deRoos P, et al. Metabolites produced by commensal bacteria promote peripheral regulatory T-cell generation. *Nature*. (2013) 504:451–5. doi: 10.1038/nature12726

69. Chassaing B, Koren O, Goodrich JK, Poole AC, Srinivasan S, Ley RE, et al. Dietary emulsifiers impact the mouse gut microbiota promoting colitis and metabolic syndrome. *Nature*. (2015) 519:92–6. doi: 10.1038/nature14232

70. Grabacka M, Płonka PM, Pierzchalska M. The PPARα Regulation of the gut physiology in regard to interaction with microbiota, intestinal immunity, metabolism, and permeability. *Int J Mol Sci*. (2022) 23:14156. doi: 10.3390/ijms232214156

71. Machiels K, Joossens M, Sabino J, De Preter V, Arijs I, Eeckhaut V, et al. A decrease of the butyrate-producing species Roseburia hominis and Faecalibacterium prausnitzii defines dysbiosis in patients with ulcerative colitis. *Gut*. (2014) 63:1275–83. doi: 10.1136/gutjnl-2013-304833

72. Louis P, Hold GL, Flint HJ. The gut microbiota, bacterial metabolites and colorectal cancer. *Nat Rev Microbiol*. (2014) 12:661–72. doi: 10.1038/nrmicro3344

73. Vijay-Kumar M, Aitken JD, Carvalho FA, Cullender TC, Mwangi S, Srinivasan S, et al. Metabolic syndrome and altered gut microbiota in mice lacking Toll-like receptor 5. *Science*. (2010) 328:228–31. doi: 10.1126/science.1179721

74. Di Marzo V, Silvestri C. Lifestyle and metabolic syndrome: contribution of the endocannabinoidome. *Nutrients*. (2019) 11:1956. doi: 10.3390/nu11081956

75. Alhamoruni A, Wright KL, Larvin M, O'Sullivan SE. Cannabinoids mediate opposing effects on inflammation-induced intestinal permeability. *Br J Pharmacol*. (2012) 165:2598–610. doi: 10.1111/j.1476-5381.2011.01589.x

76. Ueno K, Saika S, Okada Y, Iwanishi H, Suzuki K, Yamada G, et al. Impaired healing of cutaneous wound in a Trpv1 deficient mouse. *Exp Anim*. (2023) 72:224–32. doi: 10.1538/expanim.22-0124

77. Abdel-Moneim A, Bakery HH, Allam G. The potential pathogenic role of IL-17/Th17 cells in both type 1 and type 2 diabetes mellitus. *Biomed Pharmacother*. (2018) 101:287–92. doi: 10.1016/j.biopha.2018.02.103

78. Maffeis C, Martina A, Corradi M, Quarella S, Nori N, Torriani S, et al. Association between intestinal permeability and faecal microbiota composition in Italian children with beta cell autoimmunity at risk for type 1 diabetes. *Diabetes Metab Res Rev*. (2016) 32:700–9. doi: 10.1002/dmrr.v32.7

frontiers | Frontiers in Endocrinology

TYPE Original Research
PUBLISHED 02 June 2025
DOI 10.3389/fendo.2025.1492082

OPEN ACCESS

EDITED BY
Matthias Blüher,
Leipzig University, Germany

REVIEWED BY
Luis Del Carpio-Orantes,
Mexican Social Security Institute, Mexico
Éva Csajbók,
University of Szeged, Hungary

*CORRESPONDENCE
Xiufan Du
draliee@163.com

RECEIVED 06 September 2024
ACCEPTED 07 April 2025
PUBLISHED 02 June 2025

CITATION
Yan Z, Chang X, Liu Z, Liu R and Du X (2025) The association of obesity and lipid-related indicators with all-cause and cardiovascular mortality risks in patients with diabetes or prediabetes: a cross-sectional study based on machine learning algorithms. *Front. Endocrinol.* 16:1492082. doi: 10.3389/fendo.2025.1492082

The association of obesity and lipid-related indicators with all-cause and cardiovascular mortality risks in patients with diabetes or prediabetes: a cross-sectional study based on machine learning algorithms

Zhaoqi Yan[1], Xing Chang[1], Zhiming Liu[1], Ruxiu Liu[1] and Xiufan Du[2*]

[1]Guang'anmen Hospital, China Academy of Chinese Medical Sciences, Graduate School, Beijing, China, [2]The Third Hospital of Nanchang, Nanchang People's Hospital, Department of Rehabilitation Medicine, Nanchang, Jiangxi, China

Objective: This study aims to explore the associations between various obesity and lipid-related indicators in patients with diabetes or prediabetes. Specifically, the indicators examined include the triglyceride-glucose index (TyG), along with its derived metrics: TyG-BMI, TyG-WHtR, TyG-WWI, TyG-WC, lipid accumulation product (LAP), visceral adiposity index (VAI), and abdominal obesity index (ABSI), resulting in a total of eight indicators.

Methods: This study utilizes data from the NHANES conducted from 1999 to 2018, analyzing a cohort of 4,058 patients diagnosed with diabetes/prediabetes. We utilized multivariable Cox regression models to evaluate the impact of these indicators on both all-cause and cardiovascular mortality rates. Additionally, we compared the predictive performance of eight machine learning (ML) algorithms regarding mortality risk and used the SHAP method to clarify the significance of obesity and lipid-related indicators in mortality prediction.

Results: The results of the multivariable Cox regression analysis reveal significant associations between TyG, TyG-WWI, and ABSI with all-cause mortality among patients with diabetes/prediabetes. Compared to baseline levels, the HR for TyG in the fourth quartile (Q4) was 1.49, while for TyG-WWI (Q4), the HR was 1.52. Furthermore, ABSI was associated with increased all-cause mortality risk in groups Q3 and Q4, presenting risk ratios of 1.80 and 1.68, respectively. Notably, TyG (Q4) was also significantly associated with cardiovascular mortality risk, with an HR of 1.98. RCS analysis indicated a linear trend between TyG, TyG-WWI, and all-cause mortality, whereas ABSI displayed a non-linear trend. Among the ML algorithms evaluated, the XGBoost model exhibited the strongest predictive capability. The SHAP analysis indicated that the indicators with the greatest impact on all-cause mortality in patients with diabetes/prediabetes were ranked as follows: TyG > ABSI > TyG-WWI. Furthermore, sex-based subgroup analysis indicated that VAI was positively associated with

cardiovascular mortality in male patients with diabetes/prediabetes, exhibiting a linear trend.

Conclusion: TyG, TyG-WWI, ABSI, and VAI are closely linked to mortality risk in diabetes/prediabetes patients. Among these, TyG is significantly associated with both all-cause and cardiovascular mortality, showing superior predictive capability. We recommend long-term monitoring of these indicators and their inclusion in management strategies to effectively inform diabetes/prediabetes patients about their mortality risks.

KEYWORDS

obesity and lipid-related indicators, triglyceride-glucose index, abdominal obesity index, visceral adiposity index, diabetes/prediabetes, national health and nutrition examination survey; machine learning algorithms

Introduction

The global prevalence of diabetes has reached alarming levels, with an estimated 570 million cases projected by 2025 (1). Prediabetes, the precursor stage of diabetes, is primarily characterized by impaired fasting glucose (IFG) and impaired glucose tolerance (IGT). The population affected by prediabetes continues to grow (2). By 2030, the number of individuals with prediabetes is expected to exceed 470 million (3) Notably, the annual conversion rate from prediabetes to diabetes ranges from approximately 5% to 10% (4). Moreover, diabetes significantly shortens life expectancy. The World Health Organization (WHO) predicts that by 2030, diabetes will become the seventh leading cause of death globally (5). Compared to individuals with normal glucose metabolism, patients with diabetes or prediabetes (hereinafter referred to as diabetes/prediabetes) face significantly increased risks for macrovascular (6–8) and microvascular complications (9). Consequently, cardiovascular disease (CVD) a leading cause of mortality and disability among diabetes patients (10). Effectively managing diabetes or prediabetes to reduce mortality risk presents a formidable challenge.

Among the numerous factors influencing blood glucose levels, obesity is undoubtedly one of the most significant. The prevalence of diabetes/prediabetes in the United States is rising alongside obesity. Most patients with diabetes/prediabetes exhibit excessive adipose tissue, which stimulates inflammatory responses and immune dysfunction, serving as key contributors to insulin resistance (11). Although Body Mass Index (BMI) is a widely accepted standard for assessing obesity, it is inadequate for evaluating visceral fat, dyslipidemia, and insulin resistance. Consequently, several new anthropometric tools have been developed to better reflect these characteristics. For example, the abdominal obesity index (ABSI) (12), lipid accumulation product (LAP), and visceral adiposity index (VAI) (13) are considered effective new indicators for predicting diabetes risk compared to BMI (14). Additionally, the triglyceride-glucose index (TyG) (15) has advantages, such as not requiring highly precise insulin levels and overcoming poor measurement reproducibility. It is regarded as an effective alternative to traditional insulin resistance indicators, such as HOMA-IR and QUICKI (16). This advancement overcomes the limitations of traditional indicators in clinical practice (17). Furthermore, several studies have developed novel indices based on TyG by incorporating various anthropometric measurements. Examples include the triglyceride glucose-body mass index (TyG-BMI), triglyceride glucose-waist-to-height ratio (TyG-WHtR), triglyceride glucose-weight-adjusted waist circumference(TyG-WWI) and triglyceride glucose-waist circumference (TyG-WC) (18). These indices are also considered effective tools for predicting diabetes risk. Despite the varying degrees of potential these indicators have shown in predicting diabetes, there is currently no consensus on their effectiveness in predicting mortality risk among patients with diabetes/prediabetes.

This study aims to explore the predictive capabilities of obesity and lipid-related indices (TyG, TyG-BMI, TyG-WHtR, TyG-WWI, TyG-WC, LAP, VAI, and ABSI) for all-cause and cardiovascular mortality among patients with diabetes/prediabetes, utilizing the National Health and Nutrition Examination Survey (NHANES) database. Additionally, we will compare the predictive abilities of these indices using machine learning models to identify the most accurate predictive factors.

Materials and methods

Study population in NHANES

In this study, we analyzed data collected from 1999 to 2018. The criteria for excluding samples included the following (1): lack of necessary parameters for assessing obesity and lipid-related indices; (2) absence of definitional information for diabetes and prediabetes; (3) missing covariate data; (4) absence of survival data (Figure 1). The NHANES study protocol was approved by the Institutional Review

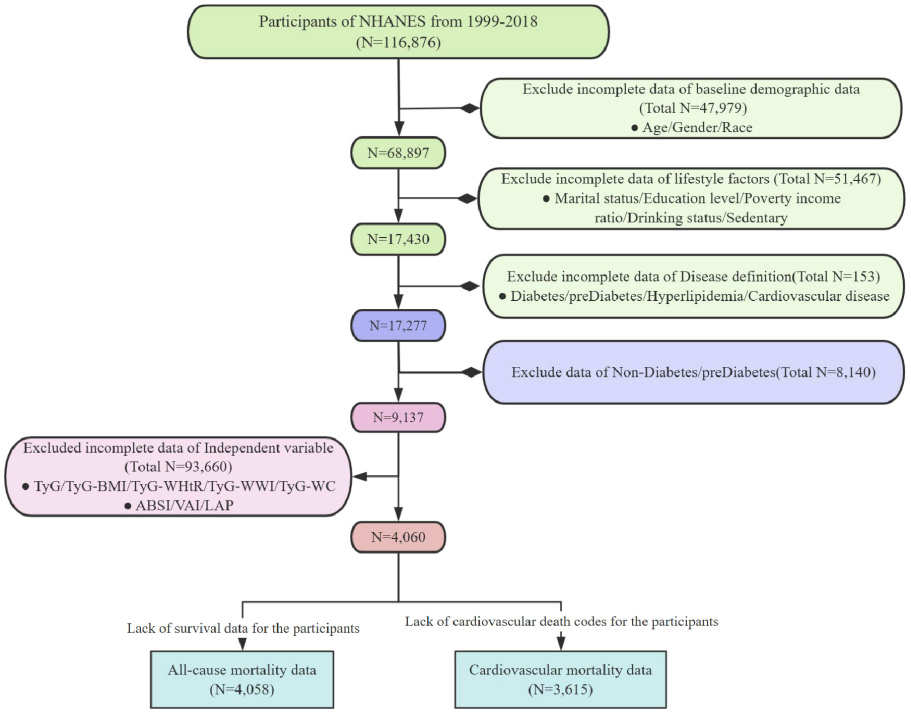

FIGURE 1
Flowchart of inclusion and exclusion criteria for the study.

Board of the National Center for Health Statistics (NCHS), and all participants provided written informed consent. For more detailed information about this study, please visit: www.cdc.gov/nchs/nhanes/irba98.htm.

Assessment of the diagnosis of prediabetes and diabetes

The diagnosis of diabetes was based on one or more of the following criteria: (1) a medical diagnosis confirmed by the patient's healthcare provider with self-reporting; (2) glycated hemoglobin (HbA1c) level ≥ 6.5%; (3) FPG level ≥ 7.0 mmol/L; (4) questionnaire results indicating that the patient is using diabetes medications. Prediabetes was defined by the following criteria: (1) a diagnosis confirmed by a healthcare professional through self-reporting; (2) HbA1c levels between 5.7% and less than 6.5%; (3) FPG levels between 100 mg/dL and 125 mg/dL (19).

Definitions of obesity and lipid-related indices

In this study, the obesity and lipid-related indices included TyG, TyG-BMI, TyG-WWI, TyG-WHtR, TyG-WC, ABSI, LAP, and VAI. The calculation methods for TyG and its related obesity indicators are as follows. Since ABSI values are typically low, the values presented in this study are shown as 10-fold multiples (18):

$$\mathrm{TyG} = \ln\left(\frac{\mathrm{Triglyceride(mg/dL)} \times \mathrm{FPG(mg/dL)}}{2}\right)$$

$$\mathrm{TyG-WHtR} = \mathrm{TyG} \times \frac{\mathrm{WC(cm)}}{\mathrm{Height(m)}}$$

$$\mathrm{TyG-BMI} = \mathrm{TyG} \times \frac{\mathrm{Weight(kg)}}{\mathrm{Height^2(m^2)}}$$

$$\mathrm{TyG-WWI} = \mathrm{TyG} \times \frac{\mathrm{WC(cm)}}{\sqrt{\mathrm{Weight(kg)}}}$$

$$\mathrm{TyG-WC} = \mathrm{TyG} \times \mathrm{WC}$$

VAI (13) is calculated as follows:

$$\mathrm{Males: VAI} = \frac{\mathrm{WC(cm)}}{39.68+(1.88\times\mathrm{BMI(kg/m^2)})} \times \left(\frac{\mathrm{Triglyceride(mmol/L)}}{1.03}\right) \times \left(\frac{1.31}{\mathrm{HDL-C(mmol/L)}}\right)$$

$$\mathrm{Females: VAI} = \frac{\mathrm{WC(cm)}}{36.58+(1.89\times\mathrm{BMI(kg/m^2)})} \times \left(\frac{\mathrm{Triglyceride(mmol/L)}}{0.81}\right) \times \left(\frac{1.52}{\mathrm{HDL-C(mmol/L)}}\right)$$

LAP (13) is calculated as follows:

$$\mathrm{Males: LAP} = (\mathrm{WC(cm)} - 65) \times \mathrm{Triglyceride(mmol/L)}$$

$$\mathrm{Female: LAP} = (\mathrm{WC(cm)} - 58) \times \mathrm{Triglyceride(mmol/L)}$$

The ABSI (12) is calculated as follows:

$$\mathrm{ABSI} = \frac{\mathrm{WC(cm)}}{\mathrm{BMI(kg/m^2)^{\frac{2}{3}}} \times \mathrm{Height(m)^{\frac{1}{2}}}}$$

FPG: Fasting blood glucose; HDL-C: High density lipoprotein cholesterol; WWI: Weight-adjusted waist circumference index; WC: Waist circumference.

Mortality

In this study, mortality data for all NHANES participants were matched with the National Death Index (NDI) using probabilistic matching methods, with a cutoff date of December 31, 2019. This process was used to calculate all-cause mortality rates. Additionally, considering the close relationship between obesity, lipid-related indices, and diabetes in relation to cardiovascular mortality risk, we used the death codes provided by the NDI to ascertain the cause of death. Causes of death were classified as cardiovascular-related according to the International Classification of Diseases, Tenth Revision (ICD-10), using relevant codes I00-I09, I11, I13, and I20-I51.

Covariates

Covariate information for this study was collected from NHANES demographic data, questionnaires, and laboratory tests. We categorized the covariates into three main groups: baseline demographic data (age, gender, race), lifestyle factors (marital status, education level, BMI, alcohol consumption, and sedentary behavior), and comorbidities (hyperlipidemia, and CVD). The specific definitions are as follows:

The original five racial classifications from NHANES were condensed into three categories: Hispanic, Non-Hispanic Black, and Non-Hispanic White and Other; Marital status was categorized as divorced, married, or unmarried; Education level was classified as Below high school (Less Than 9th Grade), High school graduate or GED (9-11th Grade, including 12th grade with no diploma), and Some college or above (Some College or AA degree/College Graduate or above); BMI classifications were defined as normal (<25 kg/m^2), obese (≥30 kg/m^2), and overweight (≥25 kg/m^2 but <30 kg/m^2); Sedentary behavior was defined as sitting or reclining for more than 480 minutes per day, or responding the questionnaire with an emphasis on a sedentary typical day; Alcohol consumption status was classified into three categories: current drinker (defined as having consumed more than 12 types of alcoholic beverages in their lifetime and currently consuming), former drinker (defined as having consumed more than 12 types of alcoholic beverages at any time during their lifetime but not in the past year), and never drinker (defined as having consumed no more than 12 types of alcoholic beverages in their lifetime); Hyperlipidemia was defined by any of the following criteria: total cholesterol levels equal to or exceeding 200 mg/dL, triglyceride levels equal to or exceeding 150 mg/dL, male HDL-C levels below 40 mg/dL, female HDL-C levels below 50 mg/dL, or low-density lipoprotein cholesterol (LDL-C) levels equal to or exceeding 130 mg/dL; CVD was defined as a positive response to any of the following questions: "Has a doctor or other health professional ever told you that you have congestive heart failure (CHF), coronary heart disease (CHD), angina, a heart attack, or a stroke?"

Statistical analysis

We employed a complex sampling design to ensure nationally representative estimates, and all analyses were adjusted for survey design and weighting variables. The new sample weights were calculated by dividing the original two-year sample weights by 20. Continuous variables are presented as means ± standard deviation (SD), while categorical variables are expressed as counts (N) and percentages (%). The obesity and lipid-related indices were categorized into four groups using quartiles. We used weighted t-tests (for continuous variables) or weighted chi-square tests (for categorical variables) to assess differences between survival and mortality group. The survival probabilities of diabetes/prediabetes patients under different obesity and lipid-related indices were compared using Kaplan-Meier (KM) curves and log-rank tests. The Cox regression model was used to analyze the mortality risk in diabetes/prediabetes patients, with model construction undergoing multiple adjustments: Model 1 adjusted for baseline demographic data; Model 2 further adjusted for lifestyle factors; and Model 3 adjusted for comorbidities on top of Model 2. A p-value of less than 0.05 was considered statistically significant for all two-sided tests. Furthermore, we employed a restricted cubic spline (RCS) model to treat obesity and lipid-related indices as continuous variables, investigating the linear and non-linear associations between these indices and mortality risk in diabetes/prediabetes patients by setting the 10th, 50th, and 90th percentiles as nodes of the RCS (20).

Machine learning

This study also employed machine learning (ML) modeling strategies to compare predictive abilities of obesity and lipid-related indices for mortality risk based on the Cox regression model. We used supervised MLs, integrating various obesity and lipid-related indices, components of each index, all covariates, and survival data into the machine learning dataset (21): extreme gradient boosting (XGBoost), decision tree (DT), robust support vector machine (RSVM), elastic net regression (Enet), multi-layer perceptron (MLP), logistic regression, random forest (RF), and k-nearest neighbors (KNN). The dataset was divided into two non-overlapping parts: a training set (60%) and a testing set (40%). In the training dataset, each model underwent automatic hyperparameter tuning using Bayesian optimization and five-fold cross-validation. When comparing the eight machine learning algorithms, we synthesized the assessment of the best algorithm using the receiver operating characteristic - area under the curve (ROC-AUC), accuracy, precision, recall, and calibration curves. We subsequently applied SHapley Additive Explanations (SHAP) to interpret the machine learning models, aiming to address the black box issue associated with these models. The Shapley value, derived

from cooperative game theory, quantifies the importance of each feature in the model by calculating marginal contributions (22). We used the "fastshap" package to generate SHAP beeswarm plots to visualize each variable's contribution to individual predictions. This clearly illustrates the significance of obesity and lipid-related indices and analyzes how the components of different indices contribute to and influence mortality risk.

Results

Baseline characteristics of study participants

This study included 4,058 participants with diabetes/prediabetes, of whom 640 (12%) died before December 31, 2019. Significant differences were observed between the mortality group and the survival group across multiple variables. First, the mortality group had a higher average age of 70.5 years and relatively fewer male survivors. Additionally, the mortality group had a higher proportion of Non-Hispanic White and other racial groups, as well as a greater proportion of married individuals. Notably, the mortality group exhibited higher rates of sedentary behavior, poverty, and low educational attainment, along with higher proportions of non-drinkers, individuals with hyperlipidemia, and CVD. Furthermore, some anthropometric measures, such as height, weight, and waist circumference, were slightly lower in the mortality group compared to the survival group. However, new anthropometric measurements derived from these indicators, such as the WWI and ABSI, were higher in the mortality group. Blood lipid and glucose levels were also significantly elevated in the mortality group. Additionally, the TyG was higher in the mortality group. Other derived anthropometric indices, such as TyG-WHtR and TyG-WWI, were also elevated compared to the survival group, with the VAI significantly higher as well. However, no significant difference was found in the LAP between the two groups (Table 1).

TABLE 1 Characteristics of participants according to All-cause mortality. (NHANES 1999-2018, N = 4,058).

Characteristic	Overall, N = 4058 (100%)[1,2]	Survival Group, N = 3418 (88%)[1,2]	Mortality Group, N = 640 (12%)[1,2]	P Value
Age (years)	54.6 (16.5)	52.4 (15.8)	70.5 (11.9)	<0.001
Sex				0.036
Female	2,470 (58%)	2,078 (58%)	392 (63%)	
Male	1,588 (42%)	1,340 (42%)	248 (37%)	
Race				<0.001
Non-Hispanic White and Other	2,033 (72%)	1,644 (71%)	389 (80%)	
Hispanic	1,085 (15%)	967 (16%)	118 (7.3%)	
Non-Hispanic Black	940 (13%)	807 (13%)	133 (13%)	
Marital				0.014
Divorced	2,232 (59%)	1,923 (60%)	309 (53%)	
Married	1,677 (39%)	1,365 (38%)	312 (45%)	
Never married	149 (2.6%)	130 (2.6%)	19 (2.3%)	
PIR				<0.001
High(>3.49)	1,040 (36%)	932 (38%)	108 (22%)	
Medium(>1.39,<=3.49)	1,573 (38%)	1,302 (37%)	271 (45%)	
Low(≤1.39)	1,445 (26%)	1,184 (25%)	261 (33%)	
Sedentary				0.001
Non Sedentary	2,895 (69%)	2,499 (73%)	396 (62%)	
Sedentary	1,163 (31%)	919 (27%)	244 (38%)	
Education				<0.001
Below high school	599 (8.4%)	456 (7.5%)	143 (15%)	
High school graduate or GED	1,611 (40%)	1,319 (39%)	292 (50%)	
Some college or above	1,848 (51%)	1,643 (54%)	205 (35%)	

(Continued)

10.3389/fendo.2025.1492082

TABLE 1 Continued

Characteristic	Overall, N = 4058 (100%)[1,2]	Survival Group, N = 3418 (88%)[1,2]	Mortality Group, N = 640 (12%)[1,2]	P Value
Weight(Kg)	86 (23)	87 (23)	79 (21)	<0.001
Height(Cm)	166 (10)	167 (10)	164 (10)	<0.001
Waist circumference	104 (17)	104 (17)	102 (16)	0.029
BMI	31 (7)	31 (7)	29 (7)	<0.001
Normal(≥18.5,<25)	799 (19%)	633 (18%)	166 (27%)	
Obese(≥30)	1,935 (49%)	1,678 (50%)	257 (40%)	
Overweight(≥25,<30)	1,292 (31%)	1,084 (31%)	208 (32%)	
Drinking status				<0.001
Current drinker	1,538 (45%)	1,411 (48%)	127 (22%)	
Former drinker	1,095 (25%)	867 (23%)	228 (35%)	
Never drinker	1,425 (30%)	1,140 (28%)	285 (42%)	
Hyperlipidemia				0.027
Hyperlipidemia	3,266 (80%)	2,729 (80%)	537 (84%)	
Non-Hyperlipidemia	792 (20%)	689 (20%)	103 (16%)	
CVD				<0.001
CVD	625 (13%)	421 (12%)	204 (32%)	
Non-CVD	3,433 (87%)	2,997 (88%)	436 (68%)	
Insulin	16 (18)	16 (18)	15 (18)	0.4
Triglyceride	128 (67)	125 (66)	150 (70)	<0.001
Blood glucose	118 (38)	117 (35)	128 (52)	<0.001
WHtR	0.63 (0.10)	0.63 (0.10)	0.63 (0.09)	0.8
WWI	11.30 (0.80)	11.26 (0.80)	11.61 (0.78)	<0.001
TyG-BMI	273 (71)	274 (72)	264 (67)	0.019
TyG-WHtR	5.51 (1.05)	5.50 (1.05)	5.65 (0.99)	0.008
TyG-WWI	99 (11)	98 (11)	105 (11)	<0.001
TyG-WC	916 (174)	915 (175)	925 (167)	0.3
TyG	8.76 (0.62)	8.73 (0.62)	9.01 (0.59)	<0.001
LAP	214 (92)	215 (92)	209 (87)	0.2
ABSI	0.82 (0.05)	0.82 (0.05)	0.85 (0.05)	<0.001
VAI	2.14 (1.53)	2.08 (1.49)	2.59 (1.78)	<0.001

[1]Mean ± SD for continuous; n (%) for categorical.
[2]t-test adapted to complex survey samples; chi-squared test with Rao & Scott's second-order correction.
triglyceride glucose-waist circumference.
TyG, Triglyceride Glucose; TyG-BMI, Triglyceride Glucose - Body Mass Index; TyG-WHtR, Triglyceride Glucose - Waist to Height Ratio; TyG-WWI, Triglyceride Glucose - Weight Adjusted Waist Index; TyG-WC, Triglyceride Glucose - Waist Circumference; ABSI, A Body Shape Index; LAP, Lipid Accumulation Product; VAI, Visceral Adiposity Index.

Survival patterns of diabetes/prediabetes patients by quartile levels of obesity and lipid-related indices

We conducted a survival analysis on the indices that demonstrated statistical differences between the survival and mortality groups in Table 1. The KM curves revealed that diabetes/prediabetes patients in the lowest quartile of TyG, TyG-WWI, and ABSI had significantly higher overall survival probabilities compared to those in the highest quartile (P = 5e-05, P < 2e-16, and P < 2e-16, respectively) (Figures 2A–C). Additionally, the TyG-BMI in the Q2 group demonstrated the

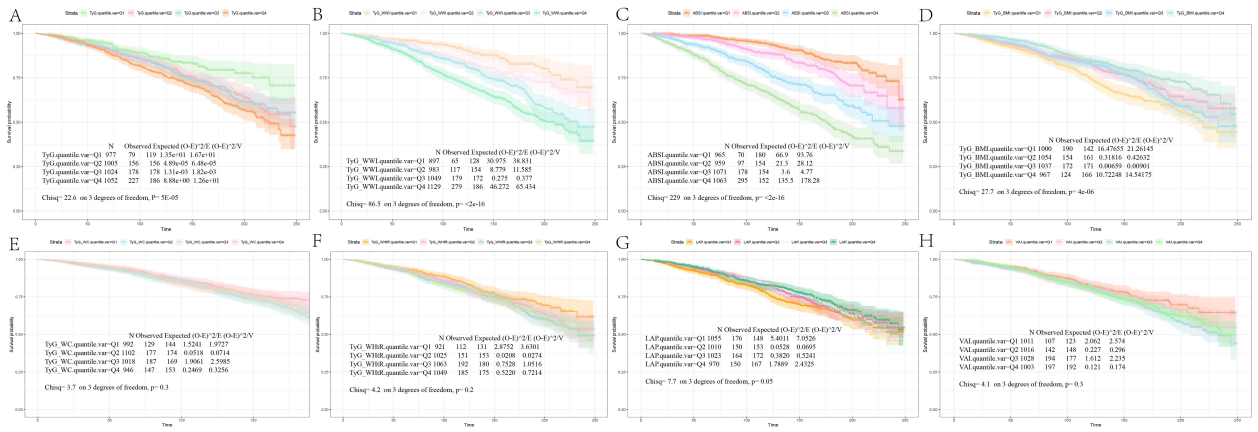

FIGURE 2
Kaplan-Meier survival analysis curves for all-Cause mortality. The Kaplan-Meier curves show the cumulative probabilities of all-cause mortality at 250 days for each group: **(A)** TyG: Q1 (6.56, 8.33), Q2 (8.34, 8.74), Q3 (8.75, 9.17), Q4 (9.18, 11.03); **(B)** TyG-WWI: Q1 (60.85, 90.83), Q2 (90.84, 98.38), Q3 (98.39, 106.25), Q4 (106.26, 144.15); **(C)** ABSI: Q1 (0.60, 0.78), Q2 (0.79, 0.81), Q3 (0.82, 0.85), Q4 (0.86, 0.99); **(D)** TyG-BMI: Q1 (115.40, 223.37), Q2 (223.38, 262.31), Q3 (262.32, 313.23), Q4 (313.24, 620.83); **(E)** TyG-WC: Q1 (453.12, 792.26), Q2 (792.27, 902.24), Q3 (902.25, 1025.15), Q4 (1025.16, 1648.81); **(F)** TyG-WHtR: Q1 (2.63, 4.73), Q2 (4.74, 5.40), Q3 (5.41, 6.14), Q4 (6.15, 10.23); **(G)** LAP: Q1 (3.07, 149.93), Q2 (149.94, 202.77), Q3 (202.78, 268.45), Q4 (268.46, 604.96); **(H)** VAI: Q1 (0.15, 1.01), Q2 (1.02, 1.68), Q3 (1.69, 2.75), Q4 (2.76, 11.39). TyG, Triglyceride Glucose; TyG-BMI, Triglyceride Glucose - Body Mass Index; TyG-WHtR, Triglyceride Glucose - Waist to Height Ratio; TyG-WWI, Triglyceride Glucose - Weight Adjusted Waist Index; TyG-WC, Triglyceride Glucose - Waist Circumference; ABSI, A Body Shape Index; LAP, Lipid Accumulation Product; VAI, Visceral Adiposity Index.

highest survival probability (P = 4e-06) (Figure 2D), while TyG-WC, TyG-WHtR, LAP, and VAI did not show significant differences (P = 0.3, P = 0.2, P = 0.05, and P = 0.3, respectively) (Figures 2E–H).

Associations between obesity and lipid-related indices and mortality

We performed a quartile-based analysis of obesity and various lipid-related indices, including TyG, TyG-BMI, TyG-WHtR, TyG-WWI, TyG-WC, LAP, VAI, and ABSI. The results from the Cox regression analysis indicated significant associations between TyG, TyG-WWI, and ABSI and all-cause mortality in diabetes/prediabetes patients. After adjustment in Model 3, compared to baseline levels (Q1), the highest quartile of TyG (Q4: 9.18, 11.03) and TyG-WWI (Q4: 106.26, 144.15) respectively increased the risk of all-cause mortality, with a HR of 1.49 (95% CI: 1.09-2.03) and 1.52 (95% CI: 1.02-2.26). Furthermore, ABSI in Q3 (0.82, 0.85) and Q4 (0.86, 0.99) also indicated increased all-cause mortality risk, with HRs of 1.80 (95% CI: 1.23-2.64) and 1.68 (95% CI: 1.17-2.41), respectively. Additionally, the analysis of ungrouped continuous variables revealed that for each one-unit increase in TyG, TyG-WWI, and ABSI, the all-cause mortality risk increased by 1.4 times, 1.02 times, and 48.6 times, respectively (Figure 3, Supplementary Table S2).

Moreover, focusing solely on patients who died from cardiovascular causes (Supplementary Table S1), the Cox regression analysis indicated a significant association between TyG and cardiovascular mortality in diabetes/prediabetes patients. After adjustment in Model 3, the highest quartile of TyG (Q4: 8.75, 11.03) was associated with an increased risk of cardiovascular mortality, with a HR of 1.98 (95% CI: 1.04-2.35). Additionally, the analysis of ungrouped continuous variables revealed that for each one-unit increase in TyG, the risk of cardiovascular mortality increased by 1.57 times (Figure 3, Supplementary Table S3). Additionally, TyG-WC in the Q4 was associated with elevated cancer-related mortality, with a HR of 3.09 (95% CI: 1.11–8.58) (Figure 3, Supplementary Table S4).

Race differences in analysis

Cox regression analysis of race revealed that race-specific associations between obesity/lipid-related indicators and mortality risks. For Hispanic populations, elevated TyG quartiles (Q4) significantly increased all-cause mortality (HR = 2.35, 95% CI: 1.18–4.68) and cardiovascular mortality (HR = 2.42, 95% CI: 1.12–5.24), with per-unit TyG increases further amplifying risks (all-cause: HR = 1.94; Cardiovascular mortality: HR = 1.69). Non-Hispanic Black groups exhibited extreme obesity-driven risks, particularly with higher ABSI quartiles (all-cause mortality Q2–Q4 HRs = 3.79–3.00, all *P < 0.05; cardiovascular mortality per-unit HR = 49.3, 95% CI: 6.19–392, ***P < 0.001). Additionally, ABSI at the Q4 level demonstrated an elevated risk of all-cause mortality in both the Hispanic and Non-Hispanic White and Other groups. Non-Hispanic White/Other populations only showed significant cancer mortality risks with TyG-WC Q4 (HR = 3.26, 95% CI: 1.03–10.34). LAP/VAI showed no significant associations across races (Tables 2–4).

Gender differences in analysis

Given that VAI and LAP were calculated based on gender, we further explored their predictive capacity for mortality through

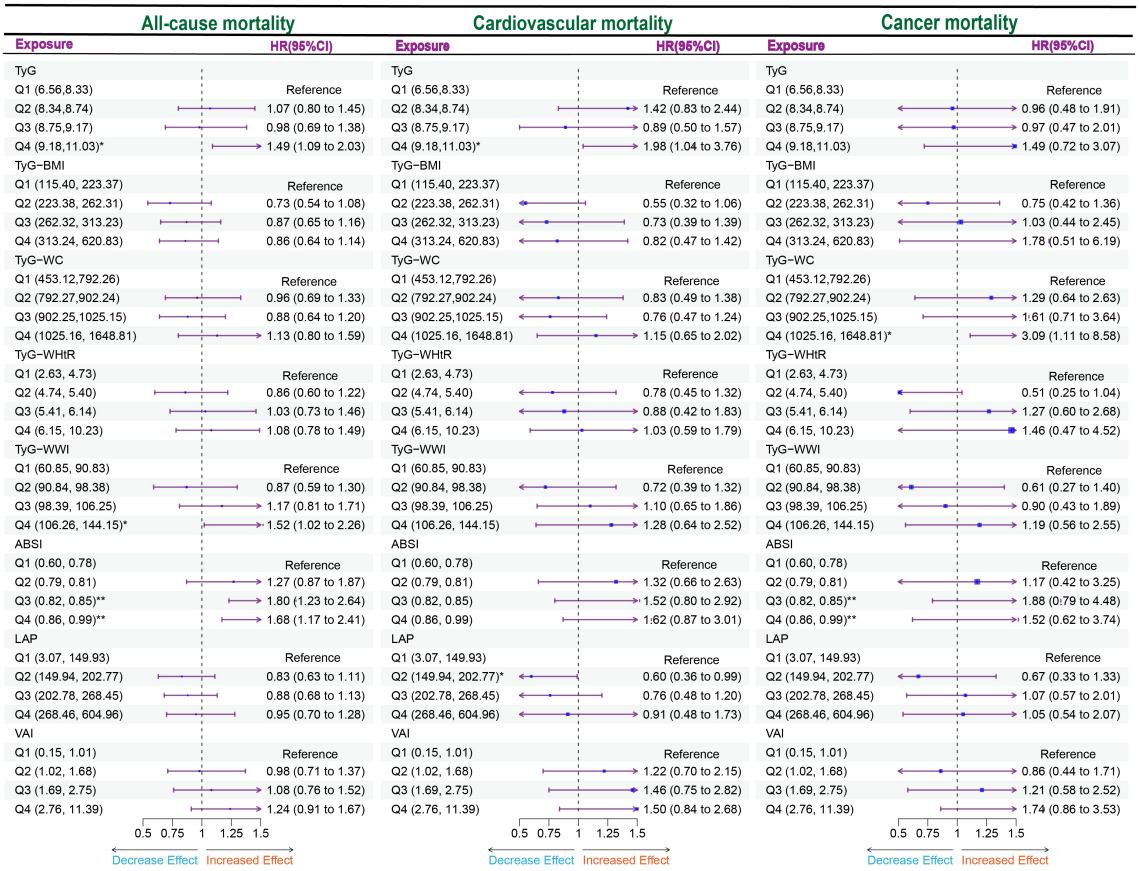

FIGURE 3
Forest plot of obesity and lipid-related indicators with mortality. Multiple Cox regression model: Model 1: Adjusted for Age, Gender, Race; Model 2: Adjusted for Age, Gender, Race, Education, Marital, PIR, Sedentary, Drinking status; Model 3: Adjusted for Age, Gender, Race, Education, Marital, PIR, Sedentary, Drinking status, Hyperlipidemia, CVD. TyG, Triglyceride Glucose; TyG-BMI, Triglyceride Glucose - Body Mass Index; TyG-WHtR, Triglyceride Glucose - Waist to Height Ratio; TyG-WWI, Triglyceride Glucose - Weight Adjusted Waist Index; TyG-WC, Triglyceride Glucose - Waist Circumference; ABSI, A Body Shape Index; LAP, Lipid Accumulation Product; VAI, Visceral Adiposity Index. *P < 0.05; **P < 0.01.

TABLE 2 Subgroup analysis of all-cause mortality risk based on race.

All-cause mortality	Hispanic	Non-Hispanic Black	Non-Hispanic White and Other
TyG			
Q1 (6.56,8.33)	Reference	Reference	Reference
Q2 (8.34,8.74)	1.66 (0.94,2.93)	0.64 (0.25,1.62)	0.95 (0.65,1.40)
Q3 (8.75,9.17)	1.73 (0.98,3.03)	0.56 (0.22,1.43)	0.88 (0.57,1.37)
Q4 (9.18,11.03)	2.35 (1.18,4.68)*	0.70 (0.29,1.68)	1.39 (0.94,2.03)
TyG(Per 1 unit increase)	1.94 (1.34,2.79)***	1.20 (0.81,1.76)	1.36 (1.09,1.70)**
TyG-BMI			
Q1 (115.40, 223.37)	Reference	Reference	Reference
Q2 (223.38, 262.31)	0.75 (0.38,1.48)	0.31 (0.13,0.77)*	0.87 (0.58,1.29)
Q3 (262.32, 313.23)	1.19 (0.60,2.35)	0.55 (0.23,1.32)	1.04 (0.61,1.78)
Q4 (313.24, 620.83)	2.22 (0.85,5.78)	0.73 (0.19,2.76)	1.01 (0.45,2.28)
TyG-BMI(Per 1 unit increase)	1.02 (1.01,1.03)***	1.01 (0.99,1.02)	1.01 (1.00,1.02)*

(Continued)

10.3389/fendo.2025.1492082

TABLE 2 Continued

All-cause mortality	Hispanic	Non-Hispanic Black	Non-Hispanic White and Other
TyG-WC			
Q1 (453.12, 792.26)	Reference	Reference	Reference
Q2 (792.27, 902.24)	0.95 (0.50,1.78)	0.77 (0.28,2.06)	1.18 (0.77,1.80)
Q3 (902.25, 1025.15)	1.48 (0.73,2.97)	0.88 (0.34,2.31)	1.12 (0.69,1.82)
Q4 (1025.16, 1648.81)	2.24 (1.03,4.89)*	2.25 (0.59,8.55)	1.68 (0.83,3.39)
TyG-WC(Per 1 unit increase)	1.00 (1.00, 1.01)***	1.00 (1.00,1.01)	1.00 (1.00, 1.00)
TyG-WHtR			
Q1 (2.63, 4.73)	Reference	Reference	Reference
Q2 (4.74, 5.40)	1.05 (0.52,2.11)	1.01 (0.32,3.20)	1.01 (0.66,1.56)
Q3 (5.41, 6.14)	1.53 (0.76,3.07)	0.71 (0.26,1.93)	1.47 (0.88,2.45)
Q4 (6.15, 10.23)	2.79 (1.24,6.24)*	1.76 (0.53,5.81)	1.66 (0.92,2.99)
TyG-WHtR(Per 1 unit increase)	2.24 (1.59,3.17)***	1.42 (0.89,2.26)	1.45 (1.13,1.86)**
TyG-WWI			
Q1 (60.85, 90.83)	Reference	Reference	Reference
Q2 (90.84, 98.38)	1.29 (0.69,2.40)	0.87 (0.20,3.69)	0.84 (0.50,1.42)
Q3 (98.39, 106.25)	2.07 (1.08,3.94)*	1.15 (0.24,5.58)	1.21 (0.72,2.01)
Q4 (106.26, 144.15)	2.22 (1.08,4.56)*	1.43 (0.29,7.01)	1.68 (0.99,2.86)
TyG-WWI(Per 1 unit increase)	1.05 (1.03,1.06)***	1.02 (0.99,1.05)	1.02 (1.01,1.04)**
ABSI			
Q1 (0.60, 0.78)	Reference	Reference	Reference
Q2 (0.79, 0.81)	1.60 (0.91,2.80)	3.79 (1.71,8.42)**	1.13 (0.65,1.95)
Q3 (0.82, 0.85)	1.89 (0.99,3.61)	2.11 (1.00,4.43)*	1.78 (1.09,2.91)*
Q4 (0.86, 0.99)	2.80 (1.56,5.03)***	3.00 (1.20,7.48)*	1.51 (1.05,1.97)*
ABSI(Per 1 unit increase)	56.1 (6.61, 476)***	49.3 (6.19, 392)***	27.83 (11.89,43.77)*
LAP			
Q1 (3.07, 149.93)	Reference	Reference	Reference
Q2 (149.94, 202.77)	0.66 (0.33,1.32)	0.54 (0.22,1.28)	0.98 (0.67,1.42)
Q3 (202.78, 268.45)	0.83 (0.43,1.62)	0.48 (0.22,1.06)	1.10 (0.77,1.59)
Q4 (268.46, 604.96)	1.16 (0.54,2.49)	0.60 (0.20,1.86)	1.21 (0.70,2.10)
LAP(Per 1 unit increase)	1.00 (1.00,1.01)	1.00 (0.99,1.00)	1.00 (1.00, 1.00)
VAI			
Q1 (0.15, 1.01)	Reference	Reference	Reference
Q2 (1.02, 1.68)	1.17 (0.69,1.98)	0.76 (0.26,2.21)	0.96 (0.65,1.43)
Q3 (1.69, 2.75)	1.60 (0.91,2.84)	1.35 (0.43,4.25)	0.99 (0.65,1.50)
Q4 (2.76, 11.39)	1.54 (0.88,2.72)	1.25 (0.41,3.82)	1.18 (0.82,1.68)
VAI(Per 1 unit increase)	1.24 (1.09,1.40)***	1.08 (0.94,1.24)	1.06 (0.99,1.13)

*P < 0.05; **P < 0.01.
Multiple Cox regression model 3: Adjusted for Age, Sex, Education, Marital, PIR, Sedentary, Drinking status, Hyperlipidemia, CVD.

10.3389/fendo.2025.1492082

TABLE 3 Subgroup analysis of cardiovascular risk based on race.

Cardiovascular mortality	Hispanic	Non-Hispanic Black	Non-Hispanic White and Other
TyG			
Q1 (6.56,8.33)	Reference	Reference	Reference
Q2 (8.34,8.74)	1.49 (0.70,3.14)	0.58 (0.08,3.98)	1.49 (0.70,3.14)
Q3 (8.75,9.17)	0.89 (0.42,1.87)	0.41 (0.07,2.55)	0.89 (0.42,1.87)
Q4 (9.18,11.03)	2.42 (1.12,5.24)*	0.47 (0.09,2.41)	2.42 (1.12,5.24)*
TyG(Per 1 unit increase)	1.69 (1.05,2.72)*	0.98 (0.41,2.38)	1.69 (1.05,2.72)*
TyG-BMI			
Q1 (115.40, 223.37)	Reference	Reference	Reference
Q2 (223.38, 262.31)	0.62 (0.29,1.31)	0.07 (0.02,0.23)***	0.62 (0.29,1.31)
Q3 (262.32, 313.23)	0.60 (0.16,2.27)	0.25 (0.07,0.93)*	0.60 (0.16,2.27)
Q4 (313.24, 620.83)	0.64 (0.10,4.12)	0.27 (0.03,2.71)	0.64 (0.10,4.12)
TyG-BMI(Per 1 unit increase)	1.02 (1.00,1.03)*	1.00 (0.97,1.03)	1.02 (1.00,1.03)*
TyG-WC			
Q1 (453.12, 792.26)	Reference	Reference	Reference
Q2 (792.27, 902.24)	0.94 (0.48,1.86)	0.67 (0.15,2.98)	0.94 (0.48,1.86)
Q3 (902.25, 1025.15)	0.82 (0.34,1.94)	0.81 (0.24,2.73)	0.82 (0.34,1.94)
Q4 (1025.16, 1648.81)	1.40 (0.36,5.47)	3.78 (0.76,18.72)	1.40 (0.36,5.47)
TyG-WC(Per 1 unit increase)	1.00 (1.00,1.00)	1.00 (1.00,1.01)	1.00(1.00, 1.00)
TyG-WHtR			
Q1 (2.63, 4.73)	Reference	Reference	Reference
Q2 (4.74, 5.40)	0.71 (0.35,1.45)	2.88 (0.64,12.93)	0.71 (0.35,1.45)
Q3 (5.41, 6.14)	1.01 (0.34,3.02)	0.35 (0.06,1.94)	1.01 (0.34,3.02)
Q4 (6.15, 10.23)	1.15 (0.37,3.63)	4.52 (0.67,30.32)	1.15 (0.37,3.63)
TyG-WHtR(Per 1 unit increase)	1.36 (0.85,2.17)	1.50 (0.65,3.48)	1.36 (0.85,2.17)
TyG-WWI			
Q1 (60.85, 90.83)	Reference	Reference	Reference
Q2 (90.84, 98.38)	0.58 (0.28,1.19)	1.41 (0.18,10.99)	0.58 (0.28,1.19)
Q3 (98.39, 106.25)	0.98 (0.49,1.93)	1.04 (0.10,10.56)	0.98 (0.49,1.93)
Q4 (106.26, 144.15)	1.26 (0.54,2.98)	2.01 (0.27,14.72)	1.26 (0.54,2.98)
TyG-WWI(Per 1 unit increase)	1.02 (0.99,1.05)	1.02 (0.98,1.07)	1.02 (0.99,1.05)
ABSI			
Q1 (0.60, 0.78)	Reference	Reference	Reference
Q2 (0.79, 0.81)	1.20 (0.50,2.88)	2.72 (0.33,22.09)	1.20 (0.50,2.88)
Q3 (0.82, 0.85)	1.21 (0.57,2.57)	2.96 (0.31,28.48)	1.21 (0.57,2.57)
Q4 (0.86, 0.99)	1.16 (0.56,2.40)	4.84 (0.56,42.09)	1.16 (0.56,2.40)
ABSI(Per 1 unit increase)	1.75 (0.04,77.20)	49.3(6.19, 392)***	1.75 (0.04,77.20)
LAP			
Q1 (3.07, 149.93)	Reference	Reference	Reference

(Continued)

TABLE 3 Continued

Cardiovascular mortality	Hispanic	Non-Hispanic Black	Non-Hispanic White and Other
LAP			
Q2 (149.94, 202.77)	0.69 (0.36,1.35)	0.26 (0.06,1.07)	0.69 (0.36,1.35)
Q3 (202.78, 268.45)	0.87 (0.42,1.78)	0.31 (0.10,0.98)*	0.87 (0.42,1.78)
Q4 (268.46, 604.96)	1.00 (0.27,3.64)	0.74 (0.13,4.22)	1.00 (0.27,3.64)
LAP(Per 1 unit increase)	1.00 (1.00,1.01)	0.99 (0.98,1.00)	1.00(1.00, 1.01)
VAI			
Q1 (0.15, 1.01)	Reference	Reference	Reference
Q2 (1.02, 1.68)	1.36 (0.68,2.72)	0.77 (0.13,4.53)	1.36 (0.68,2.72)
Q3 (1.69, 2.75)	1.58 (0.71,3.49)	1.41 (0.29,6.79)	1.58 (0.71,3.49)
Q4 (2.76, 11.39)	1.62 (0.84,3.12)	0.72 (0.14,3.63)	1.62 (0.84,3.12)
VAI(Per 1 unit increase)	1.06 (0.94,1.20)	0.98 (0.72,1.33)	1.06 (0.94,1.20)

*P < 0.05; **P < 0.01.
Multiple Cox regression model 3: Adjusted for Age, Sex, Education, Marital, PIR, Sedentary, Drinking status, Hyperlipidemia, CVD.

subgroup analysis in diabetes/prediabetes patients. The Cox regression analysis demonstrated a significant association between VAI and cardiovascular mortality specifically among males. Notably, after adjustment in Model 3, individuals in the Q3 (1.69, 2.75) and Q4 (2.76, 11.39) groups showed significantly increased cardiovascular mortality risks, with HR of 3.70 (95% CI: 1.21-11.3) and 3.43 (95% CI: 1.36-8.65), respectively. Furthermore, the analysis of ungrouped continuous variables indicated that for each one-unit increase in VAI, the cardiovascular mortality risk increased by 1.29 times. Finally, neither VAI nor LAP demonstrated significant differences in cancer-related mortality, with both showing no statistical significance (Table 5).

Trend analysis of obesity and lipid-related indices with mortality

Using multivariable-adjusted RCS analysis, we visualized the associations of various indices with all-cause and cardiovascular mortality in diabetes/prediabetes patients. The analysis of all-cause mortality revealed that both TyG and TyG-WWI displayed a linear relationship with all-cause mortality (overall P-values < 0.0001), with cutoff points where the HR exceeded 1 at 9.21 and 103.03, respectively (Figures 4A, B). In contrast, ABSI exhibited a non-linear relationship with all-cause mortality, with a non-linear P-value of 0.0391, showing cutoff points at 0.80 and 0.83 (Figure 4C).

TABLE 4 Subgroup analysis of cancer mortality risk based on race.

Cancer mortality	Hispanic	Non-Hispanic Black	Non-Hispanic White and Other
TyG			
Q1 (6.56,8.33)	Reference	Reference	Reference
Q2 (8.34,8.74)	0.54 (0.23,1.28)	2.93 (0.23,36.88)	4.42 (0.90,21.67)
Q3 (8.75,9.17)	0.65 (0.28,1.51)	2.96 (0.25,35.12)	3.67 (0.72,18.81)
Q4 (9.18,11.03)	1.17 (0.52,2.65)	1.83 (0.13,25.85)	3.86 (0.56,26.56)
TyG(Per 1 unit increase)	1.33 (0.76,2.32)	1.08 (0.50,2.34)	1.62 (0.76,3.47)
TyG-BMI			
Q1 (115.40, 223.37)	Reference	Reference	Reference
Q2 (223.38, 262.31)	0.89 (0.42,1.90)	1.44 (0.37,5.59)	0.46 (0.10,2.17)
Q3 (262.32, 313.23)	1.38 (0.44,4.28)	1.70 (0.51,5.69)	0.56 (0.16,2.04)
Q4 (313.24, 620.83)	2.52 (0.51,12.42)	1.58 (0.16,15.78)	0.73 (0.07,8.10)
TyG-BMI(Per 1 unit increase)	1.01 (0.99,1.03)	1.00 (0.98,1.03)	1.02 (0.99,1.04)

(Continued)

10.3389/fendo.2025.1492082

TABLE 4 Continued

Cancer mortality	Hispanic	Non-Hispanic Black	Non-Hispanic White and Other
TyG-WC			
Q1 (453.12, 792.26)	Reference	Reference	Reference
Q2 (792.27, 902.24)	1.53 (0.65,3.58)	1.27 (0.23,6.88)	0.88 (0.25,3.18)
Q3 (902.25, 1025.15)	1.80 (0.63,5.10)	3.64 (0.78,17.02)	1.17 (0.37,3.77)
Q4 (1025.16, 1648.81)	3.12 (0.79,12.32)	6.63 (0.39,112.03)	3.26 (1.03,10.34)*
TyG-WC(Per 1 unit increase)	1.00 (1.00,1.01)	1.00 (1.00,1.01)	1.00 (1.00,1.01)**
TyG-WHtR			
Q1 (2.63, 4.73)	Reference	Reference	Reference
Q2 (4.74, 5.40)	0.42 (0.16,1.05)	1.71 (0.37,7.85)	0.97 (0.28,3.31)
Q3 (5.41, 6.14)	1.54 (0.58,4.11)	1.29 (0.23,7.08)	1.11 (0.37,3.35)
Q4 (6.15, 10.23)	1.26 (0.27,5.83)	4.70 (0.89,24.88)	3.40 (1.00,11.63)
TyG-WHtR(Per 1 unit increase)	1.16 (0.65,2.06)	1.27 (0.54,3.00)	2.07 (1.22,3.51)**
TyG-WWI			
Q1 (60.85, 90.83)	Reference	Reference	Reference
Q2 (90.84, 98.38)	0.34 (0.11,1.02)	2.59 (0.13,51.77)	2.14 (0.82,5.58)
Q3 (98.39, 106.25)	0.58 (0.24,1.44)	1.58 (0.06,42.74)	2.92 (0.90,9.51)
Q4 (106.26, 144.15)	0.91 (0.37,2.25)	2.89 (0.08,109.86)	2.43 (0.93,6.31)
TyG-WWI(Per 1 unit increase)	1.01 (0.97,1.04)	1.01 (0.97,1.06)	1.04 (1.01,1.07)**
ABSI			
Q1 (0.60, 0.78)	Reference	Reference	Reference
Q2 (0.79, 0.81)	1.08 (0.27,4.24)	1.16 (0.17,8.10)	1.68 (0.35,8.10)
Q3 (0.82, 0.85)	1.56 (0.43,5.59)	3.19 (0.51,19.76)	3.05 (0.95,8.86)
Q4 (0.86, 0.99)	1.31 (0.38,4.51)	2.13 (0.23,19.98)	2.88 (0.86,9.64)
ABSI(Per 1 unit increase)	1.75 (0.04,77.20)	49.3 (6.19, 392)***	27.83 (0.89, 49.66)
LAP			
Q1 (3.07, 149.93)	Reference	Reference	Reference
Q2 (149.94, 202.77)	0.72 (0.31,1.64)	0.57 (0.15,2.16)	1.11 (0.32,3.89)
Q3 (202.78, 268.45)	1.41 (0.65,3.06)	0.59 (0.14,2.40)	0.98 (0.33,2.90)
Q4 (268.46, 604.96)	1.23 (0.54,2.80)	0.40 (0.06,2.78)	1.33 (0.35,5.10)
LAP(Per 1 unit increase)	1.00 (1.00,1.01)	1.00 (0.98,1.01)	1.00(0.99, 1.00)
VAI			
Q1 (0.15, 1.01)	Reference	Reference	Reference
Q2 (1.02, 1.68)	0.63 (0.26,1.53)	1.17 (0.15,8.93)	2.32 (0.80,6.74)
Q3 (1.69, 2.75)	0.84 (0.37,1.94)	4.64 (0.49,43.50)	2.66 (0.81,8.69)
Q4 (2.76, 11.39)	1.58 (0.66,3.80)	3.47 (0.27,44.20)	1.71 (0.50,5.83)
VAI(Per 1 unit increase)	1.13 (1.00,1.28)	1.22 (0.90,1.65)	1.23 (0.94,1.59)

*P < 0.05; **P < 0.01.
Multiple Cox regression model 3: Adjusted for Age, Sex, Education, Marital, PIR, Sedentary, Drinking status, Hyperlipidemia, CVD.

10.3389/fendo.2025.1492082

TABLE 5 Subgroup analysis of mortality risk based on gender.

All-cause mortality	Model 1 HR (95% CI)	Model 2 HR (95% CI)	Model3 HR (95% CI)
VAI (Female)			
Q1 (0.15, 1.02)	Reference	Reference	Reference
Q2 (1.02, 1.69)	1.26 (0.84, 1.88)	1.22 (0.80, 1.86)	1.19 (0.80, 1.77)
Q3 (1.69, 2.75)	1.22 (0.82, 1.83)	1.13 (0.75, 1.69)	1.07 (0.72, 1.58)
Q4 (2.76, 11.39)	1.33 (0.93, 1.92)	1.23 (0.84, 1.80)	1.14 (0.79, 1.65)
VAI (Per 1 unit increase)	1.07 (1.00, 1.15)*	1.06 (0.98, 1.14)	1.06 (0.98, 1.14)*
VAI (Male)			
Q1 (0.15, 1.02)	Reference	Reference	Reference
Q2 (1.02, 1.69)	0.78 (0.45, 1.33)	0.72 (0.42, 1.22)	0.79 (0.45, 1.38)
Q3 (1.69, 2.75)	1.27 (0.77, 2.09)	1.26 (0.73, 2.21)	1.44 (0.81, 2.57)
Q4 (2.76, 11.39)	1.37 (0.83, 2.27)	1.39 (0.85, 2.28)	1.69 (0.99, 2.88)
VAI (Per 1 unit increase)	1.10 (0.98, 1.23)	1.12 (1.00, 1.25)*	1.16 (1.04, 1.29)**
LAP (Female)			
Q1 (3.07, 149.94)	Reference	Reference	Reference
Q2 (149.94, 202.78)	0.83 (0.60, 1.14)	0.92 (0.61, 1.38)	0.96 (0.66, 1.40)
Q3 (202.78, 268.45)	0.78 (0.56, 1.07)	0.92 (0.61, 1.37)	0.94 (0.63, 1.42)
Q4 (268.46, 604.96)	0.85 (0.63, 1.13)	0.88 (0.58, 1.34)	0.91 (0.60, 1.38)
LAP (Per 1 unit increase)	1.00 (1.00, 1.00)	1.00 (1.00, 1.00)	1.00 (1.00, 1.00)
LAP (Male)			
Q1 (3.07, 149.94)	Reference	Reference	Reference
Q2 (149.94, 202.78)	0.68 (0.45, 1.01)	0.72 (0.44, 1.18)	0.77 (0.46, 1.28)
Q3 (202.78, 268.45)	0.88 (0.61, 1.27)	0.95 (0.55, 1.61)	1.03 (0.60, 1.78)
Q4 (268.46, 604.96)	1.26 (0.71, 2.23)	1.63 (0.55, 4.77)	1.75 (0.58, 5.25)
LAP (Per 1 unit increase)	1.00 (1.00, 1.00)	1.00 (1.00, 1.01)	1.00 (1.00, 1.01)
Cardiovascular mortality	Model 1 HR (95% CI)	Model 2 HR (95% CI)	Model3 HR (95% CI)
VAI (Female)			
Q1 (0.15, 1.02)	Reference	Reference	Reference
Q2 (1.02, 1.69)	1.08 (0.59, 1.98)	1.02 (0.54, 1.94)	0.94 (0.50, 1.77)
Q3 (1.69, 2.75)	0.93 (0.47, 1.83)	0.87 (0.41, 1.83)	0.84 (0.41, 1.71)
Q4 (2.76, 11.39)	1.03 (0.53, 2.00)	0.92 (0.47, 1.80)	0.81 (0.43, 1.55)
VAI (Per 1 unit increase)	1.01 (0.87, 1.18)	0.99 (0.85, 1.16)	0.98 (0.84, 1.14)
VAI (Male)			
Q1 (0.15, 1.02)	Reference	Reference	Reference
Q2 (1.02, 1.69)	1.59 (0.66, 3.78)	1.40 (0.52, 3.74)	1.55 (0.59, 4.07)
Q3 (1.69, 2.75)	3.51 (1.34, 9.25)*	3.71 (1.27, 10.9)*	3.70 (1.21, 11.3)*
Q4 (2.76, 11.39)	3.03 (1.28, 7.13)*	3.08 (1.20, 7.90)*	3.43 (1.36, 8.65)**
VAI (Per 1 unit increase)	1.26 (1.07, 1.49)**	1.29 (1.08, 1.55)**	1.29 (1.09, 1.52)**

(Continued)

10.3389/fendo.2025.1492082

TABLE 5 Continued

All-cause mortality	Model 1 HR (95% CI)	Model 2 HR (95% CI)	Model3 HR (95% CI)
LAP (Female)			
Q1 (3.07, 149.94)	Reference	Reference	Reference
Q2 (149.94, 202.78)	0.62 (0.33, 1.15)	0.70 (0.34, 1.44)	0.77 (0.37, 1.60)
Q3 (202.78, 268.45)	0.57 (0.33, 1.00)*	0.63 (0.33, 1.18)	0.67 (0.35, 1.31)
Q4 (268.46, 604.96)	0.72 (0.44, 1.20)	0.66 (0.30, 1.46)	0.75 (0.32, 1.76)
LAP (Per 1 unit increase)	1.00 (1.00, 1.00)	1.00 (0.99, 1.00)	1.00 (1.00, 1.00)
LAP (Male)			
Q1 (3.07, 149.94)	Reference	Reference	Reference
Q2 (149.94, 202.78)	0.35 (0.17, 0.76)**	0.33 (0.12, 0.88)*	0.36 (0.13, 0.94)*
Q3 (202.78, 268.45)	1.11 (0.62, 2.00)	0.90 (0.30, 2.70)	0.94 (0.31, 2.82)
Q4 (268.46, 604.96)	1.74 (0.65, 4.63)	1.32 (0.11, 16.4)	1.36 (0.11, 16.6)
LAP (Per 1 unit increase)	1.00 (1.00, 1.01)	1.00 (1.00, 1.01)	1.00 (1.00, 1.01)
Cancer mortality	Model 1 HR (95% CI)	Model 2 HR (95% CI)	Model 3 HR (95% CI)
VAI (Female)			
Q1 (0.15, 1.02)	Reference	Reference	Reference
Q2 (1.02, 1.69)	0.89 (0.32,2.53)	0.78 (0.26,2.33)	0.76 (0.26,2.21)
Q3 (1.69, 2.75)	1.30 (0.43,3.97)	1.29 (0.43,3.94)	1.21 (0.39,3.73)
Q4 (2.76, 11.39)	1.71 (0.66,4.42)	1.58 (0.61,4.15)	1.45 (0.53,3.96)
VAI (Per 1 unit increase)	1.19 (1.06,1.34)**	1.17 (1.04,1.32)*	1.16 (0.93,1.31)
VAI (Male)			
Q1 (0.15, 1.02)	Reference	Reference	Reference
Q2 (1.02, 1.69)	1.00 (0.39,2.55)	0.94 (0.34,2.64)	1.21 (0.43,3.43)
Q3 (1.69, 2.75)	1.12 (0.46,2.72)	1.05 (0.41,2.69)	1.41 (0.59,3.37)
Q4 (2.76, 11.39)	1.83 (0.68,4.91)	1.91 (0.58,6.26)	2.81 (0.88,8.93)
VAI (Per 1 unit increase)	1.07 (0.88,1.29)	1.06 (0.86,1.31)	1.12 (0.93,1.33)
LAP (Female)			
Q1 (3.07, 149.94)	Reference	Reference	Reference
Q2 (149.94, 202.78)	0.48 (0.19,1.19)	0.57 (0.22,1.50)	0.57 (0.22,1.45)
Q3 (202.78, 268.45)	0.99 (0.42,2.33)	1.18 (0.49,2.84)	1.09 (0.46,2.58)
Q4 (268.46, 604.96)	0.94 (0.41,2.18)	1.11 (0.47,2.61)	0.99 (0.42,2.34)
LAP (Per 1 unit increase)	1.00 (1.00,1.00)	1.00 (1.00,1.01)	1.00 (1.00,1.01)
LAP (Male)			
Q1 (3.07, 149.94)	Reference	Reference	Reference
Q2 (149.94, 202.78)	0.65 (0.26,1.62)	0.66 (0.26,1.73)	0.67 (0.25,1.76)
Q3 (202.78, 268.45)	0.80 (0.35,1.83)	0.88 (0.30,2.56)	0.92 (0.31,2.69)
Q4 (268.46, 604.96)	0.76 (0.26,2.22)	0.95 (0.29,3.16)	1.03 (0.32,3.36)
LAP (Per 1 unit increase)	1.00 (0.99,1.00)	1.00 (0.99,1.01)	1.00 (0.99,1.01)

*P < 0.05; **P < 0.01.

Multiple Cox regression model: Model 1: Adjusted for Age, Race; Model 2: Adjusted for Age, Race, Education, Marital, PIR, Sedentary, Drinking status; Model 3: Adjusted for Age, Race, Education, Marital, PIR, Sedentary, Drinking status, Hyperlipidemia, CVD.

LAP, Lipid accumulation product; VAI, Visceral adiposity index.

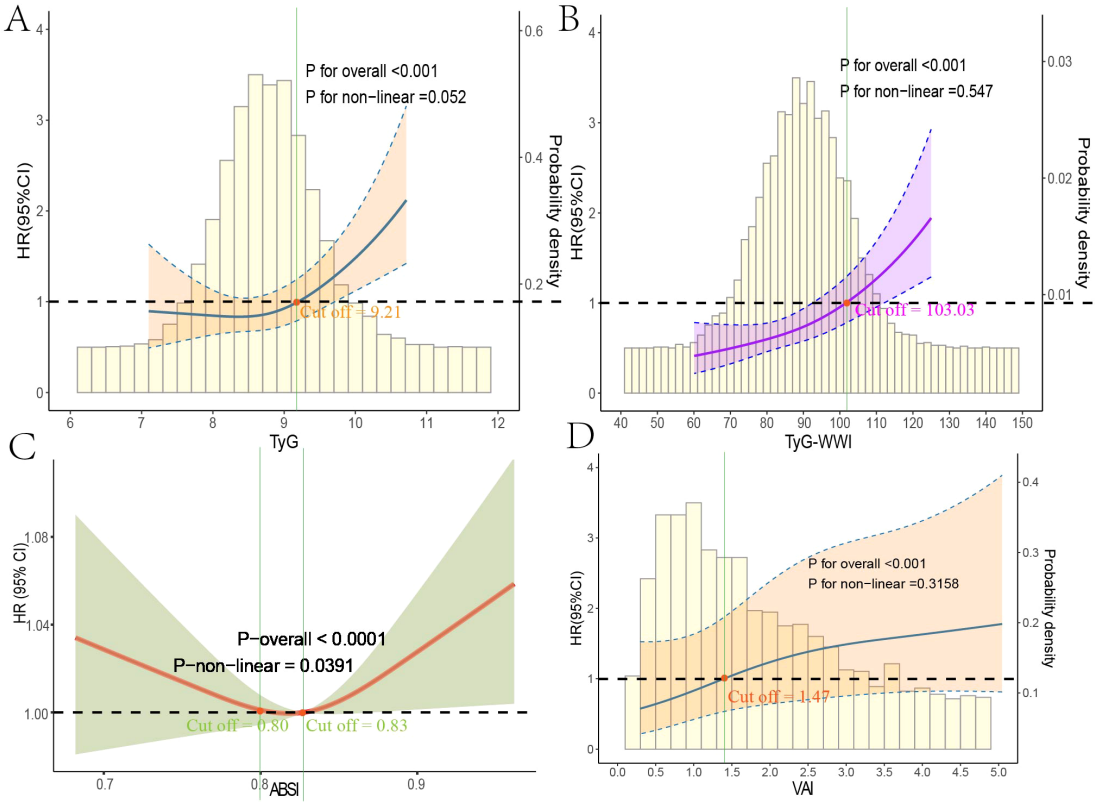

FIGURE 4
Restricted cubic spline regression analysis of obesity and lipid-related indices with mortality. This figure presents spline analysis of mortality risk for obesity and lipid-related indices, accompanied by the background frequency distribution histogram. Solid lines represent the hazard ratios (HR) adjusted for multivariable covariates (Age, Gender, Race, Education, Marital Status, Poverty Income Ratio (PIR), Sedentary Behavior, Drinking Status, Hyperlipidemia, and Cardiovascular disease (CVD)). The shaded areas indicate the 95% confidence intervals derived from the RCS regression. TyG **(A)** and TyG-WWI **(B)** show linear relationships with all-cause mortality, while ABSI **(C)** indicates a non-linear relationship. VAI **(D)** demonstrates a linear relationship with cardiovascular mortality in male patients, where all red points correspond to cutoff values for HR > 1.

Additionally, among male diabetes/prediabetes patients, moderate to high levels of VAI (Q3: 1.69, 2.75; Q4: 2.76, 11.39) were associated with a clear linear relationship to cardiovascular mortality (overall P-value < 0.0001), with a cutoff point where HR exceeded 1 at 1.47 (Figure 4D).

Evaluation of machine learning models

After determining that TyG, TyG-WWI, and ABSI are significant risk factors for all-cause mortality in diabetes/prediabetes patients, we aimed to assess the importance of these indices and their contributions to mortality risk by comparing eight ML algorithms: XGBoost, DT, SVM, Enet, MLP, RF, and KNN. The results indicated that the XGBoost model achieved the highest area under the curve (AUC) value of 0.85, with an accuracy of 0.79, precision of 0.94, and recall of 0.81, indicating strong performance across various metrics (Figures 5A, B, Supplementary Table S5). Furthermore, the calibration curve showed good consistency between the predicted probabilities from the XGBoost model and the actual probabilities (Figure 5C). Thus, we selected XGBoost as the optimal ML model for predicting mortality risk in this study. Subsequently, we used the SHAP model to interpret and visualize feature importance. The beeswarm plot illustrates the cumulative impact of each feature on mortality risk, arranged in descending order of importance. Positive SHAP values indicate that increasing feature values are directly correlated with higher mortality risk, with larger SHAP values contributing more significantly to the predictions.

In the global interpretability of the optimal XGBoost model, age emerged as the most significant contributor to mortality risk, consistent with clinical expectations. In the overall model that included covariates, the importance ranking of obesity and lipid-related indices was as follows: TyG > ABSI > TyG-WWI (Figure 5D). In the TyG-related model, apart from age, fasting blood glucose and triglycerides ranked second and third, respectively. Notably, very low fasting blood glucose also increased mortality risk (Figure 6A). A similar trend was observed in the TyG-WWI model, with fasting blood glucose and triglycerides carrying substantial weight, followed by weight and waist circumference (Figure 6B). In the ABSI model, waist circumference was the most significant factor, followed by weight

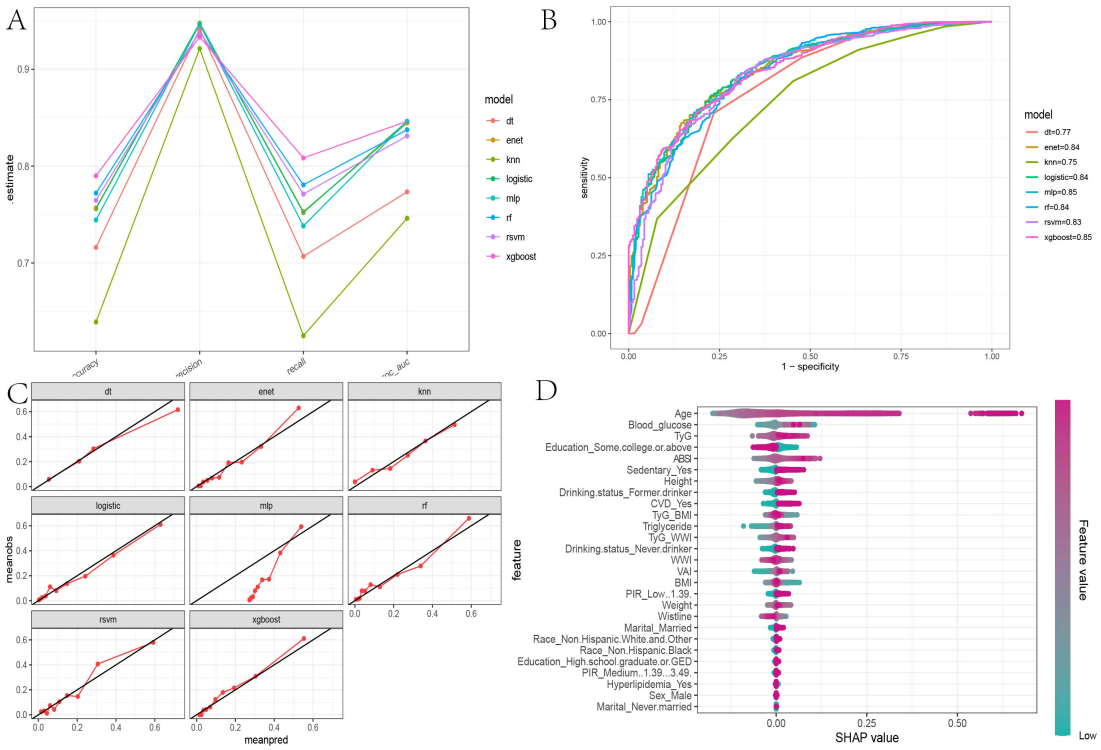

FIGURE 5
Evaluation of machine learning models and SHAP beeswarm Plot. **(A)** The parallel coordinate plot assesses the efficacy of eight machine learning algorithms based on accuracy, precision, recall, and ROC AUC calculations found in Supplementary Table S2; **(B)** Comparison of eight machine learning algorithms on ROC curves; **(C)** Calibration curves for eight machine learning algorithms; **(D)** SHAP interpretability beeswarm plot incorporating all obesity and lipid-related indices associated with mortality risk, illustrating the cumulative impact of each feature on mortality risk and sorted by importance.

and height, with very low weight significantly increasing the risk of mortality (Figure 6C).

In summary, both blood glucose-related indices and anthropometric measures substantially influence mortality risk in patients with diabetes/prediabetes. For cardiovascular mortality risk in male patients, the feature importance for VAI was ranked as follows: triglycerides, HDL-C, height, waist circumference, and weight, with triglycerides, waist circumference, and weight positively contributing to mortality risk, while other indicators showed a negative impact (Figure 6D).

Discussion

This cross-sectional study systematically explores the relationship between obesity and lipid-related indices and all-cause and cardiovascular mortality in patients with diabetes/prediabetes in the United States. Additionally, we employed machine learning methods to assess and compare the predictive capabilities of these indices regarding mortality risk. The findings indicate that TyG > 8.75, ABSI > 0.82, and TyG-WWI > 98.39 are positively correlated with all-cause mortality in diabetes/prediabetes patients, with TyG > 8.75 also showing a significant positive correlation with cardiovascular mortality. We observed a non-linear trend in the relationships between ABSI and TyG-WWI and all-cause mortality, while TyG exhibited a significant linear correlation with both all-cause and cardiovascular mortality.

Among the machine learning algorithms, the XGBoost model demonstrated the best predictive performance, and the SHAP analysis revealed that TyG is the most significant contributor to all-cause mortality in patients with diabetes/prediabetes. In addition to age, high levels of fasting blood glucose and triglycerides were significant contributors. The remaining indices were ranked in terms of their contribution as follows: ABSI, TyG-BMI, and TyG-WWI. In the subgroup analysis based on gender, we found that moderate to high levels of VAI (>1.69) were positively correlated with cardiovascular mortality in male patients with diabetes and prediabetes, displaying a linear relationship, with triglycerides being the most significant contributor.

We recognize that TyG is an important indicator of IR, a core issue in diabetes/prediabetes. The significance of TyG in predicting risk for patients with diabetes and prediabetes should not be overlooked. This study also highlights, for the first time that the TyG-related index, TyG-WWI, can effectively predict all-cause mortality risk in diabetes and prediabetes patients, and TyG can also be used to predict cardiovascular mortality risk. The effectiveness of TyG in assessing insulin resistance is partly attributed to its strong sensitivity and specificity, as well as its

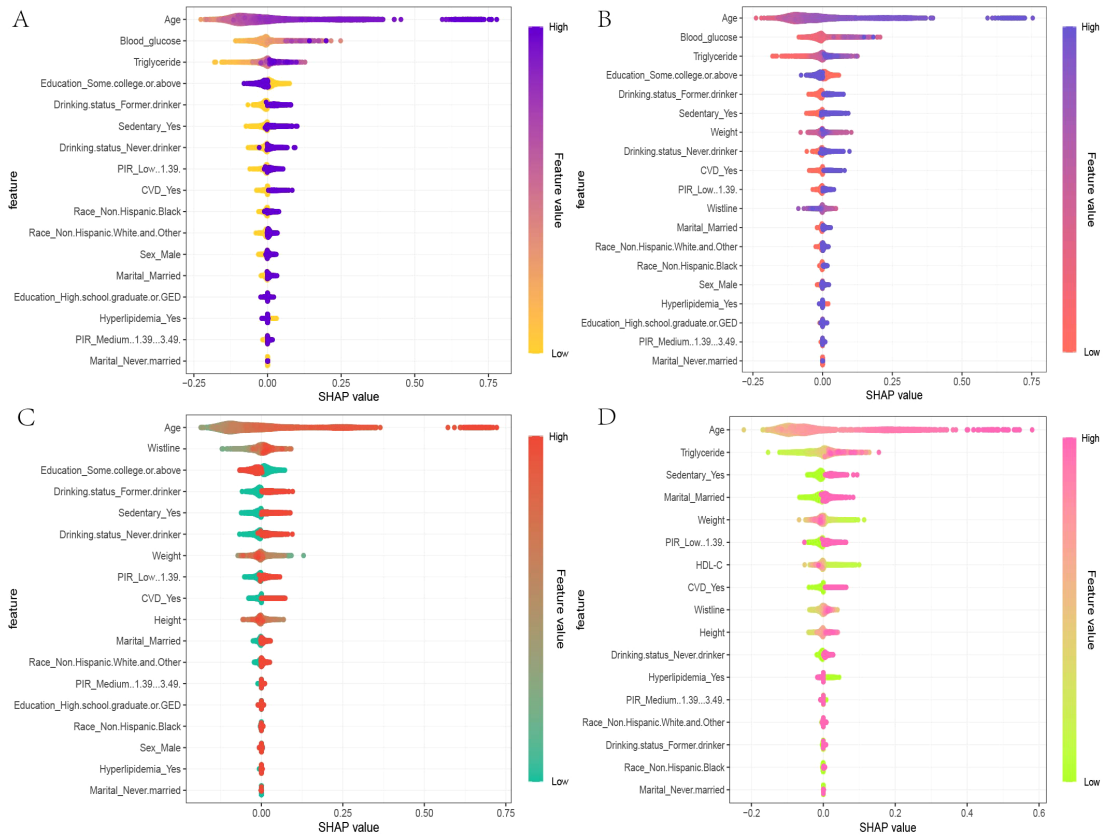

FIGURE 6
SHAP beeswarm plots for the four indices in the optimal XGBoost model. **(A)** The SHAP beeswarm plot for TyG, **(B)** TyG-WWI, **(C)** ABSI, and **(D)** VAI models provides a global interpretation of how each component of these indices predicts the risk of mortality in patients with diabetes/prediabetes. The beeswarm plots illustrate the cumulative impact of each feature on mortality risk, arranged in descending order of importance. In the plots, the Feature values are represented using a gradient color scheme that indicates the magnitude of each feature variable. Positive SHAP values imply that the feature values are positively correlated with an increased risk of mortality, with larger SHAP values contributing more significantly to mortality predictions. This visual representation helps in understanding how each component of TyG, TyG-WWI, ABSI, and VAI influences the overall risk of death among individuals diagnosed with diabetes or prediabetes.

broad clinical applicability (17). The association between TyG and mortality in diabetes patients, along with poor cardiovascular outcomes, may be influenced by various factors. First, insulin resistance leads to dysregulation of glucose and lipid metabolism, exacerbating inflammation and oxidative stress in the body, which accelerates biological aging (23) and promotes the development of atherosclerosis and CHD (24). Second, insulin resistance can elevate reactive oxygen species (ROS) levels, damaging vascular endothelium (25), leading to excessive platelet activation and potentially triggering thrombosis (26). This series of issues further contributes to cardiovascular diseases, which are among the leading causes of mortality. Therefore, this not only explains why TyG is used to predict the incidence of cardiovascular diseases (27) but also clarifies why TyG is more closely associated with cardiovascular mortality risk than other indices in this study (28).

In this study, we found that the average BMI of all participants was 31 kg/m², indicating a significant obesity risk among patients with diabetes and prediabetes in the United States. It is important to consider that BMI may not effectively distinguish between muscle and fat composition; typically, higher fat content is associated with lower life expectancy, while higher muscle mass may contribute to increased longevity (29). The relationship between BMI and mortality risk is complex, with meta-analyses suggesting a U-shaped non-linear association (30). This phenomenon partially explains the paradox whereby individuals with a high BMI may have a longer lifespan than those with a lower BMI in populations with diabetes (31). In our study, we also conducted subgroup analyses based on BMI levels and found that obesity exhibited more dangerous tendencies across several key indicators including blood glucose, insulin, and TyG index. Interestingly, we also observed that BMI levels in the mortality group were slightly lower than those in the survival group; however, the proportions of hyperlipidemia and CVD were higher. This finding suggests that, in addition to TyG, it is essential to consider other obesity-related indices in our analyses. The results also showed that TyG-WWI plays a significant role in predicting all-cause mortality risk. The WWI standardizes waist circumference relative to body weight, emphasizing abdominal obesity while minimizing the association

with BMI. Recent studies have recognized WWI as superior to BMI in predicting diabetes (32). Our research further integrates WWI with TyG to enhance predictive ability regarding mortality risk in patients with diabetes/prediabetes.

Additionally, ABSI, a newly developed body shape index based on waist circumference, weight, and height, is positively associated with visceral fat accumulation (33). Visceral fat accumulation is linked to various adverse outcomes due to excess fatty acid buildup (34), increased triglyceride synthesis and secretion (35), and lower levels of protective factors (PPAR-γ, glycogen synthase, and leptin) (36). ABSI has been validated as an independent predictor of survival rates (33). A 20-year follow-up study by Tate J demonstrated a linear positive correlation between ABSI and all-cause mortality in diabetes patients (37). A notable advantage of ABSI over TyG is its measurement is non-invasive, allowing patients with diabetes/prediabetes to conveniently track changes in this index.

In our gender-based analysis, we found that VAI was associated with cardiovascular mortality risk. Previous research, including that by Marco C, identified VAI as an important indicator of visceral fat function and insulin sensitivity (38). In our study, an association between VAI and cardiovascular mortality risk was observed only in males, similar with findings from Shi Y regarding gender differences affecting VAI (39). The impact of VAI regarding gender differences may stem from variations in insulin sensitivity and differences in body fat distribution due to hormonal levels. Relevant data indicate that, at a given body type, women usually have approximately 10% higher body fat percentages than men (40), and women's body fat percentages have consistently been higher throughout life (41). This may suggest that men are more sensitive to the health implications of visceral fat accumulation. Therefore, findings regarding gender differences in our study warrant further exploration, potentially guiding future research directions.

Indicators such as TyG, TyG-WWI, ABSI, and VAI effectively reflect individual body composition and lipid profiles in the blood. Based on our findings, we recommend weight loss interventions be prioritized in improving health outcomes for patients with diabetes and prediabetes. However, these strategies should emphasize reducing visceral fat rather than focusing solely on overall weight loss. We suggest implementing effective exercise modalities, including resistance training, aerobic exercise, and overall conditioning. The benefits of these exercise types are reflected in some indicators from our study; for instance, reducing WC can effectively lower ABSI and VAI, suggesting potential improvements in patients' life expectancy, even without significant changes in body weight.

Naturally, this study has several unresolved issues. Firstly, due to the limitations of cross-sectional study designs, we cannot establish clear causal relationships distinguishing TyG, TyG-WWI, ABSI, VAI, and their associations with mortality risk in patients with diabetes/prediabetes. However, the NHANES dataset's bolsters lies in its large and nationally representative sample, which enhances the statistical power of our analyses and bolsters the reliability of our findings. Secondly, the study population comprised individuals exclusively from the United States, limiting the generalizability of our conclusions. Responses to obesity and related metabolic indicators may differ significantly across regions, cultural backgrounds, or dietary habits. Therefore, our results may not apply to other populations, and future research should consider broader demographic studies to validate the universality and applicability of these findings.

Conclusion

This study represents the first comprehensive assessment of the associations between obesity, lipid-related indices, and all-cause and cardiovascular mortality risk in patients with diabetes/prediabetes. The results indicate that TyG is closely related to all-cause and cardiovascular mortality in patients with diabetes/prediabetes and demonstrates superior predictive capability compared to other indices. This finding underscores the potential role of TyG as an effective biomarker in the clinical management of diabetes/prediabetes. Furthermore, TyG-WWI and ABSI also effectively predict all-cause mortality risk, while VAI shows a significant association with cardiovascular mortality specifically in male patients. These indicators assess life expectancy from multiple dimensions and suggest a greater focus on the rationality of body fat distribution rather than solely on BMI or overall weight changes. This shift in focus can help optimize long-term management and intervention strategies for patients with diabetes and prediabetes.

Data availability statement

The NHANES data in this study is sourced from the Centers for Disease Control and Prevention, and all data is freely accessible at: https://wwwn.cdc.gov/Nchs/Nhanes/.

Author contributions

ZY: Data curation, Formal analysis, Funding acquisition, Methodology, Software, Visualization, Writing – original draft. XC: Formal analysis, Funding acquisition, Validation, Writing – original draft. ZL: Supervision, Validation, Visualization, Writing – review & editing. RL: Supervision, Validation, Visualization, Writing – review & editing. XD: Data curation, Formal analysis, Methodology, Software, Visualization, Writing – review & editing.

Funding

The author(s) declare that no financial support was received for the research and/or publication of this article.

Conflict of interest

The authors declare that the research was conducted in the absence of any commercial or financial relationships that could be construed as a potential conflict of interest.

Publisher's note

All claims expressed in this article are solely those of the authors and do not necessarily represent those of their affiliated organizations, or those of the publisher, the editors and the reviewers. Any product that may be evaluated in this article, or claim that may be made by its manufacturer, is not guaranteed or endorsed by the publisher.

Supplementary material

The Supplementary Material for this article can be found online at: https://www.frontiersin.org/articles/10.3389/fendo.2025.1492082/full#supplementary-material

References

1. Lin X, Xu Y, Pan X, Xu J, Ding Y, Sun X, et al. Global, regional, and national burden and trend of diabetes in 195 countries and territories: an analysis from 1990 to 2025. *Sci Rep*. (2020) 10:14790. doi: 10.1038/s41598-020-71908-9

2. Echouffo-Tcheugui JB, Perreault L, Ji L, Dagogo-Jack S. Diagnosis and management of prediabetes: A review. *JAMA*. (2023) 329:1206–16. doi: 10.1001/jama.2023.4063

3. Tabak AG, Herder C, Rathmann W, Brunner EJ, Kivimaki M. Prediabetes: a high-risk state for diabetes development. *Lancet*. (2012) 379:2279–90. doi: 10.1016/S0140-6736(12)60283-9

4. Bansal N. Prediabetes diagnosis and treatment: A review. *World J Diabetes*. (2015) 6:296–303. doi: 10.4239/wjd.v6.i2.296

5. Mohammadpour-Haratbar A, Mohammadpour-Haratbar S, Zare Y, Rhee KY, Park SJ. A review on non-enzymatic electrochemical biosensors of glucose using carbon nanofiber nanocomposites. *Biosensors (Basel)*. (2022) 12:1004. doi: 10.3390/bios12111004

6. Brunner EJ, Shipley MJ, Witte DR, Fuller JH, Marmot MG. Relation between blood glucose and coronary mortality over 33 years in the Whitehall Study. *Diabetes Care*. (2006) 29:26–31. doi: 10.2337/diacare.29.01.06.dc05-1405

7. Huang Y, Cai X, Mai W, Li M, Hu Y. Association between prediabetes and risk of cardiovascular disease and all cause mortality: systematic review and meta-analysis. *BMJ*. (2016) 355:i5953. doi: 10.1136/bmj.i5953

8. Sanchez E, Betriu A, Lopez-Cano C, Hernandez M, Fernandez E, Purroy F, et al. Characteristics of atheromatosis in the prediabetes stage: a cross-sectional investigation of the ILERVAS project. *Cardiovasc Diabetol*. (2019) 18:154. doi: 10.1186/s12933-019-0962-6

9. Tooke JE. Microvascular function in human diabetes. A physiological perspective. *Diabetes*. (1995) 44:721–6. doi: 10.2337/diab.44.7.721

10. Einarson TR, Acs A, Ludwig C, Panton UH. Prevalence of cardiovascular disease in type 2 diabetes: a systematic literature review of scientific evidence from across the world in 2007-2017. *Cardiovasc Diabetol*. (2018) 17:83. doi: 10.1186/s12933-018-0728-6

11. Wu H, Ballantyne CM. Metabolic inflammation and insulin resistance in obesity. *Circ Res*. (2020) 126:1549–64. doi: 10.1161/CIRCRESAHA.119.315896

12. Bawadi H, Abouwatfa M, Alsaeed S, Kerkadi A, Shi Z. Body shape index is a stronger predictor of diabetes. *Nutrients*. (2019) 11:1018. doi: 10.3390/nu11051018

13. Nusrianto R, Ayundini G, Kristanti M, Astrella C, Amalina N, Muhadi, et al. Visceral adiposity index and lipid accumulation product as a predictor of type 2 diabetes mellitus: The Bogor cohort study of non-communicable diseases risk factors. *Diabetes Res Clin Pract*. (2019) 155:107798. doi: 10.1016/j.diabres.2019.107798

14. Zhang X, Wang Y, Li Y, Gui J, Mei Y, Yang X, et al. Optimal obesity- and lipid-related indices for predicting type 2 diabetes in middle-aged and elderly Chinese. *Sci Rep*. (2024) 14:10901. doi: 10.1038/s41598-024-61592-4

15. Zhang L, Zeng L. Non-linear association of triglyceride-glucose index with prevalence of prediabetes and diabetes: a cross-sectional study. *Front Endocrinol (Lausanne)*. (2023) 14:1295641. doi: 10.3389/fendo.2023.1295641

16. Park HM, Lee HS, Lee YJ, Lee JH. The triglyceride-glucose index is a more powerful surrogate marker for predicting the prevalence and incidence of type 2 diabetes mellitus than the homeostatic model assessment of insulin resistance. *Diabetes Res Clin Pract*. (2021) 180:109042. doi: 10.1016/j.diabres.2021.109042

17. Matthews DR, Hosker JP, Rudenski AS, Naylor BA, Treacher DF, Turner RC. Homeostasis model assessment: insulin resistance and beta-cell function from fasting plasma glucose and insulin concentrations in man. *Diabetologia*. (1985) 28:412–9. doi: 10.1007/BF00280883

18. Huang D, Ma R, Zhong X, Jiang Y, Lu J, Li Y, et al. Positive association between different triglyceride glucose index-related indicators and psoriasis: evidence from NHANES. *Front Immunol*. (2023) 14:1325557. doi: 10.3389/fimmu.2023.1325557

19. Zhang Q, Xiao S, Jiao X, Shen Y. The triglyceride-glucose index is a predictor for cardiovascular and all-cause mortality in CVD patients with diabetes or pre-diabetes: evidence from NHANES 2001-2018. *Cardiovasc Diabetol*. (2023) 22:279. doi: 10.1186/s12933-023-02030-z

20. Marrie RA, Dawson NV, Garland A. Quantile regression and restricted cubic splines are useful for exploring relationships between continuous variables. *J Clin Epidemiol*. (2009) 62:511–7.e1. doi: 10.1016/j.jclinepi.2008.05.015

21. Lin Z, Cheng YT, Cheung BMY. Machine learning algorithms identify hypokalaemia risk in people with hypertension in the United States National Health and Nutrition Examination Survey 1999-2018. *Ann Med*. (2023) 55:2209336. doi: 10.1080/07853890.2023.2209336

22. Wang K, Tian J, Zheng C, Yang H, Ren J, Liu Y, et al. Interpretable prediction of 3-year all-cause mortality in patients with heart failure caused by coronary heart disease based on machine learning and SHAP. *Comput Biol Med*. (2021) 137:104813. doi: 10.1016/j.compbiomed.2021.104813

23. Tucker LA. Insulin resistance and biological aging: the role of body mass, waist circumference, and inflammation. *BioMed Res Int*. (2022) 2022:2146596. doi: 10.1155/2022/2146596

24. Yang Q, Vijayakumar A, Kahn BB. Metabolites as regulators of insulin sensitivity and metabolism. *Nat Rev Mol Cell Biol*. (2018) 19:654–72. doi: 10.1038/s41580-018-0044-8

25. Molina MN, Ferder L, Manucha W. Emerging role of nitric oxide and heat shock proteins in insulin resistance. *Curr Hypertens Rep*. (2016) 18:1. doi: 10.1007/s11906-015-0615-4

26. Gerrits AJ, Koekman CA, van Haeften TW, Akkerman JW. Platelet tissue factor synthesis in type 2 diabetic patients is resistant to inhibition by insulin. *Diabetes*. (2010) 59:1487–95. doi: 10.2337/db09-1008

27. Jin JL, Cao YX, Wu LG, You XD, Guo YL, Wu NQ, et al. Triglyceride glucose index for predicting cardiovascular outcomes in patients with coronary artery disease. *J Thorac Dis*. (2018) 10:6137–46. doi: 10.21037/jtd.2018.10.79

28. Liu F, Ling Q, Xie S, Xu Y, Liu M, Hu Q, et al. Association between triglyceride glucose index and arterial stiffness and coronary artery calcification: a systematic review and exposure-effect meta-analysis. *Cardiovasc Diabetol*. (2023) 22:111. doi: 10.1186/s12933-023-01819-2

29. Bigaard J, Frederiksen K, Tjonneland A, Thomsen BL, Overvad K, Heitmann BL, et al. Body fat and fat-free mass and all-cause mortality. *Obes Res*. (2004) 12:1042–9. doi: 10.1038/oby.2004.131

30. Katzmarzyk PT, Hu G, Cefalu WT, Mire E, Bouchard C. The importance of waist circumference and BMI for mortality risk in diabetic adults. *Diabetes Care*. (2013) 36:3128–30. doi: 10.2337/dc13-0219

31. Tobias DK, Manson JE. The obesity paradox in type 2 diabetes and mortality. *Am J Lifestyle Med*. (2018) 12:244–51. doi: 10.1177/1559827616650415

32. Li X, Zhao D, Wang H. Association between weight-adjusted waist index and risk of diabetes mellitus type 2 in United States adults and the predictive value of obesity indicators. *BMC Public Health*. (2024) 24:2025. doi: 10.1186/s12889-024-19576-6

33. Krakauer NY, Krakauer JC. A new body shape index predicts mortality hazard independently of body mass index. *PloS One*. (2012) 7:e39504. doi: 10.1371/journal.pone.0039504

34. Ibrahim MM. Subcutaneous and visceral adipose tissue: structural and functional differences. *Obes Rev*. (2010) 11:11–8. doi: 10.1111/j.1467-789X.2009.00623.x

35. Wajchenberg BL. Subcutaneous and visceral adipose tissue: their relation to the metabolic syndrome. *Endocr Rev*. (2000) 21:697–738. doi: 10.1210/edrv.21.6.0415

36. Lefebvre AM, Laville M, Vega N, Riou JP, van Gaal L, Auwerx J, et al. Depot-specific differences in adipose tissue gene expression in lean and obese subjects. *Diabetes*. (1998) 47:98–103. doi: 10.2337/diab.47.1.98

37. Tate J, Knuiman M, Davis WA, Davis TME, Bruce DG. A comparison of obesity indices in relation to mortality in type 2 diabetes: the Fremantle Diabetes Study. *Diabetologia*. (2020) 63:528–36. doi: 10.1007/s00125-019-05057-8

38. Amato MC, Giordano C, Galia M, Criscimanna A, Vitabile S, Midiri M, et al. Visceral Adiposity Index: a reliable indicator of visceral fat function associated with cardiometabolic risk. *Diabetes Care*. (2010) 33:920–2. doi: 10.2337/dc09-1825

39. Shi Y, Yu C, Hu L, Li M, Zhou W, Wang T, et al. Visceral adiposity index and sex differences in relation to peripheral artery disease in normal-weight adults with hypertension. *Biol Sex Differ*. (2022) 13:22. doi: 10.1186/s13293-022-00432-4

40. Womersley J. A comparison of the skinfold method with extent of 'overweight' and various weight-height relationships in the assessment of obesity. *Br J Nutr*. (1977) 38:271–84. doi: 10.1079/BJN19770088

41. Gallagher D, Visser M, Sepulveda D, Pierson RN, Harris T, Heymsfield SB. How useful is body mass index for comparison of body fatness across age, sex, and ethnic groups? *Am J Epidemiol*. (1996) 143:228–39. doi: 10.1093/oxfordjournals.aje.a008733

frontiers | Frontiers in Endocrinology

TYPE Mini Review
PUBLISHED 09 June 2025
DOI 10.3389/fendo.2025.1577505

OPEN ACCESS

EDITED BY
Robert Kiss,
McGill University, Canada

REVIEWED BY
Sergei Tevosian,
University of Florida, United States
Maria Mercedes Mori Sequeiros Garcia,
Universidad de Buenos Aires, Argentina

*CORRESPONDENCE
Vasileia Ismini Alexaki
vasileiaismini.alexaki@uniklinikum-dresden.de

RECEIVED 15 February 2025
ACCEPTED 26 May 2025
PUBLISHED 09 June 2025

CITATION
Aderhold A and Alexaki VI (2025) Lipid metabolism in the adrenal gland.
Front. Endocrinol. 16:1577505.
doi: 10.3389/fendo.2025.1577505

Lipid metabolism in the adrenal gland

Anika Aderhold and Vasileia Ismini Alexaki*

Institute for Clinical Chemistry and Laboratory Medicine, Faculty of Medicine and University Hospital Carl Gustav Carus, Technische Universität Dresden, Dresden, Germany

The adrenal gland consists of the medulla and the cortex. The chromaffin cells of the adrenal medulla release catecholamines via regulated exocytosis. Vesicle formation, trafficking, maturation and fusion with the plasma membrane are orchestrated by lipids such as cholesterol, diacylglycerol, phosphatidic acid and phosphatidylinositol-4,5-bisphosphate. On the other hand, the adrenal cortex is a highly specialized lipid-metabolizing organ secreting steroid hormones. Cholesterol, acquired from circulating lipoproteins and *de novo* biosynthesis, is mobilized from intracellular stores and transported to mitochondria to be used as a substrate for steroidogenesis. Steroidogenesis is regulated by free polyunsaturated fatty acids (PUFA) and an increased PUFA content in phospholipids promotes steroidogenesis. Cholesterol efflux and lipid-processing macrophages further contribute to lipid homeostasis in the adrenal gland. Given that lipidomics have revolutionized our perception of cell function, we anticipate that this will also hold true for the investigation of adrenocortical function. Such investigations may pinpoint novel targets for the management of abnormal adrenal function.

KEYWORDS

lipid metabolism, adrenal cortex, adrenal medulla, cholesterol metabolism, phospholipids, cortisol, aldosterone

Introduction

The adrenal gland plays a pivotal role in vertebrate physiology and survival, as it mediates responses to danger and stress. It consists of the medulla, which releases catecholamines upon activation by splanchnic nerves in the so called 'fight or flight response', and the cortex, which secretes corticoid and other steroid hormones (1–3). Here, we summarize the role of lipids in the secretory function of chromaffin cells and we review the role of lipid metabolism in adrenocortical steroidogenesis.

Lipids as regulators of catecholamine secretion

Catecholamines, i.e. adrenaline and nor-adrenaline, are released by chromaffin cells through a process that involves secretory vesicles budding off the Golgi apparatus, trafficking to the plasma membrane and their regulated exocytosis (4). Membrane lipid composition plays a key role in these processes (5). Lipid rafts in the Golgi membrane can guide protein

clustering required for vesicle formation (5). Diacylglycerol (DAG), phosphatidic acid (PA), sphingolipids and cholesterol are implicated in fission of secretory vesicles (5). After formation, granules mature through acidification and condensation, and associate with actin to be transported to the plasma membrane, where catecholamines are secreted via regulated exocytosis (4, 5). Exocytosis requires vesicle docking, priming and Ca^{2+}-dependent fusion with the plasma membrane. These processes involve the assembly of soluble N-ethylmaleimide-sensitive factor attachment protein receptor (SNARE) proteins, the synaptic vesicle VAMP (synaptobrevin), and the plasma membrane proteins syntaxin and synaptosomal-associated protein of 25Kda (SNAP-25) (4). Phospholipids, like lysophosphatidylcholine (LPC), and cone-shaped lipids, such as cholesterol, DAG and PA, play a critical role in this process by regulating protein assembly and driving negative membrane curvature, which facilitates the opening of the secretory pore (4–8). Also, increased phosphoinositide (PI) amounts in the plasma membrane and the secretory granules promote exocytosis. Particularly phosphatidylinositol-4,5-bisphosphate ($PI(4,5)P_2$) localizes at sites of exocytosis, binds to proteins such as syntaxin-1, and promotes the actin-mediated conveyance of secretory granules to the plasma membrane (4, 9–12). Similarly, PA produced from phospholipids (such as phosphatidylcholine (PC), phosphatidylethanolmine (PE), phosphatidylglycerol (PG)) by phospholipase D1 (PLD1) or from DAG by diacylglycerol kinase, accumulates at the plasma membrane near exocytotic sites and contributes to lipid bilayer bending, binds to proteins like syntaxin-1, and promotes $PtdIns(4,5)P_2$ production (4, 13). While monounsaturated PA increase the number of exocytotic events by eventually driving granule docking, polyunsaturated PA regulate fusion pore stability and expansion (14). DAG primes exocytosis via activation of protein kinase C and Munc13, which modulate the function of syntaxin isoforms (15). Polyunsaturated fatty acids (PUFAs) can also interact with syntaxin isoforms aiding SNARE complex formation (16, 17). Particularly arachidonic acid (AA) released from DAG and phospholipids during exocytosis increases SNARE complex formation and fosters granule docking and exocytosis (17, 18). During exocytosis, phospholipids are scrambled in the plasma membrane, with phosphatidylserine (PS) being externalized to the outer leaflet (19). PS clusters inhibit synaptotagmin 1 membrane penetration, which is required to promote fusion pore formation (20). Sphingosine, a releasable backbone of sphingolipids, activates vesicular synaptobrevin and promotes granule tethering (21, 22). Moreover, extracellular sphingosine-1-phosphate promotes exocytosis via activation of S1P receptors (23) and sphingomyelin derivatives enhance the frequency of fusion events in chromaffin cells (24). Finally, after completion of the secretory event, the granule membrane components are entirely recycled by DAG-driven endocytosis (25).

Steroidogenesis in the adrenal cortex

The adrenal cortex consists of the *zona glomerulosa*, which produces aldosterone, and the *zona fasciculata* that produces glucocorticoids (1, 2). In primates, a third inner zone, the *zona reticularis*, produces the steroid hormone dehydroepiandrosterone (DHEA) and its sulfate ester (DHEA-S) (3, 26). Adrenocortical function is regulated by the hypothalamic–pituitary–adrenal (HPA) axis. Stress triggers the production of corticotropin-releasing-hormone (CRH) from the hypothalamus, which induces the release of adrenocorticotropic hormone (ACTH) from the anterior pituitary that reaches the adrenal gland via the circulation and binds to its receptor (melanocortin 2 receptor, MC2R) inducing corticoid production (27). ACTH is the exclusive stimulus for glucocorticoid release, while secretion of aldosterone is mainly induced by the renin-angiotensin-aldosterone system (RAAS) via angiotensin II and elevated circulating potassium levels (27, 28).

Corticoid hormones are not stored but synthesized *de novo* from cholesterol for immediate secretion. Glucocorticoid synthesis is triggered by binding of ACTH to MC2R, a G protein-coupled receptor (GPCR) activating the cyclic adenosine monophosphate (cAMP)-protein kinase A (PKA) signaling pathway. PKA activates hormone-sensitive lipase (HSL), which hydrolyzes cholesterol esters (CEs) stored in lipid droplets. Free cholesterol is transported through a complex mechanism involving steroidogenic acute regulatory (StAR) protein into mitochondria, where it serves as a substrate for steroid biosynthesis (2, 27). Cholesterol transport into mitochondria is the rate-limiting step of steroidogenesis (2, 27). Angiotensin II binds to the angiotensin type 1 receptor (AGT1R), triggering increase of intracellular calcium levels, which leads to activation of calmodulin kinase (CaMK). The latter induces StAR activation via its phosphorylation (29). Once inside the mitochondria, cholesterol is processed by cytochrome P450scc (P450 side-chain cleavage or CYP11A1), which cleaves cholesterol's aliphatic side-chain, generating pregnenolone. CYP11A1 expression is induced by ACTH and angiotensin II via cAMP signaling (27, 30). Pregnenolone is transformed into progesterone by 3β-hydroxysteroid dehydrogenase (3β-HSD). Pregnenolone and progesterone generated in mitochondria transfer to the endoplasmatic reticulum (ER), where the next steps of steroidogenesis take place (31). In humans, progesterone is converted by CYP21 to 11-deoxycorticosterone, which is further metabolized to corticosterone by CYP11B1. Corticosterone is metabolized in the *zona glomerulosa* by CYP11B2 to aldosterone. In the *zona fasciculata*, progesterone is converted by CYP17 to 17-hydroxyprogesterone, which is processed by CYP21 to 11-deoxycortisol. In the final step of glucocorticoid synthesis, CYP11B1 converts 11-deoxycortisol to cortisol (27). While CYP11B1 is constitutively expressed in the *zona fasciculata*, CYP11B2 expression in the *zona glomerulosa* is regulated by circulating factors, such as angiotensin II, sodium and lipoproteins, like low-density lipoproteins (LDL), high-density lipoproteins (HDL) and very low-density lipoproteins (VLDL) (32–35). In the *zona reticularis*, 17-hydroxyprogesterone is converted by CYP17A1 to DHEA, which can be further metabolized to sex hormones (27).

Cholesterol homeostasis in adrenocortical cells

Cholesterol serves as a precursor for steroid hormone production (36, 37). Cholesterol availability in adrenocortical cells is covered by 1. uptake from circulating lipoproteins 2. *de novo* synthesis and 3. CEs stored in lipid droplets (30, 37) (Figure 1). However, the exact contribution of these pathways to steroidogenesis and the flexibility in switching between them at baseline or stimulated conditions, are not fully understood. Excess intracellular cholesterol is transferred to circulating HDL through cholesterol efflux (38).

Cholesterol acquisition from lipoproteins

Lipoproteins supply adrenocortical cells with cholesterol for steroid hormone production. LDL and HDL are internalized via binding to the LDL receptor (LDLR) and scavenger receptor class B type I (SCARB1), respectively, followed by endocytosis (37, 39, 40). Patients deficient for LDLR have normal serum cortisol levels but show reduced cortisol production in response to ACTH (41). Similarly, patients with SCARB1 mutation have normal cortisol concentrations, but reduced cortisol levels upon stimulation with an ACTH derivative (42). In contrast, LDLR and SCARB1 expression is increased in the adrenal cortex of patients with primary

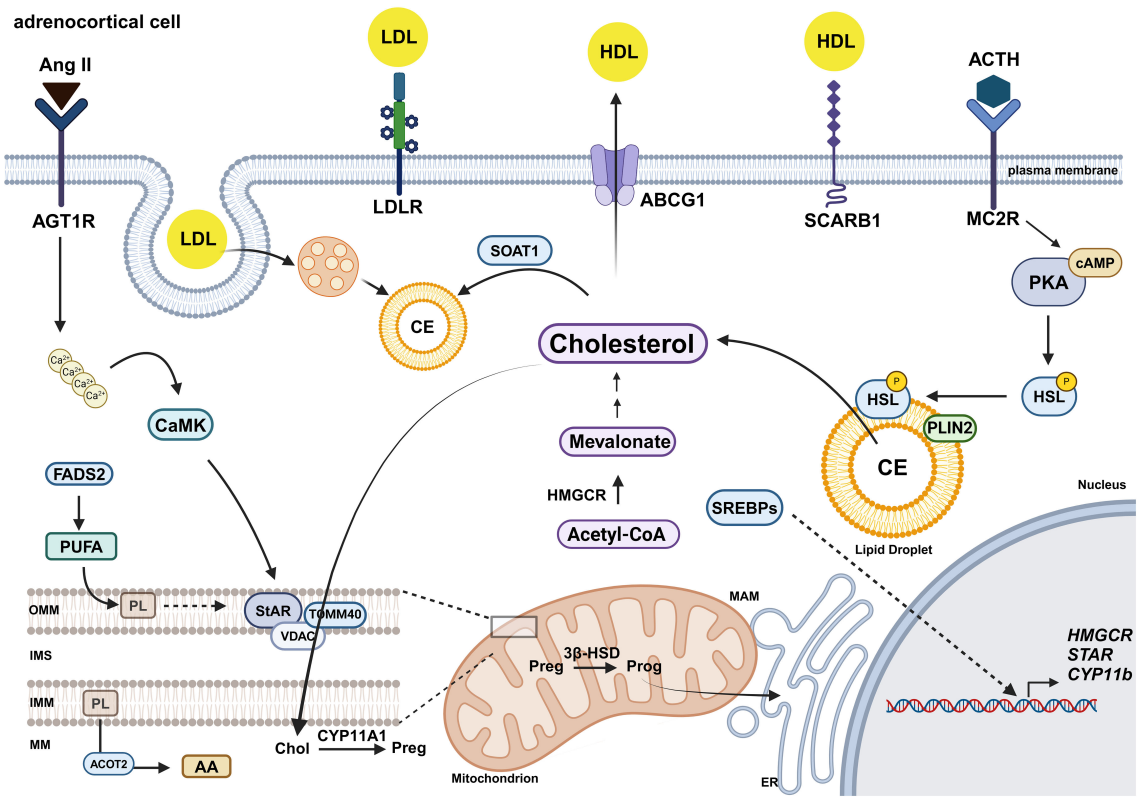

FIGURE 1
Lipid metabolism in adrenocortical cells. In adrenocortical cells, cholesterol derives from circulating lipoproteins and *de novo* biosynthesis. Low-density lipoproteins (LDLs) are internalized via the LDL receptor (LDLR) and endocytosis, while high-density lipoproteins (HDL) are taken up via scavenger receptor class B type I (SCARB1) (39, 40). Excess cholesterol is either esterified by SOAT1 and stored in lipid droplets (57) or exported via Adenosine triphosphate (ATP)-binding cassette transporter G1 (ABCG1) (85). Adrenocorticotropic hormone (ACTH) binding to melanocortin 2 receptor (MC2R) activates protein kinase A (PKA), which induces hormone-sensitive lipase (HSL) phosphorylation and translocation to the lipid droplets, assisted by perilipin 2 (PLIN2), promoting cholesterol release (66, 67). Angiotensin II (Ang II) binds to the angiotensin type 1 receptor (AGT1R), triggering the increase of intracellular calcium levels, leading to activation of calmodulin kinase (CaMK), which induces StAR activation (29). *De novo* synthesis of cholesterol is regulated by the rate-limiting conversion of acetyl-CoA to mevalonate via hydroxymethylglutaryl-CoA (HMG-CoA) reductase (HMGCR) (52). Gene expression of HMGCR and other cholesterogenic proteins is induced by Sterol regulatory element-binding proteins (SREBP) (53, 55). Free cholesterol is transported into mitochondria by steroidogenic acute regulatory (StAR) protein, through a complex process involving a number of different proteins, such as Voltage-dependent anion channels (VDAC) and translocase of the outer mitochondrial membrane 40 (TOMM40) (27, 31, 74–76, 107, 108). Cholesterol transfer from the ER to mitochondria is facilitated via ER-mitochondria contact sites, called mitochondria-associated membranes (MAMs) (31, 75). Fatty acid desaturase 2 (FADS2)-mediated increase in the PUFA content of mitochondrial phospholipids promotes cholesterol import into mitochondria (59). Moreover, arachidonic acid (AA) released from phospholipids by acyl-CoA thioesterase 2 (ACOT2) promotes steroidogenesis (96, 97). In mitochondria, steroidogenesis starts with the conversion of cholesterol to pregnenolone by CYP11A1 (27, 30).

aldosteronism (43, 44). Accordingly, angiotensin II upregulates the expression of LDLR and SCARB1 (45). Besides providing cholesterol, lipoproteins (LDL, HDL, VLDL) trigger signaling events, including mobilization of intracellular calcium and cAMP response element binding (CREB) activation, thereby inducing expression of proteins involved in steroidogenesis, such as CYP11B2 and StAR (39, 44, 46, 47). LDLR is downregulated with aging in the adrenal cortex of primates limiting cholesterol uptake and DHEA-S secretion (48). Intriguingly, cholesterol uptake was shown to be dependent on autophagy, a mechanism mediating the degradation of cellular components (49). Autophagy disruption in Leydig cells leads to down-regulation of SCARB1, inefficient cholesterol supply and reduced testosterone production (49). Moreover, in Drosophila, autophagosomes sequester and transport cholesterol for steroid synthesis, while their disruption leads to cholesterol accumulation in lipid droplets (50).

Cholesterol synthesis

Along with cholesterol imported from circulating lipoproteins, *de novo* biosynthesized cholesterol also fuels adrenocortical steroidogenesis. Acetyl-CoA, the precursor molecule of cholesterol, is produced in the cytosol by the ATP citrate lyase (ACLY) (51). The rate-limiting reaction of cholesterol synthesis is the conversion of acetyl-CoA to mevalonate by hydroxymethylglutaryl-CoA reductase (HMGCR) (52). Low sterol concentration is sensed by sterol regulatory element-binding proteins (SREBPs) that induce HMGCR expression (53). Through a cascade of reactions mevalonate is metabolized to squalene, which is processed in the ER membrane via lanosterol and desmosterol to cholesterol (52, 54). The central transcriptional activator of steroidogenesis, Steroidogenic Factor 1 (SF-1) binds to the promoter and induces the expression of several genes encoding for cholesterogenic proteins (55). Peripartum and lactation-associated adrenal gland plasticity in female rats involves downregulation of HMGCR expression and depletion of intra-adrenal cholesterol stores despite increased LDLR and SCARB1 expression; this is associated with basal hypercorticism and reduced responsiveness to ACTH, conferring postpartum anxiolysis (56). These evolutionary adaptations are overridden by feeding with a high-fat diet (HFD), which prevents the peripartum reduction of HMGCR expression and cholesterol stores (56).

Cholesterol storage and mobilization

Uptaken or synthesized cholesterol is esterified by sterol O-acyltransferase 1 (SOAT1) with fatty acids and stored in lipid droplets, which makes cholesterol rapidly available for steroidogenesis (57). Inhibition of Acyl-coenzyme A: cholesterol acyltransferase (ACAT), which converts cholesterol to CE, reduces aldosterone production via suppression of CYP11B2 expression (58). Impaired steroidogenesis, as in congenital adrenal lipoid hyperplasia, or disruption of cholesterol mobilization and mitochondrial import, for instance due to HSL or StAR deficiency, lead to increased accumulation of CEs in lipid droplets (59–63). On the other hand, depleting the intracellular cholesterol pool in steroidogenic cells leads to lipid droplet shrinkage (64). Lipid droplets share contact sites with mitochondria and the ER, thereby facilitating immediate cholesterol transport to these organelles (31). Cholesterol mobilization occurs through lipophagy, where lipid droplets are engulfed by phagosomes followed by fusion with lysosomes, or through hormonally-controlled lipolysis mediated by HSL (63, 65). ACTH stimulation triggers via PKA HSL phosphorylation, which modestly increases HSL activity and, more importantly, directs HSL to lipid droplets, a process assisted by perilipin 2 (PLIN2), which resides on the lipid droplet surface (66, 67). PLIN2 deficiency in mice leads to pronounced lipid droplet accumulation in adrenocortical cells (67).

Impaired lipid mobilization and enhanced lipid accumulation in adrenocortical cells is accompanied by increased expression of macrophage markers, suggesting a role of adrenal gland macrophages in the local lipid turnover (67, 68). Similarly to lipid-associated macrophages (LAMs) present in other tissues, such as the adipose tissue, adrenal gland macrophages are rich in lipid droplets and present LAM signatures, including expression of Triggering receptor expressed on myeloid cells 2 (*Trem2*), Lipoprotein lipase (*Lpl*), *Cd9* and *Cd36* (68–70). Removal of adrenal gland macrophages causes increased lipid accumulation in the adrenal cortex (68). Consequently, adrenal gland macrophages regulate adrenocortical steroidogenesis in acute and chronic stress conditions, like cold exposure and atherosclerosis, respectively, through a mechanism dependent on TREM2 and macrophage-specific TREM2 deletion in mice increases serum glucocorticoid levels (70). These findings underscore the critical homeostatic role of macrophages in adrenocortical lipid metabolism and steroidogenesis.

Cholesterol trafficking

Cholesterol levels are sensed by SREBPs residing in the ER (71). Cholesterol freed from CEs is transferred from lipid droplets to mitochondria by StAR. StAR mutations lead to impaired adrenal steroidogenesis, a condition termed congenital adrenal lipoid hyperplasia (72). StAR localizes at the outer mitochondrial membrane (OMM) and unfolds upon cholesterol binding at a C-terminal domain, a process requiring glucose regulatory protein-78 (GRP78) (73). Subsequently StAR mediates cholesterol transport into mitochondria through a complex and not entirely understood process involving a number of different proteins, such as Voltage-dependent anion channel 1 (VDAC1), VDAC2, mitochondrial transporter protein (TSPO), translocase of the outer mitochondrial membrane 40 (TOMM40) and GRP78 (27, 74–76). StAR-mediated cholesterol import depends on the efficiency of the electron transport chain and ATP production (77, 78). Moreover, cholesterol import into mitochondria is affected by the polyunsaturated fatty acid (PUFA) content of mitochondrial phospholipids. Reduced PUFA content in the phospholipids of mitochondrial membranes associates with diminished cholesterol import, mitochondrial membrane potential

and oxidative phosphorylation (59). Accordingly, Acyl-CoA synthetase 4 (ACSL4), which inserts CoA to PUFAs facilitating their esterification into phospholipids, is highly expressed in the adrenal gland and required for steroidogenesis (59, 79). Cholesterol is thought to be transferred through direct contact sites connecting lipid droplets, mitochondria, the ER and the plasma membrane. Mitochondria, the ER, the plasma membrane, ER-mitochondria contact sites, so called mitochondria-associated membranes (MAMs) and plasma membrane-associated membranes (PAMs) have all unique and plastic lipid compositions (80). cAMP signaling triggers the formation of plasma membrane-ER and ER-mitochondria contacts (80). Cholesterol and proteins involved in cholesterol transfer accumulate at MAMs (31, 75). Aster proteins mediate cholesterol traffic from the plasma membrane to the ER and from the ER to mitochondria (81, 82). Furthermore, syntaxin (STX)-5 and a-SNAP mediate delivery of plasma membrane cholesterol to mitochondria (83, 84).

Cholesterol efflux

Cholesterol levels in adrenocortical cells are regulated by cholesterol efflux mediated by ATP-binding cassette transporter G1 (ABCG1) and apolipoprotein E (ApoE) (85). Fasting stress reduces *Apoe* and *Abcg1* expression inhibiting cholesterol efflux (38). Adrenocortical ABCG1 deficiency leads to enhanced glucocorticoid production and, paradoxically, increased expression of genes encoding for proteins involved in cholesterol uptake, such as *Ldlr*, and cholesterol synthesis, such as *Hmgcr* and Squalene Epoxidase (*Sqle*) (85). ApoE-deficient mice present impaired cholesterol efflux associated with enhanced stress-induced glucocorticoid secretion (38). In contrast, cholesterol efflux is increased and adrenocortical steroidogenesis is reduced by synthetic HDL particles, which promote reverse cholesterol transport and thereby present a therapeutic strategy against atherosclerosis (86). Besides cholesterol homeostasis, lipoprotein release also serves long-range intercellular signaling mediated by proteins loaded onto lipoproteins. For instance, Sonic hedgehog (SHH), which is expressed in adrenocortical cells beneath the adrenal capsule, is released on lipoproteins, along with Hh pathway inhibitors regulating its long-range effects (87, 88).

Sphingolipids and phospholipids as regulators of steroidogenesis

Apart from cholesterol metabolism and steroidogenesis, also other lipid metabolic pathways are dynamically regulated and play crucial roles in adrenocortical function. The adrenal gland presents organized spatial lipid distribution of sphingolipids and phospholipids (89). ACTH and cAMP signaling reduce the amounts of several sphingolipids, including sphingomyelin, ceramides, and sphingosine, induce sphingosine kinase activity and increase released S1P, while the latter promotes StAR, TSPO, LDLR and SCARB1 expression and glucocorticoid production (90, 91). Loss-of-function mutations in S1P lyase (SGPL1), lead to accumulation of sphingolipids in lysosomes and a condition termed sphingolipidose (92). Accordingly, *Sgpl1*$^{-/-}$ mice present disrupted adrenocortical zonation and impaired steroidogenic protein expression (92).

Moreover, phospholipids can determine the steroidogenic capacity of adrenocortical cells based on their PUFA content (59). AA is one of the most abundant acyl chains in PC, PE, PG and PI in the murine adrenal gland (59). Similarly, AA is among the most abundant lipids in the human adrenal cortex (59, 93). ACSL4-mediated esterification of free AA into phospholipids promotes steroidogenesis (79, 94, 95). On the other hand, hormonal stimulation and cAMP signaling induce acyl-CoA thioesterase 2 (ACOT2)-mediated release of AA from phospholipids into mitochondria (96, 97). Moreover, AA is metabolized by lipoxygenases to lipid mediators, such as hydroxyeicosatetraenoates, which can also regulate steroidogenesis (96).

The acyl chain composition of phospholipids in the adrenal gland is under dietary influence. For instance, AA-containing phospholipids increase in the adrenal gland of mice fed a HFD, aligning with enhanced corticoid output (59). Fatty acid desaturase 2 (FADS2), the rate-limiting enzyme of PUFA synthesis, is highly expressed in the adrenal gland and is upregulated in conditions of elevated corticoid synthesis, such as obesity or adrenal adenomas. Inhibition of FADS2 perturbs cholesterol transfer into mitochondria, mitochondrial function and steroidogenesis in adrenocortical cells, while steroidogenesis is partially restored by AA supplementation. In accordance, FADS2 deficiency in mice receiving a low-PUFA diet leads to reduced amounts of AA-containing phospholipids in the adrenal cortex, reduced glucocorticoid serum levels, enhanced lipid droplet accumulation and perturbed mitochondrial structure in adrenocortical cells. Accordingly, pharmacological inhibition of FADS2 reduces corticoid production in mice with established obesity (59). Moreover, the n-3 PUFA eicosapentaenoic acid (EPA) diminishes FADS2 expression and steroidogenesis in mouse and human adrenocortical cells and icosapent ethyl, an EPA analog, which is in clinical use for reduction of cardiovascular disease risk, efficiently reduces corticosterone and aldosterone serum levels in obese animals (59). Hence, treatment with dietary adjuncts, such as icosapent ethyl, could be an appealing strategy to clinically tackle dysregulated cortisol and aldosterone production.

Diseases of disturbed lipid metabolism leading to impaired adrenocortical steroidogenesis

Disturbed lipid metabolism underlies several diseases manifested by adrenal insufficiency. Cortisol production is impaired in patients with LDLR deficiency or SCARB1 mutations (41, 42). Reduced HDL levels due to decreased hepatic lecithin-cholesterol acyltransferase (LCAT) activity in patients with liver cirrhosis associate with occurrence of relative adrenal insufficiency (RAI) (98). X-linked adrenoleukodystrophy (ALD), a disorder

characterized by primary adrenal insufficiency, hypothyroidism and neurological symptoms, is caused by pathogenic variants of ABCD1, a very-long-chain fatty acid (VLCFA) transporter, leading to VLCFA accumulation in the form of CE (99–101). SGPL1 mutations are found in patients with steroid-resistant nephrotic syndrome (SRNS), which is characterized by adrenal insufficiency and chronic kidney disease (92, 102). Mutations in lysosomal acid lipase (cholesterol esterase) that hydrolyzes CE, lead to insufficient free cholesterol available to P450scc and development of Wolman disease (primary xanthomatosis) featured by adrenal insufficiency (103). Impaired cholesterol biosynthesis due to defects in sterol 7-reductase gene, DHCR7, in the Smith-Lemli-Opitz syndrome may lead to adrenal insufficiency, especially during times of stress or if LDL is inadequate (30).

Discussion

The study of lipid metabolism has transformed our understanding of cell function. Lipids lie at the core of adrenal structure and function. Although the mechanisms involved in lipid metabolism in the adrenal gland were readily investigated during the past three decades, so far acquired knowledge has been barely therapeutically harnessed to clinically modulate adrenal function, for instance treat excessive cortisol or aldosterone production. However, lipophilic statin use in hypertensive and diabetic patients was associated with reduced basal and angiotensin II-stimulated aldosterone levels (104). Statins suppress HMGCR while they also inhibit caveolin-1-mediate endocytosis of lipoprotein receptors (104, 105). Hence, downregulation of aldosterone synthesis due to inhibition of cholesterol uptake and synthesis in adrenocortical cells may underlie the anti-hypertensive effect of statins (44). Especially lipophilic statins, such as simvastatin, which are more readily uptaken in the adrenal cortex, could be used to reduce aldosterone levels (104). Hence, preclinical and clinical studies and retrospective clinical analyses should be performed to elucidate the impact of statins in aldosterone release. As primary aldosteronism often co-occurs with cardiovascular disease and metabolic syndrome, combinatorial treatments with statins and antihypertensives could more potently reduce aldosterone levels and ameliorate the outcomes of primary aldosteronism, including ischemic heart disease or stroke (44, 106).

Moreover, modulation of the phospholipid composition of the adrenal cortex may present a means to control elevated corticoid production (59). Particularly, lowering the AA content of phospholipids through regulation of FADS2 by dietary adjuncts, such as icosapent ethyl, could be a novel strategy to regulate moderately elevated corticoid production in obesity, a concept which merits clinical investigation (59). Concluding, investigation of adrenal function under the prism of lipid metabolism may reveal new valuable concepts of endocrine regulation in normal and pathological conditions.

Author contributions

AA: Visualization, Writing – original draft. VA: Conceptualization, Funding acquisition, Project administration, Resources, Supervision, Writing – original draft, Writing – review & editing.

Funding

The author(s) declare that financial support was received for the research and/or publication of this article. The project was funded by the Deutsche Forschungsgemeinschaft AL 1686/6-1 and SFB-TRR 205 project A07 to VIA.

Conflict of interest

The authors declare absence of any commercial or financial relationships that could be construed as a potential conflict of interest.

Generative AI statement

The author(s) declare that no Generative AI was used in the creation of this manuscript.

Publisher's note

References

1. Feldman RD. Aldosterone and blood pressure regulation: recent milestones on the long and winding road from electrocortin to KCNJ5, GPER, and beyond. *Hypertension*. (2014) 63:19–21. doi: 10.1161/HYPERTENSIONAHA.113.01251

2. Lightman SL, Birnie MT, Conway-Campbell BL. Dynamics of ACTH and cortisol secretion and implications for disease. *Endocr Rev*. (2020) 41(3):bnaa002. doi: 10.1210/endrev/bnaa002

3. Prough RA, Clark BJ, Klinge CM. Novel mechanisms for DHEA action. *J Mol Endocrinol*. (2016) 56:R139–55. doi: 10.1530/JME-16-0013

4. Ammar MR, Kassas N, Chasserot-Golaz S, Bader MF, Vitale N. Lipids in regulated exocytosis: what are they doing? *Front Endocrinol (Lausanne)*. (2013) 4:125. doi: 10.3389/fendo.2013.00125

5. Tanguy E, Carmon O, Wang Q, Jeandel L, Chasserot-Golaz S, Montero-Hadjadje M, et al. Lipids implicated in the journey of a secretory granule: from biogenesis to fusion. *J Neurochem*. (2016) 137:904–12. doi: 10.1111/jnc.2016.137.issue-6

6. Bao H, Goldschen-Ohm M, Jeggle P, Chanda B, Edwardson JM, Chapman ER. Exocytotic fusion pores are composed of both lipids and proteins. *Nat Struct Mol Biol*. (2016) 23:67–73. doi: 10.1038/nsmb.3141

7. Dhara M, Mantero Martinez M, Makke M, Schwarz Y, Mohrmann R, Bruns D. Synergistic actions of v-SNARE transmembrane domains and membrane-curvature modifying lipids in neurotransmitter release. *Elife*. (2020) 9:e55152. doi: 10.7554/eLife.55152

8. Lang T, Bruns D, Wenzel D, Riedel D, Holroyd P, Thiele C, et al. SNAREs are concentrated in cholesterol-dependent clusters that define docking and fusion sites for exocytosis. *EMBO J*. (2001) 20:2202–13. doi: 10.1093/emboj/20.9.2202

9. Martin TF. PI(4,5)P(2)-binding effector proteins for vesicle exocytosis. *Biochim Biophys Acta*. (2015) 1851:785–93. doi: 10.1016/j.bbalip.2014.09.017

10. Kreutzberger AJB, Kiessling V, Liang B, Seelheim P, Jakhanwal S, Jahn R, et al. Reconstitution of calcium-mediated exocytosis of dense-core vesicles. *Sci Adv*. (2017) 3: e1603208. doi: 10.1126/sciadv.1603208

11. Walter AM, Muller R, Tawfik B, Wierda KD, Pinheiro PS, Nadler A, et al. Phosphatidylinositol 4,5-bisphosphate optical uncaging potentiates exocytosis. *Elife*. (2017) 6:e30203. doi: 10.7554/eLife.30203

12. Wen PJ, Osborne SL, Zanin M, Low PC, Wang HT, Schoenwaelder SM, et al. Phosphatidylinositol(4,5)bisphosphate coordinates actin-mediated mobilization and translocation of secretory vesicles to the plasma membrane of chromaffin cells. *Nat Commun*. (2011) 2:491. doi: 10.1038/ncomms1500

13. Tanguy E, Wang Q, Vitale N. Role of phospholipase D-derived phosphatidic acid in regulated exocytosis and neurological disease. *Handb Exp Pharmacol*. (2020) 259:115–30. doi: 10.1007/164_2018_180

14. Tanguy E, Coste de Bagneaux P, Kassas N, Ammar MR, Wang Q, Haeberle AM, et al. Mono- and poly-unsaturated phosphatidic acid regulate distinct steps of regulated exocytosis in neuroendocrine cells. *Cell Rep*. (2020) 32:108026. doi: 10.1016/j.celrep.2020.108026

15. Bauer CS, Woolley RJ, Teschemacher AG, Seward EP. Potentiation of exocytosis by phospholipase C-coupled G-protein-coupled receptors requires the priming protein Munc13-1. *J Neurosci*. (2007) 27:212–9. doi: 10.1523/JNEUROSCI.4201-06.2007

16. Darios F, Davletov B. Omega-3 and omega-6 fatty acids stimulate cell membrane expansion by acting on syntaxin 3. *Nature*. (2006) 440:813–7. doi: 10.1038/nature04598

17. Latham CF, Osborne SL, Cryle MJ, Meunier FA. Arachidonic acid potentiates exocytosis and allows neuronal SNARE complex to interact with Munc18a. *J Neurochem*. (2007) 100:1543–54. doi: 10.1111/j.1471-4159.2006.04286.x

18. Narayana VK, Tomatis VM, Wang T, Kvaskoff D, Meunier FA. Profiling of free fatty acids using stable isotope tagging uncovers a role for saturated fatty acids in neuroexocytosis. *Chem Biol*. (2015) 22:1552–61. doi: 10.1016/j.chembiol.2015.09.010

19. Zhang Z, Hui E, Chapman ER, Jackson MB. Phosphatidylserine regulation of Ca2+-triggered exocytosis and fusion pores in PC12 cells. *Mol Biol Cell*. (2009) 20:5086–95. doi: 10.1091/mbc.e09-08-0691

20. Courtney KC, Mandal T, Mehta N, Wu L, Li Y, Das D, et al. Synaptotagmin-7 outperforms synaptotagmin-1 to promote the formation of large, stable fusion pores via robust membrane penetration. *Nat Commun*. (2023) 14:7761. doi: 10.1038/s41467-023-42497-8

21. Darios F, Wasser C, Shakirzyanova A, Giniatullin A, Goodman K, Munoz-Bravo JL, et al. Sphingosine facilitates SNARE complex assembly and activates synaptic vesicle exocytosis. *Neuron*. (2009) 62:683–94. doi: 10.1016/j.neuron.2009.04.024

22. Garcia-Martinez V, Villanueva J, Torregrosa-Hetland CJ, Bittman R, Higdon A, Darley-Usmar VM, et al. Lipid metabolites enhance secretion acting on SNARE microdomains and altering the extent and kinetics of single release events in bovine adrenal chromaffin cells. *PLoS One*. (2013) 8:e75845. doi: 10.1371/journal.pone.0075845

23. Jiang ZJ, Delaney TL, Zanin MP, Haberberger RV, Pitson SM, Huang J, et al. Extracellular and intracellular sphingosine-1-phosphate distinctly regulates exocytosis in chromaffin cells. *J Neurochem*. (2019) 149:729–46. doi: 10.1111/jnc.2019.149.issue-6

24. Garcia-Martinez V, Montes MA, Villanueva J, Gimenez-Molina Y, de Toledo GA, Gutierrez LM. Sphingomyelin derivatives increase the frequency of microvesicle and granule fusion in chromaffin cells. *Neuroscience*. (2015) 295:117–25. doi: 10.1016/j.neuroscience.2015.03.036

25. Yuan T, Liu L, Zhang Y, Wei L, Zhao S, Zheng X, et al. Diacylglycerol guides the hopping of clathrin-coated pits along microtubules for exo-endocytosis coupling. *Dev Cell*. (2015) 35:120–30. doi: 10.1016/j.devcel.2015.09.004

26. Yilmaz C, Karali K, Fodelianaki G, Gravanis A, Chavakis T, Charalampopoulos I, et al. Neurosteroids as regulators of neuroinflammation. *Front Neuroendocrinol*. (2019) 55:100788. doi: 10.1016/j.yfrne.2019.100788

27. Midzak A, Papadopoulos V. Adrenal mitochondria and steroidogenesis: from individual proteins to functional protein assemblies. *Front Endocrinol (Lausanne)*. (2016) 7:106. doi: 10.3389/fendo.2016.00106

28. Barrett PQ, Guagliardo NA, Klein PM, Hu C, Breault DT, Beenhakker MP. Role of voltage-gated calcium channels in the regulation of aldosterone production from zona glomerulosa cells of the adrenal cortex. *J Physiol*. (2016) 594:5851–60. doi: 10.1113/tjp.2016.594.issue-20

29. Lymperopoulos A, Borges JI, Suster MS. Angiotensin II-dependent aldosterone production in the adrenal cortex. *Vitam Horm*. (2024) 124:393–404. doi: 10.1016/bs.vh.2023.05.001

30. Miller WL, Auchus RJ. The molecular biology, biochemistry, and physiology of human steroidogenesis and its disorders. *Endocr Rev*. (2011) 32:81–151. doi: 10.1210/er.2010-0013

31. Issop L, Rone MB, Papadopoulos V. Organelle plasticity and interactions in cholesterol transport and steroid biosynthesis. *Mol Cell Endocrinol*. (2013) 371:34–46. doi: 10.1016/j.mce.2012.12.003

32. Hattangady NG, Olala LO, Bollag WB, Rainey WE. Acute and chronic regulation of aldosterone production. *Mol Cell Endocrinol*. (2012) 350:151–62. doi: 10.1016/j.mce.2011.07.034

33. Nishimoto K, Harris RB, Rainey WE, Seki T. Sodium deficiency regulates rat adrenal zona glomerulosa gene expression. *Endocrinology*. (2014) 155:1363–72. doi: 10.1210/en.2013-1999

34. Spaulding SC, Bollag WB. The role of lipid second messengers in aldosterone synthesis and secretion. *J Lipid Res*. (2022) 63:100191. doi: 10.1016/j.jlr.2022.100191

35. Gomez-Sanchez CE, Gomez-Sanchez EP. Cholesterol availability and adrenal steroidogenesis. *Endocrinology*. (2024) 165 (4):bqae032. doi: 10.1210/endocr/bqae032

36. Chakraborty S, Doktorova M, Molugu TR, Heberle FA, Scott HL, Dzikovski B, et al. How cholesterol stiffens unsaturated lipid membranes. *Proc Natl Acad Sci U S A*. (2020) 117:21896–905. doi: 10.1073/pnas.2004807117

37. Miller WL. Steroidogenesis: unanswered questions. *Trends Endocrinol Metab*. (2017) 28:771–93. doi: 10.1016/j.tem.2017.09.002

38. Hoekstra M, Ouweneel AB, Nahon JE, van der Geest R, Kroner MJ, van der Sluis RJ, et al. ATP-binding cassette transporter G1 deficiency is associated with mild glucocorticoid insufficiency in mice. *Biochim Biophys Acta Mol Cell Biol Lipids*. (2019) 1864:443–51. doi: 10.1016/j.bbalip.2019.01.003

39. Xing Y, Rainey WE, Apolzan JW, Francone OL, Harris RB, Bollag WB. Adrenal cell aldosterone production is stimulated by very-low-density lipoprotein (VLDL). *Endocrinology*. (2012) 153:721–31. doi: 10.1210/en.2011-1752

40. Tsai YY, Rainey WE, Johnson MH, Bollag WB. VLDL-activated cell signaling pathways that stimulate adrenal cell aldosterone production. *Mol Cell Endocrinol*. (2016) 433:138–46. doi: 10.1016/j.mce.2016.05.018

41. Illingworth DR, Lees AM, Lees RS. Adrenal cortical function in homozygous familial hypercholesterolemia. *Metabolism*. (1983) 32:1045–52. doi: 10.1016/0026-0495(83)90075-6

42. Vergeer M, Korporaal SJ, Franssen R, Meurs I, Out R, Hovingh GK, et al. Genetic variant of the scavenger receptor BI in humans. *N Engl J Med*. (2011) 364:136–45. doi: 10.1056/NEJMoa0907687

43. Harashima S, Yamazaki Y, Motomura N, Ono Y, Omata K, Tezuka Y, et al. Phenotype-genotype correlation in aldosterone-producing adenomas characterized by intracellular cholesterol metabolism. *J Steroid Biochem Mol Biol*. (2022) 221:106116. doi: 10.1016/j.jsbmb.2022.106116

44. Wu H, He H, Han T, Tian X, Zhu Z. Targeting cholesterol-dependent adrenal steroidogenesis for management of primary aldosteronism. *Trends Endocrinol Metab*. (2025) S1043-2760(24)00323-0. doi: 10.1016/j.tem.2024.12.001

45. Pilon A, Martin G, Bultel-Brienne S, Junquero D, Delhon A, Fruchart JC, et al. Regulation of the scavenger receptor BI and the LDL receptor by activators of aldosterone production, angiotensin II and PMA, in the human NCI-H295R adrenocortical cell line. *Biochim Biophys Acta*. (2003) 1631:218–28. doi: 10.1016/S1388-1981(03)00020-9

46. Xing Y, Cohen A, Rothblat G, Sankaranarayanan S, Weibel G, Royer L, et al. Aldosterone production in human adrenocortical cells is stimulated by high-density lipoprotein 2 (HDL2) through increased expression of aldosterone synthase (CYP11B2). *Endocrinology*. (2011) 152:751–63. doi: 10.1210/en.2010-1049

47. Tsai YY, Rainey WE, Bollag WB. Very low-density lipoprotein (VLDL)-induced signals mediating aldosterone production. *J Endocrinol*. (2017) 232:R115–R29. doi: 10.1530/JOE-16-0237

48. Wang Q, Wang X, Liu B, Ma S, Zhang F, Sun S, et al. Aging induces region-specific dysregulation of hormone synthesis in the primate adrenal gland. *Nat Aging*. (2024) 4:396–413. doi: 10.1038/s43587-024-00588-1

49. Gao F, Li G, Liu C, Gao H, Wang H, Liu W, et al. Autophagy regulates testosterone synthesis by facilitating cholesterol uptake in Leydig cells. *J Cell Biol*. (2018) 217:2103–19. doi: 10.1083/jcb.201710078

50. Texada MJ, Malita A, Christensen CF, Dall KB, Faergeman NJ, Nagy S, et al. Autophagy-mediated cholesterol trafficking controls steroid production. *Dev Cell*. (2019) 48:659–71.e4. doi: 10.1016/j.devcel.2019.01.007

51. Mateska I, Alexaki VI. Light shed on a non-canonical TCA cycle: cell state regulation beyond mitochondrial energy production. *Signal Transduct Target Ther*. (2022) 7:201. doi: 10.1038/s41392-022-01060-5

52. Duan Y, Gong K, Xu S, Zhang F, Meng X, Han J. Regulation of cholesterol homeostasis in health and diseases: from mechanisms to targeted therapeutics. *Signal Transduct Target Ther*. (2022) 7:265. doi: 10.1038/s41392-022-01125-5

53. Brown MS, Goldstein JL. Cholesterol feedback: from Schoenheimer's bottle to Scap's MELADL. *J Lipid Res*. (2009) 50 Suppl:S15–27. doi: 10.1194/jlr.R800054-JLR200

54. Shi Q, Chen J, Zou X, Tang X. Intracellular cholesterol synthesis and transport. *Front Cell Dev Biol*. (2022) 10:819281. doi: 10.3389/fcell.2022.819281

55. Baba T, Otake H, Inoue M, Sato T, Ishihara Y, Moon JY, et al. Ad4BP/SF-1 regulates cholesterol synthesis to boost the production of steroids. *Commun Biol*. (2018) 1:18. doi: 10.1038/s42003-018-0020-z

56. Perani CV, Neumann ID, Reber SO, Slattery DA. High-fat diet prevents adaptive peripartum-associated adrenal gland plasticity and anxiolysis. *Sci Rep*. (2015) 5:14821. doi: 10.1038/srep14821

57. Ferraz-de-Souza B, Hudson-Davies RE, Lin L, Parnaik R, Hubank M, Dattani MT, et al. Sterol O-acyltransferase 1 (SOAT1, ACAT) is a novel target of steroidogenic factor-1 (SF-1, NR5A1, Ad4BP) in the human adrenal. *J Clin Endocrinol Metab*. (2011) 96:E663–8. doi: 10.1210/jc.2010-2021

58. Shimada H, Hata S, Yamazaki Y, Otsubo Y, Sato I, Ise K, et al. YM750, an ACAT inhibitor, acts on adrenocortical cells to inhibit aldosterone secretion due to depolarization. *Int J Mol Sci*. (2022) 23(21):12803. doi: 10.3390/ijms232112803

59. Witt A, Mateska I, Palladini A, Sinha A, Wolk M, Harauma A, et al. Fatty acid desaturase 2 determines the lipidomic landscape and steroidogenic function of the adrenal gland. *Sci Adv*. (2023) 9:eadf6710. doi: 10.1126/sciadv.adf6710

60. Sasaki G, Ishii T, Jeyasuria P, Jo Y, Bahat A, Orly J, et al. Complex role of the mitochondrial targeting signal in the function of steroidogenic acute regulatory protein revealed by bacterial artificial chromosome transgenesis *in vivo*. *Mol Endocrinol*. (2008) 22:951–64. doi: 10.1210/me.2007-0493

61. Miller WL, Bose HS. Early steps in steroidogenesis: intracellular cholesterol trafficking. *J Lipid Res*. (2011) 52:2111–35. doi: 10.1194/jlr.R016675

62. Mizuno Y, Ishii T, Hasegawa T. *In vivo* verification of the pathophysiology of lipoid congenital adrenal hyperplasia in the adrenal cortex. *Endocrinology*. (2019) 160:331–8. doi: 10.1210/en.2018-00777

63. Li H, Brochu M, Wang SP, Rochdi L, Cote M, Mitchell G, et al. Hormone-sensitive lipase deficiency in mice causes lipid storage in the adrenal cortex and impaired corticosterone response to corticotropin stimulation. *Endocrinology*. (2002) 143:3333–40. doi: 10.1210/en.2002-220341

64. Bassi G, Sidhu SK, Mishra S. The intracellular cholesterol pool in steroidogenic cells plays a role in basal steroidogenesis. *J Steroid Biochem Mol Biol*. (2022) 220:106099. doi: 10.1016/j.jsbmb.2022.106099

65. Weckman A, Di Ieva A, Rotondo F, Syro LV, Ortiz LD, Kovacs K, et al. Autophagy in the endocrine glands. *J Mol Endocrinol*. (2014) 52:R151–63. doi: 10.1530/JME-13-0241

66. Wang H, Hu L, Dalen K, Dorward H, Marcinkiewicz A, Russell D, et al. Activation of hormone-sensitive lipase requires two steps, protein phosphorylation and binding to the PAT-1 domain of lipid droplet coat proteins. *J Biol Chem*. (2009) 284:32116–25. doi: 10.1074/jbc.M109.006726

67. Li Y, Khanal P, Norheim F, Hjorth M, Bjellaas T, Drevon CA, et al. Plin2 deletion increases cholesteryl ester lipid droplet content and disturbs cholesterol balance in adrenal cortex. *J Lipid Res*. (2021) 62:100048. doi: 10.1016/j.jlr.2021.100048

68. Dolfi B, Gallerand A, Firulyova MM, Xu Y, Merlin J, Dumont A, et al. Unravelling the sex-specific diversity and functions of adrenal gland macrophages. *Cell Rep*. (2022) 39:110949. doi: 10.1016/j.celrep.2022.110949

69. Chavakis T, Alexaki VI, Ferrante AW Jr. Macrophage function in adipose tissue homeostasis and metabolic inflammation. *Nat Immunol*. (2023) 24:757–66. doi: 10.1038/s41590-023-01479-0

70. Xu Y, Patterson MT, Dolfi B, Zhu A, Bertola A, Schrank PR, et al. Adrenal gland macrophages regulate glucocorticoid production through Trem2 and TGF-beta. *JCI Insight*. (2024) 9(14):e174746. doi: 10.1172/jci.insight.174746

71. Brown AJ, Sun L, Feramisco JD, Brown MS, Goldstein JL. Cholesterol addition to ER membranes alters conformation of SCAP, the SREBP escort protein that regulates cholesterol metabolism. *Mol Cell*. (2002) 10:237–45. doi: 10.1016/S1097-2765(02)00591-9

72. Bose HS, Sugawara T, Strauss JF 3rd, Miller WL, International Congenital Lipoid Adrenal Hyperplasia C. The pathophysiology and genetics of congenital lipoid adrenal hyperplasia. *N Engl J Med*. (1996) 335:1870–8. doi: 10.1056/NEJM199612193352503

73. Tsujishita Y, Hurley JH. Structure and lipid transport mechanism of a StAR-related domain. *Nat Struct Biol*. (2000) 7:408–14. doi: 10.1038/75192

74. Bose HS, Bose M, Whittal RM. Tom40 in cholesterol transport. *iScience*. (2023) 26:106386. doi: 10.1016/j.isci.2023.106386

75. Prasad M, Kaur J, Pawlak KJ, Bose M, Whittal RM, Bose HS. Mitochondria-associated endoplasmic reticulum membrane (MAM) regulates steroidogenic activity via steroidogenic acute regulatory protein (StAR)-voltage-dependent anion channel 2 (VDAC2) interaction. *J Biol Chem*. (2015) 290:2604–16. doi: 10.1074/jbc.M114.605808

76. Prasad M, Pawlak KJ, Burak WE, Perry EE, Marshall B, Whittal RM, et al. Mitochondrial metabolic regulation by GRP78. *Sci Adv*. (2017) 3:e1602038. doi: 10.1126/sciadv.1602038

77. Larsen MC, Lee J, Jorgensen JS, Jefcoate CR. STARD1 functions in mitochondrial cholesterol metabolism and nascent HDL formation. Gene expression and molecular mRNA imaging show novel splicing and a 1:1 mitochondrial association. *Front Endocrinol (Lausanne)*. (2020) 11:559674. doi: 10.3389/fendo.2020.559674

78. Mateska I, Witt A, Hagag E, Sinha A, Yilmaz C, Thanou E, et al. Succinate mediates inflammation-induced adrenocortical dysfunction. *Elife*. (2023) 12:e83064. doi: 10.7554/eLife.83064

79. Mele PG, Duarte A, Paz C, Capponi A, Podesta EJ. Role of intramitochondrial arachidonic acid and acyl-CoA synthetase 4 in angiotensin II-regulated aldosterone synthesis in NCI-H295R adrenocortical cell line. *Endocrinology*. (2012) 153:3284–94. doi: 10.1210/en.2011-2108

80. Venugopal S, Galano M, Chan R, Sanyal E, Issop L, Lee S, et al. Dynamic remodeling of membranes and their lipids during acute hormone-induced steroidogenesis in MA-10 mouse leydig tumor cells. *Int J Mol Sci*. (2021) 22(5):2554. doi: 10.3390/ijms22052554

81. Sandhu J, Li S, Fairall L, Pfisterer SG, Gurnett JE, Xiao X, et al. Aster proteins facilitate nonvesicular plasma membrane to ER cholesterol transport in mammalian cells. *Cell*. (2018) 175:514–29.e20. doi: 10.1016/j.cell.2018.08.033

82. Andersen JP, Zhang J, Sun H, Liu X, Liu J, Nie J, et al. Aster-B coordinates with Arf1 to regulate mitochondrial cholesterol transport. *Mol Metab*. (2020) 42:101055. doi: 10.1016/j.molmet.2020.101055

83. Deng B, Shen WJ, Dong D, Azhar S, Kraemer FB. Plasma membrane cholesterol trafficking in steroidogenesis. *FASEB J*. (2019) 33:1389–400. doi: 10.1096/fj.201800697RRR

84. Venugopal S, Martinez-Arguelles DB, Chebbi S, Hullin-Matsuda F, Kobayashi T, Papadopoulos V. Plasma membrane origin of the steroidogenic pool of cholesterol used in hormone-induced acute steroid formation in leydig cells. *J Biol Chem*. (2016) 291:26109–25. doi: 10.1074/jbc.M116.740928

85. Liimatta J, Curschellas E, Altinkilic EM, Naamneh Elzenaty R, Augsburger P, du Toit T, et al. Adrenal abcg1 controls cholesterol flux and steroidogenesis. *Endocrinology*. (2024) 165(3):bqae014. doi: 10.1210/endocr/bqae014

86. Taylor MJ, Sanjanwala AR, Morin EE, Rowland-Fisher E, Anderson K, Schwendeman A, et al. Synthetic high-density lipoprotein (sHDL) inhibits steroid production in HAC15 adrenal cells. *Endocrinology*. (2016) 157:3122–9. doi: 10.1210/en.2014-1663

87. Mateska I, Nanda K, Dye NA, Alexaki VI, Eaton S. Range of SHH signaling in adrenal gland is limited by membrane contact to cells with primary cilia. *J Cell Biol*. (2020) 219(12):e201910087. doi: 10.1083/jcb.201910087

88. Swierczynska MM, Mateska I, Peitzsch M, Bornstein SR, Chavakis T, Eisenhofer G, et al. Changes in morphology and function of adrenal cortex in mice fed a high-fat diet. *Int J Obes (Lond)*. (2015) 39:321–30. doi: 10.1038/ijo.2014.102

89. Wang X, Han J, Pan J, Borchers CH. Comprehensive imaging of porcine adrenal gland lipids by MALDI-FTMS using quercetin as a matrix. *Anal Chem*. (2014) 86:638–46. doi: 10.1021/ac404044k

90. Ozbay T, Rowan A, Leon A, Patel P, Sewer MB. Cyclic adenosine 5'-monophosphate-dependent sphingosine-1-phosphate biosynthesis induces human CYP17 gene transcription by activating cleavage of sterol regulatory element binding protein 1. *Endocrinology*. (2006) 147:1427–37. doi: 10.1210/en.2005-1091

91. Lucki NC, Li D, Sewer MB. Sphingosine-1-phosphate rapidly increases cortisol biosynthesis and the expression of genes involved in cholesterol uptake and transport in H295R adrenocortical cells. *Mol Cell Endocrinol*. (2012) 348:165–75. doi: 10.1016/j.mce.2011.08.003

92. Prasad R, Hadjidemetriou I, Maharaj A, Meimaridou E, Buonocore F, Saleem M, et al. Sphingosine-1-phosphate lyase mutations cause primary adrenal insufficiency and steroid-resistant nephrotic syndrome. *J Clin Invest*. (2017) 127:942–53. doi: 10.1172/JCI90171

93. Sun N, Wu Y, Nanba K, Sbiera S, Kircher S, Kunzke T, et al. High-resolution tissue mass spectrometry imaging reveals a refined functional anatomy of the human adult adrenal gland. *Endocrinology*. (2018) 159:1511–24. doi: 10.1210/en.2018-00064

94. Cornejo Maciel F, Maloberti P, Neuman I, Cano F, Castilla R, Castillo F, et al. An arachidonic acid-preferring acyl-CoA synthetase is a hormone-dependent and obligatory protein in the signal transduction pathway of steroidogenic hormones. *J Mol Endocrinol*. (2005) 34:655–66. doi: 10.1677/jme.1.01691

95. Maloberti P, Castilla R, Castillo F, Cornejo Maciel F, Mendez CF, Paz C, et al. Silencing the expression of mitochondrial acyl-CoA thioesterase I and acyl-CoA synthetase 4 inhibits hormone-induced steroidogenesis. *FEBS J*. (2005) 272:1804–14. doi: 10.1111/j.1742-4658.2005.04616.x

96. Maloberti P, Cornejo Maciel F, Castillo AF, Castilla R, Duarte A, Toledo MF, et al. Enzymes involved in arachidonic acid release in adrenal and Leydig cells. *Mol Cell Endocrinol*. (2007) 265-266:113–20. doi: 10.1016/j.mce.2006.12.026

97. Castillo AF, Cornejo Maciel F, Castilla R, Duarte A, Maloberti P, Paz C, et al. cAMP increases mitochondrial cholesterol transport through the induction of arachidonic acid release inside this organelle in Leydig cells. *FEBS J*. (2006) 273:5011–21. doi: 10.1111/j.1742-4658.2006.05496.x

98. Wentworth BJ, Haug RM, Northup PG, Caldwell SH, Henry ZH. Abnormal cholesterol metabolism underlies relative adrenal insufficiency in decompensated cirrhosis. *Liver Int*. (2021) 41:1913–21. doi: 10.1111/liv.14970

99. Engelen M, van Ballegoij WJC, Mallack EJ, Van Haren KP, Kohler W, Salsano E, et al. International recommendations for the diagnosis and management of patients with adrenoleukodystrophy: A consensus-based approach. *Neurology*. (2022) 99:940–51. doi: 10.1212/WNL.0000000000201374

100. Jaspers YRJ, Yska HAF, Bergner CG, Dijkstra IME, Huffnagel IC, Voermans MMC, et al. Lipidomic biomarkers in plasma correlate with disease severity in adrenoleukodystrophy. *Commun Med (Lond)*. (2024) 4:175. doi: 10.1038/s43856-024-00605-9

101. Buda A, Forss-Petter S, Hua R, Jaspers Y, Lassnig M, Waidhofer-Sollner P, et al. ABCD1 transporter deficiency results in altered cholesterol homeostasis. *Biomolecules*. (2023) 13(9):1333. doi: 10.3390/biom13091333

102. Lovric S, Goncalves S, Gee HY, Oskouian B, Srinivas H, Choi WI, et al. Mutations in sphingosine-1-phosphate lyase cause nephrosis with ichthyosis and adrenal insufficiency. *J Clin Invest*. (2017) 127:912–28. doi: 10.1172/JCI89626

103. Aguisanda F, Thorne N, Zheng W. Targeting wolman disease and cholesteryl ester storage disease: disease pathogenesis and therapeutic development. *Curr Chem Genom Transl Med*. (2017) 11:1–18. doi: 10.2174/2213988501711010001

104. Baudrand R, Pojoga LH, Vaidya A, Garza AE, Vohringer PA, Jeunemaitre X, et al. Statin use and adrenal aldosterone production in hypertensive and diabetic subjects. *Circulation*. (2015) 132:1825–33. doi: 10.1161/CIRCULATIONAHA.115.016759

105. Haas AV, Baudrand R, Easly RM, Murray GR, Touyz RM, Pojoga LH, et al. Interplay between statins, cav1 (Caveolin-1), and aldosterone. *Hypertension*. (2020) 76:962–7. doi: 10.1161/HYPERTENSIONAHA.120.14777

106. Castellano JM, Pocock SJ, Bhatt DL, Quesada AJ, Owen R, Fernandez-Ortiz A, et al. Polypill strategy in secondary cardiovascular prevention. *N Engl J Med*. (2022) 387:967–77. doi: 10.1056/NEJMoa2208275

107. Bose M, Whittal RM, Miller WL, Bose HS. Steroidogenic activity of StAR requires contact with mitochondrial VDAC1 and phosphate carrier protein. *J Biol Chem*. (2008) 283:8837–45. doi: 10.1074/jbc.M709221200

108. Rone MB, Midzak AS, Issop L, Rammouz G, Jagannathan S, Fan J, et al. Identification of a dynamic mitochondrial protein complex driving cholesterol import, trafficking, and metabolism to steroid hormones. *Mol Endocrinol*. (2012) 26:1868–82. doi: 10.1210/me.2012-1159

Frontiers in Endocrinology

Explores the endocrine system to find new therapies for key health issues

The second most-cited endocrinology and metabolism journal, which advances our understanding of the endocrine system. It uncovers new therapies for prevalent health issues such as obesity, diabetes, reproduction, and aging.

Discover the latest Research Topics

See more →

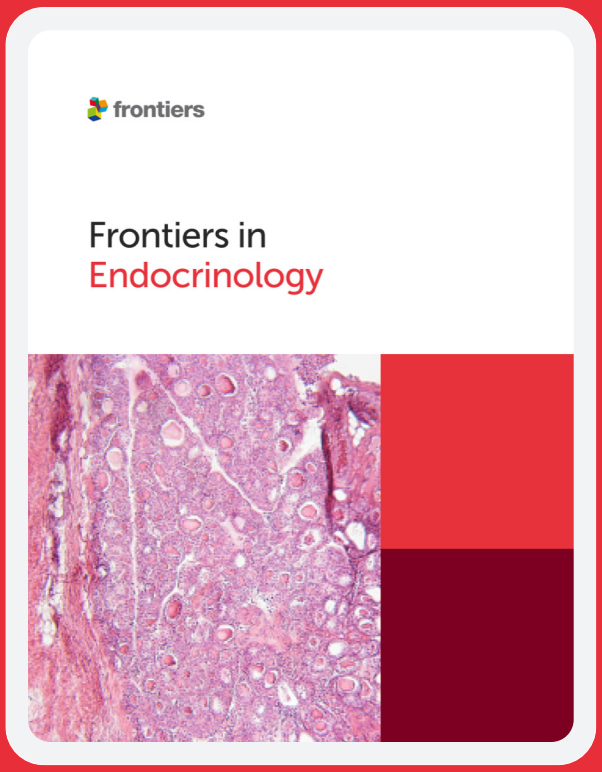

Frontiers

Avenue du Tribunal-Fédéral 34
1005 Lausanne, Switzerland
frontiersin.org

Contact us

+41 (0)21 510 17 00
frontiersin.org/about/contact